ANALYSIS OF DEFORMATION

KEITH SWAINGER
PH.D.(ENG.), LONDON
Recently Imperial Chemical Industries
Research Fellow in the University of London

ANALYSIS OF DEFORMATION

VOLUME TWO

Experiment and Applied Theory

LONDON
CHAPMAN & HALL LTD
37 Essex Street, London, W.C.2
1954

First published 1954

CATALOGUE NO. 542/4

Made and printed in Great Britain by
William Clowes and Sons, Limited, London and Beccles

PREFACE TO VOLUME TWO

'All substances deform under applied loads. This phenomenon is the aspect of natural science considered in the present work after imposing certain idealising restrictions to bring such a wide subject within the scope of one set of mathematically linear equations.' This introduced the formulation of the theory in volume I of this treatise and indicates the general attitude adopted there.

Here, the theory is applied and the available experimental evidence is examined for the equilibrium deformation of various solids having various boundary conditions. Even for economically important materials like engineering metals and rubber, there is *very little experimental evidence* at present on their behaviour under complex stresses. The present author undertook a research in the period from October 1945 to September 1950. After some preliminary simple tensile loading of engineering metals to get the 'feel' of the situation and to develop and make suitable instruments [3, 8, 9, 27], it was seen to be essential to test at least one engineering metal over as much of the stress universe as is physically possible.

The importance of using the whole strain field of the deformable body itself as a reference for the observation of stress-strain effects, rather than to use a reference fixed in space, was realised early in 1946. The consequences of this idea are examined in general terms in volume I and an extremely simple presentation of the relevant ideas is given here, in chapter II.

The classical Navier, Cauchy, Saint-Venant theory on infinitesimal elastic straining was shown to be insufficiently restrictive on the theoretical distribution of complex stresses. This criticism led to a polemical situation with the elasticians, while the analytical methods used led to controversy with the mathematicians [69, 70]. The author hopes that the first volume together with this second volume will clarify the difficulties. Further, the original three stress functions of Maxwell have been shown to remove the essential property of invariant transformability from the stress dyadic when it is expressed in terms of them. (See volume I, article II,9.) When modified suitably to a single function then there appeared inferences from the classical theory similar to those said to be unacceptable from the author's theory.

Even such a trivial case as simple tension on duralumin led to controversy when the value of the plastic transverse contraction ratio was published [84, 48] as less than $\frac{1}{2}$ for small strains. (See article I,11 here.) It was contended that plastic straining involved only a rearrangement of particles in the metal lattice so that volume change could not occur and, therefore, the plastic transverse contraction ratio could not be less than $\frac{1}{2}$. The evident weakness of the argument is in reasoning to a conclusion based on a homogeneous lattice of particles whereas the metallic body is definitely of crystalline heterogeneity. The author's use of electrical resistance-wire strain-gauges was said to be the cause of the error in the observation. Therefore considerable time was spent in designing, making and using a multiply-armed optical extensometer [3]. The same values were found. Next, it was said that the use of rectangular cross-sectioned test specimens was unsatisfactory since, undoubtedly, the plastic transverse contraction value through the smaller thickness of the section was greatly different from that across the width on which the measurements were taken. (This same statement has appeared again, elsewhere in 1950 [83], since the original discussion in 1946–47.) A check using less accurate means of measurement gave virtually the same value in both directions. It transpired that the other experimenter had tested steel and a measurement on this material did indeed give a value not much less than $\frac{1}{2}$. Tests on copper, brass and aluminium gave values well below $\frac{1}{2}$ similar to that for duralumin.

This rather trivial case demonstrates the danger of extrapolating measurements from one substance to another or, even worse, to a general conclusion which, by a coincidence, may be in accord with a preconception on what should be observed. This book is not one on strength of materials, so the experimental data in chapter I are less than those available to the author. When more tests are available then there can be written a book which is the complex stress equivalent of the familiar type of book dealing with simple loading of engineering materials. A survey of the literature shows that the necessity for a programme of *complex* stressing of materials has not been realised yet by the learned societies dealing with this topic. So very much experiment is needed on many substances!

During such experiments and while analysing the measurements, fresh directions for investigation will undoubtedly appear. The present author has dimly seen several directions for advance, from

his rudimentary experiments and the analysis of measurements by others, as the careful reader will note here. The present author hopes that he, or somebody else, will secure in the near future the experimental facilities necessary to extend knowledge in this field which affects the current ideas in so many topics discussing the change of shape of bodies under force. There is so much to be done that many workers can spend full, profitable lives without seeing the end of the task.

The few measurements that have been taken are rarely given in the memoirs published more recently. Usually, an author gives only a printed curve, so that a reader is unable to examine any alternative method of analysing the observations. The present author experienced this difficulty, so several of the experimenters were kind enough to supply their readings privately on request. For the convenience of the present reader, the measurements are given in the Tables and their sources gratefully acknowledged.

The Navier, Cauchy, Saint-Venant theory leads to equations which are mathematically necessary but are not sufficient. Even with the Saint-Venant compatibility conditions, which are less restrictive than the present author's, the usual biharmonic distribution of the Airy stress function is not sufficiently restrictive for 'plane stress'. It is shown how to utilise these 'approximate' solutions for infinitesimal strain and to extend them to finite elastic strain by using whole-body convected axes and the principle of straining equivalence of relative-displacement and straining-displacement. This shows that the orthogonal transformation, from the unstrained elastic body to the strained elastic body, is performed with precisely the same equations for any finite magnitudes of strain when the two orthogonal (usually curvilinear) grids are locked together at one arbitrary point and a 'true' strain measure is used. Thus, the immense labour expended on the solution of particular boundary problems, since the Navier, Cauchy inception of the current theory in the period 1822–27, is not completely discarded but it needs to be recognised that each solution is mathematically approximate and that it must be examined for possible error.

The impact of the present ideas on the deservedly famous theory of torsion due to Saint-Venant is seen in chapter XI. The inferences there are consistent with qualitative ideas expressed separately by Cauchy and Kelvin, but which were discarded as valueless (but, fortunately, were placed on record) because only

the insufficient compatibility conditions of Saint-Venant were available then. The modification of Saint-Venant's theory by the present author shows that radius vectors do not necessarily remain straight as hypothesised by Saint-Venant following Coulomb. Cauchy doubted the validity of such an hypothesis when considering Saint-Venant's memoir prior to publication.

Further, the unhappy Navier was not completely in error with some of his inferences, since greatest stresses on a boundary can occur at its most distant points from the axis of twist in some cases. This suits Kelvin's analogue to irrotational fluid circulation which is discarded by the Saint-Venant theory as dealing with the trivial case of zero torsion. The Saint-Venant compatibility conditions allow physically unacceptable 'dislocational rotations' to occur in general solutions. The torsion solutions illustrate this dislocational rotation on the so-called axis of twist and give point to Cauchy's query on their validity. A more general theory of torsion, with fewer arbitrary hypotheses, is then given. The Boussinesq stress function is seen to be the conjugate of a particular form of the present author's stress potential.

The self-conjugacy (i.e. symmetry) of the stress and strain dyadics allows each to be expressed in terms of three mutually orthogonal principal components. The principal directions for these two dyadics are not coaxial in anisotropic straining. One arbitrary choice of reference directions is allowable to relate these two dyadics by phenomenological stress-strain parameters. This has been discussed in volume I and is re-emphasised here, but it is not clear from the usual statement of Cauchy's generalised Hooke's law.

The recent observations, by L. R. G. Treloar, on the apparently anomalous stress-strain effects on the application of apparently homogeneous, complex, apparently 'plane' stress to a thin rubber sheet are presented in chapter X. The resolution of the difficulty is seen to be consistent with predictions from the present author's theory. This led to the reconsideration of Filon's well-known generalised plane stress theory and to the formulation of a quasi-plane stress theory. This latter suits the observations that plane strain solutions, of particular boundary value problems, are in accord with the observations of strain on the main faces of thin sheets apparently loaded with plane stress and with photo-elastic observations on relatively thick plates.

Further, consideration of the stress-strain relations derived

from strain energy functions by M. Mooney, L. R. G. Treloar, R. S. Rivlin and others using the same methods indicates that their neglect of the first stress invariant is unjustified. A zero strain energy function influencing the stress-strain relations for incompressible elastic substances, like rubber, is seen to occur. The zero component of the strain energy function for incompressible substances means that the stresses cannot be specified from observations of only strain energy and strain in such cases.

The present author's theory on the shearing of laminæ leads to an analogy with the two-dimensional flow of inviscid, irrotational, incompressible fluid. Hence, the well-known powerful methods of conformal transformation with the complex variable can be applied.

The contemporary recent writers on finite elastic strain have brought into prominence the so-called Poynting effect, due to which an elastic cylindrical rod extends under axial torsion. These writers use quadratic strain theories and introduce a third stress-strain parameter, the 'modulus of cross-elasticity', to analyse the effect. The present author points out that the Poynting effect is a stretch, rather than a normal strain, and analyses the effect by the mathematically linear theory, with only two stress-strain parameters and the further idea of strain transfer, which has no place in other theories. This leads to the theoretical derivation of Poynting's observation that, after application of axial tension to a rod, further axial stretch (referred to as 'strain' by Poynting and subsequent writers) occurs on applying a small shear stress. The increased axial stretch is proportional to the square of the shear stress.

The recent important tests by J. L. M. Morrison & W. M. Shepherd in England, and by R. W. Peters, N. F. Dow & S. B. Batdorf in America, on elasto-plastic straining in metals, emphasise further the necessity of considering strain transfer explicitly. The author's analysis [64] of these tests indicates what is to be taken as elasto-plastic 'strain' to fit the evidence and shows how to analyse the elasto-plastic displacement. A survey of the literature between 1946 and 1950 indicates a severe theoretical controversy on the plastic stress-'strain' relations. These tests appear to have concluded [64] that discussion. The plastic equivalent of the Poynting effect appears again in an example on simple shear.

The relationship between the methods of the 'stress-fluidity' school of plastic strain analysis and that of hydrodynamics, as

given originally by Tresca and Saint-Venant in 1870, seems to have been lost. Much of the controversy in the period 1946–50 can be traced to the misunderstanding arising from the use of the same terms to denote different physical situations by different analysts following upon this loss of sight of the initial formulation. (See article **IV**,16.15.) Further, the writers have not discussed all their physical assumptions, so the matter is presented briefly in article **IV**,16. It is commonly accepted as a fundamental hypothesis that plastic stress-strain relations are independent of the first stress invariant. The present author opposes this idea and presents his theoretical reasons and experimental evidence. Usually, the elastic and plastic stress-strain parameters are hypothesised as isotropic but the usual form of the stress-strain relations does not facilitate the experimental examination of this aspect. The assumed isotropy of the plastic modulus is shown to be very much an approximation. Again, it is seen that when the components of the stress dyadic have some independence of variation one from another then, correspondingly, the variations of the elasto-plastic strain dyadic show some independence one from another. This does not mean that the 'simple' superposition of elasto-plastic stress-strain effects is allowable.

It is of interest that the same sort of polemic has arisen independently in Russia. The applied-mathematician A. A. Ilyushin complained in 1949 [86] of attacks by the physicist V. D. Kuznetsov [87] and the experimentalist S. I. Ratner [88]. The physicist complained that the mathematician ignored physical evidence, had no physical 'feel' for what was happening and in consequence the mathematical theory of Ilyushin [89] did not suggest further directions for experiment but arrived at a dead end. (Quoting Pasteur in the preface of our volume I, the theory is not 'fruitful'.) The experimentalist complained that there are so many unexamined physical hypotheses and suggested tests involving the rotation of stress and strain relative to the substance (present author's 'transfer'). Ilyushin rejects [86] such a test as unenlightening. (Outside Russia such a test was accepted as crucial [64] and carried out [60, 61].) More broadly, it is seen that the quarrel between the physicist and the mathematician is only that between the atomistic and phenomenological approaches similar to the polemic between Navier and Cauchy in the nineteenth century [19], while that with the experimentalist is similar to that with the engineer Vicat [19] who stimulated Saint-Venant to

an improved theory. In fact, the first step towards synthesis of the atomistic and phenomenological approaches has been taken by A. M. Freudenthal [90].

Very steep stress gradients are possible in a deformation but do not appear to have been discussed in detail previously except in Rayleigh's theory [102] of propagation of surface strain waves and rather by implication in Griffith's idea [113] of surface energy to predict rupture of brittle solids. Their observation in experiments is likely to be extremely difficult and could be overlooked in some cases unless a theory had inferred their presence. Further, interior stresses are never measured but must be inferred from some stress-strain theory. Unfortunately, theory is not always amenable to experimental examination and even when tests are carried out the manner of their interpretation is as important as the test, which rarely gives the desired information directly.

Volume I needed to be rigorous since it considered the mathematical consistency of the present theory. This volume II is more concerned with 'practical' aspects, so that in some cases approximations have been made in the intuitive, engineering sense as required but always indicating the nature of the approximation when compared with the rigorous theory. Thus, it is hoped that the present volume supplies a need for the research engineer, experimentalists and physicists without unduly emphasising the mathematics from which this subject cannot be divorced. If the reader desires more detail of basic formulation then volume I gives it. Other topics such as thin plates, buckling, stress propagation, vibrations, etc. will be treated in subsequent volumes. The deformation of 'solids' has been considered primarily in the first two volumes even when discussing stress-fluidity or plastic flow-strain. The inclusion of elasto-viscous fluids like molten solids, pitch, oil, water, air and other gases, etc. in the present comprehensive theory is done readily in terms of the partial-increment dyadics. Volume III, now in preparation, develops the method and shows that the usual restriction to inviscid fluids is unnecessary, as the elasto-viscous flows are analysed just as readily. It is unnecessary to subdivide [156.1] a flow arbitrarily into zones within and outside a 'boundary layer' (in which velocity gradients are appreciable near a surface) as though the fluid body is inhomogeneous, nor to assume arbitrary conditions for its analysis [150, 156.2, 157]. Some deficiencies are revealed in the classical theory of hydrodyamics.

The relevant expressions are given in appendix A, of the various operators and operations in the vector analysis of curvilinear coordinates required here for the particular deformation cases analysed. This, with the appendix A of volume I, gives a concise introduction and summary of vector analysis methods for ready reference, but cannot replace one of the many excellent books on the subject.

Part of this analysis was formulated, some of the examples were worked and the experiments were performed during the author's tenure of an Imperial Chemical Industries Research Fellowship in the University of London from October 1945 to September 1950. Because the theory conflicted with the generally accepted old theories it proved impossible to have published a full account in the scientific journals, so the present treatise was undertaken. The dates for the more important unpublished matter are given in footnotes. The novelty of the ideas led to lack of support of the necessary experimental work, so that there still remains a great deal to be done. This volume was virtually complete in 1952 but, in the interim, a few articles have been added, as shown by the dates in the footnotes.

It is a pleasure to record again the continued encouragement and courtesy of the publishers, Messrs. Chapman & Hall, Ltd., and, in particular, that of Mr. G. Parr, Technical Director. Without this impartial support by the publishers, the new ideas may not have been available for the reader's consideration for many years. Mr. E. W. Hamilton, in charge of the production of the publishers' technical books, has given his helpful guidance again and expedited this volume. The printing and proof-reading by Messrs. William Clowes and Sons, Ltd., have been even more accurate and helpful in this volume, so that the author's task has been light. The author is grateful for this help.

It is hoped that the good offices of these helpers have produced an accurate text. If, however, there are any inaccuracies of presentation or printing, then, clearly, the author is responsible alone.

K. H. S.

6th July, 1954

CONTENTS

Chapter III. HOMOGENEOUS, PLANE TWO-STRESS

Chapter VI. HETEROGENEOUS TWO-STRESS EXPERIMENTS

Chapter VII. TWO-STRESS THEORETICAL EXAMPLES

Chapter VIII. THREE-STRESS EQUATIONS FOR SOLUTION

Chapter IX. THREE-STRESS ANALYSES

Chapter X. RUBBER DEFORMATION AND ITS THEORETICAL INTERPRETATION

Chapter XI. COUPLES APPLIED TO MASSIVE BODIES

Appendix B. COMPLEX VARIABLE

Appendix C. FINITE DIFFERENCES

Appendix D. FOURIER SERIES

PRINCIPAL NOTATION

$\mathbf{R}$	Current position vector of a point.
$\mathbf{R}^o$	Initial position relative to a spatially fixed reference.
$\mathbf{R}^{o\ \text{inst}}$	Initial position relative to non-deformable whole-body convected axes.
$\mathbf{R}^{o*}$	Initial position relative to the deformable reference given by the body itself.
$\mathbf{R}^{o\ \text{def}}$	Initial position relative to non-deformable whole-body convected axes for an elasto-plastic body.
$\mathbf{U}$	Spatial-displacement of a point.
$\mathbf{D}$	Straining-displacement of a point.
$\mathbf{D}^*$	Relative-displacement of a point.
$\mathbf{D}^{\text{abs}}$	Absolute-displacement of a point. The differential form $d\mathbf{D}^{\text{abs}}$ is usually considered.
$\mathbf{V}$	Deformation-displacement relative to non-deformable whole-body convected axes for an elasto-plastic body. (Also used for velocity in chapter XII.) (Also used for spatial-displacement averaged over the thickness of a plate.)
$\mathbf{C}$	Convection-displacement.
$\mathbf{C}^{\text{sp}}$	Spatial convection-displacement.
$\mathbf{C}^{\text{wb}}$, $\mathbf{C}^{\text{st}}$	Whole-body and straining convection-displacement components, respectively, of $\mathbf{C}^{\text{sp}}$.
$\mathbf{O}$	Position of the arbitrary origin of non-deformable whole-body convected axes.
$\mathfrak{M}$	Strain dyadic.
$\mathfrak{S}$	Stress dyadic.
$\mathfrak{P}$	Stress-strain parameters dyadic. Superscript M denotes the general member of E, P for elastic and plastic respectively.
$\boldsymbol{P}$	Stress-strain parameters quadadic.
$\mathfrak{I}$	Idemfactor.
$\mathfrak{Q}$	Versor operator.
Δ	Partial-increment operator.

$\boldsymbol{\nabla}$	Vector gradient operator referred to generally as 'nabla'.
$\cdot$	'Dot' of scalar product.
$\times$	'Cross' of vector product.
$:$	Double scalar product. (See volume I, article A,22.1.)
$\overset{\times}{\times}$	Double vector product. (See volume I, Article A,22.2.)
$\approx$	Sign meaning 'equivalent to'.
$\doteqdot$	Sign meaning 'approximately equal to'.
$\boldsymbol{\nabla}\cdot \equiv \text{div}$	Divergence operator.
$\boldsymbol{\nabla}\times \equiv \text{curl}$	Curl operator.
∇^2	Laplacian operator found here from $\mathfrak{J}:\boldsymbol{\nabla}\boldsymbol{\nabla}$.
$\nabla^4 \equiv \nabla^2\nabla^2$	Biharmonic operator.
$\mathcal{E}$	Displacement potential or, otherwise, the scalar potential of the strain dyadic.
H	Stress potential.
$\mathcal{A}$	Airy stress function.
α	Special form in the stress potential $H = R_z\alpha$.
β	Boussinesq stress function shown to be conjugate to α. (Also a constant of proportionality in article IV,16.)
i, j, k	Direction subscripts for cartesian axes. Each can represent the general member of *1, 2, 3*. A specialised sequence used frequently is

$i = 1$	2	3
$j = 2$	3	1
$k = 3$	1	2

x, y, z	Direction subscripts used sometimes in place of i, j, k.
$\mathbf{i}, \mathbf{j}, \mathbf{k}$	Subscripts denoting the principal directions of the self-conjugate strain dyadic.
a, b, c	Direction subscripts for the typical point in a typical curvilinear coordinates system.
r, θ, z	Direction subscripts for cylindrical coordinates (R_r, θ, R_z).
r, θ, ϕ	Direction subscripts for spherical coordinates (R_r, θ, ϕ).

$\mathbf{c}_i$ or $\mathbf{c}_x$ — Spatially fixed cartesian axes unit vectors.

$\mathbf{x}_i$ — Non-deformable whole-body convected axes unit vectors.

$\mathbf{x}_\mathbf{i}$ — Principal directions (unit vectors) of the strain dyadic.

$\mathbf{c}_a$, $\mathbf{c}_b$, $\mathbf{c}_c$ — Curvilinear coordinates unit vectors.

$\mathbf{c}_i\mathbf{c}_j$, ..., $\mathbf{c}_x\mathbf{c}_y$, ..., $\mathbf{x}_i\mathbf{x}_j$, ..., $\mathbf{x}_\mathbf{i}\mathbf{x}_\mathbf{i}$, ..., $\mathbf{c}_a\mathbf{c}_b$, ... Unit dyads for the various dyadics and directions.

$\mathbf{s}_\mathbf{i}$ — Principal directions (unit vectors) of the stress dyadic.

$\mathbf{n}$ — Unit vector normal of a surface.

$\mathbf{t}$, $\mathbf{p}$ — Orthogonal unit vectors tangential to the surface and forming a set $\mathbf{n}$, $\mathbf{t}$, $\mathbf{p}$.

n_i, ..., n_x, ..., n_a, ... Scalar components of $\mathbf{n}$ to the various coordinate directions. Also direction cosines since, for example, $n_i = \mathbf{n}\cdot\mathbf{c}_i$.

R_i, ..., R_x, ..., R_a, ... Scalar components of $\mathbf{R}$ to the various coordinate directions.

U_i, ..., U_x, ..., U_a, ...
D_i, ..., D_x, ..., D_a, ...
D_i^*, ..., D_x^*, ..., D_a^*, ...
} Scalar components of the various displacements for the various coordinate directions.

$d\mathbf{R}$ — Arbitrary, differential change of position from $\mathbf{R}$ in the *deformed* body.

$\mathbf{x}_R$ — Unit vector in the direction of $d\mathbf{R}$.

$F_{,i}$, ..., $F_{,x}$, ..., $F_{;a}$, ... Abbreviated notation for partial differentiation of any function F. For example, $F_{;i} \equiv \partial F/\partial R_i$, so that the subscript semicolon represents the operator $\partial/\partial R$ for brevity.

$\mathbf{S}$ — Vector stress. Components of the stress dyadic for various directions are $\mathbf{S}_i$, ..., $\mathbf{S}_x$, ..., $\mathbf{S}_a$, ..., $\mathbf{S}_\mathbf{i}$, ...

S — Scalar stress. Components of vector stress for various coordinate directions are S_{ij}, ..., S_{xy}, ..., S_{ab}, ..., $S_{\mathbf{ij}}$, ... When $\mathbf{S}_\mathbf{i}$ is the principal value for the stress dyadic then the scalar value is $S_\mathbf{i}$.

e — 'True' strain. Scalar components of the strain dyadic are e_{ij}, ..., e_{xy}, ..., e_{ab}, ..., $e_\mathbf{i}$, ...

a_R	Unit stretch of the *line* element, in direction $\mathbf{x}_R$, of current length dR and initial length dR^o. Thus, $d\mathbf{D}^{\text{abs}} = a_R dR \mathbf{x}_R$.
ϵ	Partial-strain component of e. Appropriate subscripts give the various directions.
ψ, q	Stress-strain parameters. Modulus and transverse contraction ratio, respectively. Superscript M denotes various 'qualities' of the strain. Direction subscripts are used when the *parameters* are not isotropic.
E, E^o	'True' and 'nominal' Young's elastic modulus, respectively. (For linear, true, elastic stress-strain relations $E \equiv \psi^{-1}$.)
P	Elasto-plastic tangent modulus.
F, G J, K	Stress-strain parameters usually as suitable combinations of the ψ's and q's. (J, K also used as geometrical quantities in article **III**,8.)
Φ, Λ	Strain transfer angle for an elastic body and an elasto-plastic body, respectively.
κ	Modulus of infinitesimal dilation.
v	Infinitesimal volumetric dilation per unit volume. (Also used for *areal* dilation in article **V**,19.)
$\mathfrak{A}^{\text{sp}}$	Infinitesimal spatial-rotation antiself-conjugate dyadic. Sometimes just $\mathfrak{A}$ for brevity.
$\omega_{ij}, \ldots$	Scalar components of $\mathfrak{A}^{\text{sp}}$ for various coordinate directions.
$\theta^{\text{sp}}, \theta^{\text{wb}}, \theta^{\text{st}}, \theta^{\text{dr}}$	Spatial-, whole-body, straining-, dislocational-rotation, respectively, of a principal element during infinitesimal elastic deformation.
e^o	'Nominal' or Cauchy strain. Appropriate subscripts of direction, similar to those for e, are inserted as required.
e^{nat} (or α)	Natural, logarithmic or Roentgen, Ludwig, Hencky strain. (α also used for the 'real' component of a complex function, as an elliptic coordinate and as Trouton's coefficient of viscous extension.)
m, m^o	Current and initial density, respectively.
$m\mathbf{B}$	Body force per unit current volume.

$\chi^{(i)}$ Three invariants of a self-conjugate dyadic.

χ^S, χ^D First invariant of the stress dyadic and strain dyadic, respectively. The superscript (1) is left off for brevity.

λ_1^o, λ_1 Extension ratio (er) and inverse extension ratio (inver), respectively, for principal directions. (λ_1^o here is A_1, the strain ellipsoid semi-axis in volume I, article **I**,4.1.)

u_1^o, u_1 Squared extension ratio (ser) and inverse squared extension ratio (invser), respectively, for principal directions.

w, w^o Strain energy per unit current and initial volumes, respectively. Referred to more briefly as current and initial unit strain energy, respectively. (w is also used for infinitesimal spatial-rotation in article **V**,19.)

w'' Zero strain energy function in article **X**,5.8.

$\mathfrak{U} = (\mathfrak{J}-\nabla\mathbf{U})\cdot(\mathfrak{J}-\mathbf{U}\nabla)$ A self-conjugate dyadic in the strain ellipsoid equation with the coordinates of the point in the *deformed* body.

$\mathfrak{U}^o = (\mathfrak{J}+\nabla^o\mathbf{U})\cdot(\mathfrak{J}+\mathbf{U}\nabla^o)$ A self-conjugate dyadic in the inverse strain ellipsoid equation with the coordinates of the point in the *undeformed* body.

ξ, ξ^o First invariant of $\mathfrak{U}$ and $\mathfrak{U}^o$, respectively.

$u_{R} = \mathbf{x}_R\cdot\mathfrak{U}\cdot\mathbf{x}_R$ Quadratic invariant (elastic) strain metric analysing spatial-displacement relative to the deformed body.

$u_R^o = \mathbf{x}_R^o\cdot\mathfrak{U}^o\cdot\mathbf{x}_R^o$ Quadratic invariant (elastic) strain metric analysing spatial-displacement relative to the undeformed body.

$\mathbf{x}_R^o$ Initial direction of a line element having current direction $\mathbf{x}_R$.

C, C^o Stress-strain parameters in chapter X. (Also used as geometrical quantities in article **III**,8.) (C also denotes the constant first stress invariant sometimes.)

$\mathbf{Q}$, Q, $\mathbf{q}$ Torque vector, scalar magnitude and direction, respectively.

$\mathbf{o}$ Octahedral unit vector.

$\mathbf{S}^{oct}$	Octahedral stress vector.
σ, τ	Octahedral normal and shear scalar stress, respectively.
ν, γ	Octahedral normal and shear strains, respectively.
$i = \sqrt{(-1)}$	Imaginary, so-called.
$c = R_x + iR_y$	Complex variable.
$c' = R_x - iR_y$	Conjugate complex variable.
γ, γ'	Function of c and c', respectively.
α, β	Real and imaginary components of γ. (Also elliptic coordinates in article **XII**,7.)
$\overset{c}{\mathbf{c}}, \overset{cc}{\mathbf{cc}}$	Complex unit vector, unit dyad, respectively.
$2\mu, \alpha$	Coefficient of fluid viscosity and viscous extension, respectively, in article **IV**,16.
$\delta f, f'\delta(\ )$	Incremental plastic parameters in article **IV**,16.
$\mathfrak{N}, \mathfrak{T}$	Strain and stress dyadic, respectively, from $\mathfrak{M}$, $\mathfrak{S}$, each averaged over the thickness of a plate.
$\mathbf{V}, V_x, \ldots$	Spatial-displacement averaged over the thickness of a plate. Vector and the scalar components, respectively.
χ^T	First invariant of $\mathfrak{T}$.
f, T'	Scalar component of $\mathfrak{N}$ and $\mathfrak{T}$, respectively, with appropriate direction subscripts. (T' is also used sometimes for shear stress.) (Again, in article **XI**,5 it is used for the infinitesimal angle of twist.)
$\mathcal{F}, \mathcal{J}$	Scalar potentials of dyadics $\mathfrak{N}$, $\mathfrak{T}$, respectively.

Chapter I

ONE-STRESS DEFINITIONS AND TESTS

1. One-stress test

Simple tension is the most usual loading to test the behaviour of common engineering substances. An extensile or tensile force is applied axially to a right cylinder of the substance and distributed as uniformly as possible over the cross-section, which is usually circular or rectangular. The changes in dimensions of the specimen are frequently very small over important ranges of the loading, so that accurate means of measurement are required.

1.1. **Extensometers.** Many optical instruments have been devised using the relative rotation between a mirror effectively fixed to the specimen and another moved by the relative displacement between two points of the loaded specimen at a distance apart known as the *gauge length*. The Martens extensometer is a typical instrument of this sort to measure longitudinal stretch, while the Lamb extensometer also measures the transverse contraction of a rectangular-sectioned specimen [1, 2].

An instrument constructed by the author [3] measures simultaneously the longitudinal stretch, transverse contraction and, also, stretch at 45° to the axis on a rectangular-sectioned specimen. Several gauge lengths are available in each of these directions, stretches of any finite magnitudes can be accommodated by means of a zero resetting device, while high sensitivity of the order 10^{-5} inches per inch is retained.

A device developed [6] from an observation by Kelvin [7] is to cement a very thin electrical resistance-wire to the surface to be strained. The stretch changes the specific resistance of the wire and this, after suitable calibration, gives a measure of the strain. Most gauges operate within the extension 0·03 inches per inch, but the author found [8, 9] wire filaments operating to 0·14 inches per inch, and then W. Weibull found [10] materials operating to 0·65 inches per inch before they ruptured.

1.2. **Simple compression test.** Axial compression is the other simple loading for a substance. This is not easy to achieve,

as it is difficult to apply the load evenly over the cross-section, to have a specimen long enough to secure a length reasonably free from the end effects, such as friction, and yet short enough to prevent unwanted 'buckling' of the specimen.

2. Normal strain

As the load increases, the simple tensile specimen extends in length and contracts in width. Thus, a short line in the direction of pull and local to a given point on the surface of the specimen increases in length, while one normal to the direction of pull decreases in length. More generally, two such initially orthogonal short lines not in the direction of nor orthogonal to the direction of pull will depart from orthogonality one to another and also change their lengths. The relative displacements between the ends of the short local lines in the direction of and orthogonal to the pull constitute *strain* at the point.†

The change in length of the lines at an angle to the pull is not 'strain', in general, but is known as *stretch*. 'Strain' is the component of a dyadic (or second-order tensor), while 'stretch' is not, as it refers only to the effects in a single line. Elaboration of this distinction, while seen to be most important subsequently, is inappropriate at this introductory phase of the discussion but is given‡ in chapter III.

2.1. **Normal strain definition.** Many mathematical definitions have been proposed for strain. Cauchy's *nominal normal strain* defined as linewise relative displacement per unit length of the *undeformed* body appears to have been the first. Other definitions can be found in the literature or, as discussed briefly, in volume I, articles **III**,8, **III**,H. Unless indicated explicitly otherwise, there is always used here a *true normal strain* defined as linewise relative displacement per unit length of the *deformed* body. Thus [5],

$$e = \begin{pmatrix}\text{Stretched}\\ \text{length}\end{pmatrix} - \begin{pmatrix}\text{Initial}\\ \text{length}\end{pmatrix} \Big/ \begin{pmatrix}\text{Stretched}\\ \text{length}\end{pmatrix} \tag{2.1}$$

The term 'true' does not imply 'falseness' for other definitions but merely that all quantities are 'actual' or 'true' in referring to the current state of strain.

† See volume I, chapters I, III.

‡ A more general discussion is given in volume I, article **III**,13.

2.2. **Comparison of nominal and true strains values.** If a line is initially straight and of length R^o while currently it is straight and of length R, with the notation $(R-R^o) = D$, then true strain

$$e = D/R \tag{2.2}$$

while nominal strain is

$$e^o = D/R^o \tag{2.3}$$

so that

$$e/e^o = R^o/R \tag{2.4}$$

Rearrangement gives

$$e = e^o/(1+e^o) \qquad e^o = e/(1-e) \tag{2.5}$$

2.3. **Extension ratio, nominal and true strains.** Recent writers [12, 13, 14, 17] on the high elasticity of substances such as rubber have used the extension ratio

$$\lambda^o = R/R^o \tag{2.6}$$

and its inverse

$$\lambda = R^o/R \tag{2.7}$$

to be related to stress when analysing the stress-strain effects. Then, true strain

$$e = 1-\lambda \tag{2.8}$$

while nominal strain

$$e^o = \lambda^o-1 \tag{2.9}$$

2.4. **Normal increment strain from a current state.** The foregoing evolves normal strain definitions regarding the initial, undeformed body as the reference from which to pass to the deformed state or conversely, so that total strains are considered. Now, regard the currently deformed body as the reference from which to pass to a state only incrementally different, so that increment strains will be considered. Thus, by definition, with δD the *increment displacement* of the point relative to the currently deformed state, the true increment strain is†

$$\delta e = \frac{(R+\delta R)-R}{(R+\delta R)} = \frac{\delta D}{R} \tag{2.10}$$

2.5. **Comparison of true total and increment strains and logarithmic strain.** Throughout the present treatise the displacement of particles, relatively one to another, is regarded as

† See volume I for a full discussion.

the primary quantity analysed. Therefore, in articles I,2.2, I,2.4 the 'strains' definitions suit this viewpoint. Thus, for example,

$$\delta e = \delta D/R + \delta(D/R) = \delta D/R - D\delta R/R^2 \qquad (2.11)$$

because $\delta(D/R)$ is an increment of true strain referred to the initially undeformed body, whereas $\delta D/R$ is a true increment strain referred to the currently deformed body.

Then, using total strain gives

$$D = Re \qquad (2.12)$$

or using increment strain

$$D = \Sigma\delta D = \Sigma R\delta e \qquad (2.13)$$

with the summation between the initial and current states.

The Roentgen [15], Ludwig [11], Hencky [12] *natural* or *logarithmic* strain is

$$e^{\text{nat}} = \operatorname*{Lim}_{\delta D \to 0} \Sigma\delta D/R = \log(R/R^o) = \log \lambda^o \qquad (2.14)$$

Comparison with I(2.11) shows that

$$\delta e^{\text{nat}} = \delta e \qquad (2.15)$$

but, because displacement D is the primary quantity here, we do not integrate δe like Roentgen but integrate δD as in I(2.13). The natural strain definition leads to rather clumsy exponential expressions to pass from strain, and therefore stress, to displacement.

3. Transverse contraction

A substance generally contracts in all directions orthogonal to an applied longitudinal stretch as in simple tension. This is the transverse contraction. For the purpose of analysis it is usually convenient to introduce a *transverse contraction ratio* q such that, when the longitudinal strain is e, then the transverse contractile strain is $-qe$, with the negative sign to indicate contraction when the positive sign indicates extension.

Sometimes it is more convenient to analyse the deformation into longitudinal increment strain δe and transverse contractile increment strain $-q\delta e$, where, however, the *transverse increment contraction ratio* q is not necessarily of the same value as that associated with e, although they all apply to the same current state.

4. Stress in simple tension

Simple tensile stress has been defined as one in which the axial force is distributed uniformly across the section. This is a convenient approximation, but it should be borne in mind that actual materials are usually crystalline, with consequent non-uniformity of loading. The *true stress* is defined as force per unit area of actual cross-section at the current strain. Thus, with cross-sectional area α and axial force F the true stress is an *average* value

$$S = F/\alpha \tag{4.1}$$

4.1. **Stress in real substances.** Fig. I,4.1 represents the crystal structure in metal, for example. The crystals vary in

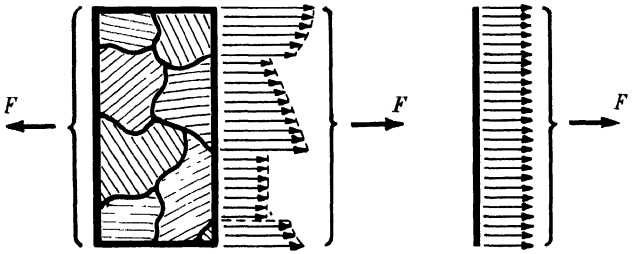

FIG. I,4.1. Crystals shown diagrammatically in a small, rectangular element of metal under simple tensile force F. The stress distribution on the faces of the small element is not uniform. However, the present theory supposes the metal to be amorphous so that stress S is assumed to be uniform on the faces of the element.

size depending on the metal and its previous treatment. As some indication for engineering metals they are classified as [43]: coarse grains $> 0{\cdot}04$ mm, fine grains $= 0{\cdot}004$ mm, very fine grains $= 0{\cdot}0004$ mm. The individual crystals have different stress-strain properties for different directions of loading on each [11], so that the force distribution cannot be strictly uniform across the section. Each crystal carries a different loading from its neighbour, depending on its orientation in the specimen. The mathematical theory evolved neglects the non-uniformity of the stress, so that it postulates an ideal substance that is effectively an amorphous continuum. This fact should be borne in mind if apparent anomaly occurs when comparing theory and experiment.

Further, it is supposed that the stress is zero transversely to the applied axial stress S. It can be seen intuitively as most unlikely that the transverse stresses are zero in such a complex arrangement of crystals in a real substance, although it seems plausible in the ideal amorphous substance postulated in the theory. W. Boas [11] studied the interaction of crystals in such an aggregate and found neighbouring crystals suffering different amounts of deformation, indicating that each carries a different load. The forces appear to act all round on a given crystal, while deformation is continuous across crystal or grain boundaries.

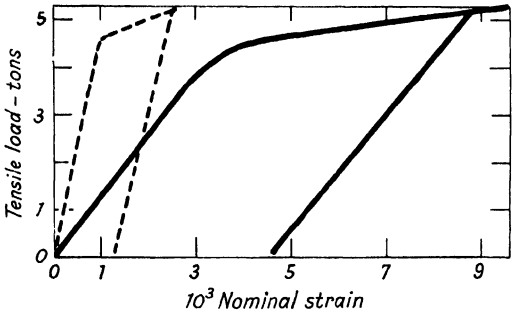

FIG. I,5.1.—Duralumin under simple tensile load. The working cross-section was 1·200 inches wide by 0·233 inches thick. The full line is that for longitudinal strain and the dotted line that for transverse strain in the width of the working section. After the almost linear primary elastic straining there appears plastic strain that remains as irreversible strain on unloading as shown. See Fig. I,5.3 for more detail and Fig. I,5.2 for a greater strain range. The departure from initial linearity occurs at approximately 34 000 pounds per square inch (psi). The primary ratio S/e is 10 10^6 psi.

4.2. **Nominal stress.** It is sometimes convenient, when discussing the properties of a substance, to refer to the *nominal stress* defined as force per initially undeformed area. Thus, with α^o the initial cross-sectional area of the simple tensile specimen and F the current force, then nominal stress is

$$S^o = F/\alpha^o \tag{4.2}$$

Hence, with I(4.1), there is found the relation

$$S/S^o = \alpha^o/\alpha \tag{4.3}$$

This is of the same form as equation I(2.4) between the true and nominal strains.

5. Duralumin under simple tension

The light alloys of aluminium known as 'duralumin' have become increasingly important in recent years because of their use in aircraft and special civil engineering structures where lightness is essential. Under simple tension the typical stress vs. strain curve has the form shown in Fig. I,5.1. The opposing arrow-heads in Fig. I,5.3 indicate that, over that part of the loading sequence, the strain is reversible or recoverable by merely

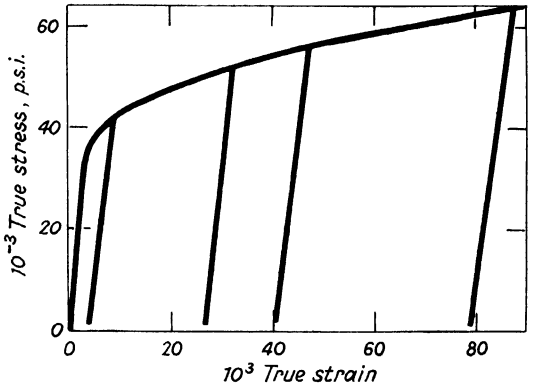

FIG. I,5.2.—The duralumin of Fig. I,5.1 for a greater strain range with four elastic unloading, loading cycles. The transition from such secondary elastic straining is not quite sharp but as shown diagrammatically in Fig. I,5.4. The unloading curve practically coincided with the loading curve in each case, so that the straining hysteresis was low. The 'loops' shown diagrammatically in Fig. I,5.4. indicate the trend in such unloading, loading cycles. The post-secondary yield curves virtually coincide with that for which unloading, loading has not occurred. Thus, the post-primary yield curve is the locus of the secondary yielding.

releasing the load, but a single arrow-head indicates that the stress-strain path cannot be retraced by mere load change. For convenience, the transverse strain is plotted as though of the same sign as the longitudinal strain, but it should be noted that it is negative.

Up to a stress of value S^{P}, say, the longitudinal strain e_L and transverse strain e_T can be removed by merely releasing the load. This is the primary elastic range, in which the longitudinal and transverse stress-strain curves are practically straight. Thus,

the elastic transverse strain contraction ratio q^E is almost constant. It is usually called 'Poisson's ratio' after the nineteenth-century mathematician [19.15] who indicated its presence from a theoretical study on the straining of an assembly of points intended to represent the idealised elastic solid.

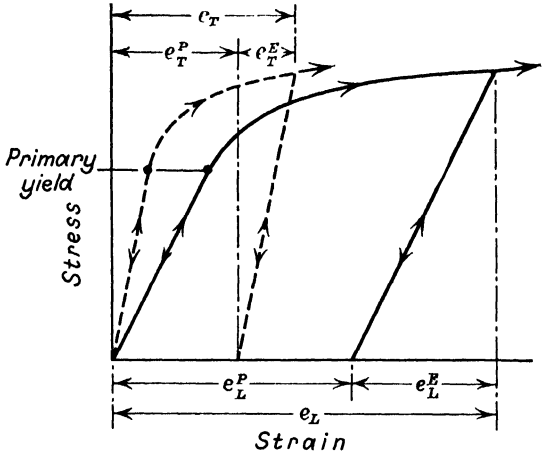

FIG. I,5.3.—Duralumin simple tensile stress vs. longitudinal strain shown as a full line and stress vs. transverse strain shown dotted. Plastic or irreversible strains occur after the elastic or reversible unloading. The stress at which plastic strains first appear is the primary yield stress, while all other post-primary yield stresses are secondary yield stresses.

5.1. **Post-yield straining.** Beyond stress S^p the strains increase more rapidly than before it, and if the stress $S > S^p$ is released then the resulting strain is not zero. This permanent strain is now usually called the *plastic strain* or, in older books, the *permanent set.* The stress-strain recovery curve for unloading is not quite coincident with that followed on reloading up to the stress from which the metal was unloaded. The narrow loop formed is the *hysteresis loop* and is a measure of energy absorbed by a sort of friction and small-scale slippage in the substance which is largely dispersed as heat. However, for the analysis developed in this treatise the hysteresis loop is neglected, so that both curves are taken to coincide on the mean curve between them. The stress S^p at which plastic strains begin to appear is the *primary yield stress.* The stress continues to increase beyond the primary yield and for this reason the duralumin is said to *work-harden.*

5.2. **Secondary yielding.** When stress S greater than S^p is released then the elastic recovery curve is followed. On reloading it is found that the *secondary yield* usually begins again at a slightly lower value than S, but soon follows a stress-strain path that is practically a continuation or a little above that of the one previous to unloading. The result is a rounded corner as in Fig. I,5.4, but this is neglected in the analysis developed here; it is supposed that the secondary yield is sharply on to a curve which is the continuation of that from which unloading occurred. Therefore, the stress-strain curve beyond primary yield can be

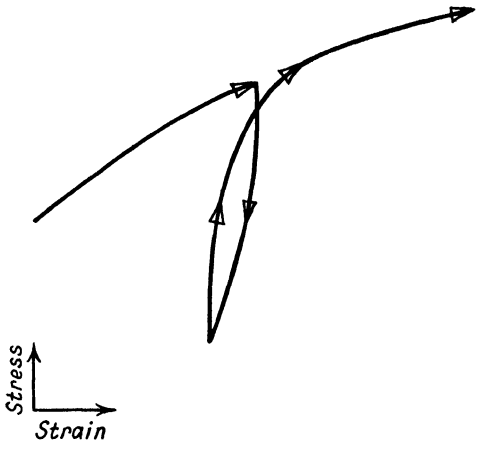

FIG. I,5.4.—Duralumin unloading, loading curve subsequent to primary yield, shown diagrammatically. The 'loop' indicates that energy is absorbed by 'solid viscosity' or frictional effects. The transition from the unloading, loading curve to the post-secondary yield curve is not very sudden but slightly rounded as shown.

regarded as the locus of all the secondary yield points for the duralumin.

The terminology 'elastic limit' has been used frequently and rather loosely in the literature on this topic when referring to primary yield, but it will be avoided in the present work because the term so easily becomes interpreted as that the duralumin, or any other metal, no longer has elastic properties. As seen already, the duralumin does retain its elastic properties even up to the verge of rupture, but some rearrangement of its particles leads to permanent changes in shape. The current elastic strain can be visualised as due to relative, reversible displacements

between the particles at any given instant after rearrangement has occurred to give the appropriate plastic strain.

5.3. **The terminology plastic 'strain' is not satisfactory.** The author feels that a new term should be coined to replace plastic 'strain', because this component of the deformation merely gives some measure of the deformation history of the specimen from an arbitrary initial time. If such a plastically strained specimen is handed to another experimenter not told of its history then he would quite happily regard it as a specimen of metal with a 'primary yield' etc. merely as noted by himself. However, the term has such general usage that it is retained here although 'plastic set' would be suitable and consistent with the older usage.

6. Steel under simple tension

Many steels have stress vs. strain curves of the same general character as that for duralumin in Fig. I,5.1 except that the elastic strains are smaller for given stress values. The common engineering material mild steel, on the other hand, usually displays effects not found in duralumin or most other engineering metals.

6.1. **Unstable primary yield.** The primary elastic range is practically linear up to an *upper yield stress* S^U that, however, is not a definite value. Quite suddenly, as in Fig. I,6.1, the load drops off the tensile specimen until it reaches a *lower yield stress* S^L which is also not quite definite, while at the same time the strain increases quite considerably. The mild steel is in an unstable condition at yield. It has been suggested that the steel would yield at a much lower stress if its atomic lattice behaved like duralumin, for example. In this case, the post-yield curve would be like that dotted in Fig. I,6.2 and joining fairly smoothly into the curve actually observed after the unstable yielding. The mild steel appears to be in a 'super-stressed' condition.

6.2. **Experiment on unstable primary yield.** The mechanically unstable character of mild steel near primary yield can be shown in the following manner.† Several specimens were cut from neighbouring positions in the same stock bar. The upper yield approximate value was found from two specimens and then

† Author, 1939.

a third specimen loaded to a value a little below the upper yield. The load was supported for several minutes without creep of the strain but immediately yielded considerably when the specimen was given a light transverse tap with a pencil. This behaviour was not repeatable at every attempt, as may be expected for an unstable condition. Various theories attempt to explain the

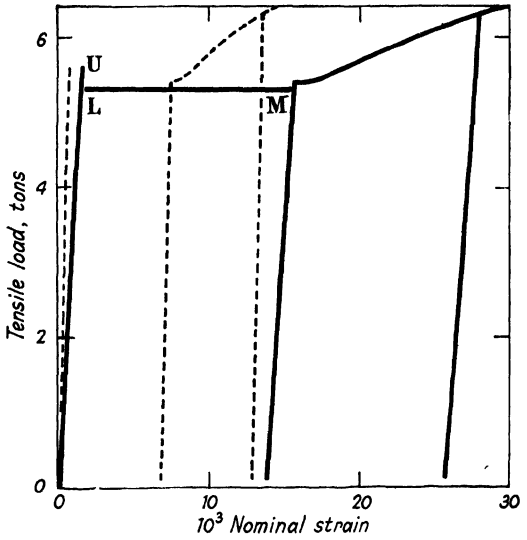

FIG. I,6.1.—Mild steel under simple tensile loading. Longitudinal strain is the full line and transverse strain in the width of the specimen is dotted. The working cross-section was 1·125 inches wide by 0·246 inches thick. Letter U indicates upper primary yield and L the lower value for which the strain was stable subsequent to the sudden, unstable primary yield. Line LM is shown full, but it was impossible to measure the sudden stress and strain changes between the limits U and M. Subsequent to this unstable primary yield the secondary yielding is fairly stable, with only small sudden changes in strain. The transverse strains do not 'follow' the longitudinal strains smoothly. Fig. I,6.3 shows the situation diagrammatically.

physics of this unstable condition for the yielding of mild steel, but the suggestion of J. Palm [44] that it is due to hydrogen in the lattice of the steel crystal seems to fit the facts.

6.3. **Transverse contraction.** The transverse contraction of mild steel frequently follows the longitudinal straining fairly faithfully, as in Fig. I,6.1, but even this is not quite predictable, as shown in a number of tests.†

† Author, 1946.

The typical measurements of longitudinal and transverse strains are shown in Fig. I,6.3. Range OA is the primary elastic with primary yield point A. At the first sudden yield over AB the longitudinal strain increased considerably but the transverse

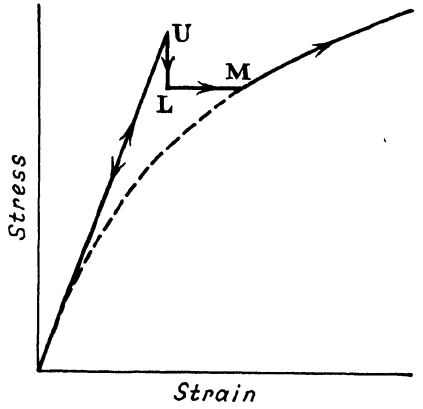

FIG. I,6.2.—Mild-steel unstable primary yielding diagrammatically from upper-value U to lower-value stress at L and on to strain value M. The dotted curve shows the possible transition from a much lower primary yield stress in the absence of any 'super' yield effects.

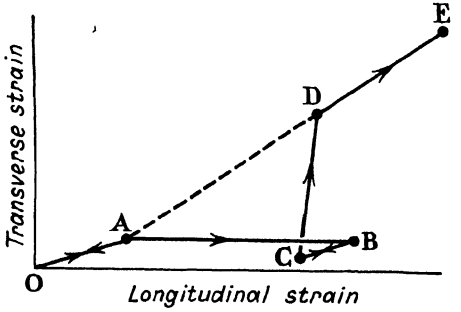

FIG. I,6.3.—Mild-steel unstable primary yielding diagrammatically. The transverse strain does not 'follow' the longitudinal strain faithfully. Primary yield is at A. Full secondary yield at D. Line ADE is that for stable yielding.

strain remained practically constant, so that the plastic straining effect was not observed equally for all directions. Decrease of load caused a normal elastic recovery over BC for both directions. On reloading to yield, the transverse strain suddenly increased but the longitudinal strain remained practically constant to reach

point D apparently on the dotted line that would have been followed if the unstable transverse and longitudinal strain effects had not been present. Path DE is the normal elasto-plastic one once yield occurs again. The foregoing is merely a fairly typical case and differs somewhat in different specimens and steels. This effect was not found to be so severe for secondary yield in the steels tested.

7. Copper and brass under simple tension

Copper is a well-behaved material without any temperamental effects like those noted for mild steel. If the simple tensile specimen is initially soft then primary yield occurs at a low load.

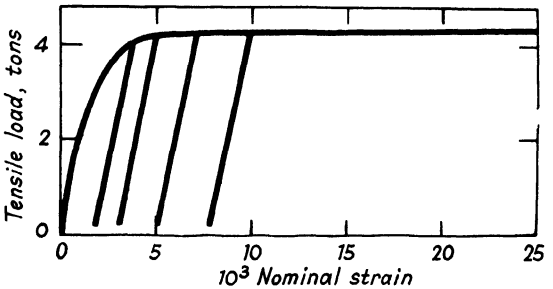

FIG. I,7.1.—Copper under a simple tensile load. Working section was 1·137 inches wide by 0·253 inches thick. When plastic straining was well established the secondary yield loading increased very little over the strain range. The yielded state was quite stable and strain increase occurred only with stress increase.

The transverse strain follows the longitudinal strain without obvious lag such as occurred for mild steel. The hysteresis loop is fairly narrow and the mean curve practically linear. Secondary yield occurs at the stress value that allows the smooth continuation of the stress-strain curve previous to unloading.

Once the deformation is well established the copper does not work-harden very much, as shown by the very small positive slope of the stress-strain curve in Fig. I,7.1. The specimen can sustain a constant load quite well, but the slightest vibration or load increase leads to appreciable strain increase.

The brasses are alloys of copper and other metals and have stress-strain curves of the same general character as duralumin, so they will not be repeated.

8. Rubberlike substances under simple tension

Rubber and substances of like character are distinguished by the very large elastic strains they can suffer before plastic strains appear. Compared with metals, for example, their extensibility is 10^3 to 10^4 times greater. Such great strains presented some difficulty of explanation, as it was fairly clear that mere interatomic relative displacements could not give such values. W. Ostwald, in 1926 [45], seems to have started theory on the mechanism of the effect by picturing the rubber to consist of a liquid and globules having micellar outer sheaths. Progress by subsequent writers modified the ideas, until now the structure is regarded as one of greatly 'kinked', very long molecules bonded to their neighbours by appropriate forces. The topic is discussed fully in L. R. G. Treloar's recent book [13] and, as the method of analysis is to be phenomenological here, the physics will not be pursued further.

TABLE I,8.1

Load, gm F_1	Extension ratio λ_1^o
58	1·056
108	1·119
158	1·192
208	1·270
258	1·364
308	1·478
358	1·613
408	1·769
458	1·939
508	2·121
558	2·305
608	2·506
658	2·686
708	2·874
758	3·056
808	3·225
858	3·383
908	3·525
958	3·680

Initial cross-sectional area 0·0688 cm^2.
Measurements by R. S. Rivlin & D. W. Saunders [16].

8.1. **Simple tensile test.** The simple tensile load-deformation curves in Figs. I,8.1, I,8.2 are for a typical rubber tested by R. S. Rivlin & D. W. Saunders [16] and given in Table I,8.1. Experiments on rubber are frequently analysed in terms of extension ratio $\lambda^o = R/R^o$, with initial length R^o and current length R of a homogeneously strained line. These curves are plotted for

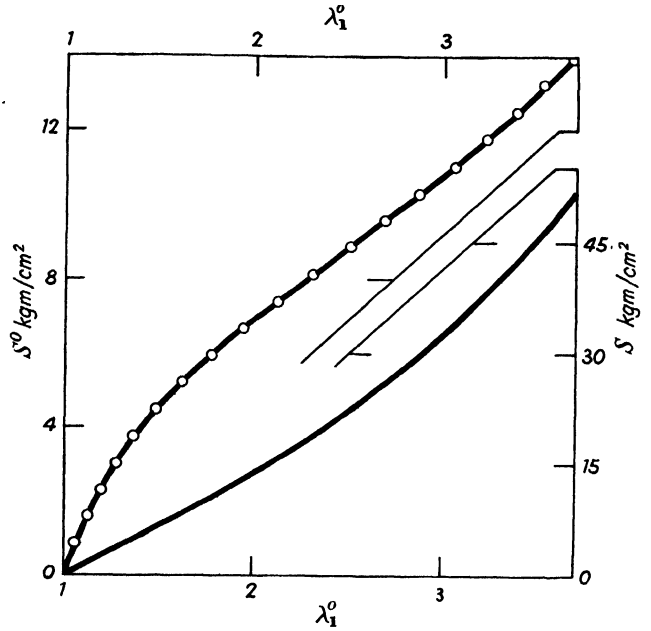

FIG. I,8.1.—The typical rubber tested under simple tension as given in Table I,8.1. Plotting the quantities nominal stress, true stress and er gives curves of different character for the same physical event. Such different plots suggest various forms for complex stress-strain relations subsequently for rubber. Note the approximately linear initial range for true stress and er, while nominal stress and er are approximately linear beyond this initial range.

the longitudinal extension ratio† λ_1^o, simple tensile nominal stress S^o, true stress S, true strain e and the ser $(\lambda_1^o)^2$.

These various plots of the same physical event show that the 'physical behaviour' observed for a substance depends, in a

† It is convenient to use a briefer terminology based on initial letters:
Er = extension ratio = λ^o
Ser = squared extension ratio = $(\lambda^o)^2$
Inver = inverse extension ratio = $(\lambda^o)^{-1} = \lambda$
Invser = inverse squared extension ratio = $(\lambda^o)^{-2} = \lambda^2$

sense, on the mode of measuring or analysing it. Thus, this rubber exhibits stress-strain curves that are concave-down and concave-up over some parts of the range, at least, depending upon which stress and which strain variables are plotted. The effects of this are seen in article I,9 when parameters to relate stress with strain are considered.

The experimental curves are accepted and fitted into the mathematical analysis of this book, but it is of interest that some success has been achieved in formulating a molecular theory to fit, or predict, the simple tensile stress-strain curve for S vs. $(\lambda_1^0)^2$ up

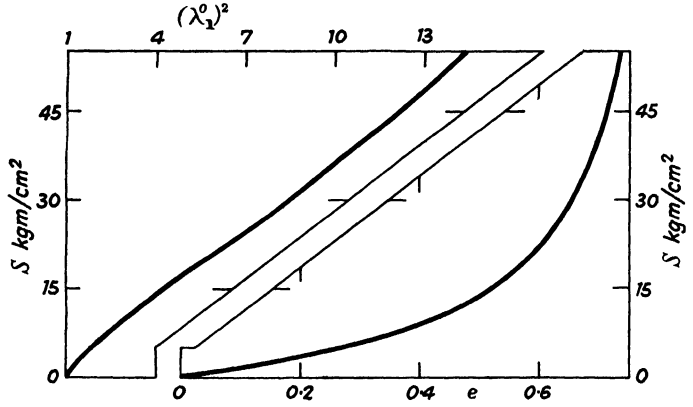

FIG. I,8.2.—The typical rubber tested under simple tension as in Table I,8.1. Note the approximate linearity of true stress and strain over the initial range, corresponding to an er of more than 1·5, while true stress and ser are approximately linear beyond this initial range. Such results suggest analytically convenient methods for complex stress and strain in rubber as in the text subsequently.

to values of λ_1^0 equal to 3 or 4. W. Kuhn [12] began the development in 1934 with a statistical analysis of the thermodynamical behaviour of an aggregate of long, kinked molecules under simple tensile stress and other writers followed to improve the approach. L. R. G. Treloar, from his viewpoint, gives a concise account [13] of the method that is otherwise widely dispersed through the scientific periodicals.

8.2. **Nominal and true stress on incompressible rubber.** Rubber is virtually incompressible for large strains, so that

$$\lambda_1^0\lambda_2^0\lambda_3^0 = 1 \qquad (8.1)$$

as shown in volume I, article III,8.5. M. Mooney [17] quotes W. L. Holt & A. T. McPherson [18] as giving the most exact experimental information on this aspect. This leads to simple formulæ to convert nominal stress to true stress. If R_2^o, R_3^o are the initial cross-sectional dimensions of the simple tensile specimen then the current simple tensile force is

$$F_1 = \lambda_2^o R_2^o \lambda_3^o R_3^o S = R_2^o R_3^o S/\lambda_1^o$$

But

$$F_1/(R_2^o R_3^o) = S^o$$

so that true stress

$$S = \lambda_1^o S^o \tag{8.2}$$

9. Elastic modulus

Hooke, in 1678 [19.16], and Mariotte independently, in 1680 [19.17], showed that the load vs. extension curve for an elastic metal spring is linear. Hooke appears to have regarded all elastic bodies as 'springs', so that the nominal stress vs. nominal strain curve was thought to be always linear, and found to be approximately so, for engineering metals at least.

Young, in 1807 [19.18], introduced his well-known modulus defined† effectively as the stress required to produce unit strain. Originally, this was based on nominal stress S^o and nominal elastic strain e^o, as in articles I,4.2, I,2.1, to give *Young's modulus*

$$E^o = S^o/e^o \tag{9.1}$$

† This is the form which Young's idea assumed with later writers and is accepted here to conform with general usage. Young originally stated that [152]: 'The modulus of the elasticity of any substance is a column of the same substance, capable of producing a pressure on its base which is to the weight causing a certain degree of compression as the length of the substance is to the diminution of its length.' Therefore, if the height of the column is h, its density m^o, cross-section of unit area and the gravitational constant g then it seems that the modulus defined by Young is

$$h = S^o/(e^o m^o g) = E^o/(m^o g)$$

so that the modern Young's modulus is, in fact, the weight $m^o gh$ of his column and not his original h. Todhunter & Pearson remark [19 18] that Young's presentation is obscure throughout his writings. He preferred the discursive mode rather than concise mathematical expression. The mathematical expression of Hooke's law requires a constant of proportionality and this is the modern modulus without any long, obscure definition.

9.1. **True Young's modulus.** In the present treatise 'true' stress S and 'true' elastic strain are used, so that, by analogy, a 'true' Young's modulus can be defined by

$$E = S/e \tag{9.2}$$

The qualifying term 'true' does not mean that the original definition is false but merely distinguishes the two. In engineering metals the elastic strains are so small that the difference between E^o and E is negligibly small. Just as the qualifying 'true' is usually left out when discussing stress and strain, then so is it also for the modulus.

9.2. **Secant modulus.** The definition of Young's modulus does not require the stress vs. strain curve to be linear. If the curve is not linear, as shown diagrammatically in Fig. I,9.1, then

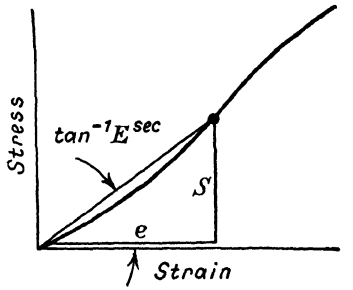

FIG. I,9.1.—A *secant* elastic modulus defined as stress divided by strain for a non-linear stress-strain relationship in an elastic substance.

the modulus of equation I(9.2) should be qualified as a secant elastic modulus. Clearly, there is no absolute merit in a particular definition of a modulus so long as it is convenient in the mathematics used to analyse the deformation.

9.3. **Tangent modulus.** Increment stress and elastic increment strain are analysed frequently, rather than the total quantities, so that it is convenient to define the corresponding tangent elastic modulus

$$E^{\tan} = \delta S/\delta e \tag{9.3}$$

as in Fig. I,9.2.

The inverse of the tangent elastic modulus is used so frequently that it is convenient to have a distinct symbol

$$\psi = 1/E^{\tan} \tag{9.4}$$

so that

$$\delta e = \psi \delta S \tag{9.5}$$

This also will be called the tangent elastic modulus, but there is no confusion with E, as the context always makes clear which is meant.

When the stress vs. elastic strain curve is linear then the Young's modulus, secant modulus and tangent modulus are all the same value at any given point on the curve.

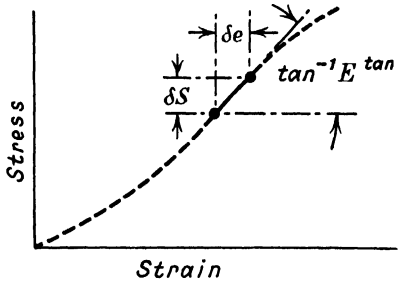

FIG. I,9.2.—A *tangent* elastic modulus defined as increment stress divided by increment strain for an elastic substance.

9.4. **Elastic tangent modulus for elasto-plastic strains.** Substances frequently have a plastic strain component as well as the elastic, so that in such cases, with δe^E the elastic increment strain, this will be related to the stress increment by the elastic modulus ψ^E. Thus,

$$\delta e^E = \psi^E \delta S \tag{9.6}$$

9.5. **Elastic modulus for duralumin.** Fig. I,9.3 gives† typical values of Young's modulus for a duralumin with the true strain range of zero to about 0·090, corresponding to the true stress 65 10^3 psi. This shows how the value of the modulus depends on the definition of stress and strain. When stress and strain are calculated on area and length in the undeformed body

† Author, 1947.

then the corresponding 'nominal' modulus E^o decreases continuously in value over the range studied. When stress and strain are 'true' then the modulus increases at about 50 10^3 psi, corresponding to a true strain of about 0·025. However, just beyond primary yield the true and nominal moduli are about equal and both decrease in value. This is of some physical interest, since it shows that the duralumin strains more easily elastically as well as more easily plastically when yield is reached.

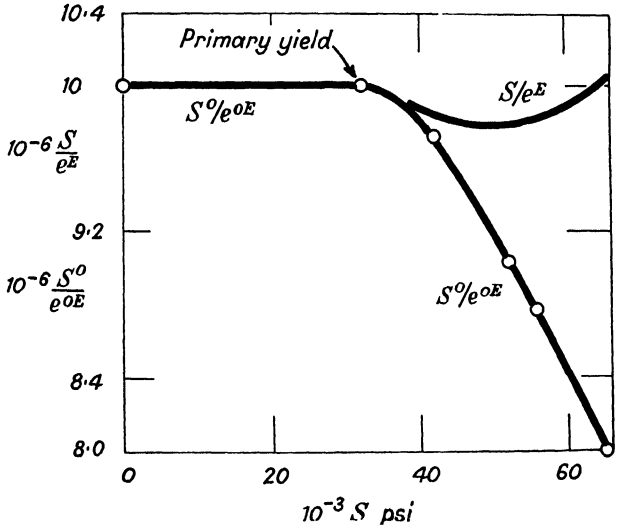

FIG. I,9.3. Duralumin elastic modulus for the metal in Fig. I,5.1. The decrease in nominal Young's modulus should be noted. The true Young's modulus remains more nearly constant over the stress range. Both nominal and true moduli decrease initially at primary yield.

9.6. **Duralumin and rubber stress-strain curves compared.** Comparison of the stress-strain curves for duralumin in article I,5 and those for rubber in article I,8 shows their difference in behaviour both qualitatively and quantitatively. The large elastic strains for rubber under quite small loads presented a difficult problem for analysis so long as the classical theory on infinitesimal strains was the only one available. Consider the various simple tensile elastic moduli that can be used to relate force and deformation, as shown in the forms of Figs. I,8.1 and I,8.2.

9.7. **Rubber stress-ser curve modulus.** True stress S vs. ser $(\lambda_1^0)^2$ in Fig. I,8.2 appears reasonably linear away from the initial curvature. A secant modulus $(\lambda_1^0)^2/S$ to relate these two quantities when plotted against S gives the curve shown in Fig. I,9.4, with quite high values for the modulus at low stresses. That is, the stress-ser curve departs definitely from linearity for fairly small stresses. However, for practical calculation, the mean curve for which the stress-ser secant modulus is of constant value

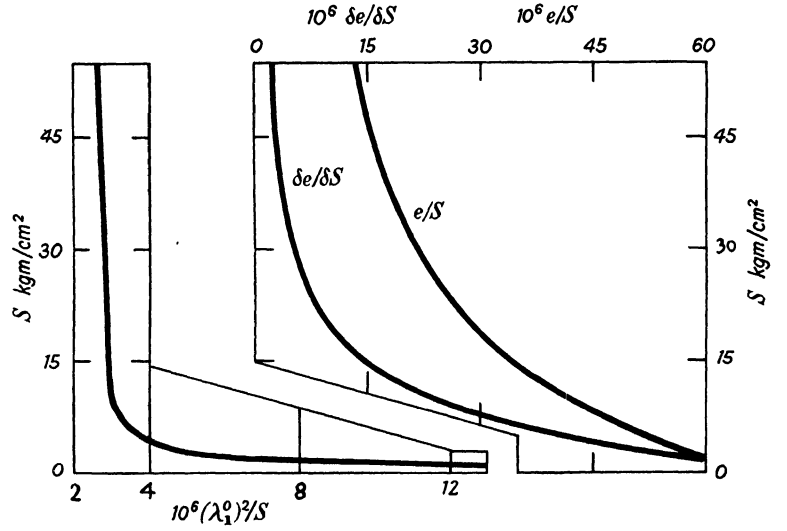

FIG. I,9.4.—Stress-strain relations for the simple tensile loading of the typical rubber as in Fig. I,8.2. The calculation of elastic moduli in terms of true stress, true strain, increments of these two and ser gives the three curves shown to relate stress and 'strain' for the same physical event.

270 10^{-6} $(\text{gm/cm}^2)^{-1}$ approximates quite well to the actual experimental results. This indicates the order of approximation introduced when constant stress-strain parameters are assumed for mere mathematical convenience to obtain solvable equations for complex straining subsequently.

9.8. **Rubber stress-strain curve modulus.** Inspection of Fig. I,8.2 shows reasonable correlation between the mean curve and the actual curve for true stress and true strain up to strain values of about 0·4 to 0·5. These are large values for many

purposes and outside the range of applicability of an infinitesimal strain theory. Displacements (i.e. change in shape) in some problems can be large although the strains fall within this range of values. The constant true stress-strain secant modulus for such a mean initial curve is 41 10^{-6} $(gm/cm^2)^{-1}$. Other moduli and plots for true stress and strain are given in Fig. I,9.5.

9.9. **Rubber stress-er curve modulus.** The approximate initial linearity of true stress S and er λ_1^q in Fig. I,8.1 suggests a mean value for the stress-er secant modulus S/λ_1^q in Fig. I,9.6.

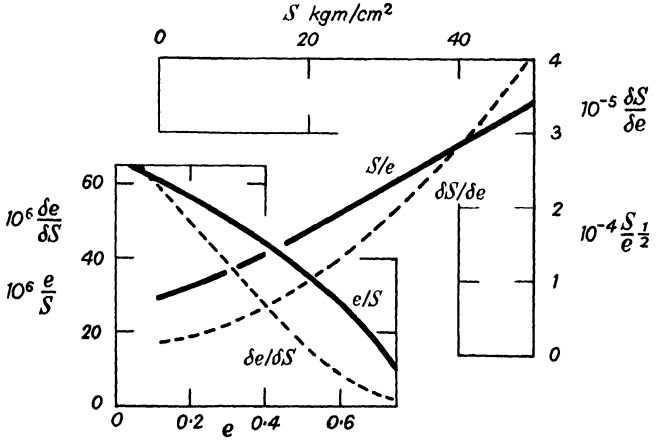

FIG. I,9.5.—The true stress and strain moduli of Fig. I,9.4 for simple tension on rubber are inverted in some cases here and plotted against other independent variables. Sometimes such replotting for a particular substance suggests the form to be adopted for the complex stress-strain relationship for the simplest analysis in a particular case. Note the approximate linearity over some ranges of stress.

The constant value 11 10^3 gm/cm^2 for the initial mean stress-er modulus gives a fair approximation to the curve up to the large strains for er value 3.

10. Plastic modulus

Plastic moduli of the 'secant' type have been used frequently [46], in the literature, but here only a tangent plastic modulus involving increment stress and increment strain is considered.

Define the slope of the elasto-plastic increment stress vs. increment strain curve, or the elasto-plastic modulus, by

$$P = \delta S/\delta e \tag{10.1}$$

so that

$$\delta e = P^{-1}\delta S \tag{10.2}$$

But, from article I,9.4,

$$\delta e^E = E^{-1}\delta S \tag{10.3}$$

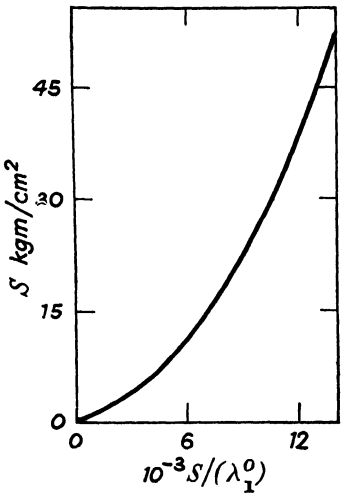

FIG. I,9.6—The elastic modulus relating true stress and er for the typical rubber in Fig. I,8.1. Note that the adoption of the constant value 8 10^3 would reasonably well represent the curve in Fig. I,8.1 for the considerable elastic er of about 2·5, although over the stress range, as here, the modulus varies from this value down to zero.

From Fig. I,10.1

$$\delta e = \delta e^E + \delta e^P \tag{10.4}$$

so then, the plastic increment strain is [47]

$$\delta e^P = (P^{-1} - E^{-1})\delta S \tag{10.5}$$

By analogy with I(9.6), I(9.4) write the *tangent plastic modulus* relating increment stress to plastic increment strain as

$$\psi^P = P^{-1} - E^{-1} \tag{10.6}$$

Then,

$$\delta e^P = \psi^P \delta S \tag{10.7}$$

10.1. **Elasto-plastic modulus is not convenient.** At this early stage of the analysis it may seem to be too artificial introducing elastic and plastic moduli where one might write, for example, $1/P = \psi = (\psi^E + \psi^P)$ and deal with δe directly as in I(10.2).

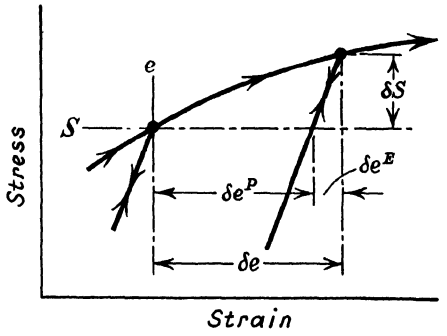

FIG. I,10.1.—An elasto-plastic increment strain due to an increment stress. The plastic increment strain is the elasto-plastic increment strain less the elastic increment strain.

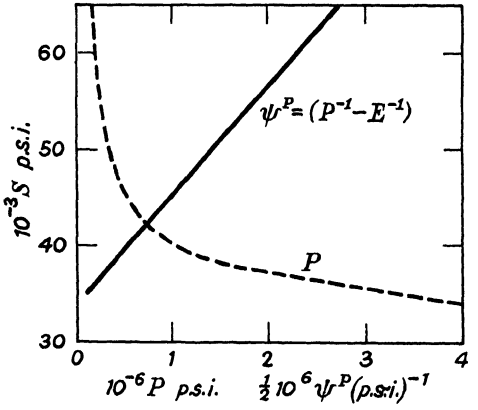

FIG. I,10.2.—Simple tensile elasto-plastic modulus P and plastic modulus ψ^P of the duralumin in Figs. I,5.1 and I,5.2.

However, this is seen to introduce difficulties when the stressing is more complicated than the present simple tension.

10.2. **Duralumin plastic modulus.** The value of P and ψ^P for the duralumin of Fig. I,5.2 is shown in Fig. I,10.2. The

virtual linearity of ψ^P when plotted against true stress is not necessarily general but applies to this specimen.

11. Elastic and plastic transverse contraction ratios

Under a simple tensile load the specimen suffers transverse contractile strain e_T as well as longitudinal extensile strain e_L as discussed in article I,3. For the infinitesimal elastic strains Poisson introduced a transverse contraction ratio bearing his name. Thus,

$$q^o = |\, e_T^o \,| \,/\, |\, e_L^o \,| \tag{11.1}$$

or, since contraction is negative in our sign convention,

$$e_T^o = -q^o e_L^o \tag{11.2}$$

11.1. **'True' elastic transverse contraction ratio.** Here, true elastic strains are used to analyse a deformation, so that it is convenient to define a 'true' elastic transverse contraction ratio by

$$q = |\, e_T \,| \,/\, |\, e_L \,| \tag{11.3}$$

or

$$e_T = -q e_L \tag{11.4}$$

11.2. **Transverse contraction ratios for elastic and plastic increment strains.** The longitudinal elasto-plastic increment strain δe_L can be resolved to elastic and plastic components δe_L^E, δe_L^P. It is convenient to regard each of these components as inducing a transverse contraction effect and write

$$\delta e_T^E = -q^E \delta e_L^E \tag{11.5}$$

$$\delta e_T^P = -q^P \delta e_L^P \tag{11.6}$$

More briefly, with $M = E, P$ to denote either symbol,

$$\delta e_T^M = -q^M \delta e_L^M \tag{11.7}$$

Now, it is clearer why an elasto-plastic modulus is not satisfactory, as mentioned in article I,10.1. As the deformation becomes more complicated it is seen to be essential to separate elastic and plastic effects. Thus, it is not convenient to define an elasto-plastic transverse contraction ratio by

$$|\, \delta e_T^E + \delta e_T^P \,| \,/\, |\, \delta e_L^E + \delta e_L^P \,|$$

11.3. **Duralumin elastic and plastic transverse contraction ratios.** Figs. I,11.1 and I,11.2 show the elastic and plastic transverse contraction ratios for the duralumin of Fig. I,5.2.

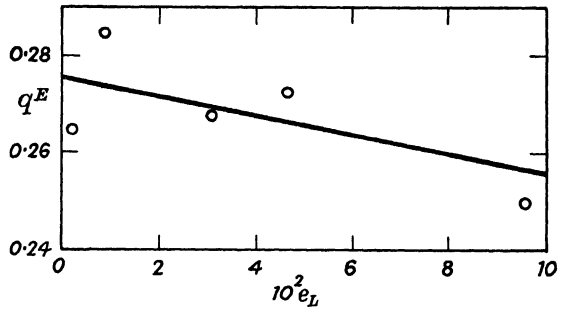

FIG. I,11.1. –Elastic transverse contraction ratio vs. true longitudinal strain for the duralumin shown in Fig. I,5.2. The values shown were found from longitudinal and transverse unloading, loading curves. The scatter of points from the mean curve appears to be a real physical effect and not mere experimental error.

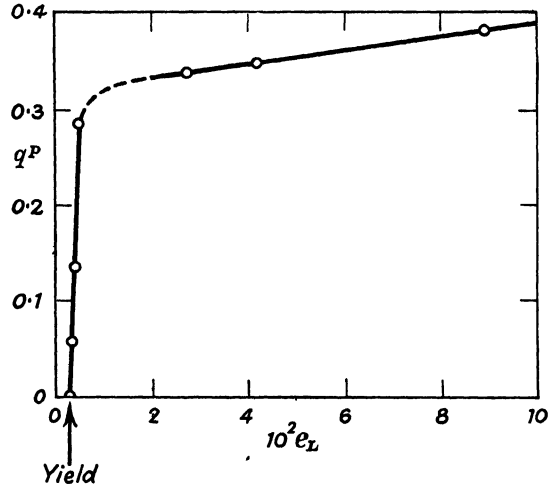

FIG. I,11.2.—True plastic transverse contraction ratio vs. true longitudinal strain for the duralumin in Figs. I,5.1 and I,5.2. At primary yield the transverse plastic strains did not develop at the same rate as the longitudinal plastic strains. The dotted part of the curve is the 'transition' to complete yielding. The values of q^P less than $\frac{1}{2}$ indicate dilation due to the plastic component of the strain.

The mean curve of the elastic transverse contraction ratio measurements is seen to decrease slightly with increase in strain. The scatter of the results is fairly high about the mean curve, indicating that the elastic transverse contraction is rather an unstable effect for this duralumin. The plastic transverse contraction ratio, however, shows an appreciable increase with increase of strain, but the curve is smooth, with slight scatter of measurements.

Chapter II

ONE-STRESS THEORETICAL CONSIDERATIONS

1. Straining - displacement, spatial - displacement and whole-body rotation in the simple tensile test

A theory of analysis is trivial for the simple tensile test, but it is convenient to illustrate here some fundamental ideas required to analyse complex stressing. The approach by other writers [13, 14, 15, 17, 31, 39, 42] using only a spatially fixed reference is simpler for formulation but tends to obscure the basic aspects,

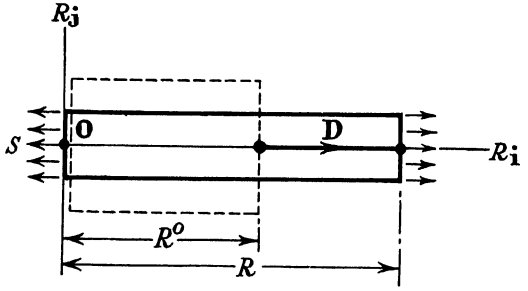

FIG. II,1.1.- A point at the scalar initial position R^o suffers *straining-displacement* D to the scalar current position R under simple tension.

leads away from simple analysis to complicated non-linear equations difficult to solve in particular cases and, according to the author's theory, leads to some erroneous inferences for complex stress. The formulation here is more elaborate but the equations found ultimately are simple.

1.1. **Straining-displacement.** Fig. II,1.1 shows an elastic sheet extended by normal stress S from an initially unstretched length R^o to currently stretched length R. Suppose the centre line of the plate remains collinear in all positions between these two states, while the point O at the end of the centre line keeps its position at the origin of two-dimensional cartesian coordinate axes OR_iR_j. The point at $R_i = R$ on the centre line of the sheet has been displaced by vector D. say, due to the strain established

throughout the sheet. Thus, it is convenient to call **D** the *straining-displacement* [5, 48] of the point at R_i relative to the axes OR_iR_j.

With D the arithmetical magnitude of vector **D** the strain for this direction is given by article I,2.2 as

$$e_i = D/R = \partial D/\partial R_i \equiv D_{;i} \qquad (1.1)$$

The partial differential coefficient form follows from the fact that the strain is constant along the direction OR_i, while the last form is the abbreviated notation used throughout this treatise. The reader will find this a convenience in the saving of labour of writing the more complicated forms.

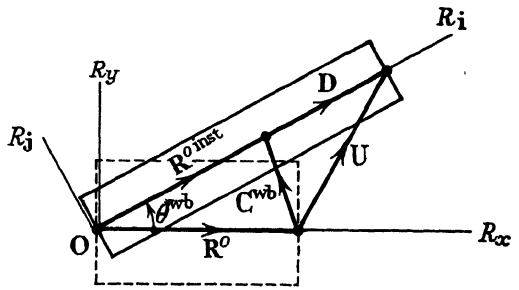

FIG. II,1.2.– Whole-body convected reference axes OR_iR_j are carried around, through angle θ^{wb} of *whole-body rotation*, with the body as it deforms. Axes OR_iR_j coincide initially with the spatially fixed axes OR_xR_y. *Spatial-displacement* **U** of a point is from spatially initial position $\mathbf{R}^o$. Straining-displacement **D** is from instantaneously initial position $\mathbf{R}^{o\,inst}$ relative to the whole-body convected axes. Whole-body convection-displacement is the difference between spatial-displacement and straining-displacement.

1.2. **Straining - displacement, spatial - displacement, whole-body rotation and whole-body convection-displacement.** Now consider a new situation. In Fig. II,1.2 the axes OR_xR_y are fixed in space. Suppose that, initially, axes OR_iR_j coincide with OR_xR_y but, during the evolution of the strain under current stress S, the two sets of axes separate by rotation through angle θ^{wb}. That is, the axes OR_iR_j are imbedded in and carried around or convected by the sheet.

Relative to the whole-body convected axes OR_iR_j the straining-displacement is still **D**, due to the establishment of the whole strain field as seen by a whole-body observer. Relative to the spatially fixed axes OR_xR_y the *spatial-displacement* of the point

is **U** as seen by a spatially fixed observer. Of course, the rectilinear vector **U** is not the path of the point but only connects the end points of the path. The difference between these two observations of displacement of the same point is $\mathbf{C}^{wb}$, conveniently called the *whole-body convection-displacement*. If the whole body is rotated back through angle θ^{wb} until OR_iR_j and OR_xR_y coincide then the whole-body rotation is zero and straining-displacement equals spatial-displacement. The whole-body rotation and, hence, whole-body convection-displacement can be any arbitrary values without affecting the strain field.

1.3. **Doublet vector fields.**† The point considered is currently at position **R** and initially at *instantaneously initial position* $\mathbf{R}^{o\,inst}$ relative to OR_iR_j, while it is at *spatially initial position* $\mathbf{R}^o$ relative to OR_xR_y. Geometrically,

$$\begin{aligned}\mathbf{R} &= \mathbf{R}^{o\,inst} + \mathbf{D} \\ &= (\mathbf{R}^{o\,inst} - \mathbf{C}^{wb}) + (\mathbf{D} + \mathbf{C}^{wb}) \\ &= \mathbf{R}^o + \mathbf{U} \end{aligned} \qquad (1.2)$$

The *pairs* of vector fields ($\mathbf{R}^{o\,inst}$, **D**) and ($\mathbf{R}^o$, **U**) are *doublet vector fields*. Merely adding the whole-body convection-displacement field to one component vector field of a doublet and subtracting it from the other component vector field allows transition from one doublet vector field to the other doublet vector field. The component vector fields of the straining doublet are in one-one correspondence with the applied force or stress; that is, to each value of stress there is a definite, unique initial position and displacement for each point. The component vector fields of the spatial doublet, however, are not one-one with the deforming forces. Therefore, observations of strain effects must be relative to whole-body convected axes unless some other condition such as infinitesimal straining and spatial-rotation is applied as in the classical Navier, Cauchy theory.‡

1.4. **Arbitrariness of straining-displacement.** The choice of position on the centre line of the sheet for the origin of whole-body axes was quite arbitrary, so that any one of the infinite number of points on the line could have been chosen. If any other point were chosen than that at the end of the line then the

† See volume I, articles **I,11.2, I,12, ..., A,32.**

‡ See [19, 23, 29, 49, 50] or volume I, articles **I,15.5, ..., III,9, VI,11.**

value of straining-displacement changes accordingly. In this sense, the straining-displacement is as arbitrary as the choice of position of origin **O** of whole-body axes, although the strain field as a whole is unique.

2. Straining-displacement, stress and instantaneously initial position in the simple tensile test

The position **R** of the typical point could have been anywhere along the centre line of the sheet without affecting the equations of article **II**,1. At another, closely adjacent point (**R**+d**R**) still on the centre line all the associated quantities will have changed differentially as in Fig. **II**,2.1. Thus, the differential of **II**(1.2)

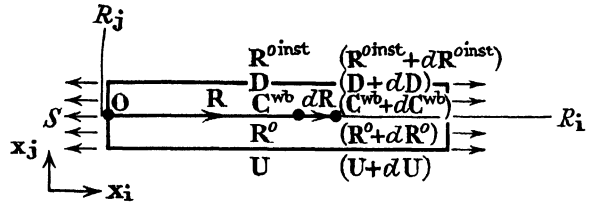

FIG. **II**,2.1.—The continuous vectors of spatially initial position, spatial-displacement, convection-displacement, instantaneously initial position and straining-displacement are all associated with the point at current position **R**. All these vectors suffer differential changes in value with differential change d**R** of position in the body.

with respect to change in position gives

$$\begin{aligned} d\mathbf{R} &= d\mathbf{R}^{o\,inst} + d\mathbf{D} \\ &= (d\mathbf{R}^{o\,inst} - d\mathbf{C}^{wb}) + (d\mathbf{D} + d\mathbf{C}^{wb}) \\ &= d\mathbf{R}^{o} + d\mathbf{U} \end{aligned} \qquad (2.1)$$

The analysis of this treatise uses the deformed body as the function domain. The current position **R** is the independent variable, while initial position, displacement, stress, etc. are the dependent variables. Thus, in Fig. **II**,2.1 all five vector fields $\mathbf{R}^{o\,inst}$, **D**, $\mathbf{C}^{wb}$, $\mathbf{R}^{o}$, **U** are associated with point **R**, while their differentially increased values are associated with (**R**+d**R**). With unit vectors $\mathbf{x}_i$, $\mathbf{x}_j$ for the cartesian axes OR_iR_j then, using equation **II**(1.1), the differential change in straining-displacement with respect to position is

$$d\mathbf{D} = dD\mathbf{x}_i = D_{;i}dR_i\mathbf{x}_i = e_i dR_i\mathbf{x}_i \qquad (2.2)$$

2.1. **Stress and straining-displacement on the centre line of the specimen.** Suppose the strain e_i is elastic and related to stress by a secant modulus ψ as in article I,9. Then,

$$d\mathbf{D} = S\psi \mathbf{x}_i dR_i \tag{2.3}$$

The straining-displacement relative to **O** is then

$$\mathbf{D} = \int_{\mathbf{O}}^{R_i} S\psi \mathbf{x}_i dR_i = S\psi \mathbf{x}_i R_i = S\psi \mathbf{R} \tag{2.4}$$

From equation II(1.2).1 the instantaneously initial position of the point currently at **R** in the deformed body on the axis OR_i is

$$\mathbf{R}^{o\ inst} = \mathbf{R}(1-S\psi) \tag{2.5}$$

2.2 **Straining-displacement at a general point.** Consider a general point **R** with components $\mathbf{R}_i$, $\mathbf{R}_j$ as in Fig. II,2.2.

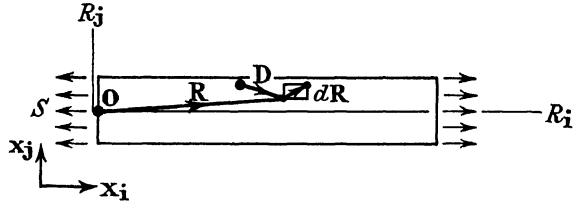

FIG. II,2.2.– Straining-displacement of a point at general position **R** under the current tensile force.

Using a transverse contraction ratio q appropriate to the secant modulus ψ, then transverse strain

$$e_j = -qe_i = -q\psi S \tag{2.6}$$

Resolve a general differential of position $d\mathbf{R}$ to components $d\mathbf{R}_i$, $d\mathbf{R}_j$, calculate the differentials of straining-displacement in each to give $d\mathbf{D}_i$, $d\mathbf{D}_j$, add to give $d\mathbf{D}$, the differential of straining-displacement, and then integrate to give the straining-displacement relative to **O** as

$$\mathbf{D} = S\psi(R_i\mathbf{x}_i - qR_j\mathbf{x}_j) \tag{2.7}$$

The instantaneously initial position is **R**—**D**.

2.3. **Strain dyadic, straining-displacement and instantaneously initial position for a general point.** Noting that

the scalar products $\mathbf{R}\cdot\mathbf{x}_i = R_i'$, $\mathbf{R}\cdot\mathbf{x}_j = R_j$, then II(2.7) can be written as

$$\mathbf{D} = \mathbf{R}\cdot\mathfrak{M} \tag{2.8}$$

with the strain dyadic

$$\mathfrak{M} = S\psi(\mathbf{x}_i\mathbf{x}_i - q\mathbf{x}_j\mathbf{x}_j) \tag{2.9}$$

Then,

$$\mathbf{R}^{o\,\text{inst}} = \mathbf{R} - \mathbf{R}\cdot\mathfrak{M} = \mathbf{R}\cdot(\mathfrak{J} - \mathfrak{M}) \tag{2.10}$$

with the idemfactor $\mathfrak{J}$ which, in scalar product with a vector, gives the vector unchanged.†

Thus, given the elastic strain dyadic throughout the deformed sheet due to the applied stresses, we may calculate the shape of the corresponding undeformed sheet if the stress-strain parameters are of secant form.

3. Spatial - displacement, straining - displacement and infinitesimal whole-body rotation

The classical theory of straining due to Navier, Cauchy and subsequent writers uses a spatially fixed reference to observe the movement of a point when the body is loaded. Consider again the point on the centre line of the sheet under simple tension as in Fig. II,1.2. The classical approach, however, focusses attention on an *element* and not on the whole body as here.

3.1. **Whole-body geometry.** Suppose the whole-body rotation angle θ^{wb} is infinitesimal, then, geometrically, the scalar components of $\mathbf{U}$ relative to axes OR_iR_j are

$$U_i = D \tag{3.1}$$

$$U_j = R^o\theta^{\text{wb}} \tag{3.2}$$

But R^o is the arithmetical magnitude of either $\mathbf{R}^o$ or $\mathbf{R}^{o\,\text{inst}}$ and, therefore, $R^o = R - D$, so that

$$U_j = (R-D)\theta^{\text{wb}} \tag{3.3}$$

3.2. **Differential geometry of an element.**‡ Fig. II,3.1 shows just an element of the body in the manner of approach of

† See volume I, article A,10 or reference [28] for a fuller discussion.
‡ See volume I, articles I,15, III,9, VI,11 for a fuller account.

the classical theory. For this line element on the centre line of the simple tensile specimen, the geometry gives

$$d\mathbf{R}^o + d\mathbf{U} = d\mathbf{R} = d\mathbf{R}^{o\,\mathrm{inst}} + d\mathbf{D} \tag{3.4}$$

Since dR^o is the arithmetical value of either $d\mathbf{R}^o$ or $d\mathbf{R}^{o\,\mathrm{inst}}$ then, relative to axes OR_iR_j,

$$d\mathbf{U} = dU_i\mathbf{x}_i + dU_j\mathbf{x}_j = dD\mathbf{x}_i + dR^o\theta^{\mathrm{wb}}\mathbf{x}_j \tag{3.5}$$

But

$$dR^o = dR - dD \tag{3.6}$$

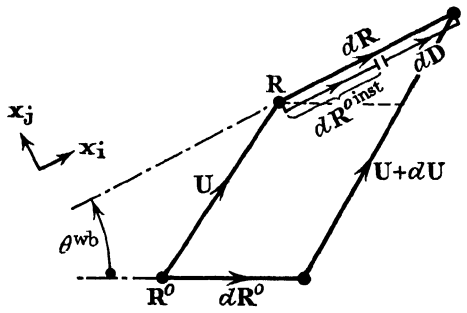

FIG. II,3.1. A line element on the centre line of the sheet under simple tension. Spatial-displacement **U** is relative to spatially fixed axes, while straining-displacement **D** is relative to whole-body axes convected through whole-body rotation angle θ^{wb}.

so that, scalarly, **II**(3.5) gives

$$dU_i = dD \tag{3.7}$$

$$dU_j = (dR - dD)\theta^{\mathrm{wb}} \tag{3.8}$$

Note carefully that, if the form of the whole strain field cannot be seen, as in this simple case, then the 'rotation' would have to be given the more general label 'spatial', so that it becomes spatial-rotation θ^{sp} relative to spatially fixed axes. Thus, according to the classical theory,

$$dU_j = (dR - dD)\theta^{\mathrm{sp}} \tag{3.9}$$

3.3. Stress and gradients of spatial-displacement and straining-displacement. Noting that, with respect to change

in position along axis OR_i, the differentials $dU_i = U_{i;i}dR_i$, etc., then, from II(3.7), II(3.9),

$$U_{i;i} = D_{;i} = e_i \tag{3.10}$$

$$U_{j;i} = (1-e_i)\theta^{sp} \tag{3.11}$$

when only a single element of the whole field is considered to formulate these differential equations. Similar expressions follow from differentiating II(3.1), II(3.3) with respect to R_i, except that then the known constant θ^{wb} replaces θ^{sp} here that must be assumed to be a function of position until it is shown otherwise.

The classical theory of infinitesimal strains neglects the products of strain and rotation, so that, in this simpler case, II(3.11) becomes

$$U_{j;i} = \theta^{sp} \tag{3.12}$$

Suppose the strain and stress are related by a secant modulus ψ as in article II,2.1. Then, II(3.10) becomes

$$U_{i;i} = \psi S = D_{;i} \tag{3.13}$$

while II(3.12) is independent of stress.

3.4. **Stress and gradients of spatial-displacement at a general point in the sheet.** Let **R** be a point not on the axis OR_i of the sheet. Let $d\mathbf{R}$ be a differential change in position from **R** as in Fig. II,2.2. The scalar components dR_i, dR_j of $d\mathbf{R}$ define an orthogonal element of the deformed sheet that is also orthogonal in the undeformed sheet. For infinitesimal strain and spatial-rotation, by methods similar to that in article II,3.3 (or with more detail in volume I, article I,15.7, applied to the present case), are found the relations for a single element

$$\left.\begin{aligned} U_{i;i} &= e_i = D_{i;i} \\ U_{j;j} &= e_j = D_{j;j} \end{aligned}\right\} \tag{3.14}$$

$$\left.\begin{aligned} U_{i;j} &= -\theta^{sp} \\ U_{j;i} &= \theta^{sp} \end{aligned}\right\} \tag{3.15}$$

Assuming the stress-strain relations of secant form, as in article II,2.2, gives

$$e_i = \psi S \qquad e_j = -q\psi S \tag{3.16}$$

Since S is constant and ψ, q assumed to be so, then, from II(3.15), II(3.14) on differentiation,

$$\left.\begin{aligned} U_{i;ij} &= 0 = -\theta^{sp}{}_{;i} \\ U_{j;ij} &= 0 = \theta^{sp}{}_{;j} \end{aligned}\right\} \tag{3.17}$$

Then, evidently, θ^{sp} is *constant* and equals θ^{wb}, as required for the geometry in article II,3.1.

3.5. **Integration of the stress, displacement equations at a general point in the sheet.** Integrating the spatial-displacement, spatial-rotation equations II(3.15) gives

$$\left.\begin{aligned} U_i &= -\theta^{wb}R_j + I(R_i) \\ U_j &= \theta^{wb}R_i + J(R_j) \end{aligned}\right\} \tag{3.18}$$

with $I(R_i)$, $J(R_j)$ the arbitrary functions of integration. Substitute II(3.16) in II(3.14) and integrate these stress, spatial-displacement relations to give

$$\left.\begin{aligned} U_i &= \psi S R_i + J'(R_j) \\ U_j &= -q\psi S R_j + I'(R_i) \end{aligned}\right\} \tag{3.19}$$

Comparison of II(3.19) and II(3.18) gives

$$\left.\begin{aligned} U_i &= -\theta^{wb}R_j + \psi S R_i \\ U_j &= \theta^{wb}R_i - q\psi S R_j \end{aligned}\right\} \tag{3.20}$$

satisfying the conditions $R_i = R_j = 0 = U_i = U_j$.

Now substitute II(3.16) in II(3.14) and integrate these stress, straining-displacement relations to give

$$\left.\begin{aligned} D_i &= \psi S R_i \\ D_j &= -q\psi S R_j \end{aligned}\right\} \tag{3.21}$$

with the correct fixing conditions $R_i = R_j = 0 = D_j = D_i$.

Inspection of the solutions II(3.21), II(3.20) shows that if the displacement, stress equations only are solved then the resulting displacement is straining-displacement and not spatial-displacement, as this latter also requires the solution of the displacement, whole-body rotation equations. Clearly, the conclusion is not altered if all the equations are transformed to another set of axes not in the directions $\mathbf{x}_i$, $\mathbf{x}_j$ and then solved for displacements relative to them.

3.6. **Displacements in the classical Navier, Cauchy infinitesimal strains theory.** The trivial example of simple tension has been chosen deliberately for its geometrical simplicity to encourage the reader to examine the fundamentals of the classical theory more closely. The classical theory considers just

one typical element, a spatially fixed reference, and formulates the equations effectively as

$$\left.\begin{aligned} U_{i;i} &= \psi S \\ U_{j;j} &= -q\psi S \\ \tfrac{1}{2}(U_{i;j}+U_{j;i}) &= 0 \end{aligned}\right\} \tag{3.22}$$

$$\tfrac{1}{2}(U_{j;i}-U_{i;j}) = \theta^{sp} \tag{3.23}$$

in a form similar to equations II(3.14), II(3.15).†

Equations II(3.22) between stress and displacement are integrated for the 'spatial-displacement' **U** and then, to put things right, since a whole-body rotation can have occurred, a 'complementary' solution like

$$\mathbf{C} = A(R_j\mathbf{x}_i - R_i\mathbf{x}_j) \tag{3.24}$$

is added with arbitrary constant A, while II(3.23) is not used explicitly.‡

However, article II,3.5 shows that the integration of II(3.22) gives straining-displacement **D** and not spatial-displacement **U**, while A in II(3.24) equals θ^{sp} in II(3.23) and cannot be calculated in terms of 'spatial-displacement' **U** found from equations II(3.22). Thus, with the classical stress-strain forms there should be solved

$$\left.\begin{aligned} D_{i;i} &= \psi S \\ D_{j;j} &= -q\psi S \end{aligned}\right\} \tag{3.25}$$

$$\tfrac{1}{2}(D_{i;j}+D_{j;i}) = 0 \tag{3.26}$$

with the addition of the arbitrary 'complementary' or whole-body convection-displacement

$$\mathbf{C}^{wb} = \theta^{wb}(R_j\mathbf{x}_i - R_i\mathbf{x}_j) \tag{3.27}$$

independent of the stress field.

3.7. Relative-displacement and straining-displacement.

The present author's theory goes a step further in pointing out that, for *infinitesimal* strain, whether it is heterogeneous or homogeneous as here, straining-displacement **D** *virtually* equals a

† See, for example, the standard works [19, 23, 29, 49, 50].
‡ See, for example, S. Timoshenko [23 6].

5.1. **Vector stress on an oblique plane.** Let unit vectors $\mathbf{n}$, $\mathbf{t}$ be in the plane of $\mathbf{x}_i$, $\mathbf{x}_j$ and consider the strip of plate of width B and unit thickness in Fig. II,5.1. Then volume I, article II,2.1 gives the *vector stress* $\mathbf{S}_n$ acting on the plane normal to $\mathbf{n}$ as

$$\mathbf{S}_n = \mathbf{n}\cdot\mathfrak{S} \tag{5.2}$$

But $\mathbf{n}\cdot\mathbf{x}_i = \cos\theta$, so that

$$\mathbf{S}_n = S_i\mathbf{x}_i \cos\theta \tag{5.3}$$

5.2. **Stress components on an oblique plane.** The scalar *normal stress* component of $\mathbf{S}_n$ is

$$S_{nn} = \mathbf{n}\cdot\mathbf{S}_n = S_i \cos^2\theta = \tfrac{1}{2}S_i(1+\cos 2\theta) \tag{5.4}$$

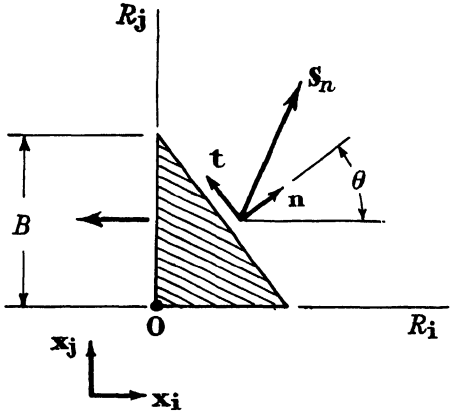

FIG. II,5.1.—Vector stress $\mathbf{S}_n$ on a plane normal to unit vector $\mathbf{n}$ in the plane of $\mathbf{x}_i$, $\mathbf{x}_j$ due to applied tensile vector stress $\mathbf{S}_i$.

while the scalar *shear stress* component is

$$S_{nt} = \mathbf{t}\cdot\mathbf{S}_n = -S_i \sin\theta \cos\theta = -\tfrac{1}{2}S_i \sin 2\theta \tag{5.5}$$

since $\mathbf{t}\cdot\mathbf{x}_i = -\sin\theta$. This shear stress has a maximum value when $\sin 2\theta = \pm 1$, so that in this case $\theta = 45°$ and $135°$. Then,

$$S_{nt}(\max) = -\tfrac{1}{2}S_i \tag{5.6}$$

5.3. **Complementary shear stresses.** Now consider the vector stress $\mathbf{S}_t$ acting on a plane normal to $\mathbf{t}$ and then resolve it to the scalar shear stress component in direction $\mathbf{n}$. Then,

$$S_{tn} = \mathbf{n}\cdot(\mathbf{t}\cdot\mathfrak{S}) = -\tfrac{1}{2}S_i \sin 2\theta \tag{5.7}$$

Therefore, with II(5.5),

$$S_{tn} = S_{nt} \tag{5.8}$$

are the complementary shear stresses in Fig. II,5.2.

5.4. **Vector stress on a more general oblique plane.** Suppose now, more generally, that $\mathbf{n}$ is not in the plane of $\mathbf{x}_i$, $\mathbf{x}_j$, so that, if $\mathbf{n}$, $\mathbf{t}$, $\mathbf{p}$ is a mutually orthogonal set to define an orthogonal element, then the vector stresses are

$$\mathbf{S}_n = \mathbf{n}\cdot\mathfrak{S} \qquad \mathbf{S}_t = \mathbf{t}\cdot\mathfrak{S} \qquad \mathbf{S}_p = \mathbf{p}\cdot\mathfrak{S} \tag{5.9}$$

The scalar stress components are $S_{nn} = \mathbf{n}\cdot(\mathbf{n}\cdot\mathfrak{S})$, ..., so that

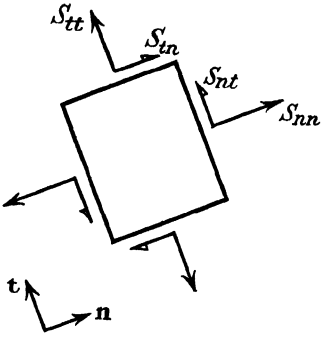

FIG. II,5.2.—Vector stresses $\mathbf{S}_n$, $\mathbf{S}_t$ acting on planes normal to unit vectors $\mathbf{n}$, $\mathbf{t}$ respectively are resolved to normal and shear components on their respective planes. Complementary, scalar shear stresses S_{nt}, S_{tn} are of equal magnitudes for rotational equilibrium of the element.

with n_i the cosine of the angle between $\mathbf{n}$ and $\mathbf{x}_i$, and so on, this then gives

$$\left.\begin{array}{llll} S_{nn} = n_i^2 S_i & & S_{nt} = S_{tn} = n_i t_i S_i \\ S_{tt} = t_i^2 S_i & & S_{tp} = S_{pt} = t_i p_i S_i \\ S_{pp} = p_i^2 S_i & & S_{pn} = S_{np} = p_i n_i S_i \end{array}\right\} \tag{5.10}$$

Notice that, similar to the conclusion in article II,5.2, the maximum arithmetical value of the shear stress is $\frac{1}{2}S_i$ on the inclined face of a cone with a vertex semi-angle of 45° and its axis in the direction of S_i.

6. Body force

Stress is the force acting across unit area of a plane described in the loaded body. Body force is the force acting on the particles

within a volume usually taken to be elemental about a given point. Such a body force is usually due to weight or some other accelerating force. If dV is an elemental volume about a typical point **R**, the density of substance is m and the body force **B** per unit mass,

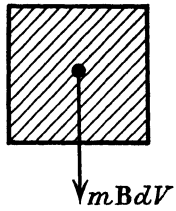

FIG. II,6.1.—Element of volume dV and density m with body force $m\mathbf{B}$ per unit volume acting on its particles.

then the force acting on the particles of the element is $m\mathbf{B}dV$. Thus, $m\mathbf{B}$ is the force per unit volume on the element particles shown diagrammatically as acting on the centre of mass of the element in Fig. II,6.1.

Chapter III

HOMOGENEOUS, PLANE TWO-STRESS

1. Stress dyadic for a two-stress system

A two-stress system is such that, at all points of the loaded body, the stress dyadic can be reduced to only two normal stresses by mere choice of direction about each point. Thus, with principal normal stresses S_i, S_j in the directions of unit vectors $\mathbf{x}_i$, $\mathbf{x}_j$ respectively, the stress dyadic is

$$\mathbf{S} = S_i\mathbf{x}_i\mathbf{x}_i + S_j\mathbf{x}_j\mathbf{x}_j \tag{1.1}$$

so that the component S_k is zero in the direction $\mathbf{x}_k$ orthogonal to the other two directions.

With $\mathbf{x}_i$, $\mathbf{x}_j$ coplanar with the constant unit reference vectors

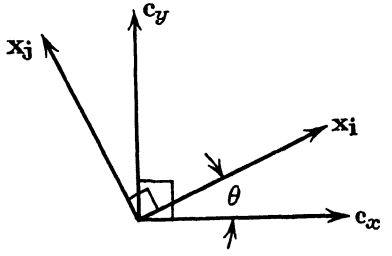

FIG. III,1.1.– Two-stress system principal normal stress directions $\mathbf{x}_i$, $\mathbf{x}_j$ and general directions $\mathbf{c}_x$, $\mathbf{c}_y$.

$\mathbf{c}_x$, $\mathbf{c}_y$ of cartesian axes OR_xR_y, then volume I shows that, on transformation,

$$\mathbf{S} = S_{xx}\mathbf{c}_x\mathbf{c}_x + S_{yy}\mathbf{c}_y\mathbf{c}_y + S_{xy}(\mathbf{c}_x\mathbf{c}_y + \mathbf{c}_y\mathbf{c}_x) \tag{1.2}$$

1.1. **Homogeneous two-stress definition.** The two-stress is homogeneous for axes OR_xR_y if all the stress components S_{xx}, S_{yy}, S_{xy} have the same values at all points of the plane sheet.

It is convenient to give here a more general definition of homogeneous two-stress for cylindrical coordinates (R_r, θ, R_z) having local unit reference vectors $\mathbf{c}_r$, $\mathbf{c}_\theta$, $\mathbf{c}_z$ and spherical coordinates (R_r, θ, ϕ) having local reference vectors $\mathbf{c}_r$, $\mathbf{c}_\theta$, $\mathbf{c}_\phi$ as in article A,7. Thus, any of the three pairs of unit vectors in each curvilinear

system replaces $\mathbf{c}_x$, $\mathbf{c}_y$ in III(1.2), while corresponding subscripts replace x, y to give the two-stress dyadic. Now, for homogeneous, curvilinear stress the scalar components S_{rr}, ... retain their values from point to point in the curvilinear coordinates system.

1.2. **Stress on a plane.** Just as in article II,5 the vector stress $\mathbf{S}_n$, acting on a plane normal to unit vector $\mathbf{n}$ in the plane of $\mathbf{c}_x$, $\mathbf{c}_y$ and from the given point at which the stress dyadic is $\mathfrak{S}$, is

$$\mathbf{S}_n = \mathbf{n}\cdot\mathfrak{S} \tag{1.3}$$

With unit vector $\mathbf{t}$ normal to $\mathbf{n}$ and in the plane of $\mathbf{c}_x$, $\mathbf{c}_y$ the normal and shear stress components of $\mathbf{S}_n$ are

$$S_{nn} = \mathbf{n}\cdot\mathfrak{S}\cdot\mathbf{n} \qquad S_{nt} = \mathbf{n}\cdot\mathfrak{S}\cdot\mathbf{t} \tag{1.4}$$

1.3. **Principal normal stresses and their directions.** Choose $\mathbf{n}$, $\mathbf{t}$ to have the particular values $\mathbf{x}_\mathbf{i}$, $\mathbf{x}_\mathbf{j}$ to give, with III(1.2),

$$\left.\begin{aligned} S_\mathbf{i} &= \mathbf{x}_\mathbf{i}\cdot\mathfrak{S}\cdot\mathbf{x}_\mathbf{i} \\ &= \tfrac{1}{2}(S_{xx}+S_{yy})+\tfrac{1}{2}(S_{xx}-S_{yy})\cos 2\theta+S_{xy}\sin 2\theta \\ S_\mathbf{j} &= \mathbf{x}_\mathbf{j}\cdot\mathfrak{S}\cdot\mathbf{x}_\mathbf{j} \\ &= \tfrac{1}{2}(S_{xx}+S_{yy})-\tfrac{1}{2}(S_{xx}-S_{yy})\cos 2\theta-S_{xy}\sin 2\theta \end{aligned}\right\} \tag{1.5}$$

while shear stress $S_{\mathbf{ij}}$ is zero for the principal directions. Thus,

$$0 = \mathbf{x}_\mathbf{i}\cdot\mathfrak{S}\cdot\mathbf{x}_\mathbf{j} = \tfrac{1}{2}(-S_{xx}+S_{yy})\sin 2\theta+S_{xy}\cos 2\theta$$

so that the principal normal stress directions are given by

$$\tan 2\theta = 2S_{xy}/(S_{xx}-S_{yy}) \tag{1.6}$$

1.4. **Partial-increment stress dyadic.** Suppose the principal normal stress directions $\mathbf{x}_\mathbf{i}$ are held constant in III(1.1) during an incremental change of the dyadic. Referring to this as a partial-increment, since the directions are unchanged, gives

$$\Delta\mathfrak{S} = \delta S_\mathbf{i}\mathbf{x}_\mathbf{i}\mathbf{x}_\mathbf{i}+\delta S_\mathbf{j}\mathbf{x}_\mathbf{j}\mathbf{x}_\mathbf{j} \tag{1.7}$$

This self-conjugate dyadic† transforms to

$$\Delta\mathfrak{S} = \delta S_{xx}\mathbf{c}_x\mathbf{c}_x+\delta S_{xy}(\mathbf{c}_x\mathbf{c}_y+\mathbf{c}_y\mathbf{c}_x)+\delta S_{yy}\mathbf{c}_y\mathbf{c}_y \tag{1.8}$$

with

$$\delta S_{xx} = \mathbf{c}_x\cdot\Delta\mathfrak{S}\cdot\mathbf{c}_x \qquad \delta S_{yy} = \mathbf{c}_y\cdot\Delta\mathfrak{S}\cdot\mathbf{c}_y \qquad \delta S_{xy} = \mathbf{c}_x\cdot\Delta\mathfrak{S}\cdot\mathbf{c}_y$$

† See article A,6 or volume I, articles A,9, A,11 for a fuller discussion.

1.5. **Principal normal increment stresses and their directions.** With $\mathbf{x}_i$, $\mathbf{x}_j$ the principal directions of the increment stress dyadic and θ the angle between $\mathbf{x}_i$ and $\mathbf{c}_x$ then, just as in article **III**,1.3 for the stress dyadic, there are found

$$\left.\begin{aligned}\delta S_i &= \tfrac{1}{2}(\delta S_{xx}+\delta S_{yy})+\tfrac{1}{2}(\delta S_{xx}-\delta S_{yy})\cos 2\theta+\delta S_{xy}\sin 2\theta\\ \delta S_j &= \tfrac{1}{2}(\delta S_{xx}+\delta S_{yy})-\tfrac{1}{2}(\delta S_{xx}-\delta S_{yy})\cos 2\theta-\delta S_{xy}\sin 2\theta\end{aligned}\right\} \quad (1.9)$$

$$\tan 2\theta = 2\delta S_{xy}/(\delta S_{xx}-\delta S_{yy}) \quad (1.10)$$

This transformation is the converse of that in article **III**,1.4.

1.6. **First invariants of the total stress dyadic and partial-increment stress dyadic.** Suppose the stress and increment stress dyadics are transformed invariantly for rotation of axes about an axis in the direction $\mathbf{c}_z = \mathbf{x}_k$, then volume I, article **II**,3 shows that, with the idemfactor in double scalar product,

$$\mathfrak{J}:\mathfrak{S} = \chi^S = S_{xx}+S_{yy} = S_i+S_j \quad (1.11)$$

$$\mathfrak{J}:\Delta\mathfrak{S} = \delta\chi^S = \delta S_{xx}+\delta S_{yy} = \delta S_i+\delta S_j \quad (1.12)$$

are the first invariants. That is, each of these sums maintains its arithmetical value whatever orthogonal axes are chosen in the (R_x, R_y) plane.

1.7. **Maximum shear stress on each of some particular planes.** Substituting **III**(1.1) in **III**(1.4).2 gives

$$S_{nt} = S_i n_i t_i + S_j n_j t_j \quad (1.13)$$

with the direction cosines notation similar to article **II**,5.4. Now choose some particular directions for the unit vectors.

(a) $\mathbf{n}$, $\mathbf{t}$ *coplanar with* $\mathbf{S}_i$, $\mathbf{S}_j$. Denote† by ϕ the angle between $\mathbf{S}_i$ and $\mathbf{n}$, so that $n_i = t_j = \cos\phi$, $n_j = -t_i = \sin\phi$. Substituting in **III**(1.13) gives

$$S_{nt} = -\tfrac{1}{2}(S_i-S_j)\sin 2\phi \quad (1.14)$$

This has the maximum value

$$S_{nt}(\max) = -\tfrac{1}{2}(S_i-S_j) \quad (1.15)$$

(b) $\mathbf{n}$, $\mathbf{t}$ *coplanar with* $\mathbf{S}_i$, $\mathbf{x}_k$. Again denote by ϕ the angle between $\mathbf{S}_i$ and $\mathbf{n}$, but now both $\mathbf{n}$ and $\mathbf{t}$ are orthogonal to $\mathbf{S}_j$.

† This avoids confusion with the principal normal stress direction in **III**,1.3.

Therefore, $n_i = \cos\phi$, $t_i = -\sin\phi$, $n_j = 0 = t_j$, to give, from III(1.13),

$$S_{nt} = -\tfrac{1}{2}S_i \sin 2\phi \tag{1.16}$$

and then

$$S_{nt}(\max) = -\tfrac{1}{2}S_i \tag{1.17}$$

(c) **n**, **t** *coplanar with* $\mathbf{S_j}$, $\mathbf{x_k}$. In this case the shear stress value is given by an appropriate expression similar to III(1.16), while

$$S_{nt}(\max) = \tfrac{1}{2}S_j \tag{1.18}$$

1.8. **Maximum shear stress in a thin sheet loaded planewise.** Note carefully that the demonstration in equations III(1.13) to III(1.18) has not necessarily shown the maximum value of S_{nt} in III(1.13). All that has been found is the maximum stress in each of three cases of a plane having a normal which is normal to one of the principal normal stress directions. Thus, geometrically, as in Mohr's construction of Fig. A,6.2 there have been considered three such figures for the cases of (S_i, S_j, ($S_k = 0$)), (S_i, ($S_k = 0$)), (S_j, ($S_k = 0$)). Which case gives the greatest arithmetical value of shear stress depends on the signs of S_i and S_j. If S_i and S_j are of *opposite* signs then III(1.15) gives the greatest of the three $S_{nt}(\max)$ found. If S_i and S_j are of the *same* sign, with the former arithmetically greater, then III(1.17) gives the greatest of the three $S_{nt}(\max)$. The general proof of these results is given in article A,6.4.

The criteria in the inequalities A(6.7), A(6.8) show when the maximum shear stress in a thin sheet is given by the difference of the planewise principal normal stresses or only the arithmetically greatest of them. Thus,

$$\left.\begin{aligned} |S_{nt}(\max)| &= |\tfrac{1}{2}(S_i - S_j)| \text{ when } |S_{xx}S_{yy}| < S_{xy}{}^2 \\ |S_{nt}(\max)| &= |\tfrac{1}{2}S_i| \text{ when } |S_{xx}S_{yy}| > S_{xy}{}^2 \end{aligned}\right\} \tag{1.19}$$

Therefore, if, for example, a photoelastic [79, 115] observation gives $(S_i - S_j)$ directly, it does not necessarily give the maximum shear stress in the sheet, since III(1.19).2 may apply.† Thus, it is necessary to find the signs of the two principal normal stresses.

† Among the recent writers (see, for example, S. Timoshenko [23.14], R. V. Southwell [29.4], A. Nadai [46.2], M. M. Frocht [115 1]) there seems to be no other explicit statement than that in III(1.15). The various writers accept the three-dimensional analyses such as in article A,6.4, so that there seems to be an inconsistency in their treatment. R. Hill [37.7] notes the need for care about signs.

2. Strain and partial-strain for a two-stress

Volume I, chapter III formulates the strain expressions in terms of a 'partial' strain [47] preparatory to relating them to stress. Reconsider, briefly here, the simplest case in which the principal normal total strains have no components due to shear stresses. Visualise the substance as elastic and that principal normal stresses S_i, S_j act parallel to the two edges of a rectangular, plane sheet in directions $\mathbf{x}_i$, $\mathbf{x}_j$.

2.1. **Elastic substance of general isotropy.** Apply partial-strains ϵ_i, ϵ_j to the sheet and allow for the fact that each induces a transverse contraction effect in the direction of the other. Then, strains

$$\left.\begin{aligned} e_i &= \epsilon_i - q_{j-i}\epsilon_j \\ e_j &= \epsilon_j - q_{i-j}\epsilon_i \\ e_k &= -q_{i-k}\epsilon_i - q_{j-k}\epsilon_j \end{aligned}\right\} \qquad (2.1)$$

These equations should be regarded as a geometrical statement on the whole complex strain state at the point.

The transverse contraction ratios have subscripts indicating that their value may differ between the various directions. Thus q_{j-i} means 'the transverse contraction ratio for the effect of ϵ_j in direction $\mathbf{x}_i$'.

2.2. **Elastic substance of restricted isotropy.** By definition, a substance of restricted isotropy is one for which the stress-strain parameters are isotropic; that is, they are independent of direction. Then, for such a case **III**(2.1) becomes

$$\left.\begin{aligned} e_i &= \epsilon_i - q\epsilon_j = (1+q)\epsilon_i - q(\epsilon_i+\epsilon_j) \\ e_j &= \epsilon_j - q\epsilon_i = (1+q)\epsilon_j - q(\epsilon_i+\epsilon_j) \\ e_k &= -q(\epsilon_i+\epsilon_j) \end{aligned}\right\} \qquad (2.2)$$

2.3. **Elastic increment deformation.** When the currently deformed elastic body is used as the reference to observe an increment deformation then the increment strains can be analysed to increment partial-strains with appropriate transverse contraction ratios. Thus, for *general isotropy*,

$$\left.\begin{aligned} \delta e_i &= \delta\epsilon_i - q_{j-i}\delta\epsilon_j \\ \delta e_j &= \delta\epsilon_j - q_{i-j}\delta\epsilon_i \\ \delta e_k &= -q_{i-k}\delta\epsilon_i - q_{j-k}\delta\epsilon_j \end{aligned}\right\} \qquad (2.3)$$

and, for *restricted isotropy*,

$$\left.\begin{aligned} \delta e_{\mathrm{i}} &= (1+q)\delta\epsilon_{\mathrm{i}} - q(\delta\epsilon_{\mathrm{i}}+\delta\epsilon_{\mathrm{j}}) \\ \delta e_{\mathrm{j}} &= (1+q)\delta\epsilon_{\mathrm{j}} - q(\delta\epsilon_{\mathrm{i}}+\delta\epsilon_{\mathrm{j}}) \\ \delta\epsilon_{\mathrm{k}} &= -q(\delta\epsilon_{\mathrm{i}}+\delta\epsilon_{\mathrm{j}}) \end{aligned}\right\} \qquad (2.4)$$

Note carefully that, in general, the q's in this article for an increment deformation are not of the same values as those for total strains as in articles **III**,2.1 and **III**,2.2

2.4. **Elasto-plastic increment deformation.** An elasto-plastic substance generally requires to be analysed incrementally, because the plastic component of the strain does not 'transfer' with the stress if this rotates relative to the substance. Article **III**,6 describes this briefly or volume I, article **III**,7 gives a fuller account.

The elasto-plastic increment strain at each point of the deformed body is resolved to its elastic and plastic components δe^E and δe^P respectively. Then, analysing these by appropriate increment partial-strains and transverse contraction ratios gives, similar to **III**(2.3),

$$\left.\begin{aligned} \delta e_{\mathrm{i}} &= (\delta\epsilon^E_{\mathrm{i}} - q^E_{\mathrm{j-i}}\delta\epsilon^E_{\mathrm{j}}) + (\delta\epsilon^P_{\mathrm{i}} - q^P_{\mathrm{j-i}}\delta\epsilon^P_{\mathrm{j}}) \\ \delta e_{\mathrm{j}} &= (\delta\epsilon^E_{\mathrm{j}} - q^E_{\mathrm{i-j}}\delta\epsilon^E_{\mathrm{i}}) + (\delta\epsilon^P_{\mathrm{j}} - q^P_{\mathrm{i-j}}\delta\epsilon^P_{\mathrm{i}}) \\ \delta e_{\mathrm{k}} &= (-q^E_{\mathrm{i-k}}\delta\epsilon^E_{\mathrm{i}} - q^E_{\mathrm{j-k}}\delta\epsilon^E_{\mathrm{j}}) + (-q^P_{\mathrm{i-k}}\delta\epsilon^P_{\mathrm{i}} - q^P_{\mathrm{j-k}}\delta\epsilon^P_{\mathrm{j}}) \end{aligned}\right\} (2.5)$$

For restricted isotropy the transverse contraction ratios are independent of direction and become q^E, q^P respectively, giving expressions similar to **III**(2.4) but with a plastic component.

2.5. **Strain dyadic.** The scalar strains in **III**(2.1) are shown, in the manner of volume I, article **III**,2.1, to be the components of the self-conjugate strain dyadic.

$$\mathfrak{M} = e_{\mathrm{i}}\mathbf{x}_{\mathrm{i}}\mathbf{x}_{\mathrm{i}} + e_{\mathrm{j}}\mathbf{x}_{\mathrm{j}}\mathbf{x}_{\mathrm{j}} + e_{\mathrm{k}}\mathbf{x}_{\mathrm{k}}\mathbf{x}_{\mathrm{k}} \qquad (2.6)$$

of similar form to the stress dyadic in **III**(1.1).

Scalar product of the stress dyadic with a unit vector gave the vector stress acting on a plane normal to the unit vector. Scalar product of the strain dyadic with a unit vector $\mathbf{n}$ gives the vector straining-displacement between its ends at unit distance apart in the present case of homogeneous strain. Thus, similar to the simpler, one-stress case in article **II**,2.3,

$$\mathbf{D} = \mathbf{n}\cdot\mathfrak{M} = n_{\mathrm{i}}e_{\mathrm{i}}\mathbf{x}_{\mathrm{i}} + n_{\mathrm{j}}e_{\mathrm{j}}\mathbf{x}_{\mathrm{j}} + n_{\mathrm{k}}e_{\mathrm{k}}\mathbf{x}_{\mathrm{k}} \qquad (2.7)$$

If, in particular, $\mathbf{n} = \mathbf{x}_i$ then

$$\mathbf{D}_i = \mathbf{x}_i \cdot \mathfrak{M} = e_i \mathbf{x}_i \tag{2.8}$$

and so on for the other two vector components analogous to the vector stress components of the stress dyadic.

2.6. **Partial-increment strain dyadic.** Similarly, the scalar increment strain components in III(2.5) are those of a self-conjugate dyadic similar to III(2.6). Its vector components can be extracted for given directions. Then, the increment strain dyadic is

$$\Delta \mathfrak{M} = \delta e_i \mathbf{x}_i \mathbf{x}_i + \delta e_j \mathbf{x}_j \mathbf{x}_j + \delta e_k \mathbf{x}_k \mathbf{x}_k \tag{2.9}$$

while the increment straining-displacement between the ends of a unit length is

$$\delta \mathbf{D} = \mathbf{n} \cdot \Delta \mathfrak{M} = n_i \delta e_i \mathbf{x}_i + n_j \delta e_j \mathbf{x}_j + n_k \delta e_k \mathbf{x}_k \tag{2.10}$$

$$\delta \mathbf{D}_i = \mathbf{x}_i \cdot \Delta \mathfrak{M} = \delta e_i \mathbf{x}_i \tag{2.11}$$

2.7. **Principal normal strains and their directions.** The principal normal strains and their directions are found for the strain dyadic just as the corresponding values were found for the two-stress dyadic in article III,1.3. Thus,

$$\left.\begin{aligned} e_i &= \tfrac{1}{2}(e_{xx}+e_{yy}) + \tfrac{1}{2}(e_{xx}-e_{yy}) \cos 2\theta + e_{xy} \sin 2\theta \\ e_j &= \tfrac{1}{2}(e_{xx}+e_{yy}) - \tfrac{1}{2}(e_{xx}-e_{yy}) \cos 2\theta - e_{xy} \sin 2\theta \end{aligned}\right\} \tag{2.12}$$

while

$$\tan 2\theta = 2e_{xy}/(e_{xx}-e_{yy}) \tag{2.13}$$

2.8. **Principal normal increment strains and their directions.** In a similar fashion the principal normal increment strains and their directions for the increment strain dyadic are

$$\left.\begin{aligned} \delta e_i &= \tfrac{1}{2}(\delta e_{xx}+\delta e_{yy}) + \tfrac{1}{2}(\delta e_{xx}-\delta e_{yy}) \cos 2\theta + \delta e_{xy} \sin 2\theta \\ \delta e_j &= \tfrac{1}{2}(\delta e_{xx}+\delta e_{yy}) - \tfrac{1}{2}(\delta e_{xx}-\delta e_{yy}) \cos 2\theta - \delta e_{xy} \sin 2\theta \end{aligned}\right\} \tag{2.14}$$

$$\tan 2\theta = 2\delta e_{xy}/(\delta e_{xx}-\delta e_{yy}) \tag{2.15}$$

3. Stress-strain relations for a two-stress

The strains of article III,2 are 'total' and 'incremental', so that the transverse contraction ratios are of corresponding 'secant' and 'tangent' form. Similarly, now use secant and

tangent moduli to relate stress and partial-strain or their increments.

3.1. **Secant elastic moduli.** The elastic partial-strains of article **III**,2.1 for *general isotropy* are now related to stress by secant moduli in

$$\epsilon_{\mathfrak{i}} = \psi_{\mathfrak{i}} S_{\mathfrak{i}} \qquad \epsilon_{\mathfrak{j}} = \psi_{\mathfrak{j}} S_{\mathfrak{j}} \tag{3.1}$$

while, for *restricted isotropy*,

$$\epsilon_{\mathfrak{i}} = \psi S_{\mathfrak{i}} \qquad \epsilon_{\mathfrak{j}} = \psi S_{\mathfrak{j}} \tag{3.2}$$

Thus, explicitly in **III**(2.2), for example,

$$e_{\mathfrak{i}} = GS_{\mathfrak{i}} + F\chi^S \qquad e_{\mathfrak{j}} = GS_{\mathfrak{j}} + F\chi^S \qquad e_{\mathfrak{k}} = F\chi^S \tag{3.3}$$

with isotropic secant stress-strain parameters

$$G = (1+q)\psi \qquad F = -q\psi \tag{3.4}$$

and first stress invariant

$$\chi^S = S_{\mathfrak{i}} + S_{\mathfrak{j}} \tag{3.5}$$

3.2. **Tangent elastic moduli.** The elastic increment partial-strains of article **III**,2.3 are related to increment stresses by tangent moduli for *general isotropy* in

$$\delta\epsilon_{\mathfrak{i}} = \psi_{\mathfrak{i}} \delta S_{\mathfrak{i}} \qquad \delta\epsilon_{\mathfrak{j}} = \psi_{\mathfrak{j}} \delta S_{\mathfrak{j}} \tag{3.6}$$

while, for *restricted isotropy*,

$$\delta\epsilon_{\mathfrak{i}} = \psi \delta S_{\mathfrak{i}} \qquad \delta\epsilon_{\mathfrak{j}} = \psi \delta S_{\mathfrak{j}} \tag{3.7}$$

Thus, explicitly in **III**(2.4), for example,

$$\delta e_{\mathfrak{i}} = G\delta S_{\mathfrak{i}} + F\delta\chi^S \qquad \delta e_{\mathfrak{j}} = G\delta S_{\mathfrak{j}} + F\delta\chi^S \qquad \delta e_{\mathfrak{k}} = F\delta\chi^S \tag{3.8}$$

with isotropic tangent stress-strain parameters

$$G = (1+q)\psi \qquad F = -q\psi \tag{3.9}$$

not equal, in general, to the secant parameters in **III**(3.4). The increment stress first invariant is

$$\delta\chi^S = \delta S_{\mathfrak{i}} + \delta S_{\mathfrak{j}} \tag{3.10}$$

3.3. **Elasto-plastic tangent moduli.** The elastic and plastic increment partial-strains components of elasto-plastic increment strain in article **III**,2.4 are similarly related to increment stresses by tangent moduli. Thus, for *general isotropy*,

$$\left.\begin{aligned} \delta\epsilon_{\mathfrak{i}}^E &= \psi_{\mathfrak{i}}^E \delta S_{\mathfrak{i}} & \delta\epsilon_{\mathfrak{i}}^P &= \psi_{\mathfrak{i}}^P \delta S_{\mathfrak{i}} \\ \delta\epsilon_{\mathfrak{j}}^E &= \psi_{\mathfrak{j}}^E \delta S_{\mathfrak{j}} & \delta\epsilon_{\mathfrak{j}}^P &= \psi_{\mathfrak{j}}^P \delta S_{\mathfrak{j}} \end{aligned}\right\} \tag{3.11}$$

Substituting in **III**(2.5) and writing explicitly for *restricted isotropy* gives

$$\left.\begin{aligned}\delta e_{\mathbf{i}} &= (G^E\delta S_{\mathbf{i}}+F^E\delta\chi^S)+(G^P\delta S_{\mathbf{i}}+F^P\delta\chi^S)\\ \delta e_{\mathbf{j}} &= (G^E\delta S_{\mathbf{j}}+F^E\delta\chi^S)+(G^P\delta S_{\mathbf{j}}+F^P\delta\chi^S)\\ \delta e_{\mathbf{k}} &= (F^E+F^P)\delta\chi^S\end{aligned}\right\}\quad(3.12)$$

3.4. **Current total stress and elasto-plastic strains relations.** In general, stress rotates relative to the substance but the plastic strain does not transfer with it, as is discussed in article **III**,6. Thus, current elasto-plastic 'strain' is the total transferred elastic strain and last plastic increment strain. Then, for restricted isotropy, with $\delta e_{\mathbf{i}}$ in **III**(3.12) this gives

$$e_{\mathbf{i}} = \int_0^{S_{\mathbf{i}}} G^E\partial S_{\mathbf{i}}+\int_0^{\chi^S} F^E\partial\chi^S+(G^P\delta S_{\mathbf{i}}+F^P\delta\chi^S)\qquad(3.13)$$

with similar integral forms for $e_{\mathbf{j}}$ and $e_{\mathbf{k}}$.

4. Shear stress on a sheet

As a particular case, suppose the principal normal stresses are equal but of opposite sign in the stress dyadic of article **III**,1. Then, with $S_{\mathbf{i}} = S = -S_{\mathbf{j}}$ the stress dyadic is

$$\mathfrak{S} = S(\mathbf{x_i x_i}-\mathbf{x_j x_j})\qquad(4.1)$$

Choosing unit vector $\mathbf{n}$ at $-45°$ and unit vector $\mathbf{t}$ at $+45°$ to $\mathbf{O}R_{\mathbf{i}}$ gives the normal stresses S_{nn}, S_{tt} as zero for these directions, while the complementary shear stresses are

$$S_{nt} = \mathbf{n}\cdot\mathfrak{S}\cdot\mathbf{t} = S_{tn} = T\qquad(4.2)$$

say, of the same arithmetical value as S. This gives the homogeneous two-stress system in Fig. **III**,4.1. See volume I, article **II**,13 for a fuller treatment.

The principal normal stresses S and $-S$ are *equivalent* to, and of the same arithmetical value as, the complementary shear stresses T. Therefore, it is convenient to call them the *auxiliary normal stresses* of the applied shear stresses.

5. Pure shear strain in a sheet

It is supposed that the current, complex, two-stress system having principal normal components S, $-S$ as in Fig. **III**,4.1

evolves from zero without the axes OR_iR_j rotating relative to the spatially fixed set OR_xR_y as in Fig. III,5.1. Thus, the squares drawn as solid lines in the deformed sheet were the parallelograms shown as dotted lines in the undeformed sheet.

At each intermediate load between zero and the current state the stresses S, $-S$ are equivalent to the intermediate-state complementary shear stresses T as in Fig. III,4.1. Such a deformation is called pure shear strain due to the applied pure shear stress. Then, relative to the whole-body convected axes OR_iR_j, that do not rotate spatially in this case, the straining-displacement of point A is **D**(A) and that of point B is **D**(B).

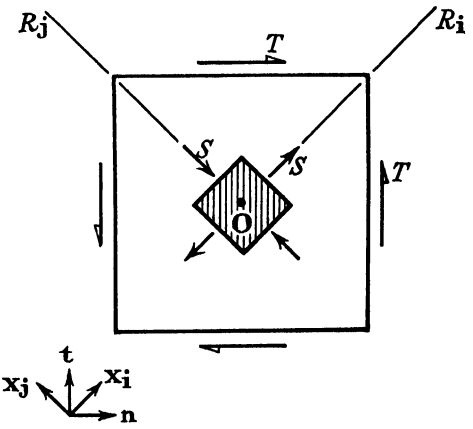

FIG. III,4.1.—The applied complementary shear stresses T can be represented by the auxiliary normal stresses S of equal magnitude to T, while one is tensile and the other compressive.

The analytical discussion of these straining-displacements is given in volume I, article III,3 and illustrated in the subsequent examples here.

6. Stress and strain transfer

In the pure shear strain of article III,5 the principal normal stresses always act on the same 'strings' of particles of the substance, while the strain and stress evolve from zero to the current values. Therefore, the stress and strain can be said to have 'not transferred'. If the principal normal stresses do not always act on the same 'strings' of particles then they 'transfer'. That is,

the principal normal stresses rotate relative to the particles of substance about the typical point considered.

Elastic strain is due to the current relative-displacement between each pair of particles constituting the body, but plastic strain is due only to their rearrangement during the strain history previous to the current state. Therefore, it is clear that only elastic strain can transfer with the stresses, while plastic strain

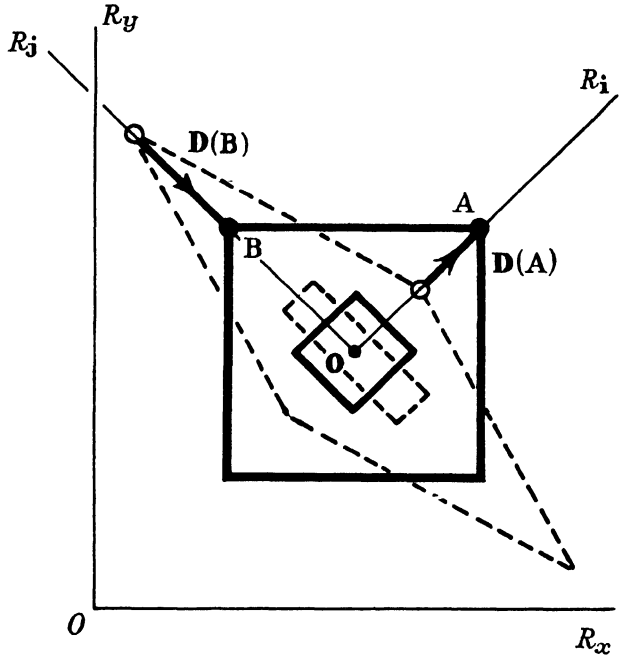

FIG. III,5.1. Pure shear strain induced by the pure shear stress system S, $-S$ of Fig. III,4.1. The unstrained lozenge shown dotted becomes the strained square shown by full lines, while the small rectangle shown dotted becomes the small square shown in solid lines.

'remains behind'. If this were not so then a square initially in the directions of the first applications of principal normal stresses would deform elasto-plastically to a rectangle always in the direction of the principal normal stresses whatever their rotation. A simple experiment with a sheet of plasticine soon disposes of such a possibility. Stress and strain transfer are discussed in more detail in volume I, articles II,10, III,7.

7. Simple shear in an elastic sheet

A simple shear of the sheet occurs under the applied complementary shear stresses T when one pair of opposite edges of the lozenge in Fig. III,5.1 remains parallel to the spatially fixed axis OR_x. This gives the situation in Fig. III,7.1. The point currently at A suffers spatial-displacement U(A) from spatially initial position A^o, while B has suffered U(B) from B^o. Relative to whole-body convected axes the straining-displacements are still

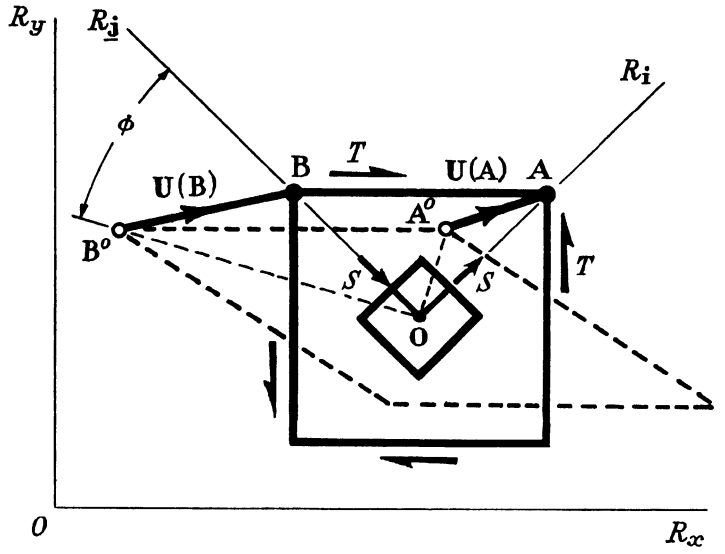

FIG. III,7.1.—Simple shear strain induced by the applied shear stress T. The initially undeformed line A^oB^o and deformed line AB remain parallel to spatially fixed axis OR_x. Directions OA^o, OB^o are the initial directions of the whole-body convected axes that are currently OR_i, OR_j. The strain 'transfers' by angle Φ.

D(A), D(B) as for pure strain shear in article III,5. The differences U(A)—D(A) and U(B)—D(B) are due to strain transfer through angle Φ.

7.1. **'Rigid-body rotation' in simple shear.** The current strain state can be visualised in two stages. If the current, deforming shear stress is removed and the whole-body convected axes held spatially fixed, then points A, B suffer elastic recovery displacements —D(A), —D(B) as in article III,5. However, side A^oB^o is not parallel to OR_x until the whole, now undeformed,

sheet is rotated back through angle Φ. This is usually referred to as the 'rigid-body rotation' of simple shear. This terminology is misleading, as it disguises the idea of strain transfer which does not occur in general for a whole-body rotation.

After application of the first incremental shear stress $\delta^{(1)}T$, say, the square of side length AB in the slightly deformed sheet does not contain the same set of particles as the same square of the same size when the shear stress reaches finite value T. At each load stage, however, between $\delta^{(1)}T$ and T the auxiliary normal stresses and principal normal strains are in the auxiliary directions at 45° and 135° respectively to OR_x. The mutually orthogonal line elements currently in these directions were mutually orthogonal at an orientation at strain transfer angle Φ from the auxiliary directions.

7.2. **Unit stretch and normal strain are not the same thing generally.** The stress dyadic with principal normal components S, $-S$ in the auxiliary directions has normal stresses S_{xx}, S_{yy} zero on transformation to axes OR_xR_y. Volume I, article III,13.2 shows that when the principal normal strains in the auxiliary directions are equal and of opposite sign then, like the stresses, the *normal strains* e_{xx}, e_{yy} *are zero*. However, line AB $\neq$ A^{o}B^o in Fig. III,7.1, so that the *unit stretch is not zero*. Similarly, line elements currently parallel to OR_y are of different length from the corresponding line elements in the undeformed sheet. Again, the depth of the dotted lozenge in Fig. III,7.1 is less than the depth of the solid-line square. This increase in width under simple shear is the Poynting effect [30], first noticed for circular cylinders under axial torsion. It is an effect of 'stretch' and not 'strain'. Recent writers have evolved quadratic strain theories introducing at least one more 'stress-strain parameter' to be 'adjusted' to allow for this 'strain'. M. Reiner [52] has called his third parameter the 'modulus of cross-elasticity' but has not noticed that the Poynting effect is explainable, in part at least, in terms of stretch and strain transfer as here.

8. Analysis† of simple shear in an elastic sheet

A shear stress T acts on the long edges of an elastic strip of depth H as in Fig. III,8.1. The straining-displacements of

† Author, 1950.

points A, B are **C**, **D** respectively relative to the whole-body convected axes OR_iR_j. The auxiliary normal stresses S, $-S$ transform the strip of depth W in the direction of unit vector **w** into the strip of depth H in direction $\mathbf{c}_y$. However, it is required that, for simple shear strain, the long edges of the strip shall be parallel in the undeformed and deformed states. Therefore, the rotation through angle Φ of strain transfer gives the geometry in Fig. III,8.2. Relative to the whole-body convected axes in their initial orientation the straining-displacements are $\mathbf{C}^o$, $\mathbf{D}^o$ as shown. The spatial-displacements are **M**, **N**, so that $(\mathbf{M}-\mathbf{C}^o)$, $(\mathbf{N}-\mathbf{D}^o)$ are the strain transfer displacements due to spatial-rotation of the whole-body convected axes.

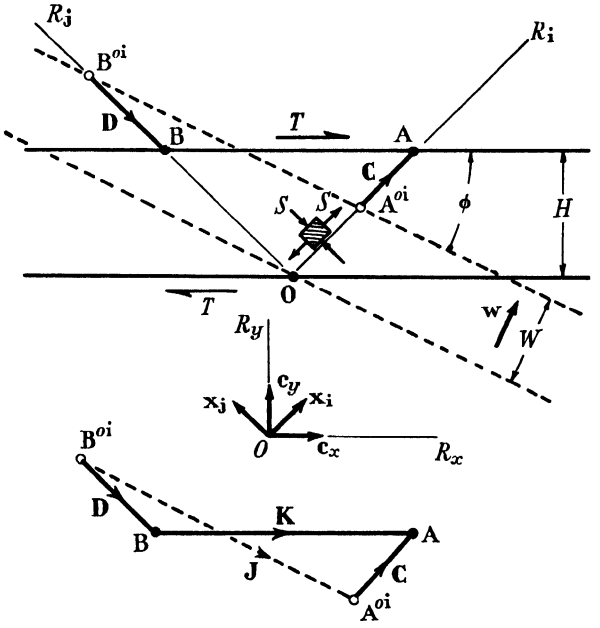

FIG. III,8.1.—An elastic strip of deformed depth H is maintained in this state by shear stress T applied to its long edges or, otherwise, by auxiliary normal tensile and compressive stresses S. Relative to whole-body convected axes in the auxiliary directions the point A suffers straining-displacement **C** and point B suffers **D**. The undeformed strip is of depth W. The shear strain is to be one of simple shear, so that the undeformed strip is incorrectly orientated by strain transfer angle Φ from the required parallelism with the spatially fixed axis OR_x.

8.1. **Strain transfer angle in terms of straining-displacement.** From Fig. III,8.1,

$$\mathbf{J} = -\mathbf{C}+\mathbf{D}+\mathbf{K} \tag{8.1}$$

Effect the 'rotation' of vector **J** into vector $\mathbf{J}^o$ through angle Φ by the 'versor operator'†

$$\mathfrak{Q} = \mathbf{c}_z\mathbf{c}_z+(\mathbf{c}_x\mathbf{c}_x+\mathbf{c}_y\mathbf{c}_y)\cos\Phi+(\mathbf{c}_y\mathbf{c}_x-\mathbf{c}_x\mathbf{c}_y)\sin\Phi \tag{8.2}$$

in prefactor scalar product. Thus,

$$\mathbf{J}^o = \mathfrak{Q}\cdot\mathbf{J} \tag{8.3}$$

Since $\mathbf{J}^o$ is parallel to **K** then their vector product is zero. Then, substituting for **J** from III(8.1) gives

$$\mathbf{K}\times\mathfrak{Q}\cdot(\mathbf{K}-\mathbf{C}+\mathbf{D}) = 0 \tag{8.4}$$

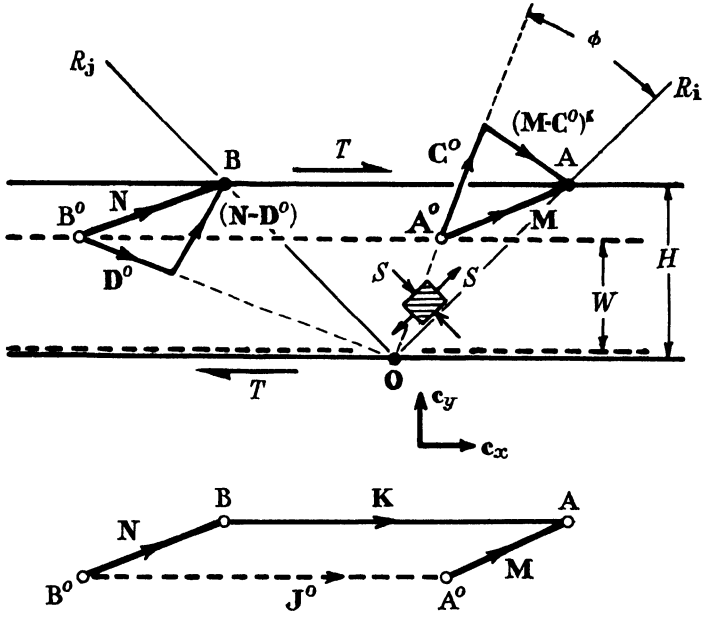

FIG. III,8.2.—Relative to the whole-body convected axes in their orientation corresponding to the orientation of the initially undeformed sheet the point A suffers straining-displacement $\mathbf{C}^o$, while point B suffers $\mathbf{D}^o$. The spatial-displacements of points A, B are **M**, **N** respectively, while $(\mathbf{M}-\mathbf{C}^o)$, $(\mathbf{N}-\mathbf{D}^o)$ are the strain-transfer displacements.

† This term is carried over from Hamilton's quaternion analysis by the present author. See volume 1, article A,14 for its formulation geometrically. Familiarity with its use will show the reader that it is a powerful and convenient mathematical device saving much avoidable geometrical analysis while economising in thought and writing.

But

$$\left.\begin{array}{lll} \mathbf{K} = 2H\mathbf{c}_x & \mathbf{C} = C\mathbf{x}_i & \mathbf{D} = -D\mathbf{x}_j \\ \mathbf{x}_i\sqrt{2} = \mathbf{c}_x+\mathbf{c}_y & \mathbf{x}_j\sqrt{2} = -\mathbf{c}_x+\mathbf{c}_y & \\ \mathbf{c}_x\times\mathbf{c}_x = 0 & \mathbf{c}_x\times\mathbf{c}_y = \mathbf{c}_z = -\mathbf{c}_y\times\mathbf{c}_x & \end{array}\right\} \quad (8.5)$$

Substituting in **III**(8.4) gives, on rearrangement,

$$\tan\Phi = (C+D)/(2H\sqrt{2}-C+D) \quad (8.6)$$

Note that C, D are the arithmetical values of **C**, **D** respectively, since the signs have already been considered.

8.2. **Change in length of the strip in terms of straining-displacement.** The change in length of the strip can be found from $(K-J)$ with K the modulus of **K** and J the modulus of **J** or $\mathbf{J}^o$. From **III**(8.1),

$$\begin{aligned} J^2 &= \mathbf{J}\cdot\mathbf{J} \\ &= C^2+D^2+K^2-2\mathbf{C}\cdot\mathbf{D}-2\mathbf{C}\cdot\mathbf{K}+2\mathbf{D}\cdot\mathbf{K} \end{aligned} \quad (8.7)$$

But **C** and **D** are orthogonal, so that their scalar product is zero, while using **III**(8.5), taking the square root, and subtracting from K gives

$$K-J = 2H-\sqrt{[C^2+D^2+4H^2+2^{-\frac{1}{2}}4H(-C+D)]}$$

Written as the change in length per unit length of deformed sheet this gives

$$J/K = \sqrt{[\tfrac{1}{4}(C^2+D^2)H^{-2}+1+(-C+D)H^{-1}2^{-\frac{1}{2}}]} \quad (8.8)$$

8.3. **Change in depth of the strip in terms of straining-displacement.** The change in depth of the strip can be measured by $(H-W)$. Depth W can be found by resolving the *vector* $\mathbf{OA}^{o\,i}$ to the direction **w** in Fig. **III**,8.1. Thus,

$$W = \mathbf{w}\cdot(\sqrt{2H}\mathbf{x}_i-\mathbf{C}) \quad (8.9)$$

with

$$\mathbf{w} = \mathbf{c}_x \sin\Phi+\mathbf{c}_y\cos\Phi$$

Substituting appropriately from equations **III**(8.5) and then substituting for $\sin\Phi$ from equation **III**(8.6) gives

$$\frac{W}{H} = \frac{(\sqrt{2}+D/H)[1-C/(\sqrt{2}H)]\cos\Phi}{\sqrt{2}-\frac{1}{2}C/H+\frac{1}{2}D/H} \quad (8.10)$$

8.4. **Unit stretches in the length and depth of the strip.** Volume I, article **III**,13 discusses the 'stretch' of a line. The

unit stretches here of the length and depth of the strip are defined by

$$a_x = (K-J)/K \qquad a_y = (H-W)/H \tag{8.11}$$

Substituting from III(8.8) and III(8.10) gives

$$\left.\begin{aligned} a_x &= 1-\sqrt{[\tfrac{1}{4}(C^2+D^2)H^{-2}+1+2^{-\frac{1}{2}}(-C+D)H^{-1}]} \\ a_y &= 1-\frac{(\sqrt{2}+D/H)[1-C/(\sqrt{2}H)]\cos\Phi}{\sqrt{2}-\frac{1}{2}C/H+\frac{1}{2}D/H} \end{aligned}\right\} \tag{8.12}$$

8.5. **Spatial-displacements of points** A, B. To find the spatial-displacement **M** of point B from its initial position B^o consider the geometry of Fig. III,8.2.

$$\mathbf{M} = \mathbf{C}^o+(\mathbf{M}-\mathbf{C}^o) \tag{8.13}$$

But

$$(\mathbf{M}-\mathbf{C}^o) = \sqrt{2}H\mathbf{x}_i-\mathfrak{Q}\cdot(\sqrt{2}H\mathbf{x}_i) = \sqrt{2}H(\mathfrak{J}-\mathfrak{Q})\cdot\mathbf{x}_i$$

with the idemfactor

$$\mathfrak{J} = \mathbf{c}_x\mathbf{c}_x+\mathbf{c}_y\mathbf{c}_y+\mathbf{c}_z\mathbf{c}_z = \mathbf{x}_i\mathbf{x}_i+\mathbf{x}_j\mathbf{x}_j+\mathbf{c}_z\mathbf{c}_z \tag{8.14}$$

while, also,

$$\mathbf{C}^o = \mathfrak{Q}\cdot\mathbf{C} \tag{8.15}$$

Then, from III(8.13),

$$\mathbf{M} = \mathfrak{Q}\cdot\mathbf{C}+\sqrt{2}H(\mathfrak{J}-\mathfrak{Q})\cdot\mathbf{x}_i \tag{8.16}$$

Similarly, the spatial-displacement of point B is

$$\mathbf{N} = \mathfrak{Q}\cdot\mathbf{D}+\sqrt{2}H(\mathfrak{J}-\mathfrak{Q})\cdot\mathbf{x}_j \tag{8.17}$$

Using III(8.5), III(8.2) to expand these two expressions to the spatially fixed axes and substituting for sin Φ from III(8.6) gives the scalar components of **M** as

$$\left.\begin{aligned} M_x &= H+(2^{-\frac{1}{2}}C-H)[1-(C+D)/(2H\sqrt{2}-C+D)]\cos\Phi \\ M_y &= H+(2^{-\frac{1}{2}}C-H)[1+(C+D)/(2H\sqrt{2}-C+D)]\cos\Phi \end{aligned}\right\} \tag{8.18}$$

while a similar form can be found for **N**.

8.6. **Spatial-displacement of a general point.** Let **R** be a general point in the sheet with components $R_i\mathbf{x}_i$, $R_j\mathbf{x}_j$ relative to the whole-body convected axes. Let **D** be the straining-displacement of **R** with components $D_i\mathbf{x}_i$, $-D_j\mathbf{x}_j$. Then, with C, D as previously,

$$\begin{aligned} \mathbf{D} &= (C\mathbf{x}_i)R_i/(\sqrt{2}H)-(D\mathbf{x}_j)R_j/(\sqrt{2}H) \\ &= (C\mathbf{x}_i\mathbf{x}_i-D\mathbf{x}_j\mathbf{x}_j)\cdot\mathbf{R}/(\sqrt{2}H) \end{aligned} \tag{8.19}$$

The instantaneously initial position of a point is

$$\mathbf{R}^{oi} = \mathbf{R} - \mathbf{D} \tag{8.20}$$

while its spatially initial position, allowing for the strain transfer of this simple shear, is

$$\mathbf{R}^{o} = \mathfrak{Q} \cdot \mathbf{R}^{oi} \tag{8.21}$$

The spatial-displacement is then

$$\begin{aligned} \mathbf{U} = \mathbf{R} - \mathbf{R}^{o} &= \mathfrak{J} \cdot \mathbf{R} - \mathfrak{Q} \cdot \mathbf{R}^{oi} \\ &= \{\mathfrak{J} - \mathfrak{Q} \cdot [\mathfrak{J} - (C\mathbf{x}_i\mathbf{x}_i - D\mathbf{x}_j\mathbf{x}_j)/(\sqrt{2}H)]\} \cdot \mathbf{R} \end{aligned} \tag{8.22}$$

Equations III(8.17), III(8.16) are seen to be special cases of this equation when $\mathbf{R}$ has the components of the particular values there. The expansion of this to the spatially fixed axes is left as an exercise for the reader.

8.7. **Straining-displacement of a general point.** The straining-displacement of a point at general position $\mathbf{R}$ is given in equation III(8.19) relative to the whole-body convected axes. Resolve the self-conjugate dyadic on the right-hand side to the spatially fixed axes. Thus, on transforming the unit vectors $\mathbf{x}_i$, $\mathbf{x}_j$,

$$\mathbf{D} = \mathfrak{M} \cdot \mathbf{R} \tag{8.23}$$

with strain dyadic

$$\mathfrak{M} = [(C-D)(\mathbf{c}_x\mathbf{c}_x + \mathbf{c}_y\mathbf{c}_y) + (C+D)(\mathbf{c}_x\mathbf{c}_y + \mathbf{c}_y\mathbf{c}_x)]/(2\sqrt{2}H) \tag{8.24}$$

8.8. **Anisotropic sheet.** A substance is anisotropic when the principal normal stresses and strains are not always coaxial as the deformation evolves but differ by phase angle θ^{ph} as in volume 1, article IV,2.1. In this case the vectors $\mathbf{C}$, $\mathbf{D}$ of Fig. III,8.1 are not in the auxiliary normal stress directions and correspondingly alter the strain transfer angle.

There appears to be no experimental evidence (March 1954) on this aspect but, in subsequent tests, it is a theoretical possibility to be borne in mind when analysing physical data. The writing out of the geometry and consequent changes in the foregoing expressions for unit stretches are left as an exercise for the reader.

9. Simple shear in an elastic sheet: theoretical examples†

The various expressions in article III,8 for the spatial-displacement of points and the unit stretch of length and depth of the

† Author, 1950.

strip are given in terms of the arithmetical magnitudes C, D of the straining-displacement of the auxiliary directions at 45°, 135° respectively to axis OR_x. Principal normal stresses and strains are coaxial, so that general, or restricted, isotropy is implied. Within this restriction, the problem is now to express the magnitudes of the current C, D in terms of the current applied shear stresses T.

The increment stress and increment strain approach is convenient here. Thus,

$$\left.\begin{aligned} \delta C &= \sqrt{2}H\delta e_i = \sqrt{2}H(\delta\epsilon_i - q_{j-i}\delta\epsilon_j) \\ \delta D &= \sqrt{2}H\delta e_j = \sqrt{2}H(\delta\epsilon_j - q_{i-j}\delta\epsilon_i) \end{aligned}\right\} \quad (9.1)$$

and these are integrated between the initial undeformed and current deformed states, since the elastic strains and elastic straining-displacement transfer as the stress system evolves.

9.1. **Constant elastic tangent modulus and restricted isotropy.** Suppose the transverse contraction ratios are isotropic of value q, as are also the tangent moduli ψ of equations **III**(3.6). The principal normal increment stresses are equal and of opposite sign, so that

$$\delta C = \sqrt{2}H(1+q)\psi\delta T = \delta D \quad (9.2)$$

Further, suppose that the stress-strain parameters are constant to give

$$C = \sqrt{2}H(1+q)\psi T = D \quad (9.3)$$

Therefore, the principal normal strain

$$e_i = C/(\sqrt{2}H) = (1+q)\psi T = f \quad (9.4)$$

say, while compressive strain e_j is of the same arithmetical value.

Substituting **III**(9.3) in **III**(8.6) together with **III**(9.4) gives the strain transfer angle Φ in

$$\tan\Phi = f \quad (9.5)$$

The unit stretches in the length and depth of the strip are given by substituting **III**(9.4), **III**(9.3) in **III**(8.12). Thus,

$$\left.\begin{aligned} a_x &= 1-\sqrt{(1+f^2)} \\ a_y &= 1-(1-f^2)\cos\Phi \end{aligned}\right\} \quad (9.6)$$

Substituting **III**(9.3) in **III**(8.23) gives the straining-displacement of the general point **R** as

$$\mathbf{D} = \mathfrak{M}\cdot\mathbf{R} \quad (9.7)$$

with strain dyadic

$$\mathfrak{M} = f(\mathbf{c}_x\mathbf{c}_y + \mathbf{c}_y\mathbf{c}_x) \tag{9.8}$$

Since the dyads $\mathbf{c}_x\mathbf{c}_x$, $\mathbf{c}_y\mathbf{c}_y$ do not appear, then the normal strains are zero in the directions of the spatially fixed axes although the unit stretches are not zero. Thus, symbolically,

$$a_x \neq 0 = e_{xx} \qquad a_y \neq 0 = e_{yy} \tag{9.9}$$

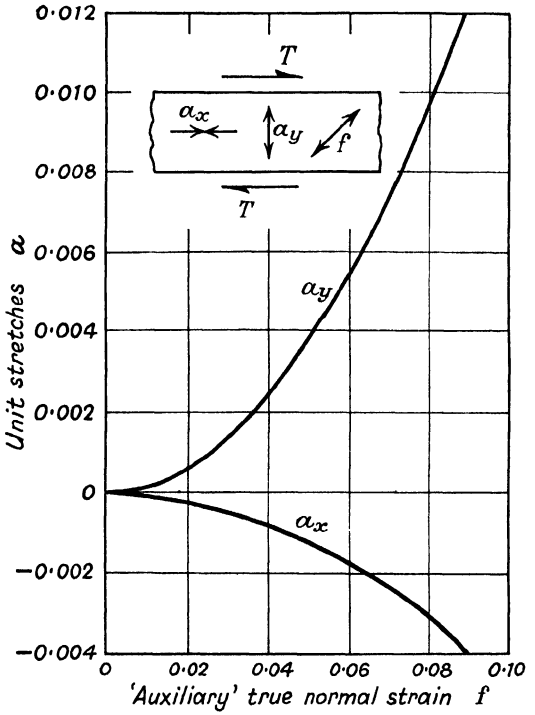

FIG. III,9.1.—Simple shear of an elastic sheet of restricted isotropy and constant stress-strain parameters. Shear strain is measured by the auxiliary normal strain f. The values of the unit stretches a_x, a_y are those for the initial, fairly small deformation.

The normal strains components of the strain dyadic are zero but the Poynting [30] 'normal strains' (as discussed recently by M. Reiner [52], for example, in terms of a modulus of cross-elasticity) are not zero. Figs. III,9.1, III,9.2 give the length and depth unit stretches vs. auxiliary normal strain as the measure of shear strain.

When the strains are small enough to neglect their squares as in classical infinitesimal strains theory then

$$a_x = 0 = e_{xx} \qquad a_y = 0 = e_{yy} \tag{9.10}$$

9.2. **Isotropic tangent modulus a function of shear stress.** Suppose, again, that the transverse contraction ratio is constant

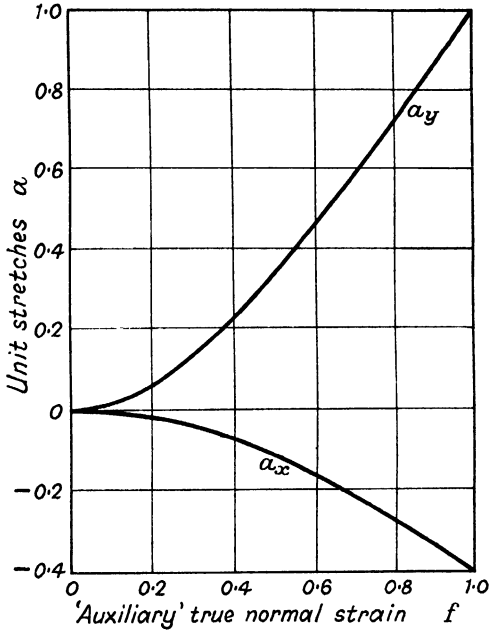

FIG. III,9.2.—Simple shear of an elastic sheet of restricted isotropy and constant stress-strain parameters. The strain range here is much greater than that in Fig. III,9.1.

while the isotropic tangent modulus ψ is a function of shear stress of the form

$$\psi = k + j \exp(hT) \tag{9.11}$$

with parameters h, j, k to be fitted to experimental measurements on the behaviour of the substance. Substitute in III(9.2) and integrate to give

$$C = \sqrt{2H(1+q)}[kT + jh^{-1} \exp(hT)] = D \tag{9.12}$$

Thus, the principal normal stress and the partial-strain are

related by a form similar to that for the rubber in article I,8. Therefore, the principal normal strain

$$e_{\mathbf{i}} = (1+q)[kT+jh^{-1}\exp(hT)] = f \tag{9.13}$$

say, while $e_{\mathbf{j}}$ is of the same magnitude but opposite sign.

From III(8.6) the angle of strain transfer is found from

$$\tan \Phi = f \tag{9.14}$$

while, from III(8.12),

$$a_x = 1-\sqrt{(1+f^2)} \qquad a_y = 1-(1-f^2)\cos\Phi \tag{9.15}$$

The relationships III(9.10), III(9.9) are found again for the present case.

9.3. **General isotropy and constant tangent moduli.** In III(9.1) suppose, for simplicity, that the q's are isotropic, as they are of less importance than the moduli, while the tangent moduli are anisotropic as in equations III(3.6). Thus,

$$\delta C = \sqrt{2H(\psi_{\mathbf{i}}+q\psi_{\mathbf{j}})}\delta T \qquad \delta D = \sqrt{2H(\psi_{\mathbf{j}}+q\psi_{\mathbf{i}})}\delta T \tag{9.16}$$

With all stress-strain parameters constant then integration gives

$$C = \sqrt{2H(\psi_{\mathbf{i}}+q\psi_{\mathbf{j}})}T \qquad D = \sqrt{2H(\psi_{\mathbf{j}}+q\psi_{\mathbf{i}})}T \tag{9.17}$$

Thus, on reinserting the sign for compression, the total strains are,

$$e_{\mathbf{i}} = (\psi_{\mathbf{i}}+q\psi_{\mathbf{j}})T \qquad e_{\mathbf{j}} = -(\psi_{\mathbf{j}}+q\psi_{\mathbf{i}})T \tag{9.18}$$

and are not equal as for restricted isotropy.

Substituting III(9.17) in III(8.6), III(8.12) gives the strain transfer angle and unit stretches respectively, while in the strain dyadic III(8.24) the normal strains are not zero. Thus, for general isotropy,

$$(a_x \neq a_y) \neq (e_{xx} = e_{yy}) \neq 0 \tag{9.19}$$

9.4. **Non-constant tangent moduli and general isotropy.** More generally, the stress-strain parameters of equations III(9.16) may be functions of current stress in the manner of article III,9.2. At present (March 1954) there seems to be no experimental evidence on anisotropic, non-constant parameters. The reader may find it an interesting exercise to assume plausible values and study their effects on strain transfer, unit stretches of the strip and the effect on the components of the strain dyadic.

10. Simple shear in an elasto-plastic sheet†

Article III,3.4 mentions that the plastic component of elasto-plastic strain does not 'transfer' when the stress and strain rotate relative to the substance about a typical point. The elastic strain adds up, or sums scalarly, as it transfers to follow the rotating stresses. Thus, the current principal normal strains at a point due to a two-stress system are given by adding the elastic total strain and the last plastic increment strain. Thus, the current straining-displacements C, D as in Figs. III,8.1, III,8.2 are

$$C = C^E + \delta C^P \qquad D = D^E + \delta D^P \tag{10.1}$$

With this restriction the equations formulated in article III,8 for an elastic sheet apply to the present elasto-plastic case.

The elasto-plastic strain transfer angle Λ, say, is given by III(8.6) from

$$\tan \Lambda = \frac{(C^E + D^E) + (\delta C^P + \delta D^P)}{2H\sqrt{2} + (-C^E + D^E) + (-\delta C^P + \delta D^P)} \tag{10.2}$$

The strain transfer versor operator is now, similar to III(8.2),

$$\mathfrak{Q} = \mathbf{c}_z\mathbf{c}_z + (\mathbf{c}_x\mathbf{c}_x + \mathbf{c}_y\mathbf{c}_y)\cos\Lambda + (\mathbf{c}_y\mathbf{c}_x - \mathbf{c}_x\mathbf{c}_y)\sin\Lambda \tag{10.3}$$

10.1. **Elasto-plastic spatial-displacement.** The current 'spatial-displacement' is now an elastic component and the last increment plastic component. Thus, from III(8.22), with $\mathfrak{Q}$ from III(10.3) and C, D from III(10.1),

$$\begin{aligned}\mathbf{U} &= \mathbf{U}^E + \delta\mathbf{U}^P \\ &= \{\mathfrak{J} - \mathfrak{Q}\cdot[\mathfrak{J} - (C^E\mathbf{x}_i\mathbf{x}_i - D^E\mathbf{x}_j\mathbf{x}_j)/(\sqrt{2}H)]\}\cdot\mathbf{R} \\ &\quad + \mathfrak{Q}\cdot[\delta C^P\mathbf{x}_i\mathbf{x}_i - \delta D^P\mathbf{x}_j\mathbf{x}_j]\cdot\mathbf{R}/(\sqrt{2}H)\end{aligned} \tag{10.4}$$

10.2. **Depth change of the elasto-plastic strip.** If, particularly,

$$\mathbf{R} = H\mathbf{c}_y \tag{10.5}$$

then the component of III(10.4) in direction $\mathbf{c}_y$ gives the elastic, or reversible, and increment plastic, or increment non-recoverable, depth changes of the strip due to the current load and its last increment. Thus, the strip of current depth H has suffered the last, permanent, incremental increase of depth

$$\delta W^P = \mathbf{c}_y\cdot\delta\mathbf{U}_y^P = 2^{-\frac{1}{2}}\mathbf{c}_y\cdot\mathfrak{Q}\cdot(\delta C^P\mathbf{x}_i\mathbf{x}_i - \delta D^P\mathbf{x}_j\mathbf{x}_j)\cdot\mathbf{c}_y$$

† Author, 1950.

But the direction cosines $\mathbf{x}_i \cdot \mathbf{c}_y = 2^{-\frac{1}{2}} = \mathbf{x}_j \cdot \mathbf{c}_y$, so that

$$\delta W^P = \tfrac{1}{2}\mathbf{c}_y \cdot \textcircled{Q} \cdot (\delta C^P \mathbf{x}_i - \delta D^P \mathbf{x}_j)$$

Substituting for $\textcircled{Q}$ from III(10.3) and $\mathbf{x}_i$, $\mathbf{x}_j$ from III(8.5) gives

$$\delta W^P = (2\sqrt{2})^{-1}[(\delta C^P - \delta D^P)\cos A + (\delta C^P + \delta D^P)\sin A] \quad (10.6)$$

Suppose the strip is still elastic but just about to yield when it is of depth W^o under shear stress T^o. Under the shear stress $(T^o + \delta^{(1)}T)$ the strip suffers an elastic increase in depth $\delta^{(1)}W^E$ and a plastic increase in depth $\delta^{(1)}W^P$ to become $(W^o + \delta^{(1)}W^E + \delta^{(1)}W^P)$. Again, let the shear stress increase by another increment $\delta^{(2)}T$, using the latter depth to calculate the new depth $(W^o + \delta^{(1)}W^E + \delta^{(2)}W^E + \delta^{(1)}W^P + \delta^{(2)}W^P)$. This incremental process can be continued to give the current depth of a strip initially of depth W^o just before plastic strains appeared.

10.3. **Length change of the elasto-plastic strip.** If, particularly,

$$\mathbf{R} = H\mathbf{c}_x \quad (10.7)$$

then this component of III(10.4) in direction $\mathbf{c}_x$ gives the elastic and last increment plastic length changes due to the current load and its last increment. Denote the increment plastic length change by δL^P and derive its form in a similar manner to the derivation of III(10.6). Thus,

$$\begin{aligned}\delta L^P &= \mathbf{c}_x \cdot \delta \mathbf{U}_x^P \\ &= (2\sqrt{2})^{-1}[(\delta C^P - \delta D^P)\cos A - (\delta C^P + \delta D^P)\sin A] \quad (10.8)\end{aligned}$$

The length change at the current state of the strip can be computed incrementally in a manner similar to that for depth change as in article III,10.2.

11. Simple shear in an elasto-plastic sheet of restricted isotropy: theoretical example†

The elasto-plastic sheet is supposed to be of restricted isotropy and have the idealised normal stress vs. normal partial-strain relationship in Fig. III,11.1, so that the elastic and plastic moduli are both constant. Further, it is supposed that the elastic and

† Author, 1950.

plastic transverse contraction ratios are equal and remain constant at value q. The constant elastic modulus is

$$\psi^E = E^{-1} \tag{11.1}$$

and we may write

$$\psi^P = (P^{-1} - E^{-1}) = h\psi^E \tag{11.2}$$

with constant ratio h. Then, in III(10.4) the elastic and plastic increment straining-displacements are

$$\left.\begin{aligned} \delta C^E = \delta D^E &= (1+q)\psi^E \delta T \sqrt{2H} \\ \delta C^P = \delta D^P &= (1+q)h\psi^E \delta T \sqrt{2H} = h\delta C^E \end{aligned}\right\} \tag{11.3}$$

with H the current depth of the strip.

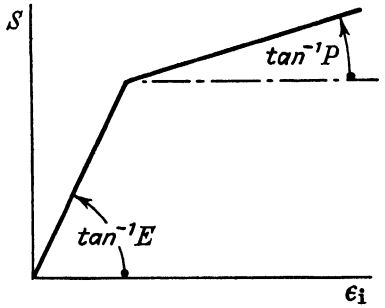

FIG. III,11.1.—Idealised elasto-plastic normal partial-strain vs. normal stress. The elastic modulus is E^{-1}, while P^{-1} is the elasto-plastic modulus. The plastic modulus is $(P^{-1}-E^{-1})$.

11.1. **Spatial-displacement of a particular point for particular increment stress-strain parameters values.** The particular point followed is initially at

$$\mathbf{R} = \mathbf{c}_y \tag{11.4}$$

when the strip is just about to yield. Its spatial-displacement is computed incrementally in equation III(10.4) using the values:

$$\left.\begin{aligned} &\text{Primary yield auxiliary normal strain } f^{(0)} = 0{\cdot}2 \\ &\text{Plastic modulus ratio } h = 10 \\ &\text{Shear stress increment } \delta = 20^{-1} \end{aligned}\right\} \tag{11.5}$$

The method of computation suggested in articles III,10.2, III,10.3 is used and gives the spatial-displacement path of the point shown as a solid line in Fig. III,11.2. The dotted curve is the trajectory

of the point when the applied shear stress is reduced to zero and shows the extent of the permanent increase in depth of the strip.

11.2. **Simple shear and reversed shear.** The spatial-displacement trajectories in Fig. III,11.3 for simple shear and reversed shear have been constructed from the analysis giving Fig. III,11.2. The trajectory FG is elastic and GHJ... is

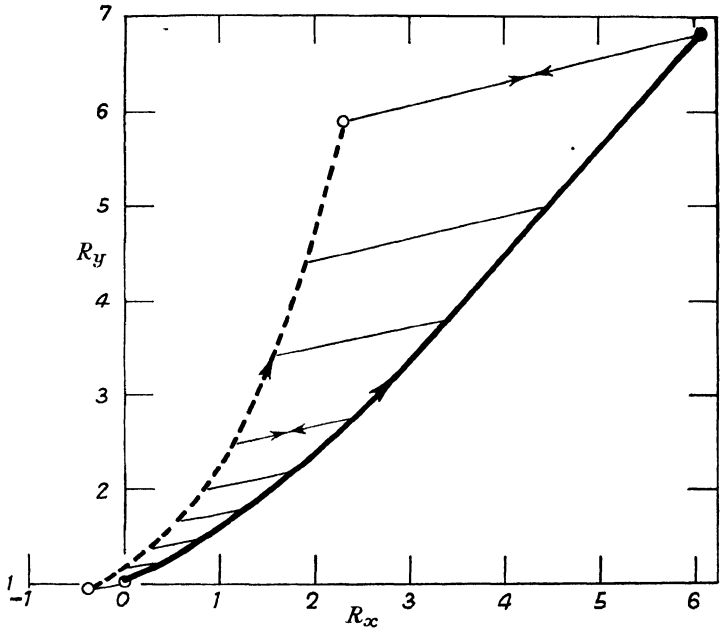

FIG. III,11.2.—The elasto-plastic trajectory of a point at initial position (0, 1) when the applied simple shear stress is just at yield. The post-yield increase of R_y with applied shear stress shows that the depth of the strip increases considerably relative to its lower edge at $R_y = 0$. The dotted trajectory is that of the point when the shear stress is reduced to zero from successive positions on the elasto-plastic trajectory.

elasto-plastic. At H unloading of the strip commences, is complete at K and again reaches yield at L under reversed shear stress, while LMN... is the elasto-plastic range as this reversed shear stress increases further. Reversal of the reversed shear stress commences at M, is complete at P, yield commences again at Q, while QR... is again the elasto-plastic strain range. The qualitative similarity of these trajectories and those noted experi-

mentally by H. W. Swift [53] for fairly small unit stretches as in article IV,4 should be noted.

12. Simple shear in a slightly elastic elasto-plastic sheet of general isotropy: theoretical example

Suppose that the yield stress and work-hardening of a substance are both 'small'. Then, in article III,10 the strain transfer angle

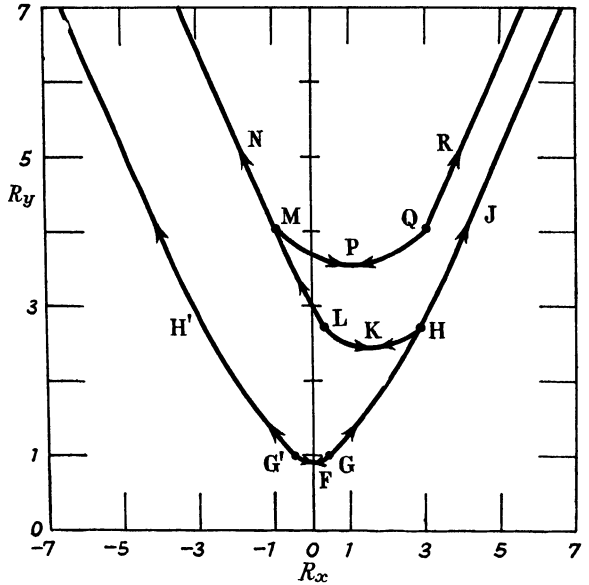

FIG. III,11.3.—Shear and reversed shear trajectories of the point in Fig. III,11.2. Segments of trajectory with arrows in both directions are those for elastic unloading, loading to yield again. The qualitative similarity of these curves to the experimental curves in Fig. IV,4.1 should be noted.

is small, so that $\tan \Lambda \doteqdot \Lambda \doteqdot \sin \Lambda$ and $\cos \Lambda \doteqdot 1$. Therefore, from articles III,10.2, III,10.3 and neglecting the products $\Lambda \delta C^P$, $\Lambda \delta D^P$ this gives

$$\delta W^P = (2\sqrt{2})^{-1}(\delta C^P - \delta D^P) = \delta L^P \qquad (12.1)$$

Suppose the plastic moduli are not isotropic but, for simplicity, that the plastic transverse contraction ratio is isotropic. Then,

$$\left.\begin{aligned} \delta C^P &= (\psi_i^P - q^P \psi_j^P)\delta T \sqrt{2H} \\ \delta D^P &= (\psi_j^P - q^P \psi_i^P)\delta T \sqrt{2H} \end{aligned}\right\} \qquad (12.2)$$

Then,

$$\delta W^P = \tfrac{1}{2}H\delta T(1+q^P)(\psi_{\mathrm{i}}^P - \psi_{\mathrm{j}}^P) = \delta L^P \qquad (12.3)$$

Therefore, the permanent change in depth of the strip is an increase or a decrease depending on the relative magnitudes of the plastic moduli in the auxiliary normal stress directions of the applied simple shear stress.

In a test by H. W. Swift [53], axial torsion was applied to a solid lead cylinder not previously worked after casting. There was an appreciable stage of zero length change and then the cylinder shortened, but no observation of the change in diameter is recorded. If the length changes of the cylinder could be analysed approximately by such as III(12.3) then, initially, $\psi_{\mathrm{i}}^P = \psi_{\mathrm{j}}^P$ and subsequently $\psi_{\mathrm{i}}^P < \psi_{\mathrm{j}}^P$.

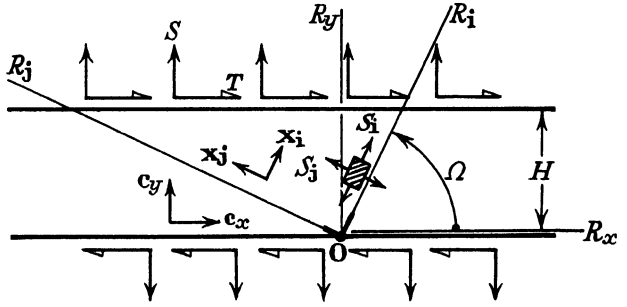

FIG. III,13.1.—Shear stress T and transverse normal stress S applied to a long, isotropic, elastic strip for which appropriate strain transfer keeps the long edges always parallel to the spatially fixed axis OR_x. The whole-body convected axes $OR_{\mathrm{i}}R_{\mathrm{j}}$ are shown in their current position in the directions of the principal normal stresses and strains.

13. Shear stress and transverse normal stress applied to an isotropic elastic strip

Consider the shear stress T and normal stress S applied to the long edges of an elastic, deformed strip as in Fig. III,13.1. The strip is to have its long edges always parallel to the spatially fixed axis OR_x between its initially undeformed and currently deformed states. This is something like the simple shear in articles III,7 and III,8, but it is not simple shear because of the presence of normal stress on planes normal to the axis OR_y.

13.1. **Stress dyadic.** For this complex stress system the stress dyadic is

$$\mathfrak{S} = S\mathbf{c}_x\mathbf{c}_x + T(\mathbf{c}_x\mathbf{c}_y + \mathbf{c}_y\mathbf{c}_x) \tag{13.1}$$

Article III,1.3 gives the principal normal stress direction $\mathbf{x}_\mathrm{i}$ at angle Ω, say, from

$$\tan 2\Omega = -2T/S \tag{13.2}$$

while the principal normal stresses are

$$\left.\begin{aligned} S_\mathrm{i} &= \tfrac{1}{2}S(1-\cos 2\Omega) + T\sin 2\Omega \\ S_\mathrm{j} &= \tfrac{1}{2}S(1+\cos 2\Omega) - T\sin 2\Omega \end{aligned}\right\} \tag{13.3}$$

The principal normal stress directions unit vectors are now

$$\left.\begin{aligned} \mathbf{x}_\mathrm{i} &= \mathbf{c}_x\cos\Omega + \mathbf{c}_y\sin\Omega \\ \mathbf{x}_\mathrm{j} &= -\mathbf{c}_x\sin\Omega + \mathbf{c}_y\cos\Omega \end{aligned}\right\} \tag{13.4}$$

13.2. **Strain transfer angle.** The principal normal strains are in the directions of principal normal stresses for an isotropic substance, so that, in Fig. III,13.1, the straining-displacements for these directions are

$$\mathbf{C} = C\mathbf{x}_\mathrm{i} \qquad \mathbf{D} = D\mathbf{x}_\mathrm{j} \tag{13.5}$$

Note that this does not take account of sign as in article III,8.

Similar to article III,8 there is found geometrically

$$\mathbf{J} = -\mathbf{C} - \mathbf{D} + \mathbf{K} \tag{13.6}$$

$$\mathbf{J}^o = \mathfrak{Q}\cdot\mathbf{J} \tag{13.7}$$

$$\mathfrak{Q} = \mathbf{c}_z\mathbf{c}_z + (\mathbf{c}_x\mathbf{c}_x + \mathbf{c}_y\mathbf{c}_y)\cos\Phi + (\mathbf{c}_y\mathbf{c}_x - \mathbf{c}_x\mathbf{c}_y)\sin\Phi \tag{13.8}$$

for strain transfer angle Φ. This is found in the tan Φ form from

$$\mathbf{K}\times\mathfrak{Q}\cdot(\mathbf{K}-\mathbf{C}-\mathbf{D}) = 0 \tag{13.9}$$

while, here,

$$\mathbf{K} = (1/\tan\Omega + \tan\Omega)H\mathbf{c}_x \tag{13.10}$$

13.3. **Length change of the strip.** The unit stretch in length of the strip is again

$$a_x = 1 - J/K \tag{13.11}$$

with

$$J = \sqrt{(\mathbf{J}\cdot\mathbf{J})} \tag{13.12}$$

and $\mathbf{J}$ from III(13.6).

13.4. **Depth change of the strip.** Similar to article III,8.3 the initial scalar depth of the strip here is

$$W = \mathbf{w}\cdot[(H\mathbf{x}_\mathbf{i}/\sin\Omega)-\mathbf{C}] \tag{13.13}$$

with

$$\mathbf{w} = \mathbf{c}_x \sin\Phi + \mathbf{c}_y \cos\Phi \tag{13.14}$$

The unit stretch in depth is, again,

$$a_y = 1 - W/H \tag{13.15}$$

13.5. **Spatial-displacement of a point.** Relative to the whole-body convected axes currently in directions $\mathbf{x}_\mathbf{i}$, $\mathbf{x}_\mathbf{j}$ the instantaneously initial position of a point at current position $\mathbf{R}$ is

$$\mathbf{R}^{o\,\mathbf{i}} = \mathbf{R}-(\mathbf{C}HR_\mathbf{i}/\sin\Omega)-(\mathbf{D}HR_\mathbf{j}/\cos\Omega) = \mathbf{R}\cdot(\mathfrak{J}-\mathfrak{M}) \tag{13.16}$$

with strain dyadic

$$\mathfrak{M} = [(\mathbf{x}_\mathbf{i}\mathbf{C}/\sin\Omega)+(\mathbf{x}_\mathbf{j}\mathbf{D}/\cos\Omega)]H \tag{13.17}$$

14. Transverse normal stress and a small shear stress applied to an isotropic elastic strip

In the applied complex stress S, T of article III,13 suppose that T is small. Then, from III(13.2), with ρ a small angle the principal normal stress direction

$$\Omega = \tfrac{1}{2}\pi - \rho \tag{14.1}$$

with

$$\rho = T/S \tag{14.2}$$

The principal normal stresses are then found from III(13.3) to be

$$S_\mathbf{i} = S+(2T^2/S) \qquad S_\mathbf{j} = -2T^2/S \tag{14.3}$$

and their directions from III(13.4) to be

$$\mathbf{x}_\mathbf{i} = (\mathbf{c}_x T/S)+\mathbf{c}_y \qquad \mathbf{x}_\mathbf{j} = -\mathbf{c}_x+(\mathbf{c}_y T/S) \tag{14.4}$$

14.1. **Strain transfer angle:** The vector of III(13.10) is now

$$\mathbf{K} = [(1/\rho)+\rho]H\mathbf{c}_x = [(S/T)+(T/S)]H\mathbf{c}_x \tag{14.5}$$

while

$$\mathbf{C} = C[(\mathbf{c}_x T/S)+\mathbf{c}_y] \qquad \mathbf{D} = D[-\mathbf{c}_x+(\mathbf{c}_y T/S)] \tag{14.6}$$

Use $\mathfrak{Q}$ from III(13.8) and with III(14.6), III(14.5) substitute in III(13.9). Neglecting T^3 and smaller terms gives the strain

transfer angle Φ from tan Φ. However, it can be approximated by Φ to give

$$\Phi = TC/(SH)+T^2D(1-C/H)/(S^2H) \tag{14.7}$$

14.2. **Length change of the strip.** From **III**(13.12), **III**(13.6)

$$J = \sqrt{(\mathbf{J}\cdot\mathbf{J})} \tag{14.8}$$

$$\mathbf{J} = \mathbf{K}-\mathbf{C}-\mathbf{D} \tag{14.9}$$

Therefore, with **III**(14.6), **III**(14.5),

$$J = \sqrt{\left\{\begin{matrix} H^2[2+(S/T)^2]+C^2+D^2+2H(-C+DS/T) \\ +(T/S)2HD+(T/S)^2[(H-C)^2+D^2] \end{matrix}\right\}} \tag{14.10}$$

The lengthwise unit stretch is

$$a_x = 1-J/K \tag{14.11}$$

while, from **III**(14.5),

$$K = [(S/T)+(T/S)]H \tag{14.12}$$

14.3. **Depth change of the strip.** Using **III**(14.1), **III**(14.4), then **III**(13.13) gives

$$W = \mathbf{w}\cdot[(\mathbf{c}_x T/S)+\mathbf{c}_y](H-C) \tag{14.13}$$

and with the small strain transfer angle then, from **III**(13.14),

$$\mathbf{w} = \mathbf{c}_x\Phi+\mathbf{c}_y \tag{14.14}$$

so that

$$W = [(\Phi T/S)+1](H-C) = [(T/S)^2(C/H)+1](H-C) \tag{14.15}$$

with **III**(14.7) and neglecting T^3 and smaller. The depthwise unit stretch is

$$a_y = 1-W/H$$

so that, with **III**(14.15), then

$$a_y = (C/H)\{1+(T/S)^2[(C/H)-1]\} \tag{14.16}$$

15. Depth change of an elastic strip of restricted isotropy due to a small shear stress and a finite transverse normal stress: theoretical example

Article **III**,14.3 gives the depthwise unit stretch of an elastic strip due to small shear stress T and finite normal stress S as

$$a_y = (C/H)\{1+(T/S)^2[(C/H)-1]\} \tag{15.1}$$

Article **III**,14 gives the principal normal stresses as

$$S_\mathbf{i} = S+(2T^2/S) \qquad S_\mathbf{j} = -2T^2/S \tag{15.2}$$

15.1. **Depthwise unit stretch.** The generalised Hooke's law is given from article III,3.1 as

$$\left.\begin{aligned} e_{\mathrm{i}} &= \psi(S_{\mathrm{i}}-qS_{\mathrm{j}}) = \psi[S+2(1+q)T^2/S] \\ e_{\mathrm{j}} &= \psi(S_{\mathrm{j}}-qS_{\mathrm{i}}) = \psi[-qS-2(1+q)T^2/S] \end{aligned}\right\} \quad (15.3)$$

The scalar straining-displacement, noting III(14.1), is

$$C = e_{\mathrm{i}}H/\sin\Omega = \psi H[S+2(1+q)T^2/S] \quad (15.4)$$

Substitution in III(15.1) and neglecting terms of order T^3 and smaller gives the depthwise unit stretch as†

$$a_y = \psi S[1+(T/S)^2(\psi S+1+2q)] \quad (15.5)$$

If, in particular, shear stress T is zero, or else if T^2 is negligible then

$$a_y = e_{\mathrm{i}} = \psi S \quad (15.6)$$

the depthwise strain due to the normal stress only.

15.2. **Depthwise normal strain.** The depthwise normal strain is found from the strain dyadic

$$\mathfrak{M} = e_{\mathrm{i}}\mathbf{x}_{\mathrm{i}}\mathbf{x}_{\mathrm{i}}+e_{\mathrm{j}}\mathbf{x}_{\mathrm{j}}\mathbf{x}_{\mathrm{j}} \quad (15.7)$$

as

$$e_{yy} = \mathbf{c}_y\mathbf{c}_y:\mathfrak{M} \quad (15.8)$$

But $\mathbf{c}_y\cdot\mathbf{x}_{\mathrm{i}} = 1$, while $\mathbf{c}_y\cdot\mathbf{x}_{\mathrm{j}} = \rho = T/S$, the small angle of article III,14, so that

$$e_{yy} = e_{\mathrm{i}}+(T/S)^2e_{\mathrm{j}} \quad (15.9)$$

Substituting III(15.3) and neglecting $(T/S)^4$ gives

$$e_{yy} = \psi S[1+(T/S)^2(2+q)] \quad (15.10)$$

Comparison with III(15.5) gives

$$\frac{a_y}{e_{yy}} = \frac{1+(T/S)^2(\psi S+1+2q)}{1+(T/S)^2(2+q)} \quad (15.11)$$

as the ratio of depthwise unit stretch to normal strain.

15.3. **Poynting effect.** Poynting[30], in 1909, extended circular rods of metal and rubber by axial tensile load that was then held constant during the application of an axial torque which induced increased change in length. While the torque is small this is rather similar to the case just discussed. Poynting found

† Author, 1950.

the unit axial stretch proportional to the square of the superimposed shear stress T, similar to the theoretical result in equation III(15.5). However, Poynting and subsequent recent writers (R. S. Rivlin [14] and M. Reiner [52], for example) have regarded the axial change of length in the cylinder (or depthwise as in the strip here) as a 'normal strain', whereas the present author treats it as a 'stretch'. 'Normal strain' is a component of the strain dyadic (or second-order tensor) as in III(15.10), calculated by invariant transformation from the unit stretches in the principal directions. M. Reiner [52], in fact, introduces a 'coefficient of cross-elasticity' as a modulus to account for this Poynting 'strain'. A survey and comparison by C. Truesdell [31], in 1952, gives the general theories proposed by the various writers. Truesdell does not remark on any distinction between normal strain and unit stretch as here.

Usually $\psi S < 1$, so that, when S becomes negative for axial compression, the additional axial unit stretch should be a compression according to III(15.5), but there is no experimental evidence at present (March 1954).

Chapter IV

HOMOGENEOUS, CURVILINEAR TWO-STRESS

1. Equilibrium stress equation

The analysis of two-stress, up to the present, has not considered the equilibrium stress equation ensuring that, if the stresses vary from point to point of the body, then each element is in equilibrium under the forces acting upon it from the surrounding, contiguous, deformed substance. Volume I, article **II**,6.2 shows that, for equilibrium,

$$\operatorname{div} \mathfrak{S} + m\mathbf{B} = 0 \tag{1.1}$$

The left-hand side of this equation is a null vector having three zero components, in general. Here, the stress dyadic $\mathfrak{S}$ is a two-stress, so that the vector stress involving one of the coordinates is put equal to zero and this gives only two zero components of the null vector. Article **A**,11 gives the divergence of a self-conjugate dyadic for curvilinear coordinates and article **VIII**,3 gives its application to the three-stress dyadic. For brevity here, accept these equations and put zero all stress components involving one coordinate subscript. Further, suppose body force is zero.

1.1. **Cartesian coordinates.** Putting $\mathbf{S}_z = 0$ gives

$$S_{xx;x} + S_{yx;y} = 0 \qquad S_{yy;y} + S_{xy;x} = 0 \tag{1.2}$$

All the plane stresses considered in chapters II, III were independent of position, so that they satisfy these equilibrium, scalar, stress equations identically.

1.2. **Cylindrical coordinates.** For cylindrical coordinates (R_r, θ, R_z) put vector stress $\mathbf{S}_r = 0$ to give a curvilinearly plane two-stress in the cylindrical surfaces having OR_z as their common axis. The three equations of article **VIII**,3 then reduce to

$$S_{\theta\theta} = 0 \tag{1.3}$$

$$S_{\theta z;z} = 0 \tag{1.4}$$

$$R_r S_{zz;z} + S_{\theta z;\theta} = 0 \tag{1.5}$$

The circumferential normal stress $S_{\theta\theta}$ is zero, while shear stress $S_{\theta z}$ is independent of R_z. Therefore, if $S_{\theta z}$ is also independent of θ, then, also, S_{zz} is independent of R_z.

Therefore, if $\mathbf{S}_r = 0 = S_{\theta\theta}$, while $S_{\theta z}$, S_{zz} have constant values at all positions in a cylindrical surface of given radius R_r, then $S_{\theta z}$, S_{zz} constitute a curvilinearly homogeneous plane two-stress system that may be a function of radius R_r without violating the equilibrium stress equations restrictions.

2. Axial torsion of an elastic, thin-walled, circular tube: approximate theoretical analysis†

Shear stress $S_{\theta z} \equiv T$ is the only non-zero stress acting in the wall of a circular cylinder of radius R_r and, further, it is independent of R_z. Article **IV**,1.2 shows that the equilibrium stress equations are satisfied under these conditions. If R is the mean radius of a thin-walled deformed tube of thickness t, then the applied axial torque

$$Q = 2\pi R^2 t T \tag{2.1}$$

The stress state is now curvilinearly plane and homogeneous, so the results of article **III**,8 analysing a *plane*, homogeneous, simple shear stress are now applied here. The unit stretches a_x, a_y there are a_θ, a_z here, while normal strains e_{xx}, e_{yy} there are $e_{\theta\theta}$, e_{zz} here. Thus, the cylinder increases in length and decreases in diameter.

2.1. **Strain transfer, circumferential and axial stretches for a substance of restricted isotropy and constant stress-strain parameters.** The results of article **III**,9.1 can be applied to give the angle of strain transfer from

$$\tan \Phi = f = (1+q)\psi T \tag{2.2}$$

while the unit stretches are

$$a_\theta = 1-\sqrt{(1+f^2)} \qquad a_z = 1-(1-f^2)\cos\Phi \tag{2.3}$$

2.2. **Relative rotation of radius vectors normal to the axis.** The radius vectors OA, OB in Fig. **IV**,2.1 coincide initially as OA^o, OB^o. In the deformed cylinder OA, OB are unit distance apart in the direction of OR_z. Angle θ is now the *angle of twist* per unit length of the cylinder.

† Author, 1950.

The present curvilinear analysis merely takes the results of the plane analysis in article III,8 'wrapped' on to the cylinder. Therefore, from this viewpoint, the arc

$$R\theta = \mathbf{c}_\theta \cdot \{\mathfrak{J} - \mathfrak{Q} \cdot [\mathfrak{J} - f(\mathbf{x}_i\mathbf{x}_i - \mathbf{x}_j\mathbf{x}_j)]\} \cdot \mathbf{c}_z$$

using III(8.22) with $H = 1$ and

$$C = D = f\sqrt{2}$$

$$\mathbf{x}_i\sqrt{2} = \mathbf{c}_\theta + \mathbf{c}_z \qquad \mathbf{x}_j\sqrt{2} = -\mathbf{c}_\theta + \mathbf{c}_z$$

$$\mathfrak{Q} = \mathbf{c}_r\mathbf{c}_r + (\mathbf{c}_\theta\mathbf{c}_\theta + \mathbf{c}_z\mathbf{c}_z)\cos\Phi + (\mathbf{c}_z\mathbf{c}_\theta - \mathbf{c}_\theta\mathbf{c}_z)\sin\Phi$$

$$\mathfrak{J} = \mathbf{c}_r\mathbf{c}_r + \mathbf{c}_\theta\mathbf{c}_\theta + \mathbf{c}_z\mathbf{c}_z$$

Using IV(2.2) gives the angle of twist per unit length of the cylinder as

$$\theta = 2(f/R)\cos\Phi \tag{2.4}$$

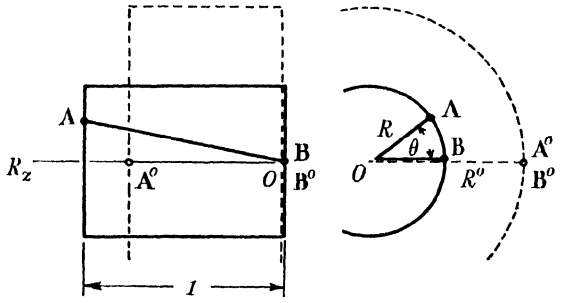

FIG. IV.2.1. The relative rotation through angle θ of two radius vectors unit distance apart axially in the *deformed*, circular, thin-walled, elastic tube due to axial torsion inducing curvilinearly plane, homogeneous shear stress. The dotted outline represents the undeformed tube of greater diameter and lesser length than the deformed tube.

2.3. **Initial radius and length.** From IV(2.3), since

$$a_\theta = 1 - R^o/R$$

then

$$R^o = R(1-a_\theta) = R(1+f^2)^{\frac{1}{2}} \tag{2.5}$$

Also,

$$a_z = 1 - H^o/H$$

so that, for $H = 1$, the corresponding undeformed length of cylinder is

$$H^o = (1-f^2)\cos\Phi \tag{2.6}$$

3. Axial torsion of an elasto-plastic, thin-walled, circular tube: approximate theoretical analysis

Article **IV**,2 adapts the analysis of plane, elastic, simple shear in article **III**,8 to the curvilinearly plane, simple shear in a thin-walled tube due to axial torsion. Similarly, the analysis of plane, elasto-plastic, simple shear in articles **III**,10 to **III**,12 can be adapted to a thin-walled, elasto-plastic tube under axial torsion.

The increase in length and decrease in diameter of brass and steel tubes, for example, has been found experimentally by H. W. Swift [53], in 1947, and explained theoretically as due to anisotropic stress-strain effects. However, such effects can be rationalised on geometrical lines as in articles **III**,10, **III**,11 for isotropic stress-strain relations, although, of course, anisotropy may be a contributory factor. Unfortunately, Swift's measurements were insufficient to attempt to assess separately the importance of the effects of geometry and anisotropy. The published results are curves not allowing satisfactory re-examination.

Swift's measurements on a solid lead cylinder showed a decrease in length but the change in diameter is not recorded. The analysis of article **III**,12 indicates the possibility of length decrease due to anisotropic stress-strain relations.

4. Axial torsion of elasto-plastic, circular metal tubes and rods: tests by H. W. Swift [53]

H. W. Swift tested 70/30 brass, stainless steel, aluminium, cupro-nickel, copper, mild steel, 0·5 per cent carbon steel and lead circular cylinders under axial torsion into the post-yield range of deformation. Because an assumption had to be made on the radial distribution of stress in a solid bar Swift tested fairly thin-walled tubes. Structural instability of the thin walls necessitated partial support by a solid core having a few thousandths of an inch clearance from the inside surface of the tube. A dial-gauge extensometer measured the changes in length, while a protractor and pointer gave the relative rotation between the planes at a distance apart equal to the gauge length of the extensometer. The effects of reversing the direction of torsion and also of annealing subsequent to yield were examined.

Table **IV**,4.1 gives 26 of the 66 measurements made on a 70/30 brass and kindly communicated privately to the writer by

Professor Swift in July 1948. Fig. IV,4.1 gives a few of the curves for reversed torsion of 70/30 brass from a greater number in figure 11 of Swift's paper. Fig. IV,4.2 gives the contraction of a solid lead cylinder as in figure 16 of Swift's paper.

Swift offers a speculative, qualitatively statistical theory of slip-

TABLE IV,4.1

Reversed torsion test on a 70/30 hard brass specimen machined from 1-inch square bar. Outside diameter 0·750 inch, inside diameter 0·531 inch, gauge length for both torsion and length change 2·8 inches. Speed of twisting $\frac{1}{4}$ r.p.m. Tests by H. W. Swift [53].

Twist (180 = $1\frac{1}{2}$ revs.)	Torque, lb-inch	Extension, thousandths of an inch
0	0	0
20	730	$\frac{1}{2}$
40	870	$1\frac{1}{2}$
60	980	3
80	1 100	4
120	1 290	$5\frac{1}{2}$
180	1 550	14
240	1 770	$23\frac{1}{2}$
300	1 960	37
360	2 100	53
420	2 210	$68\frac{1}{2}$
480	2 300	85
540	2 360	$101\frac{1}{2}$
Reversed Twist		
520	1 750	$100\frac{1}{2}$
480	2 075	92
440	2 200	84
400	2 350	78
340	2 480	$73\frac{1}{2}$
260	2 650	$68\frac{1}{2}$
180	2 820	$69\frac{1}{2}$
100	2 960	$77\frac{1}{2}$
20	3 050	91
−60	3 100	$108\frac{1}{2}$
−140	3 120	123
− 200	3 090	$133\frac{1}{2}$
−220	Broke	—

planes in each crystal of a randomly orientated aggregate to give anisotropic stress-strain relations to account for length change in the cylinder. The qualitative character of the curves in Fig. IV,4.1 should be compared with the present author's theoretical curves in Fig. III,11.3 for severe, reversed torsion deformation.

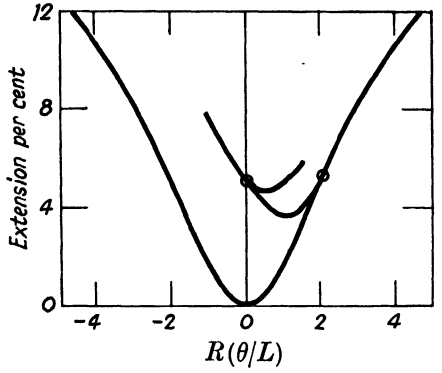

FIG. IV,4.1.—Axial extension of a 70/30 brass thin-walled tube under axial torsion. The initial outside diameter of the tube is $2R$, the initial axial distance apart of two planes is L, while θ is the relative angular rotation about the tube axis of radius vectors in the two planes. Reversal and re-reversal of applied torque are shown. Compare this qualitatively with Fig. III,11.3.

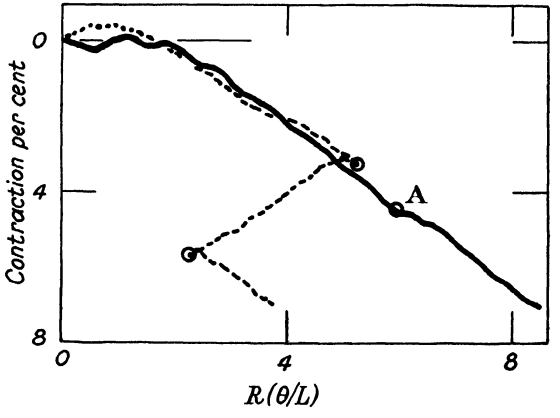

FIG. IV,4.2.— Axial contraction due to axial torsion of a solid lead cylinder. At A the specimen was removed from the test machine, turned truly cylindrical after 'wringing' from true, rested for a day and then retested. Dotted curve shows a second test with reversal and re-reversal of torque.

5. Axial torsion and tension on an elastic, thin-walled, circular tube: approximate theoretical analysis

Article IV,1.2 shows that the three, scalar, equilibrium stress equations for cylindrical coordinates are satisfied if $\mathbf{S}_r = 0 = S_{\theta\theta}$, $S_{\theta z} \neq S_{\theta z}(\theta, R_z)$, $S_{zz} \neq S_{zz}(R_z)$. Such a curvilinearly plane two-stress is rather like the plane two-stress of articles III,13 to III,15 analysing transverse normal stress and shear stress on an elastic strip. The plane strip is now 'wrapped' on to the cylinder and the analytical results applied to a thin-walled tube under axial torsion and tension.

The results of articles III,13 to III,15 are applied here but with directions $\mathbf{c}_x$, $\mathbf{c}_y$, $\mathbf{c}_z$ there becoming $\mathbf{c}_\theta$, $\mathbf{c}_z$, $\mathbf{c}_r$ here. Note that this intuitive idea is behind the use of thin-walled tubes as convenient specimens in which the separate components of the complex stress system are fairly easily controlled and most of the strains observed easily.

6. Octahedral stresses and strains

It is shown in volume I that any complex stress system at a given point can be reduced to three principal normal stresses. In the present case, the complex stress system is assumed to be two-dimensional, so that the stresses can always be reduced to two principal normal stresses $S_\mathbf{i}$, $S_\mathbf{j}$ on planes normal to the plane of the stress system, while component $S_\mathbf{k}$ mutually orthogonal to these two is zero. Volume I, article II,12 discusses the 'octahedral stress' acting on the eight octahedral planes normal to the eight octahedral directions of which each has equal angles to the principal normal stress directions.

6.1. **Octahedral normal and shear stresses.** The octahedral stress is resolved to an octahedral normal stress normal to each octahedral plane and has the same arithmetical value on each. In terms of the principal normal stresses the octahedral normal stress is

$$\sigma = \tfrac{1}{3}(S_\mathbf{i} + S_\mathbf{j}) \tag{6.1}$$

for the present two-stress system. The sum of the normal stresses is also the first stress invariant, as discussed in volume I, article II,3. The octahedral stress is resolved to the octahedral

shear stress τ tangential to the octahedral plane. Stated for principal normal stresses for a two-stress system it is

$$9\tau^2 = 2(S_i^2 - S_iS_j + S_j^2) \tag{6.2}$$

6.2. **Equivalent normal stress.** Consideration of the strain energy for an elastic substance of restricted isotropy in volume I, article **VIII**,2 gives a relationship between the octahedral shear stress τ and an equivalent normal stress S, say. Thus,

$$9\tau^2 = 2S^2 \tag{6.3}$$

It is important to notice that this relationship is independent of stress-strain parameters only in the case of restricted isotropy.

6.3. **Octahedral normal and shear strains.** Volume I, article **III**,10 discusses the differential relative-displacement between the ends of the unit vector in the octahedral direction as being of the nature of a strain. The component of this vector 'strain' normal to the octahedral plane is the octahedral normal strain and for principal normal directions is

$$\nu = \tfrac{1}{3}(e_i + e_j + e_k) \tag{6.4}$$

of the same form as **IV**(6.1) for stresses. The sum of the three normal strains is the first strain invariant, as discussed in volume I, article **III**,6.

The component of the relative-displacement tangential to the octahedral plane is the octahedral shear strain γ and is given in volume I, article **III**,10 as

$$9\gamma^2 = (e_i - e_j)^2 + (e_j - e_k)^2 + (e_k - e_i)^2 \tag{6.5}$$

6.4. **Equivalent normal strain.** Comparison of **IV**(6.2), **IV**(6.3), **IV**(6.5) suggests defining an equivalent normal strain e, say, so that

$$9\gamma^2 = 2(1+q)^2e^2 \tag{6.6}$$

with an isotropic transverse contraction ratio q. This form is chosen so that, in the case of simple tension, for example, both the equivalent normal stress and strain equal simple tensile stress and strain.

6.5. **Octahedral curve.** The plane curve of octahedral shear stress vs. octahedral shear strain is termed the octahedral curve and has been found of considerable value in correlating the results

of complex stressing of yielded metals in particular [46]. The next article and those subsequent discuss this aspect further.

7. Octahedral-parametric surface

Many experiments on various metals, in particular, have shown remarkable correlation† when the values of octahedral shear

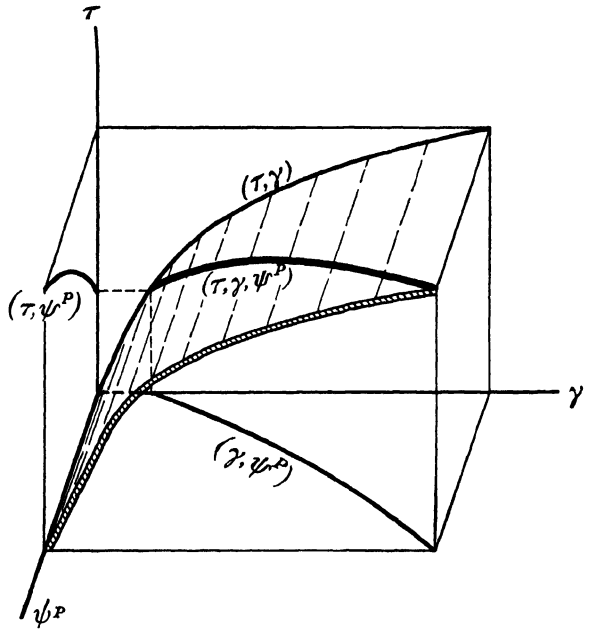

FIG. IV,7.1.—The *octahedral-parametric surface* is shown as cylindrical and normal to the octahedral shear stress, octahedral shear strain plane. The projection of the octahedral-parametric surface gives the octahedral curve (τ, γ) and the other two projections are the (τ, ψ^P) and (γ, ψ^P) plane curves respectively. The values of τ, γ, ψ^P during an experiment trace a trajectory on the octahedral-parametric surface.

stress τ and the corresponding octahedral shear strain γ are plotted as a plane octahedral curve (τ, γ) with

$$\left.\begin{aligned} 9\tau^2 &= 2(S_i^2 - S_i S_j + S_j^2) \\ 9\gamma^2 &= (e_i - e_j)^2 + (e_j - e_k)^2 + (e_k - e_i)^2 \end{aligned}\right\} \quad (7.1)$$

from article IV,6. However, these two quantities are independent of the isotropic stress-strain parameters relating the stress and strain components from which they are calculated.

† Much of this development is due to A. Nadai [55].

Volume I, article IX,9 suggests that this means that the octahedral curve (τ, γ) should be regarded as the projection of the octahedral-parametric surface on which the points have the coordinates (τ, γ, ψ^P), with the plastic modulus ψ^P regarded as the most important of the plastic stress-strain parameters. The correlation of tests on the plane octahedral curve means that this surface is a portion of a right cylindrical surface with generators normal to the octahedral curve as in Fig. IV,7.1. Similarly, a curve (τ, γ, q^P) can be plotted on the octahedral-parametric surface to relate the plastic transverse contraction ratio with the octahedral shear stress and strain.

7.1. **Restricted isotropy is assumed.** In the present article the analysis is regarded as performed with isotropic stress-strain parameters. This is, of course, an assumption that needs to be justified. Therefore, when examining test measurements in the next few articles the amount of departure of the plastic modulus from isotropy will be examined. Unfortunately, the measurements available do not give sufficient data to enable the examination of isotropy of the other stress-strain parameters. Therefore, it will be assumed that Young's elastic modulus $E = (\psi^E)^{-1}$, Poisson's elastic transverse contraction ratio q^E and the plastic transverse contraction ratio q^P are all isotropic.

7.2. **Increment stress and strain with anisotropic plastic moduli.** With these restrictions the incremental elasto-plastic stress-strain relations for a two-stress are

$$\left.\begin{aligned} \delta e_i &= \psi^E(\delta S_i - q^E \delta S_j) + \psi_i^P \delta S_i - q^P \psi_j^P \delta S_j \\ \delta e_j &= \psi^E(\delta S_j - q^E \delta S_i) + \psi_j^P \delta S_j - q^P \psi_i^P \delta S_i \end{aligned}\right\} \quad (7.2)$$

Then, with measured quantities δe_i, δe_j, δS_i, δS_j, ψ^E, q^E, q^P, these two equations are solved for the two unknowns ψ_i^P, ψ_j^P that should be approximately equal to justify the assumption of restricted isotropy.

7.3. **Octahedral shear increment stress and strain.** Volume I, article IX,9 shows that incremental forms similar to equations IV(7.1) are, with $\delta\tau^2 \equiv (\delta\tau)^2$, ..., for brevity,

$$\left.\begin{aligned} 9\delta\tau^2 &= 2(\delta S_i^2 - \delta S_i \delta S_j + \delta S_j^2) \\ 9\delta\gamma^2 &= (\delta e_i - \delta e_j)^2 + (\delta e_j - \delta e_k)^2 + (\delta e_k - \delta e_i)^2 \end{aligned}\right\} \quad (7.3)$$

8. Axial and circumferential tension on thin-walled tubes of copper and steel: tests by E. A. Davis

Tests on thin-walled tubes of copper and steel were made by E. A. Davis [54]. Internal pressure in the tubes induced circumferential tension that was regarded as constant throughout the thickness of the thin wall. Applied axial tension together with the circumferential tension induced by internal pressure was then regarded as a curvilinear *two-stress* system. Thus, it was assumed that the radial stress in the tube wall had a negligible effect on the stress-strain relations.

8.1. Mode of calculating the circumferential normal stress. The circumferential normal stress is calculated in the same way as the well-known 'hoop' stress in engineering pressure vessels. Thus, with inner radius a, internal pressure S_a and the thin cylindrical wall of thickness h, then the circumferential stress

$$S_{\theta\theta} = (a/h)S_a \tag{8.1}$$

Thus, when a is large compared with h, then S_a is small compared with $S_{\theta\theta}$. The correct distributions of $S_{\theta\theta}$ and S_{rr} are given in article **VII**,1.

8.2. Experimental results. The tubes suffered fairly large elasto-plastic strains, as recorded in Tables **IV**,8.1, **IV**,8.2 for copper and steel respectively. The arithmetical values were communicated privately to the present author by Dr. Davis. For brevity here, the number of readings for each test has been reduced from about fifteen to about ten. The readings left out fell on a smooth curve passing through the readings in the tables.

The stresses are *true*, while the strains are *nominal*. The results were supplied in this form by Dr. Davis and are given without change for analysis by others if desired.

9. Interpretation of the tests by Davis [54] on copper and steel tubes

Several experimenters [54, 56, 57] have shown that octahedral shear stress vs. octahedral shear strain for a wide range of values and combinations of stress components gives practically a single octahedral curve. The test data of article **IV**,8 have, therefore,

TABLE IV,8.1

Axial and circumferential stress and strain in thin-walled *copper* tubes under internal pressure and axial tension. The stresses are 'true' and strains are 'nominal'. The measurements are by E. A. Davis [54].

S_{zz} psi	e_{zz}	$S_{\theta\theta}$ psi	$e_{\theta\theta}$	Pressure psi
0	0	0	0	0
2 400	0	0	0	0
4 830	0·0050		−0·0015	
7 330	0·0125		−0·0049	
12 390	0·0312		−0·0157	
17 950	0·0612	0	−0·0277	0
23 950	0·1037		−0·0483	
31 450	0·1823		−0·0788	
36 700	0·2662		−0·1112	
41 300	0·3637		−0·1453	
43 000	0·4737	0	−0·1800	0
0	0	0	0	0
3 070	0	1 530	0	245
6 180	0·0050	3 080	0	490
9 330	0·0137	4 650	0	735
12 600	0·0250	6 310	0	980
15 960	0·0362	7 980	0	1 225
19 400	0·0549	9 670	0	1 470
23 360	0·0748	11 650	0	1 715
27 300	0·1047	13 650	0	1 960
31 780	0·1460	15 900	0	2 205
36 400	0·2045	18 260	0	2 390
39 770	0·2790	20 000	0	2 450
0	0	0	0	0
4 560	0·0037	4 600	0·0030	700
6 725	0·0037	6 950	0·0074	1 050
9 300	0·0075	9 430	0·0126	1 405
11 680	0·0099	11 900	0·0178	1 755
14 280	0·0174	14 680	0·0259	2 110
16 880	0·0211	17 550	0·0340	2 460
19 670	0·0298	20 700	0·0466	2 810
22 850	0·0435	24 400	0·0622	3 160
26 770	0·0622	29 300	0·0903	3 515

TABLE IV,8.2

Axial and circumferential stress and strain in thin-walled *steel* tubes under internal pressure and axial tension. The stresses are 'true' and strains are 'nominal'. The measurements are by E. A. Davis [54].

S_{zz} psi	e_{zz}	$S_{\theta\theta}$ psi	$e_{\theta\theta}$	Pressure psi
0	0	0	0	0
33 400	0·0075	0	−0·0048	0
38 200	0·0149		−0·0078	
41 000	0·0199		−0·0096	
46 400	0·0298		−0·0140	
51 900	0·0435	0	0·0204	0
57 800	0·0647		−0·0310	
63 800	0·1008		−0·0459	
69 300	0·1490		−0·0667	
76 300	0·2560		−0·1048	
79 200	0·3280	0	−0·1238	0
0	0	0	0	0
37 870	0·0112	18 730	0	3 000
43 480	0·0175	21 800	0·0070	3 440
50 020	0·0275	25 050	0·0010	3 920
64 500	0·0662	32 500	0·0022	4 850
71 030	0·1025	35 800	0·0037	5 150
75 180	0·1350	38 000	0·0045	5 280
81 900	0·2100	41 400	0·0060	5 350
86 770	0·2850	44 300	0·0081	5 310
87 400	0·3300	44 900	0·0096	5 220
0	0	0	0	0
30 950	0·0025	30 900	0·0050	4 900
35 750	0·0087	36 100	0·0090	5 620
40 600	0·0125	41 300	0·0140	6 320
45 800	0·0175	46 600	0·0210	7 020
51 450	0·0287	53 250	0·0350	7 725
56 200	0·0424	60 500	0·0550	8 250
58 000	0·0474	61 800	0·0640	8 250
61 400	0·0600	66 700	0·0850	8 430

been plotted in this form in Figs. IV,9.1, IV,9.2 for copper and steel respectively. The values in the abridged Tables IV,8.1, IV,8.2 were used to calculate the octahedral values.

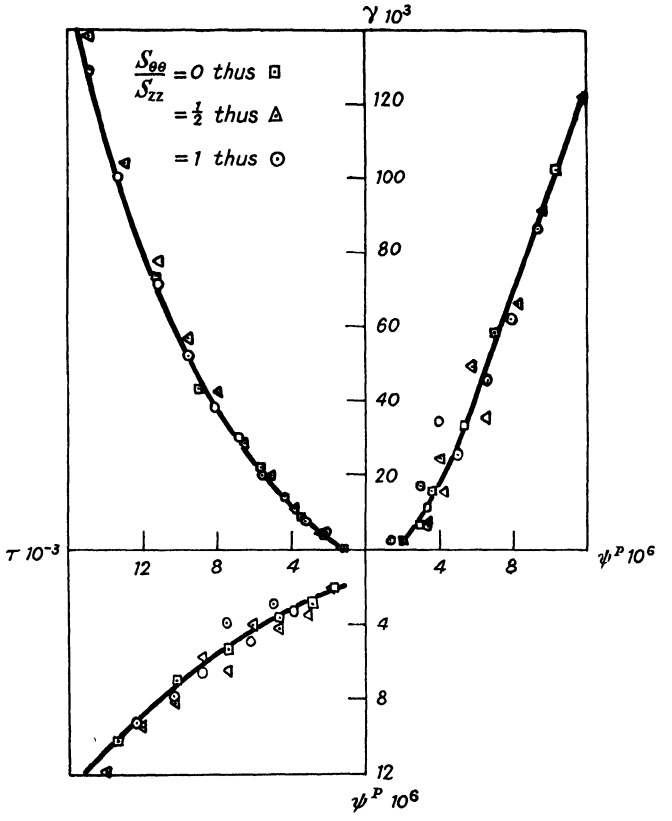

FIG. IV,9.1.—Octahedral-parametric curves for *copper* tubes under internal pressure and axial tension. The curve drawn is for simple tension. The scales numbers are for octahedral shear stress psi divided by 10^3, octahedral shear strain multiplied by 10^3, plastic modulus multiplied by 10^6. The calculated values occur around the mean curve for the three loadings in each of which the stresses remain in approximately the same ratio.

9.1. **Octahedral shear strain and stress.** With cylindrical coordinates for the present case, the octahedral shear strain γ is given in article IV,6 as

$$9\gamma^2 = (e_{\theta\theta}-e_{zz})^2+(e_{zz}-e_{rr})^2+(e_{rr}-e_{\theta\theta})^2 \qquad (9.1)$$

Measurements of radial normal strain e_{rr} are not available, so some assumption must be made. The simplest relationship between these three strains follows from supposing that the strains are sufficiently small to take dilation as their algebraic mean and then to suppose that dilation is zero. This gives

$$e_{rr} = -e_{\theta\theta} - e_{zz} \tag{9.2}$$

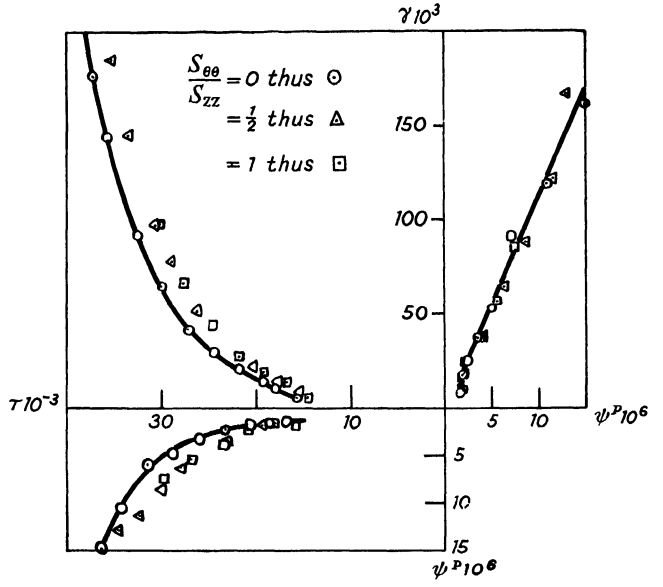

FIG. IV,9.2.—Octahedral-parametric curves for *steel* tubes under internal pressure and axial tension. The curve drawn is for simple tension. The scales numbers are for octahedral shear stress psi divided by 10^3, octahedral shear strain multiplied by 10^3, plastic modulus multiplied by 10^6. The calculated values for the three approximately constant ratios of stress tend to lie on separate curves on the octahedral stress-strain curve and on the stress-parameter plane. This indicates that all three tests do not lie on the same octahedral-parametric surface.

Note that these assumptions also imply the neglect of radial strain due to the radial stress that must accompany the pressure internal to the tube. Substituting IV(9.2) in IV(9.1) gives

$$3\gamma^2 = 2(e_{\theta\theta}^2 + e_{\theta\theta}e_{zz} + e_{zz}^2) \tag{9.3}$$

Article IV,6 gives the octahedral shear stress τ from

$$9\tau^2 = 2(S_{\theta\theta}^2 - S_{\theta\theta}S_{zz} + S_{zz}^2) \tag{9.4}$$

9.2. **Elastic increment strains.** Article IV,7.2 gives the elastic and plastic increments of the increment strains. Thus, the elastic components are

$$\delta e^E_{\theta\theta} = \delta\epsilon^E_{\theta\theta} - q^E\delta\epsilon^E_{zz} \qquad \delta e^E_{zz} = \delta\epsilon^E_{zz} - q^E\delta\epsilon^E_{\theta\theta} \tag{9.5}$$

with the increment partial-strains

$$\delta\epsilon^E_{\theta\theta} = \psi^E_{\theta\theta}\delta S_{00} \qquad \delta\epsilon^E_{zz} = \psi^E_{zz}\delta S_{zz}$$

Young's modulus was not measured in the tests, so it was supposed to be isotropic and of the typical values 30 10^6 psi for the steel. Poisson's elastic transverse contraction ratio was assumed of typical value 0·35 in both tests.

9.3. **Plastic increment strains.** The elastic increment strain components were calculated and subtracted from the elasto-plastic increment strains to give the plastic increment strain components

$$\delta e^P_{\theta\theta} = \delta\epsilon^P_{\theta\theta} - q^P\delta\epsilon^P_{zz} \qquad \delta e^P_{zz} = \delta\epsilon^P_{zz} - q^P\delta\epsilon^P_{\theta\theta} \tag{9.6}$$

with

$$\delta\epsilon^P_{\theta\theta} = \psi^P_{\theta\theta}\delta S_{00} \qquad \delta\epsilon^P_{zz} = \psi^P_{zz}\delta S_{zz}$$

The plastic transverse contraction ratio q^P was assumed of value $\frac{1}{2}$ corresponding to zero volume change in the increment of deformation.

9.4. **Plastic moduli.** The two equations IV(9.6) were solved for the two plastic moduli $\psi^P_{\theta\theta}$, ψ^P_{zz}. If the metals are behaving with restricted isotropy then these two moduli are equal. With the assumptions stated they were found to be mostly less than 5 per cent different one from the other. This was considered to be satisfactory, so the mean value was taken and plotted in the octahedral-parametric Figs. IV,9.1, IV,9.2 for copper and steel respectively.

The curves drawn in Figs. IV,9.1, IV,9.2 pass through the values for simple tension. The octahedral shear stress-strain values group fairly closely around the curve for copper but show fairly definite separation for steel. The simple tensile strain, modulus curve is practically the mean curve of the strain, modulus values for all three results from both copper and steel. The stress, modulus values group closely along the simple tensile curve for copper but exhibit definite separation for steel. S. J. Fraenkel[57] also tested thin-walled steel tubes under internal

pressure and axial tension. Analysis of his measurements in the same manner as the present author has done for Davis's tests showed separation of the stress, modulus curves as already noted.

9.5. **Tangent modulus values susceptible to small instability in the yielding.** The tangent modulus is sensitive to sudden changes of stress and strain values. Such little 'runs' or 'jerks' occur while testing metals beyond the primary yield

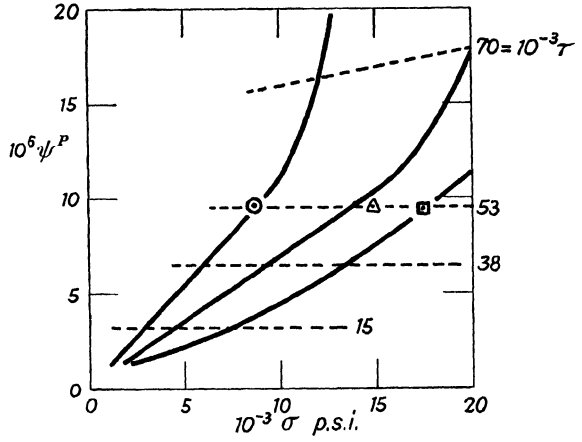

FIG. IV,9.3.—Copper tubes under axial and circumferential tension in the Davis tests. Each dotted curve shows the plastic modulus as a function of octahedral normal stress for a constant value of octahedral shear stress. The three points marked are for $10^{-3}\tau = 53$, 53, 54 respectively and the curve $10^{-3}\tau = 53$ was interpolated by eye. The other dotted curves were found similarly. Plastic modulus ψ^P is independent of octahedral normal stress σ except at the large strains for this copper, at least.

because of the rather unstable processes of 'glide' and rearrangement of crystals in the specimen. Since general laws of behaviour are sought it would be reasonable to employ some arithmetical smoothing technique for the measurements of stress and strain before analysis into octahedral-parametric values. The present author did not smooth the values but simply took differences of the stress and strain values supplied by the experimenters and this doubtless accounts for the scatter of values in the figures.

9.6. **Plastic modulus as a function of octahedral normal stress.** P. W. Bridgman, in 1912 [58], found that metals did not suffer plastic strains under great hydrostatic pressures. This can

be interpreted to mean, phenomenologically, that the plastic modulus is zero when the three principal normal stresses are compressive or negative with the sign convention of this treatise. Volume I, article IX,7 discusses this and fits the effect into the functional relationship of the plastic modulus in the stress-space at a given point of the loaded metal.

Continuity of the plastic modulus in stress-space, in relation to other experiments, suggests that the plastic modulus should

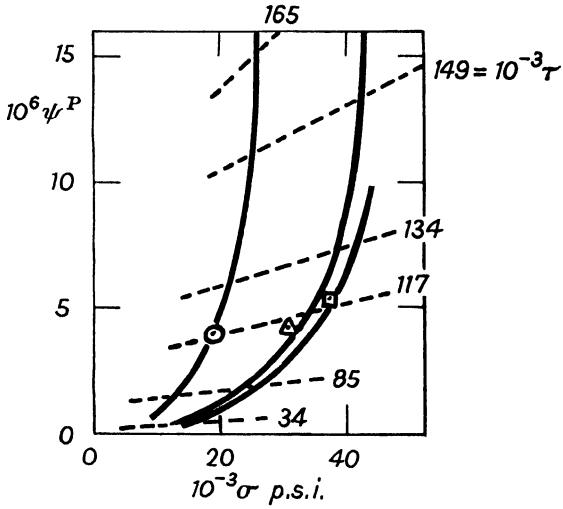

FIG. IV,9.4.– Steel tubes under axial and circumferential tension in the Davis tests. Each dotted curve shows plastic modulus as a function of octahedral normal stress for a constant value of octahedral shear stress. The three points marked are for $10^{-3}\tau = 119$, 112, 118 respectively and the curve $10^{-3}\tau = 117$ was interpolated by eye. The other dotted curves were found similarly. Plastic modulus ψ^P is a function of octahedral normal stress and increases with it for this steel, at least.

increase with the octahedral normal stress for a given value of octahedral shear stress on duralumin. The present author has no data on this metal (March 1954), but the analysis for the copper of Table IV,8.1 is given in Fig, IV,9.3 while that for the steel in Fig. IV,9.4 was done for Table IV,8.2 and is significant. The plastic modulus is seen to increase quite definitely with increase in octahedral normal stress for a given value of octahedral shear stress [48, 59]. The conclusion is presented tentatively subject to further examination at some future time when tests covering a

greater range of values and signs in the stress-space are available. A maximum of three readings define each of the dotted curves and this is insufficient.

The analysis of Table IV,8.1 for copper indicates slight change in the plastic modulus with increase of octahedral normal stress for a given value of octahedral shear stress under the tension-tension two-stress loading as here. Clearly, further tests are required to cover more of stress-space, particularly in the compression-tension zone.

10. Steel, thin-walled, circular tubes strained elasto-plastically by axial torsion and tension: experiments by J. L. M. Morrison & W. M. Shepherd [60]

In the period 1946 to 1950 there was considerable controversy between the researchers on 'plastic' straining of metals in particular. The crux of the argument lay in whether 'plastic' strains should be analysed (i.e. related to stress) as 'total' or 'incremental' values. The literature of that period is voluminous but mainly deals with theoretical or mathematical considerations, as, for example, in W. Prager's paper [62] of 1948. It became clear that a decision could not be reached by theoretical discussion only.

Almost simultaneously, searching experiments on the issues were undertaken independently by R. W. Peters, N. F. Dow & S. B. Batdorf [61] in the United States of America and by J. L. M. Morrison & W. M. Shepherd [60] in Britain. The crucial test conceived by these two groups was to rotate the complex stress system relative to the substance. Both groups used thin-walled tubes under axial torsion and endwise normal loading.

10.1. **Specimen.** J. L. M. Morrison & W. M. Shepherd [60] tested thin-walled steel tubes under combined axial torsion and tension. They were interested in the effect of loading path on the elasto-plastic stress-strain relations when the stress system 'transferred' on the deformed steel. Therefore, to avoid irrelevant complication they selected a 5 per cent nickel steel (Brit. Stand. S.90), as this has a smooth transition from primary elastic to elasto-plastic simple tensile straining. Sudden yielding such as that for the mild steel in article I,6 would have confused the investigation. Two thin-walled tubular specimens together with specimens for tests under simple tension and pure torque were

machined from adjacent lengths of a 2-inch diameter bar. The tubes were bored to 1·000 inches inside diameter and had an outside diameter of 1·040 inches ground finish.

TABLE IV,10.1

Steel, thin-walled tubes under axial torsion and tension. Tests by J. L. M. Morrison & W. M. Shepherd[60]. Stresses are 'nominal' tons per square inch (tsi). Strains are 'nominal'.

Load stage	S_{zz} tsi	e_{zz} 10^3	$S_{\theta z}$ tsi	$2e_{\theta z}$ 10^3
1	0	0	0	0
	1·748	0·132	0	0·007
	3·495	0·264	0	0·015
	5·243	0·396	0·015	0·022
2	5·155	0·391	1·416	0·294
	5·112	0·389	2·757	0·555
	5·068	0·386	4·664	0·937
	5·068	0·386	6·020	1·209
	5·024	0·385	7·510	1·506
	5·024	0·389	8·985	1·797
	5·024	0·397	$10·50_5$	2·127
	5·024	0·412	11·92	2·458
	4·981	0·438	13·41	2·893
	4·959	0·477	14·90	3·463
3	7·121	0·657	14·78	3·499
	9·306	0·848	14·74	3·565
	$11·44_7$	1·057	14·62	3·645
	$13·67_5$	1·288	14·45	3·786
	$15·81_6$	1·532	14·30	3·906
	18·00	1·795	14·10	4·073
	20·23	2·109	13·86	4·283
	22·37	2·470	13·59	4·541
	24·47	2·970	13·14	4·969
	26·69	3·528	12·69	5·365
	28·84	4·279	12·11	5·873
	30·98	5·336	11·35	6·530
	33·07	6·824	10·42	7·358
	35·15	8·990	9·18	8·60
4	34·82	9·30	10·55	9·15
	33·82	10·28	$11·90_5$	10·62
	32·85	11·24	$13·33_6$	12·23

From other tests: Young's elastic modulus 12 820 tsi
Elastic shear modulus 2(5 015) tsi

10.2. **Measurements.** The load test measurements shown in Table IV,10.1 were supplied privately to the present author by Professor Morrison and Dr. Shepherd because their paper [60] did not give the results in a form amenable to analysis by methods other than those given by them. Stresses and strains are both 'nominal', as the deformation is so small that nominal and true values are very slightly different, as a calculation will show.

The analyses of articles III,13 to III,15 and IV,5 for an elastic substance show that, generally, the change in length of a thin-walled tube is 'stretch' and not 'normal strain'. The measurements of length change are regarded as normal strain e_{zz} by Morrison & Shepherd and are still denoted by this in the table. However, the reader should have clearly in mind that the measurement e_{zz} there is, in fact, the unit stretch a_z. Future experimenters need to have this in mind when designing experiments involving large strains.

11. Interpretation [63] of the Morrison & Shepherd [60] tests on thin-walled steel tubes

These tests with the stress system 'transferring' by rotation relative to the substance were designed to check if stress and elasto-plastic 'strain' remained coaxial. It was also required to find out just what was to be taken as elasto-plastic 'strain'. These tests and those in parallel independently by Peters, Dow & Batdorf [61] were intended to examine these polemical aspects.

11.1. **Phase difference between the stress dyadic and elasto-plastic strain dyadic.** With angle A between the coordinate direction $\mathbf{c}_\theta$ and the principal normal strain direction unit vector $\mathbf{x}_i$ and B the angle between $\mathbf{c}_\theta$ and the principal normal stress direction $\mathbf{s}_i$, there follows from articles III,1.3 and III,2.7

$$\tan 2A = 2e_{\theta z}/(e_{\theta\theta}-e_{zz}) \qquad (11.1)$$

$$\tan 2B = 2S_{\theta z}/(S_{\theta\theta}-S_{zz}) \qquad (11.2)$$

The elasto-plastic strain theory formulated by the present author in volume I and previously in this volume II gives 'elasto-plastic strain' as the transferred elastic total strain coaxial with the last plastic increment strain. Thus [63, 64],

$$e_i = e_i^E + \delta e_i^P \qquad e_j = e_j^E + \delta e_j^P \qquad (11.3)$$

This strain dyadic is transformed to the coordinates directions at a point and then IV(11.1) becomes

$$\tan 2A = 2(e^E_{\theta z}+\delta e^P_{\theta z})/[(e^E_{\theta\theta}+\delta e^P_{\theta\theta})-(e^E_{zz}+\delta e^P_{zz})] \qquad (11.4)$$

Using this equation to calculate A and IV(11.2) to calculate B from the strain and stress values in Table IV,10.1 gives the phase difference $(A-B)$ as practically zero in Fig. IV,11.1. The plastic increment strains are calculated from

$$\delta e^P_{\theta\theta} = \delta e_{\theta\theta}-\delta e^E_{\theta\theta} \quad \delta e^P_{zz} = \delta e_{zz}-\delta e^E_{zz} \quad \delta e^P_{\theta z} = \delta e_{\theta z}-\delta e^E_{\theta z} \qquad (11.5)$$

$$\delta e^E_{\theta\theta} = -\psi^E q^E \delta S_{zz} \quad \delta e^E_{zz} = \psi^E \delta S_{zz} \quad \delta e^E_{\theta z} = (1+q^E)\psi^E \delta S_{\theta z} \qquad (11.6)$$

The elastic stress-strain parameters had to be assumed as isotropic in the absence of observations on this aspect. The modulus

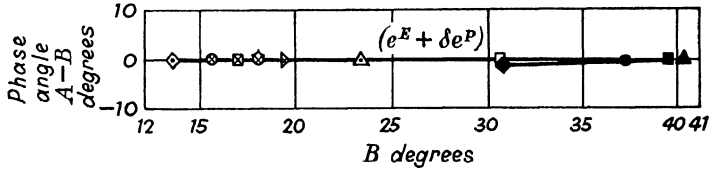

FIG. IV,11.1.—Phase angle $(A-B)$ between the principal normal stress and elasto-plastic strain directions for a thin-walled *steel* tube under axial torsion and tension. Stress is total, while *elasto-plastic strain is elastic total strain with plastic increment strain.* Angle A is that of the principal normal strain, while B is that of the principal normal stress relative to the circumferential direction. The phase difference is almost zero over a large range of loading.

ψ^E was taken as $(12\,820)^{-1}$ tsi^{-1} as in Table IV,10.1, while q^E was assumed to be $\frac{1}{3}$.

The zero value for $(A-B)$ shows that the *elastic total strain dyadic and last plastic partial-increment strain dyadic do, in fact, transfer with the stress dyadic* on this steel, at least. This fact has been used previously in this treatise to analyse elasto-plastic deformation. Explicitly, in symbols, with principal normal stress and strain directions unit vectors $\mathbf{x}_i$, $\mathbf{x}_j$ the stress dyadic

$$\mathfrak{S} = S_i\mathbf{x}_i\mathbf{x}_i+S_j\mathbf{x}_j\mathbf{x}_j \qquad (11.7)$$

the elastic strain dyadic, neglecting direction $\mathbf{x}_k$, is

$$\mathfrak{M}^E = e^E_i\mathbf{x}_i\mathbf{x}_i+e^E_j\mathbf{x}_j\mathbf{x}_j \qquad (11.8)$$

and the partial-increment plastic strain dyadic

$$\Delta\mathfrak{M}^P = \delta e_i^P \mathbf{x}_i\mathbf{x}_i + \delta e_j^P \mathbf{x}_j\mathbf{x}_j \tag{11.9}$$

while the current elasto-plastic strain dyadic is

$$\mathfrak{M} = \mathfrak{M}^E + \Delta\mathfrak{M}^P \tag{11.10}$$

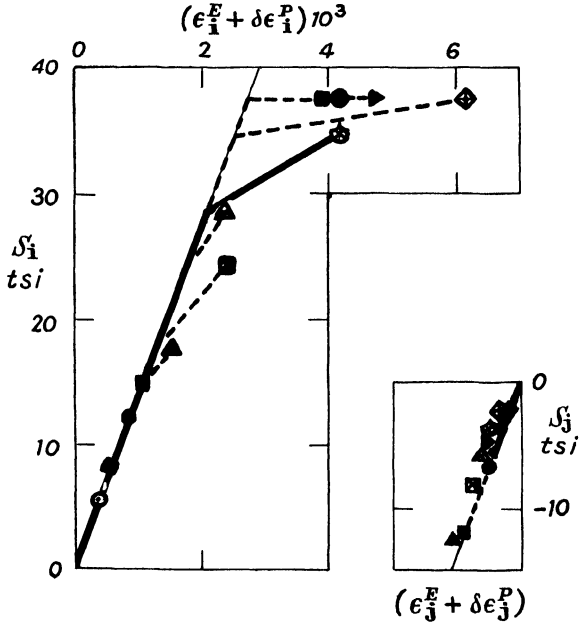

FIG. IV,11.2.—Steel, thin-walled tube loaded by axial tension and torsion. Current principal normal elasto-plastic partial-strains are plotted against principal normal stresses given as nominal tons per square inch (tsi). The elastic modulus and elastic transverse contraction ratio were assumed constant and isotropic, as was also the plastic transverse contraction ratio of value 0·34. The increase in plastic partial-strain ϵ_j^P with decrease in stress S_j may be due to the assumed values of stress-strain parameters. The experiment is deficient in this respect.

11.2. **Principal normal increment stresses and elasto-plastic increment strains.** All the two-dimensional, self-conjugate dyadics can be transformed from principal directions to the general directions $\mathbf{c}_\theta$, $\mathbf{c}_z$ by the formulæ or graphical construction of article A,6. Thus, for example,

$$\Delta\mathfrak{M}^P = \delta e_{\theta\theta}^P \mathbf{c}_\theta\mathbf{c}_\theta + \delta e_{zz}^P \mathbf{c}_z\mathbf{c}_z + \delta e_{\theta z}^P(\mathbf{c}_\theta\mathbf{c}_z + \mathbf{c}_z\mathbf{c}_\theta) \tag{11.11}$$

Then, conversely, with the double scalar product notation,

$$\delta e_{\mathrm{i}}^{P} = \mathbf{x}_{\mathrm{i}}\mathbf{x}_{\mathrm{i}}{:}\Delta\mathfrak{M}^{P}(\mathbf{c}_{\theta}, \mathbf{c}_{z}) \qquad \delta e_{\mathrm{j}}^{P} = \mathbf{x}_{\mathrm{j}}\mathbf{x}_{\mathrm{j}}{:}\Delta\mathfrak{M}^{P}(\mathbf{c}_{\theta}, \mathbf{c}_{z}) \quad (11.12)$$

Article III,13 shows that under the present loading the measured changes in length and diameter of the tube are 'unit stretches' a_z, a_θ and not 'normal strains' e_{zz}, $e_{\theta\theta}$. Similarly, the measured 'helix angle' said to measure shear strain does not in fact do so. However, for the present small strains the measured quantities are accepted as first approximations to strains. With this reservation, already accepted in IV(11.5), then IV(11.11) is calculated from

$$\Delta\mathfrak{M}^{P} = \Delta\mathfrak{M} - \Delta\mathfrak{M}^{E} \quad (11.13)$$

with the scalar, plastic increment strains given by equations IV(11.5). Substituting in IV(11.12) and using unit vectors $\mathbf{x}_{\mathrm{i}}$, $\mathbf{x}_{\mathrm{j}}$ calculated from IV(11.4) giving the direction angle A, then gives the principal normal plastic increment strains.

11.3. **Principal normal increment stresses and plastic increment partial-strains.** The principal normal increment stresses are readily calculated from $(S_{\mathrm{i}}+\delta S_{\mathrm{i}})-S_{\mathrm{i}}$ and similarly for the other direction since, for any current loading,

$$\begin{matrix} 2S_{\mathrm{i}} \\ \\ 2S_{\mathrm{j}} \end{matrix} = S_{zz} \begin{matrix} + \\ \\ - \end{matrix} (S_{zz}^{2}+4S_{\theta z}^{2})^{\frac{1}{2}} \quad (11.14)$$

using Table IV,10.1 to calculate the principal normal stresses and increment stresses.

The plastic increment partial-strains are related to the plastic increment strains by

$$\delta e_{\mathrm{i}}^{P} = \delta\epsilon_{\mathrm{i}}^{P} - q^{P}\delta\epsilon_{\mathrm{j}}^{P} \qquad \delta e_{\mathrm{j}}^{P} = \delta\epsilon_{\mathrm{j}}^{P} - q^{P}\delta\epsilon_{\mathrm{i}}^{P} \quad (11.15)$$

The plastic transverse contraction ratio has been assumed as isotropic and is taken to be of value 0·34.

The increment stress and increment partial-strain values are shown in Figs. IV,11.2, IV,11.3. These figures show the current elastic total partial-strain and last plastic increment partial-strain to give the current elasto-plastic partial-strain, of which a typical value is the heavy line. The values of S_{j} and $(\epsilon_{\mathrm{j}}^{E}+\delta\epsilon_{\mathrm{j}}^{P})$ are small, so Fig. IV,11.3 gives them to an increased scale. The elastic moduli are $\delta\epsilon_{\mathrm{i}}^{E}/\delta S_{\mathrm{i}} = \psi_{\mathrm{i}}^{E}$ and similarly for the other

direction, but these have been assumed isotropic and constant, so that S_i vs. ϵ_i^E and the similar curve for the other direction are linear as shown. Volume I, Fig. IX,15.1 also shows these values but with the plastic increment partial-strains summed to display plastic total partial-strains.

11.4. **Plastic moduli.** The plastic moduli are $\delta\epsilon_i^P/\delta S_i = \psi_i^P$ and similarly for the other direction. Inspection of Fig. IV,11.3 shows that the plastic modulus is negative over stage 3 loading

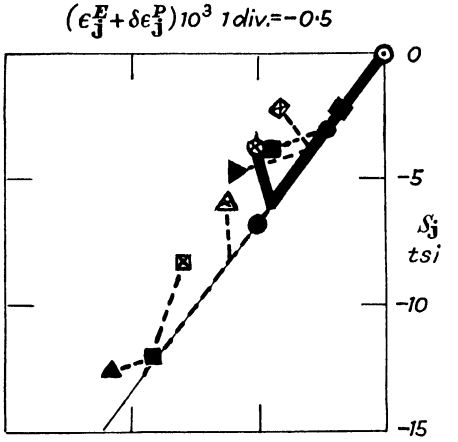

FIG. IV,11.3.—The plotting to a larger scale of the current elasto-plastic partial-strain $(\epsilon_j^E+\delta\epsilon_j^P)$ and stress S_j in Fig. IV,11.2. The negative values of ψ_j^P for stage 3 loading could be due to the value $q^P = 0{\cdot}34$ having been assumed incorrectly. Further experiments are necessary.

in which the increment stresses δS_j are positive but plastic increment partial-strains $\delta\epsilon_j^P$ are negative. That is, for this direction the plastic partial-strain increases with decrease of the stress [63].

It is clear that a change in the stress-strain behaviour occurs with change in *sign* of the increment stress. However, the change can be influenced by the value of the plastic transverse contraction ratio q^P, which was assumed to be of constant value 0·34. A greater value than this could lead to $\delta\epsilon_j^P \gtrless 0$. If the true value of q^P should give $\delta\epsilon_j^P = 0$ then the elasto-plastic element would be displaying some independence of action for the principal directions with respect to increment stresses. If the true value of q^P should

give $\delta\epsilon_j^P > 0$ then the plastic modulus would be approximately, at least, independent of sign of increment stress. There is no test data to clarify this aspect at present (March 1954). A test similar to that in article IV,8 would be best, as the complication of stress transfer would not occur and 'strains' are measured instead of 'unit stretches' as here. The internal hydraulic pressure could be decreased to give the changed sign of increment stress for one direction as required.†

12. Experimental elasto-plastic straining of thin-walled circular duralumin tubes: tests by R. W. Peters, N. F. Dow & S. B. Batdorf

The tests by R. W. Peters, N. F. Dow & S. B. Batdorf[61] were undertaken with care and attention to detail, and various types of optical and electrical deflectometers and extensometers used as a check on one another. The specimens were machined from solid billets of duralumin to give a parallel working section 12 inches long, $3\frac{3}{4}$ inches outside diameter, a wall $\frac{1}{8}$ inch thick and flat, flanged ends about $7\frac{1}{2}$ inches in diameter. The flat, flanged ends were bolted to the working heads of a combined axial torsion and compression testing machine. The rigidity of the massive machine was relied upon to ensure axial compressive loading with negligible eccentricity. Two specimens were made and one was tested twice. The second specimen denoted by 3—(*B*) was tested only once.

These are the measurements given in Table IV,12.1 as supplied to the present author by the U.S. Advisory Committee for Aeronautics because the published paper[61] gave only printed curves. The present author wondered if, for economy of space, he should abridge the table, but reflection showed that the full results of such costly, well-performed tests should be available to other analysts who may not agree with the interpretations of the author. The shear strains here are half the values of those given by Peters, Dow & Batdorf, who used the classical shear strain which is not the component of a dyadic as required for invariant transformation with reorientation of coordinate axes.

† The present author has no experimental facilities at present.

TABLE IV,12.1

Duralumin, thin-walled tube under axial *torsion* and *compression*. Measurements by R. W. Peters, N. F. Dow & S. B. Batdorf[61]. Stresses and strains are nominal but differ little from 'true' values because the strains are small. Pounds per square inch is denoted by psi. Available by courtesy of the U.S. National Advisory Committee for Aeronautics.

S_{zz} psi 10^{-3}	e_{zz} 10^3	$e_{\theta\theta}$ 10^3	$S_{\theta z}$ psi 10^{-3}	$2e_{\theta z}$ 10^3
0	0	0	0	0
1·835	0·1833	−0·0684		
2·568	0·2244	−0·0853		
2·691	0·2446	−0·0963		
2·976	0·2745	−0·1026		
3·302	0·3064	−0·1141	0	0
3·628	0·3463	−0·1256		
3·873	0·3774	−0·1371		
4·199	0·4074	−0·1486		
4·525	0·4385	−0·1599		
4·851	0·4695	−0·1713	0	0
5·259	0·4996	−0·1827		
5·707	0·5407	−0·1997		
6·196	0·5676	−0·2165		
6·808	0·6320	−0·2390		
7·256	0·6918	−0·2514	0	0
7·827	0·7539	−0·2743		
8·357	0·7950	−0·2912		
9·009	0·8559	−0·3088		
9·662	0·9074	−0·3364		
10·313	0·9673	−0·3592	0	0
11·007	1·0295	−0·3768		
11·782	1·0894	−0·4049		
12·638	1·1611	−0·4280		
13·371	1·2327	−0·4562		
14·309	1·3237	−0·4852	0	0
15·247	1·4047	−0·5140		
16·103	1·4782	−0·5528		
16·959	1·5701	−0·5818		
17·774	1·6524	−0·6155		
18·752	1·7324	−0·6442	0	0
19·567	1·8147	−0·6781		
20·423	1·8949	−0·7119		
21·361	1·9859	−0·7409		
22·299	2·0682	−0·7747		

Table IV,12.1—*contd.*

S_{zz} psi 10^{-3}	e_{zz} 10^3	$e_{\theta\theta}$ 10^3	$S_{\theta z}$ psi 10^{-3}	$2e_{\theta z}$ 10^3
23·196	2·1632	−0·8091	0	0
23·970	2·2435	−0·8428		
24·869	2·3237	−0·8766		
25·723	2·4159	−0·9108		
26·579	2·524	−0·9507		
27·435	2·6244	−0·9923	0	0
28·251	2·7315	−1·0356		
29·066	2·8381	−1·0858		
29·759	2·9726	−1·1471		
30·452	3·1131	−1·2088		
31·064	3·2879	−1·2879	0	0
31·594	3·4475	−1·3604		
32·165	3·6132	−1·4330		
32·694	3·7692	−1·5165		
33·224	3·9200	−1·5887		
33·632	4·1113	−1·6887	0	0
34·080	4·2921	−1·7720		
34·529	4·4828	−1·8568		
34·977	4·6838	−1·9520		
35·344	4·855	−2·045		
35·670	5·016	−2·139	0	0
	5·217	−2·244		
36·363	5·419	−2·334		
36·689	5·5995	−2·438		
37·016	5·832	−2·561		
37·301	6·043	−2·667	0	0
37·627	6·275	−2·788		
37·830	6·506	−2·900		
38·075	6·728	−3·000		
38·279	6·929	−3·105		
38·483	7·161	−3·223	0	0
38·687	7·383	−3·349		
38·891	7·604	−3·445		
39·094	7·795	−3·550		
39·257	7·997	−3·654		
39·462	8·219	−3·777	0	0
39·625	8·430	−3·882		
39·787	8·632	−3·977		
39·910	8·823	−4·082		
39·991	8·985	−4·176		

Table IV,12.1—*contd.*

S_{zz} psi 10^{-3}	e_{zz} 10^3	$e_{\theta\theta}$ 10^3	$S_{\theta z}$ psi 10^{-3}	$2e_{\theta z}$ 10^3
40·073	9·116	−4·247	0	0·0087
40·155	9·227	−4·303		0·0305
40·236	9·327	−4·357		0·0349
	9·428	−4·409		0·1003
	9·519	−4·458	0·1807	0·1831
40·318	9·5596	−4·480	0·4906	0·2442
40·318	9·670	−4·526	0·7230	0·3270
40·358	9·750	−4·559	0·9811	0·4011
40·358	9·821	−4·736	1·2135	0·4752
40·358	9·8814	−4·7656	1·4724	0·5537
	9·9718	4·8086	1·6784	0·6322
	10·012	4·8420	1·8844	0·7238
	10·093	−4·8846	2·1174	0·8153
	10·153	4·9196	2·2974	0·8894
	10·233	−4·9553	2·5304	0·9684
	10·305	−5·003	2·7624	1·0504
40·399	10·386	−5·055	2·9434	1·1384
40·399	10·455	−5·075	3·1504	1·2204
40·440	10·516	5·127	3·4084	1·3034
	10·607	−5·169	3·5374	1·3954
	10·708	−5·216	3·7174	1·4954
	10·778	5·262	3·9244	1·5914
	10·879	−5·311	4·0794	1·6834
	10·979	5·354	4·2344	1·7924
	11·080	−5·413	4·3634	1·8924
	11·191	5·471	4·5184	1·9794
	11·282	−5·537	4·6214	2·0794
	11·392	−5·574	4·7514	2·1844
	11·482	−5·621	4·9574	2·2934
	11·603	−5·675	5·1124	2·4114
	11·704	−5·745	5·3704	2·5594
	11·844	−5·810	5·5514	2·7164
	11·976	−5·888	5·7834	2·8604
	12·107	−5·948	5·9894	2·9864
	12·237	−6·0076	6·1194	3·1044
	12·378	−6·085	6·2744	3·2394
	12·549	−6·175	6·4034	3·3744
	12·690	−6·252	6·5324	3·5094
40·521	12·871	−6·340	6·6874	3·5754
40·644	13·042	−6·429	6·7644	3·68

Table IV,12.1—*contd.*

S_{zz} psi 10^{-3}	e_{zz} 10^3	$e_{\theta\theta}$ 10^3	$S_{\theta z}$ psi 10^{-3}	$2e_{\theta z}$ 10^3
40·684	13·193	—6·507	6·9194	3·9064
40·726	13·325	—6·590	7·0744	4·0464
	13·516	—6·674	7·2554	4·2114
	13·656	—6·761	7·4364	4·3814
	13·837	—6·841	7·6424	4·5654
	13·999	—6·935	7·8494	4·7434
	14·170	—7·019	8·0044	4·8964
	14·331	—7·107	8·1844	5·0704
	14·502	—7·186	8·3654	5·2104
	14·623	—7·263	8·5204	5·375
	14·774	—7·340	8·6754	5·5464
	14·925	—7·411	8·9074	5·7774
	15·106	—7·517	8·9594	5·8944
	15·207	—7·577	9·1394	6·0694
	15·388	—7·655	9·2694	6·2261
	15·519	—7·732	9·4234	6·4184
	15·709	—7·810	9·5524	6·5834
	15·821	—7·886	9·6044	6·6884
	15·932	—7·939	9·3984	6·7014
40·806	16·022	—7·988	9·2174	6·7144
40·888	16·092	8·024	7·5904	6·3654
40·888	16·134	-8·069	5·4736	5·8864
40·970	16·233	—8·090	1·2135	4·8444
41·051	16·244	—8·112	1·1359	4·8264
41·133	16·304	—8·136	0·4906	4·7604
41·255	16·324	—8·154	0·2324	4·5604
41·255	16·345	—8·171	0·1033	4·5174
40·399	16·315	—8·170	0·0775	4·4864
39·462	16·215	—8·133	0·0259	4·4644
38·524	16·115	—8·097	0·0259	4·4474
37·505	16·024	—8·049	0	
36·526	15·914	-8·011	-0·0258	
36·445	15·814	—7·964		
35·262	15·673	—7·903		4·4384
33·632	15·523	—7·861		4·4254
31·797	15·352	—7·792		4·4164
29·840	15·192	—7·709		4·4164
27·639	14·981	—7·629		4·4034
25·479	14·721	—7·538		4·3904
23·237	14·520	—7·442		4·3813

Table IV,12.1--*contd.*

S_{zz} psi 10^{-3}	e_{zz} 10^3	$e_{\theta\theta}$ 10^3	$S_{\theta z}$ psi 10^{-3}	$2e_{\theta z}$ 10^3
20·587	14·230	—7·344		4·3734
17·774	13·940	—7·229		4·3604
14·472	13·569	—7·092		4·2944
12·230	13·268	—6·965	—0·1549	4·1984
10·191	13·008	—6·869		4·1904
8·3567	12·787	—6·766		4·1814
6·645	12·586	—6·682		4·1724
5·055	12·345	—6·591		4·1684
3·179	12·016	—6·496		4·1684
—1·019	11·934	—6·404		4·1724
—1·019	11·883	—6·369		4·1854
—0·9787	11·873	—6·357		4·1854

13. Experimental elasto-plastic straining of thin-walled, circular duralumin tubes: tests by J. L. M. Morrison & W. M. Shepherd [60]

J. L. M. Morrison and W. M. Shepherd tested two thin-walled duralumin tubes under combined axial torsion and axial tension. The two specimens were machined from the core of a 5-inch diameter billet. The parallel working section was 2 inches long, with an inside diameter of 1 inch and a wall thickness of 0·050 inch. Optical extensometers of comparator type were used to measure the fairly small strains. These tests are of importance because they used axial tension where Peters, Dow & Batdorf used axial compression, so that some comparative analysis is possible. Further, Morrison & Shepherd followed a more complicated load path than Peters, Dow & Batdorf.

13.1. **Measurements.** Table IV,13.1 gives the nominal stresses and strains calculated by Professor Morrison and Dr. Shepherd from their test specimen S.A.1 and supplied privately to the present author. The shear strain used in the present treatise is half that used by Morrison & Shepherd to ensure that it is a component of a self-conjugate dyadic that will transform invariantly as noted in volume I, article III,H.

TABLE IV,13.1

Duralumin, thin-walled tube under axial *torsion* and *tension*. Stresses and strains are nominal. Tons per square inch is denoted by tsi with a ton of 2 240 pounds. The measurements are by J. L. M. Morrison & W. M. Shepherd [60].

Load stage	S_{zz} tsi	e_{zz} 10^3	$S_{\theta z}$ tsi	$2e_{\theta z}$ 10^3
1	0	0	0	0
	0·2	0·040		not
	0·4	0·080		read
	0·6	0·124		—
	0·8	0·173		—
	1·0	0·221	0	0·015
	1·2	0·279		0·011
	1·4	0·328		0·015
	1·6	0·390		—
	1·983	0·533		0·034
	2·383	0·726	0	0·056
	2·767	0·946		0·079
	3·175	1·254		0·109
	3·55	1·669		0·090
	3·99	2·246		0·075
10-min. pause	3·98	2·275	0	0·075
2	3·965	2·298	0·206	0·195
	3·95	2·309	0·317	0·262
	3·94	2·328	0·428	0·341
	3·92	2·356	0·550	0·439
	3·90	2·395	0·665	0·551
	3·87	2·419	0·66	0·593
	3·85	2·423	0·63	0·585
	3·85	2·434	0·69	0·623
	3·695	2·761	1·34	1·56
	3·66	2·830	1·48	1·79
	3·615	2·946	1·63	2·16
	3·50	3·153	1·855	2·88
	3·455	3·264	1·945	3·25
	3·39	3·415	2·08	3·82
	3·32	3·559	1·92	4·21

Table IV,13.1—*contd.*

Load stage	S_{zz} tsi	e_{zz} 10^3	$S_{\theta z}$ tsi	$2e_{\theta z}$ 10^3
2 (*contd.*)	3·28	3·658	2·225	4·84
	3·215	3·802	2·44	5·53
	3·04	4·200	2·70	7·60
	2·845	4·646	3·01	10·22
	2·845	4·667	3·00	10·30
7-min. pause				
3	3·31	4·844	2·945	10·45
	3·79	5·150	2·83	10·80
	4·22	5·653	2·65	11·31
	4·675	6·277	2·46	11·82
	5·13	7·130	2·26	12·30
	5·60	8·225	2·06	12·87

From other tests: Young's elastic modulus 4 900 tsi
Elastic shear modulus 2(1 724) tsi

Unfortunately, Morrison & Shepherd did not measure circumferential strain, so that it is necessary to use a guessed value of elastic and plastic transverse contraction ratios. The elastic (Poisson) ratio can be inferred from the Young's elastic modulus and elastic shear modulus for initial strain values and then it can be assumed that these apply over the load path.

14. Interpretation of the axial tension, compression and torsion tests on thin-walled duralumin tubes

A primary object of the tests on duralumin tubes by Peters, Dow & Batdorf [61] given in article IV,12 and by Morrison & Shepherd [60] given in article IV,13 was to examine the coaxiality or otherwise of various 'strain' dyadics and the total stress dyadic as hypothesised by various contemporary theories. Thus, denoting by f's the scalar components of the various 'strain' dyadics for principal and general directions respectively gives

$$f_i\mathbf{x}_i\mathbf{x}_i+f_j\mathbf{x}_j\mathbf{x}_j = f_{\theta\theta}\mathbf{c}_\theta\mathbf{c}_\theta+f_{zz}\mathbf{c}_z\mathbf{c}_z+f_{\theta z}(\mathbf{c}_\theta\mathbf{c}_z+\mathbf{c}_z\mathbf{c}_\theta) \qquad (14.1)$$

The angle A between $\mathbf{c}_\theta$ and $\mathbf{x}_i$, similar to article IV,11.1, is given by

$$\tan 2A = 2f_{\theta z}/(f_{\theta\theta}-f_{zz}) \qquad (14.2)$$

The total stress dyadic is

$$S_i\mathbf{s}_i\mathbf{s}_i+S_j\mathbf{s}_j\mathbf{s}_j = S_{\theta\theta}\mathbf{c}_\theta\mathbf{c}_\theta+S_{zz}\mathbf{c}_z\mathbf{c}_z+S_{\theta z}(\mathbf{c}_\theta\mathbf{c}_z+\mathbf{c}_z\mathbf{c}_\theta) \quad (14.3)$$

The angle B between $\mathbf{c}_\theta$ and $\mathbf{s}_i$ is given by

$$\tan 2B = 2S_{\theta z}/(S_{\theta\theta}-S_{zz}) \quad (14.4)$$

Plastic total strains were calculated from such as

$$e^P_{\theta\theta} = e_{\theta\theta}-e^E_{\theta\theta} \quad (14.5)$$

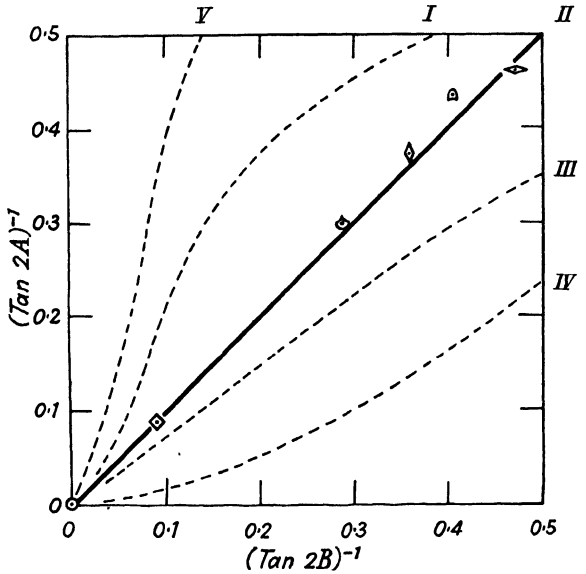

FIG. IV,14.1.—The angle between the circumferential direction is A for principal normal elasto-plastic 'strain' and B for principal normal stress due to axial torsion and compression on a thin-walled duralumin tube. A point on the heavy line indicates coaxiality of the elasto-plastic 'strain' and stress dyadics. The curve numbers correspond to elasto-plastic 'strain' supposed as: I, (δe^P); II, $(e^E+\delta e^P)$; III, (e^E+e^P); IV, (e^P); V, $(\delta e^E+\delta e^P)$. Curves I, IV are due to Peters, Dow & Batdorf [61], while II, III, V are due to the present writer [64].

with

$$e^E_{\theta\theta} = \psi^E(-q^E S_{zz}) \qquad e^E_{zz} = \psi^E S_{zz} \qquad e^E_{\theta z} = \psi^E(1+q^E)S_{\theta z} \quad (14.6)$$

Plastic increment strains were calculated from equations of the same form as these but with the e's replaced by δe's and the S's by δS's. For the Peters, Dow & Batdorf tests Young's modulus $E = (\psi^E)^{-1} = 10{\cdot}7\ 10^6$ psi and Poisson's ratio $q^E = 0{\cdot}34$.

14.1. **Principal directions for total stress and various 'strains'.** Fig. IV,14.1 shows the values [64] $(\tan 2A)^{-1}$ vs.

$(\tan 2B)^{-1}$ when the f's on the right-hand side of equations IV(14.1), IV(14.2) are assumed to have various values calculated from IV(14.5), IV(14.6) and the corresponding increment strain forms using the values in Table IV,12.1. Similar results follow from using the Table IV,13.1. Comparison of results is done most conveniently in Table IV,14.1.

TABLE IV,14.1

Curve No.	'Strain' f assumed as	Coincidence of principal directions for total stress and 'strain' dyadics
I	δe^P	$\mathbf{x}_i \neq \mathbf{s}_i$
II	$e^E + \delta e^P$	$\mathbf{x}_i = \mathbf{s}_i$
III	$(e^E + e^P) = e$	$\mathbf{x}_i \neq \mathbf{s}_i$
IV	e^P	$\mathbf{x}_i \neq \mathbf{s}_i$
V	$(\delta e^E + \delta e^P) = e$	$\mathbf{x}_i \neq \mathbf{s}_i$

14.2. **Plastic moduli.** Analysing the measurements in Table IV,12.1 in the manner of articles IV,11.2 to IV,11.4 gave the values of the plastic moduli ψ_i^P, ψ_j^P in Fig. IV,14.2 plotted against the equivalent normal stress of article IV,6.2. The calculation of these plastic moduli is not entirely satisfactory (as already noted in article IV,11.4 for similar calculations), because the values of elastic modulus, elastic and plastic transverse contraction ratios had to be assumed isotropic and constant in the absence of experimental data. However, the probable change in the values of parameters as a result of future tests should not change the order of magnitude of the plastic moduli nor the qualitative deductions from Fig. IV,14.2 showing the range when axial torque is applied increasingly with axial compression virtually constant.

The elastic modulus $\psi^E = 0{\cdot}0934$ $(10^6 \text{ psi})^{-1}$ and $\psi_i^P = 4{\cdot}215$ $(10^6 \text{ psi})^{-1}$ when torque, and hence S_j, is zero, showing that the duralumin is well into the elasto-plastic stage of deformation. With the advent of tensile stress $S_j > 0$ the duralumin becomes plastically 'stiffer', as shown by the decrease in the value of ψ_i^P. The elasto-plastic duralumin behaves virtually elastically so far

as the incoming tensile stress S_j is concerned, as shown by ψ_j^P of order 0·15 $(10^6 \text{ psi})^{-1}$. Towards the end of the range both $\psi_i^{l'}$, $\psi_j^{l'}$ show increase, indicating that the transition stage for the incoming stress is passing and the duralumin is beginning to behave homogeneously elasto-plastically. Presumably, further increase of S_j would bring $\psi_j^{l'}$ more nearly equal to ψ_i^P for a state approaching restricted isotropy.

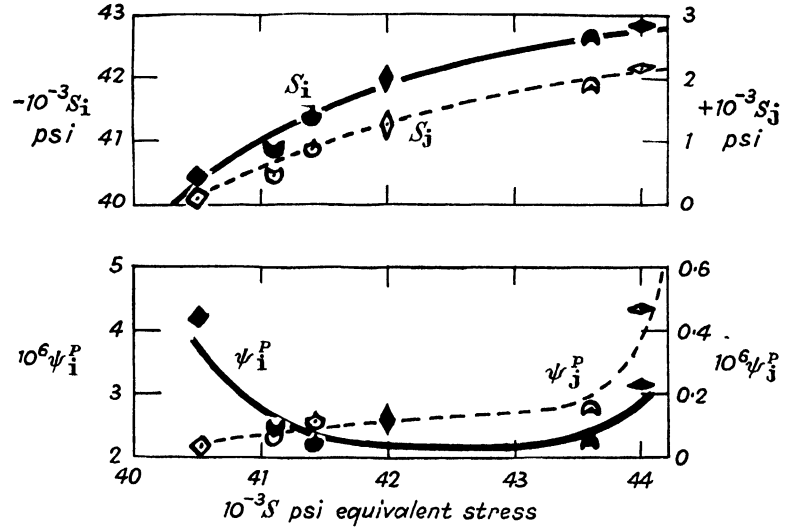

FIG. IV,14.2.— Plastic moduli for thin-walled duralumin tubes under axial torsion and compression from the tests by Peters, Dow & Batdorf given in Table IV,12.1. Stress S_j is zero when S_i is simple axial compression. Axial compression remains almost constant, while axial torque increases to give S_i an increasing compression and S_j a small increasing tension. Over most of the range shown the substance becomes plastically 'stiffer' with the small applied tension, as shown by ψ_i^P decreasing. The substance behaves almost elastically towards S_j, as shown by ψ_j^P of the order of $\psi^E = 0{\cdot}0934\ (10^6 \text{ psi})^{-1}$.

15. Conclusions from the tests on thin-walled metal tubes

It is convenient to bring together the results of the tests discussed in this chapter preparatory to the solution of theoretical examples of heterogeneous straining and to indicate where further experimental research is necessary.

15.1. **Coaxiality of stress and strain dyadics.** The tests of steel and duralumin by Morrison & Shepherd [60] and Peters, Dow & Batdorf [61] show that, as the principal directions of the stress

dyadic rotate relative to metals, the elasto-plastic strain dyadic having elastic total strain and plastic increment strain dyadics as its components remains coaxial with the total stress dyadic. Denoting the principal stress directions briefly by $\mathbf{s}_i$ and the general coordinates directions by $\mathbf{c}_\theta$, this means that Figs. IV,11.1, IV,14.1 imply that, with

$$\mathfrak{M} = \mathfrak{M}^E + \Delta\mathfrak{M}^P \qquad \Delta\mathfrak{M} = \Delta\mathfrak{M}^E + \Delta\mathfrak{M}^P$$

then

$$\mathfrak{M}(\mathbf{s}_i) \to \mathfrak{M}(\mathbf{c}_\theta) \tag{15.1}$$

$$\Delta\mathfrak{M}(\mathbf{s}_i) \to \Delta\mathfrak{M}(\mathbf{c}_\theta) \tag{15.2}$$

$$\Delta\mathfrak{M}^P(\mathbf{s}_i) \to \Delta\mathfrak{M}^P(\mathbf{c}_\theta) \tag{15.3}$$

15.2. **Non-coaxiality of stress and 'strain' dyadics.** The tests by Morrison & Shepherd, and Peters, Dow & Batdorf showed that some of the current theories intended to analyse 'isotropic' stress-strain relationships are invalid and also that care is necessary in the interpretation of experimental observations. Thus, denoting the general strain dyadic of Fig. IV,14.1 by $\mathfrak{F}$, say, then for all but $\mathfrak{M}$ of equation IV(15.1)

$$\mathfrak{F}(\mathbf{c}_\theta) \to \mathfrak{F}(\mathbf{x}_i') \tag{15.4}$$

where the principal directions of the strain dyadic

$$\mathbf{x}_i' \neq \mathbf{s}_i \tag{15.5}$$

the directions of principal normal stress.

If the scalar coefficients of $\mathfrak{F}(\mathbf{c}_\theta)$ are taken to be elasto-plastic total strain $e_{\theta\theta} = e^P_{\theta\theta} + e^E_{\theta\theta}$, ..., or plastic total strain $e^P_{\theta\theta}$, ..., then IV(15.5) shows that the plastic total strain does not transfer with stress, as is obvious intuitively.

If the scalar coefficients of $\mathfrak{F}(\mathbf{c}_\theta)$ are taken to be elasto-plastic increment strain $\delta e_{\theta\theta} = \delta e^P_{\theta\theta} + \delta e^E_{\theta\theta}$, ..., or plastic increment strain $\delta e^P_{\theta\theta}$, ..., then IV(15.5) shows that the plastic increment strains cannot be considered apart from the current total stresses so far as *directions* are concerned. More explicitly, the incremental strain dyadics must be partially-incremental as for the elasto-plastic dyadic, for example,

$$(\delta e_i \mathbf{s}_i \mathbf{s}_i + \ldots) \neq (\delta e_i' \mathbf{x}_i' \mathbf{x}_i' + \ldots) \tag{15.6}$$

15.3. **Isotropy of stress-strain parameters.** The tests by Davis [54] on copper and steel, given in article IV,8 and interpreted in IV,9, show that the plastic modulus ψ^P is approximately isotropic within the restriction that the values and isotropy of elastic modulus ψ^E, elastic and plastic transverse contraction ratios q^E, q^P were assumed on the basis of initial values usually found from a one-stress loading. Further, the stresses do not transfer in these tests.

The Morrison & Shepherd, and Peters, Dow & Batdorf tests on steel and duralumin given in articles IV,10, IV,12, IV,13 and interpreted in articles IV,11, IV,14 indicate anisotropy of the plastic modulus, but there, again, too many assumptions were necessary about the values of the other stress-strain parameters. The anisotropy of the plastic modulus may be a genuine effect due to stress and strain transfer and reversal of sign of increment stress at some stage of the loading, but the present state of experimental knowledge † is too slight and sketchy to form firm opinions on general stress-strain relations.

15.4. **Stress-strain parameters as functions of the octahedral normal and shear stresses.** The interpretation in article IV,9 of Davis's tests on copper and steel in article IV,8 gives the plastic modulus as a function of octahedral shear and normal stresses. All the copper results plotted reasonably well on to a single octahedral-parametric surface. The results for steel indicated that the measurements for simple tension are on one octahedral-parametric surface, while those for tension-tension complex stresses are on another surface. This needs further examination.

Copper seems to have a plastic modulus independent of octahedral normal stress until the 'small' strains range is exceeded. The *plastic modulus of steel is a function of octahedral normal stress* for a given value of octahedral shear stress.

† When the present author intensified his research on elasto-plastic strains in 1945 it was hoped to clarify some of the difficulties apparent at even that time. Lack of mechanic assistance and meagre financial support forced the author back to analytical methods and the gleaning of measurements from other experimenters as further difficulties became obvious and demanded a programme requiring physical effort by more than one man. The methodical survey of the stress-strain behaviour of one metal, at least, over two-dimensional stress-space, that should have been done between 1945 and 1950, still needs to be done in March 1954.

This controverts the hypothesis of other writers [35, 36, 37, 38, 46, 55, 65] that plastic stress-strain relations are independent of octahedral normal stress. Such an hypothesis has arisen from an idea that, since the first stress invariant, and hence octahedral normal stress, is isotropic, or invariant with reorientation of axes, it will have the same physical effect of not influencing plastic straining just as is found experimentally for isotropic, hydrostatic pressure [58]. In fact, the first stress invariant and hydrostatic pressure (apart from sign) are similar in merely a mathematical sense but are physically different. The first stress invariant has three directional components, in general, whereas hydrostatic pressure is truly scalar in character.

16. The Tresca, Saint-Venant, Lévy, Prandtl, Reuss incremental plastic strain theory and the tests on thin-walled metal tubes

Volume I, article **IX**,H gives the history of this incremental theory very briefly. The relationship between the experimental evidence subsequently submitted here and the form the theory has assumed with present-day writers requires a brief recapitulation of the Tresca, Saint-Venant theory, given in 1870 [32], and its subsequent development by Lévy in 1870 [33]. Body force was considered by Saint-Venant but it will be neglected here to simplify the equations without losing the essentials of the argument. Notation is changed to suit the present treatise.

16.1. **Hydrodynamical theory for an incompressible fluid.** The flow of metals during extrusion tests by Tresca, in 1870 [19.8], suggested using the kinematical ideas of classical hydrodynamics. Thus, the *motion equation* of a 'particle' of fluid is

$$\operatorname{div}(H\mathfrak{J}) = m[(\mathbf{U}_{;t})_{;t} + \mathbf{U}_{;t} \cdot \nabla \mathbf{U}_{;t}] \tag{16.1}$$

with H the negative of hydrostatic pressure, $\mathfrak{J}$ the idemfactor, m the fluid density, $\mathbf{U}$ the spatial-displacement, t time, $\mathbf{U}_{;t}$ the spatial-velocity. In fact, the left-hand side is usually given as $\nabla(H) = \operatorname{div}(H\mathfrak{J})$.

The *continuity equation* for an incompressible fluid, ensuring that as much matter flows out of an arbitrarily described, spatially fixed surface described in the field of flow as flows into it, is

$$\operatorname{div}(\mathbf{U}_{;t}) = 0 \tag{16.2}$$

16.2. **Data from extrusion tests.** Tresca considered the shape of jets of flowing metal during extrusion and reached two fundamental conclusions, given by Todhunter & Pearson [19.8]. With a constant K

Maximum shear (stress) across any face $= K$. (16.3)

Maximum shear (stress) and maximum slide-velocity are co-directional. (16.4)

Tresca [19.9] suggested that these apply when the metal is in a *fluid*† state and that between this and the primary elastic state there is an *intermediate*‡ state.

Tresca, however, neglected the intermediate state and assumed abrupt yield with continued flow (or zero work-hardening in more recent terms). There seems to be no reference to the fact that **IV**(16.3) is Coulomb's maximum shear-stress yield criterion of 1773 [19.10], so presumably it had been forgotten and overlooked.

16.3. **Tresca, Saint-Venant plastic flow theory.** Neglecting vector stress $\mathbf{S}_z$ and assuming two-dimensional flow with cartesian coordinates $OR_xR_yR_z$, the following mathematical theory was formulated [19.11]. Using the methods of stress extraction in article **III**,1.2 with **IV**(16.3) gives

$$S_{xy}{}^2+\tfrac{1}{4}(S_{xx}-S_{yy})^2 = K^2 \tag{16.5}$$

Treating the strains of article **III**,2.5 as strain-velocity, extracting the shear strain-velocity (the 'slide-velocity'), finding the direction for a maximum and equating to the direction for maximum shear stress to satisfy **IV**(16.4) gives§

$$2e_{xy;t}/(e_{xx;t}-e_{yy;t}) = 2S_{xy}/(S_{xx}-S_{yy}) \tag{16.6}$$

This is precisely the statement for coaxiality of principal normal strain-velocity and stress as in articles **III**,2.8, **III**,1.3.

The continuity condition **IV**(16.2) gives

$$(\mathbf{U}_{x;t})_{;x}+(\mathbf{U}_{y;t})_{;y} = 0$$

or, for infinitesimal strains,

$$e_{xx;t}+e_{yy;t} = 0 \tag{16.7}$$

† Present author refers to this as 'flow-strain' in volume I.

‡ This is the stable, elasto-plastic state of the present treatise.

§ The $2e_{xy;t}$ here is given as $e_{xy;t}$ by Saint-Venant. Without the 2 the shear strain-velocity is not the component of a dyadic transformable invariantly with reorientation of axes. See volume I, article **III**,H.

Tresca attempted to proceed on purely kinematical lines, considering only strain-velocities without reference to stress except, rather vaguely, in relation to the 'plastic modulus' K in **IV**(16.5), while his motion equation was to be just **IV**(16.1) as for an inviscid fluid. Saint-Venant† replaced the hydrostatic dyadic $(H\mathfrak{J})$ in **IV**(16.1) by the stress dyadic $\mathfrak{S}$ so that it applied to the viscous case. This gives‡

$$\left.\begin{aligned} S_{xx;x}+S_{xy;y} &= m[(U_{x;t})_{;t}+U_{x;t}(U_{x;t})_{;x}+U_{y;t}(U_{x;t})_{;y}] \\ S_{yy;y}+S_{yx;x} &= m[(U_{y;t})_{;t}+U_{y;t}(U_{y;t})_{;y}+U_{x;t}(U_{y;t})_{;x}] \end{aligned}\right\} (16.8)$$

Equations **IV**(16.5) to **IV**(16.8) give the basis on which others, as well as Saint-Venant, built further.

16.4. **Lévy's extension to three-dimensional flow.** Lévy, in 1870 [19.13, 33], extended the Tresca, Saint-Venant theory to three-dimensional flow. The equation analogous to **IV**(16.5) is complicated, of fourth degree in K and sixth degree in the stress components. It is of interest that the so-called *deviatoric normal stresses* like

$$S_{xx}' = S_{xx}-\sigma \qquad (16.9)$$

to use a modern term, make their appearance with the octahedral normal stress

$$\sigma = \tfrac{1}{3}(S_{xx}+S_{yy}+S_{zz}) \qquad (16.10)$$

Lévy finds the six forms like the two in **IV**(16.6) ensuring coaxiality of maximum shear strain-velocity and maximum shear stress (or else coaxiality of principal normal strain-velocities and stresses). However, he rearranges the equations as

$$e_{xy;t}/S_{xy} = (e_{xx;t}-e_{yy;t})/(S_{xx}-S_{yy}) = \ldots \qquad (16.11)$$

with four more similar terms.

The coefficient of fluid viscosity 2μ is defined as the shear stress per unit time-rate of change of shear strain. Therefore, **IV**(16.11) can be written as

$$e_{xy;t} = \tfrac{1}{2}\mu^{-1}S_{xy} \qquad e_{xx;t}-e_{yy;t} = \tfrac{1}{2}\mu^{-1}(S_{xx}-S_{yy}) \qquad (16.11')$$

† Saint-Venant [19.12] generously 'attributes to Tresca a keen appreciation of theory; he was no mere empiricist, as many have erroneously believed'.

‡ Application of this equation to constant, simple tensile stress, with zero body force and Trouton's coefficient of viscous extension, leads to an anomaly if the non-linear term $\mathbf{U}_{;t}\cdot\nabla\mathbf{U}_{;t}$ (of Euler, in 1755 [153]) of the acceleration is retained. Navier, in 1822 [154], and Cauchy, in 1827 [155], gave **IV**(16.8). Volume III on 'Fluidity' in the present treatise discusses the matter. (Author, February 1954.)

with four more similar terms. Otherwise, with a flow transverse contraction ratio $q^F = \frac{1}{2}$ for an incompressible substance there can be used Trouton's *coefficient of viscous extension* [66, 67], say,

$$\alpha = 2\mu/(1+q^F) = 4\mu/3 \qquad (16.11'')$$

16.5. **Lévy criticises Saint-Venant.** For the plane flow treated by Saint-Venant

$$e_{zz;t} = 0 \qquad (16.12)$$

and the continuity condition **IV**(16.7) gives

$$e_{yy;t} = -e_{xx;t} \qquad (16.13)$$

From two of the terms in the coaxiality equations **IV**(16.11), together with **IV**(16.13),

$$2e_{xx;t}/(S_{xx}-S_{yy}) = -e_{xx;t}/(-S_{zz}+S_{yy})$$

or

$$S_{zz} = \tfrac{1}{2}(S_{xx}+S_{yy}) \qquad (16.14)$$

Lévy [19.14] derived this and criticised Saint-Venant for neglecting to discuss it in his paper.

16.6. **Quasi-stationary flow.** Saint-Venant, in 1871 [19.14], proposed that, when velocity $\mathbf{U}_{;t}$ is small, then it and $\mathbf{U}_{;tt}$ should be neglected in **IV**(16.8) to give the right-hand side quasi-zero. The two quasi-equilibrium stress equations could be solved by an Airy stress function to be found from the second-order second-degree partial-differential equation given when it is substituted in the yield criterion **IV**(16.5).

16.7. **Stress discontinuity.** The physical hypothesis that the substance is either in the elastic or in the fluid (i.e. plastic) state introduces stress discontinuities at the surfaces separating elastic and plastic zones. Saint-Venant [19.14] examined this effect mathematically.

16.8. **Mises incremental plasticity theory.** Noting that $(e_{xy;t})\delta t = \delta e_{xy}$, ..., the increments of strain in time δt, then the coaxiality equations **IV**(16.11) become

$$\delta e_{xy}/S_{xy} = (\delta e_{xx}-\delta e_{yy})/(S_{xx}-S_{yy}) = \ldots \qquad (16.15)$$

If Lévy's deviatoric normal stresses in **IV**(16.9) are substituted in these coaxiality equations the form is not altered.

Again, if each of the terms is equated to a first-order small-quantity *flow modulus* δf, then there are six equations like

$$\delta e_{xy} = \delta f(S_{xy}) \qquad \delta e_{xx} - \delta e_{yy} = \delta f(S_{xx}' - S_{yy}') \qquad (16.16)$$

R. von Mises [34], in 1913, suggested that differences in the normal stress equations could be separated to give six expressions like

$$\left.\begin{aligned} \delta e_{xy} &= \delta f S_{xy} \\ \delta e_{xx} &= \delta f S_{xx}' = \delta f[S_{xx} - \tfrac{1}{3}(S_{xx} + S_{yy} + S_{zz})] \end{aligned}\right\} (16.17)$$

This suits the hypothesis that the octahedral normal stress σ, of **IV**(16.10), does not influence the plastic stress-strain relations. The idea follows from the identification of σ with a 'hydrostatic' stress because of its invariant value with reorientation of axes and equality on the eight octahedral planes and the experimental fact that great hydrostatic pressure does not induce yield. Further, a 'hydrostatic' stress cannot induce volume change or dilation in an incompressible substance.

16.9. **Prandtl, Reuss elasto-plastic incremental theory** The Tresca, etc., von Mises flow theory implies an ideally plastic (or flowing) substance without an elastic strain component. L. Prandtl [35], in 1924, introduced an incremental elastic strain and used **IV**(16.17) explicitly for the plastic component in plane strain. A. Reuss [36], in 1930, generalised the theory for three dimensions. Thus, there are six equations like

$$\left.\begin{aligned} \delta e_{xy} &= \delta e_{xy}^{P} + \delta e_{xy}^{E} \\ &= \delta f S_{xy} + (1+q^{E})\psi^{E}\delta S_{xy} \\ \delta e_{xx} &= \delta e_{xx}^{P} + \delta e_{xx}^{E} \\ &= \delta f S_{xx} - \tfrac{1}{3}\delta f(S_{xx} + S_{yy} + S_{zz}) \\ &\quad + (1+q^{E})\psi^{E}\delta S_{xx} - q^{E}\psi^{E}(\delta S_{xx} + \delta S_{yy} + \delta S_{zz}) \end{aligned}\right\} (16.18)$$

16.10. **Contemporary writers.** The book by R. Hill [37],† in 1950, uses the Reuss theory exclusively. The genealogy of the theory from the Tresca flow seems to be not understood by Hill when the following quotation [37:1] is considered:‡

'The reader should guard against a facile analogy with the

† Explicit reference is given to this book because the relevant topics are otherwise diffused.

‡ The notation and equation number are altered to suit that of the present treatise.

equations for a Newtonian viscous fluid: $e_{xy;t} = S_{xy}'/2\mu$ where the viscosity μ is a material constant, and the rate of shear is directly linked with the applied stress. Although IV(16.17) can be written as $e_{xy;t} = f_{;t}S_{xy}'$ the relations between stress and strain are still independent of time since they are dimensionally homogeneous. Also f is certainly not a material constant, but varies during the deformation.'

Noting the step taken in article IV,16.8 to give increments of strain in time δt rather than time-rate of strain, it is not surprising that time does not appear explicitly in the Reuss theory, although it is certainly implicit since it deals with flow. Hill's statement that f is not a material constant is considered in relation to experiment in article IV,16.13. Comparison of IV(16.16) with IV(16.11′) shows that, in fact, for the fluid state treated by Lévy and, hence, Mises,

$$\delta f = \tfrac{1}{2}\mu^{-1}\delta t = 3\delta t/(2\alpha) \qquad (16.19)$$

with Trouton's coefficient of viscous extension α. Again, for example, the book by W. Prager [38], in 1951, uses the Mises theory for 'ideal plasticity' with δf not a material constant (i.e. it is not a stress-strain parameter).

16.11. **A formulation† alternative to that of Mises.** An alternative step is allowable in place of that taken in passing from IV(16.15) to IV(16.16). In place of δf use the first-order small quantity of $f'\delta(\ )$, with f' a scalar plastic flow function and $\delta(\ )$ a first-order small-quantity incremental operator on any function introduced within the brackets. Equating each term of IV(16.15) to $f'\delta(\ )$ then gives the coaxiality conditions

$$\left.\begin{aligned} \delta e_{xy} &= f'\delta(S_{xy}) = f'\delta S_{xy} \\ \delta e_{xx} - \delta e_{yy} &= f'\delta(S_{xx}' - S_{yy}') = f'(\delta S_{xx}' - \delta S_{yy}') \end{aligned}\right\} (16.20)$$

with four more similar equations.

Separating the normal increment stress terms as in Mises' hypothetical approach gives the increment stress, increment strain equations

$$\left.\begin{aligned} \delta e_{xy} &= f'\delta S_{xy} \\ \delta e_{xx} &= f'[\delta S_{xx} - \tfrac{1}{3}(\delta S_{xx} + \delta S_{yy} + \delta S_{zz})] \end{aligned}\right\} (16.21)$$

with four more similar expressions. The extension to elasto-plastic flow is done readily as in article IV,16.9.

† Author, 1950.

16.12. **The Mises, Prandtl, Reuss formulation for elasto-plastic strain compared with the alternative formulation.** More briefly, with the partial-increment strain and stress dyadics $\Delta\mathfrak{M}$, $\Delta\mathfrak{S}$, stress dyadic $\mathfrak{S}$, idemfactor $\mathfrak{J}$, the elastic 'tangent' stress-strain parameters $G^E = (1+q^E)\psi^E$, $F^E = -q^E\psi^E$, the Mises etc. theory of article **IV**,16.9 has a partial-increment elastic strain dyadic equal to that of the alternative formulation in article **IV**,16.11. Thus, in both theories,

$$\Delta\mathfrak{M}^E = (G^E+F^E\mathfrak{J}\mathfrak{J}:)\Delta\mathfrak{S} \tag{16.22}$$

The partial-increment plastic strain dyadics for the two theories are

$$\Delta\mathfrak{M}^P(\text{Mises etc.}) = \delta f(1-\tfrac{1}{3}\mathfrak{J}\mathfrak{J}:)\mathfrak{S} \tag{16.23}$$

$$\Delta\mathfrak{M}^P(\text{Altern.}) = f'(1-\tfrac{1}{3}\mathfrak{J}\mathfrak{J}:)\Delta\mathfrak{S} \tag{16.24}$$

while, for both theories,

$$\Delta\mathfrak{M} = \Delta\mathfrak{M}^I+\Delta\mathfrak{M}^E \tag{16.25}$$

Comparison with volume I, article **IV**,4 shows that, in **IV**(16.23), the Mises etc. 'plastic' strain theory is essentially the 'flow' theory of the present author. Thus, for an incompressible flow

$$\Delta\mathfrak{M}^P(\text{Mises etc.}) = \Delta\mathfrak{M}^P(\text{Author}) \tag{16.26}$$

while, for stable, incompressible 'plastic' straining,

$$\Delta\mathfrak{M}^P(\text{Altern.}) = \Delta\mathfrak{M}^P(\text{Author}) \tag{16.27}$$

16.13. **Theoretical values of the stress-strain parameters.** R. Hill, for example, states emphatically that 'f is certainly not a material constant', as in article **IV**,16.10, but from equation **IV**(16.19), with Trouton's coefficient of viscous extension α,

$$\delta f = 3\delta t/(2\alpha)$$

so that

$$f = 3(\delta t = 1)/(2\alpha) \tag{16.28}$$

Write **IV**(16.23), **IV**(16.24) for the principal directions in a plane two-stress using the present author's

$$f' = (1+q^P)\psi^P = 3\psi^P/2 \tag{16.29}$$

with $q^P = \frac{1}{2}$ for an incompressible substance. Thus, without writing the increments of strain for the third direction,

$$\left.\begin{aligned}\delta e_i^P(\text{Mises etc.}) &= (\delta t/\alpha)(S_i-\tfrac{1}{2}S_j)\\ \delta e_j^P(\text{Mises etc.}) &= (\delta t/\alpha)(S_j-\tfrac{1}{2}S_i)\end{aligned}\right\} \tag{16.30}$$

$$\left.\begin{aligned}\delta e_i^P(\text{Altern.}) &= \psi^P(\delta S_i-\tfrac{1}{2}\delta S_j)\\ \delta e_j^P(\text{Altern.}) &= \psi^P(\delta S_j-\tfrac{1}{2}\delta S_i)\end{aligned}\right\} \tag{16.31}$$

If the stresses and increment strains are known experimentally then the value of α, and hence f, can be examined as a material parameter, in denial of Hill's hypothetical statement.

Both theories deal with restricted isotropy, so that the hypothetical isotropy of the stress-strain parameters needs experimental justification. Introducing the 'partial-strains' of article III,2 and attaching appropriate directional subscripts to α and f gives

$$\left.\begin{aligned} \frac{\delta\epsilon_j^P S_i}{\delta\epsilon_i^P S_j} &= \frac{\alpha_i}{\alpha_j} = \frac{f_j}{f_i} = \beta(\text{Mises etc.}) \\ \frac{\delta\epsilon_j^P \delta S_i}{\delta\epsilon_i^P \delta S_j} &= \frac{\psi_j^P}{\psi_i^P} = \beta(\text{Altern.}) \end{aligned}\right\} \quad (16.32)$$

say. The ratio β is unity if isotropy of parameters is justified, so that directional subscripts can be removed.

Again, Hill states[37.4] hypothetically '. . . the ratios of the components of the plastic strain-increment are functions of the current stress but not of the stress-increment'. The present author has already examined the experimental functional relationship of increment stress and plastic increment strain in this chapter, so no further comment is required. The experimental relationship between plastic increment strain and total stress is given in article IV,16.14.

Yet again, Hill states [37.2, 37.3] hypothetically that f is a function of only the second and third invariants of the deviatoric stress dyadic (for which the first invariant is zero). That is, f is independent of $(S_{xx}+S_{yy}+S_{zz}) = 3\sigma$. This follows from assuming that σ is physically analogous to hydrostatic pressure H (or its negative), but the present author denies this. Although the experimental evidence is scrappy (March 1954), the present author has already shown tentatively that ψ^P is a function of σ. Whether f is or is not a function of σ needs experimental examination and is not amenable to mere hypothesis.

16.14. **Experimental examination of isotropy of the stress-strain parameters.** The test by Peters, Dow & Batdorf applying axial torsion and compression on a thin-walled duralumin tube was analysed for isotropy of the flow modulus f over the loading range shown in Fig. IV,14.2. Substituting the experimental values of stress and increment partial-strains in

equations IV(16.32) gives the values of the ratios f_j/f_i and ψ_j^P/ψ_i^P in Fig. IV,16.1.

Since the ratio f_j/f_i is not unity then flow modulus f is not isotropic, as hypothesised for duralumin by Hill, for example. The erratic variation in the ratio seems to indicate that the 'flow' theory of equation IV(16.23) is not applicable to the thin-walled tubes tests in which the strain state was stable (i.e. independent of time) under a given load and did not flow (i.e. depend on time) indefinitely with maintenance of load, as implied by the flow theory [37.5], to give a corresponding coefficient of viscous traction

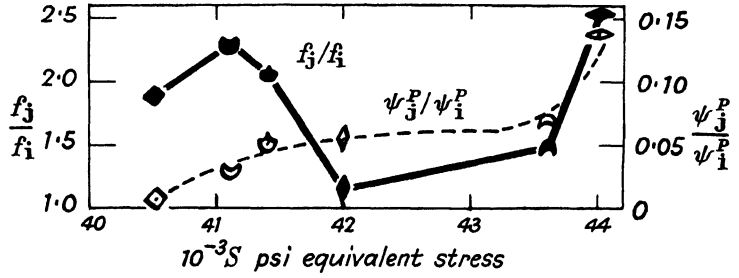

FIG. IV,16.1.—The plastic flow modulus f of the Mises, Prandtl theory is isotropic when the ratio f_j/f_i equals unity. The erratic changes in value of the ratio suggest that total stress and plastic increment strain are not related functionally in the *stable* straining of thin-walled metal tubes, at least. The plastic modulus ψ^P is, also, not isotropic, but this is readily rationalised physically from Fig. IV,14.2, as the duralumin does not behave elasto-plastically homogeneously initially towards a stress superimposed on an existing stress state.

for the 'stress-fluidity' state of duralumin. Analysis of the results for steel gives an even more anisotropic [63] flow modulus.

The reason for the zero value of ψ_j^P/ψ_i^P when S_j is zero and its increase with this stress is discussed in article IV,14.2. There is a functional relationship between increment stress and plastic increment strain in denial of Hill's hypothesis [37.4] quoted in article IV,16.13.

16.15. **A possible confusion due to terminology.** Consideration of articles IV,16.1 to here shows that some confusion could arise due to using 'plasticity' to mean two distinct physical processes. Tresca visualised three states for a metal [19.9], (i) elastic, (ii) transition from elastic to fluid, (iii) fluid (i.e. stress-fluidity, say), to suit the visual effects in extrusion. Saint-

Venant [19.9] first called the *stress-fluidity* 'hydrostereo-dynamics' and then 'plastico-dynamics', while Pearson, in 1893 [19.9], called it just 'plasticity'. The reader should note that 'plasticity' is still stress-fluidity in which deformation continues indefinitely with time according to contemporary writers [37.5].

Subsequent to Pearson, writers and experimenters on small, stable, permanent strains, in metals particularly, have referred to them as 'plastic'. These are clearly Tresca's transition range of strain that he, Saint-Venant and others onward simply neglected. Thus, R. Hill [37.6], for example, states that: 'In tension, for example, if the stress is maintained at the yield point an arbitrary amount of extension may be produced.' This is clearly stress-fluidity with an abrupt primary yield and no work-hardening. In particular problems, such as pressure in holes internal to a body, the stress-fluidity theory leads to discontinuities of stress and/or its gradients at the interfaces between elastic and stress-fluidic zones [46.1]. The application of a stress-fluidic theory to cases where experiment shows that the straining is stable is undesirable. (See also volume I, pp. 226, 267.)

The present writer has treated Tresca's 'transition' as elasto-plastically stable (see volume I, chapter IX) and the stress-fluidic straining is referred to as 'flow-strain' for such a time-dependent effect. (See volume I, chapter IV.) Stress discontinuities do not occur at elastic, elasto-plastic interfaces nor at elasto-plastic, flow-strain interfaces.

17. Yield criteria

The necessity for a criterion able to predict the appearance of permanent or plastic deformation was seen by the earliest writers on strength of materials. (See volume I, chapter VIII.) The two approaches, (i) atomistic, (ii) phenomenological, appear to have arisen more or less together in the eighteenth century but came into violent, apparent conflict in the nineteenth century largely on the question of elastic stress-strain relationships.

17.1. **Atomistic approach.** The phenomenological approach is used in this treatise because there is still insufficient knowledge of atomic physics to formulate a theory analysing the deformation of all real substances. However, some of the effects and ideas should be remembered to avoid rigidity of thinking.

Newton's ideas on interatomic forces were adapted and modified gradually [19] to the conception of a *potential trough* [116] between two adjacent atoms. At zero linewise relative displacement (or linewise force) between the two atoms the potential is a minimum. Decrease of interatomic distance (compression) or increase (extension) increases the potential from its 'trough' value. This leads to the idea that an attractive force (following one law of change with interatomic distance) cancels a repulsive force (following another law of change) at their equilibrium distance apart. According to this, a compression requires increasing force but an extension requires a tensile force reaching a maximum from which it decreases with increasing distance. This maximum is the *yield force* for the two atoms.

The occurrence of 'slip' along definite planes at the inception of yield in macroscopic specimens of engineering metals was noted by Lüders in 1860 [117]. Such specimens are an aggregate of small crystals, so, in the second quarter of this century, several physicists examined the simpler case of large single crystals of metal grown especially for the purpose, as these would seem to be ideal, or perfect, *atomic lattices*. Under simple loading, slip was found to occur along definite crystallographic planes [116.2] but it did not proceed smoothly; a series of many audible 'clicks' [118] were noted at each 'jump' of slip.

The single crystals were found to work-harden, and this presents a difficulty for explanation if the crystal lattice is perfect. K. Yamaguchi [119] and G. I. Taylor [120] independently, in 1928, suggested *local distortions* of the atomic lattice with the local stresses greater than the average for the plane. This concept was extended in 1934 by G. I. Taylor [121], M. Polanyi [122] and E. Orowan [123] independently, by allowing the local distortions or *dislocations* to migrate up to the crystal boundary.

The mere diffusion of such dislocations does not explain changes in volume during the plastic straining of engineering metals [84, 48]. W. Boas, in 1948 [11], studied aggregates of metal crystals and found that slide strain (and hence dislocations effectually, presumably) are propagated across crystal boundaries and initiate severe residual strains that can cause macroscopic plastic volume change. Thus, the analysis of yielding of an aggregate of crystals needs more data than that given by studies of single crystals. Such work is proceeding in several countries [137 to 140].

17.2. **Phenomenological approach to yield.** Just as rapid progress was made by Cauchy in adopting the phenomenological approach to stress, then so is rapid progress possible to secure a criterion of yield inception by phenomenological observations on the substances concerned. The acceptance of macroscopic effects is statistical in the sense that no account is taken of atomistic details. Therefore, attention must be given to phenomenological stress, elastic strain and energy of elastic straining and one or more of these used as a yield criterion.

P. W. Bridgman, in 1912 [58], showed that substances do not yield under great hydrostatic pressures. This led to the rejection of a number of hypotheses involving various observable quantities but the retention of *maximum shear stress* and *distortional energy* as criteria. Volume I, chapter VIII discusses this in detail for three-stress. The experimental evidence available (March 1954) is for virtually two-stress only, so here the detailed discussion covers only this latter case.

17.3. **Maximum shear stress criterion of yield inception.** Coulomb, in 1773 [19.10], suggested the maximum shear stress as a criterion of yield inception. Denoting the arithmetical value of the shear stress for *primary yield* by T gives, from article III,1.8 for a two-stress,

$$\left.\begin{array}{ll} T = |\tfrac{1}{2}(S_{\mathrm{i}}-S_{\mathrm{j}})| & \text{when } S_{\mathrm{i}},\ S_{\mathrm{j}} \text{ are of opposite signs so that } |S_{xx}S_{yy}| < S_{xy}{}^2 \\ T = |\tfrac{1}{2}S_{\mathrm{i}}| & \text{when } S_{\mathrm{i}},\ S_{\mathrm{j}} \text{ are of the same sign with } S_{\mathrm{i}} \text{ arithmetically the greatest so that } |S_{xx}S_{yy}| > S_{xy}{}^2 \\ T = |\tfrac{1}{2}S_{\mathrm{j}}| & \text{when } S_{\mathrm{i}},\ S_{\mathrm{j}} \text{ are of the same sign with } S_{\mathrm{j}} \text{ arithmetically the greatest so that } |S_{xx}S_{yy}| > S_{xy}{}^2 \end{array}\right\} \quad (17.1)$$

The six-sided figure in Fig. IV,17.1(a) is given on using these three conditions with T held constant in each of the three cases.

This six-sided figure is the intersection by the plane $S_{\mathrm{k}} = 0$ of the hexagonal right cylinder with its axis in the octahedral direction of the stress space, as in Fig. IV,17.1(b), viewing in the negative octahedral direction.

17.4. **Distortional energy criterion of yield inception.** This criterion was enunciated by Maxwell in 1856 [144] but appears

to have been overlooked or insufficiently publicised. Independently, from slightly different approaches, it was proposed again by M. T. Huber in 1904 [145], R. von Mises in 1913 [34] and H. Hencky in 1924 [146]. Volume I, article **VIII**,3.3 gives the two-stress distortional energy yield criterion as

$$S_i^2 - S_i S_j + S_j^2 = S^2 \qquad (17.2)$$

with S the simple tensile yield stress. This is the equation of the ellipse in Fig. **IV**,17.1(a) with the positive, major semi-axis at

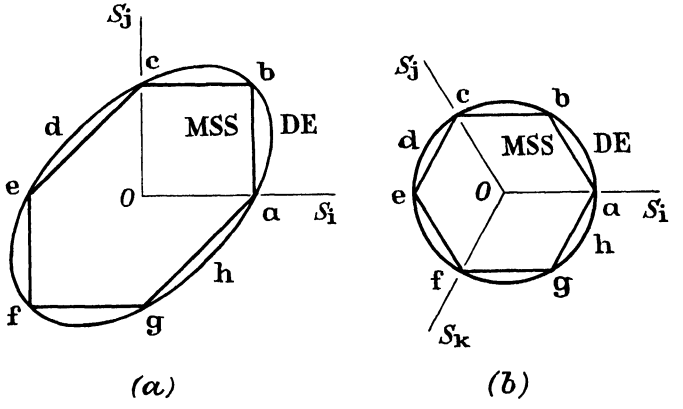

FIG. **IV**,17.1.—Surfaces of yield for the maximum shear stress (MSS) and deformational energy (DE) criteria. Fig. (a) is for two-stress with the six-sided figure for maximum shear stress and the ellipse for deformational energy. Fig. (b) is a view along the axis of the right circular and hexagonal cylinders of yield in the three-stress space. The intersection of these cylinders by the plane resulting when one stress is zero gives Fig. (a).

45° to S_i and the ratio of the length of the axes equal to $\sqrt{3}$. This circumscribes the six-sided figure of the maximum shear stress criterion.

The ellipse is the intersection of the plane $S_k = 0$ with the right circular cylinder shown in Fig. **IV**,17.1(b) of radius $\sqrt{(2/3)}S$. The circular cylinder circumscribes the hexagonal cylinder. The analysis of experimental results is done more conveniently by 'flattening' the mutually orthogonal axes of Fig. **IV**,17.1(b) into the octahedral plane, so that the circle in Fig. **IV**,17.2 is $\sqrt{(3/2)}$ times greater in radius than Oa. (See volume I, article **VIII**,3.6.) This allows a direct plot of stress values along the oblique axes.

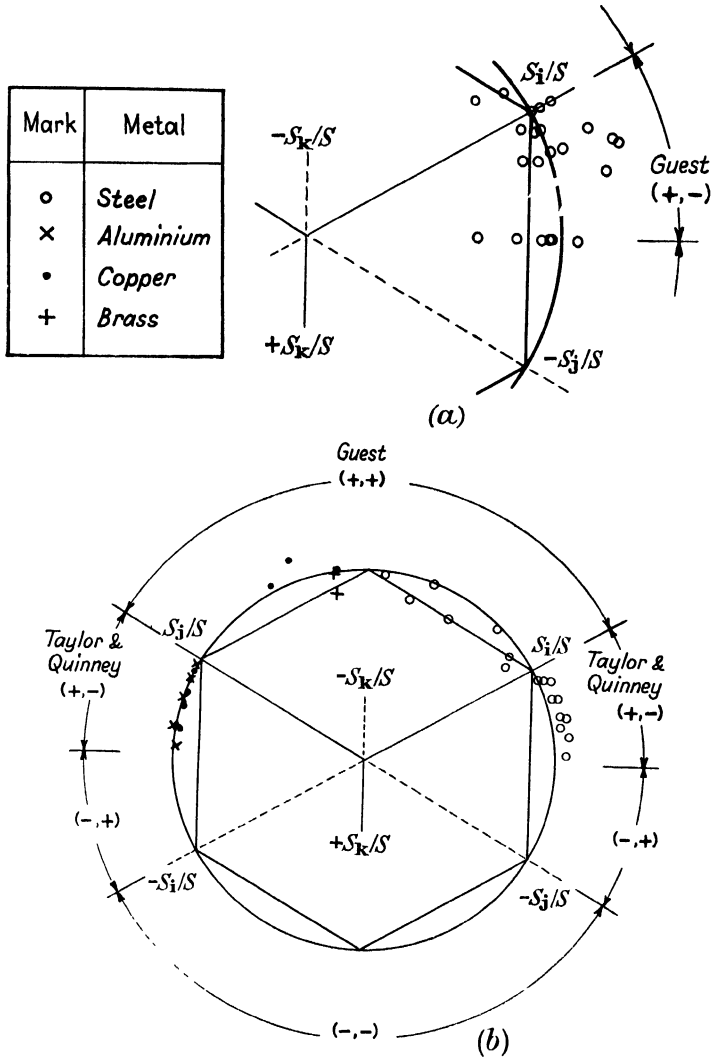

FIG. IV,17.2.—The hexagon for the MSS theory and the circle for the DE theory as in Fig. IV,17.1(*b*). The DE circle is of unit radius because each principal normal stress has been divided by the appropriate simple tensile primary yield stress. The figure has been used as virtually two-stress since S_k is negligible in the tests considered. There are no available measurements to cover the (−, +) and (−, −) zones or for other materials than those shown. There are no measurements for three-stress loading.

Note that, for three-stress, a point on the plane circle is the projection of the generator of the cylinder, so that an indefinite number of three-stress values can be associated with it. However, codes are readily devised to show the number of positive and negative components for each observation.

17.5. **Experiments to test the yield criteria.** Thin-walled tubes can be loaded with fairly well determined stress distributions induced by axial tension or compression, axial torsion, internal and/or external pressure. For any one or combination of these loads the average stresses induced can be calculated directly from the loads and the dimensions of the tube. This assumes that there are no steep stress gradients at the 'skin', as discussed in article VII,6.5.

Solid or thick-walled hollow bars submitted to axial tension or compression, axial torsion, flexure, internal and/or external pressure are not satisfactory tests, because a theory of stress and strain is required to give the stress distribution. Assumptions (i.e. distributions given by a theory) for the stress distribution due to torsion, for example, may be astray. (See the discussion of Saint-Venant's theory of torsion in chapters XI, XII presenting alternatives from the present author's viewpoint.)

Because of this possible difficulty in knowing the stress distributions, the tests by E. L. Hancock [125], W. A. Scoble [126], L. B. Turner [128], W. J. Crawford [129], G. Cook & A. Robertson [130], J. Seigle & F. Cretin [132] and M. Ennslin [136] during the period 1906–28 will not be discussed here in detail. A concise account is given by E. H. Salmon [1.1]. For the same reason, the meticulous tests of mild steel by J. L. M. Morrison, in 1940 [134], are not presented here. The apparent effect of specimen size, as noted by Morrison, may be attributable to using the Saint-Venant distribution of torsional stresses.

Tests applying tension and torsion singly and in pairs on thin-walled steel tubes by E. L. Hancock [125], in 1906, gave results similar to those of J. J. Guest [124], in 1900, so they are not repeated here. Subsequent to Guest, who gave his measurements clearly in tabular form, writers (or, perhaps, editors) have given results in the form of curves not allowing analysis or replotting in other forms by other writers following the original author to check his conclusions from other viewpoints. For this reason and/or the foregoing objections to the form of specimen, the tests by

W. Mason [127], W. Lode[141], G. Sachs [137], H. L. Cox & D. G. Sopwith [138], J. M. Lessells & C. W. Macgregor [142], E. A. Davis [143], U. Dehlinger [139], N. K. Snitko [140], in the period 1909–48, will not be discussed here.

This sifting leaves only the tests by J. J. Guest in 1900 and those of G. I. Taylor & H. Quinney [133] in 1934. This latter must be objected to as not giving tabulated measurements, but the printed curves are clear enough to extract fairly accurate values for plotting into Fig. IV,17.2.

17.6. **J. J. Guest.** In 1900 [124], J. J. Guest performed the first comprehensive series of tests to examine the criteria of yield inception. Guest loaded thin-walled tubes of steel, copper and brass with axial tension, axial torsion and internal fluid pressure. These loads were applied singly and in pairs. Considering Fig. IV,17.1(*a*) shows that such loading can cover the zone h...a...b...c...d of that two-stress space.

Each tube was subjected to a sequence of different loadings numbering from six to twenty but without methodical changes of the stress components. Guest states [135] that the tubes were annealed lightly between each test. However, the simple tensile yield stress of the same tube was significantly different, depending on the previous tests, so that the annealing was not effective. Thus, the simple tensile yield in pounds per square inch for his steel tube number II is 60 500, 55 500, 57 800; for III is 34 400, 33 000; for VII is 39 200, 38 100; for VIII is 40 200, 41 200; for IX is 34 000, 36 100; for his copper tube X is 10 630, 12 050, 12 750; for his brass tube XII is 17 400, 20 100.

The unmethodical applications of load and the ineffective annealing make it difficult to analyse Guest's tests either dimensionally or non-dimensionally. Fig. IV,17.2(*a*) gives 22 of his 101 measurements on steel using the lowest value of simple tensile yield in each tube to allow comparable plotting in the (+, −) zone of the two-stress space. The scatter is seen to be too serious to allow examination of the relative merits of the MSS and DE criteria of yield inception.

No other measurements are available (March 1954) for the (+, +) zone of Fig. IV,17.2, so Guest's were used as follows. The (+, +) loading immediately preceding or succeeding a simple tensile test of a given tube was plotted as shown using that simple tensile stress to give the non-dimensional values.

Even with this favourable treatment the measurements scatter badly.

17.7. **G. I. Taylor & H. Quinney.** In 1934[133], G. I. Taylor & H. Quinney tested thin-walled tubes of steel, copper and aluminium by applied axial tension and torsion singly and together. Each tube was annealed carefully to standardise the materials as far as possible. The loading covered h...a or c...d of the two-stress space in Fig. IV,17.1(*a*).

The object of their tests was to find out if the DE theory of primary yield inception is superior to the MSS theory and to compare the results with those of W. Lode[141], whose measurements were suspected as influenced by anisotropy of his iron, copper and nickel tubes. Lode applied axial tension and fairly small internal pressure to induce circumferential tension in the thin-walled tubes. Thus, his curvilinear, virtually two-stress loading falls into zone a...b...c of Fig. IV,17.1(*a*) or the (+, +) of Fig. IV,17.2. Therefore, the Taylor & Quinney tests, which fall into the (+, −) zone, are strictly not comparable with those of Lode in another part of stress space.

Taylor & Quinney plotted as orthogonal coordinates the non-dimensional stresses $S_{z\theta}/S$, S_{zz}/S with applied shear stress $S_{z\theta}$, applied axial normal stress S_{zz} and simple tensile yield stress S. The MSS theory defines an ellipse with semi-axes of lengths 1, $\frac{1}{2}$, while the DE theory defines an ellipse with semi-axes of lengths 1, 0·577 for these coordinates. Their results for copper and aluminium are almost coincident with their DE ellipse, but those for steel lie consistently outside it.

The measurements extracted from the curves of Taylor & Quinney are plotted in Fig. IV,17.2 to show their position in the stress space.

17.8. **Conclusions.** The tests by Taylor & Quinney establish the superiority of the DE theory over the MSS theory in the (+, −) zone of the stress space for carefully annealed copper, aluminium and steel. Increase of the simple tensile yield stress S by only about 5 per cent could bring their readings for steel on to the DE circle in Fig. IV,17.2. Such an error in estimation is possible for steel.

The tests by Guest, even when selected rather arbitrarily in their favour, have too great a scatter in the (+, +) zone for

copper, brass and steel to distinguish between the DE and MSS theories of yield inception. Although the tests by Lode cannot be plotted here they apparently justify the DE theory for copper, nickel and iron in the (+, +) zone.

Fig. IV,17.2 has no readings in the (−, +) or (−, −) zones, although the tests by W. Mason[127], in 1909, applying axial tension or compression and internal or external pressure on unannealed and annealed mild-steel tubes would fall into these zones if his results could be plotted here.

For the metals steel, iron, copper, brass, aluminium and nickel mentioned here there are still needed measurements in the (−, +) and (−, −) zones of the two-stress space to justify the DE theory. The DE theory has not been justified for any substance for three-stress loading, although axial tension or compression and pressure internal and/or external to thin-walled tubes can cover all of three-stress space except the (+, +, +) zone.

The DE theory has been justified as superior to the MSS theory over part of stress space for carefully standardised metals. However, the engineer frequently uses metals as supplied in a state approximating to, or worse than, Guest's specimens in view of the preceding processes like extrusion, rolling, etc. and yet he must still predict their behaviour in use. The wide scatter in Guest's measurements, as in Fig. IV,17.2(*a*) for less carefully prepared specimens, suggests that too great an apparent accuracy and complication of mathematical forms in yield prediction could be misleading and time-wasting from the engineer's viewpoint.† There is required a comprehensive programme of tests over two-stress space, at least, of engineering materials as used in practice to give the scatter to be expected. It is likely that the mathematically simple MSS theory is sufficiently accurate in such circumstances. Otherwise, a point in stress space on the MSS hexagon of Fig. IV,17.1(*b*) can be 'factored' to bring it on to the DE circle to take advantage of the physical superiority of the latter theory.

† Professor Guest's paper of 1940 [135] re-examines minutely some of his measurements made in 1900. On this basis, he questions the justification of the DE theory by the tests of Taylor & Quinney and attacks other well-known writers for supporting the DE theory. The present author feels that he is not justified in view of the wide scatter of his measurements when taken as a whole.

Chapter V

HETEROGENEOUS TWO-STRESS EQUATIONS FOR SOLUTION

1. Physical concepts expressed in the two-stress equations of equilibrium deformation

The application of force to the surfaces and particles of a body is visualised as inducing a stress field throughout the deformed body. It is expressed as the stress dyadic $\mathfrak{S}$, of article **III**,1, constituted by the forces acting on the surface of an element locally about the point considered. In the *heterogeneous two-stress* considered here, the magnitudes and directions of the principal normal stresses change from point to point of the coordinate space in either the rectilinearly plane or curvilinearly plane senses. The equilibrium stress equation ensures that each element of the body is in equilibrium under the surrounding applied forces and is, similar to article **IV**,1,

$$\operatorname{div} \mathfrak{S} + m\mathbf{B} = 0 \tag{1.1}$$

The stress acting on a surface of the body with $\mathbf{n}$ the outward unit normal at the point is

$$\mathbf{S}_n = \mathbf{n} \cdot \mathfrak{S} \tag{1.2}$$

This is zero or non-zero at each point of the surface depending on the prescribed loading conditions there.

1.1. **Strain and stress.** The aggregate of relative displacements between each pair of points in the locality of the point considered constitutes the state of strain expressed in the strain dyadic $\mathfrak{M}$ of article **III**,2.5. When it is a two-stress then the strain dyadic is a three-strain; that is, $\mathfrak{M}$ has three principal normal strain components. Conversely, when $\mathfrak{M}$ is a two-strain then $\mathfrak{S}$ is a three-stress. In a sufficiently small locality about the typical point the stress and strain states are quasi-homogeneous. (See volume I, article **I**,4.2.)

The stress-strain relations have been considered in articles **III**,2, **III**,3 for homogeneous stress and strain and can be stated briefly as

$$\mathfrak{M} = \boldsymbol{P} : \mathfrak{S} \tag{1.3}$$

with the stress-strain parameters quadadic $\boldsymbol{P}$ and are applied to the quasi-homogeneous state about each point of the heterogeneously strained body.

1.2. **Strains compatibility.** The strain dyadic must be single-valued and continuous from point to point of the deformed body. Volume I, article III,5.3 shows that this is satisfied when

$$\text{curl } \mathfrak{M} = 0 = \text{curl } (\boldsymbol{P} : \mathfrak{S}) \tag{1.4}$$

This is the strains compatibility condition.

1.3. **Displacements of points.** The analysis of deformation involves the observation of the displacement of points of the body, relative to some suitable reference frame, and relating these displacements to the forces causing them. The trivial, but easily visualised, case of simple tension of article II,3.5 shows that the use of a spatially fixed reference to observe spatial-displacement **U** allows the appearance of whole-body convection-displacement $\mathbf{C}^{wb}$, due to whole-body rotation, as a component of **U** which cannot be related to the stress field and hence to the applied forces relative to the body. The stresses, and hence forces, must be related to straining-displacement **D** observed relative to the whole-body convected axes as in Fig. II,1.2.

Simple tension is homogeneous stress and strain, whereas the heterogeneous case is considered here. This heterogeneity causes the principal directions line elements to have different directions in the strained and unstrained states, in general, relative to the whole-body convected axes. This is straining-rotation and introduces the straining convection-displacement $\mathbf{C}^{st}$ component of **D**. The difference,

$$\mathbf{D}^* = \mathbf{D} - \mathbf{C}^{st} \tag{1.5}$$

is relative-displacement and shown† to be that given by summing together all the local, differential, relative-displacement observations $d\mathbf{D}^*$ of local observers using locally convected axes to observe strain, and stress, effects. Stated otherwise, the unstrained and strained principal normal strain trajectories constitute a deformable reference relative to which $\mathbf{D}^*$ is observed or, more strictly, is calculated from the $d\mathbf{D}^*$. That is, the deformable body is its own reference to give $\mathbf{D}^*$.

† See volume I, article I,8.

It is very important to notice that *both* **D** *and* **D*** *are in one-one correspondence with the applied forces, and hence with the stress field which is one-one with the strain field.* Therefore, both **D** and **D*** are one-one with the strain field.

1.4. **Doublet vector fields.** Note carefully that **D** cannot be any, arbitrary, continuous vector field function because it must satisfy the geometrical relationship.

$$(\mathbf{R}^{o\ \mathrm{inst}}+\mathbf{D}) = \mathbf{R} = (\mathbf{R}^{o*}+\mathbf{D}^{*}) \tag{1.6}$$

In this sense, the theoretical deformation problem is to establish the two complementary doublet vector fields in the brackets.

Geometrically,

$$\left.\begin{aligned} \mathbf{R}^{o\ \mathrm{inst}}+\mathbf{C}^{\mathrm{st}} &= \mathbf{R}^{o*} \\ \mathbf{D}-\mathbf{C}^{\mathrm{st}} &= \mathbf{D}^{*} \end{aligned}\right\} \tag{1.7}$$

This mere addition and subtraction of the straining convection-displacement field to the components of a doublet allows transition to its complementary doublet.

1.5. **Strain and relative-displacement.** The strain dyadic and relative-displacement are related physico-mathematically by

$$\nabla\mathbf{D}^{*} = \mathfrak{M} \tag{1.8}$$

while

$$\mathbf{D}^{*} = \int_{\mathbf{O}}^{\mathbf{R}} d\mathbf{D}^{*} = \int_{\mathbf{O}}^{\mathbf{R}} d\mathbf{R}\cdot\nabla\mathbf{D}^{*} = \int_{\mathbf{O}}^{\mathbf{R}} d\mathbf{R}\cdot\mathfrak{M} \tag{1.9}$$

with **R** the point to which the value **D*** applies and **O** is the origin of whole-body convected axes.

1.6. **Equivalence of relative-displacement and straining-displacement.** For limiting small deformation $\mathbf{C}^{\mathrm{st}}$ is quasi-zero in comparison with **D**, **D***, $\mathbf{R}^{o\ \mathrm{inst}}$, $\mathbf{R}^{o*}$ as discussed in volume I. It appears physically as the deformation becomes greater, without, however, altering the mathematical equations between the doublet fields in which $\mathbf{C}^{\mathrm{st}}$ is 'concealed' between the components. Thus, in this sense, **D** and **D*** are 'equivalent' and each is in one-one correspondence with the applied forces and, hence, with the stresses. However, these two displacements are physically distinct. (A somewhat similar situation has already been observed in chapter III, where the Poynting effect is shown to be

a 'stretch' and not a 'normal strain' effect, although the two are quasi-equal for a sufficiently small simple shear.)

Thus,

$$\mathbf{D}\left\{\begin{matrix}=\\ \neq\end{matrix}\right\}\mathbf{D}^{*} \text{ for } \left\{\begin{matrix}\text{Infinitesimal}\\ \text{Finite}\end{matrix}\right\}\text{deformation} \qquad (1.10)$$

while, generally, with the sign for 'equivalent to',

$$\mathbf{D} \approx \mathbf{D}^{*} \qquad (1.11)$$

1.7. **Boundary value problems.** Prescribed loading to satisfy $\mathbf{S}_n$ in V(1.2) must also be related to the stress dyadic $\mathfrak{S}$ satisfying the equilibrium stress equation V(1.1) throughout the deformed body.

The substance will have prescribed stress-strain behaviour given in the quadadic $\boldsymbol{P}$, so that the stress dyadic then gives the strain dyadic throughout the deformed body. The quadadic $\boldsymbol{P}$ cannot be completely arbitrary, as it must satisfy the strains compatibility condition V(1.4) throughout the deformed body.

Having $\mathfrak{M}$ then gives $\mathbf{D}^{*}$ by solution of V(1.8) or the consistent statement V(1.9) when the origin of whole-body convected axes has been chosen.

Having $\mathbf{D}^{*}$ then gives $\mathbf{R}^{o*}$ in V(1.6) and using V(1.11) for equivalence of $\mathbf{D}^{*}$ and $\mathbf{D}$, or equivalence of $\mathbf{R}^{o*}$ and $\mathbf{R}^{o\,\mathrm{inst}}$, gives the required doublet field ($\mathbf{R}^{o\,\mathrm{inst}}$, $\mathbf{D}$).

Usually it is easier to solve a given boundary value problem when one coordinate of a given coordinate system remains constant on the boundary surface of the deformed body. Thus, when solving cases of loading on circular holes in plates, for example, it is more convenient to use cylindrical coordinates rather than cartesian coordinates. The various equations will be given explicitly in cartesian, cylindrical and spherical coordinates, while the more general curvilinear equations can be derived as required from the methods in Appendix A.

1.8. **Virtually irrotational strain and partial-increment dyadics.** Relative to whole-body convected axes the principal normal strain trajectories remain virtually parallel between the unstrained and strained states for an (elastic) infinitesimal deformation or between the current finite strain state and the previous state only differentially different. This leads to the partial-increment dyadics of stress $\Delta\mathfrak{S}$ and strain $\Delta\mathfrak{M}$. A set of incremental equations is then found with these partial-increment

dyadics replacing $\mathfrak{S}$ and $\mathfrak{M}$ in the corresponding total stress and total strain equations just given.

2. Two-stress dyadic

The two-stress dyadic for rectilinearly plane two-stress, for cartesian axes $OR_xR_yR_z$ with unit vectors $\mathbf{c}_x$, $\mathbf{c}_y$, $\mathbf{c}_z$, is discussed in article **III**,1. Thus, vector stress

$$\mathbf{S}_z = \mathbf{c}_z \cdot \mathfrak{S} = 0 \tag{2.1}$$

as also, of course, are the complementary shear stresses S_{xz}, S_{yz}. Then, the cartesian two-stress dyadic

$$\mathfrak{S} = S_{xx}\mathbf{c}_x\mathbf{c}_x + S_{yy}\mathbf{c}_y\mathbf{c}_y + S_{xy}(\mathbf{c}_x\mathbf{c}_y + \mathbf{c}_y\mathbf{c}_x) \tag{2.2}$$

2.1. **Curvilinear stresses.** The form of the stress dyadic for curvilinear coordinates is precisely the same as that for cartesian coordinates, except that the unit vectors are local values at a given point in the coordinate space. Thus, with the cylindrical coordinates unit vectors $\mathbf{c}_r$, $\mathbf{c}_\theta$, $\mathbf{c}_z$ of Fig. **A**,7.1, the spherical coordinates unit vectors $\mathbf{c}_r$, $\mathbf{c}_\theta$, $\mathbf{c}_\phi$ of Fig. **A**,7.2 or $\mathbf{c}_a$, $\mathbf{c}_b$, $\mathbf{c}_c$ for any orthogonal coordinates, then the zero stress is

$$\mathbf{S}_c = \mathbf{c}_c \cdot \mathfrak{S} = 0 \tag{2.3}$$

which gives the stress dyadic

$$\mathfrak{S} = S_{aa}\mathbf{c}_a\mathbf{c}_a + S_{bb}\mathbf{c}_b\mathbf{c}_b + S_{ab}(\mathbf{c}_a\mathbf{c}_b + \mathbf{c}_b\mathbf{c}_a) \tag{2.4}$$

2.2. **Plane polar stresses.** With $\mathbf{c}_c$ equal to $\mathbf{c}_z$ of cylindrical coordinates (R_r θ, R_z) gives the plane polar coordinates two-stress dyadic

$$\mathfrak{S} = S_{rr}\mathbf{c}_r\mathbf{c}_r + S_{\theta\theta}\mathbf{c}_\theta\mathbf{c}_\theta + S_{r\theta}(\mathbf{c}_r\mathbf{c}_\theta + \mathbf{c}_\theta\mathbf{c}_r) \tag{2.5}$$

2.3. **Cylindrical stresses.** With $\mathbf{c}_c$ equal to $\mathbf{c}_r$ of the cylindrical coordinates gives the curvilinearly plane cylindrical coordinates two-stress dyadic

$$\mathfrak{S} = S_{\theta\theta}\mathbf{c}_\theta\mathbf{c}_\theta + S_{zz}\mathbf{c}_z\mathbf{c}_z + S_{\theta z}(\mathbf{c}_\theta\mathbf{c}_z + \mathbf{c}_z\mathbf{c}_\theta) \tag{2.6}$$

2.4. **Principal normal stresses.** With θ the angle between $\mathbf{c}_a = \mathbf{c}_r$ (cylindrical), for example, and the principal normal stress S_{I}, then article **III**,1.3 gives tan 2θ and S_{I}, S_{J} in terms of S_{ab}, ... The rectilinear S_{xy}, ... there are merely replaced by the curvilinear S_{ab}, ... here.

2.5. **First stress invariant.** With reorientation of axes, the first stress invariant which is the sum of the normal stresses remains constant. Then, similar to article **III**,1.6,

$$\mathfrak{J}:\mathfrak{S} = \chi^S = S_{aa}+S_{bb} = S_{\mathbf{i}}+S_{\mathbf{j}} \tag{2.7}$$

2.6. **Partial-increment two-stress dyadic.** The partial-increment two-stress dyadic is

$$\begin{aligned}\Delta\mathfrak{S} &= \delta S_{\mathbf{i}}\mathbf{x}_{\mathbf{i}}\mathbf{x}_{\mathbf{i}}+\delta S_{\mathbf{j}}\mathbf{x}_{\mathbf{j}}\mathbf{x}_{\mathbf{j}} \\ &= \delta S_{aa}\mathbf{c}_a\mathbf{c}_a+\delta S_{bb}\mathbf{c}_b\mathbf{c}_b+\delta S_{ab}(\mathbf{c}_a\mathbf{c}_b+\mathbf{c}_b\mathbf{c}_a)\end{aligned} \tag{2.8}$$

Note that, scalarly, the general directions components are six, such as

$$\delta S_{ab} = \mathbf{c}_a\mathbf{c}_b:\Delta\mathfrak{S}(\mathbf{x}_{\mathbf{i}}, \mathbf{x}_{\mathbf{j}}) \tag{2.9}$$

3. Equilibrium two-stress equations

The equilibrium two-stress equation **V**(1.1) has been given in article **IV**,1 for cartesian and cylindrical coordinates when body force is zero. Retaining body force, they are restated here fully for convenient reference. The operator div is given in article **A**,8 for cartesian and cylindrical coordinates. These operate on a self-conjugate dyadic in article **A**,11. Apply these to the stress case and leave out the appropriate zero terms.

3.1. **Cartesian stresses.** Put as zero all stresses involving subscript z. Then,

$$\left.\begin{aligned}S_{xx;x}+S_{yx;y}+mB_x &= 0 \\ S_{yy;y}+S_{xy;x}+mB_y &= 0\end{aligned}\right\} \tag{3.1}$$

3.2. **Plane polar stresses.** Put as zero all stresses involving subscript z. Then,

$$\left.\begin{aligned}S_{rr;r}+R_r^{-1}S_{r\theta;\theta}+R_r^{-1}(S_{rr}-S_{\theta\theta})+mB_r &= 0 \\ R_r^{-1}S_{\theta\theta;\theta}+S_{r\theta;r}+2R_r^{-1}S_{r\theta}+mB_\theta &= 0\end{aligned}\right\} \tag{3.2}$$

3.3. **Cylindrical stresses.** Put as zero all stresses involving subscript r. Then,

$$\left.\begin{aligned}-R_r^{-1}S_{\theta\theta}+mB_r &= 0 \\ R_r^{-1}S_{\theta\theta;\theta}+S_{\theta z;z}+mB_\theta &= 0 \\ S_{zz;z}+R_r^{-1}S_{\theta z;\theta}+mB_z &= 0\end{aligned}\right\} \tag{3.3}$$

4. Strain dyadic for a two-stress dyadic

A two-stress dyadic induces a three-strain dyadic with one principal normal strain in the direction $\mathbf{c}_c$ due to the transverse strain effects induced by the stresses on planes normal to the curvilinear directions $\mathbf{c}_a$, $\mathbf{c}_b$. Thus, for rectilinear or curvilinear coordinates, with $\mathbf{c}_c = \mathbf{x}_k$,

$$\begin{aligned}\mathfrak{M} &= e_i\mathbf{x}_i\mathbf{x}_i + e_j\mathbf{x}_j\mathbf{x}_j + e_k\mathbf{x}_k\mathbf{x}_k \\ &= e_{aa}\mathbf{c}_a\mathbf{c}_a + e_{bb}\mathbf{c}_b\mathbf{c}_b + e_{ab}(\mathbf{c}_a\mathbf{c}_b + \mathbf{c}_b\mathbf{c}_a) + e_k\mathbf{c}_c\mathbf{c}_c \qquad (4.1)\end{aligned}$$

The subscripts a, b, c are x, y, z for cartesian coordinates and r, θ, z for cylindrical coordinates.

4.1. **Partial-increment dyadic for strain.** Similar to the partial-increment dyadic for stress in article V,2.6 the partial-increment dyadic $\Delta\mathfrak{M}$ for strain is given by replacing the e's of V(4.1) by δe's.

5. Two-stress and three-strain relations

The stress-strain parameters quadadic in article V,1.1 is of 'secant' form to simplify the description leading to article V,1.7 giving the steps to solve a boundary value problem. It is more general to deal with a 'tangent' parameters quadadic to relate the partial-increment dyadics $\Delta\mathfrak{M}$, $\Delta\mathfrak{S}$ for strain and stress respectively. Thus,

$$\Delta\mathfrak{M} = \boldsymbol{P}:\Delta\mathfrak{S} = (\boldsymbol{P}^E + \boldsymbol{P}^P):\Delta\mathfrak{S} \qquad (5.1)$$

with $\boldsymbol{P}^E$, $\boldsymbol{P}^P$ the elastic and plastic stress-strain parameters quadadics respectively and either of these denoted by $\boldsymbol{P}^M$. The first elements of these have been given in article III,3.3 for the principal directions in a homogeneous strain field.

5.1. **Principal directions for general isotropy.** For the principal normal strain directions $\mathbf{x}_i$, $\mathbf{x}_j$, $\mathbf{x}_k$ the increment partial-strains are, for general isotropy,

$$\left.\begin{aligned}\delta\epsilon_i^M &= \psi_i^M\delta S_i = \psi_i^M\mathbf{x}_i\mathbf{x}_i:\Delta\mathfrak{S} \\ \delta\epsilon_j^M &= \psi_j^M\delta S_j = \psi_j^M\mathbf{x}_j\mathbf{x}_j:\Delta\mathfrak{S} \\ \delta\epsilon_k^M &= 0\end{aligned}\right\} \qquad (5.2)$$

while

$$\left.\begin{aligned}\delta e_i^M &= \delta\epsilon_i^M - q_{j\text{-}i}^M\delta\epsilon_j^M \\ \delta e_j^M &= \delta\epsilon_j^M - q_{i\text{-}j}^M\delta\epsilon_i^M \\ \delta e_k^M &= -q_{i\text{-}k}^M\delta\epsilon_i^M - q_{j\text{-}k}^M\delta\epsilon_j^M\end{aligned}\right\} \qquad (5.3)$$

and

$$\Delta\mathfrak{M}^M = \mathbf{x}_i\mathbf{x}_i\delta e_i^M + \mathbf{x}_j\mathbf{x}_j\delta e_j^M + \mathbf{x}_k\mathbf{x}_k\delta e_k^M \tag{5.4}$$

Substituting V(5.2) in V(5.3) and then in V(5.4) and then comparing with V(5.1) gives the stress-strain parameters quadadic

$$\begin{aligned}\boldsymbol{P}^M = {} & \mathbf{x}_i\mathbf{x}_i(\psi_i^M\mathbf{x}_i\mathbf{x}_i - q_{j-i}^M\psi_j^M\mathbf{x}_j\mathbf{x}_j) + \mathbf{x}_j\mathbf{x}_j(\psi_j^M\mathbf{x}_j\mathbf{x}_j - q_{i-j}^M\psi_i^M\mathbf{x}_i\mathbf{x}_i) \\ & + \mathbf{x}_k\mathbf{x}_k(-q_{i-k}^M\psi_i^M\mathbf{x}_i\mathbf{x}_i - q_{j-k}^M\psi_j^M\mathbf{x}_j\mathbf{x}_j)\end{aligned} \tag{5.5}$$

5.2. **General directions for general isotropy.** Usually the stress-strain relations are required for rectilinear or curvilinear directions denoted generally by $\mathbf{c}_a$, $\mathbf{c}_b$, $\mathbf{c}_c$ with $\mathbf{c}_c = \mathbf{x}_k$. The partial-increment dyadics for stress and strain are given for general directions in articles V,2.6, V,4.1 and denoted briefly by $\Delta\mathfrak{S}(\mathbf{c}_a, \mathbf{c}_b, \mathbf{c}_c)$, $\Delta\mathfrak{M}(\mathbf{c}_a, \mathbf{c}_b, \mathbf{c}_c)$. Use these in V(5.1) and then extract the scalar increment strains

$$\left.\begin{aligned}\delta e_{aa}^M &= \mathbf{c}_a\mathbf{c}_a{:}\Delta\mathfrak{M}^M = \mathbf{c}_a\mathbf{c}_a{:}\boldsymbol{P}^M(\mathbf{x}_i, \ldots){:}\Delta\mathfrak{S}(\mathbf{c}_a, \ldots) \\ \delta e_{bb}^M &= \mathbf{c}_b\mathbf{c}_b{:}\boldsymbol{P}^M(\mathbf{x}_i, \ldots){:}\Delta\mathfrak{S}(\mathbf{c}_a, \ldots) \\ \delta e_{cc}^M &= \delta e_k^M = \mathbf{c}_c\mathbf{c}_c{:}\boldsymbol{P}^M(\mathbf{x}_i, \ldots){:}\Delta\mathfrak{S}(\mathbf{c}_a, \ldots) \\ \delta e_{ab}^M &= \tfrac{1}{2}(\mathbf{c}_a\mathbf{c}_b + \mathbf{c}_b\mathbf{c}_a){:}\boldsymbol{P}^M(\mathbf{x}_i, \ldots){:}\Delta\mathfrak{S}(\mathbf{c}_a, \ldots)\end{aligned}\right\} \tag{5.6}$$

With $a_i = \mathbf{c}_a{\cdot}\mathbf{x}_i, \ldots$, the cosine of the angle between $\mathbf{c}_a$ and $\mathbf{x}_i, \ldots$, this gives

$$\begin{aligned}\delta e_{aa}^M = {} & a_i^2\left[\begin{matrix}\psi_i^M(a_i^2\delta S_{aa} + b_i^2\delta S_{bb} + a_ib_i\delta S_{ab}) \\ -q_{j-i}^M\psi_j^M(a_j^2\delta S_{aa} + b_j^2\delta S_{bb} + a_jb_j\delta S_{ab})\end{matrix}\right] \\ & + a_j^2\left[\begin{matrix}\psi_j^M(a_j^2\delta S_{aa} + b_j^2\delta S_{bb} + a_jb_j\delta S_{ab}) \\ -q_{i-j}^M\psi_i^M(a_i^2\delta S_{aa} + b_i^2\delta S_{bb} + a_ib_i\delta S_{ab})\end{matrix}\right]\end{aligned} \tag{5.7}$$

The expansion of the other three expressions is left as an exercise for the reader.

5.3. **Principal directions for restricted isotropy.** Article III,3.3 discusses these conditions, so they are now rewritten for convenient reference later.

$$\left.\begin{aligned}\delta e_i^M &= G^M\delta S_i + F^M\delta\chi^S \\ \delta e_j^M &= G^M\delta S_j + F^M\delta\chi^S \\ \delta e_k^M &= F^M\delta\chi^S\end{aligned}\right\} \tag{5.8}$$

$$G^M = (1+q^M)\psi^M \qquad F^M = -q^M\psi^M \tag{5.9}$$

5.4. **General directions for restricted isotropy.** Trans formation of V(5.8) to general directions is not as convenient in

terms of a stress-strain parameters quadadic as to notice that these three equations are the scalar components of the dyadic

$$\Delta\mathfrak{M}^M = G^M\Delta\mathfrak{S}+F^M\delta\chi^S\mathfrak{I} \tag{5.10}$$

The scalar components are readily extracted as

$$\left.\begin{array}{ll}\delta e^M_{aa} = G^M\delta S_{aa}+F^M\delta\chi^S & \delta e^M_{bb} = G^M\delta S_{bb}+F^M\delta\chi^S \\ \delta e^M_{cc} = F^M\delta\chi^S & \delta e^M_{ab} = G^M\delta S_{ab}\end{array}\right\}(5.11)$$

5.5. **Constant elastic parameters and restricted isotropy.** Elastic strain transfers, with rotation of the stress relative to the substance, and therefore sums to give total elastic strain as in article **III**,3.4. Therefore, if G^E, F^E are constant, then, from article **III**,3.4, the current elasto-plastic strain is

$$\left.\begin{array}{l}e_{\mathbf{i}} = (G^ES_{\mathbf{i}}+F^E\chi^S)+(G^P\delta S_{\mathbf{i}}+F^P\delta\chi^S) \\ e_{\mathbf{j}} = (G^ES_{\mathbf{j}}+F^E\chi^S)+(G^P\delta S_{\mathbf{j}}+F^P\delta\chi^S) \\ e_{\mathbf{k}} = F^E\chi^S+F^P\delta\chi^S\end{array}\right\} \tag{5.12}$$

Transformation of these dyadics to the general directions, as in article **V**,5.4, gives

$$\left.\begin{array}{l}e_{aa} = (G^ES_{aa}+F^E\chi^S)+(G^P\delta S_{aa}+F^P\delta\chi^S) \\ e_{bb} = (G^ES_{bb}+F^E\chi^S)+(G^P\delta S_{bb}+F^P\delta\chi^S) \\ e_{cc} = e_{\mathbf{k}} = F^E\chi^S+F^P\delta\chi^S \\ e_{ab} = G^ES_{ab}+G^P\delta S_{ab}\end{array}\right\} \tag{5.13}$$

The converse with stresses in terms of strains is useful sometimes and is given in dyadic form for brevity. Multiplying each of the equations **V**(5.12) by the appropriate unit dyad and adding, then rearranging, gives

$$\mathfrak{S}+\Delta\mathfrak{S} = (J^E\mathfrak{M}^E+K^E\chi^{DE}\mathfrak{I})+(J^P\Delta\mathfrak{M}^P+K^P\delta\chi^{DP}\mathfrak{I}) \tag{5.14}$$

with stress-strain parameters, for $M = E, P$,

$$\left.\begin{array}{l}J^M = (G^M)^{-1} = [(1+q^M)\psi^M]^{-1} \\ K^M = -F^M(G^M)^{-1}(G^M+3F^M)^{-1} = q^M[(1+q^M)(1-2q^M)\psi^M]^{-1}\end{array}\right\} \tag{5.15}$$

and

$$\chi^{DM} = e^M_{aa}+e^M_{bb}+e^M_{cc} = e^M_{\mathbf{i}}+e^M_{\mathbf{j}}+e^M_{\mathbf{k}} \tag{5.16}$$

the first invariant of the strain dyadic component $\mathfrak{M}^M$, while $\delta\chi^{DM}$ is the first invariant of the partial-increment strain dyadic component $\Delta\mathfrak{M}^M$ with δe^M's replacing the e^M's in **V**(5.16).

6. Compatibility of two-stress strains

The strains compatibility condition V(1.4) is expanded from article A,12 with the appropriate zero components of the self-conjugate dyadic corresponding to those in V(4.1).

6.1. Cartesian stresses

$$\left.\begin{array}{lll} e_{xx;y} = e_{xy;x} & e_{yy;x} = e_{xy;y} & e_{xy;z} = 0 \\ e_{zz;x} = 0 = e_{zz;y} & e_{xx;z} = 0 = e_{yy;z} & \end{array}\right\} \quad (6.1)$$

6.2. Plane polar stresses

$$\left.\begin{array}{lll} R_r^{-1}(e_{rr,\theta} - 2e_{r\theta}) = e_{r\theta;r} & & \\ e_{\theta\theta;r} = R_r^{-1}(e_{r\theta;\theta} + e_{rr} - e_{\theta\theta}) & e_{r\theta;z} = 0 & \\ e_{zz;r} = 0 = e_{zz;\theta} & e_{rr;z} = 0 = e_{\theta\theta;z} & \end{array}\right\} \quad (6.2)$$

6.3. Cylindrical stresses

$$\left.\begin{array}{ll} e_{\theta\theta;r} = R_r^{-1}(e_{rr} - e_{\theta\theta}) & e_{\theta\theta;z} = R_r^{-1} e_{\theta z;\theta} \\ e_{\theta z;z} = R_r^{-1} e_{zz;\theta} & e_{\theta z;r} = -R_r^{-1} e_{\theta z} \\ e_{rr;\theta} = 0 = e_{rr;z} & e_{zz;r} = 0 \end{array}\right\} \quad (6.3)$$

6.4. **Increment strains compatibility for cartesian, plane polar and cylindrical stresses.** The continuity of the partial-increment strain dyadic leads to precisely the same compatibility form as V(1.4) with $\Delta\mathfrak{M}$ replacing $\mathfrak{M}$ there. Thus, in V(6.1) to V(6.3) the e's are replaced by δe's for the increment strains compatibility conditions for appropriate increment two-stress.

6.5. **Compatibility of increment stresses and stress-strain parameters for general isotropy.** The appropriate terms like V(5.7) involving increment stresses, stress-strain parameters and direction cosines for the orientation of the partial-increment strain dyadic relative to the chosen coordinate system must satisfy the increment strains compatibility conditions. Therefore, the stress-strain parameters cannot be chosen arbitrarily but must satisfy the compatibility conditions.

6.6. **Restricted isotropy compatibility of increment stresses with stress-strain parameters independent of position.** Suppose the stress-strain parameters F^M, G^M are independent of position in the body, then, for cartesian coordinates, putting δe's into V(6.1) gives

$$\delta e_{zz;x} = F^M \delta\chi^S{}_{;x} = 0 = F^M \delta\chi^S{}_{;y} = \delta e_{zz;y} \quad (6.4)$$

so that, on cancelling the common factor G^M on each side of each equation, this gives

$$\delta S_{xx;y} = \delta S_{xy;x} \qquad \delta S_{yy;r} = \delta S_{xy;y} \tag{6.5}$$

The remaining three conditions are satisfied if the increment stresses are independent of R_z.

Equations V(6.4) show that the first invariant of the increment stresses is constant throughout the deformed body when the stress-strain parameters are of restricted isotropy and independent of position.

7. Relative-displacement and strain for a two-stress

Relative-displacement and strain are related by equation V(1.8). Article A,14 gives the vector gradient of a vector for the various coordinate systems.

7.1. Cartesian stresses

$$\left.\begin{aligned} e_{xx} &= D^*_{x;x} \qquad e_{yy} = D^*_{y;y} \\ e_{xy} &= D^*_{x;y} = D^*_{y;x} \end{aligned}\right\} \tag{7.1}$$

$$\left.\begin{aligned} e_{zz} &= D^*_{z;z} \\ e_{zx} &= 0 = D^*_{z;x} = D^*_{x;z} \\ e_{zy} &= 0 = D^*_{y;z} = D^*_{z;y} \end{aligned}\right\} \tag{7.1'}$$

7.2. Plane polar stresses

$$\left.\begin{aligned} e_{rr} &= D^*_{r;r} \qquad e_{\theta\theta} = R_r^{-1}(D^*_r + D^*_{\theta;\theta}) \\ e_{r\theta} &= D^*_{\theta;r} = R_r^{-1}(D^*_{r;\theta} - D^*_\theta) \end{aligned}\right\} \tag{7.2}$$

$$\left.\begin{aligned} e_{zz} &= D^*_{z;z} \\ e_{zr} &= 0 = D^*_{z;r} = D^*_{r;z} \\ e_{\theta z} &= 0 = R_r^{-1} D^*_{z;\theta} = D^*_{\theta;z} \end{aligned}\right\} \tag{7.2'}$$

7.3. Cylindrical stresses

$$\left.\begin{aligned} e_{zz} &= D^*_{z;z} \qquad e_{\theta\theta} = R_r^{-1}(D^*_r + D^*_{\theta;\theta}) \\ e_{\theta z} &= R_r^{-1} D^*_{z;\theta} = D^*_{\theta;z} \end{aligned}\right\} \tag{7.3}$$

$$\left.\begin{aligned} e_{rr} &= D^*_{r;r} \\ e_{r\theta} &= 0 = D^*_{\theta;r} = R_r^{-1}(D^*_{r;\theta} - D^*_\theta) \\ e_{zr} &= 0 = D^*_{z;r} = D^*_{r;z} \end{aligned}\right\} \tag{7.3'}$$

7.4. **Increment relative-displacement and increment strain.** The partial-increment strain dyadic and the partial-increment relative-displacement are related by just the same form as the strain dyadic and the relative-displacement. Therefore, in this case the e's are replaced by δe's and the D^*'s by δD^*'s in V(7.1) to V(7.3′).

8. Displacement potential and relative-displacement

Volume I, article I,7 shows, generally, that since

$$D^*_{x;y} = D^*_{y;x}$$

in equation V(7.1), then we may represent the lamellar, relative-displacement vector by

$$\mathbf{D}^* = \nabla\mathcal{E} \tag{8.1}$$

with displacement potential $\mathcal{E}$. Write out scalarly for the present two-stress systems.

8.1. Cartesian stresses

$$D^*_x = \mathcal{E}_{;x} \qquad D^*_y = \mathcal{E}_{;y} \qquad D^*_z = \mathcal{E}_{;z} \tag{8.2}$$

8.2. Plane polar and cylindrical stresses

$$D^*_r = \mathcal{E}_{;r} \qquad D^*_\theta = R_r^{-1}\mathcal{E}_{;\theta} \qquad D^*_z = \mathcal{E}_{;z} \tag{8.3}$$

8.3. **Increment displacement potential and increment relative-displacement.** Relative to whole-body convected axes an increment in deformation gives a partial-increment of V(8.1). Thus,

$$\Delta\mathbf{D}^* = \Delta\nabla\mathcal{E} = \nabla\delta\mathcal{E} \tag{8.4}$$

Then, for the various coordinate systems replace $\mathcal{E}$ and the D^*'s in V(8.1) to V(8.3) by $\delta\mathcal{E}$ and δD^*'s for this case.

9. Strain and displacement potential

Substituting equation V(8.1) in V(1.8) gives the self-conjugate strain dyadic represented by

$$\mathfrak{M} = \nabla\nabla\mathcal{E} \tag{9.1}$$

Volume I, appendix C discusses this representation as an extension of potential theory analogous to the representation of the lamellar vector as in V(8.1) for relative-displacement.

Substituting V(8.2), V(8.3) appropriately in V(7.1) to V(7.3′) gives the strains in terms of displacement potential. The forms are similar to those for non-zero stresses in article V,10.

10. Stress potential and stress

The representation of the strain dyadic in terms of displacement potential is given in V(9.1) as an extension of potential theory. Similarly, represent the stress dyadic by means of stress potential H in

$$\mathfrak{S} = \nabla\nabla H \tag{10.1}$$

Article A,9 gives $\nabla\nabla$ expanded for the various coordinate systems. The two-stress dyadic is given by taking H as independent of one coordinate.

10.1. **Cartesian stresses.** $H = H(R_x, R_y)$.

$$S_{xx} = H_{;xx} \qquad S_{yy} = H_{;yy} \qquad S_{xy} = H_{;xy} \tag{10.2}$$

10.2. **Plane polar stresses.** $H = H(R_r, \theta)$.

$$S_{rr} = H_{;rr} \qquad S_{\theta\theta} = R_r^{-2}H_{;\theta\theta} + R_r^{-1}H_{;r} \qquad S_{r\theta} = (R_r^{-1}H_{;\theta})_{;r} \tag{10.3}$$

10.3. **Cylindrical stresses.** $H = H(\theta, R_z)$.

$$S_{\theta\theta} = R_r^{-2}H_{;\theta\theta} \qquad S_{zz} = H_{;zz} \qquad S_{\theta z} = R_r^{-1}H_{;\theta z} \tag{10.4}$$

11. Law of distribution of the two-stress potential

Volume I, article II,7.3 shows that representation of the stress dyadic as in V(10.1) and representation of the body force $m\mathbf{B}$ (when it is lamellar) by $\nabla\mathcal{B}$ and substitution in V(1.1) gives, with constant C, the poissonian equation

$$\nabla^2 H + \mathcal{B} = C \tag{11.1}$$

11.1. **Cartesian stresses**

$$\nabla^2 H = H_{;xx} + H_{;yy} \tag{11.2}$$

11.2. **Plane polar stresses**

$$\nabla^2 H = H_{;rr} + R_r^{-1}H_{;r} + R_r^{-2}H_{;\theta\theta} \tag{11.3}$$

11.3. **Cylindrical stresses**

$$\nabla^2 H = R_r^{-2}H_{;\theta\theta} + H_{;zz} \tag{11.4}$$

11.4. Distribution of the first stress invariant

$$\nabla^2 H = \mathfrak{J}:\nabla\nabla H = \mathfrak{J}:\mathfrak{S} = \chi^S \tag{11.5}$$

Therefore, with V(11.1),

$$\chi^S = C - \mathcal{B} \tag{11.6}$$

In particular, for zero body force $\mathcal{B}$ is zero to give the first stress invariant constant throughout the deformed body. Similarly, in this case, for the partial-increment stress dyadic

$$\delta\chi^S = \delta C \tag{11.7}$$

12. Displacement potential from the two-stress potential

The stress-strain relations are easily integrated in some special cases.

12.1. **Restricted isotropy, stress-strain parameters independent of position and with zero body force.** For the general member of the elasto-plastic increment strain

$$\nabla\nabla\delta\mathcal{E}^M = G^M\nabla\nabla\delta H + F^M\delta\chi^S\mathfrak{J} \tag{12.1}$$

Integration gives, for cartesian coordinates (R_x, R_y, R_z),

$$\delta\mathcal{E}^M = G^M\delta H + \tfrac{1}{2}F^M\delta\chi^S(R_x^2+R_y^2+R_z^2) + W_xR_x + W_yR_y + W_zR_z \tag{12.2}$$

with three arbitrary constants W_x, ... Vectorially,

$$\delta\mathcal{E}^M = G^M\delta H + \tfrac{1}{2}F^M\delta\chi^S\mathbf{R}\cdot\mathbf{R} + \mathbf{W}\cdot\mathbf{R} \tag{12.3}$$

with position vector $\mathbf{R}$ and $\mathbf{W}$ a constant vector allowing for a possible *whole-body translation* or else a shift of origin of coordinate axes if this would be convenient. This last form allows easy transformation to curvilinear coordinates.

If, as a further restriction on the behaviour of the substance, the elastic stress-strain parameters F^E, G^E are constant as the deformation evolves, then $\mathcal{E}^E$, H replace $\delta\mathcal{E}^E$, δH for this particular component of the elasto-plastic strain.

13. Airy two-stress function

Volume I, article II,9 gives the Airy stress function for curvilinear coordinates in the form

$$\mathfrak{S} = \mathbf{c}_c\mathbf{c}_{c^\times}^{\times}\nabla\nabla\mathcal{A} \tag{13.1}$$

with $\mathcal{A}(R_a, R_b)$ representing the stress dyadic because the divergence of this is identically zero to satisfy the equilibrium stress equation when body force is zero. Operator $\nabla\nabla$ is given in article A,9 for the various coordinate systems.

13.1. **Cartesian stresses.** $\mathcal{A} = \mathcal{A}(R_x, R_y)$, $\mathbf{c}_c = \mathbf{c}_z$.

$$S_{xx} = \mathcal{A}_{;yy} \qquad S_{yy} = \mathcal{A}_{;xx} \qquad S_{xy} = -\mathcal{A}_{;xy} \tag{13.2}$$

13.2. **Plane polar stresses.** $\mathcal{A} = \mathcal{A}(R_r, \theta)$, $\mathbf{c}_c = \mathbf{c}_z$.

$$\left.\begin{aligned} S_{rr} &= R_r^{-2}\mathcal{A}_{;\theta\theta} + R_r^{-1}\mathcal{A}_{;r} \\ S_{\theta\theta} &= \mathcal{A}_{;rr} \qquad S_{r\theta} = -(R_r^{-1}\mathcal{A}_{;\theta})_{;r} \end{aligned}\right\} \tag{13.3}$$

13.3. **Cylindrical stresses.** $\mathcal{A} = \mathcal{A}(\theta, R_z)$, $\mathbf{c}_c = \mathbf{c}_r$.

$$S_{\theta\theta} = \mathcal{A}_{;zz} \qquad S_{zz} = R_r^{-2}\mathcal{A}_{;\theta\theta} \qquad S_{\theta z} = -R_r^{-1}\mathcal{A}_{;\theta z} \tag{13.4}$$

14. Solutions by the Navier, Cauchy approximate theory

The Navier, Cauchy theory of infinitesimal strains is formulated from the observation of the infinitesimal spatial-displacement **U** of each point relative to a spatially fixed reference frame. Article II,3 shows, for the trivial case of simple tension, that an attempt to relate **U** and stress (or strain) actually leads to the relating of straining-displacement **D** and stress (or strain) to the exclusion of infinitesimal whole-body rotation. Volume I, article I,15.5 gives the Navier, Cauchy infinitesimal self-conjugate strain dyadic

$$\begin{aligned} \mathfrak{M} &= \tfrac{1}{2}(\nabla\mathbf{U} + \mathbf{U}\nabla) = \tfrac{1}{2}(\nabla\mathbf{D} + \mathbf{D}\nabla) \\ &= \tfrac{1}{2}(\nabla\mathbf{D}^* + \mathbf{D}^*\nabla) = \nabla\mathbf{D}^* \end{aligned} \tag{14.1}$$

14.1 **Saint-Venant's strains compatibility condition.** On the supposition that $\mathfrak{M}$ is related to spatial-displacement **U** the Saint-Venant strains compatibility condition, independent of **U**, is given in volume I, article III,9.1 as

$$(\nabla\times\mathfrak{M})\times\nabla = 0 \tag{14.2}$$

The conjugate curl operator $(\ )\times\nabla$ is necessary to remove the term $\mathbf{U}\nabla$, but $\nabla\times\mathfrak{M}$ is zero already, since $\nabla\times\nabla\mathbf{D}^*$ is zero. Therefore, the operation $(\ )\times\nabla$ is unnecessary to give a set of equations involving strains only. It is sufficient for strains compatibility that

$$\nabla\times\mathfrak{M} = 0 \tag{14.3}$$

as the symbolic form of that in article V,1.2. Therefore, a set

of strains proposed as a solution of a given problem may be spurious if they satisfy the Saint-Venant condition V(14.2) but not the more searching condition V(14.3).

14.2. **Straining-displacement.** Volume I, articles I,15.8, VI,6.9 show that for infinitesimal strain the straining-displacement **D** relative to a non-deformable, whole-body, convected reference is quasi-equal to relative-displacement $\mathbf{D}^*$ relative to a deformable, convected reference. Therefore, in V(14.1), for infinitesimal strain,

$$\mathfrak{M} = \tfrac{1}{2}(\nabla\mathbf{D}+\mathbf{D}\nabla) = \nabla\mathbf{D} = \nabla\mathbf{D}^* = \tfrac{1}{2}(\nabla\mathbf{D}^*+\mathbf{D}^*\nabla) \qquad (14.4)$$

Volume I, article I,13 shows that **D**, from the strain field viewpoint, is equivalent to $\mathbf{D}^*$, since a solution gives a doublet vector field, as mentioned in article V,1.6 here, to effect the 'orthogonal transformation' of the unstrained principal normal strain trajectories to the corresponding strained set. Therefore a solution of

$$\mathfrak{M} = \tfrac{1}{2}(\nabla\mathbf{D}^*+\mathbf{D}^*\nabla) \qquad (14.5)$$

for $\mathbf{D}^*$ also gives, for finite strain,

$$\mathbf{D} \approx \mathbf{D}^* \qquad (14.6)$$

14.3. **Approximate solutions.** Solutions of V(14.5) satisfying Saint-Venant's strains compatibility condition are given by the many theoretical solutions available for boundary value problems analysed by the classical infinitesimal strains theory. As seen, such analyses are mathematically unsatisfactory, may even be spurious, but nevertheless may check quite closely with experiments examining the main features of the solution. Some will be given in following articles, with this reservation on their validity, and then extended to finite strain by the straining equivalence principle in V(14.6).

15. Saint-Venant's strains compatibility conditions for a two-stress system

The strains compatibility conditions V(14.2) for a two-stress in cartesian axes $OR_xR_yR_z$ are shown in volume I, article VI,14.1 to be the four scalar conditions

$$e_{xx;yy}+e_{yy;xx} = 2e_{xy;xy} \qquad (15.1)$$

$$e_{zz;xx} = 0 \qquad e_{zz;yy} = 0 \qquad e_{zz;xy} = 0 \qquad (15.2)$$

15.1. **Restricted isotropy, constant elastic stress-strain parameters.** From equations V(15.2) it is seen that e_{zz} and, hence, χ^S are linear in R_x, R_y. With the Airy stress function, then

$$\chi^S = \nabla^2 \mathcal{A} = C + J_x R_x + J_y R_y \tag{15.3}$$

a Poisson's equation with arbitrary constants C, J_x, J_y. The Airy stress function in V(15.1) gives the biharmonic equation

$$\nabla^2 \nabla^2 \mathcal{A} \equiv \nabla^4 \mathcal{A} = 0 \tag{15.4}$$

A solution of V(15.3) for $\mathcal{A}$ satisfies V(15.4), but a solution of V(15.4) for $\mathcal{A}$ may not satisfy V(15.3).

The literature contains many solutions of the biharmonic applied to plane two-stress, although the more restrictive condition V(15.3) is not satisfied. If a plate is infinite, as in many examples, then the first stress invariant becomes infinite with the right-hand side of V(15.3). This is not allowable, so that the J's must be zero in this case, at least, to give the result already found in article V,11.4 that the first stress invariant is constant under the conditions here.

15.2. **Plane strain.** Let the substance have the same properties as in article V,15.1. Suppose e_{zz} is zero as well as e_{zx}, e_{yz} so that only V(15.1) remains of the original six Saint-Venant conditions. The Airy stress function can be used again, to solve V(3.1) with zero body force, and now obeys the biharmonic law V(15.4) for plane strain. Strictly, plane strain is a three-stress with normal stress

$$S_{zz} = -F(S_{xx} + S_{yy})/(F+G) \tag{15.5}$$

whereas this stress is zero for plane two-stress.

15.3. **Approximate solutions for stresses in thin, plane sheets.** The solution of the biharmonic V(15.4) has been applied frequently to the planewise loading of thin sheets, ignoring the plane strain normal stress S_{zz}. The few experimental examinations available for the strains on the main faces of the sheet show fair check of theory. Although experiments on thickness change have not been published as agreeing with theory, the present author's analysis in article X,3 of a quasi-homogeneous plane stress experiment in article X,1 suggests that they will probably differ. There appears to be at least normal stress S_{zz} in the interior of the sheet, but its effect on strains in the main faces is slight.

Biharmonic solutions will be applied to thin sheets with this qualification in mind. This further approximation must be noted, as well as the approximation due to using the Navier, Cauchy strains definitions and the Saint-Venant strains compatibility conditions as discussed in article V,14.3.

15.4. **Geometry and strains of contiguous elements.** The principal normal strain trajectories define a set of (curvilinear) orthogonal elements that were initially orthogonal (of different curvilinearity) in the unstrained state. The Navier, Cauchy theory for infinitesimal strain and infinitesimal spatial-rotation angle θ^{sp} considers a single, typical element of the whole assembly. Volume I, article I,15.4 shows geometrically that

$$e_{xx} = U_{x;x} \qquad e_{xy} = U_{x;y} + \theta^{sp} \tag{15.6}$$

$$e_{yy} = U_{y;y} \qquad e_{xy} = U_{y;x} - \theta^{sp} \tag{15.7}$$

Differentiating suitably gives

$$e_{xx;y} = U_{x;xy} \qquad e_{xy;x} = U_{x;yx} + \theta^{sp}{}_{;x} \tag{15.8}$$

$$e_{yy;x} = U_{y;yx} \qquad e_{xy;y} = U_{y;xy} - \theta^{sp}{}_{;y} \tag{15.9}$$

Therefore, with equations V(7.1),

$$\theta^{sp}{}_{;x} = 0 = \theta^{sp}{}_{;y} \tag{15.10}$$

so that

$$\theta^{sp} = \text{constant} \tag{15.11}$$

But with whole-body rotation angle θ^{wb} constant and straining-rotation θ^{st} due to the strain field, then

$$\theta^{sp} = \theta^{wb} + \theta^{st} \tag{15.12}$$

Then V(15.11) gives

$$\theta^{st} = 0 \tag{15.13}$$

or, more strictly, it is quasi-zero as in volume I, articles I,15, VI,6 or, less directly, in III,14.

15.5. **Dislocational rotation and Saint-Venant's strains compatibility conditions.** Quite arbitrarily add to the right-hand side of V(15.12) a dislocational rotation component θ^{dr} supposed to be independent of the stress and strain distribution. Thus,

$$\tfrac{1}{2}(U_{y;x} - U_{x;y}) = \theta^{sp} = \theta^{wb} + \theta^{st} + \theta^{dr} \tag{15.14}$$

as in volume I, article III,9.4. Differentiating equations V(15.8), V(15.9) again suitably gives

$$e_{xx;yy} = U_{x;xyy} \qquad e_{yy;xx} = U_{y;xxy} \tag{15.15}$$

$$U_{x;xyy} + \theta^{\mathrm{dr}}{}_{;xy} = e_{xy;xy} = U_{y;xxy} - \theta^{\mathrm{dr}}{}_{;xy} \tag{15.16}$$

From these two pairs of equations by addition

$$e_{xx;yy} + e_{yy;xx} = (U_{x;y} + U_{y;x})_{;xy} \tag{15.17}$$

$$2e_{xy;xy} = (U_{x;y} + \theta^{\mathrm{dr}} + U_{y;x} - \theta^{\mathrm{dr}})_{;xy} \tag{15.18}$$

Equating these two expressions gives Saint-Venant's strains compatibility condition in V(15.1). Note that θ^{dr} is merely implicit in V(15.18) because it cancels, just as θ^{sp} cancels in forming the Cauchy shear strain definition

$$e_{xy} = \tfrac{1}{2}(U_{x;y} + \theta^{\mathrm{sp}} + U_{y;x} - \theta^{\mathrm{sp}}) \tag{15.19}$$

from V(15.6).2 and V(15.7).2.

This re-emphasises that the *Saint-Venant compatibility conditions cannot ensure continuity of the strain dyadic but merely continuity of spatial-displacement* which can have a component independent of whole-body rotation, the strain field, stress and strain. Such an anomalous component of spatial-displacement is allowed to enter through the Cauchy strain definition. Saint-Venant's torsion theory in article XII,7.5 illustrates this aspect.

16. Navier, Cauchy strain definitions and spatial-rotation for a two-stress

Expansion of equation V(14.1) gives strains in terms of spatial-displacement for a two-stress in which $e_{bc} = 0 = e_{ca}$. The spatial-rotations are the scalar components ω_{ab}, ..., of the antiself-conjugate dyadic $\frac{1}{2}(\nabla\mathbf{U} - \mathbf{U}\nabla)$.

16.1. Cartesian stresses. $\mathbf{S}_z = 0$.

$$\left.\begin{aligned} e_{xx} &= U_{x;x} \qquad e_{yy} = U_{y;y} \\ e_{xy} &= \tfrac{1}{2}(U_{x;y} + U_{y;x}) \end{aligned}\right\} \tag{16.1}$$

$$\left.\begin{aligned} e_{zz} &= U_{z;z} \\ e_{zx} &= 0 = \tfrac{1}{2}(U_{z;x} + U_{x;z}) \\ e_{yz} &= 0 = \tfrac{1}{2}(U_{y;z} + U_{z;y}) \end{aligned}\right\} \tag{16.2}$$

$$\left.\begin{aligned} \omega_{xy} &= \tfrac{1}{2}(U_{y;x} - U_{x;y}) \\ \omega_{yz} &= \tfrac{1}{2}(U_{z;y} - U_{y;z}) \\ \omega_{zx} &= \tfrac{1}{2}(U_{x;z} - U_{z;x}) \end{aligned}\right\} \tag{16.3}$$

16.2. Plane polar and cylindrical stresses

Plane polar stresses: $\mathbf{S}_z = 0$, $e_{\theta z} = 0 = e_{zr}$.

Cylindrical stresses: $\mathbf{S}_r = 0$, $e_{r\theta} = 0 = e_{zr}$.

$$\left.\begin{aligned} e_{rr} &= U_{r;r} \\ e_{\theta\theta} &= R_r^{-1}(U_r + U_{\theta;\theta}) \\ e_{zz} &= U_{z;z} \end{aligned}\right\} \quad (16.4)$$

$$\left.\begin{aligned} e_{r\theta} &= \tfrac{1}{2}(R_r^{-1}U_{r;\theta} - R_r^{-1}U_\theta + U_{\theta;r}) \\ e_{\theta z} &= \tfrac{1}{2}(U_{\theta;z} + R_r^{-1}U_{z;\theta}) \\ e_{zr} &= \tfrac{1}{2}(U_{z;r} + U_{r;z}) \end{aligned}\right\} \quad (16.5)$$

$$\left.\begin{aligned} \omega_{r\theta} &= \tfrac{1}{2}(U_{\theta;r} - R_r^{-1}U_{r;\theta} + R_r^{-1}U_\theta) \\ \omega_{\theta z} &= \tfrac{1}{2}(R_r^{-1}U_{z;\theta} - U_{\theta;z}) \\ \omega_{zr} &= \tfrac{1}{2}(U_{r;z} - U_{z;r}) \end{aligned}\right\} \quad (16.6)$$

17. Generalised plane stress theory of Filon

L. N. G. Filon, in 1903 [80] and 1931 [79], gave a theory in which the stresses in moderately thick plates were taken as not independent of position between the two main faces as is assumed for plane stress. The generalised Hooke's law for an elastic substance of restricted isotropy, with the Navier, Cauchy strains definitions and the equilibrium stress equation, were considered. Thus, with the stress-strain parameters F, G, then

$$\tfrac{1}{2}(\boldsymbol{\nabla}\mathbf{U} + \mathbf{U}\boldsymbol{\nabla}) = \mathfrak{M} = G\mathfrak{S} + F\chi^S\mathfrak{J} \quad (17.1)$$

$$\boldsymbol{\nabla}\cdot\mathfrak{S} = 0 \quad (17.2)$$

In fact, Filon included body force in the latter, but it is neglected here to simplify the exposition without losing any essential of the theory.

With the origin of axes OR_xR_y, of axes $OR_xR_yR_z$, in the middle plane of a plate of thickness $2h$ with stress-free main faces, then Filon proposed to consider stresses and strains averaged over the thickness. Thus, average strain and stress dyadics are, say,

$$\mathfrak{N} = \frac{1}{2h}\int_{-h}^{+h} \mathfrak{M}\,\partial R_z \qquad \mathfrak{T} = \frac{1}{2h}\int_{-h}^{+h} \mathfrak{S}\,\partial R_z \quad (17.3)$$

while he considered

$$\frac{1}{2h}\int_{-h}^{+h} \boldsymbol{\nabla}\cdot\mathfrak{S}\,\partial R_z = 0 \quad (17.4)$$

17.1. **Formulation.**† Suppose that, for convenient formulation,

$$\mathfrak{M} = \mathfrak{M}' + \mathfrak{M}'' \qquad \mathfrak{S} = \mathfrak{S}' + \mathfrak{S}'' \tag{17.5}$$

with

$$\mathfrak{M}' = G\mathfrak{S}' + F\chi^S\mathfrak{J} \tag{17.6}$$

$$\mathfrak{M}'' = G\mathfrak{S}'' \tag{17.7}$$

$$\mathfrak{S}' = S_{xx}\mathbf{c}_x\mathbf{c}_x + S_{yy}\mathbf{c}_y\mathbf{c}_y + S_{xy}(\mathbf{c}_x\mathbf{c}_y + \mathbf{c}_y\mathbf{c}_x) \tag{17.8}$$

$$\mathfrak{S}'' = S_{zz}\mathbf{c}_z\mathbf{c}_z + S_{zx}(\mathbf{c}_z\mathbf{c}_x + \mathbf{c}_x\mathbf{c}_z) + S_{yz}(\mathbf{c}_y\mathbf{c}_z + \mathbf{c}_z\mathbf{c}_y) \tag{17.9}$$

With V(17.3), V(17.6), V(17.8),

$$\mathfrak{R}' = G\mathfrak{T}' + F\chi^T\mathfrak{J} \tag{17.10}$$

with the average stress first invariant

$$\chi^T = T_{xx} + T_{yy} + T_{zz} \tag{17.11}$$

With V(17.8) in V(17.4),

$$\frac{1}{2h}\int_{-h}^{+h} \boldsymbol{\nabla}\cdot\mathfrak{S}'\,\partial R_z = \boldsymbol{\nabla}\cdot\mathfrak{T}' \tag{17.12}$$

With V(17.3), V(17.7), V(17.9),

$$\mathfrak{R}'' = G\mathfrak{T}'' \tag{17.13}$$

while, explicitly,

$$\mathfrak{T}'' = T_{zz}\mathbf{c}_z\mathbf{c}_z + T_{zx}(\mathbf{c}_z\mathbf{c}_x + \mathbf{c}_x\mathbf{c}_z) + T_{yz}(\mathbf{c}_y\mathbf{c}_z + \mathbf{c}_z\mathbf{c}_y) \tag{17.14}$$

With V(17.9) in V(17.4), noting that at the limits of integration S_{zz}, S_{zx}, S_{zy} are zero, then

$$\frac{1}{2h}\int_{-h}^{+h} \boldsymbol{\nabla}\cdot\mathfrak{S}''\,\partial R_z = (T_{zx;x} + T_{yz;y})\mathbf{c}_z \tag{17.15}$$

Substituting V(17.13), V(17.10) in V(17.5) and V(17.3) gives the average strain dyadic

$$\mathfrak{R} = G(\mathfrak{T}' + \mathfrak{T}'') + F\chi^T\mathfrak{J} \tag{17.16}$$

Substituting V(17.15), V(17.12) in V(17.4) gives the equilibrium stress equation

$$\boldsymbol{\nabla}\cdot\mathfrak{T}' + (T_{zx;x} + T_{yz;y})\mathbf{c}_z = 0 \tag{17.17}$$

† The formulation by vector methods in this article and V,17.2 was done by the present author in 1951, and differs from the scalar methods of Filon in the references given, but the final results are the same.

17.2. **Filon's assumptions.** The aim was to derive equations of two-dimensional form so, firstly, by stating arbitrarily that the coefficient of $\mathbf{c}_z$ in V(17.17) is† [79.1] '. . . not required, as it does not involve T_{xx} or T_{yy}' this quantity was assumed to be zero.

Again, it was assumed that S_{zz}, and hence T_{zz}, is identically zero [79.2].

Also, without saying so explicitly,‡ Filon either ignores or puts as zero the mean stresses T_{zx}, T_{yz} in V(17.14).

Thus, by the foregoing extremely arbitrary processes Filon derives the two-dimensional mean stress-strain and equilibrium equations,

$$\mathfrak{N} = G\mathfrak{T}' + F\chi'^{T}\mathfrak{J} \tag{17.18}$$

$$\left.\begin{aligned} \chi'^{T} &= T_{xx}+T_{yy} \\ \mathfrak{T}' &= T_{xx}\mathbf{c}_x\mathbf{c}_x+T_{yy}\mathbf{c}_y\mathbf{c}_y+T_{xy}(\mathbf{c}_x\mathbf{c}_y+\mathbf{c}_y\mathbf{c}_x) \end{aligned}\right\} \tag{17.19}$$

$$\nabla\cdot\mathfrak{T}' = 0 \tag{17.20}$$

These are essentially the equations given by Filon, except that he gives the converse form of mean stresses in terms of mean strains. In his formulation, Filon emphasises the spatial-displacement **U** and considers its mean value **V**, say, averaged with respect to R_z. Thus he finds§ the mean strains, say,

$$f_{xx} = V_{x;x} \qquad f_{yy} = V_{y;y} \qquad f_{xy} = \tfrac{1}{2}(V_{x;y}+V_{y;x}) \tag{17.21}$$

Filon thus arrives at a set of equations of precisely the same form as those for plane stress, but here quantities averaged with respect to plate thickness replace the actual quantities for plane stress. The 'elemental volume' of the generalised plane stress theory is a rectangular block of edge lengths dR_x, dR_y, $2h$, while for plane stress it is dR_x, dR_y, dR_z.

17.3. **Compatibility of average strains.** The continuity of spatial-displacement **U** in the Navier, Cauchy strains is assured by the Saint-Venant strains compatibility condition

$$(\nabla\times\mathfrak{M})\times\nabla = 0 \tag{17.22}$$

† The notation for stresses is changed here.

‡ This is assumed also in the more recent standard works by A. E. H. Love [50] and R. V. Southwell [29.2].

§ The $\frac{1}{2}$ has been inserted in the Navier, Cauchy shear strain definition to make it the component of a self-conjugate dyadic, as noted in volume I, article III,H.

as in volume 1, article III,9.2. Similarly, the continuity of the average spatial-displacement **V** is assured by

$$(\nabla\times\mathfrak{R})\times\nabla = 0 \tag{17.23}$$

For the generalised plane stress mean strain expressions **V**(17.21) with **V**(17.18) there occur the four relations

$$f_{xx;yy}+f_{yy;xx} = 2f_{xy;xy} \tag{17.24}$$

$$f_{zz;xx} = 0 \qquad f_{zz;yy} = 0 \qquad f_{zz;xy} = 0 \tag{17.25}$$

Filon does not consider the compatibility conditions in his formulation [79].

17.4. **Airy stress function and its distribution.** In terms of an Airy stress function $\mathcal{A}(R_x, R_y)$ equation **V**(17.20) is satisfied identically by

$$T_{xx} = \mathcal{A}_{;yy} \qquad T_{yy} = \mathcal{A}_{;xx} \qquad T_{xy} = -\mathcal{A}_{;xy} \tag{17.26}$$

From **V**(17.18),

$$f_{zz} = F(T_{xx}+T_{yy}) = F\nabla^2\mathcal{A} \tag{17.27}$$

Therefore, from **V**(17.25), the law of distribution of $\mathcal{A}$ is

$$\nabla^2\mathcal{A} = C+J_xR_x+J_yR_y \tag{17.28}$$

with arbitrary constants C, J_x, J_y, while to suit **V**(17.24) it is

$$\nabla^2\nabla^2\mathcal{A} = \nabla^4\mathcal{A} = 0 \tag{17.29}$$

less restrictive on $\mathcal{A}$ than **V**(17.28), which must, therefore, be obeyed.

Filon uses only **V**(17.21) in **V**(17.18) without considering f_{zz}, eliminates V_x, V_y between the three scalar equations and finds **V**(17.29) the biharmonic law of distribution of $\mathcal{A}$, which is seen to be not sufficiently restrictive on it when all the non-zero compatibility conditions are considered.†

Many problems are considered in which the outer boundaries are taken to be at infinity. Therefore, as position **R** approaches infinity the first stress invariant of equation **V**(17.28) also approaches infinity and this is not allowable. Therefore, in such cases at least, $J_x = 0 = J_y$, to leave the average stress first invariant χ^T constant throughout the plate.

† A. E. H. Love [50] implicitly, and R. V. Southwell [20.3] explicitly, in their books do the same thing as Filon.

18. Quasi-plane stress

On theoretical grounds, the present author concluded, in 1948, that heterogeneous plane stress does not occur generally [70],† while from the experimental observations on a plane rubber sheet given in article X,1 it was concluded‡ that an average transverse stress existed normal to the plane of the sheet if restricted isotropy is justified. This led to the following analysis, seen to be related to, but differing from, Filon's generalised plane stress theory in article V,17.

18.1. **Average stresses and strains.**‡. The formulation in article V,17.1 places no restrictions on the distribution of the stresses with respect to R_z except that $\mathbf{S}_z$ is zero on the stress-free main faces $R_z = \pm h$ of the moderately thick sheet. Thus, with F, G the stress-strain parameters, are found the average stress and strain relations

$$\mathfrak{N} = G(\mathfrak{T}' + \mathfrak{T}'') + F\chi^T \mathfrak{J} \tag{18.1}$$

$$\left.\begin{aligned} \mathfrak{T}' &= T_{xx}\mathbf{c}_x\mathbf{c}_x + T_{yy}\mathbf{c}_y\mathbf{c}_y + T_{xy}(\mathbf{c}_x\mathbf{c}_y + \mathbf{c}_y\mathbf{c}_x) \\ \mathfrak{T}'' &= T_{zz}\mathbf{c}_z\mathbf{c}_z + T_{zx}(\mathbf{c}_z\mathbf{c}_x + \mathbf{c}_x\mathbf{c}_z) + T_{yz}(\mathbf{c}_y\mathbf{c}_z + \mathbf{c}_z\mathbf{c}_y) \\ \chi^T &= T_{xx} + T_{yy} + T_{zz} \end{aligned}\right\} \tag{18.2}$$

while the average stress equilibrium equation is

$$\nabla\cdot\mathfrak{T}' + (T_{zx;x} + T_{yz;y})\mathbf{c}_z = 0 \tag{18.3}$$

Now, assume that the average shear stresses are zero. Thus,

$$T_{zx} = 0 = T_{yz} \tag{18.4}$$

More particularly, suppose that both S_{zx}, S_{yz} are odd in R_z, so that they have equal values but opposite signs at opposite positions R_z about the middle plane as in Fig. V,18.1, and then each of their average values is zero as in V(18.4). Again, assume that S_{zz} is even in R_z as in Fig. V,18.1, so that the average stress T_{zz} must be taken for physico-mathematical convenience, as acting on the main faces that are, in fact, physically stress-free.

With these assumptions,

$$\mathfrak{T}'' = T_{zz}\mathbf{c}_z\mathbf{c}_z \tag{18.5}$$

† The present author's statement in 1950 [70] that '. . . a "plane stress" condition is not possible in a heterogeneous stress distribution' is too restrictive. It should read '. . . is not *generally* possible . . .'.

‡ Author, 1951.

while the average stress equilibrium equation becomes two-dimensional in

$$\nabla \cdot \mathbb{T}' = 0 \tag{18.6}$$

The three-dimensional stress system in the interior of the plate has now been reduced to a quasi-plane system except for normal stress T_{zz} required to keep the thickness changes correct in the plate. This stress does not affect the equilibrium equation for the 'element' of edges dR_x, dR_y, $2h$ as in Fig. V,18.1.

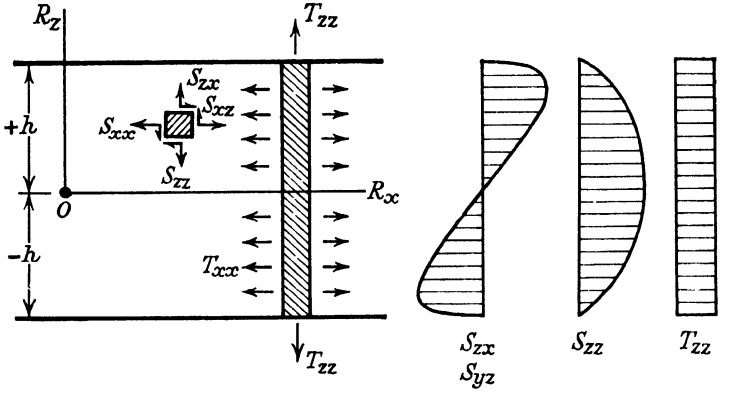

FIG. V,18.1. A three-dimensional stress system in a plane plate of moderate thickness $2h$ is reduced to a quasi-plane, average two-stress with a transverse, normal, average stress to give the correct thickness changes. For simplicity, the shear stresses S_{zx}, S_{yz} are assumed to be odd with respect to position about the middle plane, while the normal stress S_{zz} is even. All stresses and strains are averaged with respect to thickness to give the quasi-plane set.

18.2. **Average relative-displacement, average strain dyadic, average displacement potential.** The strain dyadic $\mathfrak{M}$, relative-displacement $\mathbf{D}^*$, displacement potential $\mathcal{E}$ are related by

$$\mathfrak{M} = \nabla \mathbf{D}^* = \nabla\nabla\mathcal{E}$$

Similarly, the corresponding average functions are, say, $\mathfrak{N}$, $\mathbf{E}^*$, $\mathcal{F}$ in

$$\mathfrak{N} = \nabla \mathbf{E}^* = \nabla\nabla\mathcal{F} \tag{18.7}$$

18.3. **Compatibility of average strains.** Similar to the author's compatibility condition for strains, the continuity of the average strain dyadic is assured by

$$\nabla \times \mathfrak{N} = 0 \tag{18.8}$$

For cartesian coordinates article A,12.1 gives, scalarly, for the non-zero terms after noting that the average values here are independent of R_z,

$$f_{xy;x} = f_{xx;y} \qquad f_{xy;y} = f_{yy;x} \qquad f_{zz;x} = 0 = f_{zz;y} \tag{18.9}$$

18.4. **Average stress potential.** The stress dyadic $\mathfrak{S}$ is represented in terms of stress potential H in

$$\mathfrak{S} = \nabla\nabla H$$

Similarly, with the corresponding terms $\mathfrak{T}'$, $\mathcal{J}(R_x, R_y)$,

$$\mathfrak{T}' = \nabla\nabla\mathcal{J} \tag{18.10}$$

or scalarly,

$$T'_{xx} = \mathcal{J}_{;xx} \qquad T_{yy} = \mathcal{J}_{;yy} \qquad T_{xy} = \mathcal{J}_{;xy} \tag{18.11}$$

Substituting V(18.10) in V(18.6) gives, with arbitrary constant C', the law of distribution,

$$\nabla^2\mathcal{J} = C' = \chi'^T = T_{xx} + T_{yy} \tag{18.12}$$

18.5. **Average stress potential and average strains compatibility.** From V(18.1) the scalar average stress-strain relations are

$$\left.\begin{aligned} f_{xx} &= GT_{xx} + F(\chi'^T + T_{zz}) \\ f_{yy} &= GT_{yy} + F(\chi'^T + T_{zz}) \\ f_{xy} &= GT_{xy} \\ f_{zz} &= (G+F)T_{zz} + F\chi'^T \end{aligned}\right\} \tag{18.13}$$

Using V(18.11), V(18.12) and substituting in V(18.9) gives

$$T_{zz;y} = 0 = T_{zz;x} \tag{18.14}$$

so that T_{zz} is independent of R_x, R_y. That is,

$$T_{zz} \neq T_{zz}(R_x, R_y) \tag{18.14'}$$

Therefore, noting equation V(18.13).4, the change in thickness of the moderately thick plate is constant at all positions on the stress-free main faces if a two-constant theory of restricted isotropy is to be justified. Thus, the average stress first invariant χ^T is constant, just as is the first stress invariant for plane stress.

18.6. **Average displacement potential in terms of the average stress potential.** Substituting V(18.14'), V(18.10),

V(18.7) in V(18.1) gives an equation that can be integrated readily. Thus,

$$\mathcal{F} = [G\mathcal{J}+\tfrac{1}{2}F\chi'^{T}\mathbf{R}\cdot\mathbf{R}+\mathbf{W}\cdot\mathbf{R}']+\tfrac{1}{2}T_{zz}(GR_z^2+F\mathbf{R}\cdot\mathbf{R}) \quad (18.15)$$

with $\mathbf{R}' = (R_x\mathbf{c}_x+R_y\mathbf{c}_y)$ and $\mathbf{W}$ an arbitrary, constant vector.

19. Complex variable solutions of plane problems using the Saint-Venant compatibility conditions

The complex variable appears to have been introduced into deformation analysis by Clebsch, in 1862 [19.21], for the torsion problem. The following application to plane problems is due to S. Timoshenko in 1931 [23.8]. Here, the treatment is by vector analysis for brevity and more generality in the first place.

The equations considered are the converse stress-strain equation of article V,5.5, the equilibrium stress equation and the Navier, Cauchy strains definition. That is, for elastic strains only, so that qualifying superscripts can be left off the stress-strain parameters J, K,

$$\mathfrak{S} = J\mathfrak{M}+K\chi^{D}\mathfrak{J} \quad (19.1)$$

$$\nabla\cdot\mathfrak{S} = 0 \quad (19.2)$$

$$\mathfrak{M} = \tfrac{1}{2}(\nabla\mathbf{U}+\mathbf{U}\nabla) = \nabla\mathbf{U}-\tfrac{1}{2}(\nabla\mathbf{U}-\mathbf{U}\nabla) \quad (19.3)$$

$$\chi^{D} = U_{x;x}+U_{y;y}+U_{z;z} \quad (19.4)$$

while the infinitesimal spatial-rotation antiself-conjugate dyadic is

$$\mathfrak{A} = \tfrac{1}{2}(\nabla\mathbf{U}-\mathbf{U}\nabla) \quad (19.4')$$

The essential step is to eliminate stresses from V(19.2) in favour of spatial-displacement gradients and to solve the resulting equation. Substituting V(19.4), V(19.3) in V(19.1) in V(19.2), noting that $\nabla\cdot\mathfrak{J} = \nabla$, while $\nabla\cdot\nabla = \nabla^2$, gives

$$(K/J)\nabla\chi^{D}+\nabla^2\mathbf{U}-\nabla\cdot\mathfrak{A} = 0 \quad (19.5)$$

19.1. **Plane stress and strain formulations from the classical viewpoint.** Suppose the stress dyadic in V(19.1) is two-dimensional, so that mixed subscripts involving z do not appear. For such plane stress the transverse normal strain is

$$e_{zz} = K(J+K)^{-1}(e_{xx}+e_{yy}) \quad (19.6)$$

Writing the infinitesimal *areal* dilation as

$$v = U_{x;x}+U_{y;y} \quad (19.7)$$

and the only non-zero spatial-rotation component as, say,

$$w = \tfrac{1}{2}(U_{y;x} - U_{x;y}) \tag{19.8}$$

and with Poisson's ratio q, then equation V(19.5), for *plane stress* [23.9], gives

$$\left.\begin{aligned}(1-q)^{-1}v_{;x} - w_{;y} &= 0\\ (1-q)^{-1}v_{;y} + w_{;x} &= 0\end{aligned}\right\} \tag{19.9}$$

With $e_{zz} = 0$, the transverse stress is given by V(19.1) as

$$S_{zz} = K(e_{xx} + e_{yy})$$

so that V(19.5) gives [23.8], for *plane strain*,

$$\left.\begin{aligned}(1-q)(1-2q)^{-1}v_{;x} - w_{;y} &= 0\\ (1-q)(1-2q)^{-1}v_{;y} + w_{;x} &= 0\end{aligned}\right\} \tag{19.10}$$

With the complex variable c of appendix B and with $i = \sqrt{(-1)}$, then a function of c can be written as

$$\gamma = \alpha + i\beta \tag{19.11}$$

and is differentiable when the Cauchy-Riemann conditions are satisfied. These are, from article **B**,3,

$$\alpha_{;x} = \beta_{;y} \qquad -\alpha_{;y} = \beta_{;x} \tag{19.12}$$

Comparison with V(19.10) gives, for *plane strain*,

$$(1-q)(1-2q)^{-1}v = \alpha \qquad w = \beta \tag{19.13}$$

while, for *plane stress*,

$$(1-q)^{-1}v = \alpha \qquad w = \beta \tag{19.14}$$

19.2. **A solution for displacements for plane stress.** S. Timoshenko [23.10] gives a solution which will be given now, and then examined critically. Substituting V(19.7), V(19.8) in V(19.9), multiplying through by 2 and then comparing with the Cauchy-Riemann conditions V(19.12) gives

$$\left.\begin{aligned}U_{x;x} + U_{y;y} &= \tfrac{1}{2}(1-q)\alpha\\ U_{y;x} - U_{x;y} &= \beta\end{aligned}\right\} \tag{19.15}$$

(Note that the α, β here differ by a numerical constant from those in V(19.14).)

The particular integral of these equations is given by

$$\left.\begin{aligned}U_x^p &= -\tfrac{1}{4}(1+q)R_y\beta^p + \tfrac{1}{2}A\\ U_y^p &= -\tfrac{1}{4}(1+q)R_y\alpha^p + \tfrac{1}{4}(1-q)B\end{aligned}\right\} \tag{19.16}$$

say, with the complex function

$$C = \int \gamma^p dc = A + iB \tag{19.17}$$

Substituting V(19.16) in V(19.15) and using the relationships between $A_{;x}$, ... and α, ... given in article B,3 shows that V(19.15) is satisfied.

The complementary solution of V(19.15) is given by equating the left-hand side of each equation to zero. In this case, the displacement components satisfy the Cauchy-Riemann conditions, so that the complementary integral is, say,

$$U_x^c = \beta^c \qquad U_y^c = \alpha^c \tag{19.18}$$

with the arbitrary complex function

$$\gamma^c = \alpha^c + i\beta^c$$

By adding V(19.18) to V(19.16), the spatial-displacement components are given in a complex form as

$$U_y + iU_x = -\tfrac{1}{4}(1+q)R_y\gamma^p + \tfrac{1}{4}(1-q)B + i\tfrac{1}{2}A + \gamma^c \tag{19.19}$$

19.3. **A solution for Navier, Cauchy strains for plane stress.** The two-dimensional, self-conjugate strain dyadic components are, for the Navier, Cauchy strains definitions, say,

$$\left.\begin{aligned} e_{xx}^p &= U_{x;x}^p = \tfrac{1}{4}(1+q)R_y\alpha_{;y}^p + \tfrac{1}{2}\alpha^p \\ e_{yy}^p &= U_{y;y}^p = -\tfrac{1}{4}(1+q)R_y\alpha_{;y}^p - \tfrac{1}{2}q\alpha^p \\ e_{xy}^p &= \tfrac{1}{2}(U_{x;y}^p + U_{y;x}^p) = -\tfrac{1}{4}(1+q)R_y\alpha_{;x}^p - \tfrac{1}{2}(1+q)\beta^p \end{aligned}\right\} \tag{19.20}$$

for the particular integral solution V(19.16), while for the complementary integral solution V(19.18) they are, say,

$$\left.\begin{aligned} e_{xx}^c &= \beta_{;x}^c \qquad e_{yy}^c = \alpha_{;y}^c \\ e_{xy}^c &= \tfrac{1}{2}(\beta_{;y}^c + \alpha_{;x}^c) = \beta_{;y}^c = \alpha_{;x}^c \end{aligned}\right\} \tag{19.20'}$$

The strains must satisfy at least the Saint-Venant strains compatibility conditions ensuring continuity of infinitesimal spatial-displacement. Article V,15 gives these as the four equations

$$e_{xx;yy} + e_{yy;xx} = 2e_{xy;xy} \tag{19.21}$$

$$e_{zz;xx} = 0 \qquad e_{zz;yy} = 0 \qquad e_{zz;xy} = 0 \tag{19.21'}$$

The particular integral strains satisfy V(19.21) but do not satisfy V(19.21') unless α^p is linear in R_x, R_y. Thus, α^p can be only such a specialised solution of the governing laplacian equation. If this is true, then α^p approaches infinity with the position vector **R**. But e_{zz}^p and areal dilation v^p are only different from α^p by constant stress-strain parameters multipliers, so that they also, approach infinity with **R**. This is not allowable physically,

so that, in infinite plates at least, the α^p cannot be more general than a constant value. This corresponds with the inference drawn in article V,15.1. Thus, for an infinite plate at least, equations V(19.20) become

$$e^p_{xx} = \tfrac{1}{2}\alpha^p \qquad e^p_{yy} = -\tfrac{1}{2}q\alpha^p \qquad e^p_{xy} = -\tfrac{1}{2}(1+q)\alpha^p \qquad (19.22)$$

so that this component of the strain field is homogeneous with special ratios between its component strains.

With V(19.12) in V(19.20′), it is seen that areal dilation, and hence e^c_{zz}, are zero to satisfy the three conditions V(19.21′). The complementary integral strains obey all four conditions of strains compatibility according to Saint-Venant. In fact, from V(19.20′), they satisfy the more restricted conditions

$$e^c_{xx;y} = e^c_{xy;x} \qquad e^c_{yy;x} = e^c_{xy;y} \qquad (19.23)$$

which are those of the present author, as seen in article V,6.

19.4. **Conclusions on the proposed solution.** The solution proposed by S. Timoshenko for spatial-displacement, as in article V,19.2, is not as general as it appears to be at first sight. The particular integral part of the solution does not satisfy the Saint-Venant conditions for strains compatibility for plane stress except for a linear distribution of areal dilation or transverse strain. The particular integral strains and stresses must be homogeneous if the plate is infinite and with special ratios between the component strains.

The present author did not notice† this fact in 1943 and applied these equations in the general form to solve for the stresses in a thin, large (but not infinite) plate due to a rivet pulled planewise [81, 82]. In spite of this deficiency of formulation, a good qualitative agreement was found between the theoretical solution and an experimental study using the brittle-coat technique. This is consistent with the observation by H. Kolsky, in 1952 [91], that a plane strain solution of the problem of contact between elastic bodies, as given by Hertz in 1881 [92], checked closely with a photo-elastic test on a fairly thin plate. The three conditions V(19.21′) do not appear for plane strain.

† The validity of the *formulation* of this theory was not questioned, since it had not been questioned by the prominent writers. The present author's task, at that time, was *application* to a specific problem.

20. Complex variable solutions of plane problems using relative-displacement

Article V,19.1 gives infinitesimal areal dilation and spatial-rotation as

$$v = U_{x;x}+U_{y;y} \qquad w = \tfrac{1}{2}(U_{y;x}-U_{x;y}) \tag{20.1}$$

Putting both of these zero gives, from V(19.5),

$$\nabla^2\mathbf{U} = 0 \tag{20.2}$$

consistent with the complementary integral displacements of article V,19.2 giving

$$U_x = \beta \qquad U_y = \alpha \tag{20.3}$$

$$\left.\begin{aligned} \alpha+i\beta &= \gamma(c) & c &= R_x+iR_y \\ \alpha-i\beta &= \gamma'(c') & c' &= R_x-iR_y \end{aligned}\right\} \tag{20.4}$$

since α, β are both laplacian. Then,

$$\mathbf{U} = \beta\mathbf{c}_x+\alpha\mathbf{c}_y \approx i\gamma' = \beta+i\alpha \tag{20.5}$$

treating this latter complex function as a *vector* with the real, imaginary components in directions $\mathbf{c}_x$, $\mathbf{c}_y$ respectively.

From article V,19.3 the scalar strains are, using V(20.3),

$$\left.\begin{aligned} e_{xx} &= \beta_{;x} = -\alpha_{;y} \\ e_{yy} &= -\beta_{;x} = \alpha_{;y} \\ e_{xy} &= \beta_{;y} = \alpha_{;x} \end{aligned}\right\} \tag{20.6}$$

Putting this into two-dimensional dyadic form it can easily be rearranged to give,† on using V(20.4),

$$\mathfrak{M} = \nabla\beta\cdot\mathfrak{J}\mathbf{c}_x+\nabla\alpha\cdot\mathfrak{J}\mathbf{c}_y = \nabla(\beta\mathbf{c}_x+\alpha\mathbf{c}_y) = \nabla\mathbf{U} \tag{20.7}$$

Comparison with the complex potential analysis in B,6 shows that the spatial-displacement and the strain dyadic can be found by a different process. Thus, with the complex vector

$$\overset{\circ}{\mathbf{c}} = \mathbf{c}_x+i\mathbf{c}_y = (\mathbf{c}_r+i\mathbf{c}_\theta)\exp(i\theta)$$

and total differentiation denoted briefly by the subscript solidus, then the complex displacement and complex strain dyadic are

$$\left.\begin{aligned} \overset{\circ}{\mathbf{U}} &= \nabla\gamma' = \overset{\circ}{\mathbf{c}}\gamma_{/c} \\ \overset{\circ}{\mathfrak{M}} &= \nabla\overset{\circ}{\mathbf{U}} = \overset{\circ}{\mathbf{c}}\overset{\circ}{\mathbf{c}}\gamma_{/cc} \end{aligned}\right\} \tag{20.7'}$$

Two complementary solutions result from the separation of the real and imaginary parts of each equation.

† Author, 1952.

20.1. **Infinitesimal spatial-displacement, finite straining-displacement, relative-displacement and strains compatibility.** When whole-body rotation is zero, then spatial-displacement **U** equals straining-displacement **D**. When strains are infinitesimal, then **D** virtually equals $\mathbf{D}^*$ the relative-displacement. Therefore, **V**(20.5) gives a relative-displacement lamellar vector field in which the strain and two-stress first invariants are zero. Thus, there is established the correspondence relationships allowing the orthogonal transformation from the pattern of principal normal strain trajectories in the strained elastic sheet to the set in the unstrained sheet. The principle of straining equivalence between finite $\mathbf{D}^*$, **D** and $\mathbf{R}^{o*}$, $\mathbf{R}^{o\,\mathrm{inst}}$ applies because straining convection-displacement $\mathbf{C}^{\mathrm{st}}$ does not appear explicitly in the complementary doublet vector fields, and so gives the unstrained shape for finite strain.

As 'true' strains, the expressions **V**(20.6) are compatible in the author's conditions

$$\left.\begin{aligned} e_{xx;y} = e_{xy;x} = \beta_{;xy} = -\alpha_{;yy} = \alpha_{;xx} \\ e_{yy;x} = e_{xy;y} = \alpha_{;xy} = \beta_{;yy} = -\beta_{;xx} \end{aligned}\right\} \quad (20.8)$$

more restrictive than those of Saint-Venant in article **V**,19.3.

Chapter VI

HETEROGENEOUS TWO-STRESS EXPERIMENTS

1. Simple tension on a thin sheet around a hole which is circular in the deformed state [68]

A sheet of rubber 0·006 inch thick by 6 inches wide and 9½ inches long was stretched severely by a simple tensile pull parallel to the

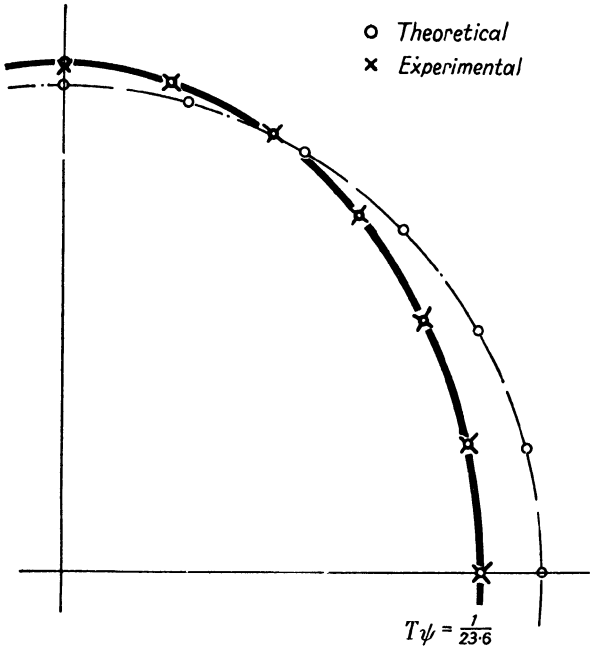

FIG. VI,1.1.—A hole in a thin, rectangular rubber sheet under approximately simple tensile stress T. The hole is *circular* in the *deformed* state and is shown by the chain-dot line. Elastic modulus ψ was not found directly, but the value of $T\psi$ was calculated from the theory and experiment at $\theta = 0$ on the axis of symmetry. This calibration at one point gives good fit between theory and experiment at all the other points observed.

9½-inch side of the sheet. A sheet of clear celluloid held the thin rubber sheet flat while a circular hole was cut in the deformed sheet by successive small cuts. The hole was circular at a diameter of 1·69 inches. The boundary of the hole was marked with

a fine ink line every 15°. The load was removed and the displacement of points on the hole boundary measured with an engineer's steel rule graduated to 0·01 inch assisted by a hand magnifying lens. The values measured are indicated by crosses

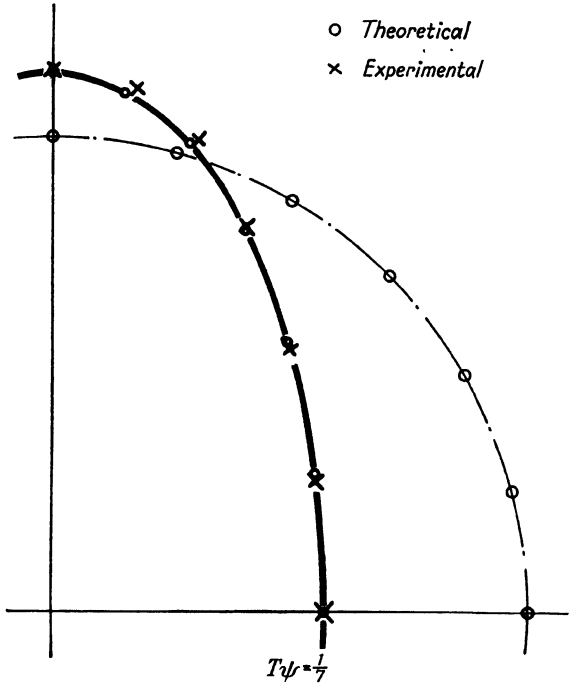

FIG. VI,1.2.— Conditions and calibration the same as those for Fig. VI,1.1 when the simple tension is increased as here. Lack of fit at $\theta = 60°$, 75° mainly due to experimental difficulty in cutting the circular deformed hole.

in Fig. VI,1.1. The circles show theoretical values found in article VII,3.

The sheet was strained still more severely and the deformed hole was nearly circular after cutting to 2·20 inches diameter. By eye, it was seen that the boundary of the hole did not change smoothly at $\theta = 60°$, 75° where the points are, in fact, not on the smooth, theoretical curve in Fig. VI,1.2, but it was difficult experimentally to correct it while the sheet was strained because each cut induced fairly large redistribution of strain in the sheet. For the severe state of strain the displacements were measured

at various points in the sheet and the values not too far from the hole are shown in Fig. VI,1.3.

2. Duralumin plate yielded by radial pressure in a circular hole†

The theoretical solution is found readily for a heterogeneous two-stress (plane stress) induced by radial pressure in a circular hole in an infinite, or finite, thin sheet. This suggested trying to examine such loading experimentally for comparison with the theory.

2.1. **Segmented collet.** Actual hydraulic radial pressure is not easy to apply in such a case, so it was decided to expand a

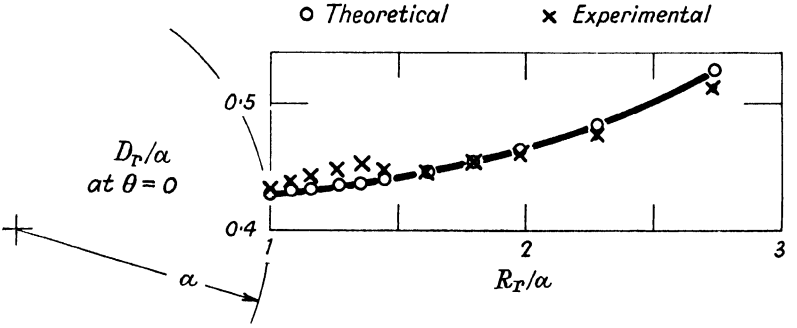

FIG. VI,1.3.—For the tension in Fig. VI,1.2, these are the straining-displacements of points on the axis of pull. The circular deformed hole is of radius a.

twelve-segmented, hardened steel collet by axial loading on a tapered mandrel as shown diagrammatically in Fig. VI,2.1. Colloidal graphite lubrication was used between the sliding tapered surfaces, but the right cylindrical surfaces between the collet and the hole in the plate were left dry so that the electrical strain-gauges would not be affected mechanically for adhesion or electrically for insulation. The use of twelve segments gave a collet segment of practicable size and yet sufficiently small to ensure that stress diffusion would give reasonably uniform 'radial pressure' at positions not too close to the boundary of the hole.

† Author, 1947. Experimental measurements unpublished.

2.2. **Strain measurements.** Measurements† of strain were made with circumferential Minalpha[8,9], resistance-wires of 0·001 inch diameter on one face of the plate. The bare resistance-

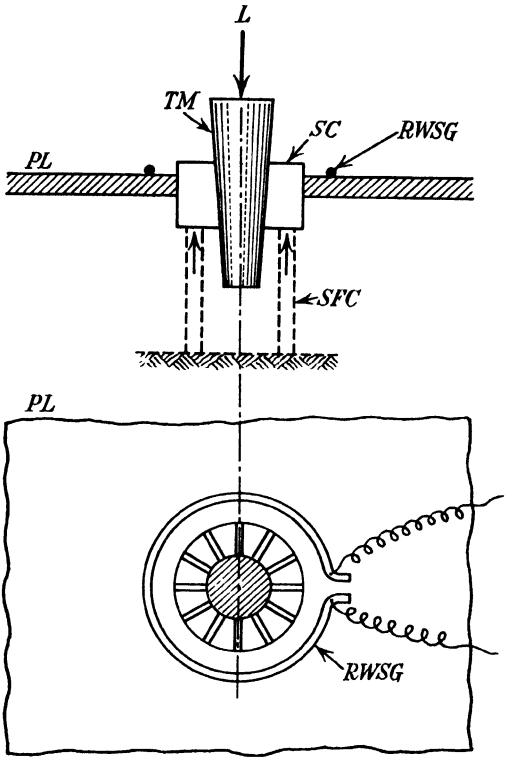

FIG. VI,2.1.– A twelve-segmented collet (or plug) expanded in a duralumin plate by axial load on the tapered mandrel lubricated by colloidal graphite. Circumferential strains were measured by resistance-wire strain-gauges at various radii on one main face of the plate. The notation is: *PL* = plate, *SC* = segmented collet, *TM* = tapered mandrel, *SFC* = support for collet, *L* = load, *RWSG* = resistance-wire strain-gauge.

wires were insulated from the metal test plate by condenser tissue 0·001 inch thick. The paper was cemented to the plate and the resistance-wires to the paper by 'Durofix' cellulose

† Mr. C. R. Urwin suggested the use of the Kelvin double bridge to minimise the unwanted resistance changes in the switch contacts. The present author suggested a much simpler arrangement giving the same advantages by using 'potential' leads to a modified Wheatstone bridge using high-ratio arms[27].

acetate cement. Once the plate had yielded there was no way of checking if the gauges were still behaving correctly. Therefore, the mean diameter of the collet was measured at each load stage and used in the analysis to give some check on the gauges. The gauges appear to have behaved correctly, since their readings, together with the tangential strain calculated from the collet diameter, define a smooth curve for all loadings. The measurements are given in Table VI,2.2 with the initial sizes in Table VI,2.1. Changes in thickness of the plate were not measured.

TABLE VI,2.1

Initial sizes

Collet diameter, inches	Electrical strain-gauges radius, inches									
	No. 1	2	3	4	5	6	7	8	9	10
1·372	0·751	0·814	0·938	1·127	1·376	1·752	2·250	3·000	4·250	5·739

The collet segments shattered at the greatest axial load, so that observations with release of load were impossible.

2.3. **Radial pressure in the hole.** The radial pressure between the cylindrical face of the collet and the cylindrical surface of the hole in the plate was not measured but estimated from the value of the coefficient of friction of metal surfaces lubricated by colloidal graphite, accepted as about 0·073. A check was given at pre-yield loading by the solution for radial pressure inducing elastic strains throughout the plate of closely the same value as that using the axial loading, taper of the mandrel and the accepted coefficient of friction. After primary yield the position of the yield boundary between the elastic and elasto-plastic zones was estimated from the gauge readings and the elastic strain theory for radial pressure at the yield boundary.

2.4. **Plate proportions.** Since a plane polar two-stress analysis was to be examined it seemed desirable to have a plate as 'thin' as possible. A duralumin plate 36 inches in diameter by $\frac{1}{4}$ inch thick with a 3-inch diameter central hole was prepared with elaborate electrical resistance strain-gauges in the circumferential and radial directions built on to one main surface. A 3-inch

TABLE VI,2.2

Axial load, lbs	1 170	2 590	4 550	6 580	9 290	11 390	13 330	17 930	26 860	30 390
Mandrel axial movement, inches	0·090	0·173	0·280	0·400	0·704	1·086	1·406	1·796	not read	not read
Collet diameter, inches	1·372	1·375	1·377	1·381	1·390	1·405	1·416	1·432	1·447	1·465
Electrical gauges circumferential nominal strain 10^3										
No. 1	1·518	2·668	4·517	6·610	12·53	20·18	26·52	34·62	45·40	55·70
2	1·340	2·375	3·928	5·715	10·72	16·94	22·05	28·50	36·68	44·62
3	1·060	1·899	2 968	4·260	7·745	12·30	16·06	20·50	26·16	31·44
4	0·759	1·358	2·125	2·861	4·960	7·683	10·08	12·78	16·37	19·53
5	0·518	0·963	1·469	1·960	3·115	4·618	5·835	7·330	9·280	11·12
6	0·294	0·579	0·955	1·246	1·975	2·752	3·392	4·176	5·155	6·095
7	0·202	0·363	0·606	0·809	1·245	1·744	2·088	2·513	3·012	3·477
8	0·135	0·257	0·427	$0·486_5$	0·783	1·106	1·344	1·616	1·936	2·208
9	$0·079_8$	$0·141_7$	0·233	$0·263_8$	0·428	0·603	0·728	0·878	1·049	1·108
10	$0·043_9$	$0·087_8$	0·143	0·163	$0·264_8$	0·378	0·454	$0·544_5$	0·651	0·740

diameter twelve-segmented collet, etc., was built. Almost as soon as axial load was applied to the tapered mandrel the test plate buckled up to the shape of a truncated cone! Pilot tests with small collets and plates indicated that the plate should be of a thickness approximately equal to the radius of the hole to ensure large strains near the hole without plate buckling. The plate used was duralumin $\frac{5}{8}$ inch thick and the initially unstrained hole was about $1\frac{3}{8}$ inches diameter. This was the only practicable plate thickness available at the time (1947). An outer diameter of about 12 inches was large enough for this stress-free boundary to have little effect on the stress and strain near the hole.

2.5. **Control test on the duralumin.** The theoretical stresses are almost equal tension and compression, so that the loading of the duralumin was practically equivalent to pure shear stress. With the equipment available only a simple tensile test was possible and is discussed in article I,5 with Figs. I,5.1, I,5.2 showing the stress-strain curves for the initial and whole strain range respectively. The primary and secondary values of the elastic modulus ψ^E are given in article I,9.5 with Fig. I,9.3. The plastic modulus ψ^P for simple tension is given in article I,10.2 with Fig. I,10.2. The elastic and plastic transverse contraction ratios are given in article I,11.3 with Figs. I,11.1, I,11.2.

Single-filament resistance-wire strain-gauges similar to those on the specimen plate were used to measure the strains and were calibrated and checked by the optical triple-armed extensometer [3] mentioned in article I,1.1. It was found† that a filament could be straight without end loops to act as 'anchors' and that it could be loaded by just the cement on its surface joining it to the paper base. Further, if the joint between the filament and the outgoing wire to the electrical measuring bridge is arranged to be unstrained [8, 9] then the strain range for a given material is doubled approximately in comparison to that with a strained joint.

† Author, 1946.

Chapter VII

TWO-STRESS THEORETICAL EXAMPLES

1. Normal loading on the cylindrical faces of an annulus of elastic substance of restricted isotropy and constant stress-strain parameters

When the substance is elastic, of restricted isotropy and constant stress-strain parameters, then the analysis of deformation is comparatively simple because the total stresses and strains may be used in the calculation. The analysis must cover the steps given in article V,1. The simple case of normal stress applied to the cylindrical faces of an annulus will illustrate the heterogeneous strain theory when strain transfer is zero. Plane polar stresses will be assumed with body force zero.

1.1. **Stress equations.** From axial symmetry, it is concluded that the shear stress is zero, and this requires the stress potential H to be independent of coordinate θ. Then, from article V,10.2, the non-zero stresses are

$$S_{rr} = H_{;rr} \qquad S_{\theta\theta} = R_r^{-1} H_{;r} \tag{1.1}$$

Article V,11 gives the equilibrium stress equation as

$$H_{;rr} + R_r^{-1} H_{;r} = C \tag{1.2}$$

Arbitrary constant C will be determined from the geometry of the boundaries and the boundary stresses.

1.2. **Stress potential and stresses.** Choosing

$$H = \tfrac{1}{4} C R_r^2 \tag{1.3}$$

gives the particular integral of VII(1.2). Choosing

$$H = -J \log R_r + K \tag{1.4}$$

with arbitrary constants J, K gives the complementary solution of VII(1.2) when the left-hand side is zero. The complete solution of VII(1.2) is, therefore,

$$H = \tfrac{1}{4} C R_r^2 - J \log R_r + K \tag{1.5}$$

Substituting in VII(1.1) gives the stresses

$$S_{rr} = \tfrac{1}{2} C + J R_r^{-2} \qquad S_{\theta\theta} = \tfrac{1}{2} C - J R_r^{-2} \tag{1.6}$$

1.3. **Boundary stresses.** Let the inner and outer boundaries of the annulus be of radii a, b respectively and the applied normal stresses A, B that are positive when radially tensile as in Fig. VII,1.1. Substituting these values for the radial stress and radii in VII(1.6).1 and solving the resulting two equations for the two constants gives

$$C = 2(Ba^{-2}-Ab^{-2})/(a^{-2}-b^{-2}) \qquad J = (A-B)/(a^{-2}-b^{-2}) \quad (1.7)$$

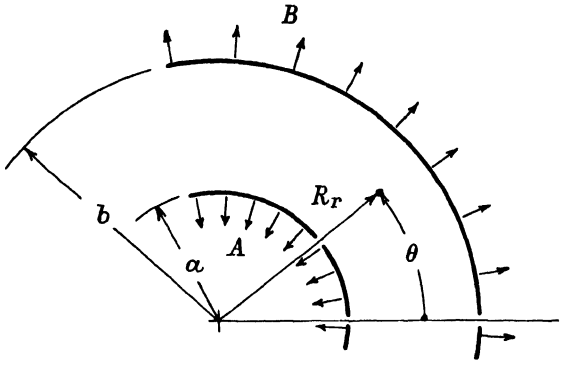

FIG. VII,1.1.— Radial tensions A, B on the inner and outer boundaries of an annulus of inner and outer radii a, b. Plane polar two-stress is induced.

1.4. **Strains.** From article V,5.5, ignoring the plastic increment strains and leaving off the unnecessary superscripts from the stress-strain parameters F, G gives the stress-strain relations

$$\left.\begin{aligned} e_{rr} &= GS_{rr}+F(S_{rr}+S_{\theta\theta}) \\ e_{\theta\theta} &= GS_{\theta\theta}+F(S_{rr}+S_{\theta\theta}) \\ e_{r\theta} &= 0 \qquad e_{zz} = F(S_{rr}+S_{\theta\theta}) \end{aligned}\right\} \quad (1.8)$$

Substituting from article VII,1.2 for stresses gives

$$\left.\begin{aligned} e_{rr} &= JGR_r^{-2}+C(F+\tfrac{1}{2}G) \\ e_{\theta\theta} &= -JGR_r^{-2}+C(F+\tfrac{1}{2}G) \\ e_{zz} &= C(F+\tfrac{1}{2}G) \end{aligned}\right\} \quad (1.9)$$

The transverse strain e_{zz} is constant, so that the deformed annulus of constant thickness is also of constant thickness when unloaded to its undeformed state.

1.5. **Displacement potential and relative-displacement.** From article V,12.1, for the present case, the displacement

potential is independent of θ from physical symmetry, as in Fig. **VII**,1.2, and gives with Hf from article **VII**,1.2,

$$\mathcal{E} = GHf + \tfrac{1}{2}FC(R_r^2 + R_z^2) + W_r R_r + W_z R_z \qquad (1.10)$$

The relative-displacement components are given in article **V**,8.2 as

$$D_r^* = \mathcal{E}_{;r} \qquad D_z^* = \mathcal{E}_{;z} \qquad (1.11)$$

Substituting **VII**(1.10) gives

$$D_r^* = -GJR_r^{-1} + (F + \tfrac{1}{2}G)CR_r + W_r \qquad D_z^* = FCR_z + W_z \qquad (1.12)$$

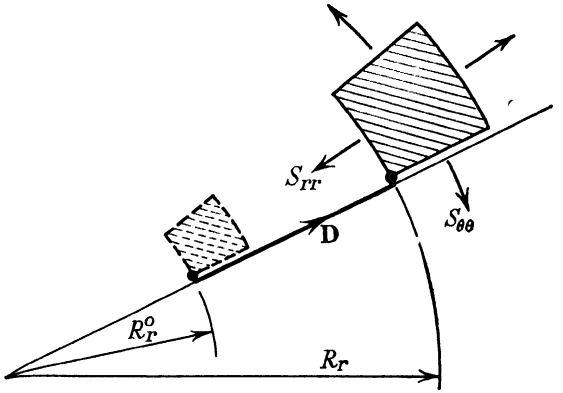

FIG. **VII**,1.2.—The dotted, orthogonal, plane polar, curvilinear element is the unstrained element that becomes the strained element of the elastic annulus with radial tension on its boundaries. The straining-displacement **D** is radial and equals the relative-displacement **D*** because straining-rotation is zero. Whole-body rotation is zero because at least one principal element suffers zero spatial-rotation.

The fixing condition that the deformed and undeformed annuli shall be coaxial is satisfied with $W_r = 0$. If the planes $R_z = 0$ coincide in these two states then $W_z = 0$. Then,

$$D_r^* = -GJR_r^{-1} + (F + \tfrac{1}{2}G)CR_r \qquad D_z^* = FCR_z \qquad (1.12')$$

Straining-rotation is zero throughout the annulus since the principal, curvilinear elements are curvilinearly parallel, although of different sizes, in the deformed and undeformed states. Therefore, relative-displacement **D*** and straining-displacement **D** are equal for all values of strain. Again, all points suffer no spatial-rotation and, therefore, whole-body rotation is zero (noting that, for this condition, only *one* point need have zero spatial-rotation).

1.6. **Solid disc.** When the inner radius is zero, then the analysis deals with radial tension B on the outer boundary of a solid disc. Then, with $a = 0$,

$$J = 0 \qquad \tfrac{1}{2}C = B \tag{1.13}$$

$$S_{rr} = B = S_{\theta\theta} \tag{1.14}$$

and the true stresses are isotropic in the plane (R_r, θ) and equal to the applied tension on the outer boundary. The relative-displacements are

$$D_r^* = (2F+G)BR_r \qquad D_z^* = 2FBR_z \tag{1.15}$$

1.7. **Hollow disc loaded on the outer boundary.** Let $A = 0$ in **VII**(1.7) and then

$$\left.\begin{aligned} S_{rr} &= B(1-a^2R_r^{-2})/(1-a^2b^{-2}) \\ S_{\theta\theta} &= B(1+a^2R_r^{-2})/(1-a^2b^{-2}) \end{aligned}\right\} \tag{1.16}$$

with

$$\tfrac{1}{2}C = Ba^{-2}/(a^{-2}-b^{-2}) \qquad J = -B/(a^{-2}-b^{-2}) \tag{1.17}$$

From **VII**(1.12′), when $R_r = a$ then D_r^* equals D_a^* and when $R_r = b$ then it equals D_b^*. Thus,

$$\left.\begin{aligned} D_a^* &= -GJa^{-1}+(F+\tfrac{1}{2}G)Ca \\ D_b^* &= -GJb^{-1}+(F+\tfrac{1}{2}G)Cb \end{aligned}\right\} \tag{1.18}$$

Let a^o, b^o be the inner and outer radii when the annulus is unloaded and then

$$a = a^o+D_a^* \qquad b = b^o+D_b^* \tag{1.19}$$

Substituting these expressions for a, b in **VII**(1.18) gives two equations to determine the values of D_a^*, D_b^* and hence a, b when the initial proportions a^o, b^o are prescribed. Numerical or graphical methods of solution appear to be indicated and will be left to the reader as an exercise when the initial proportions have been decided and the values of the stress-strain parameters found. With rubber, for example, it is a reasonable approximation to take the true stress-strain parameters as constant for strains up to the order 50 to 75 per cent in the 'nominal' measure.

1.8. **Infinite disc loaded on the inner boundary.** When the outer radius is so large that b^{-2} and Ab^{-2} are negligible, while the outer boundary stress B is zero, then

$$S_{rr} = Aa^2R_r^{-2} \qquad S_{\theta\theta} = -Aa^2R_r^{-2} \tag{1.20}$$

with $C = 0$, $J = Aa^2$ and

$$D_r^* = -GAa^2R_r^{-1} \tag{1.21}$$

1.9. **Thin-walled tube loaded on the inner surface.** The solution given in article **VII**,1.2 applies to a tube when there is no applied axial normal stress. Specialise the case to zero external stress and the thin wall of thickness h, so that $b = a+h$. Suppose radial position R_r now equals $a+j$ with $0 \leqq j \leqq h$. Suppose j and h sufficiently small to neglect their products and powers. To this degree of approximation are found

$$S_{rr} = A(1-j/h) \qquad S_{\theta\theta} = A(-a/h-1+j/h) \tag{1.22}$$

The stresses are seen to vary linearly with position through the tube wall, while $S_{\theta\theta}$ does not change greatly since, usually, a/h is great compared with unity. The applied stress A will usually be negative, for pressure, because the thin-walled tube is liable to unstable collapse under internal radial tension.

The tangential strain at the inner surface $R_r = a$ is

$$e_{\theta\theta} = 1-a^o/a = GS_{\theta\theta}+F(S_{rr}+S_{\theta\theta})$$

to give the expansion ratio

$$a/a^o = [1+AG+Aa(F+G)/h]^{-1} \tag{1.23}$$

2. Normal and shear loading on the cylindrical faces of an annulus of elastic substance of restricted isotropy and constant stress-strain parameters

When shear stress as well as normal stress is applied to the cylindrical faces of an annulus of deformed elastic substance then straining-rotation of principal elements occurs one to another. This is more complicated than the preceding example, in article **VII**,1, where straining-rotation is zero at all points, for all states, between the initially undeformed and currently deformed state. Here, the unloaded annulus is not circular and not of constant radial width.

2.1. **Stress equations.** The stresses are now to be functions of θ in the plane polar coordinates (R_r, θ) and article **V**,10.2 gives

$$S_{rr} = H_{;rr} \qquad S_{\theta\theta} = R_r^{-2}H_{;\theta\theta}+R_r^{-1}H_{;r} \qquad S_{r\theta} = (R_r^{-1}H_{;\theta})_{;r} \tag{2.1}$$

From article **V**,11.2 the stress potential obeys

$$H_{;rr}+R_r^{-1}H_{;r}+R_r^{-2}H_{;\theta\theta} = C \tag{2.2}$$

2.2. **Stress potential and stresses.** Choose a stress potential to give S_{rr} even in θ, with stresses decreasing with radius and with

constant C put as zero so that VII(2.2) becomes Laplace's equation. Choose as a simple example

$$H = \tfrac{1}{2}AR_r^{-1}\cos\theta \tag{2.3}$$

with arbitrary constant A. Substituting in VII(2.2) gives correctly

$$\nabla^2 H = 0 \tag{2.4}$$

Substituting VII(2.3) in VII(2.1) gives

$$S_{rr} = AR_r^{-3}\cos\theta \qquad S_{\theta\theta} = -AR_r^{-3}\cos\theta \qquad S_{r\theta} = AR_r^{-3}\sin\theta \tag{2.5}$$

2.3. **Boundary stresses.** If the plate is infinite then the outer boundary is stress-free. With an inner boundary of radius a in the deformed plate then the stresses acting upon it are

$$S_{aa} = Aa^{-3}\cos\theta \qquad S_{a\theta} = Aa^{-3}\sin\theta \tag{2.6}$$

2.4. **Strains.** The constant C equals the first stress invariant and, since this is zero, then the stress-strain relations of article V,5.5 become

$$\left.\begin{aligned} e_{rr} &= GS_{rr} = GAR_r^{-3}\cos\theta \\ e_{\theta\theta} &= GS_{\theta\theta} = -GAR_r^{-3}\cos\theta \\ e_{r\theta} &= GS_{r\theta} = GAR_r^{-3}\sin\theta \\ e_{zz} &= 0 \end{aligned}\right\} \tag{2.7}$$

The sheet does not change in thickness, since e_{zz} is zero.

2.5. **Displacement potential and relative-displacement.** The constant C is zero, so that, from article V,12.1 with equation VII(2.3), the displacement potential is

$$\mathcal{E} = \tfrac{1}{2}GAR_r^{-1}\cos\theta + W_xR_r\cos\theta + W_yR_r\sin\theta + W_zR_z \tag{2.8}$$

Article V,8.2 gives the relative-displacement components as

$$\left.\begin{aligned} D_r^* &= \mathcal{E}_{;r} = -\tfrac{1}{2}GAR_r^{-2}\cos\theta + W_x\cos\theta + W_y\sin\theta \\ D_\theta^* &= R_r^{-1}\mathcal{E}_{;\theta} = -\tfrac{1}{2}GAR_r^{-2}\sin\theta - W_x\sin\theta + W_y\cos\theta \\ D_z^* &= \mathcal{E}_{;z} = W_z \end{aligned}\right\} \tag{2.9}$$

Assume the boundary conditions such that the relative-displacement is zero at infinity while D_z^* is zero. Then,

$$D_r^* = -\tfrac{1}{2}GAR_r^{-2}\cos\theta \qquad D_\theta^* = -\tfrac{1}{2}GAR_r^{-2}\sin\theta \qquad D_z^* = 0 \tag{2.10}$$

2.6. **Straining-displacement and instantaneously initial position.** The relatively initial position, as in article V,1.4, is

$$\begin{aligned}\mathbf{R}^{o*} &= \mathbf{R}-\mathbf{D}^* \\ &= (R_r+\tfrac{1}{2}GAR_r^{-2}\cos\theta)\mathbf{c}_r+\tfrac{1}{2}GAR_r^{-2}\sin\theta\mathbf{c}_\theta+R_z\mathbf{c}_z \quad (2.11)\end{aligned}$$

When the deformation is infinitesimal, then each component of the doublet ($\mathbf{R}^{o*}$, $\mathbf{D}^*$) is quasi-equal to the corresponding component of the doublet ($\mathbf{R}^{o\,\mathrm{inst}}$, $\mathbf{D}$). This establishes the correspondence between the two fields using the deformable and non-deformable convected references. As the deformation increases

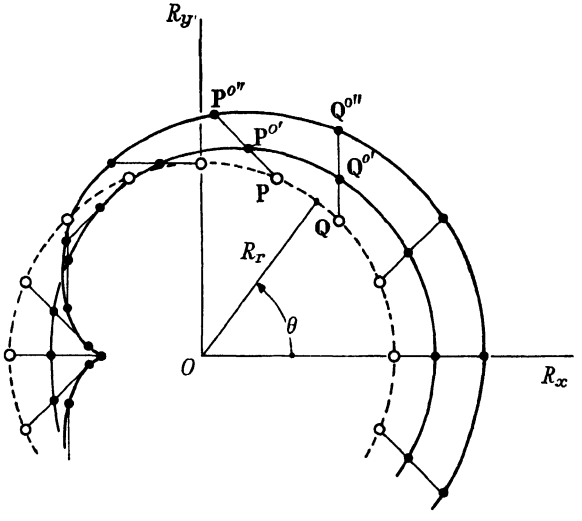

FIG. VII,2.1.—The dotted circle is defined in a deformed, highly elastic sheet and is concentric with a circular hole on which is applied normal and shear stresses loading. The solid curves correspond to the dotted circle for two degrees of severity of deformation. Alternatively, they correspond to two 'stiffnesses' of the substance in the sheet. Typical line element PQ suffers two amounts of strain and 'convection' due to establishment of the whole strain field in the two cases.

the straining convection-displacement $\mathbf{C}^{\mathrm{st}}$ increases but never appears explicitly, as it is the solenoidal component, equal but of opposite sign in each component of the doublet ($\mathbf{R}^{o\,\mathrm{inst}}$, $\mathbf{D}$).

Using the straining equivalence of $\mathbf{D}$, $\mathbf{D}^*$ and $\mathbf{R}^{o\,\mathrm{inst}}$, $\mathbf{R}^{o*}$ gives the two curves in Fig. VII,2.1 corresponding to the deformed circle of radius R_r for two degrees of severity of deformation. Alternatively, each solid curve corresponds to a different value of

GA with the parameter A including load and the stress-strain properties in G.

2.7. **Convection of line elements.** The infinite sheet does not displace at infinity, so that all movement of line elements is due to the establishment of the whole field of strain throughout the sheet. Suppose, for example, that the dotted circle in Fig. VII,2.1 is that of the circular hole of radius a in the deformed sheet. Suppose that the deformed arc PQ is typical and that, as P approaches Q, then PQ is a typical line element.

For a fairly severe deformation PQ becomes $P^{o''}Q^{o''}$ in the corresponding undeformed sheet. When the deformation is less severe, then PQ becomes $P^{o'}Q^{o'}$ in a corresponding undeformed sheet of another shape different from that corresponding to the severer deformation. Note carefully that the line element is convected from $P^{o'}Q^{o'}$ or $P^{o''}Q^{o''}$ into PQ by reason of the stretch set up in all the other typical elements other than PQ. The line element PQ is convected by the establishment of the whole strain field and is not related to the straining in PQ except to the extent that the strain field is continuous in a continuous body.

2.8. **Infinitesimal deformation and Navier, Cauchy spatial-rotation.** For finite deformation, when whole-body rotation is zero, then

$$\mathbf{D}^* \approx \mathbf{D} = \mathbf{U} \tag{2.12}$$

When the deformation is infinitesimal, then

$$\mathbf{D}^* = \mathbf{D} = \mathbf{U} \tag{2.13}$$

Substituting in the Navier, Cauchy infinitesimal spatial-rotation expressions in article V,16.2 shows that they are zero.

Thus, from either the viewpoint of the present author's theory or the classical approach of Navier, Cauchy the heterogeneous infinitesimal strains† are 'irrotational'.

This means that the straining-rotation is zero for the heterogeneous straining in the author's terminology. The physical impossibility of such a situation appears to have been the main argument in the polemical letter by A. N. Gordon [69] (apparently representing contemporary opinion in 1950) attacking the linear, finite strain theory given in the present treatise. It was attempted

† As in article VII,2.4 specialised to 'small' strains.

to show there that only homogeneous strain could be irrotational together with only a whole-body rotation. Notice that the example in article **VII**,1 is also heterogeneous, irrotational strain.

3. Simple tension at infinity on an elastic sheet of restricted isotropy around a circular, cylindrical hole: theoretical solution by the classical approximate theory.

A circular, cylindrical, stress-free hole occurs in an infinite sheet acted on by a simple tensile stress T at infinity in direction OR_x. This boundary-value problem was solved by Kirsch, in 1898 [71], for the Navier, Cauchy infinitesimal strain definitions of article **V**,16.2 and the biharmonic distribution of the Airy stress function of article **V**,15.1. There are two mathematical inexactnesses: firstly, the Navier, Cauchy strains definitions lead to the insufficiently restrictive Saint-Venant compatibility conditions; and, secondly, for a plane, polar two-stress the biharmonic distribution of the Airy stress function is insufficiently restrictive even from the viewpoint of the classical theory.

In spite of these mathematical deficiencies the theoretical solution checks well with experiment, as in Figs. **VI**,1.1 to **VI**,1.3 when it is extended to finite strain by means of the straining-equivalence principle discussed in article **V**,14.2. The usual solution using the Airy stress function will be given rather than that using the stress potential, so that the reader will see how to utilise for finite strain the many particular solutions of the classical theory but recognising that experimental check or comparison with a similar solution for the rigorous theory must finally justify the solution.

3.1. Boundary conditions for the plane two-stress.

At infinity, it is supposed that only normal stress $T = S_{xx}$ acts on the sheet. The methods of article **II**,5 then give the radial, circumferential shear stresses respectively as

$$S_{rr} = \tfrac{1}{2}T(1+\cos 2\theta) \quad S_{\theta\theta} = \tfrac{1}{2}T(1-\cos 2\theta) \quad S_{r\theta} = -\tfrac{1}{2}T \sin 2\theta \tag{3.1}$$

With the circular hole of radius a in the deformed sheet then the boundary condition at the hole is

$$R_r = a \qquad S_{aa} = 0 = S_{a\vartheta} \tag{3.2}$$

3.2. **Kirsch's method of solution.** Each of the stresses in **VII**(3.1) is resolved to two components like $S_{rr} = S_{rr}' + S_{rr}''$ with

$$S_{rr}' = \tfrac{1}{2}T \qquad S_{\theta\theta}' = \tfrac{1}{2}T \qquad S_{r\theta}' = 0 \tag{3.3}$$

$$S_{rr}'' = \tfrac{1}{2}T\cos 2\theta \quad S_{\theta\theta}'' = -\tfrac{1}{2}T\cos 2\theta \quad S_{r\theta}'' = -\tfrac{1}{2}T\sin 2\theta \tag{3.4}$$

Application of a normal stress $-\frac{1}{2}T$ on the cylindrical surface $R_r = a$ cancels S_{aa}'. Application of normal stress $-\frac{1}{2}T\cos 2\theta$ and shear stress $+\frac{1}{2}T\sin 2\theta$ on $R_r = a$ cancels S_{aa}'', $S_{a\theta}''$. The hole is then stress-free. The solution for applied stress $-S_{aa}'$ has been found already in article **VII**,1.8 to be

$$S_{rr} = -\tfrac{1}{2}Ta^2R_r^{-2} \qquad S_{\theta\theta} = \tfrac{1}{2}Ta^2R_r^{-2} \tag{3.5}$$

3.3. **Airy stress function for the axially unsymmetrical stresses.** To apply stresses $-S_{aa}''$, $-S_{a\theta}''$ the forms in **VII**(3.4), together with

$$\left.\begin{aligned} S_{rr} &= R_r^{-1}\mathcal{A}_{;r} + R_r^{-2}\mathcal{A}_{;\theta\theta} \\ S_{\theta\theta} &= \mathcal{A}_{;rr} \qquad S_{r\theta} = -(R_r^{-1}\mathcal{A}_{;\theta})_{;r} \end{aligned}\right\} \tag{3.6}$$

from article **V**,13.2, suggests taking the Airy stress function, with an undetermined function $f(R_r)$ of radius, in the form

$$\mathcal{A} = f(R_r)\cos 2\theta \tag{3.7}$$

The biharmonic distribution of $\mathcal{A}$ in article **V**,15.1 is accepted, so that

$$\nabla^2\nabla^2\mathcal{A} = 0 \tag{3.8}$$

with

$$\nabla^2(\ ) = (\ )_{;rr} + R_r^{-1}(\ )_{;r} + R_r^{-2}(\ )_{;\theta\theta}$$

Substitution from **VII**(3.7) gives an ordinary fourth-order differential equation of which the solution is

$$f(R_r) = AR_r^2 + BR_r^4 + JR_r^{-2} + K \tag{3.9}$$

with arbitrary constants A, B, J, K.

Substituting this in **VII**(3.7), in **VII**(3.6) gives the stresses

$$\left.\begin{aligned} S_{rr} &= (-2A - 4KR_r^{-2} - 6JR_r^{-4})\cos 2\theta \\ S_{\theta\theta} &= (2A + 12BR_r^2 + 6JR_r^{-4})\cos 2\theta \\ S_{r\theta} &= (2A + 6BR_r^2 - 2KR_r^{-2} - 6JR_r^{-4})\sin 2\theta \end{aligned}\right\} \tag{3.10}$$

The arbitrary constants are found from the stresses $-S_{aa}''$, $-S_{a\theta}''$ at the hole and that these axially unsymmetrical stresses vanish at infinity. Then,

$$A = 0 \qquad B = 0 \qquad J = -\tfrac{1}{4}a^4T \qquad K = \tfrac{1}{2}a^2T \tag{3.11}$$

3.4. **Kirsch's stress distribution.** Substituting VII(3.10), VII(3.5) in VII(3.1) gives the required stress distribution throughout the plate as

$$\left.\begin{aligned}(2/T)S_{rr} &= (1-a^2R_r^{-2})+(1-4a^2R_r^{-2}+3a^4R_r^{-4})\cos 2\theta\\ (2/T)S_{\theta\theta} &= (1+a^2R_r^{-2})+(-1-3a^4R_r^{-4})\cos 2\theta\\ (2/T)S_{r\theta} &= (-1-2a^2R_r^{-2}+3a^4R_r^{-4})\sin 2\theta\end{aligned}\right\} \quad (3.12)$$

The first stress invariant is

$$\chi^S = T(1-2a^2R_r^{-2}\cos 2\theta) \quad (3.13)$$

3.5. **Spatial-displacement from the Kirsch solution for plane two-stress.** From articles V,16.2, V,5.5 the stress, infinitesimal spatial-displacement relations for an elastic substance of restricted isotropy and constant stress-strain parameters are

$$\left.\begin{aligned}U_{r;r} &= GS_{rr}+F\chi^S\\ R_r^{-1}(U_r+U_{\theta;\theta}) &= GS_{\theta\theta}+F\chi^S\\ \tfrac{1}{2}(U_{\theta;r}+R_r^{-1}U_{r;\theta}-R_r^{-1}U_\theta) &= GS_{r\theta}\end{aligned}\right\} \quad (3.14)$$

$$\left.\begin{aligned}U_{z;z} &= F\chi^S \qquad \tfrac{1}{2}(U_{z;r}+U_{r;z}) = 0\\ \tfrac{1}{2}(U_{\theta;z}+R_r^{-1}U_{z;\theta}) &= 0\end{aligned}\right\} \quad (3.15)$$

Substituting VII(3.12) in VII(3.14), integrating and determining the resulting arbitrary constants from the symmetry conditions along planes $R_x = 0$, $R_y = 0$ gives [68]

$$\left.\begin{aligned}(Ta)^{-1}2U_r &= [G(a^{-1}R_r-a^3R_r^{-3})+4(F+G)aR_r^{-1}]\cos 2\theta\\ &\quad +(2F+G)a^{-1}R_r+GaR_r^{-1}\\ (Ta)^{-1}2U_\theta &= [-G(a^{-1}R_r+a^3R_r^{-3})-2(2F+G)aR_r^{-1}]\sin 2\theta\end{aligned}\right\} \quad (3.16)$$

independent of R_z like the stresses.

From VII(3.15).1 with VII(3.13)

$$U_z = FT(1-2a^2R_r^{-2}\cos 2\theta)R_z+g(R_r,\theta) \quad (3.17)$$

with arbitrary function $g(R_r, \theta)$. Since U_r, U_θ are independent of R_z, then the last two of VII(3.15) give

$$U_{z;r} = 0 = U_{z;\theta} \quad (3.18)$$

These two conditions require

$$\left.\begin{aligned}(4FTa^2R_r^{-3}\cos 2\theta)R_z+g_{;r} &= 0\\ (4FTa^2R_r^{-2}\sin 2\theta)R_z+g_{;\theta} &= 0\end{aligned}\right\} \quad (3.19)$$

These can be satisfied only when

$$R_z = 0 \qquad g = \text{constant} \quad (3.20)$$

with the last constant zero, for zero whole-body translation in direction OR_z. Therefore, the Kirsch plane, two-stress distribution and Navier, Cauchy strains, spatial-displacement relations can be satisfied for a plate of zero thickness only for even the simplest generalised Hooke's law form.

3.6. **Saint-Venant strains compatibility and the Kirsch plane two-stress solution.** Article V,15.1 shows that, for plane two-stress, the Saint-Venant compatibility conditions require the first stress invariant to be distributed linearly at least with respect to R_x, R_y; that is, for $R_r \cos\theta$, $R_r \sin\theta$. But VII(3.13) shows that χ^S is not linear in these terms. Therefore, the Kirsch, plane, two-stress solution does not satisfy the Saint-Venant strains compatibility conditions. Further, article V,15.1 shows that for an infinite plate, as here, the first stress invariant must be constant to avoid infinite values.

This indicates a reason that the calculated value of U_z in article VII,3.5 is anomalous. The Kirsch two-stress solution is given in the standard works by S. Timoshenko [23.3] or R. V. Southwell [29.1] for example, without reference to the foregoing anomalies.

3.7. **Kirsch's solution for plane strain.**† Article V,15.2 shows that for plane strain in which $U_z = 0$, $U_x \neq U_x(R_z)$, $U_y \neq U_y(R_z)$, $S_{zx} = 0 = S_{zy}$, $S_{xx} \neq S_{xx}(R_z)$, $S_{yy} \neq S_{yy}(R_z)$, $S_{xy} \neq S_{xy}(R_z)$, then the Airy stress function does obey the biharmonic law of distribution in VII(3.8), while

$$(F+G)S_{zz} = -F(S_{xx}+S_{yy}) = -F(S_{rr}+S_{\theta\theta}) \qquad (3.21)$$

The boundary conditions are just as in article VII,3.1 at $R_r = a$, but in direction OR_x at infinity the stresses acting are $T = S_{xx}$ applied but, also, with a stress

$$S_{zz} = -FT/(F+G) \qquad (3.22)$$

acting in direction OR_z and independent of R_z. Therefore, with this provision the stresses are otherwise just as in equations VII(3.12).

Now, however, the first stress invariant

$$\chi^S = S_{rr}+S_{\theta\theta}+S_{zz} = T[1-F(F+G)^{-1}-2a^2R_r^{-2}\cos 2\theta] \qquad (3.23)$$

† Author, 1950.

3.8. **Stress, spatial-displacement relations for the Kirsch plane strain solution.** The equations are still just as in VII(3.12), except that now χ^S is given by VII(3.23). Component U_z is zero in the two last equations of VII(3.15), so that $U_r \neq U_r(R_z)$, $U_\theta \neq U_\theta(R_z)$. Integration of the equations relating spatial-displacement and the stresses gives, for plane strain,

$$\left.\begin{aligned}(Ta)^{-1}2U_r &= [G(a^{-1}R_r - a^3R_r^{-3}) + 4(F+G)aR_r^{-1}]\cos 2\theta \\ &\quad + [(2F+G) - 2F^2(F+G)^{-1}]a^{-1}R_r + GaR_r^{-1} \\ (Ta)^{-1}2U_\theta &= [-G(a^{-1}R_r + a^3R_r^{-3}) - 2(2F+G)aR_r^{-1}]\sin 2\theta \\ (Ta)^{-1}2U_z &= 0\end{aligned}\right\} \quad (3.24)$$

3.9. **Comparison of plane two-stress and plane strain solutions for spatial-displacement.** Comparison of VII(3.24) with VII(3.16) gives

$$\left.\begin{aligned}U_r(\text{plane strain}) - U_r(\text{plane two-stress}) &= -F^2(F+G)^{-1}TR_r \\ U_\theta(\text{plane strain}) - U_\theta(\text{plane two-stress}) &= 0\end{aligned}\right\} \quad (3.25)$$

Thus, only one component U_r is different in one coefficient for the two solutions.

When strains are small then $F = -q\psi$, $G = (1+q)\psi$, with Poisson's ratio q and elastic modulus ψ. Then, in VII(3.24).1 and VII(3.16).1 the coefficients of $a^{-1}R_r$ are

$$\begin{aligned}(2F+G) - 2F^2(F+G)^{-1} &= (1-q)\psi - 2q^2\psi \\ 2F+G &= (1-q)\psi\end{aligned}$$

Since $\frac{1}{4} \leqq q \leqq \frac{1}{2}$ is the usual range of values, then the term $2q^2\psi$ is fairly small compared with $(1-q)\psi$, so that there is only a small difference between the strains observed on the main faces of a sheet for either strain state.

This conclusion is similar to that reached in interpreting the 'homogeneous two-stress' tests on a plane, thin rubber sheet by L. R. G. Treloar and given in article X,3.4. The presence, or not, of a transverse stress S_{zz} makes little difference to the observations of strain on the main faces of the sheet, although, of course, the transverse strain e_{zz} depends on the case considered. Therefore, the observations on the main faces are much the same for plane two-stress or the quasi-plane stress of article V,18.

3.10. **Straining-displacement.** Article V,14 discusses the mode of applying the classical analyses, such as that of Kirsch

just given, to give finite strains solutions that are approximate to the extent that the Navier, Cauchy strain definitions and Saint-Venant compatibility conditions are erroneous in each particular application, which must be considered on its own merits. In the present case, whole-body rotation is zero since at least one point

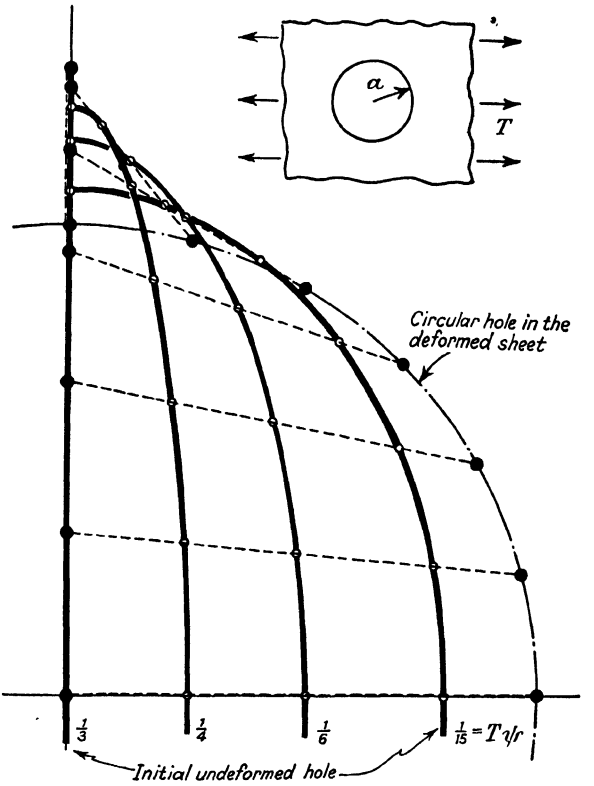

FIG. VII,3.1.– A family of holes in undeformed plates corresponding to a circular hole of radius a in an infinite plate under simple tensile stress T at infinity. The elastic modulus is ψ.

suffers zero spatial-rotation, so that **U** equals straining-displacement **D** equal to relative-displacement $\mathbf{D}^*$ for infinitesimal strain. This gives the equal doublet vector fields ($\mathbf{R}^{o*}$, $\mathbf{D}^*$), ($\mathbf{R}^{o\,inst}$, **D**) each in one-one correspondence with the applied forces. Thus, the displacements in **VII**(3.16) for plane two-stress or **VII**(3.24) for the three-stress plane strain case are, in fact, $\mathbf{D}^* \approx \mathbf{D}$.

3.11. **Numerical calculations and experimental examination.** Fig. VII,3.1 shows a family of holes of which each member becomes a circular hole in the deformed sheet. Each hole is an initial, undeformed hole for the deformed, circular hole corresponding to a particular load or 'stiffness' of the substance.

Choosing $q = \frac{1}{2}$ to suit the virtually incompressible increment straining of rubber, then equations VII(3.16) give the curves in Fig.VII,3.1. As the load increases then the corresponding undeformed hole becomes more nearly equal to the slot found for $T\psi = \frac{1}{3}$. For values of this parameter greater than $\frac{1}{3}$ the case can be regarded physically as that of a semi-infinite plate loaded on its edge $\theta = \pm\frac{1}{2}\pi$ with stresses given by article VII,3.4 and with a stress-free semicircular 'dent' which is half the 'hole'.

The same straining-displacement expressions were used to calculate the shapes of the holes in Figs. VI,1.1, VI,1.2 and the displacements in Fig. VI,1.3. The value of the parameter $T\psi$ was found by fitting the theoretical expression for D_r to the experimental value at $\theta = 0$, $R_r = a$. This avoided the necessity of actually calibrating the rubber in a simple tensile test, for example. The theory still had to predict the shape of each hole away from $\theta = 0$ and good check is found. In Fig. VI,1.2 strains of the order 65 per cent Cauchy measure occur at $\theta = 90°$, while at $\theta = 60°$ the straining-rotation is of the order 30°. These are large values beyond the scope of the strains analysable by purely classical theory.

4. Quadrantal, deformed, elastic cantilever: theoretical solution by the classical, approximate theory

The boundary-value problem of a deformed, quadrantal cantilever under shear load F per unit thickness, as in Fig. VII,4.1, was solved for the Navier, Cauchy strains with the biharmonic Airy stress function, as in equation VII(3.8), by Golovin [72, 23.7] in 1881. The discussion of article V,15.2 shows that the Saint-Venant strains compatibility conditions require the solution to be that for plane strain. When the assumption that plane stress operates, then the cantilever must be of infinitesimal thickness only. However, the observations of strain in the planes R_z = constant differ little for plane stress or plane strain, although the transverse strain e_{zz} is greatly changed. S. Timoshenko [23.5], for example, treats the solution as that for plane stress.

4.1. **Boundary conditions.** The arcual planes must be stress-free, so that

$$\left.\begin{array}{ll} R_r = a & S_{aa} = 0 = S_{a\theta} \\ R_r = b & S_{bb} = 0 = S_{b\theta} \end{array}\right\} \qquad (4.1)$$

The shear stresses S_{r_0} over the plane $\theta = \frac{1}{2}\pi$ must give force F per unit thickness, while the normal stress $S_{0\theta}$ is zero. Thus,

$$\theta = \tfrac{1}{2}\pi \qquad \int_a^b S_{r\theta}\partial R_r = F \qquad S_{0\theta} = 0 \qquad (4.2)$$

Whatever distribution of shear stress appears from the solution for $\theta = \frac{1}{2}\pi$ must be accepted and, similarly, for the built-in face

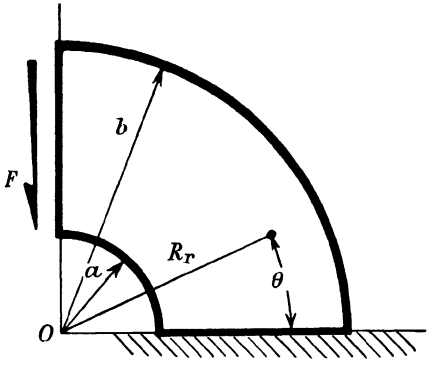

FIG. VII,4.1.—A deformed, elastic cantilever of quadrantal form held in this shape by a shear load F distributed over the radial plane shown.

at $\theta = 0$ the values of both normal and shear stresses S_{00}, S_{r0} must be accepted.

Because $R_r = a$ is stress-free the complementary shear stress S_{0r} must be zero like S_{r0}. Therefore, only normal stress $S_{\theta\theta}$ acts at $R_r = a$, $\theta = 0$, so that this is a convenient situation for the origin of whole-body convected axes as in Fig. VII,4.2 because the complication of following strain transfer is avoided [68]. The prevention of spatial-rotation at this one point gives zero whole-body rotation for the cantilever, although, of course, straining-rotation is not zero at all the other points of the body. Thus, spatial-displacement equals straining-displacement. The fixing conditions are, therefore,

$$R_r = a,\ \theta = 0 \qquad D_r^* = 0 = D_\theta^* \qquad D_{0;r}^* = 0 \qquad (4.3)$$

4.2. **Golovin's solution for plane stresses.** The geometry of the boundaries suggests using plane polar coordinates as in article **VII**,3.1. Here, we take the Airy stress function in the form

$$\mathcal{A} = f(R_r) \sin \theta \tag{4.4}$$

Substitute in **VII**(3.8) and solve the ordinary differential equation for $f(R_r)$. The expression for $\mathcal{A}(R_r, \theta)$ with four undetermined, arbitrary constants A, B, J, K is then substituted in **VII**(3.6) to give the plane stresses

$$\left.\begin{aligned} S_{rr} &= (2AR_r - 2BR_r^{-3} + KR_r^{-1}) \sin \theta \\ S_{\theta\theta} &= (6AR_r + 2BR_r^{-3} + KR_r^{-1}) \sin \theta \\ S_{r\theta} &= (-2AR_r + 2BR_r^{-3} - KR_r^{-1}) \cos \theta \end{aligned}\right\} \tag{4.5}$$

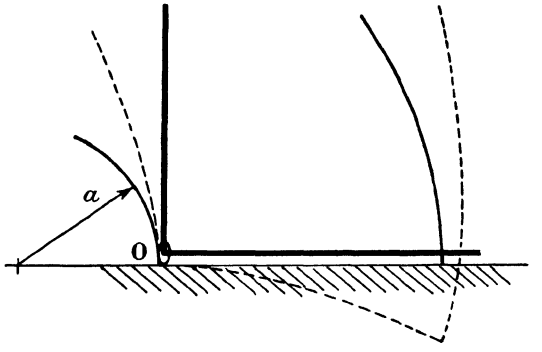

FIG. **VII**,4.2.—Whole-body convected axes with their origin **O** at $R_r = a$, $\theta = 0$. This position is chosen because shear stress is zero, so that the complication of following strain transfer is avoided.

Boundary conditions **VII**(4.1), **VII**(4.2) give

$$\left.\begin{aligned} A &= \tfrac{1}{2}F/N \qquad B = -\tfrac{1}{2}Fa^2b^2/N \qquad K = -F(a^2+b^2)/N \\ N &= a^2 - b^2 + (a^2+b^2) \log (b/a) \end{aligned}\right\} \tag{4.6}$$

4.3. **Spatial-displacements for Golovin's plane two-stress solution.** Stresses **VII**(4.5) in equations **VII**(3.14) only, then integrated with fixing conditions **VII**(4.3), give [68]

$$\left.\begin{aligned} D_r^* &= \left[\begin{aligned} &(2F+G)K \log R_r + (4F+G)AR_r^2 \\ &+GBR_r^{-2} + (F+G)L \end{aligned}\right] \sin \theta \\ &\quad -2(F+G)K\theta \cos \theta \\ D_\theta^* &= \left[\begin{aligned} &-(4F+5G)AR_r^2 - GBR_r^{-2} + GK \\ &+(2F+G)K \log R_r + (F+G)L \end{aligned}\right] \cos \theta \\ &\quad +(F+G)(2K\theta \sin \theta + HR_r) \end{aligned}\right\} \tag{4.7}$$

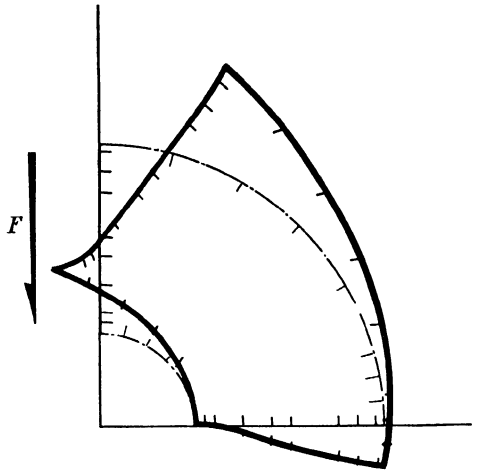

FIG. VII,4.3.—The undeformed shape of the elastic cantilever when the parameter $F\psi = 0{\cdot}1$. The short lines from the boundaries are corresponding line elements in the undeformed and deformed states.

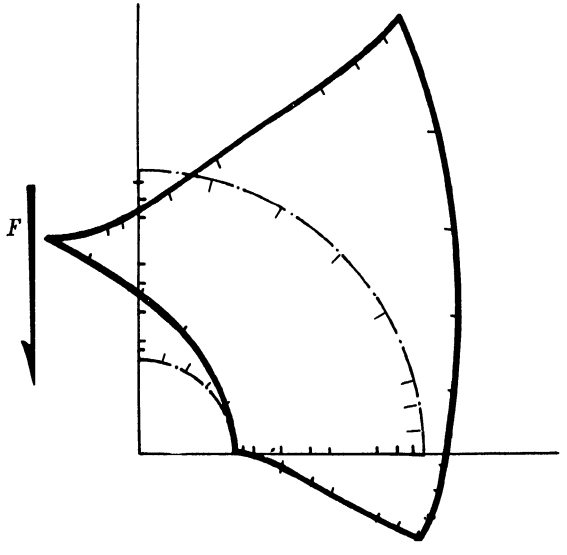

FIG. VII,4.4.—The undeformed shape of the elastic cantilever when the parameter $F\psi = 0{\cdot}2$. Note that the straining-rotation is about 90° at $R_r = a$, $\theta = \frac{1}{2}\pi$.

with

$$\left.\begin{aligned} H &= 2(4F+5G)aA-2Ga^{-3}B-(2F+G)a^{-1}K \\ L &= -(F+G)aH+(4F+5G)a^2A+Ga^{-2}B \\ &\quad +[-(2F+G)\log a-G]K \end{aligned}\right\} (4.8)$$

and F, G the stress-strain parameters of article V,5.5.

4.4. **Numerical calculations.** With the elastic modulus ψ, the spatial-displacement components (or the equal straining-displacement components) of article VII,4.3 were used to calculate the initial shapes of the cantilever for two different loads as in Figs. VII,4.3, VII,4.4 [68]. Notice the straining-rotation of the order 90° at $R_r = a$, $\theta = \frac{1}{2}\pi$, when $F\psi = 0{\cdot}2$ particularly, while the strains at the same position are of several hundred per cent Cauchy measure.

5. Circular, right, hollow cylinder generated from a flat plate: theoretical solution using the Navier, Cauchy strains definitions

This is an interesting example, as it gives a method [73] of dealing with straining-displacement directly, rather than with relative-displacement and then using the straining-equivalence principle. Further, for the classical infinitesimal strains theory, the application of bending moment to radial planes of a hollow, circular cylinder was given by Golovin [72], in 1881, and this is adapted to finite strain as in article VII,4.

5.1. **Method.** Fig. VII,5.1 shows the case treated. From symmetry, points on the plane $\theta = 0$ suffer zero spatial-rotation, so that whole-body rotation is zero and straining-displacement **D** equals spatial-displacement **U**.

The major part of **D** is **A** and **w** is a 'small' displacement necessary to keep all equations compatible when **A** is guessed, or estimated, geometrically from initial position $\mathbf{R}^o$. Thus, assume that **A** is the displacement of a point due to generating the cylinder from the flat plate with the middle plane of the same length in each case and radial planes of the cylinder normal to the plane of the flat plate. Then,

$$\mathbf{D} = \mathbf{A}+\mathbf{w} \qquad (5.1)$$

If **w** proved to be not small then the estimate for **A** would have been a bad choice and another would be necessary.

The equilibrium stress equations are solved for the cylinder with the Airy stress function having a biharmonic distribution, so that the case is one of plane strain. The stresses are related to straining-displacement in the Navier, Cauchy strains definitions, so that the Saint-Venant strains compatibility equations must be used. Thus, the estimated cylinder is being used as a currently deformed reference for the increment deformation leading to the correct current shape under the current load as in Fig. **VII**,5.2.

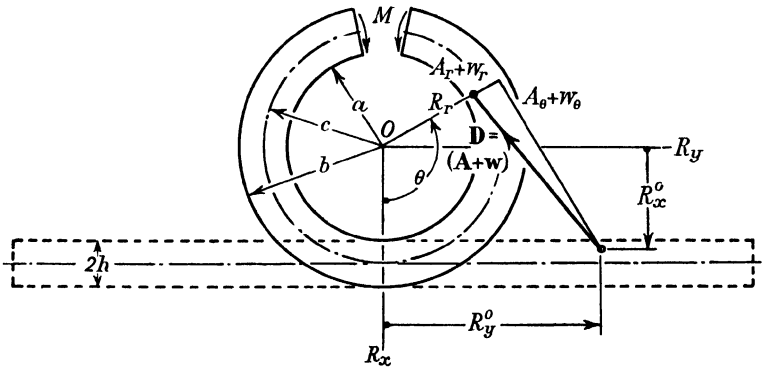

FIG. VII,5.1.—A circular, right, hollow cylinder generated from a flat plate by pure bending moment M per unit length of plate in direction OR_z. The straining-displacement is **D**, its major component **A** is calculated with an inextensile middle plane of radius c in the deformed state, while **w** is a 'small' correction to ensure compatibility of straining-displacement and stresses. The initial position of the typical point is at R_x^o, R_y^o.

5.2. **Estimated straining-displacement.** From Fig. **VII**,5.1 for no stretch of the middle plane

$$R_y^o = c\theta \qquad R_x^o = R_r \tag{5.2}$$

while

$$R_r\mathbf{c}_r = \mathbf{R}' = \mathbf{R}^o + \mathbf{A}$$

so that, scalarly,

$$A_r = R_r(1-\cos\theta) - c\theta\sin\theta \qquad A_\theta = R_r\sin\theta - c\theta\cos\theta \tag{5.3}$$

while

$$D_r = A_r + w_r \qquad D_\theta = A_\theta + w_\theta \tag{5.4}$$

5.3. **Stresses.** It is supposed that the stress system and hence the Airy stress function are independent of angular position θ. Hence, from article V,13.2, $S_{r\theta}$ is zero, while

$$S_{rr} = R_r^{-1}\mathcal{A}_{;r} \qquad S_{\theta\theta} = \mathcal{A}_{;rr} \tag{5.5}$$

From article V,15.1,

$$\nabla^2\nabla^2\mathcal{A} = 0 \tag{5.6}$$

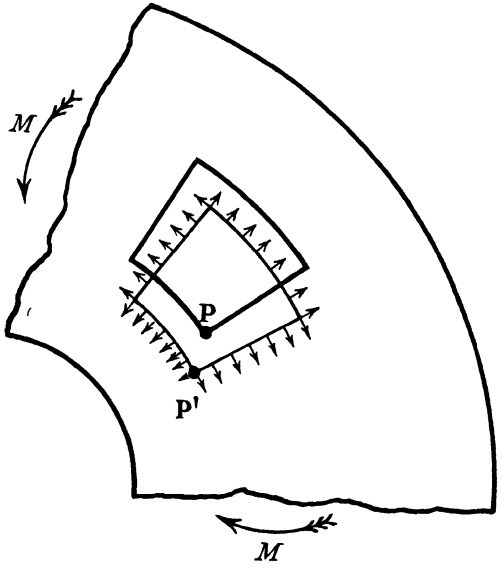

FIG. VII.5.2.—The typical point is estimated to be at P′ from the geometry of Fig. VII.5.1. The solution of the equations relating stresses and strains shows that, in fact, it is at a closely adjacent point P. The stress equations are solved with the point at P′, so that the *estimated shape* of the cylinder is used as the current reference for the calculation of the small correction deformation.

with

$$\nabla^2(\ ) = (\ )_{;rr} + R_r^{-1}(\ )_{;r}$$

The solution of the fourth-order ordinary differential equation VII(5.6) is

$$\mathcal{A} = (J + KR_r^2)\log R_r + XR_r^2 + Y \tag{5.7}$$

with arbitrary constants J, K, X, Y. Then, from VII(5.5),

$$\left.\begin{aligned} S_{rr} &= JR_r^{-2} + K(1 + 2\log R_r) + 2X \\ S_{\theta\theta} &= -JR_r^{-2} + K(3 + 2\log R_r) + 2X \end{aligned}\right\} \tag{5.8}$$

5.4. **Stresses, boundary conditions and arbitrary constants.** The boundary conditions on the stresses on the arcual planes are

$$R_r = a, b \qquad S_{rr} = 0 \tag{5.9}$$

It is supposed that the stresses $S_{\theta\theta}$ on the radial planes have no resultant but constitute a pure couple M, say, per unit thickness in the direction OR_z. For no resultant

$$\int_a^b S_{\theta\theta} \partial R_r = 0 \tag{5.10}$$

The couple is given by

$$\int_a^b S_{\theta\theta} R_r \partial R_r = M \tag{5.11}$$

Condition VII(5.10) is seen to be satisfied identically by virtue of VII(5.5).1 with the two equations VII(5.9). Equation VII(5.11) and the two in VII(5.9) are sufficient to determine the three constants as

$$\left.\begin{aligned} J &= -4ML^{-1}a^2b^2 \log (b/a) \qquad K = -2ML^{-1}(b^2-a^2) \\ X &= ML^{-1}[b^2-a^2+2(b^2 \log b - a^2 \log a)] \\ L &= (b^2-a^2)^2 - 4a^2b^2[\log (b/a)]^2 \end{aligned}\right\} \tag{5.12}$$

5.5. **Straining-displacement correction terms.** Recall that relative-displacement gradient and relatively initial position are related to the stresses relative to the deformable whole-body convected reference. For infinitesimal deformation the relative-displacement virtually equals the straining-displacement and relatively initial position virtually equals instantaneously initial position relative to a non-deformable whole-body convected reference. This establishes the mathematical form of the relation between these two patterns of points. Physical increase in the magnitudes of the four quantities in the two doublet vector fields does not affect their mathematical relationship because the straining convection-displacement never appears explicitly.

Applying the Navier, Cauchy strain relations of article V,16.2 to relative-displacement, the stress-strain relations of article

V,5.5, the straining equivalence of $\mathbf{D}^*$ and $\mathbf{D}$, then equations VII(5.4), VII(5.3) give

$$\left.\begin{aligned} w_{r;r} &= GS_{rr}+F\chi^S-A_{r;r} \\ R_r^{-1}(w_r+w_{\theta;\theta}) &= GS_{\theta\theta}+F\chi^S-R_r^{-1}(A_r+A_{\theta;\theta}) \\ R_r^{-1}(w_{r;\theta}-w_\theta)+w_{\theta;r} &= -R_r^{-1}(A_{r;\theta}-A_\theta)-A_{\theta;r} \end{aligned}\right\} (5.13)$$

Integrating these three equations and using the fixing conditions

$$\left.\begin{aligned} R_r &= R_r \quad \theta = 0 \quad w_\theta = 0 \\ R_r &= c \quad \theta = 0 \quad w_r = 0 \\ R_r &= c \quad \theta = \pi \quad w_r = 0 \end{aligned}\right\} \qquad (5.14)$$

gives

$$\left.\begin{aligned} w_r &= -JGR_r^{-1}+[(F+G)(K+2X)+F(3K+2X)]R_r \\ &\quad +2(2F+G)KR_r(\log R_r-1)+N\cos\theta-A_r \\ w_\theta &= 4(F+G)KR_r\theta-N\sin\theta-A_\theta \end{aligned}\right\} (5.15)$$

with

$$\begin{aligned} N = {} & JG/c-[(F+G)(K+2X)+F(3K+2X)]c \\ & -2(2F+G)Kc(\log c-1) \end{aligned}$$

5.6. **Applied bending moment.** Using condition VII(5.14).3 with VII(5.15).1 gives the applied bending moment for a 'radius of curvature' c as

$$M = 2c/\left[\begin{aligned} & -GJ/(cM)+(F+G)c[(K/M)+2(X/M)] \\ & +Fc[3(K/M)+2(X/M)]-N \\ & +2[(2F+G)(K/M)c(\log c-1)] \end{aligned}\right] \qquad (5.16)$$

of the same value on all radial sections.

5.7. **Magnitude of the correction term for straining-displacement.** The correction term $\mathbf{w}$ for straining-displacement must be small for justification of the foregoing analysis. With $q = \frac{1}{3}$, as a typical value, then, at $\theta = \pi$

$$w_\theta = -\pi c(32MhR_r\psi N^{-1}+1) \qquad (5.17)$$

For a duralumin plate, for example, when $R_r = c$, $c = 100h$, $h = 1$, then

$$w_\theta = 0{\cdot}0144 \qquad (5.18)$$

as in Fig. VII,5.3. This is sufficiently small to justify the analysis.

5.8. **Comparison with the Bernoulli simple theory of pure bending of a straight beam.** The well-known 'engineering' theory of pure bending of a straight beam assumes that plane sections remain plane as in the calculation for **A** here. On the hypothesis that only the longitudinal fibres, in direction OR_y of Fig. **VII**,5.1, are loaded by normal stress, $S_{yy} \equiv S_{\theta\theta}$ here for $c \to \infty$, while $S_{xx} \equiv S_{rr}$ here is zero. It is left as an exercise for the reader to decide if S_{rr} is small enough to neglect as $c \to \infty$ to give the straight plate or beam.

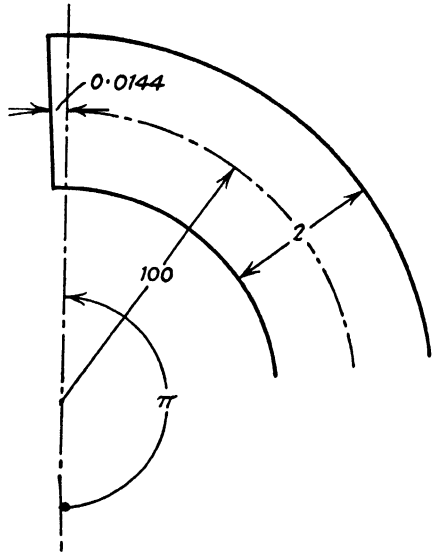

FIG. **VII**,5.3.—The small correction for a duralumin plate, of radius of curvature 100 and thickness 2, at the longitudinal 'seam' in the hollow cylinder.

6. Residual stresses in an annulus: theoretical

Consider a circular, plane annulus of inner radius a and outer radius b. The surfaces are all stress-free and body force is taken as zero, so that there is no applied loading. However, this does not mean that the body is necessarily stress-free throughout. Sometimes, in practice, if a cut is made into such an annulus it changes shape and so indicates the presence of internal self-straining due to residual stresses. This is discussed in general terms in volume I, article **IV**,9. It is of interest to construct an example to indicate something of the possible nature of such stresses.

Suppose the stresses are plane polar as defined in article V,2.2. Article V,11.4 gives the sum of the normal stresses as constant when body force is zero. From article V,11.2 if, further, the stress potential is independent of θ, there follows

$$\nabla^2 H = H_{;rr} + R_r^{-1} H_{;r} = C \tag{6.1}$$

in which

$$S_{rr} = H_{;rr} \qquad S_{\theta\theta} = R_r^{-1} H_{;r} \tag{6.2}$$

A solution is required for these equations such that when

$$R_r = a, b, \qquad S_{rr} = 0 \tag{6.3}$$

6.1. **Inadmissible solution.** The complete solution of VII(6.1) is given in article VII,1.2. The corresponding stresses S_{rr}, $S_{\theta\theta}$ follow in equations VII(1.6) with two undetermined, arbitrary constants C, J. Then, applying conditions VII(6.3) gives

$$Ca^2 + 2J = 0 = Cb^2 + 2J$$

The only solutions for these two equations are

$$C = 0 = J \text{ or } a = b$$

The last is trivial, while the first two mean that the stresses are zero throughout the annulus when the cylindrical boundaries are stress-free. This is consistent with the applied stresses $A = 0 = B$ in equations VII(1.7). Therefore, the stress potential in equation VII(1.5) is only for induced stresses which vanish with the applied stresses and cannot lead to residual stresses.

6.2. **Laplacian stresses.** When $C = 0$ then the Poisson's equation VII(6.1) degenerates to Laplace's equation. Thus, with the first stress invariant

$$\nabla^2 H = 0 = \chi^S \tag{6.4}$$

Multiply by R_r^2 and transform the independent variable to

$$t = \log R_r \qquad R_r = \exp t \tag{6.5}$$

This gives

$$R_r^2 \nabla^2 H = H_{;tt} = 0 \tag{6.6}$$

while

$$R_r^2 S_{rr} = H_{;tt} - H_{;t} \qquad R_r^2 S_{\theta\theta} = H_{;t} \tag{6.7}$$

or

$$R_r^2 S_{rr} = -H_{;t} \qquad S_{\theta\theta} = -S_{rr} \tag{6.7'}$$

The radial stress S_{rr} is to be zero at the cylindrical boundaries and, therefore, the circumferential stress $S_{\theta\theta}$ also vanishes there.

The cylindrical boundary surfaces are absolutely free of stress and strain.

6.3. **Harmonic solution not satisfying the boundary conditions.** The harmonic function solution of **VII**(6.6), with the arbitrary constants adjusted to give the distribution in the t-space as in Fig. **VII**,6.1(b) between the radii $t_a = \log a$ and $t_b = \log b$, is

$$H = (2t - t_a - t_b)L/(t_a - t_b) \tag{6.8}$$

From equations **VII**(6.7′),

$$S_{rr} = 2LR_r^{-2}(t_a - t_b)^{-1} \qquad S_{\theta\theta} = -S_{rr} \tag{6.9}$$

When $R_r = a, b$ then $S_{rr} \neq 0$ as in Fig. **VII**,6.1(d), although these boundary stresses are required to be zero as in conditions **VII**(6.3). Therefore, this solution is not sufficient as it stands.

6.4. **Fourier representation harmonic solution satisfying the boundary conditions.**† Suppose the function $H(t)$ is extended to have a periodic interval of $2(t_a - t_b)$ and maximum values $\pm L$ as shown in Fig. **VII**,6.1(b). Now represent this even function $H(t)$ by a Fourier cosine series $\mathcal{T}(t)$, say, with constant coefficients X_n. Thus, as in article **D**,1,

$$\mathcal{T}(t) = \tfrac{1}{2}X_0 + \sum_{n=1,2,3\ldots} X_n \cos\left[n\pi(t - t_a)/(t_b - t_a)\right] \tag{6.10}$$

with the periodic interval $2(t_b - t_a)$ and the values of the X's determined in terms of the periodic interval and the numbers n.

Since $H(t)$ is continuous in the periodic interval and at its ends, then, as in article **D**,1,

$$H(t) = \mathcal{T}(t) \qquad 2t_a - t_b \leqq t \leqq t_a \leqq t \leqq t_b \tag{6.11}$$

Discontinuities of dH/dt occur at $t = 2t_a - t_b$, t_a, t_b. But, at all points $d^2H/dt^2 = 0$ and therefore, from article **D**,2.2, since this second derivative exists to the right and to the left of each of the three points where the first derivative has a discontinuity, then the mean of the derivatives to the right and left is the derivative at the point. Thus, at $t = t_a$, noting **VII**(6.11), **VII**(6.8) and Fig. **VII**,6.1(b) give

$$\left(\frac{dH(t)}{dt}\right)_{t=t_a} = \left(\frac{d\mathcal{T}(t)}{dt}\right)_{t=t_a} = \tfrac{1}{2}\left[\left(\frac{dH}{dt}\right)_{t=t_a+0} + \left(\frac{dH}{dt}\right)_{t=t_a-0}\right]$$
$$= \tfrac{1}{2}[2L/(t_a - t_b) - 2L/(t_a - t_b)] = 0 \tag{6.12}$$

† Author, 1953.

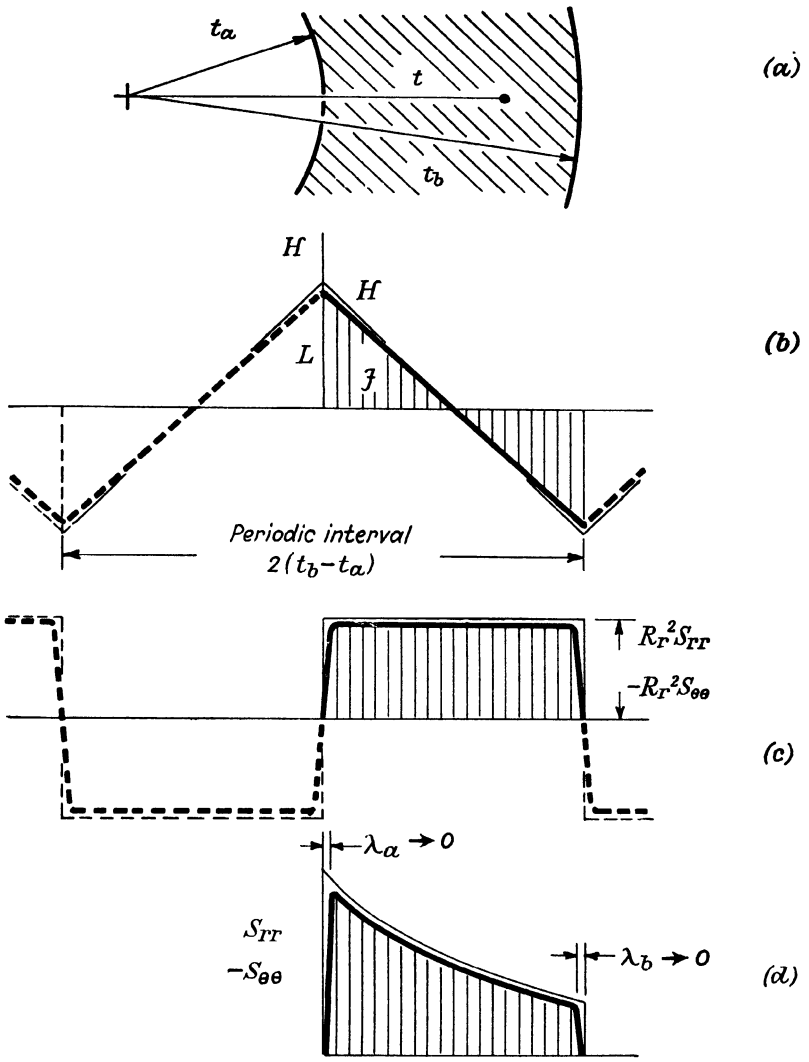

FIG. VII,6.1.—Residual stresses in the circular annulus of which an arc is shown in (*a*) in logarithmic t-space. The abscissæ of the other diagrams also correspond to the t-space. The finer lines in (*b*), (*c*), (*d*) are for the stress potential H, which does not satisfy the condition that the cylindrical boundaries are stress-free. The firm lines in (*b*), (*c*), (*d*) are for the Fourier representation stress function $\mathcal{J}$ giving stress-free cylindrical boundaries. In the Fourier sense, the stress functions H and $\mathcal{J}$ are equal, their derivatives are equal *within* the annulus, but differ *at* and *near* the boundaries. The stresses become zero *at* the boundary by virtue of very steep (but finite) stress gradients through the 'skin' of *small* thickness λ. The periodic interval of H was chosen as in (*b*) to ensure the correct boundary conditions for stress from the Fourier representation.

Similarly, the first derivative is zero at the two end-points of the periodic interval.

The second derivative d^2H/dt^2 is zero to the right and left of $t = t_a$, for example, the derivative d^3H/dt^3 exists (and is, in fact, zero) to the right and left and, therefore,

$$\left(\frac{d^2H}{dt^2}\right)_{t=t_a} = \tfrac{1}{2}\left[\left(\frac{d^2H}{dt^2}\right)_{t=t_a+0} + \left(\frac{d^2H}{dt^2}\right)_{t=t_a-0}\right] = 0 \qquad (6.13)$$

Similarly, the second derivative is zero at the end-points of the periodic interval. Therefore, the Laplace's equation **VII**(6.6) is satisfied at all points in the periodic interval and at its ends and, therefore, at all points interior to and on the boundaries of the annulus.

From **VII**(6.7′), **VII**(6.8), **VII**(6.11),

$$\left.\begin{aligned} R_r^2 S_{rr} &= 2L/(t_b - t_a) \\ R_r^2 S_{\theta\theta} &= -2L/(t_b - t_a) \end{aligned}\right\} t_a + 0 \leqq t \leqq t_b - 0 \qquad (6.14)$$

$$S_{rr} = 0 = S_{\theta\theta} \qquad t = t_a,\ t_b \qquad (6.15)$$

Therefore, the Fourier representation of the stress potential gives the same harmonic solution as that in article **VII**,6.3 but, unlike the stresses there, the boundaries are now stress-free.

6.5. **Skin effects.** Equations **VII**(6.15), **VII**(6.14) and Fig. **VII**,6.1(*d*) give the stress distribution at all points of the annulus and its boundaries. Very steep stress gradients occur at the boundary when the stresses decrease rapidly to zero over the small distances λ_a, λ_b, which will be called *skin thicknesses*.

The theory of Fourier series gives no precise value for the skin thickness except that it approaches zero. Physically, the skin thickness can be so small that it could be overlooked in an experiment not designed especially to examine it.†

Strain-gauge measurements cannot be made over such short gauge lengths. Photo-elastic observations are always (March 1954) unreliable very close to boundaries. This is usually stated to be due to residual strains induced by the cutting of the transparent material to make the test specimen, but it may be that much is due to steep (but finite) stress gradients or, otherwise, if they mutually prevent observation of the two effects.

† The possibility of such steep stress gradients was mentioned several times in reviews by the present author between 1947 and 1952. See *Appl. Mech. Reviews, U.S.A.*, for example.

Always, in passing from theoretical inference to experimental observation, the hypotheses of the theory should be kept in mind. In the present case, for example, there are the assumptions that the substance is an amorphous continuum while the stresses are strictly two-dimensional. Real, non-amorphous, non-continuous substances may have a different skin mechanism, such as the sort of 'surface tension' hypothesised by Griffith [113] to analyse the rupture of brittle substances. The assumption of plane stress removes an important degree of freedom for the distribution.

6.6. **Pseudo-harmonic solutions satisfying the boundary conditions.** Article C,7.2 shows that any smooth curve satisfies the one-dimensional Laplace's equation in the interior of the function space. Further, at any point in the annulus here, $H_{;t}$ and hence the laplacian stresses of equations VII(6.7′) are zero when the function has zero slope. Therefore, any term of the Fourier series VII(6.10) can be taken as a solution for the laplacian stress function for the residual stresses in the annulus from the point of view of finite differences. Thus, in this sense,

$$H = X_n \cos\left[n\pi(t-t_a)/(t_b-t_a)\right] \qquad (n = 1, 2, \ldots) \qquad (6.16)$$

$$S_{rr} = \frac{n\pi X_n}{t_b-t_a} \sin\left(\frac{n\pi(t-t_a)}{t_b-t_a}\right) \qquad S_{\theta\theta} = -S_{rr} \qquad (6.17)$$

is a satisfactory solution with the stresses vanishing at the boundaries.

However, formally,

$$H_{;tt} = -\left(\frac{n\pi}{t_b-t_a}\right)^2 X_n \cos\left(\frac{n\pi(t-t_a)}{t_b-t_a}\right) \neq 0 \qquad (6.18)$$

generally, as is required for a true harmonic function satisfying Laplace's equation. Therefore, it is convenient to refer to H in VII(6.16) as a *pseudo-harmonic* as in article C,7.2.

As R. V. Southwell observes [77] (see article C,4.5) when developing the relaxation technique, the precise mathematical form of the stress potential (and hence the stresses, here) does not need to be known so long as the governing equation VII(6.6) is determined to the desired order of arithmetical accuracy, which will be governed by the accuracy of the data given by physical observation. Thus, we do not need to know that the harmonic function VII(6.8), linear in t, should be found strictly. Any term or sum of terms of the Fourier series VII(6.10) will suffice for the physical observations possible.

7. Two-stress yielding due to pressure in a circular hole in a duralumin plate: theoretical and experimental

The experiment described in article VI,2 simulates the two-stress yielding of a fairly thin duralumin plate around a circular hole containing pressure. This inner-boundary normal stress is negative, while the outer boundary is stress-free as in Fig. VII,7.1. The relationship between the measured strains and the theoretical stress distribution is now considered.

7.1. **Physical concepts.** Article II,4 discusses the various types of displacement of points in a homogeneous straining. Here,

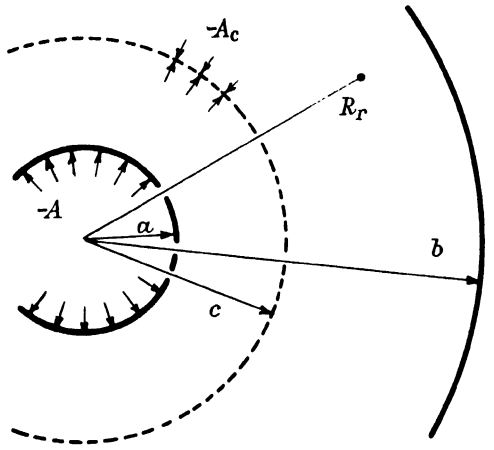

FIG. VII,7.1.—An annular plane-parallel plate with a radial pressure $-A$ applied to the inner cylindrical face. The zone from a to c is elasto-plastic and that from c to b is elastic.

the ideas need to be extended to heterogeneous straining in the annulus.

When pressure is applied to the inner boundary the initially homogeneous, stress-free plate remains elastic throughout until a critical, primary yield load is reached. Thereafter, on removal of the load, the diameter of the hole is found to be greater than it was initially. Suppose the pressure is applied again, up to a value just less than $-A$ from which it was unloaded, and then decreased again to zero. During this loading-unloading the strains are elastic or reversible. Therefore, if this 'new' annulus is homogeneous and elastic then the stresses and strains induced

by the applied pressure can be found as in article VII,1. Typical values are shown in Fig. VII,7.2 for stress and in Figs. VII,7.3, VII,7.4 for elastic strains on assuming restricted isotropy for the constant elastic stress-strain parameters. The dotted curve in Fig. VII,7.3 is for the calculated elastic strains.

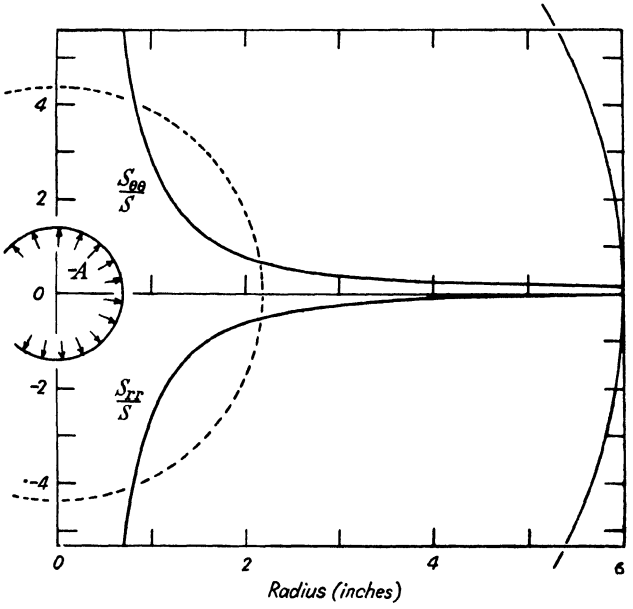

FIG. VII,7.2.—Radial and circumferential stresses in the duralumin annular plate of article VI,2 in which the pressure $-A$ in the inner hole is simulated by expanding a segmented collet. The stress S is that for simple tensile primary yield of value 34 000 psi. The stresses shown (as ordinates) are for the yield boundary radius of 2·19 inches with the inner radius 0·716 inch when the axial load on the mandrel was 17 930 pounds. When the yield boundary is at the inner boundary of radius 0·687 inch then the stresses are approximately $\frac{1}{10}$ of the values shown. More accurately, at the inner boundary $-A/S = 0{\cdot}570$, 5·34 for the lesser, greater loads respectively.

The measured elasto-plastic strains are greater than the elastic, and this is best visualised in terms of the 'migration' of particles in an ideal atomic lattice. (See volume I, article IV,1.3 or, here, article IV,17.) Consider an increment of elasto-plastic straining of a narrow annulus around the hole, for example. The circumference of the annulus increases, while its width decreases. This can be visualised as due to the migration of particles to account for its permanent, plastic change of shape into a 'new' elastic

annular band able to support the stresses just less than those from which it was unloaded.

Note carefully that the migration, or plastic straining, cannot influence the current elastic strains except to the extent that they may change the value of the elastic modulus (see Fig. I,9.3, for

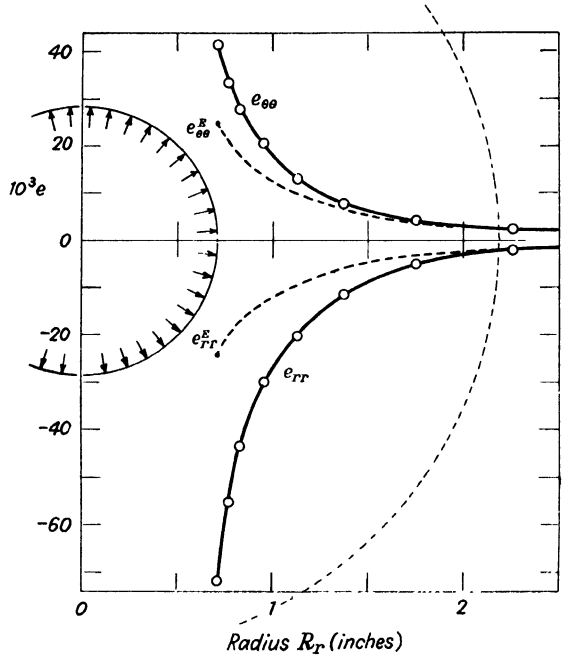

FIG. VII,7.3.—Measured elasto-plastic strains in the duralumin plate of article VI,2 when the axial load is 17 930 pounds on the tapered mandrel. The yield boundary radius is 2·19 inches and the inner boundary radius 0·716 inch. The calculated elastic strains are shown as dotted curves corresponding to the stresses in Fig. VII,7.2. The elastic stress-strain parameters are assumed to be isotropic and homogeneous of the same values as those for simple tension in chapter I. The total plastic 'strain' is the difference of the elasto-plastic and elastic strains. Note that the plastic radial strain increases more rapidly than the plastic circumferential strain.

example) or the transverse contraction ratio (see Fig. I,11.1, for example) or allow the support of greater load due to work-hardening (see Fig. I,5.2 and article IV,17.1, for example).

Therefore, all such plastic strains in the plate lead to just a new' elastic † plate able to support greater stresses, where they

† Author, 1951.

occur, due to the previous plastic straining inducing work-hardening of an appropriate amount. If such a plate is 'annealed' or 'normalised' by heat treatment it suffers little change in size † but regains its initial elastic modulus, transverse contraction ratio and yield-stress values. Thus, the work-hardened elastic plate becomes a plate of virtually the same size, but now of the initial

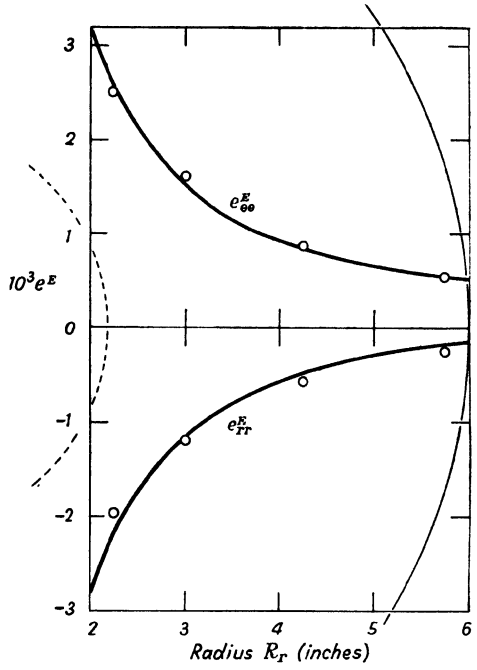

FIG. VII,7.4. - Elastic zone strains when the mandrel axial load is 17 930 pounds and the yield boundary radius is 2·19 inches. The points shown are experimental. The curves are theoretical but are also good mean curves for the observed values.

elastic substance. The plastic migration of the particles has merely led to a current elastic plate of different size from the initial elastic plate.

The foregoing physical reasoning guides the analysis that now follows.

7.2. **Stress distribution.** Articles VII,1.2, VII,1.3 give the stresses in such an elastic annulus. Retaining the internal-

† The present author can find no satisfactory, quantitative, metallurgical statements on this aspect.

boundary normal stress A as positive, for the present, while the outer-boundary applied stress is zero, gives the induced stresses

$$S_{rr} = \tfrac{1}{2}C + JR_r^{-2} \qquad S_{\theta\theta} = \tfrac{1}{2}C - JR_r^{-2} \tag{7.1}$$

with

$$C = -2A/[(b/a)^2 - 1] \qquad J = Aa^2/[1 - (a/b)^2]$$

At the yield boundary, of radius c,

$$A_c \equiv (S_{rr})_c = \tfrac{1}{2}C + Jc^{-2} \qquad (S_{\theta\theta})_c = \tfrac{1}{2}C - Jc^{-2} \tag{7.2}$$

Alternatively, the elastic zone of the plate can be regarded as an annulus with inner-, outer-boundary radii c, b loaded with normal stresses A_c, 0, while the elasto-plastic zone is an annulus with inner-, outer-boundary radii a, c loaded with normal stresses A, A_c.

7.3. Yield boundary determined theoretically by the stresses. The radius of the yield boundary is a function of the yield criterion used. The maximum shear stress criterion of yield inception, given in article **IV**,17.3, is the most convenient here for arithmetical computation. The signs of the stresses in **VII**(7.2) or **VII**(7.1) are opposite, so the first of **IV**(17.1) gives the criterion here as

$$\tfrac{1}{2}S = |\tfrac{1}{2}(S_{rr} - S_{\theta\theta})_c|$$

with S the simple tensile primary yield stress. Since the stresses here always fall approximately on the radius vector passing through point h in the stress-space diagram of Fig. **IV**,17.1, then it is convenient to use the more exact factored maximum shear stress criterion of article **IV**,17.8. The factor here is about $\sqrt{(4/3)}$, to give the yield criterion

$$|(S_{rr} - S_{\theta\theta})_c| = \sqrt{(4/3)}S \tag{7.3}$$

Substituting **VII**(7.2) gives

$$c^2 = 3^{\frac{1}{2}}(J/S) \tag{7.4}$$

to determine the yield boundary radius in terms of the current geometry and simple tensile yield properties of the plate.

Substituting for J in **VII**(7.1) from **VII**(7.4) gives the applied radial stress in the hole as

$$A = 3^{-\frac{1}{2}}Sa^{-2}[1 - (a/b)^2]c^2 \tag{7.5}$$

7.4. **Elastic strains.** With the generalised Hooke's law for restricted isotropy the elastic strains are

$$e^E_{rr} = G^E S_{rr} + F^E \chi \qquad e^E_{\theta\theta} = G^E S_{\theta\theta} + F^E \chi \tag{7.6}$$

$$\chi = S_{rr} + S_{\theta\theta} \qquad G^E = (1+q^E)\psi^E \qquad F^E = -q^E \psi^E$$

with the elastic modulus $\psi^E = E^{-1}$, with E = Young's modulus and q^E the elastic transverse contraction ratio or Poisson's ratio.

From VII(7.6) in VII(7.3) the yield criterion in terms of elastic strains, with simple tensile yield strain e, is

$$|(e^E_{rr} - e^E_{\theta\theta})_c| = G^E \sqrt{(4/3)} S = (1+q^E)\sqrt{(4/3)} e \tag{7.7}$$

7.5. **Yield boundary located experimentally from the strains.** Equation VII(7.7) can be used graphically to locate the yield boundary. A disadvantage is that only the circumferential strains have been measured, so that the radial strains must be inferred. A more direct method is as follows:

The stresses $(S_{rr})_c$, $(S_{\theta\theta})_c$ are calculated in terms of b, c, S and substituted in VII(7.6).2 to give

$$(e_{\theta\theta})_c = -\frac{\psi^E S}{\sqrt{3}}\left[\frac{(b/c)^2+1}{(b/c)^2-1} + q^E\right]\left[1-\left(\frac{c}{b}\right)^2\right] \tag{7.8}$$

Choose appropriate values of c and calculate $(e_{\theta\theta})_c$. Plot these values in a diagram of $e_{\theta\theta}$ vs. R_r. This curve intersects each of the family of experimental curves $e_{\theta\theta}$ vs. R_r for a given state of loading as in Table VI,2.2. The intersection is the yield boundary radius c for each axial load L on the mandrel. Using $\psi^E = 0{\cdot}10\ 10^{-6}$ (psi)$^{-1}$ from Fig. I,9.3, $q^E = 0{\cdot}28$ from Fig. I,11.1, $b = 6$ inches and $S = 34\,000$ psi gives the values of c vs. L in Fig. VII,7.5.

The yield boundary has been located as though the duralumin plate is an ideal, amorphous continuum. In practice, the boundary could not be defined sharply. A microscopic examination of the metal before and after loading could show that at a certain radius yield had definitely occurred, while at some greater radius it had definitely not occurred. The annular region between these two radii is a transition zone in which many crystals remain unyielded. Intuitively, it may be guessed that this zone will be about 0·1 to 0·3 inch, depending on the metal.

7.6. **Yield boundary and axial load.** If the yield boundary has been located correctly for each load then, according to

VII(7.5), the radial stress A is proportional to c^2. From Fig. VI,2.1, the radial stress will be proportional to L. Therefore, if the coefficient of friction is constant for the lubricated faces of the tapered mandrel and the segmented collet, then L is proportional to c^2. The curve drawn in Fig. VII,7.5 is for $L = 4000\,c^2$ and fits the experimental points reasonably well. Thus, 4000 psi

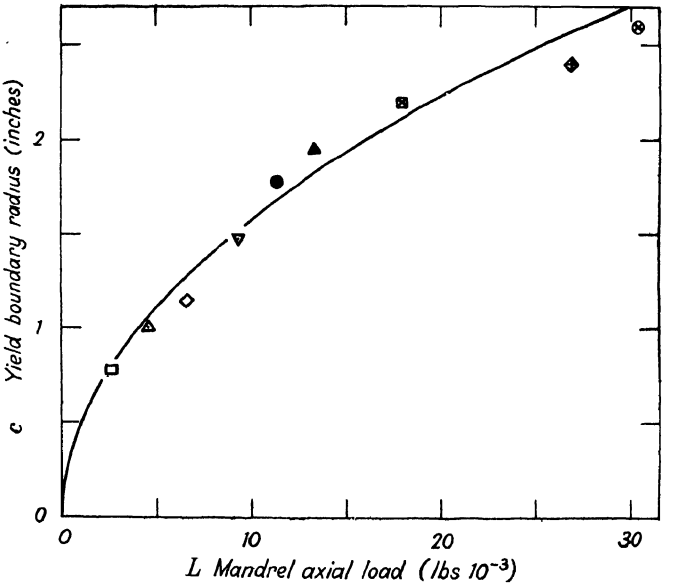

FIG. VII,7.5. Mandrel axial load L vs. yield boundary radius c. The curve shown has the equation $L = 4000\,c^2$. The theory gives the axial load L on the mandrel as proportional to c^2. The experimental values of c are found from the strain measurements and the 'factored' maximum shear stress criterion of yield inception. The collet cracked several times just before the second highest load and disintegrated just before the highest load. This may account for these two points being of greater deviation than the others.

can be taken as the calibration constant for the experimental rig and used to calculate radial stress $-A$ from the axial load.

The fit of theory to experiment in Fig. VII,7.5 is good when the experimental difficulties are noted. As the segmented collet expanded the conical face of each segment tended to lose contact with the conical surface of the mandrel and ride on its sharp edges as larger diameters of the mandrel entered the collet. Such sharp edges could not be lubricated satisfactorily and the

mandrel showed just such deep grooving from this effect. Further, the contiguous cylindrical faces of the collet and hole in the plate had to be left unlubricated, so that unaccounted shear stresses probably acted between them. Also, the parts of the hole between the expanded collet segments were unloaded.

7.7. **Calculation of the radial strain.** The radial strain was not measured, but it is readily inferred from the measured circumferential strain in the present case of cylindrical axial symmetry. Article **V**,7.2 gives the strains in terms of relative-displacement $\mathbf{D}^*_{,1}$. The straining-rotation is zero here, so that relative-displacement equals straining-displacement **D**. The whole-body rotation is zero, so that straining-displacement equals spatial-displacement **U**, except for a possible whole-body translation. The experimental strains in Table **VI**,2.2 are nominal, so that it is convenient to take the coordinates of each point to be in the undeformed body. The nominal strains are, therefore,

$$e^o_{rr} = \partial U/\partial R^o \qquad e^o_{\theta\theta} = U/R^o \tag{7.9}$$

The scalar initial radii R^o are given in Table **VI**,2.1. The scalar spatial-displacement U was calculated from the second equation, the result plotted against R^o, a smooth curve was drawn through the points and then the slope was measured to give the graphical differentiation for nominal radial strain. Typical values of true strain are given in Figs. **VII**,7.3, **VII**,7.4 for the same mandrel load of 17 930 pounds.

7.8. **Elastic strains.** The elastic strains throughout the annulus are calculated from **VII**(7.6) with the elastic stress-strain parameters as in article **VII**,7.5 and the stress in the hole given by equation **VII**(7.5). Fig. **VII**,7.3 shows typical measured strains in the elasto-plastic zone with the calculated elastic strains curve shown dotted. Fig. **VII**,7.4 shows the calculated elastic zone strains for the same load as a full line with a scale ten times greater for convenience.

7.9. **Planewise plastic strains.** The planewise strains need to be considered incrementally as in article **V**,5.1. Suppose that the plastic transverse contraction ratio is isotropic, to give the principal normal plastic increment strains

$$\left.\begin{aligned} \delta e^{P}_{rr} &= \delta\epsilon^{P}_{rr} - q^P \delta\epsilon^{P}_{\theta\theta} & \delta e^{P}_{\theta\theta} &= \delta\epsilon^{P}_{\theta\theta} - q^P \delta\epsilon^{P}_{rr} \\ \delta\epsilon^{P}_{rr} &= \psi^{P}_{rr}\delta S_{rr} & \delta\epsilon^{P}_{\theta\theta} &= \psi^{P}_{\theta\theta}\delta S_{\theta\theta} \end{aligned}\right\} \tag{7.10}$$

Fig. VII,7.6 is the typical member of these two increment partial-strains plotted against total stress. For example, with subscript $\mathbf{i} = \theta\theta$, the diagram is that for one of the circumferential strain-gauges when the transverse strain effects from the radial partial-strain are removed. The dotted curve is followed during elasto-plastic straining.

Now suppose that, for the particle of substance to which VII(7.10) applies, the plastic modulus remains constant between

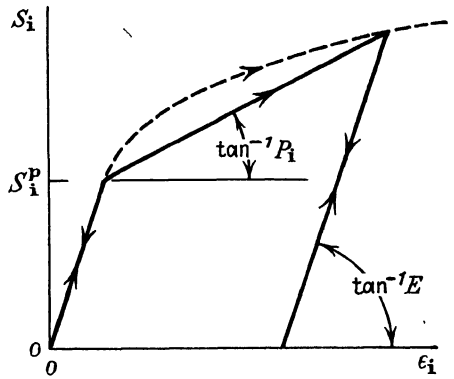

FIG. VII,7.6.—Principal normal stress vs. principal normal elasto-plastic partial-strain diagrammatically for a *point* of the body as the load changes. The subscript denotes either radial or circumferential directions for the yielded annulus problem. The dotted elasto-plastic curve is that which would be observed. For computational convenience, the straight, full elasto-plastic line is taken to pass through the primary yield and current values. This allows the definition of a current plastic secant modulus $\psi^P_{\mathbf{i}} = (P_{\mathbf{i}}{}^{-1} - E^{-1})$ with the isotropic elastic modulus $\psi^E = E^{-1}$ assumed of the same value throughout.

the primary yield and current states. Then summation of the increment strains gives

$$\left.\begin{aligned} e^P_{rr} &= \psi^P_{rr}(S_{rr} - S^{\mathrm{p}}_{rr}) - q^P\psi^P_{\theta\theta}(S_{\theta\theta} - S^{\mathrm{p}}_{\theta\theta}) \\ e^P_{\theta\theta} &= \psi^P_{\theta\theta}(S_{\theta\theta} - S^{\mathrm{p}}_{\theta\theta}) - q^P\psi^P_{rr}(S_{rr} - S^{\mathrm{p}}_{rr}) \end{aligned}\right\} \quad (7.11)$$

This means that, for greater convenience, the current elasto-plastic stress-strain effects are plotted along the straight secant shown in Fig. VII,7.6 instead of along the dotted actual curve. Thus, the ψ^P's in VII(7.11) are current secant moduli, whereas those in VII(7.10) are current tangent moduli.

7.10. **Compatibility of planewise plastic strains.** The current elasto-plastic strains must satisfy the compatibility conditions with respect to change of position in the currently deformed body. Thus, strictly, the partial-increment plastic strains dyadic $\Delta\mathfrak{M}^P$, of which VII(7.10) gives the scalar components, must have a zero curl. Alternatively, noting the assumption allowing the consideration of total plastic 'strains' in VII(7.11), the curl of $\mathfrak{M}^P$ can be considered. Thus, from article V,6.2, the only non-zero planewise condition here is

$$R_r e^P_{\theta\theta;r} = e^P_{rr} - e^P_{\theta\theta} \tag{7.12}$$

As a typical result, the measurements given in Fig. VII,7.3 have been analysed. Taking

$$e^P_{rr} = e_{rr} - e^E_{rr} \qquad e^P_{\theta\theta} = e_{\theta\theta} - e^E_{\theta\theta} \tag{7.13}$$

plotting the last against current radial position, differentiating graphically and then plotting VII(7.12) gives the points marked in Fig. VII,7.7. The line drawn is for the exact satisfaction of the

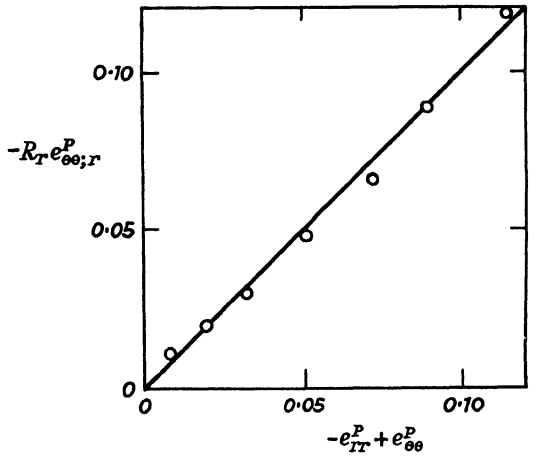

FIG. VII,7.7.—Compatibility of *total plastic* 'strains'. The full line is theoretical for complete satisfaction. The points shown are calculated from the observations and fall well on to the theoretical line.

compatibility conditions and is, in fact, a good mean curve for the experimental observations. Therefore, the total plastic planewise strains dyadic has a zero curl, as is required for compatibility.

7.11. **Plastic moduli.** The equations VII(7.11) can be solved for the two unknowns ψ^P_{rr}, $\psi^P_{\theta\theta}$ if the value of q^P is known. This

ratio is assumed to be 0·35, the mean value for simple tension given in Fig. I,11.2. As a typical case, the strains in Fig. VII,7.3 and the stresses in Fig. VII,7.2 are substituted in VII(7.11). The primary yield stresses are given closely by equations VII(7.2) when c there has the value R_r to which equations VII(7.11) are to apply in calculating the values of the plastic moduli.

Fig. VII,7.8 gives the values of the two moduli for plastic general isotropy. The very small values of $\psi^P_{\theta\theta}$ with tensile stress $S_{\theta\theta}$ in comparison with ψ^P_{rr} with compressive stress S_{rr} should be noted as qualitatively consistent with the values in Fig. IV,14.2

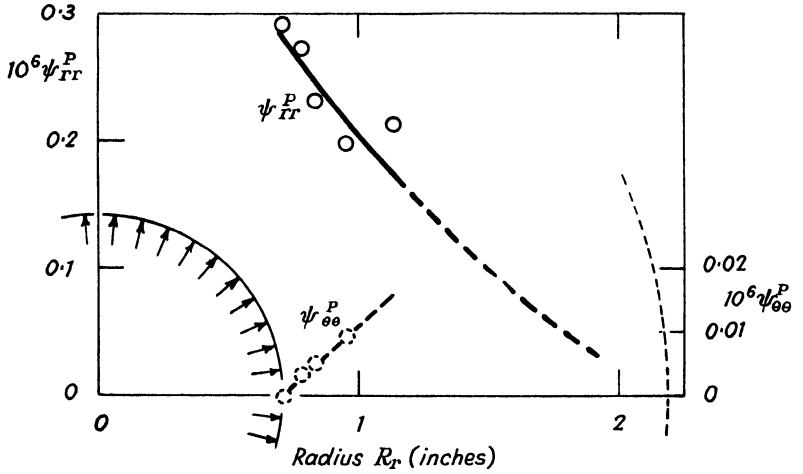

FIG. VII,7.8.- Plastic moduli for general isotropy of the plastic strains given from Fig. VII,7.3. The low values of the circumferential plastic modulus are qualitatively consistent with those in Fig. IV,14.2.

for thin-walled duralumin tubes. In fact, if it is supposed that $\psi^P_{\theta\theta} = 0$ in VII(7.11), then the two equations and the observations are still reasonably consistent. That is, the duralumin acts almost 'elastically' only to induced tensile increment stress $\delta S_{\theta\theta}$ but plastically towards the compressive increment stress δS_{rr}.

7.12. **Thickness changes.** The thickness strain

$$e_{zz} = e^E_{zz} + \int \partial e^P_{zz} \tag{7.14}$$

is the third principal normal component of the strain dyadic and has not been considered up to the present.

Similar to equations **VII**(7.6) for restricted isotropy of elastic strains

$$e_{zz}^{E} = F^{E}\chi = F^{E}C \tag{7.15}$$

with

$$C = -2A/[(b/a)^2-1]$$

The elastic thickness change is constant throughout the plate and proportional to the applied stress in the hole.

Assuming isotropy of the plastic transverse contraction ratio, then, similar to **VII**(7.10),

$$\delta e_{zz}^{P} = -q^{P}(\delta\epsilon_{rr}^{P}+\delta\epsilon_{\theta\theta}^{P}) \doteq -q^{P}\delta\epsilon_{rr}^{P} \tag{7.16}$$

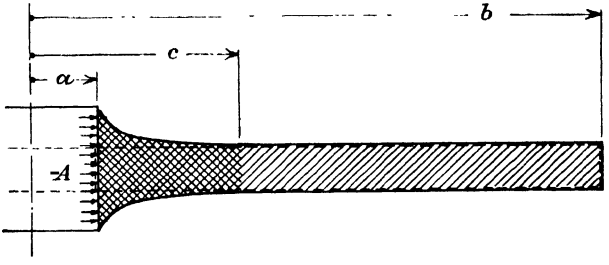

FIG. **VII**,7.9. Theoretical thickness changes due to the inequality of the plastic moduli in the initially plane-parallel duralumin annulus. The scale of the thickness change is large to display the distribution. In fact, the thickness strain is nowhere greater than a few per cent.

with

$$\delta\epsilon_{rr}^{P} = \psi_{rr}^{P}\delta S_{rr}$$

on noting the small values of $\psi_{\theta\theta}^{P}$ in article **VII**,7.11. Then, similar to **VII**(7.11),

$$e_{zz}^{P} = -q^{P}\psi_{rr}^{P}S_{rr} \tag{7.17}$$

This plastic thickness strain is fairly small even at the boundary of the hole, so that it makes little difference if the plate is taken as currently or initially plane-parallel. Fig. **VII**,7.9 shows the theoretical thickness change to a large scale for the stresses given in Fig. **VII**,7.2 and the plastic moduli in Fig. **VII**,7.8. Experimental observations are not available for comparison, as their importance in determining stress-strain parameters was not fully realised at that time (1947).

The compatibility conditions for the plastic strains are given

by article V,6.2. All are identically zero here except VII(7.12) and

$$e^P_{zz;r} = 0 \tag{7.18}$$

This condition is not satisfied by e^P_{zz} in VII(7.17). Therefore, the foregoing analysis which assumes that the stresses are plane and makes arbitrary assumptions for the stress-strain parameters is not strictly true. However, the main, planewise features of the experiment and theory are consistent, so until further tests give more data the analysis is sufficient.

7.13. **Other solutions of this problem.** Several solutions of this problem of yielding around a hole due to pressure have been proposed, but the present author's measurements of strain across the plane face of the annulus seem to be all that are available.

A. Nadai, in 1947 [55], extended to a plate his analysis for a thick-walled tube as given in 1931 [46]. Restricted isotropy with homogeneous elastic and plastic stress-strain parameters was assumed. The compatibility of the strains was not discussed. The value of A/S (see equation VII(7.5) here) is given as 1·16 by Nadai and 1·76 by the present author when $c/a = 1{\cdot}75$. Nadai gave the circumferential stress $S_{\theta\theta}$ as much less at the hole than at the yield boundary, whereas the present author gives it as much greater. Nadai gives $S_{\theta\theta}$ as negative at the hole when $c/a = 1{\cdot}75$, whereas the present author gives it as positive.

A. Winzer & W. Prager, in 1947 [147], used plastic stress-strain relations suggested by A. A. Ilyushin in 1946 [148]. This leads to $S_{\theta\theta} = 0$ throughout the annulus. Winzer & Prager then suggested another stress-strain relation, and this led to $S_{\theta\theta}$ almost constant throughout the elasto-plastic zone and of the value at the yield boundary. From either stress-strain relation Winzer & Prager gave the value A/A_c (see equation VII(7.2).1) as 1·60, whereas the present author gives 1·77 when $c/a = 1{\cdot}33$.

G. I. Taylor, in 1948 [149], considered † the severe expansion of a circular hole due to internal pressure. Attention is focussed on the total stresses and the 'velocities' they generate. Great thickening near the hole is considered but with the hypothesis that plane polar stresses are maintained there. Restricted isotropy seems to be implied. Compatibility conditions are not given. Towards the yield boundary the elasto-plastic region is found to suffer no

† The method is reproduced in the book by R. Hill [37 9] in 1950.

thickening. The stresses are shown to have a peculiar distribution inside the yield boundary. Moving from the yield boundary inwards to the hole the negative stress S_{rr} increases negatively, then remains constant and then decreases. The positive circumferential stress $S_{\theta\theta}$ decreases to zero, discontinuously becomes negative, increases to zero and, after a discontinuity of slope, increases positively.

The present author, in 1945 [47], gave a solution with $S_{\theta\theta}$ almost constant throughout the elasto-plastic zone. Then, in 1948 [106, 59], a solution was given with $S_{\theta\theta}$ a little less than that in Fig. VII,7.2. Restricted isotropy was assumed for the plastic strains. Strains compatibility conditions were not considered.

7.14. **Conclusions.** This is one of the simplest cases of heterogeneous elasto-plastic straining and yet there is *not even qualitative agreement among the various writers* on the stress distribution. It seems desirable to study this case further before proceeding to more difficult problems. The reader could regard as an extensive exercise the attempt to relate the various theories with the available measurements in article VI,2.

The tests need to be repeated taking care that the unloading case is included. The presence, magnitude and distribution of residual elastic strains should be established. The question needs to be considered of whether these strains (if found to be of an important magnitude) are due to non-homogeneous elastic stress-strain properties induced by the straining or to the preceding elasto-plastic straining, as other writers' theories imply. That is, whether the physical concepts in VII,7.1 are correct in regarding the plate as merely a 'new' elastic one at each load stage. Thickness changes should be observed.

Auxiliary tests on thin-walled tubes should be made with equal and opposite two-stress loading to verify the anisotropy of the plastic moduli but without the complication of strain transfer as in article IV,14. Further, are the elastic stress-strain parameters isotropic and homogeneous?

Chapter VIII

THREE-STRESS EQUATIONS FOR SOLUTION

1. The physical concepts expressed in the general equations of equilibrium deformation

Article V,1 discusses briefly the physical concepts of deformation under a two-stress system in terms of vectors, dyadics and appropriate operators. Here we deal with a three-stress distribution and an accompanying three-strain system. Therefore, it is only necessary to let all dyadics and vectors be three-dimensional and the discussion of article V,1 applies here directly, so that representation is unnecessary.

Curvilinear coordinates are frequently useful for particular problems, but, for brevity, the full scalar expansions will not be given usually in this chapter, as was done in chapter V for two-stress. Instead, the closed form will be given and it will be indicated where the expansion can be found in appendix A, as this will save repetition of the same mathematical forms for different physical aspects. Where expanded forms are given explicitly, the general directions $\mathbf{c}_a$, $\mathbf{c}_b$, $\mathbf{c}_c$ for either the constant unit vectors of rectilinear cartesian coordinates or the variable local unit vectors of curvilinear coordinates will be used in the manner of article A,2.

Where statements here seem to be too arbitrary, then the proofs will be found in volume I.

2. Three-stress dyadic

The three-stress dyadic $\mathfrak{S}$ is self-conjugate of the form in article A,6 with the C's there replaced by S's here. It can always be reduced from its nonion form to a principal form in which only the principal normal stresses $S_{\mathbf{i}}$ in directions $\mathbf{s}_{\mathbf{i}}$ appear. During the transformation from one set of axes to another there are found three invariants, of which the most important is the first stress invariant

$$\chi^{S(1)} = \sum_{\mathbf{i}} S_{\mathbf{i}} = \sum_{a} S_{aa} \tag{2.1}$$

2.1. **Vector stress on a plane.** The vector stress acting on a plane normal to unit vector $\mathbf{n}$ at the point to which the stress dyadic applies is

$$\mathbf{S}_n = \mathbf{n}\cdot\mathfrak{S} \tag{2.2}$$

2.2. **Partial-increment stress dyadic.** When whole-body convected axes are the reference for observation, then the principal normal strain trajectories are virtually parallel before and after an increment deformation from the current state. Thus, the principal normal strain directions $\mathbf{x}_i$ are quasi-constant during the increment deformation. If, particularly, principal normal stresses and strains are coaxial, then the stress dyadic suffers a partial-increment

$$\Delta\mathfrak{S} = \sum_i \delta S_i \mathbf{x}_i\mathbf{x}_i \tag{2.3}$$

3. Equilibrium three-stress equation

The equation ensuring that a point and its neighbourhood are in equilibrium is

$$\operatorname{div}\mathfrak{S} + m\mathbf{B} = 0 \tag{3.1}$$

The vector $\operatorname{div}\mathfrak{S}$ is given in article A,11 for the common coordinate systems.

4. Strain dyadic

The strain dyadic $\mathfrak{M}$ is self-conjugate of the form in article A,6 with the C's there replaced by e's here. It can always be reduced from its nonion form to a principal form in which only the principal normal strains e_i in directions $\mathbf{x}_i$ appear. During the transformation from one set of axes to another there are found three invariants, of which the most important is the first strain invariant

$$\chi^{D(1)} = \sum_i e_i = \sum_a e_{aa} \tag{4.1}$$

4.1. **Differential relative-displacement for a given direction.** The differential vector relative-displacement of one end of differential position vector $d\mathbf{R} = dR\mathbf{n}$ is

$$d\mathbf{D}^* = dR\mathbf{n}\cdot\mathfrak{M} \tag{4.2}$$

Note the similarity to equation VIII(2.2).

4.2. **Partial-increment strain dyadic.** Relative to whole-body convected axes the principal normal strain directions $\mathbf{x}_i$ are quasi-constant during an increment deformation. Thus, the partial-increment strain dyadic is, similar to equation VIII(2.3),

$$\Delta\mathfrak{M} = \sum_i \delta e_i \mathbf{x}_i\mathbf{x}_i \tag{4.3}$$

5. Three-stress and three-strain relations

Partial-increment stress dyadic $\Delta\mathfrak{S}$ is related to the partial-increment strain dyadic $\Delta\mathfrak{M}$ by a stress-strain parameters quadadic $\boldsymbol{P}$. Thus, as in article V,5,

$$\Delta\mathfrak{M} = \boldsymbol{P}:\Delta\mathfrak{S} = (\boldsymbol{P}^E+\boldsymbol{P}^P):\Delta\mathfrak{S} \tag{5.1}$$

5.1. **Principal directions for general isotropy.** The principal normal increment partial-strains are

$$\delta\epsilon_i^M = \psi_i^M \delta S_i = \psi_i^M \mathbf{x}_i\mathbf{x}_i:\Delta\mathfrak{S} \tag{5.2}$$

while

$$\delta e_i^M = \delta\epsilon_i^M - q_{j-i}^M \delta\epsilon_j^M - q_{k-i}^M \delta\epsilon_k^M \tag{5.3}$$

The general component of the stress-strain parameters quadadic is then

$$\boldsymbol{P}^M = \sum_{i,j,k} \mathbf{x}_i\mathbf{x}_i(\psi_i^M \mathbf{x}_i\mathbf{x}_i - q_{j-i}^M \psi_j^M \mathbf{x}_j\mathbf{x}_j - q_{k-i}^M \psi_k^M \mathbf{x}_k\mathbf{x}_k) \tag{5.4}$$

5.2. **General directions for general isotropy.** The unit vectors $\mathbf{x}_i$ in the stress-strain parameters quadadic are transformed to the general directions $\mathbf{c}_a$. The partial-increment stress and strain dyadics are similarly transformed to directions $\mathbf{c}_a$. Then, for the general directions the stress-strain parameters quadadic $\boldsymbol{P}^M(a)$ includes direction cosines, like $\mathbf{c}_a\cdot\mathbf{x}_i$ to the fourth degree, and the stress-strain parameters ψ_i^M, q_{j-i}^M, ... as in article V,5.2.

5.3. **Principal directions for restricted isotropy.** The direction subscripts can be left off the parameters in article VIII,5.1 to give simply

$$\delta e_i^M = G^M \delta S_i + F^M \delta\chi^S \tag{5.5}$$

with

$$G^M = (1+q^M)\psi^M \qquad F^M = -q^M\psi^M \tag{5.6}$$

and

$$\delta\chi^S = \sum_i \delta S_i \tag{5.7}$$

the increment stress first invariant.

5.4. **General directions for restricted isotropy.** Equation VIII(5.5) in VIII(5.1) then transformed to the general axes gives normal, shear increment strains

$$\delta e^M_{aa} = G^M \delta S_{aa} + F^M \delta \chi^S \qquad \delta e^M_{ab} = G^M \delta S_{ab} \tag{5.8}$$

In dyadic form

$$\Delta \mathfrak{M}^M = (G^M + F^M \mathfrak{JJ}:) \Delta \mathfrak{S} \tag{5.9}$$

5.5 **Constant elastic parameters and restricted isotropy.** The elastic strains transfer as the deformation evolves. Therefore, if the elastic parameters are constant then the current elasto-plastic strain for the principal directions is

$$e_i = (G^E S_i + F^E \chi^S) + (G^P \delta S_i + F^P \delta \chi^S) \tag{5.10}$$

with the plastic parameter referring to the last increment deformation.

The dyadics transform to give, for general directions,

$$\left.\begin{aligned} e_{aa} &= (G^E S_{aa} + F^E \chi^S) + (G^P \delta S_{aa} + F^P \delta \chi^S) \\ e_{ab} &= G^E S_{ab} + G^P \delta S_{ab} \end{aligned}\right\} \tag{5.11}$$

In dyadic form

$$\mathfrak{M} = (G^E + F^E \mathfrak{JJ}:) \mathfrak{S} + (G^P + F^P \mathfrak{JJ}:) \Delta \mathfrak{S} \tag{5.12}$$

6. Compatibility of three-stress strains

Continuity of the strain dyadic with position leads to the consideration of $\nabla \mathfrak{M}$. However, the same continuity is assured when

$$\nabla \times \mathfrak{M} = 0 \tag{6.1}$$

Article A,12 gives the expanded form for various coordinate systems when the a's there become the e's here.

6.1. **Compatibility of increment stresses and stress-strain parameters for general isotropy.** Similarly, compatibility of the partial-increment strain dyadic is assured by

$$\nabla \times \Delta \mathfrak{M} = 0 \tag{6.2}$$

with δe's replacing a's in article A,12.

Substituting the component δe^M's from article VIII,5 gives the compatibility conditions for increment stresses and stress-strain parameters. In dyadic form, for each component of the elasto-plastic strain,

$$\nabla \times (\boldsymbol{P}^M : \Delta \mathfrak{S}) = 0 \tag{6.3}$$

6.2. Restricted isotropy compatibility of increment stresses with stress-strain parameters independent of position. From VIII(6.2) there are found *nine* scalar equations like

$$\delta e^M_{ii;j} = \delta e^M_{ij;i} \qquad \delta e^M_{ij;k} = \delta e^M_{jk;i} \tag{6.4}$$

for cartesian axes. With F^M, G^M independent of position in the body at the current state of deformation, then substitution of equations VIII(5.8) gives

$$\left.\begin{aligned} G^M(\delta S_{ii;j} - \delta S_{ij;i}) &= -F^M \delta\chi^S{}_{;j} \\ G^M(\delta S_{ij;k} - \delta S_{jk;i}) &= 0 \end{aligned}\right\} \tag{6.5}$$

for increment strains compatibility.

Article VIII,10 gives the representation of the partial-increment stress dyadic in terms of increment stress potential δH by

$$\Delta\mathfrak{S} = \nabla\nabla\delta H \tag{6.6}$$

or scalarly,

$$\delta S_{ij} = \delta H_{;ij} \qquad (i = \text{or} \neq j) \tag{6.6'}$$

Then the left-hand side of each equation in VIII(6.5) is zero, so that, from the first equation,

$$\delta\chi^S = \text{constant} \tag{6.7}$$

throughout the current, deformed body. This is consistent with the integration of the increment stress equilibrium equation for zero body force as in article VIII,11.

Article VIII,13 gives the representation of the partial-increment stress dyadic in terms of a modified Maxwell increment stress function $\delta\mathcal{A}$ by

$$\Delta\mathfrak{S} = \mathfrak{J}_\times^\times \nabla\nabla\delta\mathcal{A} \tag{6.8}$$

since its divergence is zero as required when body force is zero. Scalarly,

$$\delta S_{ii} = \delta\mathcal{A}_{;jj} + \delta\mathcal{A}_{;kk} \qquad \delta S_{ij} = -\delta\mathcal{A}_{;ij} \tag{6.8'}$$

Substituting in VIII(6.5).1 gives

$$\tfrac{1}{2}(G^M + 2F^M)\delta\chi^S{}_{;j} = 0 \tag{6.9}$$

while VIII(6.5).2 is identically zero. Equation VIII(6.9) shows that the first invariant of the increment stresses is constant as in VIII(6.7).

7. Relative-displacement and strain

Relative-displacement $\mathbf{D}^*$ and the strain dyadic are related by

$$\mathfrak{M} = \nabla\mathbf{D}^* \tag{7.1}$$

The expansion of $\nabla\mathbf{D}^*$ is given in article A,14 when the F's there are replaced by D^*'s here. The self-conjugate strain dyadic $\mathfrak{M}$ is similar to that in article A,6 with C's there replaced by e's here. Equating the coefficients of like dyads on each side of VIII(7.1) gives the required scalar strains in terms of relative-displacement gradients.

8. Displacement potential and relative-displacement

Relative-displacement $\mathbf{D}^*$ and displacement potential $\mathcal{E}$ are related by

$$\mathbf{D}^* = \nabla\mathcal{E} \tag{8.1}$$

Article A,8 gives operator ∇ for various coordinate systems. Allowing this to operate on $\mathcal{E}$ and equating the components of the vector on each side of the equation gives D^*'s in terms of $\mathcal{E}$.

9. Strain and displacement potential

The strain dyadic and displacement potential are related by

$$\mathfrak{M} = \nabla\nabla\mathcal{E} \tag{9.1}$$

Article A,9 gives operator $\nabla\nabla$ for various coordinate systems. Equating the coefficients of like dyads on each side of the equation gives strains in terms of displacement potential.

10. Stress potential and stress

Consistent with the form for representation of the strain dyadic in terms of displacement potential the stress dyadic is represented in terms of the stress potential by

$$\mathfrak{S} = \nabla\nabla H \tag{10.1}$$

Article A,9 gives the operator $\nabla\nabla$ for various coordinate systems. Equating the coefficients of like dyads on each side of the equation gives stress in terms of stress potential.

11. Law of distribution of the three-stress potential

Similar to article V,11,

$$\nabla^2 H + \mathcal{B} = C \tag{11.1}$$

The laplacian operator ∇^2 is given in article A,9 for various coordinate systems. But

$$\nabla^2 H = \chi^S \tag{11.2}$$

the first stress invariant, and this is constant when body force is zero.

12. Displacement potential from the three-stress potential

The treatment is similar to article V,12 for a two-stress system.

12.1. **Restricted isotropy, stress-strain parameters independent of position and zero body force.** The increment displacement potential component $\delta\mathcal{E}^M$ of the elasto-plastic deformation is related to the increment stress potential by

$$\delta\mathcal{E}^M = G^M \delta H + \tfrac{1}{2} F^M \delta\chi^S \mathbf{R}\cdot\mathbf{R} + \mathbf{W}\cdot\mathbf{R} \tag{12.1}$$

with $\mathbf{R}$ the current position vector and $\mathbf{W}$ an arbitrary vector of whole-body translation.

If the elastic parameters remain constant during the evolution of the elasto-plastic deformation then $\mathcal{E}^E$, H, χ^S replace $\delta\mathcal{E}^E$, δH, $\delta\chi^S$ for the elastic component of the current strain.

13. Modified Maxwell three-stress function

Volume I, article II,9.4 shows that the three Maxwell stress functions employed to represent the stress dyadic will not transform with reorientation of axes. However, employing one function $\mathcal{A}$ (conveniently called the modified Maxwell stress function) in the same fashion is seen to be the three-dimensional analogue of the Airy stress function in article V,13 here. Thus

$$\mathbb{S} = \mathbb{J} \overset{\times}{\times} \nabla\nabla\mathcal{A} \tag{13.1}$$

With idemfactor

$$\mathbb{J} = \sum_i \mathbf{c}_i \mathbf{c}_i$$

and $\nabla\nabla$ from article A,9 for cartesian coordinates gives, scalarly,

$$S_{ii} = \mathcal{A}_{;jj} + \mathcal{A}_{;kk} \qquad S_{ij} = -\mathcal{A}_{;ij} \tag{13.2}$$

Similar forms are found for the common curvilinear coordinates when $\mathbb{J}$ and $\nabla\nabla$ are expressed in them.

14. Solutions by the Navier, Cauchy approximate theory

Article V,14 on a two-stress system discusses the classical infinitesimal strains analysis and its extension to finite strain in terms of vectors and dyadics. Expressing all those quantities three-dimensionally, then precisely the same discussion applies here to three-stress. The mathematically approximate character of the classical theory must be borne in mind. Remember that it must, in fact, deal with straining-displacement rather than spatial-displacement related to stress, that the Cauchy strain definitions are a sort of doublet in which can be 'concealed' a 'dislocational' rotation not revealed by the Saint-Venant compatibility conditions, as these consider continuity of spatial-displacement rather than continuity of the strain dyadic.

15. Saint-Venant's strains compatibility conditions for a three-stress system

For strain dyadic $\mathfrak{M}$ to ensure continuity of spatial-displacement

$$(\nabla\times\mathfrak{M})\times\nabla = 0 \tag{15.1}$$

From article A,13.3, for cartesian coordinates there are found the six conditions given briefly as

$$\left.\begin{aligned} e_{ii;jj}+e_{jj;ii}-2e_{ij;ij} &= 0 \\ e_{ii;jk}+e_{jk;ii}-e_{ki;ij}-e_{ij;ki} &= 0 \end{aligned}\right\} \tag{15.2}$$

15.1. **Restricted isotropy, constant elastic stress-strain parameters.** From article VIII,5.5, briefly,

$$e_{ii} = GS_{ii}+F\chi^S \qquad e_{ij} = GS_{ij} \tag{15.3}$$

From article VIII,13, the modified Maxwell stress function gives briefly

$$S_{ii} = \mathcal{A}_{;jj}+\mathcal{A}_{;kk} \qquad S_{ij} = -\mathcal{A}_{;ij} \tag{15.4}$$

and

$$\nabla^2\mathcal{A} = \tfrac{1}{2}\chi^S \tag{15.5}$$

Substituting VIII(15.3) to VIII(15.5) in VIII(15.2) gives the six equations

$$\chi^S{}_{;ii}+\chi^S{}_{;jj} = 0 \tag{15.6}$$

$$\chi^S{}_{;ij} = 0 \tag{15.7}$$

Solving the three equations VIII(15.6) algebraically gives the three equations

$$\chi^S{}_{;ii} = 0 \tag{15.8}$$

From VIII(15.7), VIII(15.8) it is seen that the three-stress first invariant χ^S is linear in the cartesian coordinates R_i. Then, with VIII(15.5), the arbitrary, constant, scalar C and the arbitrary, constant, vector $\mathbf{J}$, with position vector $\mathbf{R}$, gives

$$\nabla^2 \mathcal{A} = C + \mathbf{J} \cdot \mathbf{R} \tag{15.9}$$

This is the same form as that for two-stress in article V,15.1. The expressions for ∇^2 in various coordinate systems are given in article A,9. Note that as $\mathbf{R} \to \infty$ then the first stress invariant also approaches infinity. This is not allowable physically, so that in the many problems in which boundaries are at infinity the constant vector $\mathbf{J}$ must be zero. Thus, in these cases at least, the first stress invariant is constant, as was concluded generally from the stress potential H.

16. Navier, Cauchy strains definitions and spatial-rotation for a three-stress

The Navier, Cauchy strains definitions and spatial-rotation are the self-conjugate and antiself-conjugate dyadics

$$\mathfrak{M} = \tfrac{1}{2}(\boldsymbol{\nabla}\mathbf{U} + \mathbf{U}\boldsymbol{\nabla}) \tag{16.1}$$

$$\mathfrak{A} = \tfrac{1}{2}(\boldsymbol{\nabla}\mathbf{U} - \mathbf{U}\boldsymbol{\nabla}) \tag{16.2}$$

The expansions of these are given in article A,15 for various coordinate systems with the F's there becoming U's here. The scalar components of $\mathfrak{M}$ are e_{aa}, e_{ab} and of $\mathfrak{A}$ are ω_{ab} for the general curvilinear coordinates.

Chapter IX

THREE-STRESS ANALYSES

1. Normal loading on hollow and solid elastic spheres: theoretical

Spherical coordinates (R_r, θ, ϕ) are appropriate and point symmetry for stresses is assumed. Then article **VIII**,11 gives the law of distribution of stress potential H as

$$\nabla^2 H = H_{;rr} + 2R_r^{-1} H_{;r} = C \tag{1.1}$$

The particular integral is $\frac{1}{6}CR_r^2$, the complementary function is $JR_r^{-1} + K$ with arbitrary constants J, K of integration, so that the complete solution is

$$H = \tfrac{1}{6}CR_r^2 + JR_r^{-1} + K \tag{1.2}$$

The stresses are given by article **VIII**,10 as

$$\left.\begin{aligned} S_{rr} &= H_{;rr} = \tfrac{1}{3}C + 2JR_r^{-3} \\ S_{\theta\theta} &= S_{\phi\phi} = R_r^{-1} H_{;r} = \tfrac{1}{3}C - JR_r^{-3} \end{aligned}\right\} \tag{1.3}$$

1.1. Stresses induced by normal stresses applied to both surfaces of a hollow sphere.

The internal, external radii of a hollow sphere are a, b and the corresponding applied normal stresses are A, B. Using the boundary conditions $R_r = a$, $S_{rr} = A$, $R_r = b$, $S_{rr} = B$ gives

$$2J = (A - B)/(a^{-3} - b^{-3}) \qquad \tfrac{1}{3}C = (Aa^3 - Bb^3)/(a^3 - b^3) \tag{1.4}$$

for substitution in **IX**(1.3).

1.2. Particular cases

(i) When $A = B$, then $J = 0$ and the three normal stresses have the same isotropic value B.

(ii) When $a = 0$ to give a solid sphere, then $J = 0$ and the three normal stresses have the isotropic value B.

(iii) When $b \to \infty$ and $B = 0$ gives normal stress on a spherical hole in an infinite solid stress-free at infinity, then $C = 0$, $2J = Aa^3$.

(iv) When $b \to \infty$ and $A = 0$ gives a stress-free spherical hole in a solid loaded at infinity by normal stress B to give $\frac{1}{3}C = B$, $2J = -Ba^3$.

1.3. **Displacement potential for restricted isotropy, stress-strain parameters independent of position and zero body force.** From article **VIII**,12.1, with $\mathbf{W} = 0$ for zero whole-body translation, the elastic displacement potential is

$$\mathcal{E} = GH + \tfrac{1}{2}F\chi^S R_r^2 \tag{1.5}$$

Relative-displacement $\mathbf{D}^*$ equals straining-displacement $\mathbf{D}$ because straining-rotation is zero. Straining-displacement equals spatial-displacement $\mathbf{U}$ because whole-body rotation is zero. Then, with the $\boldsymbol{\nabla}$ operator form in article **A**,8.2,

$$\mathbf{D} = \boldsymbol{\nabla}\mathcal{E} = \mathbf{c}_r \mathcal{E}_{;r} \tag{1.6}$$

With $\chi^S = C$, then substituting **IX**(1.2) in **IX**(1.5) gives, scalarly,

$$D_r = C(\tfrac{1}{3}G + F)R_r - JGR_r^{-2} \tag{1.7}$$

The strains are given from article **VIII**,9 as

$$\left.\begin{aligned} e_{rr} &= \mathcal{E}_{;rr} = C(\tfrac{1}{3}G + F) + 2JGR_r^{-3} \\ e_{\theta\theta} &= e_{\phi\phi} = R_r^{-1}\mathcal{E}_{;r} = C(\tfrac{1}{3}G + F) - JGR_r^{-3} \end{aligned}\right\} \tag{1.8}$$

1.4. **Pressure inside a thin shell of restricted isotropy and zero body force.** Put $B = 0$ and $A = -A$ for pressure. Put $b = a + h$, with h small compared with a, and $R_r = a + j$, with $0 \leqq j \leqq h$. Then, neglecting squares and products of h, j, there are found, from **IX**(1.3),

$$\left.\begin{aligned} S_{\theta\theta} &= S_{\phi\phi} = \tfrac{1}{2}A[(a/h) + 1 - (j/h)] \\ S_{rr} &= A[-1 + (j/h)] \end{aligned}\right\} \tag{1.9}$$

To this degree of approximation the stresses vary linearly through the thickness of the shell. Term a/h is large compared with unity or j/h, so that $S_{\theta\theta}$, $S_{\phi\phi}$ do not change much with position through the thickness of the shell. For the same reason S_{rr} is small compared with $S_{\theta\theta}$.

The average value of $S_{\theta\theta}$ is, say,

$$S_{\theta\theta}' = \tfrac{1}{2}A[(a/h) + \tfrac{1}{2}] \tag{1.10}$$

The usual engineering approximation would calculate the average circumferential stress by calculating the total force on the diametral plane due to A as $\pi a^2 A$ and divide by $2\pi ah$ the area of shell intersected by the plane. Then the engineering average stress is, say,

$$S_{\theta\theta}'' = \tfrac{1}{2}Aa/h \tag{1.11}$$

The difference

$$S_{\theta\theta}' - S_{\theta\theta}'' = \tfrac{1}{4}A \tag{1.12}$$

is fairly small compared with $S_{\theta\theta}'$. A typical toy rubber balloon for example, has values of a/h of the order 50 to 1000 and greater.

The circumferential strain at $R_r = b$ is

$$1-(b^o/b) = e_{\theta\theta} = GS_{\theta\theta}+F(S_{rr}+S_{\theta\theta}+S_{\phi\phi})$$

giving

$$Kb^2-(1+K)hb+b^oh = 0 \tag{1.13}$$

with $K = (\frac{1}{2}G+F)A$. The average radial strain is

$$1-(h^o/h) = e_{rr} = -\tfrac{1}{2}GA+FAa/h$$

giving

$$h = (h^o+AFb)/(1+K) \tag{1.14}$$

Substituting **IX**(1.14) in **IX**(1.13) gives an equation from which to find, (i) b^o in terms of b, A, h^o, F, G, or (ii) b in terms of b^o, A, h^o, F, G. The solution for b^o in (i) is only a single value, so no difficulty arises, but b occurs in a quadratic form for solution (ii), so that two values are found. One value can be discarded as physically unacceptable by examining which value suits solution (i) here.

Chapter X

RUBBER DEFORMATION AND ITS THEORETICAL INTERPRETATION

1. Experimental planewise complex straining of a thin rubber sheet

Rubber is such a common substance and, generally, suffers such a large elastic strain under quite small applied loads that it is an attractive material on which to experiment. The simplest form

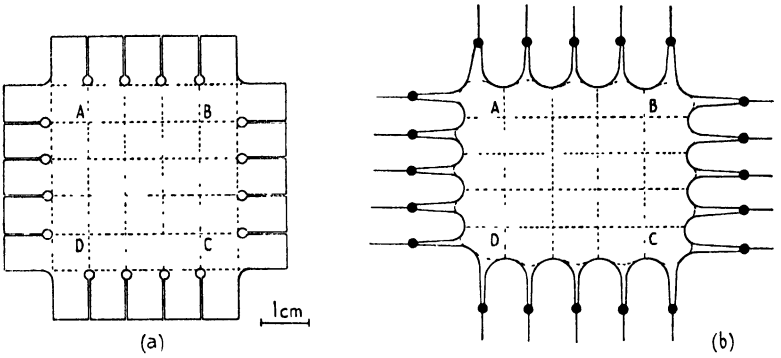

FIG. X,1.1.—A thin rubber sheet stretched in two directions by strings tied to lugs. The initial shape is shown in (*a*) and the deformed shape in (*b*). The nine squares in boundary ABCD of the undeformed sheet deform to rectangles in the loaded sheet. Tests showed that the three middle strings carrying load F_1 was effectively that on AB. Similarly, F_2 acted on side BC. The area outside ABCD acted as a 'diffusion' zone through which the stresses diffused from the point loads of the strings to virtually uniform loading on the sides of ABCD. (After L. R. G. Treloar [13] without change.)

of complex loading would appear to be homogeneous two-stress in a thin sheet. Such considerations led L. R. G. Treloar [74, 13] to attempt the test, but it was difficult to devise satisfactory means of applying such stresses. A compromise was reached with the test specimen shown in Fig. X,1.1(*a*). Strings were tied to the lugs and, on being pulled equally, gave much the shape in Fig. X,1.1(*b*).

Treloar satisfied himself experimentally that the loads in the

middle three strings on each side were inducing the deformation in the nine sub-rectangles shown for the rectangle ABCD. Thus, the non-homogeneously strained zone outside ABCD is excluded and regarded as a 'guard ring' or diffusion zone in which the stresses change rapidly away from the 'point' loads of the strings to spread out to a virtually homogeneous stressing inside ABCD. Treloar assumes that there are no stresses acting on planes parallel to the flat faces of the sheet because these main faces are stress-free. The present author's interpretation of the measurements questions the validity of this assumption in article X,3.

Table X,1.1 gives Treloar's measurements for a typical rubber

TABLE X,1.1

'Homogeneous plane two-stress' loading on a thin, plane rubber sheet by L. R. G. Treloar [74, 13]. The initial cross-sectional area for each direction was 0·0648 cm² and initial thickness 0·082 cm. The extension ratios were independent of sequence of load application.

Tensile Load, gm		Extension Ratio	
F_1	F_2	λ_1^o	λ_2^o
100	100	$1{\cdot}07_0$	$1{\cdot}08_3$
100	200	$0{\cdot}97_8$	$1{\cdot}29_7$
200	200	$1{\cdot}16_7$	$1{\cdot}20_9$
300	200	$1{\cdot}46_0$	$1{\cdot}09_1$
300	100	$1{\cdot}58_2$	$0{\cdot}90_5$
300	300	$1{\cdot}35_0$	$1{\cdot}37_0$
300	400	$1{\cdot}18_3$	1·88
200	400	$0{\cdot}93_3$	2·04
100	400	$0{\cdot}78_3$	2·14
400	400	1·60	$1{\cdot}72_5$
500	400	2·24	$1{\cdot}51_3$
500	300	2·42	$1{\cdot}09_6$
500	200	2·51	$0{\cdot}87_5$
500	100	2·64	$0{\cdot}72_5$
500	500	2·07	2·10
600	500	2·68	$1{\cdot}87_5$
400	600	$1{\cdot}25_0$	2·98
300	600	$0{\cdot}98_0$	3·06
200	600	$0{\cdot}79_1$	3·14
100	600	$0{\cdot}67_9$	3·21
600	600	2·34	2·63

with loads applied in the order shown. The load F_1, for example, is the total on the three strings on one side of rectangle ABCD, while F_2 is the total load for the middle three strings on the other side. The strains in the rubber sheet were found to be functions of the current loads and independent of the sequence in which they were applied[13.4]. Extension ratio λ_1^o equals R_1/R_1^o, with R_1 the current length of the side of the rectangle parallel to the force F_1, while R_1^o is the initial length of the same side. Thus, $\lambda_1^o \equiv \sqrt{u_1^o}$ of volume I, article I,4.4, and is used here for brevity. Extension ratio λ_2^o is defined similarly.

Nominal stresses S_1^o, S_2^o are found by dividing the appropriate forces by the initial cross-sectional area. The virtual incompressibility of rubber gives (see volume I, article III,8.5) the relation

$$\lambda_1^o \lambda_2^o \lambda_3^o = 1 \tag{1.1}$$

Then, as in article I,8, the true stresses are found from

$$S_1 = \lambda_1^o S_1^o \qquad S_2 = \lambda_2^o S_2^o \tag{1.2}$$

2. A quadratic strain theory †

For infinitesimal straining, the nominal strain e^o and true strain e are quasi-equal, as also are nominal stress S^o and true stress S. The secant moduli principal normal stress-strain forms of article VIII,5.5 are, in this case,

$$e_1 = GS_1 + F\chi^S \tag{2.1}$$

with the stress-strain parameters F, G and the first stress invariant

$$\chi^S = \sum_1 S_1$$

In dyadic form,

$$\mathfrak{M} = G\mathfrak{S} + F\mathfrak{J}\mathfrak{J}:\mathfrak{S} \tag{2.2}$$

2.1. **Stress-ser relations.** The approximate linearity of the simple tensile true stress vs. elastic ser ‡ $u_1^o = (\lambda_1^o)^2$ in Fig. I,8.2 suggests the formulation of a 'secant' stress-ser relation for complex stresses. Thus, the three scalar equations

$$u_1^o = 2GS_1 + 2F\chi^S + 1 \tag{2.3}$$

or the dyadic form

$$\mathfrak{U}^o = 2G\mathfrak{S} + 2F\mathfrak{J}\mathfrak{J}:\mathfrak{S} + \mathfrak{J} \tag{2.4}$$

† Author, 1951.

‡ ser ≡ 'squared extension ratio' is a coined word, convenient for brevity, and its form suggesting the full expression.

with the ser dyadic, having current principal directions $\mathbf{x}_i$, as

$$\mathfrak{U}^o = \sum_i u_i^o \mathbf{x}_i \mathbf{x}_i \tag{2.5}$$

Equations X(2.3) reduce to just X(2.1) for infinitesimal strains since, then, neglecting squares of strains,

$$e_i^o = \lambda_i^o - 1 \qquad u_i^o = 1 + 2e_i^o \tag{2.6}$$

From X(2.3) are found readily

$$\chi^S = \tfrac{1}{2}(\xi^o - 3)/(G + 3F) \tag{2.7}$$

$$\xi^o = \mathfrak{U}^o : \mathfrak{J} \tag{2.8}$$

$$2G\mathfrak{S} = \mathfrak{U}^o - [F(G+3F)^{-1}(\mathfrak{U}^o : \mathfrak{J} - 3) + 1]\mathfrak{J} \tag{2.9}$$

2.2 **Inverse strain ellipsoid.** Volume I, article I,4.2 shows that $\mathfrak{U}^o$ is the self-conjugate dyadic of the inverse strain ellipsoid in the undeformed body corresponding to an elemental sphere in the deformed body when strain transfer has not occurred.

Continuity of the ser dyadic must be assured in a heterogeneous straining, but this will not be pursued, as only homogeneous straining and the stress-ser relations are discussed here.

3. Quasi-plane and plane stress

It is attempted to impose a plane, homogeneous two-stress on a thin sheet, as in L. R. G. Treloar's test in article X,I, and to relate stresses and strains. Following most experimenters, and Treloar in particular, in such a case suppose that the principal normal stress S_3 normal to the plane of the thin sheet is zero because the main faces of the sheet are stress-free. Denote this zero stress explicitly by T_3.

3.1. **Infinitesimal straining observations.** From equations X(2.1),

$$e_1 = GS_1 + F\chi^S \qquad e_2 = GS_2 + F\chi^S \qquad e_3 = GT_3 + F\chi^S \tag{3.1}$$

with

$$\chi^S = S_1 + S_2 + T_3$$

The experimental measurements give e_1, e_2 on the main faces, e_3 as a change in thickness observed by the relative movements of the main faces normally one to another, S_1, S_2 as average values not directly observable. The remaining three quantities are *two* stress-strain parameters F, G and the assumed zero value T_3.

Three equations, in general, relate three unknowns or satisfy consistency conditions. Therefore, if the theory uses only two stress-strain parameters then the stress T_3 cannot be assumed arbitrarily as zero.†

3.2. **Analysis of infinitesimal straining observations.** Taking

$$(e_1-e_2) = G(S_1-S_2) \tag{3.2}$$

eliminates χ^S in which T_3 appears. Plotting (e_1-e_2) against (S_1-S_2) will show if G is a constant or not.

Now, take

$$(e_1-e_3) = G(S_1-T_3) \tag{3.3}$$

and T_3 appears explicitly. If T_3 is not zero then, clearly, anomalous results will be found if (e_1-e_3) is plotted against S_1 only. This is virtually what Treloar noted, as in article X,3.4, and discussed in his book [13] at length, without seeing the reason for the anomaly. Similarly, of course, there must be considered

$$(e_2-e_3) = G(S_2-T_3) \tag{3.3'}$$

in which T_3 appears. Also, relating the first invariants of stress and strain,

$$\sum_1 e_1 = (3F+G)\chi^S \tag{3.4}$$

3.3. **Analysis of finite straining.** Now, consider the quadratic strain expressions X(2.3) supposing S_3 to be zero in a thin sheet test and denote it explicitly by T_3. Thus,

$$\left.\begin{aligned} u_1^2 &= 2GS_1+2F\chi^S+1 \\ u_2^2 &= 2GS_2+2F\chi^S+1 \\ u_3^2 &= 2GT_3+2F\chi^S+1 \end{aligned}\right\} \tag{3.5}$$

Then, similar to X(3.2) to X(3.3'),

$$(u_1^2-u_2^2) = 2G(S_1-S_2) \tag{3.6}$$

$$(u_1^2-u_3^2) = 2G(S_1-T_3) \tag{3.7}$$

$$(u_2^2-u_2^2) = 2G(S_2-T_3) \tag{3.7'}$$

Rubber is virtually incompressible and this requires

$$u_1^2u_2^2u_3^2 = 1 \tag{3.8}$$

and so determines the transverse ser u_3^2 for given values of the other two ser.

† Author, 1951.

3.4. **Observations analysed.** Plotting the ser and stress differences of X(3.6) in Fig. X,3.1 shows that the stress-ser parameter $2G$ is practically constant of value 544 10^{-6} $(\text{gm/cm}^2)^{-1}$ over the stress range considered. However, plotting the ser and stress differences of X(3.7) in Fig. X,3.2 with the assumption that T_3 is zero gives the discontinuous curves shown [74, 13]. If the

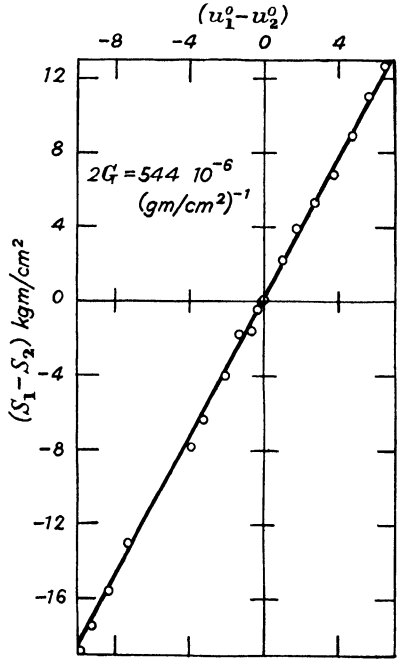

FIG. X,3.1.—Planewise stress-ser differences for a thin rubber sheet tested by L. R. G. Treloar [74, 13] under apparently plane two-stress homogeneous loading. Such plotting of differences eliminates the isotropic stress component and determines the main stress-ser parameter $2G$. For limiting small strains G is the shear modulus.

values of stress difference (S_1-T_3) are calculated from the values of ser difference $(u_1^0-u_3^0)$ using $2G$ of value 544 10^{-6}, then the dotted line is found. Then, denoting the value of T_3 by $T_3(1)$ to satisfy X(3.7), this is the difference between the discontinuous lines and the dotted line in Fig. X,3.2.

Almost the same values of $T_3(2)$ are found as the difference between a similar set of discontinuous curves (S_2-T_3) vs. $(u_2^0-u_3^0)$

and a dotted line of stress difference of value $2G(u_2^0 - u_3^0)$. Differences between $T_3(1)$ and $T_3(2)$ are found because the three equations X(3.5) have not been solved as a group, but this is not important at present. Treloar tested other specimens of rubber and the curves in Fig. X,3.3 are taken from his book [13]. It is

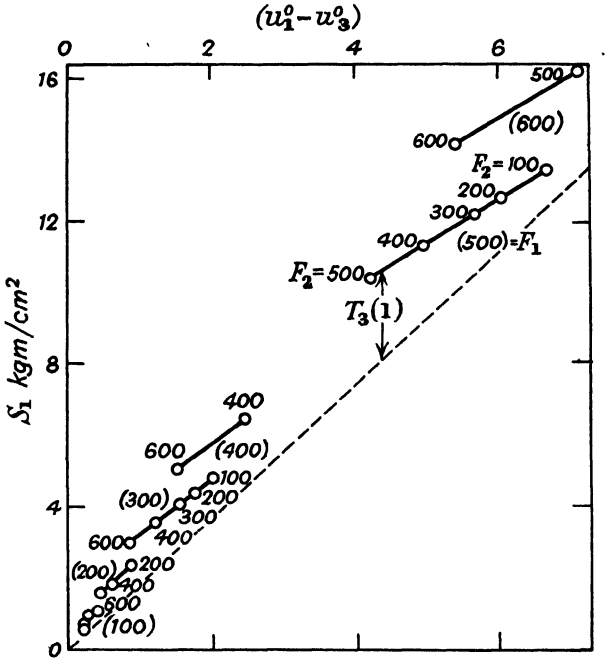

FIG. X,3.2.—One component of the apparently plane, homogeneous two-stress plotted against the corresponding ser reduced by the ser value of the thickness when the rubber is incompressible. This assumes that the stresses on planes in the interior of the sheet and parallel to the main faces are zero to give a 'plane' two-stress. Stress $T_3(1)$ is the *average* through the sheet thickness of the *non-zero* third principal normal stress. This shows that the stresses are, in fact, *quasi-plane*. The dotted line is that for constant value $2G = 544\ 10^{-6}$ $(\text{gm/cm}^2)^{-1}$ used to calculate stress from ser values.

of interest that when the applied stress tended to a one-stress then the transverse stress T_3 approached zero.

3.5. **Physical examination of the anomaly.** Treloar made a careful examination of the phenomenon and concluded that the discontinuity of the curves was a real effect and not due to something overlooked in the experimental technique. The possibility

that relaxation effects gave the discontinuity was removed by using a specimen of rubber swollen with medicinal paraffin to about twice its initial volume, as this was known to reduce relaxation times considerably, and yet the same phenomenon was observed.

Simultaneous measurement of optical double refraction disposed of the possibility of crystallisation. An experiment on latex sheet gave the same effect and so disposed of possible initial anisotropy. The same values were found for the same rubber in an inflation test for which the strains were not homogeneous but for which the stresses were calculated from the engineering

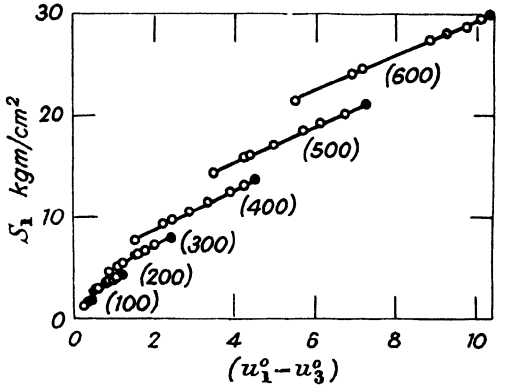

FIG. X,3.3.—Another set of values, similar to Fig. X,3.2, from other tests by L. R. G. Treloar. The black dots are the values for simple tension (not available for the rubber giving Fig. X,3.2), indicating zero values of the transverse stress T_3 for such loading.

formula of article IX,1.4 for curvilinearly, homogeneously strained spheroidal balloons.

The effect for the flat sheet was independent of order of application of forces [13.4] to the sheet, as may be seen by comparing Table X,1.1 with Fig. X,3.2. It should be noted that, in all Treloar's tests, the sheet thickness was not measured but calculated on other evidence of incompressibility, such as that by W. L. Holt & A. T. McPherson [18], for example.

3.6. **Comparison of main observations for plane and quasi-plane stress.** The constant values $2G = 544\ 10^{-6}$ and $2F = 83\ 10^{-6}$ $(\text{gm/cm}^2)^{-1}$ were used in the first two equations of X(3.5) to calculate ser values u_1^o to u_2^o and plotted in Fig. X,3.4

to compare them with the measured values. Whether plane stress is assumed with T_3 zero, or quasi-plane stress with T_3 of the values already found to suit the three equations X(3.5), the values of u_1^o, u_2^o calculated are practically the same. This is an important inference, because it means that if a complex stress distribution is assumed to be plane then the strains observed experimentally on the stress-free main faces of a thin sheet should correspond closely

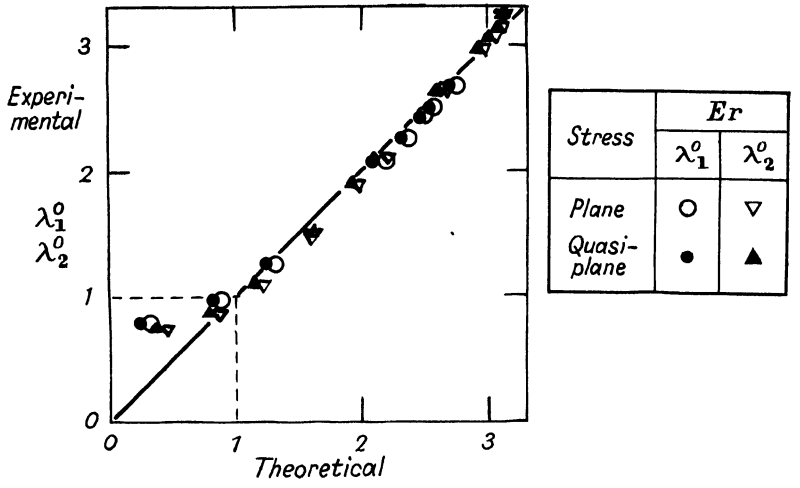

FIG. X,3.4.—Experimental values of planewise er vs. theoretical values, assuming the constant values $2G = 544\ 10^{-6}$, $2F = 83\ 10^{-6}$ for the stress-ser parameters. Two sets of theoretical values are calculated: one set for plane two-stress and one set for quasi-plane two-stress for which the transverse stress is included in the first stress invariant. Er less than unity is for compression, while a value greater than unity is for tension. There is little difference for strains *observed* for plane and quasi-plane two-stress systems. Fair correlation of experimental and theoretical values is seen for tension, but the fit is not as good for compression with the assumed constant parameters.

to those predicted by a correct theoretical solution. However, the predicted changes in thickness may be quite seriously in error because the stress distribution is, in fact, quasi-plane.

3.7. **Physical significance of the transverse normal stress.** The integration of the equilibrium stress equation by means of the stress potential shows that the first stress invariant is constant throughout a deformed body when body forces are zero. The

value of this constant depends on the geometry of the boundary of the deformed body and the applied surface stresses, as, for example, for the sphere in article **IX**,1. Again, when stress-strain parameters are isotropic and independent of position in a body, then strains compatibility, as in article **VIII**,6 for example, requires that the first stress invariant shall be constant.

Then, in the thin rubber sheet strained by planewise strings tied to lugs on the four sides, the value of the constant is determinded by the extremely complicated 'boundary' stresses and strain. Therefore, the interior of the thin sheet can feasibly have a complicated stress distribution. The stresses on interior faces parallel to the main, stress-free faces of the sheet can decrease very rapidly (but not, of course, at infinitely large rates) to zero at the main faces. The normal stresses S_1, S_2 should be regarded as average values equivalent to some more complicated distribution. Similarly, the transverse stress T_3 should be thought of as an average normal stress equivalent to a complicated thickness-wise distribution and required to complete the average stress dyadic to give the strains observed on the stress-free main faces and through the thickness. Therefore, the stresses here are essentially the quasi-plane distribution of article **V**,18, whereas Filon's generalised plane stress could not suit the data because the transverse stress S_{zz} is there hypothesised as identically zero.

4. Relation between stress-strain and stress-ser parameters for plane stress

The relation between the stress-strain and stress-ser parameters of the linear and quadratic theories of article **X**,2 is found readily. With qualifying superscripts to distinguish the F's and G's, add together the three equations of each theory to give

$$\chi^S = \tfrac{1}{2}(u_1^o+u_2^o+u_3^o-3)/(G^u+3F^u) = (e_1+e_2+e_3)/(G^e+3F^e) \quad (4.1)$$

Taking the difference of the two equations applying to observations on the main faces of a sheet gives

$$\tfrac{1}{2}(u_1^o-u_2^o)/G^u = (e_1-e_2)/G^e \quad (4.2)$$

Thus, with G^u, F^u known, then F^e, G^e can be found. Constancy of the parameters in one theory clearly precludes the constancy of the parameters in the other theory.

5. Strain energy, extension ratios and the definition of stress

Elastic strain energy, in particular, is considered frequently in the literature [13, 14, 17, 31, 39] in terms of extension ratios, so it is of interest to consider it here.

5.1. **Strain energy per unit initial volume.** Suppose an initial unit cube is stretched to a rectangular block having edges of length λ_i^o by current true stresses S_i. The force on the plane normal to direction λ_i^o is $S_i\lambda_j^o\lambda_k^o$. Now, allow an incremental change in the forces and corresponding extension ratios. Neglecting second and higher order small quantities gives the increment work done per unit initial volume, briefly, as

$$\delta w^o = \sum_{i,j,k} S_i\lambda_j^o\lambda_k^o\delta\lambda_i^o \tag{5.1}$$

The current strain energy per unit initial volume follows by integrating this expression between the initial and current values of stresses and extension ratios.

5.2. **Strain energy per unit current volume.** The volume considered now is always unity or virtually so for a current cube of deformed substance. Therefore, from instant to instant, as the deformation evolves, the unit cube of a deformable body does not consist of the same particles, as some migrate in and others migrate out.

The force on a typical face is now S_i. The increment work done per unit deformed volume in an increment deformation is

$$\delta w = \sum_i S_i\delta R_i \tag{5.2}$$

with δR_i the differential changes in length of the unit sides of the cube, regarding the current state as reference. Then, instantaneously, with the currently deformed body as the reference, the initial length R_i^o can be treated as a constant with respect to the increment deformation, so that

$$\lambda_i^o = R_i/R_i^o \tag{5.3}$$

$$\delta\lambda_i^o = \delta R_i/R_i^o = \lambda_i^o\delta R_i/R_i = \lambda_i^o\delta R_i \tag{5.4}$$

since the R_i are *unity*. Then

$$\delta w = \sum_i S_i\delta\lambda_i^o/\lambda_i^o \tag{5.5}$$

The current strain energy per unit current volume follows by integrating between the initial and current values of stresses and extension ratios.

5.3. **Stresses and the strain energy.** When unit energy is supposed to be a function of only the extension ratios, then the total differential of 'initial' unit energy w^o is

$$\delta w^o = \sum_i (\partial w^o/\partial \lambda_i^o)\delta\lambda_i^o \tag{5.6}$$

Comparison with equation X(5.1), and noting that the three $\delta\lambda_i^o$ are arbitrary, gives

$$S_i = (\partial w^o/\partial \lambda_i^o)/(\lambda_j^o \lambda_k^o) \tag{5.7}$$

defining the true stresses in terms of rate of change of strain energy with respect to extension ratios and initial volume.

Writing a total differential for δw similar to X(5.6) and equating with X(5.5) gives the true stresses as

$$S_i = \lambda_i^o(\partial w/\partial \lambda_i^o) \tag{5.8}$$

Equating X(5.8), X(5.7) gives

$$\partial w^o/\partial \lambda_i^o = \lambda_1^o \lambda_2^o \lambda_3^o (\partial w/\partial \lambda_i^o) \tag{5.9}$$

A change of variable is sometimes convenient. Write

$$\lambda_i^o = \exp \alpha_i \tag{5.10}$$

or

$$\alpha_i = \log \lambda_i^o \tag{5.10'}$$

is the 'natural' or 'logarithmic' strain definition of Ludwig [41], also defined independently by Hencky [42] and used methodically in his finite elastic strains theory. Then, in equation X(5.8),

$$S_i = \partial w/\partial \alpha_i \tag{5.11}$$

In dyadic form, with $\mathbf{x}_i$ the unit vectors in the principal normal strain directions for isotropy, this gives a sort of 'dyadic gradient operator' in strain-space in

$$\mathfrak{S} = \sum_i x_i x_i \partial w/\partial \alpha_i \tag{5.11'}$$

5.4. **Incompressible substances.** If the substance is incompressible then

$$\lambda_1^o \lambda_2^o \lambda_3^o = 1 \tag{5.12}$$

Using this with its differential gives a condition to be satisfied by

the differentials of the extension ratios for an incompressible substance such as rubber, for example,

$$\sum_{\mathbf{i}}(\lambda_{\mathbf{i}}^{o})^{-1}\delta\lambda_{\mathbf{i}}^{o} = 0 \tag{5.13}$$

The logarithm of **X**(5.12) considered with **X**(5.10) gives the incompressibility condition as

$$\sum_{\mathbf{i}}\alpha_{\mathbf{i}} = 0 \tag{5.14}$$

while

$$\sum_{\mathbf{i}}\delta\alpha_{\mathbf{i}} = 0 \tag{5.15}$$

5.5. **Stresses in incompressible substances.** Equation **X**(5.12) in **X**(5.9) gives, for an incompressible substance,

$$\partial w^{o}/\partial\lambda_{\mathbf{i}}^{o} = \partial w/\partial\lambda_{\mathbf{i}}^{o} \tag{5.16}$$

From article **X**,1

$$S_{\mathbf{i}} = S_{\mathbf{i}}^{o}\lambda_{\mathbf{i}}^{o} \tag{5.17}$$

so that in **X**(5.7), **X**(5.8) with **X**(5.16) the nominal stress is

$$S_{\mathbf{i}}^{o} = \partial w^{o}/\partial\lambda_{\mathbf{i}}^{o} = \partial w/\partial\lambda_{\mathbf{i}}^{o} \tag{5.18}$$

5.6. **Strain energy for rubber under simple normal stress.** A simple case of strain energy is that for rubber under simple tension $S_{\mathbf{1}}$, say. Article **I**,8 shows that true stress is almost linearly proportional to ser. Then, with constant C, write

$$S_{\mathbf{1}} = C[(\lambda_{\mathbf{1}}^{o})^{2}-1] \tag{5.19}$$

With $S_{\mathbf{2}}$, $S_{\mathbf{3}}$ zero in **X**(5.5) substitute for $S_{\mathbf{1}}$ and integrate to give

$$w = \int_{1}^{\lambda_{\mathbf{1}}^{o}} C(\lambda_{\mathbf{1}}^{o}-\lambda_{\mathbf{1}}^{o-1})d\lambda_{\mathbf{1}}^{o} = C\{\tfrac{1}{2}[(\lambda_{\mathbf{1}}^{o})^{2}-1]-\log\lambda_{\mathbf{1}}^{o}\} \tag{5.20}$$

As an academic example suppose the $S_{\mathbf{1}}$ vs. $\lambda_{\mathbf{1}}^{o}$ curve for simple normal stress on a highly elastic substance is fitted by

$$S_{\mathbf{1}} = C+J\lambda_{\mathbf{1}}^{o}+K(\lambda_{\mathbf{1}}^{o})^{2}+L(\lambda_{\mathbf{1}}^{o})^{3} \tag{5.21}$$

with constants J, K, L. Then, with $-C = J+K+L$ for zero stress with zero strain, on integrating the increments of strain energy,

$$w = C\log\lambda_{\mathbf{1}}^{o}+J(\lambda_{\mathbf{1}}^{o}-1)+\tfrac{1}{2}K[(\lambda_{\mathbf{1}}^{o})^{2}-1]+\tfrac{1}{3}L[(\lambda_{\mathbf{1}}^{o})^{3}-1] \tag{5.22}$$

Generally, with constants $C^{(n)}$, the simple normal curve is fitted by

$$S_1 = \sum^{n} C^{(n)}(\lambda_1^o)^n \tag{5.23}$$

so that

$$w = C^{(0)} \log \lambda_1^o + \sum^{m\neq 0} m^{-1} C^{(m)}[(\lambda_1^o)^m - 1] \tag{5.24}$$

$$C^{(0)} = -\sum^{m\neq 0} C^{(m)}$$

5.7. **Three-stress strain energy for a rubberlike substance.** From X(2.9) write

$$S_1 = J(u_1^o - 1) + K\left(\sum_i u_i^o - 3\right) \tag{5.25}$$

with the stress-strain parameters

$$J = \tfrac{1}{2}G^{-1} \qquad K = -\tfrac{1}{2}FG^{-1}(3F+G)^{-1}$$

Substituting in X(5.5) gives

$$\delta w = \sum_{i,j,k}\{(J+K)\lambda_1^o + [K[(\lambda_j^o)^2 + (\lambda_k^o)^2 - 3] - J](\lambda_i^o)^{-1}\}\delta\lambda_i^o$$

Integrating partially with respect to λ_i^o between the limits 1, λ_i^o gives

$$w = \tfrac{1}{2}(J+K)\left[\sum_i (\lambda_i^o)^2 - 3\right] + \sum_{i,j,k}\{K[(\lambda_j^o)^2 + (\lambda_k^o)^2 - 3] - J\}\log \lambda_i^o \tag{5.26}$$

Rearranging and introducing the ser first invariant gives

$$w = \tfrac{1}{2}J(\xi^o - 3 - \sum_i \log u_i^o) + \tfrac{1}{2}K(\xi^o - 3)(1 + \sum_i \log u_i^o) - \tfrac{1}{2}K\sum_i u_i^o \log u_i^o \tag{5.26'}$$

From X(5.25) the first stress invariant is

$$\chi^S = (J+3K)(\xi^o - 3) \tag{5.27}$$

and substituting in X(5.26′) gives the unit energy in terms of the first stress invariant.

5.8. **Incompressible substances three-stress strain energy.** The incompressibility conditions are

$$u_1^o u_2^o u_3^o = 1 \qquad \sum_i \log u_i^o = \log(u_1^o u_2^o u_3^o) = 0 \tag{5.28}$$

From X(5.26′),

$$w = w' + w'' \tag{5.29}$$

$$w' = \tfrac{1}{2}(J+K)(\xi^o - 3) - \tfrac{1}{2}K\sum_i u_i^o \log u_i^o \tag{5.30}$$

$$w'' = \tfrac{1}{2}[-J + K(\xi^o - 3)] \log(u_1^o u_2^o u_3^o) = 0 \tag{5.31}$$

with the last using X(5.28).

From X(5.8) the stresses are

$$S_i = \lambda_i^o \partial w/\partial \lambda_i^o \tag{5.32}$$

Substituting for w from X(5.26′) gives S_i in X(5.25), from which the unit energy was calculated, but with $w'' = 0$, the w' in X(5.32) gives a stress S_i' not equal to the stress S_i in X(5.25), from which X(5.29) was calculated. Thus,

$$S_i' = u_i^o(J - K \log u_i^o) \tag{5.33}$$

More generally than X(5.31), write the *zero strain energy function* with an arbitrary function $W(u_i^o)$ of the three u_i^o as

$$w'' = \tfrac{1}{2} W(u_i^o) \log (u_1^o u_2^o u_3^o) = 0 \tag{5.34}$$

Then, using X(5.32) and X(5.28), the corresponding stresses are

$$S_i'' = W(u_i^o) \tag{5.35}$$

or as a stress dyadic, for isotropic stress W which is generally an arbitrary function of the ser's varying from point to point in a heterogeneously deformed body,

$$\mathbf{S}'' = W\mathbf{I} \tag{5.35′}$$

Therefore, *in an incompressible body, the absolute stresses acting cannot be prescribed by a strain energy function.* For example, in an experiment on rubber, if the strain energy and ser's are measured, then the zero strain energy function w'' escapes measurement † and the experimenter must, of necessity, calculate the stresses from w' in X(5.32), which gives $S_i' \neq S_i$, the absolute stresses acting. If the stress-ser relation X(5.25) applies then, from X(5.26′),

$$W = -J + K(\xi^o - 3) \tag{5.36}$$

6. Other quadratic theories on strain

This brief article cannot include all the writers on quadratic theories of strain or do full justice to the labours of those quoted. A recent survey and critical comparison of various theories on finite elastic strain are given by C. Truesdell [31] with a fairly comprehensive list of references which the reader can use as a starting-point from which to form his own ‡ opinions.

† Author, 1952.

‡ Professor Truesdell shows a predilection for quadratic theories on strain and he does not notice the deficiency in R. S. Rivlin's only independent, fundamental postulate, as given in article X,6.6 here. Again, on the present author's work, nothing is given on which a reader can form his

It is convenient to introduce coined words as abbreviations to describe various deformation effects related to stress by the several writers. Thus,

er = extension ratio,
ser = squared extension ratio,
inver = inverse extension ratio,
invser = inverse squared extension ratio.

6.1. **Cauchy, Green.** Cauchy, in 1827 [19.19], derived the relationship defining a strain ellipsoid or the quadratic strain metric

$$\mathbf{x}_R \cdot \mathfrak{U} \cdot \mathbf{x}_R = (dR^o/dR)^2 = u_R \tag{6.1}$$

while Green, in 1839 [19.20], found the relationship defining the inverse strain ellipsoid

$$\mathbf{x}^o_R \cdot \mathfrak{U}^o \cdot \mathbf{x}^o_R = (dR/dR^o)^2 = u^o_R \tag{6.2}$$

with

$$\left.\begin{aligned} \mathfrak{U} &= (\mathfrak{J} - \nabla\mathbf{U}) \cdot (\mathfrak{J} - \mathbf{U}\nabla) \\ \mathfrak{U}^o &= (\mathfrak{J} + \nabla^o\mathbf{U}) \cdot (\mathfrak{J} + \mathbf{U}\nabla^o) \end{aligned}\right\} \tag{6.3}$$

These are formulated in volume I, article I,2.

With the unit vector successively in the principal directions there are given the principal normal invser and ser values

$$u_\mathfrak{i} = \mathbf{x}_\mathfrak{i}\mathbf{x}_\mathfrak{i} : \mathfrak{U} = (dR^o_\mathfrak{i}/dR_\mathfrak{i})^2 \tag{6.4}$$

$$u^o_\mathfrak{i} = \mathbf{x}^o_\mathfrak{i}\mathbf{x}^o_\mathfrak{i} : \mathfrak{U}^o = (dR_\mathfrak{i}/dR^o_\mathfrak{i})^2 = u_\mathfrak{i}^{-1} \tag{6.5}$$

The first invariants of $\mathbf{X}(6.3)$ are

$$\left.\begin{aligned} \xi &= \mathfrak{J} : \mathfrak{U} = \sum_\mathfrak{i} u_\mathfrak{i} \\ \xi^o &= \mathfrak{J} : \mathfrak{U}^o = \sum_\mathfrak{i} u^o_\mathfrak{i} \end{aligned}\right\} \tag{6.6}$$

Saint-Venant, in 1847 [19.20], attempted to use the ser with Cauchy's nominal strain to analyse finite strain but, in error, actually treated infinitesimal strain with finite spatial-displacement, as was pointed out by Pearson in 1886 [19.20].

6.2. **B. R. Seth.** In 1935 [75], B. R. Seth used strains defined by the dyadic $\frac{1}{2}(\mathfrak{J} - \mathfrak{U})$ to express stress. Rearranging, for convenience here, his stress-invser relations are of the form

$$\mathfrak{U} = 2G\mathfrak{S} + 2F\mathfrak{J}\mathfrak{J} : \mathfrak{S} + \mathfrak{J} \tag{6.7}$$

own opinion, and Truesdell shows no understanding of the few aspects of the present theory which did secure publication. (See references [5, 70], for example.)

This is similar to X(2.4) except that, here, the invser dyadic is used in place of the ser dyadic there.

From this equation there follows readily

$$\chi^S = \tfrac{1}{2}(3F+G)^{-1}(\xi-3) \tag{6.8}$$

$$\mathfrak{S} = J\mathfrak{U}+[K(\xi-3)-J]\mathfrak{J} \tag{6.9}$$

$$J = \tfrac{1}{2}G^{-1} \qquad K = -\tfrac{1}{2}FG^{-1}(3F+G)^{-1}$$

It will be useful to have the unit strain energy for such a substance. Substituting in X(5.5) gives

$$\delta w = \sum_{i,j,k}\{(J+K)(\lambda_i^o)^{-3}+[K[(\lambda_j^o)^{-2}+(\lambda_k^o)^{-2}-3]-J](\lambda_i^o)^{-1}\}\delta\lambda_i^o$$

Integrating partially with respect to λ_i^o between the limits 1, λ_i^o gives

$$w = w'+w'' \tag{6.10}$$

$$w' = \tfrac{1}{2}(J+K)(3-\xi)+\tfrac{1}{2}K\sum_i u_i \log u_i$$

$$w'' = \tfrac{1}{2}[J+K(3-\xi)]\log(u_1u_2u_3)$$

6.3. **F. D. Murnaghan.** In 1937 [39], F. D. Murnaghan analysed an increment of strain energy in an isothermal deformation using both the dyadics $\frac{1}{2}(\mathfrak{J}-\mathfrak{U})$ and $\frac{1}{2}(\mathfrak{U}^o-\mathfrak{J})$ as strain measures. An isotropic substance is defined as one in which the strain energy w^m per unit mass is unaffected by transformation of the initial coordinates R_i^o. On this basis, it is concluded that the unit strain energy must be a function of only the scalar invariants of $\frac{1}{2}(\mathfrak{J}-\mathfrak{U})$. With true density m, and writing

$$2f_i = 1-u_i \tag{6.11}$$

then Murnaghan finds the principal normal stresses as [39.1]

$$S_i = m(1-2f_i)(\partial w^m/\partial f_i) \tag{6.12}$$

Using X(6.11) and its differential gives †

$$S_i = -2mu_i(\partial w^m/\partial u_i) \tag{6.13}$$

Change the variable with

$$u_i = \exp(-2\alpha_i) \tag{6.14}$$

and then

$$S_i = m(\partial w^m/\partial\alpha_i) \tag{6.15}$$

† Author, 1950.

When the substance is incompressible, so that m is constant, while strain per unit volume is

$$w = mw^m \tag{6.16}$$

then,

$$S_i = \partial w/\partial \alpha_i \tag{6.17}$$

This is precisely equation X(5.11) formulated simply in terms of logarithmic strain without consideration of compressibility or otherwise.

Murnaghan's formulation is complicated, but to see if it is justified for physico-mathematical consistency, the reader should consult his book, of 1951 [40].

6.4. **M. Mooney.** In 1940 [17], M. Mooney considered the finite straining of rubber using three postulates [17.1]: (i) 'the material is isotropic . . .'; (ii) 'the deformations are . . . without change in volume'; (iii) 'the traction in simple shear . . . is proportional to the shear'. He concludes [17.1] from (i) that w must be symmetric in the er. He gives a circular, cylindrical element an initial axial er λ_1^o, uses (ii) and defines shear strain as $(\lambda_1^o)^{\frac{1}{2}}(\lambda_2^o - \lambda_3^o)$.

By rather involved reasoning, which the present author cannot follow completely, Mooney considers strain energy involving several arbitrary functions for which the existence conditions are considered and he concludes that their form must require, generally,

$$w = C^o(\xi^o - 3) + C(\xi - 3) \tag{6.18}$$

with ξ^o, ξ the ser and invser first invariants in equation X(6.6) while C^o, C are arbitrary constants which, effectively, are stress-strain parameters.

By reasoning involving the differential form of the incompressibility condition and holding one λ_i^o constant, then Mooney finds [17.2, 17 3]

$$S_i - S_j = \lambda_i^o(\partial w/\partial \lambda_i^o) - \lambda_j^o(\partial w/\partial \lambda_j^o) \tag{6.19}$$

(This can be found simply by just taking the difference of any two of the three equations X(5.8).) Mooney states that [17.3] the stresses S_i cannot be found from the strain energy function but only their difference $(S_i - S_j)$, because '*the strain energy is independent of the mean tension or hydrostatic pressure*'.

6.5. **W. Kuhn, L. R. G. Treloar.** In 1934–36 [12], W. Kuhn formulated a thermodynamical, statistical theory for the calculation of simple tensile stress-strain relations in substances possessing

long-chain molecules. L. R. G. Treloar, in 1943–44 and 1949 [13], applied the theory to rubber and extended it to three-stress relations. Placing some restrictions on the undeformed and deformed shapes of a long-chain molecule and assuming incompressibility gave [13.1] the unit energy

$$w^o = C^o(\xi^o - 3) \tag{6.20}$$

where C^o is a constant involving the number of molecules per unit volume, Boltzmann's constant and constant temperature.

Treloar then finds [13.2] the stress difference

$$S_1 - S_3 = 2C^o(u_1^o - u_3^o) \tag{6.21}$$

or

$$S_1 = 2C^o u_1^o + H \tag{6.21'}$$

where H is described [13.2] as '. . . an arbitrary stress in the nature of a hydrostatic pressure . . . (which) will have no effect on the stresses . . .'.

6.6. **R. S. Rivlin.** In 1948–54 [14], R. S. Rivlin considered a strain energy function to be the correct starting-point for a theory rather than any specific load-deformation experimental relationship. To restrict the mathematical form of the function, from a generality which is difficult to apply in particular cases, Rivlin gave two fundamental postulates: (i) the strain energy function must be symmetric in the ser's; (ii) the strain energy function involves only the ser's or the three invariants of the ser dyadic (i.e. the er's do not occur but only the (er's)^2).

Comparison with article **X**,6.4 shows that postulate (i) is also Mooney's (i). Rivlin accepts zero volume change but seems to reject Mooney's postulate (iii). Rivlin arrives at postulate (ii) by assuming that the scalar er's

$$\lambda_1^o = dR_1/dR_1^o \tag{6.22}$$

change sign with rotation of the element through 180°. This is incorrect, as one may see by simply asking, 'What is an extension ratio of -3, for example?' Rivlin has confused scalar and vector quantities. Mooney [17.4] states, explicitly, that the λ_1^o are always positive. On this fallacious reasoning Rivlin finds Mooney's strain energy function **X**(6.18) and regards it as that for general deformation without noting that Mooney's form followed from a particular deformation.

Using the well-known increment strain energy form in terms of

the λ_i^o Rivlin finds Mooney's form X(6.19) but, like Treloar in X(6.21′), he separates the two stresses to give

$$S_i = 2(C^o u_i^o - C u_i) + H \tag{6.23}$$

with H an 'arbitrary hydrostatic pressure'.

Except for the fallacious postulate (ii) which he introduces independently, Rivlin's theory and end results are just those of Mooney. Further, for the incompressible substance considered in most of Rivlin's work, article X,5.8 shows that the strain energy function cannot be taken as the starting-point for a theory (without further qualification) in denial of his initial reasoning.

6.7. **Collected formulæ for an incompressible substance.** For convenience of comparison, collect the relevant expressions for the various theories on incompressible substances. A superscript ^{o} is placed on the present author's stress-ser parameters to distinguish them from Seth's, while, here, $C^o = \frac{1}{2}(J^o + K^o)$, $C = -\frac{1}{2}(J + K)$ for better comparison with Mooney.

Author (articles X,5.8, X,5.7):

$$\left.\begin{aligned} w &= w' + w'' \\ w' &= C^o(\xi^o - 3) - \tfrac{1}{2}K^o \textstyle\sum_i u_i^o \log u_i^o \\ w'' &= 0 = \tfrac{1}{2}[-2C^o + K^o + K^o(\xi^o - 3)] \log (u_1^o u_2^o u_3^o) \\ S_i &= (2C^o - K^o)(u_i^o - 1) + K^o(\xi^o - 3) \\ \chi^S &= 2(C^o + K^o)(\xi^o - 3) \end{aligned}\right\} \tag{6.24}$$

Seth (article X,6.2):

$$\left.\begin{aligned} w &= w' + w'' \\ w' &= C(\xi - 3) + \tfrac{1}{2}K \textstyle\sum_i u_i \log u_i \\ w'' &= 0 = \tfrac{1}{2}[-2C - K - K(\xi - 3)] \log (u_1 u_2 u_3) \\ S_i &= -(2C + K)(u_i - 1) + K(\xi - 3) \\ \chi^S &= 2(-C + K)(\xi - 3) \end{aligned}\right\} \tag{6.25}$$

Kuhn, Treloar (article X,6.5):

$$\left.\begin{aligned} w &= C^o(\xi^o - 3) \\ S_i &= 2C^o u_i^o + H \\ S_i - S_j &= 2C^o(u_i^o - u_j^o) \\ \chi^S &= 2C^o \xi^o + 3H \end{aligned}\right\} \tag{6.26}$$

Mooney, Rivlin (articles **X**,6.4, **X**,6.6):

$$\left.\begin{aligned} w &= C^o(\xi^o-3)+C(\xi-3) \\ S_i-S_j &= 2C^o(u_i^o-u_j^o)-2C(u_i-u_j) \\ S_i &= 2C^o u_i^o-2Cu_i+H \\ \chi^S &= 2C^o\xi^o-2C\xi+3H \end{aligned}\right\} \quad (6.27)$$

Author: The theory in equations **X**(6.24) evolved from the simple tensile test. Inspection of Seth's equations for stress in **X**(6.25) suggests that they may fit compression tests better than tensile. Therefore, a combination of the two theories may give good fit over both the compressive and extensive ranges of deformation. Then, since the same physical event is analysed by each, they may be added and the factor $\frac{1}{2}$ absorbed into each parameter throughout to give,†

$$\left.\begin{aligned} w &= w'+w'' \\ w' &= C^o(\xi^o-3)+C(\xi-3)-\tfrac{1}{2}\textstyle\sum_i (K^o u_i^o+Ku_i)\log u_i^o \\ w'' &= 0 = \tfrac{1}{2}\begin{bmatrix} -2(C^o-C)+K^o+K \\ +K^o(\xi^o-3)+K(\xi-3) \end{bmatrix}\log(u_1^o u_2^o u_3^o) \\ S_i &= (2C^o-K^o)(u_i^o-1)+(-2C-K)(u_i-1) \\ &\quad +K^o(\xi^o-3)+K(\xi-3) \\ \chi^S &= 2(C^o+K^o)(\xi^o-3)+2(-C+K)(\xi-3) \end{aligned}\right\} \quad (6.28)$$

6.8. **Comparative comments.** A stress-strain theory on the finite straining of a substance of restricted isotropy should reduce to the generally accepted Hooke's law form for infinitesimal straining. The theories of Seth, Murnaghan and the present author do reduce to the correct form in which occurs the first stress invariant. The theories of Mooney, Treloar, Rivlin do not reduce to a form in which occurs the first stress invariant unless the 'arbitrary hydrostatic pressure' is identified to include it.

The idea that the first stress invariant is physically like a hydrostatic pressure and does not influence the finite elastic deformation of an incompressible substance appears to have been introduced by Mooney and propagated by Treloar and Rivlin, who simply neglect it and so find theoretically [13.3] that there is no unique relationship between stress and strain, because it depended on the loading sequence for a complex stress system, although

† Author, 1952.

Treloar's own tests (see article X,3.5) showed that the strains in rubber are uniquely the same for any sequence of load application. Inspection of these authors' own equations X(6.26), X(6.27) shows that the first stress invariant can be introduced into any of the strain energy and stress-strain equations so that the statement and their formulation are inconsistent. The erroneous idea appears to be an extrapolation from infinitesimal straining in which the first stress invariant and first strain invariant, giving the value of the zero dilation, are related by a modulus of dilation. Thus,

$$\chi^D = \psi(1-2q)\chi^S \qquad (6.29)$$

But for an incompressible substance $q = \frac{1}{2}$, so that the modulus becomes zero and allows the first stress invariant to be of any arbitrary finite value without affecting the dilational relationship. However, this does not mean that the first stress invariant does not enter into the stress-strain relationships. Further, the first strain invariant does not measure dilation in finite strain.

The incompressibility condition does lead to the existence of arbitrary stresses, but through a zero strain energy function as in X(6.24), X(6.25), X(6.28), and not through the first stress invariant. The 'arbitrary hydrostatic pressure' H in X(6.26) appears to be due to Treloar's generalisation and not due to Mooney who, explicitly, gives stress differences only. The idea of a zero strain energy function affecting the stress-strain relationships does not enter into the Mooney, Treloar, Rivlin theory.

The strain energy function for the one-constant theory of Treloar in X(6.26) is found from the author's two-constant theory in X(6.24) by putting constant $K^o = 0$. The strain energy function for the two-constant theory of Mooney in X(6.27) is found from the author's four-constant theory in X(6.28) by putting $K^o = 0 = K$.

6.9. **Compatibility of quadratic strains.** The solution of a problem in heterogeneous equilibrium straining requires the satisfaction of the equilibrium stress equation, stress-strain relations, strain-displacement relations and boundary conditions on stress and/or strain and/or displacement. Suppose such a solution is available. The problem has not been solved unless the strain dyadic is single-valued and continuous. This is not necessarily ensured by Saint-Venant's conditions even for infinitesimal strains, as in article VIII,15, but it is convenient to follow the

same processes here for finite quadratic strains to allow a comparison.

Equation X(6.28).4 is seen to include, as particular cases, the preceding four theories giving true stress S_i in terms of principal normal ser u_i^o and invser u_i. Multiplying both sides by $\mathbf{x}_i\mathbf{x}_i$, adding the three such equations and rearranging gives the dyadic form

$$\begin{aligned}\mathfrak{S} = &(-2C-K+K\mathfrak{J}\mathfrak{J}:)\mathfrak{U}\\ &+(2C^o-K^o+K^o\mathfrak{J}\mathfrak{J}:)\mathfrak{U}'\\ &+2(C-K-C^o-K^o)\mathfrak{J}\end{aligned} \tag{6.30}$$

From volume I, articles I,2 and I,4,

$$\left.\begin{aligned}\mathfrak{U} &= \mathfrak{J}-(\nabla\mathbf{U}+\mathbf{U}\nabla)+(\nabla\mathbf{U})\cdot(\mathbf{U}\nabla)\\ \mathfrak{U}' &= \sum_i \mathbf{x}_i\mathbf{x}_i u_i^o = (\sum_i \mathbf{x}_i\mathbf{x}_i\mathbf{x}_i^o\mathbf{x}_i^o):\mathfrak{U}^o\\ \mathfrak{U}^o &= \mathfrak{J}+(\nabla^o\mathbf{U}+\mathbf{U}\nabla^o)+(\nabla^o\mathbf{U})\cdot(\mathbf{U}\nabla^o)\end{aligned}\right\} \tag{6.31}$$

Equilibrium of an element requires that

$$\operatorname{div}\mathfrak{S} \equiv \nabla\cdot\mathfrak{S} = 0 \tag{6.32}$$

The independent variable coordinates in the 'nabla' operator ∇ are those of the point in the deformed body, whereas in ∇^o the coordinates are those of the point in the undeformed body. All writers agree on the necessity for using ∇ in X(6.32) and not ∇^o. Therefore it seems rational to use ∇ consistently in formulating strains compatibility conditions for the scalar components u_{ij}, u_{ij}^o $(i = \text{ or } \neq j)$ of $\mathfrak{U}$, $\mathfrak{U}'$ respectively for general directions $\mathbf{c}_i$.

Following the mode of approach to formulate Saint-Venant's compatibility conditions for infinitesimal strains we try to eliminate $\mathbf{U}$ from $\mathfrak{U}$ by taking the curl and conjugate curl. Then,

$$\nabla\times\mathfrak{U}\times\nabla = \nabla\times[(\nabla\mathbf{U})\cdot(\mathbf{U}\nabla)]\times\nabla \neq 0 \tag{6.33}$$

The elimination of the product term evidently needs compatibility conditions on $\mathfrak{U}$ even more complicated than those of Saint-Venant. Again, if we try to eliminate $\mathbf{U}$ from $\mathfrak{U}'$ the relationships are even more complicated because there occur such as ∇ operating on ∇^o.

F. D. Murnaghan [40] has, in fact, found the compatibility conditions for $\mathfrak{U}^o$ using ∇^o (while actually using advanced tensor analysis) but warns the reader of the complications. When the strains are infinitesimal then Murnaghan's relations reduce to the Saint-Venant form

$$\nabla^o\times\mathfrak{U}^o\times\nabla^o = 0 \tag{6.34}$$

The solutions of particular, heterogeneous, finite strains problems as given by F. D. Murnaghan [40] and R. S. Rivlin [14, 16]†, for example, have not been subjected to the test of satisfying compatibility conditions. (Rivlin, in fact, does not appear to have formulated any compatibility conditions.) From the present author's viewpoint, the compatibility conditions proposed, but not applied, by Murnaghan must suffer from the same deficiency as Saint-Venant's in not ensuring differentiability of the strain dyadic. (See article V,15.5 and the discussion of dislocational rotation in Saint-Venant's theory of torsion in articles XI,5.13 and XII,7.5 or in volume I, article III,9.)

7. Theory for physically non-linear stress-strain relations and mathematically linear strains relations

The mathematically linear strains theory formulated in volume I and here, except for article X,6, considered total strains as *linear* in the stresses when secant moduli were used. The formulation of quadratic theories, as in article X,6, leads to great mathematical difficulties when the compatibility of heterogeneous strains is considered. The compatibility of mathematically linear strains is fairly readily examined, so that it is now appropriate to generalise the theory to include strains physically non-linear in stresses. A simple case is that for one-stress in Fig. I,8.2.

Only the elastic case is considered here, so that qualitative superscripts are unnecessary. Further, isotropy is assumed, so that the principal normal stress and strain dyadics are coaxial.

7.1. Formulæ from the physically linear theory. Chapter VIII gives the cross-references to the formulation of the following formulæ.

The relative-displacement $\mathbf{D}^*$ and the strain dyadic $\mathfrak{M}$ are related by

$$\nabla\mathbf{D}^* = \mathfrak{M} = \sum_i e_i \mathbf{x}_i \mathbf{x}_i \tag{7.1}$$

while, with the straining equivalence principle for straining-displacement $\mathbf{D}$, then

$$\mathbf{D} \approx \mathbf{D}^* = \int_{\mathbf{O}}^{\mathbf{R}} d\mathbf{R} \cdot \mathfrak{M} \tag{7.2}$$

† See volume I, reference [24] for a more complete list.

The single-valuedness and continuity of the strain dyadic is assured if

$$\operatorname{curl} \mathfrak{M} = 0 \tag{7.3}$$

The stress dyadic $\mathfrak{S}$ obeys the law

$$\operatorname{div} \mathfrak{S} = \operatorname{div} \sum_{i} S_i \mathbf{x}_i \mathbf{x}_i = 0 \tag{7.4}$$

for equilibrium when body force is zero. This can be integrated by using the extended potential theory† to represent the stress dyadic. Thus,

$$\mathfrak{S} = \nabla\nabla H \tag{7.5}$$

while

$$\nabla^2 H = C = \chi = \mathfrak{I} : \mathfrak{S} \tag{7.6}$$

with χ the first stress invariant and arbitrary constant C.

The stress-strain relation is

$$e_i = \mathfrak{P}_i : \mathfrak{S} \tag{7.7}$$

with the stress-strain parameters dyadic, for general isotropy, as

$$\mathfrak{P}_i = \psi_i \mathbf{x}_i \mathbf{x}_i - q_{j-i}\psi_j \mathbf{x}_j \mathbf{x}_j - q_{k-i}\psi_k \mathbf{x}_k \mathbf{x}_k \tag{7.8}$$

7.2. **Physically non-linear stress-strain relations.** The formulation of equations X(7.1) to X(7.6) did not require any knowledge of the stress-strain properties of the substance, so they are still valid for a body of substance having physically non-linear stress-strain properties. Therefore, any change needs to be in equations X(7.7) and X(7.8).

Suppose that each principal normal strain can be resolved to a spectrum of components $e_i^{(n)}$ of which the n'th involves the stresses to the n'th degree. Thus,

$$e_i = \sum^{n} e_i^{(n)} \qquad (n = 1, 3, 5, \ldots) \tag{7.9}$$

with

$$e_i^{(n)} = \mathfrak{P}_i^{(n)} : \mathfrak{S}^n \tag{7.10}$$

and

$$\left.\begin{aligned} \mathfrak{S}^n &= \mathfrak{S}\cdot\mathfrak{S}\cdot\mathfrak{S}\cdot \ldots \text{ (n terms)} = \sum_{i} S_i{}^n \mathbf{x}_i \mathbf{x}_i \\ \mathfrak{P}_i^{(n)} &= \psi_i^{(n)} \mathbf{x}_i \mathbf{x}_i - q_{j-i}^{(n)} \psi_j^{(n)} \mathbf{x}_j \mathbf{x}_j - q_{k-i}^{(n)} \psi_k^{(n)} \mathbf{x}_k \mathbf{x}_k \end{aligned}\right\} \tag{7.11}$$

or

$$e_i^{(n)} = \psi_i^{(n)} S_i{}^n - q_{j-i}^{(n)} \psi_j^{(n)} S_j{}^n - q_{k-i}^{(n)} \psi_k^{(n)} \mathbf{S}_k{}^n \tag{7.12}$$

The moduli $\psi_i^{(n)}$ and transverse contraction ratios $q_{i-k}^{(n)}$ are phenomenologically appropriate to the stresses $S_i{}^n$ of degree n. The n is

† See volume I, appendix C.

odd in X(7.9) because the partial-strains must change sign with the stresses.

If restricted isotropy can be postulated, then there occurs the simpler form

$$\left.\begin{aligned} e_i^{(n)} &= G^{(n)}S_i{}^n + F^{(n)}\chi^{(n)} \\ G^{(n)} &= (1+q^{(n)})\psi^{(n)} \qquad F^{(n)} = -q^{(n)}\psi^{(n)} \\ \chi^{(n)} &= \sum_i S_i{}^n = \mathfrak{J}:\mathfrak{S}^n \end{aligned}\right\} \quad (7.13)$$

7.3. **Compatibility conditions.** The reader should note carefully that the stress-strain parameters cannot be chosen arbitrarily, as they must comply with X(7.3) at least. Thus,

$$\operatorname{curl} \sum_i^n \sum_1 \mathfrak{P}_i^{(n)} : \mathfrak{S}^n \mathbf{x}_i \mathbf{x}_i = 0 \qquad (7.14)$$

Further, for rubber the condition of incompressibility may be imposed. The satisfaction of X(7.14) may be exact or else approximately so in the 'applied theory' sense of being within a stated order of numerical accuracy. (See article C,4.5 for a general discussion.) When a valid strain distribution has been found, then the initial, undeformed shape, corresponding to the current, deformed shape, is found from X(7.2).

Chapter XI

COUPLES APPLIED TO MASSIVE BODIES

1. Two couples applied to one or more surfaces of a body

As particular cases, the torsion of thin-walled circular tubes by forces applied to planes normal to the axis is given in chapter IV. Another common example is that of a stick gripped between the hands and twisted about its axis by shear stresses applied to its cylindrical surface. Again, a finger thrust into a tube and rotated axially can supply axial torque by circumferential shear stresses on the inner surface of the tube. Torsion can be applied to a ball held in cupped hands which are then rotated in opposite directions about an axis joining them. Further, the gripped stick can be 'bowed' due to bending as well as twisted due to torque. The reader will be familiar with many such homely cases of couples applied to bodies.

The problem is to give them, in general, convenient mathematical form for analysis of such special cases. The feature common to all these cases is that each surface of the body can be subdivided into two parts of areas A', A'' loaded by surface stresses $\mathbf{S}_n'$, $\mathbf{S}_n''$ respectively, while a third part of the area is A''' left unloaded or constituting the boundary between A' and A'' where these are contiguous.

1.1. **Moment of an elemental force.** In Fig. XI,1.1, dA is an elemental area with unit normal $\mathbf{n}$ and on which acts stress $\mathbf{S}_n$. The moment of the elemental force $\mathbf{S}_n dA$ about a point O is

$$\begin{aligned} d\mathbf{Q} = dQ\mathbf{q} &= (S_n dA)R \sin [\mathbf{R}, \mathbf{S}_n]\mathbf{q} \\ &= \mathbf{R}\times\mathbf{S}_n dA = \mathbf{R}\times\mathfrak{S}\cdot d\mathbf{A} \end{aligned} \tag{1.1}$$

with stress dyadic $\mathfrak{S}$, the elemental vector area $d\mathbf{A} = \mathbf{n}dA$ and vector product denoted by the 'cross'.

The points O and $\mathbf{R}$ are in translatory equilibrium, so force $-\mathbf{S}_n dA$ acting at O will be the equilibrating force for $\mathbf{S}_n dA$, while these two equal and opposite forces constitute a couple of arm $R \sin [\mathbf{R}, \mathbf{S}_n]$.

1.2. **Moments due to the surface forces in each zone.** Use XI(1.1) to calculate the moment $\mathbf{Q}'$ at a point O' due to surface stresses $\mathbf{S}_n'$ acting on surface A'. Thus,

$$\mathbf{Q}' = \int_{A'} \mathbf{R}' \times \mathbf{S}' \cdot dA' \tag{1.2}$$

and similarly for area A'',

$$\mathbf{Q}'' = \int_{A''} \mathbf{R}'' \times \mathbf{S}'' \cdot dA'' \tag{1.3}$$

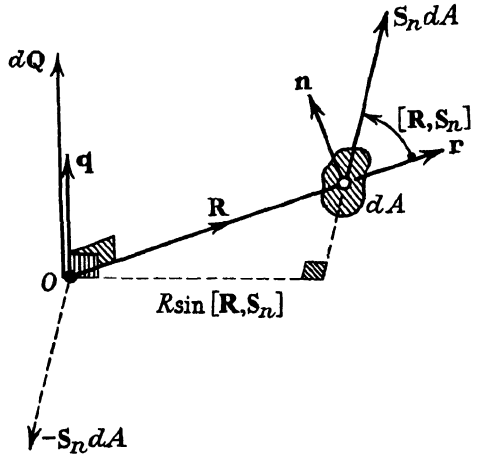

FIG. XI,1.1.—The elemental torque due to an elemental force given by stress acting on an elemental area. The direction of the elemental torque is normal to the plane of the stress vector and the position vector.

Notice for future applications that surface area A is composed of all exterior and interior surfaces of the body, while the subareas A', A'', A''' of A are arbitrary for the particular problem. Thus, for the tube twisted axially by loading on the exterior and interior surfaces, on the exterior surface $A' \neq 0 \neq A'''$, $A'' = 0$, while on the interior surface $A'' \neq 0 \neq A'''$, $A' = 0$.

For equilibrium,

$$\mathbf{q}'' = -\mathbf{q}' \qquad Q'' = Q' \tag{1.4}$$

Notice that the axes of these two couples are only required to be parallel and not necessarily coaxial.

1.3. **Body in translatory equilibrium.** The body is required to be in translatory equilibrium, so that the sum of the integrals of the forces over A' and A'' is zero. However, for the present case of couples only applied to the body there is the further restriction that each integral shall vanish. Thus,

$$\int_{A'} \mathbf{S}' \cdot d\mathbf{A}' = 0 = \int_{A''} \mathbf{S}'' \cdot dA'' \tag{1.5}$$

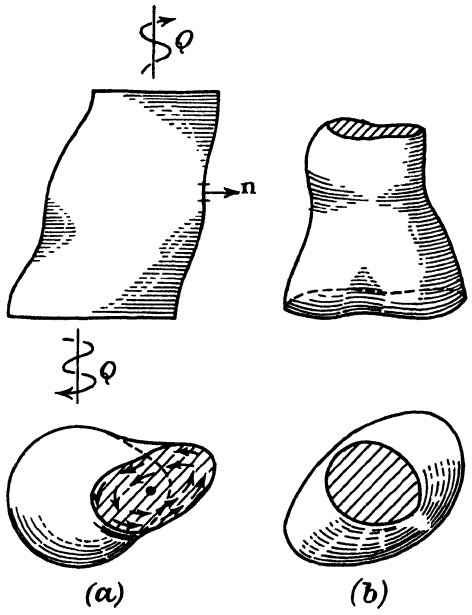

FIG. XI,2.1.—The diagrammatic *deformed* shape of an elastic body under torque Q due to shear stresses only on the plane ends of the body is shown in (*a*). Unit vector $\mathbf{c}_z$ is normal to the plane ends of the body. Unit vector $\mathbf{n}$ is a typical unit vector normal to the stress-free surface of the body at that typical point. Release of load gives the diagrammatic shape of the body in (*b*). In general, all the plane sections of the deformed body are warped in the unloaded body.

2. Torque applied to plane sections of bodies

Fig. XI,2.1(*a*) shows diagrammatically a deformed elastic body with plane, parallel end surfaces on which act shear stresses of which the aggregate constitute an applied torque Q of the same magnitude on each end surface. There is no resultant extensile

force or 'bending' moment because the normal stresses on the plane ends are zero. Fig. XI,2.1(*b*) shows diagrammatically the elastic body when the torque Q is removed. In general, the loaded plane ends will not be plane in the unloaded state. Similarly, all other sections will 'warp' in general from the unloaded to the loaded state.

It is important to notice that only the stresses applied to the ends of the body are under the control of an experimenter. Any hypothesis on the value of stresses internal to the body needs justification. The reason for an explicit statement of such a truism is clear by considering the Saint-Venant approach discussed in article XI,5.

2.1. **Mathematical form.** Suppose the upper, plane end of the body is A' with unit normal $\mathbf{c}_z$, the lower plane end is A'' with unit normal $-\mathbf{c}_z$, while the stress-free surface is A''' with unit normal $\mathbf{n}$. Stresses $\mathbf{S}_z'$, $\mathbf{S}_z''$ are shear stresses, so that

$$S_{zz}' = 0 = S_{zz}'' \tag{2.1}$$

Resolve $\mathbf{S}_z'$, $\mathbf{S}_z''$, $\mathbf{R}'$, $\mathbf{R}''$ to the general, curvilinear directions $\mathbf{c}_a$, $\mathbf{c}_b$ (as in article A,7) in the plane ends of the body, and then $dA' = dR_a'dR_b'$, $dA'' = dR_a''dR_b''$ are the elemental curvilinear areas. Expanding the integrands in article XI,1.2 gives

$$\left.\begin{aligned} \mathbf{Q}' &= \mathbf{c}_z \iint_{A'} (R_a'S_{zb}' - R_b'S_{za}')dR_a'dR_b' \\ \mathbf{Q}'' &= -\mathbf{c}_z \iint_{A''} (R_a''S_{zb}'' - R_b''S_{za}'')dR_a''dR_b'' \end{aligned}\right\} \tag{2.2}$$

with the restriction that

$$\iint_{A'} = \iint_{A''} \tag{2.3}$$

There must be no resultant force on each plane end, so, further,

$$\iint_{A'} \mathbf{S}_z'dR_a'dR_b' = 0 = \iint_{A''} \mathbf{S}_z''dR_a''dR_b'' \tag{2.4}$$

Also, the area A''' must be stress-free, so, there,

$$\mathbf{n}\cdot\mathbb{S}''' = 0 \tag{2.5}$$

2.2. **Stress-free surfaces and the stress potential.** Consider the stress-free surface of the body in terms of the stress potential H. Then,

$$\mathbf{S}_n = \mathbf{n}\cdot\nabla\nabla H = \mathbf{n}\cdot\nabla(\nabla H) = 0 \tag{2.6}$$

Choose a pair of unit vectors **l**, **m** tangential to the stress-free surface at the point for which the normal unit vector is **n**. Then, **l**, **m**, **n** constitute a mutually orthogonal set at the point. Define a set of orthogonal lines, generally curvilinear, in the surface and of lengths L, M and of length N in the volume enclosed and tangential to **l**, **m**, **n** respectively at the typical point. Then, at this point,

$$\nabla(\ ) = \mathbf{n}(\ )_{;N} + \mathbf{m}(\ )_{;M} + \mathbf{l}(\ )_{;L}$$
$$\mathbf{n}\cdot\nabla(\ ) = (\ )_{;N} \tag{2.7}$$

Therefore, for the surface to be stress-free at the point

$$(\nabla H)_{;N} = 0 \tag{2.8}$$

3. Torsion of a frustum of a hollow, elastic sphere of restricted isotropy: theoretical

An exact solution of the torsion equations of article **XI**,2 will be sought by first postulating a simple form for the stress potential in cylindrical coordinates (R_r, θ, R_z) and then finding the shape of the deformed body having the required stress-free surfaces A'''.

3.1. **Stresses.** Choose the stress potential

$$H = KR_z\theta \tag{3.1}$$

with undetermined constant K. For cylindrical coordinates, articles **VIII**,10, **A**,9.1 show that the only non-zero stresses are

$$\left.\begin{aligned} S_{r\theta} &= (R_r^{-1}H_{;\theta})_{;r} = -KR_zR_r^{-2} \\ S_{z\theta} &= (R_r^{-1}H_{;\theta})_{;z} = KR_r^{-1} \end{aligned}\right\} \tag{3.2}$$

Article **VIII**,11 shows that integration of the equilibrium stress equations gives the first stress invariant

$$\chi^S = \nabla^2 H = C = 0 \tag{3.3}$$

a zero constant here, since all the normal stresses are zero.

3.2. **Stress-free surfaces.** Article **XI**,2.2 shows that the stress is zero at a point of a surface normal to **n** when

$$(\nabla H)_{;N} = 0 \tag{3.4}$$

From article A,8.1 with H independent of R_r

$$\nabla H = R_r^{-1}\mathbf{c}_\theta H_{;\theta} + \mathbf{c}_z H_{;z} = K(R_r^{-1}R_z\mathbf{c}_\theta + \mathbf{c}_z\theta) \tag{3.5}$$

Then, with $\mathbf{c}_z$ constant,

$$(\nabla H)_{;N} = K(-R_r^{-2}R_z R_{r;N} + R_r^{-1}R_{z;N})\mathbf{c}_\theta + KR_r^{-1}R_z\mathbf{c}_{\theta;N} + K\theta_{;N}\mathbf{c}_z = 0 \tag{3.6}$$

Choose $\mathbf{n}$, and hence dN, to lie in the plane θ = constant, so that $\theta_{;N} = 0 = \mathbf{c}_{\theta;N}$, to give on rearranging,

$$\frac{R_{z;N}}{R_{r;N}} = \frac{R_z}{R_r} = \tan\Phi \tag{3.7}$$

say. Fig. XI,3.1 shows that this is satisfied when the stress-free

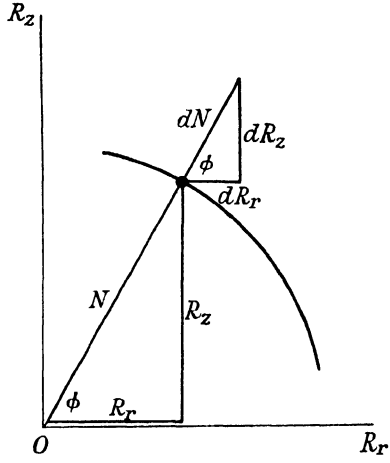

FIG. XI,3.1. With a point moving over a spherical surface so that N is constant, then R_z/R_r equals $(dR_z/dN)/(dR_r/dN)$ as required for the stress-free surface of the torsion problem when the stress potential is $K\theta R_z$.

surface is spherical, of radius N. Some representative shapes of the resulting family are shown in Fig. XI,3.2.

3.3. **Torque.** The torque on any plane with inner, outer radii b_i, b_o of a given hollow sphere of radii a_i, a_o is given from equation XI(2.2), XI(3.2).2 as

$$Q = \int_0^{2\pi}\int_{b_i}^{b_o} S_{z\theta}R_r^2\partial\theta\partial R_r = \pi K(b_o^2 - b_i^2) \tag{3.8}$$

But, with h the height of the plane from the plane $R_z = 0$,

$$b_o^2 = a_o^2 - h^2 \qquad b_i^2 = a_i^2 - h^2 \tag{3.9}$$

so that the applied torque, of the same value on each plane, is

$$Q = K\pi(a_o^2 - a_i^2) \tag{3.10}$$

3.4. **Strains.** Since, in **XI**(3.3), the first stress invariant is zero, then the elastic strain dyadic with stress-strain parameter G similar to that in article **VIII**,5.5 specialised, is

$$\mathfrak{M} = G\mathfrak{S} = G\nabla\nabla H \tag{3.11}$$

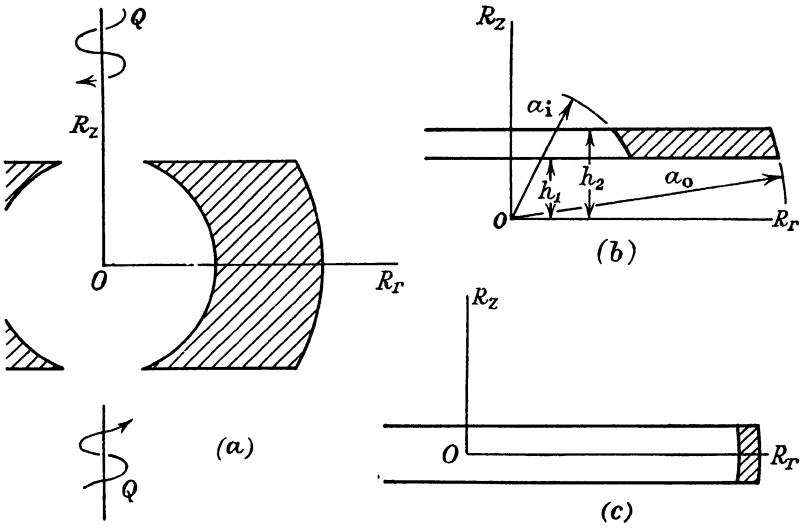

FIG. XI,3.2. Representative shapes for a family of frustums of hollow spheres with axial torque Q applied as an appropriate circumferential shear stress distribution on the plane ends and independent of circumferential position. The spherical surfaces are stress-free.

Using the cylindrical coordinates form of $\nabla\nabla$ in article **A**,9.1 with H from **XI**(3.1) gives all strains zero except

$$e_{r\theta} = -GKR_zR_r^{-2} \qquad e_{z\theta} = GKR_r^{-1} \tag{3.11'}$$

3.5. **Displacement potential and relative-displacement.** From article **VIII**,12, with arbitrary vector **W** and χ^S zero, then the displacement potential is

$$\mathcal{E} = GH \tag{3.12}$$

The relative-displacement

$$\mathbf{D}^* = \nabla\mathcal{E} = GK(R_r^{-1}R_z\mathbf{c}_\theta + \theta\mathbf{c}_z) \tag{3.13}$$

The stresses and strains are zero at $R_r \to \infty$, so that whole-body rotation is zero because there is at least one point suffering zero spatial-rotation even if it is at infinity. Therefore, spatial-displacement

$$\mathbf{U} = \mathbf{D} \approx \mathbf{D}^* \tag{3.14}$$

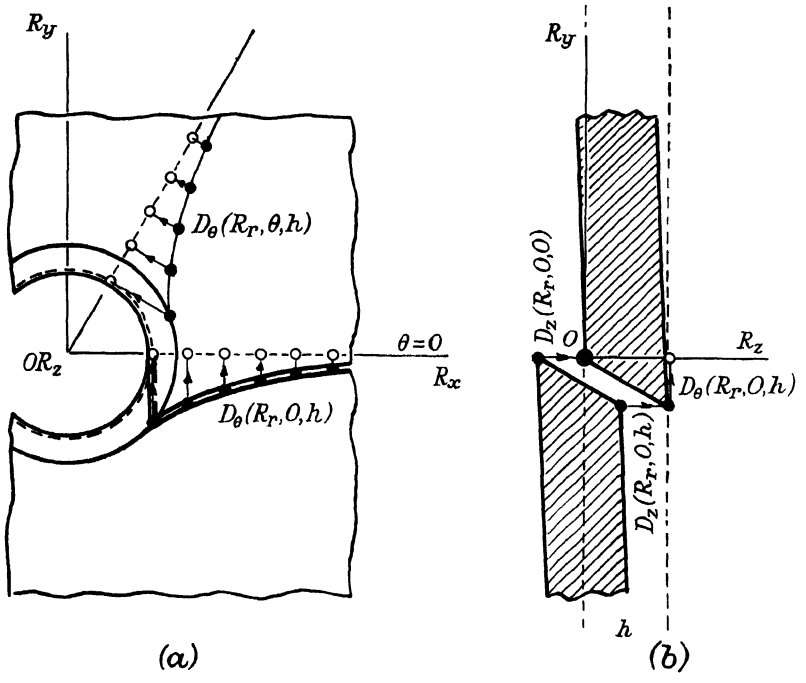

FIG. XI,3.3.—A lamina of thickness h at the basal plane position in a frustum of a hollow sphere. The dotted lines give the shape under the applied torsion, while the full lines are those correspondingly in the undeformed lamina. A physical discontinuity occurs at $\theta = 0$ although the stresses have the same value on each side of the 'slot', which opens when the applied torque is removed.

Fig. XI,3.3 shows diagrammatically the straining-displacement adjacent to the inner boundary. Since D_z has different values at $\theta = 0$, $\theta = 2\pi$, this means that the hollow sphere has a physical discontinuity or 'cut' along the plane $\theta = 0$. The two planes $\theta = 0$, $\theta = 2\pi$ are in contact when the body is deformed by the applied torque and in this sense the body is sensibly continuous.

Such a solution is 'dislocational' in the Volterra theory, which would suppose the body to be physically continuous at $\theta = 0$. This fallacious theory is discussed in volume I, article VI,12.

The reader may find it of interest to use $H = KR_z\theta \log R_r = \mathcal{E}/G$ and find discontinuity of stresses as well as displacements at $\theta = 0$.

3.6. **Inherent or residual stresses.** Suppose the initially unstrained body is made of the required shape and loaded appropriately with torque on the planes normal to OR_z and with the same values of $S_{r\theta}$, $S_{z\theta}$ as in XI(3.2) on each side of the slot at θ zero. Now, to all external appearances, the hollow sphere is continuous with continuous stresses since the slot has closed up. Suppose a perfect weld is made to join the two contiguous faces of the slot and leave a homogeneous hollow sphere with the stresses unchanged. If, now, the applied torque is removed the body cannot assume a stress-free state because the two faces of what was the slot at $\theta = 0$ cannot separate and be unloaded as part of the surface under the control of an experimenter. Thus, removal of torque gives a body having inherent or residual stresses.

Thus, the arbitrary restriction that the internal stresses $S_{z\theta}$ of the body should be independent of R_z leading to $KR_z\theta$ as a choice of stress potential leads to a problem in residual stresses if the body from which applied surface loading has been removed is to be solid. This problem of evaluating the change in stresses from the initial residual values to the current values and the change in shape to give the required spherical form has not been solved.

4. Further consideration of the approximate analysis of torsion of a thin-walled, right, circular cylinder: theoretical

Articles III,7 to III,12 consider the shear stress S_{xy} equal to T, say, acting on a strip of thin sheet. In terms of the stress potential for cartesian axes $OR_xR_yR_z$ with the main faces of the sheet parallel to the plane OR_xR_y this is

$$T = S_{xy} = H_{;xy} \tag{4.1}$$

so

$$H = TR_xR_y \tag{4.2}$$

gives the correct shear stress and all other stress components are zero.

4.1. **Plane stress solution adapted to cylindrical coordinates.** This plane analysis was adapted to give an approximate analysis of the axial torsion of a thin-walled tube with axis OR_z that of the tube when using cylindrical coordinates (R_r, θ, R_z). Thus axis OR_y of the plane analysis becomes OR_z, while R_x of the plane analysis becomes the length $R_r\theta$ in the cylindrical coordinates with R_r the radius of the tube. The axis OR_z of the plane analysis is in the radial direction for the tube. Then, for this adaptation **XI**(4.2) gives

$$H = TR_r\theta R_z \tag{4.3}$$

Provided that this stress potential is a suitable Poisson solution the cylindrical stresses are found by suitable differentiation as in article **VIII**,10. This gives the non-zero stresses

$$S_{\theta\theta} = TR_r^{-1}\theta R_z \qquad S_{\theta z} = T \qquad S_{zr} = T\theta \tag{4.4}$$

4.2. **Deficiencies of the adapted solution.** Article **VIII**,11 shows that the sum of the normal stresses must be constant but, in fact, equals $TR_r^{-1}R_z\theta$ here, so that the adapted stress potential is not suitable. The strains for such a stress distribution will not satisfy the compatibility conditions. Further, some of the stresses are not independent of θ as required.

Therefore, the intuitive wrapping of the plane sheet under shear stress only into a thin-walled tube acted upon by circumferential shear stress only is not formally allowable. Only when the radius of the tube is infinite does the stress $S_{\theta\theta}$ vanish in **XI**(4.4) while S_{zr} is independent of R_r and has a discontinuity at $\theta = 0, 2\pi$. The stress-potential function $KR_z\theta$ of article **XI**,3 gives the circumferential shear stress K/R_r as the only non-zero stress when the R_z coordinate is zero. Thus, a narrow frustum of the sphere of that article approximates to a similar short length of the thin-walled right tube.

5. Saint-Venant's theory of torsion of right cylinders of arbitrary cross-section

5.1. **Coulomb's theory for the torsion of circular cylindrical threads.** Coulomb, in 1777[19.1], gave a theory for the torsion of threads or rods of circular cross-section. This assumes that a plane passing through the axis of the initially untwisted thread deforms to a helical surface in which the *initial radius vectors remain straight*. Then, geometrically, with T the constant,

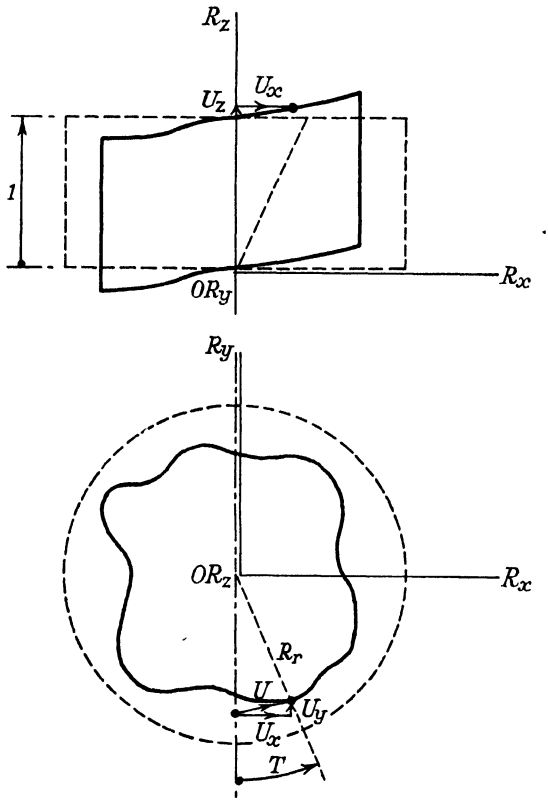

FIG. XI,5.1.—The dotted lines show the loaded, infinitesimally strained, right, circular cylinder of unit length of the Coulomb theory on torsion. When the boundary of the cross-section is of arbitrary shape as in Saint-Venant's theory, then the corresponding unloaded body is shown by full lines. Plane cross-sections 'warp', but the displacements observed in the lower view are those for the theory of Coulomb or that of Saint-Venant, as both assume that radius vectors remain straight. The 'angle of twist' T is that relatively between radius vectors unit distance apart axially.

infinitesimal angle of twist † per unit length of rod (as in Fig. XI,5.1), the infinitesimal circumferential spatial-displacement of a point at radius R_r is of magnitude

$$U = R_r T R_z \qquad (5.1^o)$$

when the axis of the rod is in direction OR_z of the spatially fixed

† This symbol has been used for shear stress in article XI,4.

cartesian axes $OR_xR_yR_z$. Thus, initially plane sections normal to OR_z are assumed to remain plane. With U_x, U_y, U_z, the spatial-displacement scalar components, then, on resolution of U,

$$U_x = -TR_yR_z \qquad U_y = TR_zR_x \qquad U_z = 0 \tag{5.1}$$

5.2. **Saint-Venant's extension of the Coulomb theory.** Saint-Venant extended the Coulomb theory to right cylinders of rectangular and elliptical cross-sections in 1847 [19.2] and then to any arbitrary cross-section in 1855 [19.7]. Saint-Venant accepted the Coulomb form for U_x, U_y in **XI**(5.1) but supposed that U_z is a function $U_z(R_x, R_y)$ independent of R_z. Therefore, generally, the initially plane sections normal to OR_z do not remain plane under load but all 'warp' to the same shape. This followed from an approximate analysis by Cauchy [19.5] in which Saint-Venant noticed that the warping of sections was implied. Thus, it is assumed that there is a line, within the cylinder and parallel to the surface generators, that remains straight and is an axis about which all sections rotate without change of shape (except for warping) under the torsion. This is the so-called *axis of twist*.

Cauchy doubted the validity of Saint-Venant's assumptions that the projection of radius vectors on planes normal to OR_z should remain straight after torsion of the arbitrary cylinder [19.6]. This assumption is important, so that a quotation † from the "History" of Todhunter & Pearson is worth while: '. . . Saint-Venant assumes that the angle of torsion T, corresponding to a unit length is *constant*; Cauchy proposes to generalise this by assuming T to be a function of the distance of the point from the axis. Saint-Venant himself pursues this suggestion in a note on pages 341–343 of his *Torsion*, and shows that it does not lead to any results of practical value.'

The present author arrived independently at Cauchy's doubt and shows in article **XII**,1 that Cauchy's suggestion is most valuable, since it leads to an analogy with flows of irrotational fluid as originally suggested qualitatively by Thomson & Tait [19.1] and giving important practical solutions. Saint-Venant's analysis will lead to analogy with the flow of rotational fluid of constant vorticity, but this is not as easy to achieve experimentally as the irrotational flows.

† The symbol T here is given as τ by Todhunter & Pearson.

5.3. **General equations required for particularisation to Saint-Venant's theory.** The further inferences that follow from the theory can be followed more closely if there are collected here the various general expressions to be particularised for torsion. The generalised Hooke's law is, with the first stress invariant

$$\left.\begin{aligned} \chi^S &= S_{xx}+S_{yy}+S_{zz} \\ U_{x;x} &= e_{xx} = GS_{xx}+F\chi^S \\ \tfrac{1}{2}(U_{x;y}+U_{y;x}) &= e_{xy} = GS_{xy} \end{aligned}\right\} \qquad (5.2)$$

with four more similar expressions for e_{yy}, e_{zz}, e_{yz}, e_{zx}. The equilibrium stress equations with zero body force are three such as

$$S_{xx;x}+S_{yx;y}+S_{zx;z} = 0 \qquad (5.3)$$

The stress-free cylindrical surface for which the typical normal unit vector is $\mathbf{n}$ normal to the axis OR_z requires

$$S_{xx}n_x+S_{xy}n_y = 0 \qquad S_{yy}n_y+S_{xy}n_x = 0 \qquad S_{yz}n_y+S_{zx}n_x = 0 \qquad (5.4)$$

with n_x, n_y the direction cosines of $\mathbf{n}$ with respect to OR_x, OR_y respectively. Saint-Venant's strains compatibility conditions are six such as

$$\left.\begin{aligned} e_{xx;yy}+e_{yy;xx} &= 2e_{xy;xy} \\ e_{xx;yz}+e_{yz;xx} &= e_{zx;xy}+e_{xy;zx} \end{aligned}\right\} \qquad (5.5)$$

with the other four expressions found by cyclic interchange of the subscripts x, y, z.

5.4. **Infinitesimal spatial-displacement, strain and stress relations.** The first two equations of **XI**(5.1) and the assumption on U_z then reduce equations **XI**(5.2) to

$$e_{xx} = 0 = e_{yy} \qquad e_{xy} = 0 = e_{zz} \qquad (5.6)$$

$$U_{z;x}-TR_y = 2GS_{zx} \qquad U_{z;y}+TR_x = 2GS_{yz} \qquad (5.7)$$

The six strains compatibility conditions, with **XI**(5.6), reduce to two non-zero expressions

$$e_{yz;xx} = e_{zx;xy} \qquad e_{yz;xy} = e_{zx;yy} \qquad (5.8)$$

5.5. **Stress assumptions and boundary conditions.** Saint-Venant now assumes, further, that

$$S_{xx} = 0 = S_{yy} \qquad S_{xy} = 0 = S_{zz} \qquad (5.9)$$

to satisfy all of the four equations **XI**(5.6) when considered with

XI(5.2). This assumption reduces the equilibrium stress equations to

$$S_{zx;z} = 0 \qquad S_{yz;z} = 0 \tag{5.10}$$

$$S_{zx;x} + S_{yz;y} = 0 \tag{5.11}$$

and the boundary conditions XI(5.4) to

$$S_{yz} n_y + S_{zx} n_x = 0 \tag{5.12}$$

But, from Fig. XI,5.2,

$$n_x = dR_y/dL \qquad n_y = -dR_x/dL \tag{5.13}$$

5.6. **Laplacian equation and boundary conditions for the warping displacement.** Differentiating the two equations

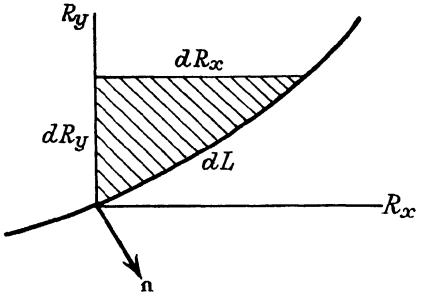

FIG. XI,5.2.— An elemental length of the boundary of the cylinder, with elemental lengths in the directions of the coordinate axes in the plane of a cross-section, define an elemental area adjacent to the boundary for which the unit outward normal is **n**.

XI(5.7) with respect to R_x, R_y respectively, adding together and using XI(5.11) gives

$$U_{z;xx} + U_{z;yy} \equiv \nabla^2 U_z = 0 \tag{5.14}$$

while XI(5.7) with XI(5.13) in XI(5.12) gives the boundary condition

$$(U_{z;x} - TR_y)(dR_y/dL) - (U_{z;y} + TR_x)(dR_x/dL) = 0 \tag{5.15}$$

These are the two equations given originally by Saint-Venant [19.2].

5.7. **Boussinesq stress function and its boundary value.** Boussinesq, in 1871 [19.3], introduced a stress function β to satisfy XI(5.11) identically. Thus, with β a function of R_x, R_y only,

$$S_{zy} = -\beta_{;x} \qquad S_{zx} = \beta_{;y} \tag{5.16}$$

Substituting in **XI**(5.7), differentiating suitably and subtracting to eliminate U_z gives

$$\nabla^2\beta = -T/G \tag{5.17}$$

Substituting **XI**(5.16) in the boundary condition **XI**(5.12) with **XI**(5.13) gives

$$\beta_{;x}(dR_x/dL)+\beta_{;y}(dR_y/dL) = d\beta/dL = 0 \tag{5.18}$$

and so the stress function β is constant along the boundary. This constant value can be zero without loss of generality.

If β is a laplacian then the right-hand side of **XI**(5.17) must be zero with $T = 0$. But a zero T means that the cylinder is not deformed and so represents a trivial case for Saint-Venant's theory of torsion.

5.8. **Spatial-displacement by integration.** The spatial-displacement component is found by substituting from **XI**(5.16) in **XI**(5.7) and then integrating the resulting two equations. The components U_x, U_y are just as in **XI**(5.1). Collect for future reference:

$$\left.\begin{array}{ll} U_x = -TR_yR_z & U_y = TR_zR_x \\ U_{z;x} = TR_y+2G\beta_{;y} & U_{z;y} = -TR_x-2G\beta_{;x} \end{array}\right\} \tag{5.19}$$

5.9. **Torque.** The torque is given by article **XI**,2.1 with article **XI**,5.7 as

$$Q = \iint_A (R_xS_{zy}-R_yS_{zx})\partial R_x\partial R_y$$

$$= -\iint_A (R_x\beta_{;x}+R_y\beta_{;y})\partial R_x\partial R_y$$

Integrating by parts gives

$$\iint_A R_x\beta_{;x}\partial R_x\partial R_y = \int_{R_y(-)}^{R_y(+)} [R_x\beta]_{\beta(-)}^{\beta(+)}\partial R_y - \iint_A \beta\partial R_x\partial R_y$$

$$= -\iint_A \beta\partial R_x\partial R_y$$

with $\beta(-)$, $\beta(+)$ zero on the boundary at the limits of integration and $R_y(-)$, $R_y(+)$ the limits for the direction OR_y. Similarly,

$$\iint_A R_y \beta_{;y} \partial R_x \partial R_y = -\iint_A \beta \partial R_x \partial R_y$$

Therefore,

$$Q = 2\iint_A \beta \partial R_x \partial R_y \tag{5.20}$$

5.10. **Membrane analogic solution.** An analogy between the Saint-Venant theory of torsion and uniform transverse pressure P on a slightly deflected membrane having a boundary of the same shape as the right cylinder cross-section was introduced by L. Prandtl [25] in 1903. This is merely summarised here to indicate its nature, so the reader should consult the book by S. Timoshenko [23.1] for a clear, concise account.

Denote by Z the small transverse deflection of the membrane under the uniform pressure. If H is the uniform tension in the curvilinear membrane, then the equilibrium of an element yields the equation

$$\nabla^2 Z \equiv Z_{;xx} + Z_{;yy} = -P/H \tag{5.21}$$

Comparison with **XI**(5.17) gives the required analogue,

$$Z = \beta \qquad P/H = T/G \tag{5.22}$$

The contour lines Z constant correspond to the stress-function trajectories β constant. The value of the resultant shear stress at a point is given by the maximum slope of the membrane at that point.

The foregoing applies to a singly connected cross-section of the cylinder; that is, one without holes inside the outer boundary. When there are holes so that the cross-section is multiply-connected, then the membrane analogy becomes inelegant because the height Z at each interior boundary needs to be adjusted and this is not easy experimentally.

5.11. **Constant-vorticity, inviscid, incompressible fluid analogic solution.** If ω is the 'rigid-body' angular velocity of an element of fluid, then the vorticity of the element in a two-dimensional flow is

$$2\omega = V_{y;x} - V_{x;y} \tag{5.23}$$

with V_x, V_y the velocity components at the given point. The condition of continuity for the incompressible fluid, ensuring that the same volume of fluid flows away from the point as to it, is

$$V_{x;x}+V_{y;y}=0 \tag{5.24}$$

Satisfy this equation with the stream function β by substituting

$$V_x=-\beta_{;y} \qquad V_y=\beta_{;x} \tag{5.25}$$

Substituting these expressions in XI(5.23) gives

$$\nabla^2\beta\equiv\beta_{;xx}+\beta_{;yy}=2\omega \tag{5.26}$$

J. Larmour, in 1892 [26], pointed out that this is analogous to XI(5.17) if ω is constant. Thus, in the analogic sense, together with XI(5.16),

$$-T/G=2\omega \qquad \beta_{;y}=S_{zx}=-V_x \qquad -\beta_{;x}=S_{zy}=-V_y \tag{5.27}$$

5.12. **Experimental circulation of constant-vorticity fluid.** H. Lamb [150] considers the irrotational motion of fluid contained in a boundary of arbitrary, fixed shape that rotates with constant angular velocity ω relative to fixed space about a point within the boundary [21.9]. The details of finding the complex potential are not given here, but article XI,7.6 illustrates the stream function in such a case for an elliptic boundary. The stream function for flow relative to the rotating cylinder is analogous to the Boussinesq stress function for torsion. The constant vorticity is given by, quite literally, rotating at constant angular velocity the fluid within a boundary of the same shape as the cross-section of the cylinder. The velocity relative to the rotating boundary gives the stresses as in XI(5.27).

This analogy appears to have advantages over the membrane analogy of article XI,5.10. The membrane is usually a soap bubble that is rather fragile, while its shape, the slope, contour, etc., are not easy to measure. The membrane analogue is particularly difficult when there are holes in the cross-section. A shallow tank of the required cross-sectional shape filled with water can be rotated at constant speed ω. Dye that does not disperse too quickly can be injected to define streamlines that can be photographed by a camera rotating with the tank. Velocities can be measured by hot resistance-wires, for example, and their readings taken via slip-rings to the outside measuring

bridge.† Holes of any shape and size are represented by cylindrical obstacles placed appropriately in the circulatory flow.

5.13. **The laplacian Boussinesq stress function and a modification‡ of the Saint-Venant theory.** The solution of the present torsional deformation problem requires the satisfaction of:

(i) Equilibrium stress equations.
(ii) Cylindrical boundaries are stress-free.
(iii) Saint-Venant's compatibility conditions for the Navier, Cauchy strains.
(iv) Stress-strain relations for restricted isotropy.

Saint-Venant assumed that

$$\text{(A)} \quad S_{xx} = 0 = S_{yy} \qquad S_{xy} = 0 = S_{zz}$$

With these assumptions on the stresses then (i), (ii), (iii) are satisfied by

$$\left.\begin{aligned} S_{zx} &= \beta_{;y} \qquad S_{zy} = -\beta_{;x} \\ \beta &= \text{constant on the boundary} \\ S_{zx} &= e_{zx}/G = \tfrac{1}{2}(U_{z;x}+U_{x;z})/G \\ S_{zy} &= e_{zy}/G = \tfrac{1}{2}(U_{z;y}+U_{y;z})/G \end{aligned}\right\} \tag{5.28}$$

with stress-strain parameter G.

Condition (iv) needs closer examination. Suppose that:

(a) β is the imaginary part of γ, a function of the complex variable c.

Then, with $i = \sqrt{(-1)}$ and the two-dimensional laplacian operator,

$$\left.\begin{aligned} \gamma &= \alpha+i\beta \qquad c = R_x+iR_y \\ \alpha_{;x} &= \beta_{;y} \qquad \alpha_{;y} = -\beta_{;x} \\ \nabla^2\alpha &= 0 = \nabla^2\beta \end{aligned}\right\} \tag{5.29}$$

From the last two equations of **XI**(5.28),

$$\tfrac{1}{2}(U_{z;x}+U_{x;z})/G = \alpha_{;x} \qquad \tfrac{1}{2}(U_{z;y}+U_{y;z})/G = \alpha_{;y} \tag{5.30}$$

† Mr. C. R. Urwin [27] suggested the Kelvin double bridge for such conditions where resistance changes at the brushes are superimposed on the small resistance changes at the hot wire. The present author suggested the modification of the simpler Wheatstone bridge by potential leads and high-ratio arms.

‡ Author, 1951.

If β has been chosen so that whole-body rotation is zero, then $\mathbf{U} = \mathbf{D}$, the straining-displacement. This is assured if, for example, the stresses vanish at infinity or at the origin of coordinates on the 'axis of twist', so that at least one point suffers zero spatial-rotation. Further, for infinitesimal strains as assumed by Saint-Venant $\mathbf{D} = \mathbf{D}^*$, the relative-displacement, while $D^*_{x;z} = D^*_{z;x}$, ... Then **XI**(5.30) gives

$$U_z = 2\alpha G \qquad U_x = 2R_z\alpha_{;x}G + X \qquad U_y = 2R_z\alpha_{;y}G + Y \quad (5.31)$$

with X, Y each arbitrary functions of both R_x and R_y. Comparison with **XI**(5.1) shows that α would be second-degree only in R_x. R_y for radius vectors to remain straight. Function α can be of any degree to suit **XI**(5.29), so that *radius vectors do not remain straight* in general. As noted, Cauchy felt intuitively that this should be so and doubted the validity of Saint-Venant's assumption.

Notice that, apart from the theory formulated in this treatise for convected axes, etc., it could have been assumed that

$$\text{(b)} \quad U_{z;x} = U_{x;z} \qquad U_{z;y} = U_{y;z} \quad (5.32)$$

without being more arbitrary than Saint-Venant in assuming that

$$\text{(B)} \quad U_x = -TR_yR_z \qquad U_y = TR_zR_x \quad (5.33)$$

This arbitrary assumption by Saint-Venant led to the poissonion distribution of β in **XI**(5.17), while the present author's (b) led to the laplacian distribution in **XI**(5.29). With $T = 0$, for **XI**(5.17) to be laplacian gives the trivial case of zero deformation according to the Saint-Venant theory.

Article **XII**,7.5 discusses further peculiarities of Saint-Venant's theory in leading to physically unacceptable 'dislocational rotations' independent of stress. Further, maximum shear stress does not necessarily occur at the point of the boundary closest to the axis of twist, as predicted by Boussinesq from the Saint-Venant theory. Filon, in 1899 [109], questioned the validity of Boussinesq's general inference and gave an example to illustrate his objection.

6. A specialised theory † of torsion of non-cylindrical bodies

The shear stresses S_{zx}, S_{zy} in terms of the stress potential H are

$$S_{zx} = H_{;zx} \qquad S_{zy} = H_{;zy} \quad (6.1)$$

† Author, 1951.

for cartesian coordinates $OR_xR_yR_z$. Suppose these stresses are independent of R_z as in Saint-Venant's theory of torsion.

6.1. **Stress potential function.** This condition is satisfied by

$$H = R_z\alpha(R_x, R_y) \tag{6.2}$$

with $\alpha(R_x, R_y)$ a function of R_x and R_y only, to give

$$S_{zx} = \alpha_{;x} \qquad S_{zy} = \alpha_{;y} \tag{6.3}$$

This supposition must be noted as an arbitrary restriction on the distribution of the stresses in the body interior, although, strictly, only the stresses applied to the end surfaces are under the control of an experimenter, as noted in article **XI**,2.

6.2. **Boussinesq stress function is the conjugate of the stress-potential function.** Comparison with the Boussinesq stress function $\beta(R_x, R_y)$ of article **XI**,5.7 shows that

$$-\beta_{;x} = \alpha_{;y} \qquad \beta_{;y} = \alpha_{;x} \tag{6.4}$$

These are the Cauchy-Riemann conditions of article **B**,3 ensuring that

$$\gamma(c) = \alpha(R_x, R_y) + i\beta(R_x, R_y) \tag{6.5}$$

is differentiable with respect to the complex variable

$$c = R_x + iR_y \tag{6.6}$$

The functions α, β are said to be conjugate. Article **B**,4 shows that the family of curves α = constant intersects orthogonally the family of curves β = constant. Article **B**,5 shows that α, β are both laplacian, so that, with the two-dimensional laplacian operator,

$$\nabla^2\alpha = 0 = \nabla^2\beta \tag{6.7}$$

6.3. **Stresses in terms of the stress-potential function and its conjugate.** Differentiating the stress-potential function suitably gives the rest of the components of the stress dyadic as in the first two columns of Table **XI**,6.1. More briefly, this means that the stress dyadic is represented by

$$\nabla\nabla(R_z\alpha) = \mathfrak{S} = -\mathbf{c}_z\times\nabla\nabla(R_z\beta)$$

with the *three-dimensional* operator $\nabla\nabla$ in each expression.

The first two lines of Table **XI**,6.1 are identical with equations **XI**(6.4) and **XI**(6.3). Differentiating each of these two lines

TABLE XI,6.1

Stress potential	Stress component	Conjugate stress potential
$\alpha_{;x}$	S_{zx}	$\beta_{;y}$
$\alpha_{;y}$	S_{yz}	$-\beta_{;x}$
$R_z\alpha_{;xy}$	S_{xy}	$-R_z\beta_{;xx}$ and $R_z\beta_{;yy}$
0	S_{zz}	0
$R_z\alpha_{;xx}$	S_{xx}	$R_z\beta_{;xy}$
$R_z\alpha_{;yy}$	S_{yy}	$-R_z\beta_{;xy}$

suitably in turn gives the remaining four expressions in column three for the stresses in terms of the conjugate stress potential. Notice that these results are consistent with the two laplacian equations in **XI**(6.7). The second equation shows that the first stress invariant $(S_{xx}+S_{yy}+S_{zz})$ is zero, but, in general, S_{xy} is not zero, nor are S_{xx} and S_{yy}, as assumed in the Saint-Venant theory of article **XI**,5.5.

6.4. **Stress-free surface.** With **n** the normal unit vector for the typical point of the stress-free surface of the twisted body, then, as in **XI**(2.6),

$$\mathbf{S}_n = 0 = \mathbf{n}\cdot\nabla\nabla H \tag{6.8}$$

For cartesian coordinates this gives the three scalar equations

$$\left.\begin{aligned} 0 &= n_x\alpha_{;x}+n_y\alpha_{;y} \\ 0 &= n_xR_z\alpha_{;xy}+n_yR_z\alpha_{;yy}+n_z\alpha_{;y} \\ 0 &= n_xR_z\alpha_{;xx}+n_yR_z\alpha_{;xy}+n_z\alpha_{;x} \end{aligned}\right\} \tag{6.8'}$$

These three homogeneous, linear equations with the direction cosines n_x, n_y, n_z of **n** as independent variables are consistent and solvable if their determinant is zero [20]. Thus,

$$\begin{vmatrix} \alpha_{;x} & \alpha_{;y} & 0 \\ R_z\alpha_{;xy} & R_z\alpha_{;yy} & \alpha_{;y} \\ R_z\alpha_{;xx} & R_z\alpha_{;xy} & \alpha_{;x} \end{vmatrix} = 0$$

$$= R_z(\alpha_{;x}\alpha_{;x}\alpha_{;yy}+\alpha_{;y}\alpha_{;y}\alpha_{;xx}-2\alpha_{;x}\alpha_{;y}\alpha_{;xy}) \tag{6.9}$$

6.5. **Basal solution for the stress-free surface.** The solution $R_z = 0$ is best treated as a special case by reverting to **XI**(6.8′) to give

$$\left.\begin{aligned} 0 &= n_x\alpha_{;x}+n_y\alpha_{;y} \\ n_z\alpha_{;y} &= 0 = n_z\alpha_{;x} \end{aligned}\right\} \tag{6.10}$$

If **n** is normal to OR_z then the last two expressions are satisfied, while with **XI**(5.13) and **XI**(6.4) the first equation of **XI**(6.10) gives

$$\beta_{;x}(dR_x/dL)+\beta_{;y}(dR_y/dL) = d\beta/dL = 0 \tag{6.11}$$

just as in **XI**(5.18) in Saint-Venant's theory. This states that β is a constant along the boundary of the section $R_z = 0$ of the twisted body, while α and β are conjugate harmonic functions. Further, Table **XI**,6.1 shows that stresses S_{xx}, S_{yy}, S_{xy} are zero in this 'basal' plane just as in Saint-Venant's hypothesis for all planes of his right cylindrical twisted body.

6.6. **General solution for the stress-free surface.** The second solution for **XI**(6.9) is given by putting as zero the expression in the brackets. Thus, for any value of R_z,

$$\alpha_{;x}\alpha_{;x}\alpha_{;yy}+\alpha_{;y}\alpha_{;y}\alpha_{;xx}-2\alpha_{;x}\alpha_{;y}\alpha_{;xy} = 0 \tag{6.12}$$

The selected stress potential α will contain at least one parameter that can take a constant value on each of a family of curves given by this latter equation. The value of n_y/n_x at any typical point on any particular one of these curves is given from **XI**(6.8′).1 as

$$n_y/n_x = \alpha_{;x}/\alpha_{;y} \tag{6.13}$$

with the partial-differential coefficients calculated at that point.

From either of the last two equations of **XI**(6.8′) there is found n_z/n_x. Thus,

$$\begin{aligned} -(\alpha_{;xy}+\alpha_{;yy}n_y/n_x)R_z/\alpha_{;y} &= n_z/n_x \\ &= -(\alpha_{;xx}+\alpha_{;xy}n_y/n_x)R_z/\alpha_{;x} \end{aligned} \tag{6.14}$$

Using **XI**(6.13) in this equation and cancelling terms common to both sides gives

$$\alpha_{;x}\alpha_{;x}\alpha_{;yy} = \alpha_{;y}\alpha_{;y}\alpha_{;xx} \tag{6.15}$$

Substituting in **XI**(6.12) gives the family of curves

$$\alpha_{;x}(\alpha_{;x}\alpha_{;yy}-\alpha_{;y}\alpha_{;xy}) = 0 \tag{6.16}$$

for R_z constant, on which are to be determined the direction cosines ratios n_y/n_x from **XI**(6.13) and, from **XI**(6.14),

$$n_z/n_x = -R_z(\alpha_{;xx}/\alpha_{;x}+\alpha_{;xy}/\alpha_{;y}) \tag{6.17}$$

But the scalar product

$$\mathbf{n}\cdot\mathbf{n} = n_x^2+n_y^2+n_z^2 = 1$$

so that substituting from XI(6.13) and XI(6.17) gives

$$n_x^2 = [1+(\alpha_{;x}/\alpha_{;y})^2+R_z^2(\alpha_{;xx}/\alpha_{;x}+\alpha_{;xy}/\alpha_{;y})^2]^{-1} \qquad (6.18)$$

to determine n_x, except for the sign, which is readily found by inspection in a particular problem. The normal unit vector is now given by

$$\mathbf{n} = n_x\mathbf{c}_x+n_y\mathbf{c}_y+n_z\mathbf{c}_z \qquad (6.19)$$

6.7. **Boundary curve of a plane section of the body.** The shape of the surface of the twisted, non-cylindrical body is most readily given in terms of the boundary curve of the typical section R_z = a constant. At the typical point of such a curve the unit vector $\mathbf{t}$ tangential to the boundary curve is normal to both $\mathbf{c}_z$ and $\mathbf{n}$. Therefore, the vector product

$$\mathbf{c}_z\times\mathbf{n} = \mathbf{t}\sin[\mathbf{c}_z, \mathbf{n}] = \mathbf{V} \qquad (6.20)$$

say, with $[\mathbf{c}_z, \mathbf{n}]$ the angle between $\mathbf{c}_z$ and $\mathbf{n}$ with the vectors in the right-handed screw sequence $\mathbf{c}_z$, $\mathbf{n}$, $\mathbf{t}$. But, to find the unit vector $\mathbf{t}$, denote the arithmetical magnitude of $\mathbf{V}$ by V, and then

$$\mathbf{V} = V\mathbf{t} \qquad V = \sqrt{(\mathbf{V}\cdot\mathbf{V})} \qquad \mathbf{t} = \mathbf{V}/\sqrt{(\mathbf{V}\cdot\mathbf{V})}$$

Therefore, from XI(6.20),

$$\mathbf{t} = (\mathbf{c}_z\times\mathbf{n})/\sqrt{|(\mathbf{c}_z\times\mathbf{n})\cdot(\mathbf{c}_z\times\mathbf{n})|} \qquad (6.21)$$

But

$$\mathbf{c}_z\times\mathbf{n} = n_x\mathbf{c}_y-n_y\mathbf{c}_x$$

so that

$$\mathbf{t} = (n_x\mathbf{c}_y-n_y\mathbf{c}_x)/\sqrt{(n_x^2+n_y^2)} \qquad (6.22)$$

6.8. **Torque.** The torque on a cross-section of area A normal to axis OR_z is given from article XI,5.9 as

$$Q = \iint_A (R_xS_{zy}-R_yS_{zx})\partial R_x\partial R_y \qquad (6.23)$$

Substituting from Table XI,6.1 gives

$$Q = \iint_A (R_x\alpha_{;y}-R_y\alpha_{;x})\partial R_x\partial R_y \qquad (6.24)$$

With dL an elemental length of the boundary and the com-

ponents of the vector in article A,17.1 as $-\mathbf{c}_x R_x \alpha$, $-\mathbf{c}_y R_y \alpha$, then the surface integral is converted to a line integral

$$Q = \oint_L \mathbf{t}\cdot\mathbf{R}\alpha_L dL = \oint_L \alpha_L R t_R dL = \oint_L \alpha_L R dR \qquad (6.25)$$

with t_R the cosine of the angle between $\mathbf{t}$ and $\mathbf{R}$ and, since $t_R dL = dR$, the change in the modulus of radius vector $\mathbf{R}$.

Now calculate the torque again, using the conjugate function β. Substituting from Table XI,6.1 in equation XI(6.23) gives

$$Q = -\iint_A (R_x\beta_{;x} + R_y\beta_{;y})\partial R_x \partial R_y = Q_1 + Q_2 \qquad (6.26)$$

$$Q_1 = -\iint_A [(R_x\beta)_{;x} + (R_y\beta)_{;y}]\partial R_x \partial R_y \qquad Q_2 = 2\iint_A \beta \partial R_x \partial R_y$$

For Q_1 take $\mathbf{c}_x R_x\beta$, $\mathbf{c}_y R_y\beta$ as the components of the vector in equation A(17.5), while, here, the outward unit normal vector is $\mathbf{t}\times\mathbf{c}_z$ when $\mathbf{t}\times\mathbf{c}_z$, $\mathbf{t}$, $\mathbf{c}_z$ form an orthogonal set. Then, as a line integral on the boundary,

$$Q_1 = -\oint_L \mathbf{t}\times\mathbf{c}_z\cdot\mathbf{R}\beta_L dL = -\oint_L \beta_L \mathbf{t}\cdot(\mathbf{c}_z\times\mathbf{R})dL$$

since the dot and cross can be interchanged in the scalar triple product. But with $\mathbf{R} = R\mathbf{r}$, then $\mathbf{t}\cdot(\mathbf{c}_z\times\mathbf{r})dL = Rd\theta$ if $d\theta$ is the angle swept by the radius vector as the point on the boundary changes from L to $L+dL$. Positive rotation is anticlockwise viewed in the direction $-\mathbf{c}_z$. So,

$$Q_1 = -\int_0^{2\pi} \beta_L R^2 d\theta$$

The torque is therefore

$$Q = -\int_0^{2\pi} \beta_L R^2 d\theta + 2\iint_A \beta \partial R_x \partial R_y \qquad (6.27)$$

6.9. **Curvilinear coordinates.** The equations for this theory on torsion have been formulated for cartesian coordinates, but these are not always the most convenient for a particular problem.

The solution for the frustum of a sphere is a solution for the present theory, since the stress potential $\alpha = KR_z\theta$ is the real component of $-iKR_z \log c$ when $c = R_r \exp(i\theta)$. The unit vector normal to the stress-free surface is there the spherically radial unit vector. Cartesian coordinates in that case would have been clumsy. As an exercise, the reader can formulate the equations for any particular coordinates by writing $H = R_z\alpha$ as before and then expressing α and the operator $\nabla\nabla$ in the desired curvilinear coordinates. Forming the scalar product with $\mathbf{n}$ as in XI(6.8) then gives three scalar equations analogous to XI(6.8′), but with the direction cosines now relative to the local unit vectors of the curvilinear coordinates.

6.10. **Displacements.** For an elastic substance of restricted isotropy, with a zero first stress invariant as here, stress-strain parameter G and constant, arbitrary vector $\mathbf{W}$, article VIII,12.1 gives the displacement potential

$$\mathcal{E} = GH + \mathbf{W}\cdot\mathbf{R} = GR_z\alpha + \mathbf{W}\cdot\mathbf{R} \tag{6.28}$$

Relative-displacement for whole-body convected cartesian axes is

$$\mathbf{D}^* = \nabla\mathcal{E} = (GR_z\alpha_{;x} + W_x)\mathbf{c}_x + (GR_z\alpha_{;y} + W_y)\mathbf{c}_y + (G\alpha + W_z)\mathbf{c}_z \tag{6.29}$$

The straining-displacement $\mathbf{D}$ is given by the straining-equivalence principle, but whether this equals spatial-displacement $\mathbf{U}$ in a particular case depends on whether whole-body rotation is zero. Notice that if α is chosen so that it has a discontinuity at a point, then so will D_z^* be discontinuous and the body has a physical discontinuity at that point.

The 'angle of twist' is not a fundamental idea in this theory, nor is it constrained to be constant as in the Coulomb, Saint-Venant approach. The particular cases in chapter XII show how radius vectors of a cross-section warp in their plane as visualised by Cauchy. His intuitive idea was not developed further because the Saint-Venant compatibility conditions, shown by the present author to be necessary but insufficient, were the only set available at that time and since.

7. Torsion of a solid right cylinder of elliptical cross-section: Saint-Venant's solution

A solution for the torsion by infinitesimal strain of a right cylinder of elliptical cross-section will be found for Saint-Venant's

theory using the Boussinesq stress function of article XI,5.7. Originally, in 1847 [19.2], Saint-Venant solved equations XI(5.14), XI(5.15) to give the warping displacement in XI(7.7) here.

7.1. **Stress function.** The stress function β is to have zero value on the elliptical boundary and satisfy

$$\nabla^2\beta = \beta_{;xx}+\beta_{;yy} = -T/G \tag{7.1}$$

with T the infinitesimal angle of twist per unit length and G the shear stress-strain, isotropic, constant parameter.

With a, b the major and minor semi-axes of the external boundary of the elliptical cross-section, then the stress function

$$\beta = K(1-R_x^2/a^2-R_y^2/b^2) \tag{7.2}$$

with

$$K = Ta^2b^2/[2G(a^2+b^2)] \tag{7.3}$$

satisfies the required conditions.

7.2. **Stresses.** The shear stresses are given by

$$S_{zx} = \beta_{;y} = -2KR_y/b^2 \qquad S_{zy} = -\beta_{;x} = 2KR_x/a^2 \tag{7.4}$$

from article XI,5.7 with equation XI(7.2). All other stresses have been assumed zero as in article XI,5.5. The shear stresses are zero at the origin of coordinates and independent of R_z. From XI(7.4) it is seen that the maximum stress occurs at the end of the minor axis, where $S_{zy} = 0$ and $S_{zx} = 2K/b$. The minimum stress occurs at the end of the major axis, where $S_{zx} = 0$ and $S_{zy} = 2K/a$.

If the shear-stress trajectories are ellipses geometrically similar to the outer boundary, then their equation will be

$$1-R_x^2/(ka)^2-R_y^2/(kb)^2 = 0 \tag{7.5}$$

with $0 < k \leqq 1$. The slope of this curve is

$$dR_y/dR_x = -(b/a)^2R_x/R_y = S_{zy}/S_{zx} \tag{7.6}$$

with the last ratio following from XI(7.4). Therefore, the shear-stress trajectories are, in fact, ellipses of geometrically the same shape as the outer boundary.

7.3. **Torque.** The torque applied to the cross-section of the solid right cylinder is given in article XI,5.9 with equations XI(7.4) as

$$Q = 2\iint_A \beta\partial R_x\partial R_y = \pi Kab \tag{7.5}$$

7.4. **Angle of twist.** The angle of twist per unit length of the right cylinder is given from **XI**(7.5) and **XI**(7.3) as

$$T = 2G(a^2+b^2)Q/(\pi a^3 b^3) \tag{7.6}$$

if the applied torque is given.

7.5. **Infinitesimal spatial-displacement.** From **XI**(5.19),

$$U_{z;x} = TR_y + 2G\beta_{;y} = TR_y - 4GKR_y/b^2$$
$$U_{z;y} = -TR_x - 2G\beta_{;x} = -TR_x + 4GKR_x/a^2$$

Integration gives the 'warping' displacement

$$U_z = -T(a^2-b^2)R_xR_y/(a^2+b^2) \tag{7.7}$$

giving the departure of plane sections of the deformed body from their initially non-planar undeformed shape. Also, from **XI**(5.19), are found Saint-Venant's assumed spatial-displacements

$$U_x = -TR_yR_z \qquad U_y = TR_zR_x \tag{7.8}$$

7.6. **Constant-vorticity, inviscid, incompressible fluid analogic solution.** Consider the solution of torsion of the solid, elliptic cylinder by the analogue of article **XI**,5.11. H. Lamb [150] gives the stream function β for the flow of fluid relative to an elliptic boundary rotating at constant angular velocity ω as [21.10]

$$\beta = (1-R_x^2/a^2-R_y^2/b^2)a^2b^2\omega/(a^2+b^2) \tag{7.9}$$

Comparison with **XI**(7.2) shows that it is the Boussinesq stress function for this case, with

$$\omega = \tfrac{1}{2}T/G \tag{7.10}$$

This is similar to **XI**(5.27) except for the unimportant change in sign of T. The streamlines β constant are geometrically similar to the outer boundary just as the shear stress trajectories are in article **XI**,7.2.

8. Torsion of a right, hollow cylinder of elliptical cross-section with geometrically similar inner and outer boundaries: Saint-Venant's solution

The analysis of this case follows directly from the analysis for the solid cylinder given in article **XI**,7.

8.1. **Stresses and stress-free boundaries.** Article **XI**,7.2 gives the torsional shear stress components and shows that their

resultant is linear with respect to position, zero at the axis of twist and tangential to the ellipse

$$1-R_x^2/(ka)^2-R_y^2/(kb)^2 = 0 \tag{8.1}$$

with $0 < k \leqq 1$, geometrically similar to the outer boundary and passing through the given point. Therefore, every such ellipse within the outer boundary can be chosen as the projection of a stress-free cylindrical boundary defining the elliptical hole in the hollow cylinder. On each ellipse the minimum, maximum stresses occur at the ends of the major, minor semi-axes respectively.

8.2. **Torque.** The torque is found in a similar manner to that in article **XI**,7.3 with the integration over the area (A_o-A_i) with A_o, A_i the areas enclosed by the outer, inner boundaries respectively. For the inner boundary let the parameter k have value k_i, and then

$$Q = (1-k_i^4)\pi Kab \tag{8.2}$$

8.3. **Angle of twist and infinitesimal spatial-displacement.** The infinitesimal angle of twist T per unit length of cylinder can be regarded as given when assuming the infinitesimal spatial-displacement values as in article **XI**,7.5. Nothing changes for the hollow, elliptical section here, so that the values U_x, U_y, U_z of the spatial-displacement components there also apply here, so they will not be repeated. For a given angle of twist the torque is reduced by the factor $(1-k_i^4)$, as in **XI**(8.2), for the hollow shaft as compared with the solid shaft.

Chapter XII

SHEARING THIN, PLANE LAMINÆ

1. A particular form from the specialised theory on torsion and a hydrodynamical analogy †

Consider again the basal solution for the particular plane $R_z = 0$ giving equations **XI**(6.10), **XI**(6.11). In this case the normal unit vector $\mathbf{n}$ is chosen to be normal to axis OR_z, while the conjugate stress potential β is constant along the one or more boundaries of the cross-section.

1.1. **Stresses in terms of the stress potential and its conjugate.** With $\mathbf{S}_z$ the resultant shear stress at a point in the plane, Table **XI**,6.1 gives

$$\alpha_{;x} = S_{zx} = \beta_{;y} \qquad \alpha_{;y} = S_{zy} = -\beta_{;x} \tag{1.1}$$

or, vectorially, with the two-dimensional nabla operator,

$$\nabla\alpha = \mathbf{S}_z = (\nabla\times\mathbf{c}_z)\beta \tag{1.1'}$$

while, with $0 \leqq R_z \leqq \delta R_z$,

$$\delta S_{xy} \to 0 = S_{zz} \qquad \delta S_{xx} \to 0 \leftarrow \delta S_{yy} \tag{1.2}$$

with the δ indicating quantities having values in the range from zero to first-order smallness with R_z. Thus, in the stress dyadic all stresses are zero or negligible in comparison with the finite shear stress $\mathbf{S}_z$ on the plane.

Since $\mathbf{n}$ is normal to $\mathbf{c}_z$, then from equations **XI**(6.8′) the boundary is stress-free when

$$0 = n_x\alpha_{;x} + n_y\alpha_{;y} = \mathbf{n}\cdot\nabla\alpha = \mathbf{n}\cdot\mathbf{S}_z \tag{1.3}$$

Therefore the shear stress $\mathbf{S}_z$ is tangential to the boundary.

1.2. **Hydrodynamical analogue.** Since α, β obey the Cauchy-Riemann conditions in **XII**(1.1), then they are both solutions of the laplacian

$$\nabla^2\alpha = 0 = \nabla^2\beta \tag{1.4}$$

† Author, 1951.

With $i = \sqrt{(-1)}$, then the complex variable solution is

$$\gamma(c) = \alpha(R_x, R_y) + i\beta(R_x, R_y) \qquad c = R_x + iR_y \tag{1.5}$$

with the trajectories β constant and α constant intersecting orthogonally as in article **B**,4.

This is analogous to irrotational, inviscid fluid motion with α the velocity potential and β the stream function. On a streamline β is constant while α varies. On an equipotential trajectory orthogonal to the streamline α is constant while β varies.

The negative vector gradient of the velocity potential will be used to conform with common usage in fluid mechanics. Thus, the fluid velocity

$$\mathbf{V} = -\nabla\alpha \tag{1.6}$$

so that, with **XII**(1.1′),

$$\left.\begin{aligned} V_x &= -\alpha_{;x} = -\beta_{;y} = -S_{zx} \\ V_y &= -\alpha_{;y} = \beta_{;x} = -S_{zy} \end{aligned}\right\} \tag{1.7}$$

while speed V equals the resultant shear stress S_z tangential to the streamline.

1.3. **Solutions for irrotational, inviscid fluid motion.** There are available many mathematical solutions for irrotational, inviscid fluid motion.† Thus, the mathematical solution for the circulation of fluid in concentric, circular paths [21.1, 150] gives a solution of torsion of a circular cross-section. The complex variable is a powerful technique to use in studying other shapes of streamlines.

It has been found experimentally that, for moderate speeds, fluid such as water, and gas such as air have the velocities predicted by irrotational flow theory so long as solid surfaces are not approached too closely. The water or air is stationary in the layer in contact with the solid surface but attains the predicted velocities outside a thin *boundary layer* in which the velocity gradients are large in the direction normal to the surface. Therefore, in a problem for which the cross-section is of such a shape that mathematical analysis is not convenient, the setting up of a suitable flow in which the speed, and hence shear stress, can be measured gives the solution with the streamlines defining the

† References [150, 21, 151] were consulted for the methods of formulation of the particular flows here. The reader should consult these books or others on classical hydrodynamics for a fuller discussion than is appropriate here.

shear stress trajectories. Alternatively, the recent elaboration of numerical methods of solving† Laplace's equation by A. Thom [76], R. V. Southwell [77] and others allows the analysis of complicated cross-sectional shapes.

The analogue presented here was anticipated qualitatively by Thomson & Tait, in 1867 [19.4], in the following words: '. . . the actual *shear* ‡ of the solid, in any infinitely thin plate of it between two normal sections, will at each point be, when reckoned as a differential sliding parallel to their planes, equal to and in the same direction § as the velocity of the liquid relatively to the containing box ||'.

1.4. **Formulæ for fluid motion.** Now determine the velocity and speed [21.2] at a point and the streamline pattern [21.3] and hence, by analogy, the magnitude and direction of the shear stress $\mathbf{S}_z$ and the shear-stress trajectories.

The additive properties of complex numbers are similar to those of vectors, so that we may write

$$\mathbf{V} = V_x + iV_y \tag{1.8}$$

while its conjugate, as in Fig. **XII**,1.1, is

$$\mathbf{V}' = V_x - iV_y \tag{1.9}$$

But, from the complex potential,

$$\gamma = \alpha + i\beta$$
$$\alpha_{;x} + i\beta_{;x} = \gamma_{;x} = (d\gamma/dc)c_{;x} = d\gamma/dc \tag{1.10}$$

since

$$c = R_x + iR_y$$

Substituting from **XII**(1.7) in **XII**(1.10) gives the conjugate velocity

$$\mathbf{V}' = -d\gamma/dc \tag{1.11}$$

† The reader should consider the objections raised in articles **C**,4.5, **C**,7.2, **C**,7.3 here.

‡ This means *shear strain*, that is linearly proportional to shear stress for the small, elastic straining of an isotropic solid with which Thomson & Tait dealt.

§ Opposite direction to that in **XII**(1.6) because of the negative sign introduced there.

|| That is, the enclosing solid boundary.

To find the velocity the sign of i must be changed throughout. That is, $\gamma(c)$ must be changed to $\gamma'(c')$ with the conjugate of c as

$$c' = R_x - iR_y \tag{1.12}$$

Then,

$$\mathbf{V} = -d\gamma'/dc' \tag{1.13}$$

To find the speed, note that

$$V^2 = V_x^2 + V_y^2 = (V_x + iV_y)(V_x - iV_y) = (d\gamma/dc)(d\gamma'/dc') \tag{1.14}$$

with the last following from **XII**(1.13), **XII**(1.11). Sometimes it is useful to have the reciprocal form

$$V^{-2} = (dc/d\gamma)(dc'/d\gamma') \tag{1.15}$$

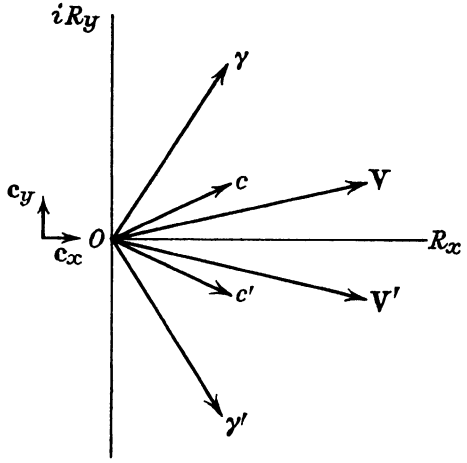

FIG. XII,1.1.—The conjugate complex number c' is given by reversing the imaginary component of the complex number c. Similarly, the conjugate complex function γ' is given by reversing the imaginary component. The conjugate vector $\mathbf{V}'$ is given by reversing the V_y component of $\mathbf{V}$.

1.5. **Equations of the streamlines.** With X, Y the real and imaginary parts of $\exp \gamma$, then

$$X = \exp \alpha \cos \beta \qquad Y = \exp \alpha \sin \beta \tag{1.16}$$

so that

$$Y = X \tan \beta \tag{1.17}$$

Therefore, if $\tan \beta$ is given a constant value on the streamline β equals a constant, then this equation is that of the streamline [21.4]. When $\beta = 0, \pi, \ldots$, then $Y = 0$ are the corresponding streamlines. When $\beta = \frac{1}{2}\pi, \frac{3}{2}\pi, \ldots$, then $X = 0$ are the corresponding streamlines.

1.6. **Displacements.** From article **XI**,6.10 the relative-displacement $\mathbf{D}^* \to \mathbf{D}_z^*$ as $R_z \to \delta R_z \to 0$ when whole-body translation is zero. Thus,

$$\mathbf{D}^* \to G\alpha \mathbf{c}_z \tag{1.18}$$

The velocity-potential function to give this warping component of relative-displacement is found most easily, in some cases, from the form **XII**(1.16). Thus,

$$X^2+Y^2 = \exp(2\alpha)$$

so

$$\alpha = \log \sqrt{(X^2+Y^2)}$$

1.7. **Warping and residual stresses.** The loaded, elastic, plane lamina will not remain plane, in general, after unloading. If it is constrained to remain more or less plane like a glue layer, for example, then the removal of the applied surface stresses S_{zx}, S_{zy} will not leave the lamina stress-free. Alternatively, if the stress-free lamina is plane and remains plane when loaded, then the stresses in article **XII**,1.1 will not maintain the deformation. Intuitively, it appears that a small normal stress S_{zz} is required to 'flatten' the lamina.

2. Shearing of a long, plane, strip lamina: theoretical

Choose,

$$\gamma = \alpha+i\beta = Sc = S(R_x+iR_y) \tag{2.1}$$

so that the velocity potential and stream function are, respectively,

$$\alpha = SR_x \qquad \beta = SR_y \tag{2.2}$$

From **XII**(1.7),

$$-V_x = S_{zx} = \alpha_{;x} = S \qquad -V_y = S_{zy} = \alpha_{;y} = 0 \tag{2.3}$$

Further, all other stress components are zero, and not merely negligible by being first-order small quantities, so that the applied stresses are as in Fig. **XII**,2.1. The streamlines β constant are straight and parallel to the axis OR_x.

The relative-displacement magnitude

$$D_z^* = G\alpha = GSR_x \tag{2.4}$$

shows that the lamina remains flat but it is to suffer zero spatial-rotation while the load is being applied, so that allowance must be made for strain transfer as in articles **III**,6, **III**,8.

3. Shearing of an infinite, plane lamina containing a circular hole: theoretical

The hydrodynamical analogy shows that the shearing of an infinite, plane lamina containing a circular hole is mathematically similar to the uniform two-dimensional flow around an obstacle of circular cross-section. For such a case the complex potential [21.5, 150]

$$\gamma = S(c+a^2/c) \tag{3.1}$$

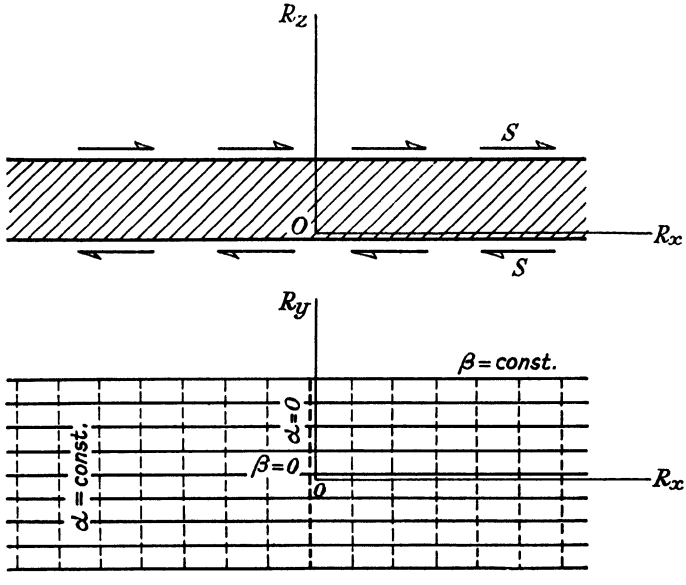

FIG. XII,2.1.—Shear stress S in direction OR_x on a lamina with its main faces normal to OR_z. Trajectories for the conjugate stress potential β = constant are those for shear stress shown as solid lines. The dotted lines are trajectories of stress potential α = constant. Any line β = constant can be taken as in a stress-free surface normal to OR_y.

with S the uniform speed in the negative direction of OR_x at infinity and a the radius of the obstacle. Separating this into real and imaginary parts gives the velocity potential and stream function respectively as

$$\left.\begin{aligned} \alpha &= S[R_x+a^2R_x/(R_x^2+R_y^2)] = S[R_r\cos\theta+(a^2/R_r)\cos\theta] \\ \beta &= S[R_y-a^2R_y/(R_x^2+R_y^2)] = S[R_r\sin\theta-(a^2/R_r)\sin\theta] \end{aligned}\right\} \tag{3.2}$$

The OR_x axis for $-\infty \leqq R_x \leqq -a$ and $a \leqq R_x \leqq \infty$ together

with the circle $R_r = a$ constitute the streamline $\beta = 0$. Several streamlines are shown in Fig. XII,3.1.

3.1. **Speeds.** The speed is given by

$$V^2 = (d\gamma/dc)(d\gamma'/dc') = S^2(1-a^2/c^2)(1-a^2/c'^2)$$

so that

$$(V/S)^2 = 1-2a^2R_r^{-2}\cos 2\theta+a^4R_r^{-4} \qquad (3.3)$$

The speed is zero at the points $R_r = a$, $\theta = 0$ and π. These are

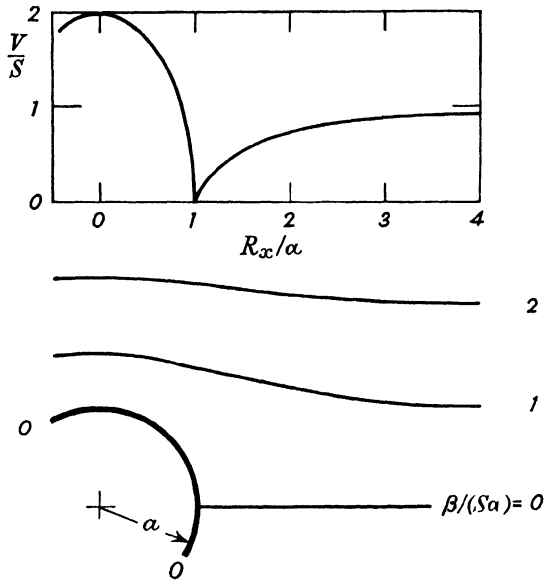

FIG. XII,3.1.—Shear stress S applied at infinity to a lamina having a stress-free circular hole of radius a. The lower view shows some shear-stress trajectories on each of which the conjugate stress potential has a constant value. The upper view gives the distribution of local shear stress V on the trajectory formed by the axis OR_x and the circumference of the hole. The maximum value is twice the value of the uniform shear stress at infinity.

the 'stagnation' points of the flow. The speed or shear stress is shown in Fig. XII,3.1 for various distances along the OR_x axis on streamline $\beta = 0$. The maximum velocity occurs at $R_r = a$, $\theta = \frac{1}{2}\pi$, $\frac{3}{2}\pi$ and is of value $2S$.

For the shearing case, the velocity at infinity must be reversed to give the shearing stress, while the local velocity must also be reversed to give the local shear stress. Then, the values of V/S

are found from XII(3.3) with the maximum shear stress of value $2S$ at $R_r = a$, $\theta = \frac{1}{2}\pi, \frac{3}{2}\pi$. The shear stress rapidly approaches the value for uniform shearing with increase of radial position. Thus, at $R_r/a = 2$ the shear stress approaches the value S. Equation XII(3.3) shows that the shear-stress ratio V/S is independent of the size of the hole.

4. Shearing of a long, strip lamina with a semicircular indentation of one edge

This case is readily analysed with the solution in article XII,3. Any shear-stress trajectory (i.e. any streamline by analogy) can

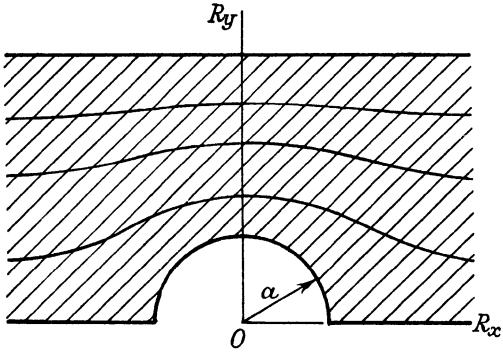

FIG. XII,4.1.—The shear-stress distribution in Fig. XII,3.1 can also be used to give that in a strip having a semicircular indentation in one edge as shown. The disturbance due to the indentation decreases rapidly with position along OR_y. The shear stress very quickly becomes virtually uniform as it is at infinity, so that the upper edge is virtually straight to define a strip.

be taken as defining the right, cylindrical stress-free face of the lamina. Therefore, the line β zero gives the indented edge in Fig. XII,4.1. The shear-stress trajectories rapidly become virtually straight and parallel with increase of R_y and, therefore, one of the streamlines can be chosen as the upper edge of the strip parallel to the OR_x axis. The stress values are precisely as in article XII,3.

5. Shearing of a long, strip lamina changing width abruptly

Consider the two-dimensional flow in a straight channel with an abrupt change in width [21.6], as in Fig. XII,5.1. With S the

velocity at infinity, where the channel is of width h, while the channel is of width k after the abrupt change in width, the complex potential is given from

$$c = \frac{h}{\pi}\left(\log\frac{1+t}{1-t} - \frac{1}{a}\log\frac{a+t}{a-t}\right) \tag{5.1}$$

with

$$t^2 = \frac{\exp\left[\gamma\pi/(Sh)\right]-a^2}{\exp\left[\gamma\pi/(Sh)\right]-1} \tag{5.2}$$

The speed can be found from

$$V^{-2} = (dc/d\gamma)(dc'/d\gamma') \tag{5.3}$$

as in XII(1.15). The form found is complicated, but the reader may find it an interesting exercise to carry out the differentiations

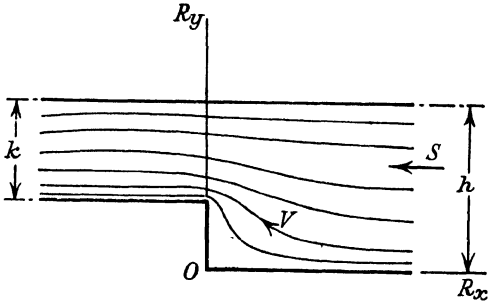

FIG. XII,5.1.—Shearing of a strip that changes width abruptly from width h to width k. Uniform shear stress S is applied at infinity to the strip of width h, and uniform shear stress Sh/k at infinity to the width k. A few shear-stress trajectories are shown diagrammatically.

and then examine the velocities in the neighbourhood of the change in width.

This problem is easily examined experimentally with a two-dimensional flow of water, for example, although the formal mathematical treatment is complicated. Sources of dye upstream will define the streamlines, while the speed can be measured at each position by a pitot-tube or hot wire, etc.

6. Shearing of an infinite, plane lamina containing an elliptical hole

The solution for two-dimensional flow past an elliptical obstacle is known [21.7, 150] and described most easily in terms of elliptic coordinates.

6.1. **Elliptic coordinates.** Thus, with

$$c = a \cosh \zeta \qquad \zeta = \xi + i\eta \tag{6.1}$$

then, by successive elimination there occur the two equations

$$R_x^2/(a^2 \cosh^2 \xi) + R_y^2/(a^2 \sinh^2 \xi) = 1 \tag{6.2}$$

$$R_x^2/(a^2 \cos^2 \eta) - R_y^2/(a^2 \sin^2 \eta) = 1 \tag{6.3}$$

For a given value of $\xi = \xi_0$ equation **XII**(6.2) is that of an ellipse with semi-axes $(a \cosh \xi_0)$ and $(a \sinh \xi_0)$. Equation **XII**(6.3) is that for an hyperbola and is orthogonal to and confocal with the ellipses. The foci of both systems of curves are $2a$ apart on the real axis. The point at which the ellipse ξ_0 constant intersects the hyperbola η_0 constant is said to have the elliptic coordinates (ξ_0, η_0). A more detailed description is given in references [21.8, 150], for example.

6.2. **Flow past an inclined ellipse.** The complex potential for flow, at angle ϕ to the axis OR_x, past an elliptical obstacle with its major axis in the direction OR_x is

$$\alpha + i\beta = \gamma = Sa(\cosh \xi_0 + \sinh \xi_0) \cosh (\zeta - \xi_0 - i\phi) \tag{6.4}$$

with S the uniform speed at infinity.

The velocity can be found as described in article **XII**,1.4 but will not be detailed here. The reader may find it as an exercise. The main concern here is with the maximum velocities and these occur on the ellipse ξ_0 constant. On the elliptical boundary,

$$\left(\frac{V}{S}\right)^2 = \frac{(\cosh \xi_0 + \sinh \xi_0) \sin^2 (\eta - \alpha)}{(\cosh \xi_0 - \sinh \xi_0)(\sinh^2 \xi_0 + \sin^2 \eta)} \tag{6.5}$$

The hydrodynamical analogue gives the local speed V equal to the local shear stress.

6.3. **Flow past an inclined plate.** As ξ_0 is chosen smaller the ellipse becomes more nearly a line of length $2a$ for which $\xi_0 = 0$. Thus, in the limit the flow is past a flat plate. However, this cannot correspond to reality because the speed tends to infinity at the ends of the plate. The plate corresponds to a straight crack of length $2a$ for the case of shear.

7. Axial torsion of a hollow, elliptical lamina

The hydrodynamical analogue to circulation of irrotational fluid allows a known solution [21.4, 150] to be applied to torsion.

7.1. **Complex potential.** Take the complex variable as a function of the complex potential in the form

$$c = k \cos \gamma \tag{7.1}$$

with k an undetermined constant. Noting that $\cos i\beta = \cosh \beta$ and $\sin i\beta = i \sinh \beta$ and separating the real and imaginary parts gives

$$R_x = k \cos \alpha \cosh \beta \qquad R_y = -k \sin \alpha \sinh \beta \tag{7.1'}$$

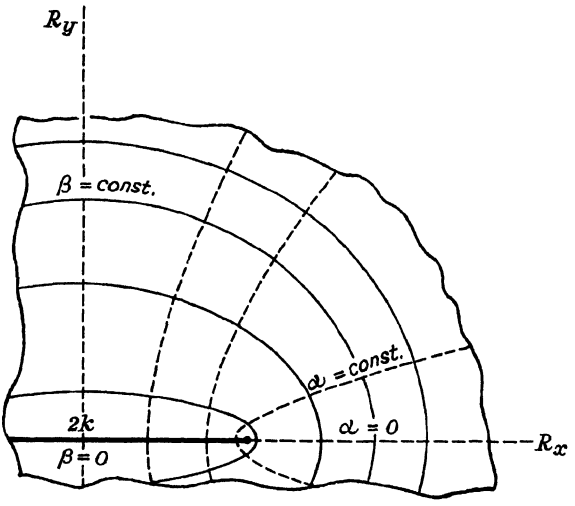

FIG. XII,7.1.—A family of confocal ellipses with foci $2k$ apart are shown as full lines. A family of confocal hyperbolæ with foci $2k$ apart are shown as dotted lines. The intersection of the ellipse for β = constant and the hyperbola α = constant gives a point located by the elliptic coordinates (α, β).

7.2. **Streamlines and equipotential lines.** Eliminating the velocity potential α gives the family of confocal ellipses, with semi-axes $k \cosh \beta$, $k \sinh \beta$,

$$R_x^2/(k^2 \cosh^2 \beta) + R_y^2/(k^2 \sinh^2 \beta) = 1 \tag{7.2}$$

as the equation for the family of streamlines on each of which the stream function β has a constant value. Taking $\beta = 0$ gives the limiting case of a line of length $2k$ along the axis OR_x.

Eliminating the stream function β in XII(7.1') gives the family of confocal hyperbolæ

$$R_x^2/(k^2 \cos^2 \alpha) - R_y^2/(k^2 \sin^2 \alpha) = 1 \tag{7.3}$$

on each of which the velocity potential α has a constant value.

These equipotential trajectories are orthogonal to the streamlines given by **XII**(7.2). Fig. **XII**,7.1 shows diagrammatically some of the streamlines and equipotential lines.

7.3. **Speed.** From article **XII**,1.4, with equation **XII**(7.1), the speed is found from

$$(k/V)^2 = \sin\gamma \sin\gamma' = \tfrac{1}{2}(\cosh 2\beta - \cos 2\alpha) \qquad (7.4)$$

The value of the speed is also the value of the resultant shear stress, and Fig. **XII**,7.2 shows Vk vs. R_x/k for a few values of β. The streamlines rapidly become very good approximations to circles with increase of the radius. When β equals 2, then the streamline is almost circular and the tangential speed almost constant. At the smaller values of β the speed changes considerably with position on the streamline and becomes theoretically infinite at the ends of the straight line $\beta = 0$. The value of the parameter k can be chosen arbitrarily of any positive value. When k is very small, but not zero, then the straight line $\beta = 0$ becomes short, while the streamlines become virtually circular of small radius. For example, choosing $k = 0{\cdot}10$, then the streamline $\beta = 2$ occurs at a radius of about 0·36, with the speed, and hence shear stress, virtually constant of value about 2·6. Outside this streamline the streamlines are even more closely circular, with speeds decreasing fairly slowly with radius. The largest speed, and hence shear stress, occurs at the end of the major axis for a given streamline.

7.4. **Hollow, elliptical lamina.** Any of the elliptical streamlines can be taken as a stress-free boundary. For a given value of k in **XII**(7.2) the radial position (R_x, R_y) increases with increase of the value of stream function β. Equation **XII**(7.4) and Fig. **XII**,7.2 indicate that the stresses tend to infinite values as $\beta \to 0$, so that there must be an inner boundary for the lamina on which $\beta > 0$. Equation **XII**(7.4) gives the distribution of the shear stresses decreasing with increase of radius to zero at infinity.

7.5. **Comparison with Saint-Venant's solution.** Saint-Venant's solution for the hollow elliptical cross-section with geometrically similar inner and outer boundaries is given in article **XI**,8.1. There the stresses increase with increase of radius, whereas here they decrease. There the stresses are a

maximum at the ends of the minor axis, whereas here they are a maximum at the ends of the major axis.

The reason can be seen by considering this solution with the present author's modification of Saint-Venant's solution in article

I,7.2

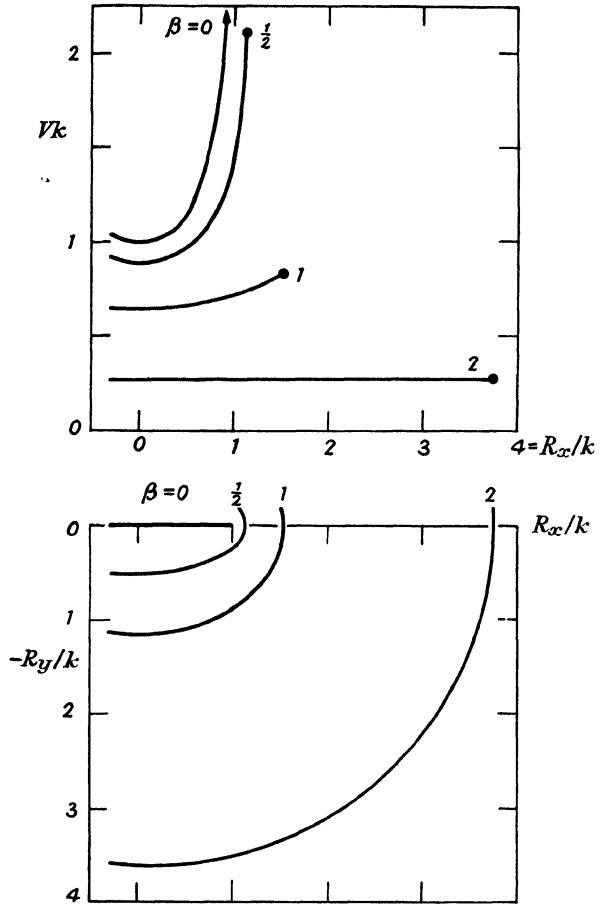

FIG. XII,7.2.—Shear-stress trajectories shaped as confocal ellipses are analogous to the circulation of inviscid, irrotational fluid around a plate of length $2k$ as in the lower figure. The ellipses rapidly become virtually circular with increase of radial position. The upper figure shows the distribution of shear stress on the corresponding elliptical trajectories in the lower figure. The shear stresses rapidly become virtually independent of angular position with increase of radial position.

XI,5.13. In this lamina, the conditions on stress, strain and the conjugate stress-potential function are just as in Saint-Venant's solution, but here some of the stress gradients with respect to R_z are not zero. The solution there shows most difference from the one here in the making of arbitrary assumptions on displacements by Saint-Venant and on displacement gradients by the present author. These latter lead to a laplacian solution for β, as here or in article **XI**,5.13, whereas Saint-Venant's assumptions on constancy of angle of twist per unit length lead to a poissonian equation.

The stress-free fibre on the axis of twist suffers twist according to Saint-Venant's solution. The present author regards this as an anomaly that Cauchy [19.6], presumably intuitively, could not accept, as is mentioned in article **XI**,5.2. The present particular solution leads to Navier's conclusion, in 1864 [24], on the high stressing of most distant parts of a given boundary, although this is not necessarily true in general as inferred by Navier, as may be seen at orthogonal corners where the shear stresses must be zero. Navier's inference followed from assuming, fallaciously, that plane sections always remained plane as in Coulomb's theory, although Saint-Venant's solution for rectangular and elliptical sections was published seventeen years earlier and was justified, qualitatively at least, by experiments with rubber showing the 'warping' of planes.

The author's solution here is compatible in Saint-Venant's strains compatibility conditions, but Saint-Venant's solution is not compatible in the author's more restrictive conditions. Therefore, the Saint-Venant compatibility conditions allow the acceptance of the 'dislocational rotation' of a stress-free fibre where this is rejected by the author's compatibility conditions. Dislocational rotation is discussed in article **V**,15.5 and volume I, article **III**,9.4

Appendix A

VECTOR ANALYSIS

1. Introduction

The deformation problem deals continually with dependent variable vector functions having a definite value at each point of the function space. Such a vector function is said to constitute a *vector field* in the space and its change in value from point to point must be considered.

Volume I, appendix A treats the cartesian forms for the vector analysis used in this treatise. The solution of particular problems is frequently more convenient in appropriate, curvilinear, orthogonal coordinates, so the various operators and the results of their operations are now formulated explicitly for cylindrical and spherical coordinates and the general curvilinear forms indicated.

If the presentation here of expressions formulated in volume I is too terse, then volume I or a standard work such as *Vector Analysis* (G. Bell & Sons, 1921 and subsequently), by C. E. Weatherburn, for example, should be consulted. The present writer has derived so much instruction and pleasure from this latter book that explicit references are given to it in volume I and here.

2. Notation

Vectors are denoted by bold upright capitals, their arithmetical magnitude or modulus by the corresponding italic capital and the unit vector in the direction of the vector, or briefly its 'direction', by the lower-case upright bold. Thus, for example,

$$\mathbf{A} = A\mathbf{a} \tag{2.1}$$

Orthogonal *cartesian* unit vectors are $\mathbf{c}_1$, $\mathbf{c}_2$, $\mathbf{c}_3$, denoted briefly by $\mathbf{c}_i$ or $\mathbf{c}_j$ or $\mathbf{c}_k$. For physical applications a particular sequence is more convenient, as in the table

$i = 1$	2	3
$j = 2$	3	1
$k = 3$	1	2

(2.2)

Sometimes $\mathbf{c}_x$, $\mathbf{c}_y$, $\mathbf{c}_z$ may be used in place of $\mathbf{c}_i$.

The orthogonal unit vectors of curvilinear coordinates take special values, in general, for each point of the coordinate space. Where brevity is secured by using general subscripts for cylindrical, spherical, . . . coordinates they are $\mathbf{c}_a$, $\mathbf{c}_b$, $\mathbf{c}_c$.

Dyadics have been denoted by an Old English face, like $\mathfrak{A}$ for example, while quadadics are shown by bold italic sanserif, like $\boldsymbol{A}$ for example.

3. Scalar product

The scalar product C of vectors $\mathbf{A}$, $\mathbf{B}$, with [A,B] the angle between them, is

$$C = \mathbf{A}\cdot\mathbf{B} = AB\cos[\mathbf{A},\mathbf{B}] = \sum_a A_a B_a = \mathbf{B}\cdot\mathbf{A} \tag{3.1}$$

since

$$\mathbf{A} = \sum_a A_a \mathbf{c}_a \qquad \mathbf{B} = \sum_a B_a \mathbf{c}_a \tag{3.2}$$

and

$$\mathbf{c}_a\cdot\mathbf{c}_b = \left.\begin{matrix}1 \text{ when } \mathbf{c}_a = \mathbf{c}_b \\ 0 \text{ when } \mathbf{c}_a \neq \mathbf{c}_b\end{matrix}\right\} = \mathbf{c}_b\cdot\mathbf{c}_a \tag{3.3}$$

The scalar product sign is referred to as 'dot' so that the term 'dot product' is sometimes used.

4. Vector product

The vector product $\mathbf{Q}$ of two vectors $\mathbf{A}$, $\mathbf{B}$ is

$$\mathbf{Q} = \mathbf{A}\times\mathbf{B} = \mathbf{q}AB\sin[\mathbf{A},\mathbf{B}] = -\mathbf{q}BA\sin[\mathbf{B},\mathbf{A}] = -\mathbf{B}\times\mathbf{A} \tag{4.1}$$

and, also,

$$\mathbf{Q} = \sum_{a,b,c} \mathbf{c}_a (A_b B_c - A_c B_b) \tag{4.2}$$

since

$$\left.\begin{aligned}\mathbf{c}_a\times\mathbf{c}_a &= 0 \\ \mathbf{c}_a\times\mathbf{c}_b &= \mathbf{c}_c = -\mathbf{c}_b\times\mathbf{c}_a\end{aligned}\right\} \tag{4.3}$$

The vector product sign is referred to as 'cross' so that the term 'cross product' is sometimes used.

5. Passive † product

The passive product $\mathfrak{C}$ of vectors **A**, **B** is

$$\mathfrak{C} = \mathbf{AB} = AB\mathbf{ab} = \sum_{a,b,c}(A_aB_a\mathbf{c}_a\mathbf{c}_a + A_aB_b\mathbf{c}_a\mathbf{c}_b + A_aB_c\mathbf{c}_a\mathbf{c}_c) \tag{5.1}$$

This is a *dyad*. In general,

$$\mathbf{BA} \neq \mathbf{AB} \tag{5.2}$$

Similarly, a quadad is given by the passive product of four vectors. Thus,

$$\mathbf{E} = \mathbf{ABCD} = \sum_{a,b,c}(A_aB_aC_aD_a\mathbf{c}_a\mathbf{c}_a\mathbf{c}_a\mathbf{c}_a + \ldots) \tag{5.3}$$

and the sequence must be retained because, generally,

$$\mathbf{ACBD} \neq \mathbf{ABCD} \neq \ldots \tag{5.4}$$

6. Self-conjugate dyadic transformation

The dyadic,

$$\mathfrak{C} = \sum_{a,b}[C_{aa}\mathbf{c}_a\mathbf{c}_a + C_{ab}(\mathbf{c}_a\mathbf{c}_b + \mathbf{c}_b\mathbf{c}_a)] \tag{6.1}$$

is self-conjugate, because interchange of unit vectors in each unit dyad leaves the dyadic unchanged. The idemfactor $\mathfrak{J}$ is a special case with the 'mixed' coefficients zero and the 'unmixed' equal to unity. (See volume I, articles A,10 and A,23 for its properties.)

6.1. Mohr's construction for a two-dimensional dyadic.

If the self-conjugate dyadic is two-dimensional, then

$$\mathfrak{C} = C_{aa}\mathbf{c}_a\mathbf{c}_a + C_{bb}\mathbf{c}_b\mathbf{c}_b + C_{ab}(\mathbf{c}_a\mathbf{c}_b + \mathbf{c}_b\mathbf{c}_a) = C_{\mathrm{i}}\mathbf{x}_{\mathrm{i}}\mathbf{x}_{\mathrm{i}} + C_{\mathrm{j}}\mathbf{x}_{\mathrm{j}}\mathbf{x}_{\mathrm{j}} \tag{6.2}$$

with the last its 'principal' form, as shown in volume I, article A,9, with directions $\mathbf{x}_{\mathrm{i}}$, $\mathbf{x}_{\mathrm{j}}$ in the plane of $\mathbf{c}_a$, $\mathbf{c}_b$ as in Fig. A,6.1.

Using,

$$\left.\begin{aligned} \mathbf{c}_a\cdot\mathbf{x}_{\mathrm{i}} &= \cos\theta & \mathbf{c}_a\cdot\mathbf{x}_{\mathrm{j}} &= -\sin\theta \\ \mathbf{c}_b\cdot\mathbf{x}_{\mathrm{i}} &= \sin\theta & \mathbf{c}_b\cdot\mathbf{x}_{\mathrm{j}} &= \cos\theta \end{aligned}\right\} \tag{6.3}$$

then, with the double product notation of volume I, article A.22.1,

$$\left.\begin{aligned} C_{aa} &= \mathbf{c}_a\mathbf{c}_a : \mathfrak{C} = \tfrac{1}{2}(C_{\mathrm{i}}+C_{\mathrm{j}}) + \tfrac{1}{2}(C_{\mathrm{i}}-C_{\mathrm{j}})\cos 2\theta \\ C_{bb} &= \mathbf{c}_b\mathbf{c}_b : \mathfrak{C} = \tfrac{1}{2}(C_{\mathrm{i}}+C_{\mathrm{j}}) - \tfrac{1}{2}(C_{\mathrm{i}}-C_{\mathrm{j}})\cos 2\theta \\ C_{ab} &= \mathbf{c}_a\mathbf{c}_b : \mathfrak{C} = \tfrac{1}{2}(C_{\mathrm{i}}-C_{\mathrm{j}})\sin 2\theta \end{aligned}\right\} \tag{6.4}$$

† Other writers refer to this as the 'dyadic product' because, historically, second-order -adics (or second-order tensors) were the only ones analysed [28]. However, we deal with triads, quadads, . . ., so that a more general, self-explanatory term like 'passive product' is convenient.

These relationships are amenable to easy geometrical interpretation on a plane diagram due to Mohr [78], in 1882. Set off C_i, C_j coinitially as in Fig. A,6.2 for *positive* values of these quantities. Draw a circle of radius $\frac{1}{2}(C_i - C_j)$ as shown. A radius vector is described at angle 2θ to C_i to give C_{aa}, C_{bb}, C_{ab} as shown. The construction for the converse transformation to pass from C_{aa}, C_{bb}, C_{ab} to C_i, C_j is evident from the figure.

Volume I, article A,9, shows that when a self-conjugate dyadic is transformed from one set of axes to another set, there are three combinations of the scalar coefficients which retain their arithmetical values for any axes. These are the three invariants of

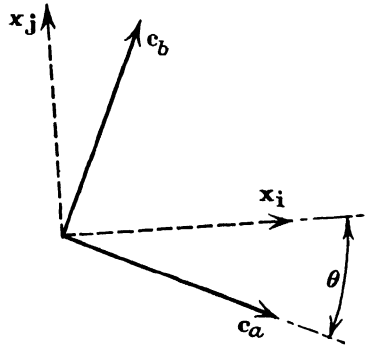

FIG. A,6.1. Unit vectors $\mathbf{x}_i$, $\mathbf{x}_j$ are the principal directions for a two-dimensional self-conjugate dyadic. The unit vectors $\mathbf{c}_a$, $\mathbf{c}_b$ are the coordinate directions and θ gives the orientation of the dyadic relative to them.

which the first $\chi^{(1)}$ is the most important in deformation analysis. Thus, from A(6.4),

$$\mathfrak{I}:\mathfrak{C} = \chi^{(1)} = C_{aa} + C_{bb} = C_i + C_j \tag{6.4'}$$

for the present two-dimensional dyadic.

6.2. **Principal components explicitly in terms of the general components.** Geometrically, from Fig. A,6.2,

$$\left.\begin{aligned} C_i &= \tfrac{1}{2}(C_{aa}+C_{bb}) - \sqrt{[\tfrac{1}{4}(C_{aa}-C_{bb})^2 + C_{ab}^2]} \\ C_j &= \tfrac{1}{2}(C_{aa}+C_{bb}) + \sqrt{[\tfrac{1}{4}(C_{aa}-C_{bb})^2 + C_{ab}^2]} \end{aligned}\right\} \tag{6.5}$$

When $(C_{aa}+C_{bb}) = 0 = (C_i+C_j)$, then the first invariant of $\mathfrak{C}$ is zero to give

$$-C_i = C_j = \sqrt{[\tfrac{1}{4}(C_{aa}-C_{bb})^2 + C_{ab}^2]} \tag{6.6}$$

The principal normal components are equal but of opposite sign, as also are the general normal components. The origin of Fig. A,6.2 is at the centre of the circle of a radius equal to the magnitude of the principal normal components and of the maximum shear component. This latter acts on planes at 45° and 135° to the principal directions.

When, on the right-hand side of A(6.5), the square root is less than the first term, then C_i and C_j are of the same sign. Thus,

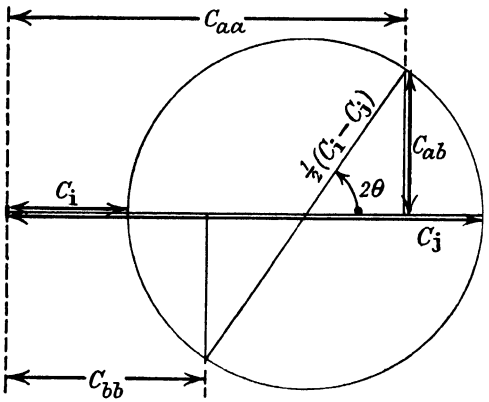

FIG. A,6.2.—Mohr's construction for invariant transformation of a two-dimensional self-conjugate dyadic. The scalar, principal components are C_i, C_j, while the general components are C_{aa}, C_{bb}, C_{ab}. Angle θ is that in Fig. A,6.1.

explicitly, forming the inequality, squaring both sides, cancelling common terms on each side and transposing suitably gives

$$|C_{aa}C_{bb}| > C_{ab}^2 \text{ for } C_i, C_j \text{ of the } \textit{same} \text{ sign} \qquad (6.7)$$

Similarly, from A(6.5),

$$|C_{aa}C_{bb}| < C_{ab}^2 \text{ for } C_i, C_j \text{ of } \textit{opposite} \text{ signs} \qquad (6.8)$$

6.3. **Vector component of a self-conjugate dyadic.** By definition,† the vector component of $\mathfrak{C}$ in direction $\mathbf{n}$ is

$$\mathbf{C}_n = \mathbf{n}\cdot\mathfrak{C} \qquad (6.9)$$

The *normal component* of this is, scalarly,

$$C_{nn} = \mathbf{n}\cdot\mathbf{C}_n = \mathbf{nn}:\mathfrak{C} \qquad (6.10)$$

† Author, 1948. See volume I, article A,7.2.

If $\mathbf{t}$ is a unit vector orthogonal to $\mathbf{n}$ then the *tangential component* of $\mathbf{C}_n$ is

$$C_{nt} = \mathbf{t}\cdot\mathbf{C}_n = \mathbf{tn}:\mathfrak{C} \tag{6.11}$$

Again, this latter is the modulus of the vector

$$\mathbf{C}_{nt} = \mathbf{C}_n - \mathbf{C}_{nn} \tag{6.12}$$

having the direction $\mathbf{t}$. Then,

$$C_{nt} = \mathbf{t}\cdot(\mathbf{n}\cdot\mathfrak{C} - \mathbf{nnn}:\mathfrak{C}) = \mathbf{tn}:\mathfrak{C} \tag{6.13}$$

as in A(6.11), since $\mathbf{t}\cdot\mathbf{n} = 0$. Otherwise, without the explicit appearance of $\mathbf{t}$,

$$\begin{aligned} C_{nt} &= \pm\sqrt{(\mathbf{C}_{nt}\cdot\mathbf{C}_{nt})} = \pm\sqrt{[(\mathbf{n}\cdot\mathfrak{C} - \mathbf{nn}:\mathfrak{C}\mathbf{n})\cdot(\mathfrak{C}\cdot\mathbf{n} - \mathbf{nnn}:\mathfrak{C})]} \\ &= \pm\sqrt{[\mathbf{n}\cdot\mathfrak{C}\cdot\mathfrak{C}\cdot\mathbf{n} - \mathbf{nn}:\mathfrak{C}\mathfrak{C}:\mathbf{nn}]} \end{aligned} \tag{6.13'}$$

The scalar tangential component is thus determined in terms of one direction $\mathbf{n}$ only, but the extraction of the square root introduces ambiguity of its sign.

6.4. Maximum scalar value of the tangential component of the vector component of the self-conjugate dyadic. Transform the nonion form of $\mathfrak{C}$ in A(6.1) to its principal form (see volume I, article A,9). Thus,

$$\mathfrak{C} = \sum_i C_i \mathbf{x}_i \mathbf{x}_i \tag{6.14}$$

(i) Substituting in A(6.11) gives C_{nt} in terms of the C_i and six direction cosines t_i, n_i. However, these are not independent but are constrained by

$$\sum_i n_i t_i = 0 \qquad \sum_i t_i^2 = 1 \tag{6.15}$$

$$\sum_i n_i^2 = 1 \tag{6.16}$$

These can be used to remove n_3, t_3, t_2, for example, from A(6.11). The resulting expression is differentiated with respect to n_1 and then equated to zero for an extreme value. This is repeated for n_2 and t_1 and the resulting three equations solved with n_1, n_2, t_1 as the unknowns. This is complicated, so a simpler proof due to S. Timoshenko [23.12] is now given.

(ii) Substitute A(6.14) in A(6.13′) to give

$$C_{nt}^2 = \sum_i C_i^2 n_i^2 - (\sum_i C_i n_i^2)^2 \tag{6.17}$$

involving only three direction cosines n_i.

One of these, n_3 say, can be eliminated by using A(6.16) to

leave only two unknowns n_1, n_2 in A(6.17). Differentiate and equate to zero for an extreme value of ${C_{nt}}^2$ with respect to the two unknowns. This gives the simultaneous equations

$$\left.\begin{aligned} n_1[(C_1-C_3){n_1}^2+(C_2-C_3){n_2}^2-\tfrac{1}{2}(C_1-C_3)] &= 0 \\ n_2[(C_1-C_3){n_1}^2+(C_2-C_3){n_2}^2-\tfrac{1}{2}(C_2-C_3)] &= 0 \end{aligned}\right\} \quad (6.18)$$

A factor (C_1-C_3) has been cancelled from the first equation and (C_2-C_3) from the second because solutions from putting such terms as zero give symmetrical stress distributions which are not general.

A solution is given by $n_1 = 0 = n_2$ and these values in A(6.16) give $n_3 = 1$. Thus, $\mathbf{n} = \mathbf{x}_3$, the principal direction for which $C_{3t} = 0$, so that this solution for $\mathbf{n}$ corresponds to a minimum for ${C_{nt}}^2$ and not the maximum value being sought.

Assuming both direction cosines are distinct and non-zero, then A(6.18) gives

$$\tfrac{1}{2}(C_1-C_3) = (C_1-C_3){n_1}^2+(C_2-C_3){n_2}^2 = \tfrac{1}{2}(C_2-C_3) \quad (6.19)$$

These simultaneous equations are inconsistent except for zero stress differences and such symmetrical cases are neglected here as not general.

Now assume $n_2 = 0 \neq n_1$ and A(6.18) gives $n_1 = \pm\sqrt{\tfrac{1}{2}}$ and these values in A(6.16) give $n_3 = \pm\sqrt{\tfrac{1}{2}}$. These values in A(6.17) give

$${C_{nt}}^2(\max) = \tfrac{1}{4}(C_3-C_1)^2 \quad (6.20)$$

If, instead of eliminating ${n_3}^2$ in A(6.17), either ${n_1}^2$ or ${n_2}^2$ is eliminated in turn and the procedure leading to equations A(6.18) to A(6.20) is repeated, then similar results are found with subscripts **1, 2, 3** interchanged cyclically. Thus, the three minimum values of the tangential component are zero and occur on the principal planes, while three maximum values

$$C_{nt}(\max) = |\tfrac{1}{2}(C_i-C_j)| \text{ when } \mathbf{n} = (\mathbf{x}_i+\mathbf{x}_j)\sqrt{\tfrac{1}{2}} \quad (6.21)$$

Therefore, the *absolute maximum* is half the greatest algebraic difference of the principal scalar components of the self-conjugate dyadic. This result was given by Hopkins[114] in 1847 for the case of the stress dyadic.

7. Elemental line lengths and changes in unit reference vectors with position in orthogonal reference systems

The various operators are readily put into the form appropriate to the particular coordinate system when the elemental line

lengths are given in terms of the coordinate parameters and the rates of change of the non-constant unit reference vectors have been found.

7.1. **Cylindrical coordinates.** In Fig. A,7.1, R_r = constant is a right cylindrical surface with axis OR_z, θ = constant is a plane passing through axis OR_z, while R_z = constant is a plane normal to OR_z. All these level surfaces intersect orthogonally. The cylindrical scalar coordinates (R_r, θ, R_z) for point **R** are shown in Fig. A,7.1.

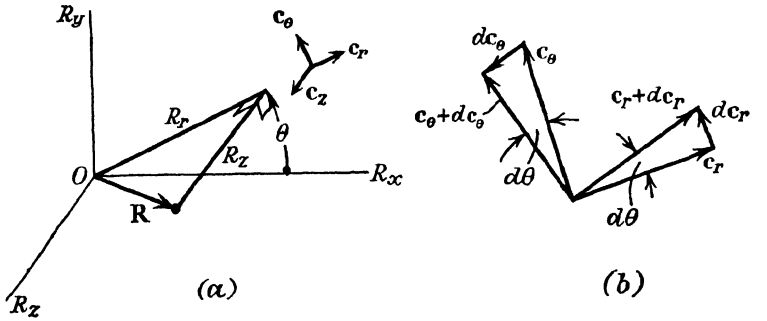

FIG. A,7.1.—Cylindrical coordinates (R_r, θ, R_z) are shown in (*a*). Component R_r lies in the plane $R_z = 0$, while R_z is normal to it. The unit vectors $\mathbf{c}_r$, $\mathbf{c}_\theta$, $\mathbf{c}_z$ are mutually orthogonal and parallel to the coordinate lines. For a differential change of position in the coordinate space the unit vectors change differentially to correspond and give the geometrical relationship in (*b*).

Passing from **R** to **R**+d**R** the coordinate parameters change by dR_r, $d\theta$, dR_z. Hence, write the elemental line lengths as

$$dR_a = dR_r \qquad dR_b = dR_\theta = R_r d\theta \qquad dR_c = dR_z \tag{7.1}$$

The differential changes in the unit vectors with these differential changes of position are found geometrically to be

$$d\mathbf{c}_r = \mathbf{c}_\theta d\theta \qquad d\mathbf{c}_\theta = -\mathbf{c}_r d\theta$$

and hence

$$\mathbf{c}_{r;\theta} = \mathbf{c}_\theta \qquad \mathbf{c}_{\theta;\theta} = -\mathbf{c}_r \tag{7.2}$$

Change of position along any other edge of the differential orthogonal element does not change the unit vectors because they

do not suffer relative rotations in the process. Hence, writing rates of change of the c's schematically gives

	$\mathbf{c}_r$	$\mathbf{c}_\theta$	$\mathbf{c}_z$
$\dfrac{\partial}{\partial R_r}$	0	0	0
$\dfrac{\partial}{\partial \theta}$	$\mathbf{c}_\theta$	$-\mathbf{c}_r$	0
$\dfrac{\partial}{\partial R_z}$	0	0	0

(7.3)

7.2. **Spherical coordinates.** The coordinates (R_r, θ, ϕ) denote a point **R** in the spherical system of Fig. A,7.2. The surface

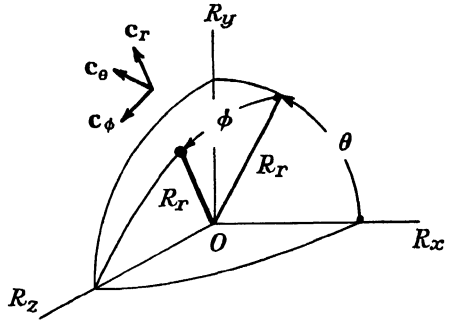

FIG. A,7.2.—Spherical coordinates (R_r, θ, ϕ) are shown. Coordinate R_r is the radius of a spherical surface. Angle θ is described in the plane $R_z = 0$, while ϕ is in the plane in which is described the great circle of radius R_r passing through point (R_r, θ) in the plane $R_z = 0$. Unit vectors $\mathbf{c}_r$, $\mathbf{c}_\theta$, $\mathbf{c}_\phi$ are mutually orthogonal and apply to point (R_r, θ, ϕ) shown. Unit vector $\mathbf{c}_\theta$ is normal to the plane in which ϕ is described, while $\mathbf{c}_\phi$ is tangential to the great circle for ϕ.

R_r = constant is a sphere about the origin, θ = constant is a plane, while ϕ = constant is a cone. All these level surfaces intersect orthogonally. Elemental coordinate line lengths are

$$dR_a = dR \qquad dR_b = dR_\theta = R_r \cos\phi d\theta \qquad dR_c = dR_\phi = R_r d\phi \tag{7.4}$$

In a geometrical manner similar to that in equation A(7.2), the rates of change of the unit vectors follow the scheme

	$\mathbf{c}_r$	$\mathbf{c}_\theta$	$\mathbf{c}_\phi$
$\dfrac{\partial}{\partial R_r}$	0	0	0
$\dfrac{\partial}{\partial \theta}$	$\mathbf{c}_\theta \cos\phi$	$-\mathbf{c}_r \cos\phi$ $+\mathbf{c}_\phi \sin\phi$	$-\mathbf{c}_\theta \sin\phi$
$\dfrac{\partial}{\partial \phi}$	$\mathbf{c}_\phi$	0	$-\mathbf{c}_r$

(7.5)

8. Operators, grad, div, curl

These operators are defined for cartesian coordinates in volume I, articles A,5, A,13. With the curvilinear coordinates they become, briefly,

$$\left.\begin{aligned} \text{grad}\,(\ ) &= \nabla(\ ) = \sum_a \mathbf{c}_a (\ )_{;a} \\ \text{div}\,(\ ) &= \nabla\cdot(\ ) = \sum_a \mathbf{c}_a \cdot (\ )_{;a} \\ \text{curl}\,(\ ) &= \nabla\times(\ ) = \sum_a \mathbf{c}_a \times (\ )_{;a} \end{aligned}\right\} \tag{8.1}$$

Using the appropriate unit vectors and differential coordinate lines lengths dR_a, ... as in article A,7 gives the particular curvilinear forms.

8.1. Cylindrical coordinates

$$\left.\begin{aligned} \text{grad}\,(\ ) &= \mathbf{c}_r (\ )_{;r} + \mathbf{c}_\theta R_r^{-1} (\ )_{;\theta} + \mathbf{c}_z (\ )_{;z} \\ \text{div}\,(\ ) &= \mathbf{c}_r \cdot (\ )_{;r} + R_r^{-1} \mathbf{c}_\theta \cdot (\ )_{;\theta} + \mathbf{c}_z \cdot (\ )_{;z} \\ \text{curl}\,(\ ) &= \mathbf{c}_r \times (\ )_{;r} + R_r^{-1} \mathbf{c}_\theta \times (\ )_{;\theta} + \mathbf{c}_z \times (\ )_{;z} \end{aligned}\right\} \tag{8.2}$$

8.2. Spherical coordinates

$$\left.\begin{aligned} \text{grad}\,(\ ) &= \mathbf{c}_r (\ )_{;r} + (R_r \cos\phi)^{-1} \mathbf{c}_\theta (\ )_{;\theta} + R_r^{-1} \mathbf{c}_\phi (\ )_{;\phi} \\ \text{div}\,(\ ) &= \mathbf{c}_r \cdot (\ )_{;r} + (R_r \cos\phi)^{-1} \mathbf{c}_\theta \cdot (\ )_{;\theta} + R_r^{-1} \mathbf{c}_\phi \cdot (\ )_{;\phi} \\ \text{curl}\,(\ ) &= \mathbf{c}_r \times (\ )_{;r} + (R_r \cos\phi)^{-1} \mathbf{c}_\theta \times (\ )_{;\theta} + R_r^{-1} \mathbf{c}_\phi \times (\ )_{;\phi} \end{aligned}\right\} \tag{8.3}$$

9. Second-order operators grad grad, laplacian

The second-order operators grad grad and the laplacian are found readily in cartesian coordinates because, there, the unit reference vectors are constant throughout the coordinate space. In curvilinear coordinates, however, the rates of change of the unit vectors must be considered.

9.1. **Cylindrical coordinates.** With the cylindrical coordinates in Fig. A,7.1, equation A(8.2).1 (operating on a dummy function F to allow the brief notation for differentiation) gives

$$\nabla\nabla F = \left[\mathbf{c}_r\frac{\partial}{\partial R_r}+\mathbf{c}_\theta R_r^{-1}\frac{\partial}{\partial\theta}+\mathbf{c}_z\frac{\partial}{\partial R_z}\right][\mathbf{c}_r F_{;r}+\mathbf{c}_\theta R_r^{-1}F_{;\theta}+\mathbf{c}_z F_{;z}]$$

Scheme A(7.3) gives the rates of change of the unit vectors and so the operator grad grad is

$$\begin{aligned}\nabla\nabla F = {} & F_{;rr}\mathbf{c}_r\mathbf{c}_r+(R_r^{-1}F_{;\theta})_{;r}(\mathbf{c}_r\mathbf{c}_\theta+\mathbf{c}_\theta\mathbf{c}_r)\\ & +(R_r^{-2}F_{;\theta\theta}+R_r^{-1}F_{;r})\mathbf{c}_\theta\mathbf{c}_\theta+R_r^{-1}F_{;\theta z}(\mathbf{c}_\theta\mathbf{c}_z+\mathbf{c}_z\mathbf{c}_\theta)\\ & +F_{;zz}\mathbf{c}_z\mathbf{c}_z+F_{;zr}(\mathbf{c}_z\mathbf{c}_r+\mathbf{c}_r\mathbf{c}_z)\end{aligned} \tag{9.1}$$

The *laplacian* is the scalar of the 'spherical' part of $\nabla\nabla$ and is found as †

$$\nabla^2 F = \mathfrak{J}:\nabla\nabla F = F_{;rr}+R_r^{-1}F_{;r}+R_r^{-2}F_{;\theta\theta}+F_{;zz} \tag{9.2}$$

by double scalar product with the idemfactor. (See volume I, article A,23.3.) The same expression is found by performing the operation div grad F, as is more usual to derive the laplacian.

9.2. **Spherical coordinates.** From A(8.3).1 for spherical coordinates as in Fig. A,7.2, and using the scheme A(7.5) for rate of change of unit vectors gives, with dummy function F,

$$\begin{aligned}\nabla\nabla F = {} & F_{;rr}\mathbf{c}_r\mathbf{c}_r+\sec\phi(FR_r^{-1})_{;r\theta}(\mathbf{c}_r\mathbf{c}_\theta+\mathbf{c}_\theta\mathbf{c}_r)\\ & +(R_r^{-1}F_{;r}+R_r^{-2}\sec^2\phi F_{;\theta\theta}-R_r^{-2}\tan\phi F_{;\phi})\mathbf{c}_\theta\mathbf{c}_\theta\\ & +R_r^{-2}\sec\phi(F_{;\theta\phi}+F_{;\theta}\tan\phi)(\mathbf{c}_\theta\mathbf{c}_\phi+\mathbf{c}_\phi\mathbf{c}_\theta)\\ & +(R_r^{-2}F_{;\phi\phi}+R_r^{-1}F_{;r})\mathbf{c}_\phi\mathbf{c}_\phi\\ & +(FR_r^{-1})_{;\phi r}(\mathbf{c}_\phi\mathbf{c}_r+\mathbf{c}_r\mathbf{c}_\phi)\end{aligned} \tag{9.3}$$

The laplacian scalar operator acting on the dummy F is

$$\nabla^2 F = F_{;rr}+2R_r^{-1}F_{;r}+R_r^{-2}\sec^2\phi F_{;\theta\theta}+R_r^{-2}(F_{;\phi\phi}-\tan\phi F_{;\phi}) \tag{9.4}$$

† Author, 1950.

10. Vector gradient of a self-conjugate dyadic

The continuity of a self-conjugate dyadic $\mathfrak{Q}$ is examined so frequently in the analysis of deformation that it is useful to have its vector gradient explicitly for the common coordinate systems. The expressions for curvilinear coordinates are not as concise as those for cartesian, so that it is convenient to write the scalar coefficients of $\nabla\mathfrak{Q}$ schematically. The scheme will be made clear by expanding the form for cartesian coordinates.

10.1. **Cartesian coordinates.** Using the cartesian coordinates (R_1, R_2, R_3) with unit vectors $\mathbf{c}_1, \mathbf{c}_2, \mathbf{c}_3$ constant throughout, then

$$\nabla\mathfrak{Q} =$$

	$\mathbf{c}_1\mathbf{c}_1$	$\mathbf{c}_2\mathbf{c}_2$	$\mathbf{c}_3\mathbf{c}_3$
$\mathbf{c}_1$	$a_{11;1}$	$a_{22;1}$	$a_{33;1}$
$\mathbf{c}_2$	$a_{11;2}$	$a_{22;2}$	$a_{33;2}$
$\mathbf{c}_3$	$a_{11;3}$	$a_{22;3}$	$a_{33;3}$

$+$

	$(\mathbf{c}_1\mathbf{c}_2+\mathbf{c}_2\mathbf{c}_1)$	$(\mathbf{c}_2\mathbf{c}_3+\mathbf{c}_3\mathbf{c}_2)$	$(\mathbf{c}_3\mathbf{c}_1+\mathbf{c}_1\mathbf{c}_3)$
$\mathbf{c}_1$	$a_{12;1}$	$a_{23;1}$	$a_{31;1}$
$\mathbf{c}_2$	$a_{12;2}$	$a_{23;2}$	$a_{31;2}$
$\mathbf{c}_3$	$a_{12;3}$	$a_{23;3}$	$a_{31;3}$

(10.1)

Thus, from the second row, third column, for example, the coefficient of the triad $\mathbf{c}_2\mathbf{c}_3\mathbf{c}_3$ is $a_{33;2}$.

10.2. **Cylindrical coordinates.** The cylindrical coordinates (R_r, θ, R_z) for which the unit vectors are $\mathbf{c}_r$, $\mathbf{c}_\theta$, $\mathbf{c}_z$ are given in Fig. A,7.1. Use the grad operator from article A,8.1 and the rates of change of the unit vectors from article A,7.1. From the self-conjugate dyadic

$$\begin{aligned}\mathfrak{Q} = {} & a_{rr}\mathbf{c}_r\mathbf{c}_r + a_{r\theta}(\mathbf{c}_r\mathbf{c}_\theta + \mathbf{c}_\theta\mathbf{c}_r) \\ & + a_{\theta\theta}\mathbf{c}_\theta\mathbf{c}_\theta + a_{\theta z}(\mathbf{c}_\theta\mathbf{c}_z + \mathbf{c}_z\mathbf{c}_\theta) \\ & + a_{zz}\mathbf{c}_z\mathbf{c}_z + a_{zr}(\mathbf{c}_z\mathbf{c}_r + \mathbf{c}_r\mathbf{c}_z)\end{aligned} \tag{10.2}$$

there follows readily

$\nabla\mathfrak{Q} =$

	$\mathbf{c}_r\mathbf{c}_r$	$\mathbf{c}_\theta\mathbf{c}_\theta$	$\mathbf{c}_z\mathbf{c}_z$
$\mathbf{c}_r$	$a_{rr;r}$	$a_{\theta\theta;r}$	$a_{zz;r}$
$R_r^{-1}\mathbf{c}_\theta$	$a_{rr;\theta}-2a_{r\theta}$	$a_{\theta\theta;\theta}+2a_{r\theta}$	$a_{zz;\theta}$
$\mathbf{c}_z$	$a_{rr;z}$	$a_{\theta\theta;z}$	$a_{zz;z}$

$+$

	$(\mathbf{c}_r\mathbf{c}_\theta+\mathbf{c}_\theta\mathbf{c}_r)$	$(\mathbf{c}_\theta\mathbf{c}_z+\mathbf{c}_z\mathbf{c}_\theta)$	$(\mathbf{c}_z\mathbf{c}_r+\mathbf{c}_r\mathbf{c}_z)$
$\mathbf{c}_r$	$a_{r\theta;r}$	$a_{\theta z;r}$	$a_{zr;r}$
$R_r^{-1}\mathbf{c}_\theta$	$a_{r\theta;\theta}+a_{rr}-a_{\theta\theta}$	$a_{\theta z;\theta}+a_{zr}$	$a_{zr;\theta}-a_{\theta z}$
$\mathbf{c}_z$	$a_{r\theta;z}$	$a_{\theta z;z}$	$a_{zr;z}$

(10.3)

10.3. **Spherical coordinates.** The spherical coordinates (R_r, θ, ϕ) are given in Fig. A,7.2 with unit vectors $\mathbf{c}_r$, $\mathbf{c}_\theta$, $\mathbf{c}_\phi$. From the self-conjugate dyadic

$$\begin{aligned}\mathfrak{Q} = {} & a_{rr}\mathbf{c}_r\mathbf{c}_r+a_{r\theta}(\mathbf{c}_r\mathbf{c}_\theta+\mathbf{c}_\theta\mathbf{c}_r)\\ & +a_{\theta\theta}\mathbf{c}_\theta\mathbf{c}_\theta+a_{\theta\phi}(\mathbf{c}_\theta\mathbf{c}_\phi+\mathbf{c}_\phi\mathbf{c}_\theta)\\ & +a_{\phi\phi}\mathbf{c}_\phi\mathbf{c}_\phi+a_{\phi r}(\mathbf{c}_\phi\mathbf{c}_r+\mathbf{c}_r\mathbf{c}_\phi)\end{aligned} \tag{10.4}$$

with the rate of change of unit vectors from article A,7.2, there follows readily

$\nabla\mathfrak{Q} =$

	$\mathbf{c}_r\mathbf{c}_r$	$\mathbf{c}_\theta\mathbf{c}_\theta$	$\mathbf{c}_\phi\mathbf{c}_\phi$
$\mathbf{c}_r$	$a_{rr;r}$	$a_{\theta\theta;r}$	$a_{\phi\phi;r}$
$(R_r\cos\phi)^{-1}\mathbf{c}_\theta$	$a_{rr;\theta}-2a_{r\theta}\cos\phi$	$a_{\theta\theta;\theta}$ $+2a_{r\theta}\cos\phi$ $-2a_{\theta\phi}\sin\phi$	$a_{\phi\phi;\theta}$ $+2a_{\theta\phi}\sin\phi$
$R_r^{-1}\mathbf{c}_\phi$	$a_{rr;\phi}-2a_{\phi r}$	$a_{\theta\theta;\phi}$	$a_{\phi\phi;\phi}+2a_{\phi r}$

$+$

	$(\mathbf{c}_r\mathbf{c}_\theta+\mathbf{c}_\theta\mathbf{c}_r)$	$(\mathbf{c}_\theta\mathbf{c}_\phi+\mathbf{c}_\phi\mathbf{c}_\theta)$	$(\mathbf{c}_\phi\mathbf{c}_r+\mathbf{c}_r\mathbf{c}_\phi)$
$\mathbf{c}_r$	$a_{r\theta;r}$	$a_{\theta\phi;r}$	$a_{\phi r;r}$
$(R_r\cos\phi)^{-1}\mathbf{c}_\theta$	$a_{r\theta;\theta}$ $-a_{\phi r}\sin\phi$ $+(a_{rr}-a_{\theta\theta})\cos\phi$	$a_{\theta\phi;\theta}$ $+a_{\phi r}\cos\phi$ $+(a_{\theta\theta}-a_{\phi\phi})\sin\phi$	$a_{\phi r;\theta}$ $-a_{\theta\phi}\cos\phi$ $a_{r\theta}\sin\phi$
$R_r^{-1}\mathbf{c}_\phi$	$a_{r\theta;\phi}-a_{\theta\phi}$	$a_{\theta\phi;\phi}+a_{r\theta}$	$a_{\phi r;\phi}$ $+(a_{rr}-a_{\phi\phi})$

(10.5)

11. Divergence of a self-conjugate dyadic

The definition in article A,8 gives the divergence of self-conjugate dyadic $\mathfrak{Q}$ as the vector $\nabla\cdot\mathfrak{Q}$. This is found readily by forming the scalar product between the first and second unit vectors in each triad of the triadic $\nabla\mathfrak{Q}$ of article A,10. The scalar product of orthogonal unit vectors is zero, while it is unity when they are equal.

11.1. Cartesian coordinates

$$\begin{aligned}\nabla\cdot\mathfrak{Q} = {} & (a_{11;1}+a_{12;2}+a_{31;3})\mathbf{c}_1 \\ & +(a_{22;2}+a_{23;3}+a_{12;1})\mathbf{c}_2 \\ & +(a_{33;3}+a_{31;1}+a_{23;2})\mathbf{c}_3\end{aligned} \tag{11.1}$$

11.2. Cylindrical coordinates

$$\begin{aligned}R_r\nabla\cdot\mathfrak{Q} = {} & (R_r a_{rr;r}+a_{r\theta;\theta}+R_r a_{zr;z}+a_{rr}-a_{\theta\theta})\mathbf{c}_r \\ & +(a_{\theta\theta;\theta}+R_r a_{\theta z;z}+R_r a_{r\theta;r}+2a_{r\theta})\mathbf{c}_\theta \\ & +(R_r a_{zz;z}+R_r a_{zr;r}+a_{\theta z;\theta}+a_{zr})\mathbf{c}_z\end{aligned} \tag{11.2}$$

11.3. Spherical coordinates

$$\begin{aligned}R_r\nabla\cdot\mathfrak{Q} = {} & \left(\begin{matrix}R_r a_{rr;r}+a_{r\theta;\theta}\sec\phi+a_{\phi r;\phi} \\ +2a_{rr}-a_{\theta\theta}-a_{\phi\phi}-a_{\phi r}\tan\phi\end{matrix}\right)\mathbf{c}_r \\ & +\left(\begin{matrix}a_{\theta\theta;\theta}\sec\phi+a_{\theta\phi;\phi}+R_r a_{r\theta;r} \\ +3a_{r\theta}-2a_{\theta\phi}\tan\phi\end{matrix}\right)\mathbf{c}_\theta \\ & +\left(\begin{matrix}a_{\phi\phi;\phi}+R_r a_{\phi r;r}+a_{\theta\phi;\theta}\sec\phi \\ +(a_{\theta\theta}-a_{\phi\phi})\tan\phi+3a_{\phi r}\end{matrix}\right)\mathbf{c}_\phi\end{aligned} \tag{11.3}$$

12. Curl of a self-conjugate dyadic

The definition in article A,8 gives the curl of a self-conjugate dyadic $\mathfrak{Q}$ as the dyadic $\nabla\times\mathfrak{Q}$. This is found readily by forming the vector product between the first and second unit vectors in each triad of the triadic $\nabla\mathfrak{Q}$ in article A,10. The vector products of like vectors are zero.

12.1. Cartesian coordinates

$$\begin{aligned}\nabla\times\mathfrak{Q} = {} & (a_{31;2}-a_{12;3})\mathbf{c}_1\mathbf{c}_1+(a_{12;3}-a_{23;1})\mathbf{c}_2\mathbf{c}_2+(a_{23;1}-a_{31;2})\mathbf{c}_3\mathbf{c}_3 \\ & +(a_{23;2}-a_{22;3})\mathbf{c}_1\mathbf{c}_2+(a_{31;3}-a_{33;1})\mathbf{c}_2\mathbf{c}_3+(a_{12;1}-a_{11;2})\mathbf{c}_3\mathbf{c}_1 \\ & +(a_{11;3}-a_{31;1})\mathbf{c}_2\mathbf{c}_1+(a_{22;1}-a_{12;2})\mathbf{c}_3\mathbf{c}_2+(a_{33;2}-a_{23;3})\mathbf{c}_1\mathbf{c}_3\end{aligned} \tag{12.1}$$

12.2. Cylindrical coordinates

$$\begin{aligned}\nabla\times\mathfrak{D} = {} & [R_r^{-1}(a_{zr;\theta}-a_{\theta z})-a_{r\theta;z}]\mathbf{c}_r\mathbf{c}_r \\ & +[-a_{\theta z;r}+a_{r\theta;z}]\mathbf{c}_\theta\mathbf{c}_\theta \\ & +[a_{\theta z;r}-R_r^{-1}(a_{zr;\theta}-a_{\theta z})]\mathbf{c}_z\mathbf{c}_z \\ & +[-a_{\theta\theta;z}+R_r^{-1}(a_{\theta z;\theta}+a_{zr})]\mathbf{c}_r\mathbf{c}_\theta \\ & +[-a_{zz;r}+a_{zr;z}]\mathbf{c}_\theta\mathbf{c}_z \\ & +[-R_r^{-1}(a_{rr;\theta}-2a_{r\theta})+a_{r\theta;r}]\mathbf{c}_z\mathbf{c}_r \\ & +[a_{rr;z}-a_{zr;r}]\mathbf{c}_\theta\mathbf{c}_r \\ & +[a_{\theta\theta;r}-R_r^{-1}(a_{r\theta;\theta}+a_{rr}-a_{\theta\theta})]\mathbf{c}_z\mathbf{c}_\theta \\ & +[R_r^{-1}a_{zz;\theta}-a_{\theta z;z}]\mathbf{c}_r\mathbf{c}_z \end{aligned} \tag{12.2}$$

12.3. Spherical coordinates

$$\begin{aligned}\nabla\times\mathfrak{D} = {} & \left[\begin{array}{l}-R_r^{-1}(a_{r\theta;\phi}-a_{\theta\phi}) \\ \quad +(R_r\cos\phi)^{-1}(a_{\phi r;\theta}-a_{\theta\phi}\cos\phi+a_{r\theta}\sin\phi)\end{array}\right]\mathbf{c}_r\mathbf{c}_r \\ & +[R_r^{-1}(a_{r\theta;\phi}-a_{\theta\phi})-a_{\theta\phi;r}]\mathbf{c}_\theta\mathbf{c}_\theta \\ & +[a_{\theta\phi;r}-(R_r\cos\phi)^{-1}(a_{\phi r;\theta}-a_{\theta\phi}\cos\phi+a_{r\theta}\sin\phi)]\mathbf{c}_\phi\mathbf{c}_\phi \\ & +\left[\begin{array}{l}-R_r^{-1}a_{\theta\theta;\phi}+(R_r\cos\phi)^{-1}a_{\theta\phi;\theta}+a_{\phi r}\cos\phi \\ \quad +a_{\theta\theta}\sin\phi-a_{\phi\phi}\sin\phi\end{array}\right]\mathbf{c}_r\mathbf{c}_\theta \\ & +[-a_{\phi\phi;r}+R_r^{-1}(a_{\phi r;\phi}+a_{rr}-a_{\phi\phi})]\mathbf{c}_\theta\mathbf{c}_\phi \\ & +[-(R_r\cos\phi)^{-1}(a_{rr;\theta}-2a_{r\theta}\cos\phi)+a_{r\theta;r}]\mathbf{c}_\phi\mathbf{c}_r \\ & +\left[\begin{array}{l}a_{\theta\theta;r}-(R_r\cos\phi)^{-1}a_{r\theta;\theta}-a_{\phi r}\sin\phi \\ \quad +a_{rr}\cos\phi-a_{\theta\theta}\cos\phi\end{array}\right]\mathbf{c}_\phi\mathbf{c}_\theta \\ & +[R_r^{-1}a_{rr;\phi}-a_{\phi r;r}]\mathbf{c}_\theta\mathbf{c}_r \\ & +\left[\begin{array}{l}(R_r\cos\phi)^{-1}(a_{\phi\phi;\theta}+2a_{\theta\phi}\sin\phi) \\ \quad -R_r^{-1}(a_{\theta\phi;\phi}+a_{r\theta})\end{array}\right]\mathbf{c}_r\mathbf{c}_\phi \end{aligned} \tag{12.3}$$

13. Conjugate curl of a dyadic

The conjugate curl operator is defined by

$$(\ )\times\nabla = \sum_a (\ )_{;a}\times\mathbf{c}_a \tag{13.1}$$

Let this operate on a dyadic

$$\begin{aligned}\mathfrak{F} = {} & f_{aa}\mathbf{c}_a\mathbf{c}_a+f_{ab}\mathbf{c}_a\mathbf{c}_b+f_{ac}\mathbf{c}_a\mathbf{c}_c \\ & +f_{bb}\mathbf{c}_b\mathbf{c}_b+f_{bc}\mathbf{c}_b\mathbf{c}_c+f_{ba}\mathbf{c}_b\mathbf{c}_a \\ & +f_{cc}\mathbf{c}_c\mathbf{c}_c+f_{ca}\mathbf{c}_c\mathbf{c}_a+f_{cb}\mathbf{c}_c\mathbf{c}_b \end{aligned} \tag{13.2}$$

13.1. Cartesian coordinates

$$\begin{aligned}\mathfrak{F}\times\nabla = {} & (f_{12;3}-f_{13;2})\mathbf{c}_1\mathbf{c}_1+(f_{23;1}-f_{21;3})\mathbf{c}_2\mathbf{c}_2+(f_{31;2}-f_{32;1})\mathbf{c}_3\mathbf{c}_3 \\ & +(f_{13;1}-f_{11;3})\mathbf{c}_1\mathbf{c}_2+(f_{21;2}-f_{22;1})\mathbf{c}_2\mathbf{c}_3+(f_{32;3}-f_{33;2})\mathbf{c}_3\mathbf{c}_1 \\ & +(f_{22;3}-f_{23;2})\mathbf{c}_2\mathbf{c}_1+(f_{33;1}-f_{31;3})\mathbf{c}_3\mathbf{c}_2+(f_{11;2}-f_{12;1})\mathbf{c}_1\mathbf{c}_3 \end{aligned} \tag{13.3}$$

13.2. **Cylindrical and spherical coordinates.** These are complicated expressions rather like those in articles A,12.2, A,12.3 for the curl operator. They are left for the reader as an exercise in expansion of the operators.

13.3. **The dyadic as the curl of a self-conjugate dyadic.** If the dyadic $\mathfrak{F}$ is chosen as the $\nabla\times\mathfrak{Q}$ of article A,12.1, then the coefficients of the dyads there are substituted for the f's here. For example, substitute $(a_{23;2}-a_{22;3})$, the coefficient of $\mathbf{c}_1\mathbf{c}_2$, in place of f_{12} in equation A(13.3). Then, for self-conjugate dyadic $\mathfrak{Q}$, for cartesian coordinates,

$$\begin{aligned}(\nabla\times\mathfrak{Q})\times\nabla = {} & (a_{23;23}+a_{23;23}-a_{22;33}-a_{33;22})\mathbf{c}_1\mathbf{c}_1 \\ & +(a_{31;31}+a_{31;31}-a_{33;11}-a_{11;33})\mathbf{c}_2\mathbf{c}_2 \\ & +(a_{12;12}+a_{12;12}-a_{11;22}-a_{22;11})\mathbf{c}_3\mathbf{c}_3 \\ & +(a_{33;12}+a_{12;33}-a_{23;31}-a_{31;23})(\mathbf{c}_1\mathbf{c}_2+\mathbf{c}_2\mathbf{c}_1) \\ & +(a_{11;23}+a_{23;11}-a_{31;12}-a_{12;31})(\mathbf{c}_2\mathbf{c}_3+\mathbf{c}_3\mathbf{c}_2) \\ & +(a_{22;31}+a_{31;22}-a_{12;23}-a_{23;12})(\mathbf{c}_3\mathbf{c}_1+\mathbf{c}_1\mathbf{c}_3)\end{aligned} \tag{13.4}$$

For cylindrical, spherical coordinates the expressions for $\nabla\times\mathfrak{Q}$ in articles A,12.2, A,12.3 are substituted in the corresponding coordinate forms for $(\ )\times\nabla$ when written out in article A,13.2. This is left as an exercise for the reader.

14. Vector gradient of a vector

The vector gradient $\nabla\mathbf{F}$ of a vector $\mathbf{F}$o ccurs frequently in the deformation problem. Using the various forms for ∇ from article A,8 and the rates of change of the unit vectors with position, as in article A,7, gives the required forms.

14.1. **Cartesian coordinates**

$$\begin{aligned}\nabla\mathbf{F} = {} & F_{1;1}\mathbf{c}_1\mathbf{c}_1+F_{1;2}\mathbf{c}_2\mathbf{c}_1+F_{1;3}\mathbf{c}_3\mathbf{c}_1 \\ & +F_{2;1}\mathbf{c}_1\mathbf{c}_2+F_{2;2}\mathbf{c}_2\mathbf{c}_2+F_{2;3}\mathbf{c}_3\mathbf{c}_2 \\ & +F_{3;1}\mathbf{c}_1\mathbf{c}_3+F_{3;2}\mathbf{c}_2\mathbf{c}_3+F_{3;3}\mathbf{c}_3\mathbf{c}_3\end{aligned} \tag{14.1}$$

14.2. **Cylindrical coordinates**

$$\begin{aligned}\nabla\mathbf{F} = {} & F_{r;r}\mathbf{c}_r\mathbf{c}_r+R_r^{-1}(F_{r;\theta}-F_\theta)\mathbf{c}_\theta\mathbf{c}_r+F_{r;z}\mathbf{c}_z\mathbf{c}_r \\ & +F_{\theta;r}\mathbf{c}_r\mathbf{c}_\theta+R_r^{-1}(F_{\theta;\theta}+F_r)\mathbf{c}_\theta\mathbf{c}_\theta+F_{\theta;z}\mathbf{c}_z\mathbf{c}_\theta \\ & +F_{z;r}\mathbf{c}_r\mathbf{c}_z+R_r^{-1}F_{z;\theta}\mathbf{c}_\theta\mathbf{c}_z+F_{z;z}\mathbf{c}_z\mathbf{c}_z\end{aligned} \tag{14.2}$$

14.3. Spherical coordinates

$$\begin{aligned}\nabla\mathbf{F} = {} & F_{r;r}\mathbf{c}_r\mathbf{c}_r+(R_r\cos\phi)^{-1}(F_{r;\theta}-F_\theta\cos\phi)\mathbf{c}_\theta\mathbf{c}_r+(F_{r;\phi}-F_\phi)\mathbf{c}_\phi\mathbf{c}_r\\ & +F_{\theta;r}\mathbf{c}_r\mathbf{c}_\theta+(R_r\cos\phi)^{-1}(F_{\theta;\theta}+F_r\cos\phi-F_\phi\sin\phi)\mathbf{c}_\theta\mathbf{c}_\theta+F_{\theta;\phi}\mathbf{c}_\phi\mathbf{c}_\theta\\ & +F_{\phi;r}\mathbf{c}_r\mathbf{c}_\phi+(R_r\cos\phi)^{-1}(F_{\phi;\theta}+F_\theta\sin\phi)\mathbf{c}_\theta\mathbf{c}_\phi+(F_{\phi;\phi}+F_r)\mathbf{c}_\phi\mathbf{c}_\phi\end{aligned} \tag{14.3}$$

15. Self-conjugate and antiself-conjugate components of the vector gradient of a vector

$$\nabla\mathbf{F} = \tfrac{1}{2}(\nabla\mathbf{F}+\mathbf{F}\nabla)+\tfrac{1}{2}(\nabla\mathbf{F}-\mathbf{F}\nabla) \tag{15.1}$$

with the conjugate dyadic $\mathbf{F}\nabla$. The term $\frac{1}{2}(\nabla\mathbf{F}+\mathbf{F}\nabla)$ is the self-conjugate component of $\nabla\mathbf{F}$, while $\frac{1}{2}(\nabla\mathbf{F}-\mathbf{F}\nabla)$ is the antiself-conjugate component. Using the results in article A,14 gives the components in the several coordinate systems.

15.1. Cartesian coordinates

$$\begin{aligned}\tfrac{1}{2}(\nabla\mathbf{F}+\mathbf{F}\nabla) = {} & F_{1;1}\mathbf{c}_1\mathbf{c}_1+F_{2;2}\mathbf{c}_2\mathbf{c}_2+F_{3;3}\mathbf{c}_3\mathbf{c}_3\\ & +\tfrac{1}{2}(F_{1;2}+F_{2;1})(\mathbf{c}_1\mathbf{c}_2+\mathbf{c}_2\mathbf{c}_1)\\ & +\tfrac{1}{2}(F_{2;3}+F_{3;2})(\mathbf{c}_2\mathbf{c}_3+\mathbf{c}_3\mathbf{c}_2)\\ & +\tfrac{1}{2}(F_{3;1}+F_{1;3})(\mathbf{c}_3\mathbf{c}_1+\mathbf{c}_1\mathbf{c}_3)\end{aligned} \tag{15.2}$$

$$\begin{aligned}\tfrac{1}{2}(\nabla\mathbf{F}-\mathbf{F}\nabla) = {} & \tfrac{1}{2}(F_{2;1}-F_{1;2})(\mathbf{c}_1\mathbf{c}_2-\mathbf{c}_2\mathbf{c}_1)\\ & +\tfrac{1}{2}(F_{3;2}-F_{2;3})(\mathbf{c}_2\mathbf{c}_3-\mathbf{c}_3\mathbf{c}_2)\\ & +\tfrac{1}{2}(F_{1;3}-F_{3;1})(\mathbf{c}_3\mathbf{c}_1-\mathbf{c}_1\mathbf{c}_3)\end{aligned} \tag{15.3}$$

15.2. Cylindrical coordinates

$$\begin{aligned}\tfrac{1}{2}(\nabla\mathbf{F}+\mathbf{F}\nabla) = {} & F_{r;r}\mathbf{c}_r\mathbf{c}_r+R_r^{-1}(F_{\theta;\theta}+F_r)\mathbf{c}_\theta\mathbf{c}_\theta+F_{z;z}\mathbf{c}_z\mathbf{c}_z\\ & +\tfrac{1}{2}[R_r^{-1}(F_{r;\theta}-F_\theta)+F_{\theta;r}](\mathbf{c}_r\mathbf{c}_\theta+\mathbf{c}_\theta\mathbf{c}_r)\\ & +\tfrac{1}{2}[F_{\theta;z}+R_r^{-1}F_{z;\theta}](\mathbf{c}_\theta\mathbf{c}_z+\mathbf{c}_z\mathbf{c}_\theta)\\ & +\tfrac{1}{2}[F_{r;z}+F_{z;r}](\mathbf{c}_z\mathbf{c}_r+\mathbf{c}_r\mathbf{c}_z)\end{aligned} \tag{15.4}$$

$$\begin{aligned}\tfrac{1}{2}(\nabla\mathbf{F}-\mathbf{F}\nabla) = {} & \tfrac{1}{2}[F_{\theta;r}+R_r^{-1}(-F_{r;\theta}+F_\theta)](\mathbf{c}_r\mathbf{c}_\theta-\mathbf{c}_\theta\mathbf{c}_r)\\ & +\tfrac{1}{2}[R_r^{-1}F_{z;\theta}-F_{\theta;z}](\mathbf{c}_\theta\mathbf{c}_z-\mathbf{c}_z\mathbf{c}_\theta)\\ & +\tfrac{1}{2}[F_{r;z}-F_{z;r}](\mathbf{c}_z\mathbf{c}_r-\mathbf{c}_r\mathbf{c}_z)\end{aligned} \tag{15.5}$$

15.3. Spherical coordinates

$$\begin{aligned}\tfrac{1}{2}(\nabla\mathbf{F}+\mathbf{F}\nabla) = {} & F_{r;r}\mathbf{c}_r\mathbf{c}_r+(R_r\cos\phi)^{-1}(F_{\theta;\theta}+F_r\cos\phi-F_\phi\sin\phi)\mathbf{c}_\theta\mathbf{c}_\theta\\ & +(F_{\phi;\phi}+F_r)\mathbf{c}_\phi\mathbf{c}_\phi\\ & +\tfrac{1}{2}[(R_r\cos\phi)^{-1}(F_{r;\theta}-F_\theta\cos\phi)+F_{\theta;r}](\mathbf{c}_r\mathbf{c}_\theta+\mathbf{c}_\theta\mathbf{c}_r)\\ & +\tfrac{1}{2}[(R_r\cos\phi)^{-1}(F_{\phi;\theta}+F_\theta\sin\phi)+F_{\theta;\phi}](\mathbf{c}_\theta\mathbf{c}_\phi+\mathbf{c}_\phi\mathbf{c}_\theta)\\ & +\tfrac{1}{2}[F_{\phi;r}+F_{r;\phi}-F_\phi](\mathbf{c}_\phi\mathbf{c}_r+\mathbf{c}_r\mathbf{c}_\phi)\end{aligned} \tag{15.6}$$

$$\tfrac{1}{2}(\nabla\mathbf{F}-\mathbf{F}\nabla) = \tfrac{1}{2}[(R_r\cos\phi)^{-1}(F_{r;\theta}-F_\theta\cos\phi)+F_{\theta;r}](\mathbf{c}_r\mathbf{c}_\theta-\mathbf{c}_\theta\mathbf{c}_r)$$
$$+\tfrac{1}{2}[(R_r\cos\phi)^{-1}(F_{\phi;\theta}+F_\theta\sin\phi)+F_{\theta;\phi}](\mathbf{c}_\theta\mathbf{c}_\phi-\mathbf{c}_\phi\mathbf{c}_\theta)$$
$$+\tfrac{1}{2}[F_{r;\phi}+F_{\phi;r}-F_\phi](\mathbf{c}_\phi\mathbf{c}_r-\mathbf{c}_r\mathbf{c}_\phi) \qquad (15.7)$$

16. Divergence and curl of a vector

The divergence of a vector $\mathbf{F}$ is $\nabla\cdot\mathbf{F}$ and the curl is $\nabla\times\mathbf{F}$. Article A,14 gives $\nabla\mathbf{F}$ for the various curvilinear coordinate systems. The divergence of the vector is found by forming the scalar product between the two vectors in each dyad of $\nabla\mathbf{F}$. The curl of the vector is found by forming the vector product between the two vectors of each dyad in $\nabla\mathbf{F}$.

17. Two-dimensional forms of the theorems of Stokes and Gauss on related line, surface and volume integrals

Volume I, articles A,20, A,21 give the three-dimensional forms of these theorems, but for some applications two dimensions are required.

17.1. **Stokes's theorem.** For the finite, single-valued point function $\mathbf{F}$, with C a closed curve and S any surface with C as boundary and $d\mathbf{R}$ a differential change in position along C,

$$\oint_C d\mathbf{R}\cdot\mathbf{F} = \int_S d\mathbf{S}\cdot\nabla\times\mathbf{F} \qquad (17.1)$$

with the surface integral over *one side* of S.

Let C, S be in the plane $R_z = 0$, while $\mathbf{F}$ is a function of R_x, R_y only for cartesian axes. Then, with dC an element of C with unit tangent $\mathbf{t}$ and direction cosines t_x, t_y, A(17.1) becomes

$$\oint_C (t_xF_x+t_yF_y)dC = \iint_S (F_{y;x}-F_{x;y})\partial R_x\partial R_y \qquad (17.2)$$

17.2. **Gauss's theorem.** With volume V enclosed by a surface S, then

$$\int_S d\mathbf{S}\cdot\mathbf{F} = \int_V \nabla\cdot\mathbf{F}dV \qquad (17.3)$$

Let the lamina of article A,17.1 now be of arbitrarily small

thickness h, the volume element $h\delta R_x \delta R_y$, the surface with $\mathbf{c}_z$ as its outward normal be S^+, that with normal $-\mathbf{c}_z$ be S^-, while an element of area on the cylindrical surface is hdC with outward normal direction $\mathbf{n}$. Then, in A(17.3),

$$\int_S = \int_{S^+} + \int_{S^-} + h\oint_C \mathbf{n}\cdot\mathbf{F}dC \tag{17.4}$$

But $\int_{S^-} = -\int_{S^+}$, so that, with n_x, n_y the direction cosines of $\mathbf{n}$, the common factor h cancels on each side of A(17.3) to give

$$\oint_C (n_x F_x + n_y F_y)dC = \iint_S (F_{x;x} + F_{y;y})\partial R_x \partial R_y \tag{17.5}$$

with S, here, the area enclosed by C as in equation A(17.2).

But

$$n_x = t_y \qquad n_y = -t_x \tag{17.6}$$

to give the left-hand side of A(17.5) in terms of the tangential vector $\mathbf{t}$ in place of normal vector $\mathbf{n}$. Then, in closed, *two-dimensional* form, A(17.5) is also

$$\oint_C \mathbf{c}_z\cdot(\mathbf{F}\times d\mathbf{R}) = \int_S \nabla\cdot\mathbf{F}dS \tag{17.7}$$

But, since the dot and cross can be interchanged in the product of the three terms under the integral sign on the left-hand side, then also

$$\oint_C \mathbf{c}_z\times\mathbf{F}\cdot d\mathbf{R} = \int_S \nabla\cdot\mathbf{F}dS \tag{17.8}$$

to give a tangential line-integral form for Gauss's two-dimensional divergence theorem.

Appendix B

COMPLEX VARIABLE

1. Complex variable

The complex variable evolved from the extraction of roots from algebraic equations. There occurred forms such as $\sqrt{(-1)}$, not being a physical quantity, although it had to be given mathematical meaning to ensure that an equation of degree n had n roots. Thus, the so-called 'imaginary' is

$$i = \sqrt{(-1)} \qquad i^2 = -1 \tag{1.1}$$

With R_x, R_y the cartesian components of position vector **R**, then the complex variable

$$c = R_x + iR_y \tag{1.2}$$

Comparison of **B**(1.1) with the Hamiltonian forms in volume I, article **A**,1 shows that quaternions can be thought of as a further generalisation of complex numbers. Alternatively, the 'rotating' effect of unit vectors in vector product can be used to interpret i into vector analysis terms, but this is not pursued here. In plane polar coordinates in which $R_r = R$, then

$$c = R\cos\theta + iR\sin\theta = R\exp(i\theta) \tag{1.3}$$

1.1. **Conjugate complex variable.** The complex position

$$c' = R_x - iR_y = R(\cos\theta - i\sin\theta) = R\exp(-i\theta) \tag{1.4}$$

is the reflection of c in the 'real' axis OR_x and is the conjugate of c.

2. Function of the complex variable

A function $\gamma(c)$ of c can always be resolved to 'real' and 'imaginary' components $\alpha(R_x, R_y)$, $\beta(R_x, R_y)$. That is,

$$\gamma = \alpha + i\beta \tag{2.1}$$

2.1. **Conjugate function.** By definition, the conjugate of γ is this function with the sign of i changed. Thus,

$$\gamma' = \alpha - i\beta \tag{2.2}$$

Therefore, $\gamma'(c')$ is of the same functional form as $\gamma(c)$.

3. Differentiability of a function of the complex variable

If $d\gamma/dc$, the rate of change of γ with respect to c, is to be uniquely defined at a point, then it must not depend on the way c changes by change in the value of either, or both, R_x and iR_y. Thus,

$$\frac{d\gamma}{dc} = \frac{\partial\gamma}{\partial R_x} = \frac{\partial\gamma}{\partial(iR_y)} \tag{3.1}$$

so that

$$\frac{\partial\alpha}{\partial R_x}+i\frac{\partial\beta}{\partial R_x} = \frac{\partial\alpha}{\partial(iR_y)}+i\frac{\partial\beta}{\partial(iR_y)} \tag{3.2}$$

Therefore, equating reals and imaginaries on each side gives the Cauchy-Riemann conditions, briefly, as

$$\alpha_{;x} = \beta_{;y} \qquad -\alpha_{;y} = \beta_{;x} \tag{3.3}$$

The integral of a complex function must be differentiable, so consider

$$\int\gamma dc = C = A+iB \tag{3.4}$$

and, similar to **B**(3.1), **B**(3.3),

$$\gamma = \frac{dC}{dc} = \frac{\partial A}{\partial R_x}+i\frac{\partial B}{\partial R_x} = \frac{\partial A}{\partial(iR_y)}+i\frac{\partial B}{\partial(iR_y)}$$

$$\alpha = A_{;x} = B_{;y} \qquad \beta = B_{;x} = -A_{;y} \tag{3.5}$$

4. Orthogonality of the trajectories of the components of a function of the complex variable

Let the coplanar curves α = constant, β = constant intersect at point **R**. Let $\delta\mathbf{R}_\beta$ be a differential change in position along β = constant during which α changes to $\alpha+\delta\alpha$. Then the unit vector tangential to β = constant is

$$\mathbf{t}_\beta = \delta\mathbf{R}_\beta/\delta\alpha \tag{4.1}$$

Similarly, the unit tangent to α = constant is

$$\mathbf{t}_\alpha = \delta\mathbf{R}_\alpha/\delta\beta \tag{4.2}$$

Resolving the δ**R**'s to cartesian axes OR_xR_y, form the scalar product of the **t**'s and equate to zero on the assumption that they are orthogonal. There follows, on slight rearrangement,

$$\alpha_{;x}/\beta_{;y} = -\alpha_{;y}/\beta_{;x} \tag{4.3}$$

But these are the Cauchy-Riemann conditions rearranged so that α = constant, β = constant are orthogonal.

5. Distribution law for components of a function of a complex variable

By differentiating and adding suitably, equations **B**(3.3) give

$$\nabla^2\alpha = 0 = \nabla^2\beta \tag{5.1}$$

with the two-dimensional laplacian operator

$$\nabla^2(\ ) = (\ )_{;xx}+(\ )_{;yy} \tag{5.2}$$

6. Complex potential

Either of the conjugate components of a complex function can be used as a potential function in the analysis of a deformation. This restricts the corresponding self-conjugate dyadic to have a zero first invariant. Thus,

$$\mathfrak{J}:(\nabla\nabla\alpha+i\nabla\nabla\beta) = \mathfrak{J}:\nabla\nabla\gamma = 0 \tag{6.1}$$

in view of **B**(5.1).

6.1. Vector gradient of a complex function. Noting **B**(3.1) gives

$$\nabla\gamma = \mathbf{c}_x\gamma_{;x}+\mathbf{c}_y\gamma_{;y} = \overset{\circ}{\mathbf{c}}\gamma_{/c} \tag{6.2}$$

with total differentiation denoted briefly by $(\ )_{/c}$ and the *complex unit vector*

$$\overset{\circ}{\mathbf{c}} = \mathbf{c}_x+i\mathbf{c}_y \tag{6.3}$$

Transformation to plane, polar coordinates gives

$$\overset{\circ}{\mathbf{c}} = (\mathbf{c}_r+i\mathbf{c}_\theta)\exp(i\theta) \tag{6.4}$$

The complex vector **B**(6.2) has complementary, lamellar components. (See volume I, article **A**,18.)

6.2. Grad grad of a complex function. Similar to **B**(6.2),

$$\nabla\nabla\gamma = \nabla(\nabla\gamma) = \overset{\circ\circ}{\mathbf{cc}}\gamma_{/cc} \tag{6.5}$$

with the complex unit dyad

$$\begin{aligned}\overset{\circ\circ}{\mathbf{cc}} &= [\mathbf{c}_x\mathbf{c}_x-\mathbf{c}_y\mathbf{c}_y+i(\mathbf{c}_x\mathbf{c}_y+\mathbf{c}_y\mathbf{c}_x)]\\ &= [\mathbf{c}_r\mathbf{c}_r-\mathbf{c}_\theta\mathbf{c}_\theta+i(\mathbf{c}_r\mathbf{c}_\theta+\mathbf{c}_\theta\mathbf{c}_r)]\exp(i2\theta)\end{aligned} \tag{6.6}$$

Self-conjugate dyadics are usually found far more easily as in **B**(6.5) rather than by extracting the complementary components of the complex function and performing the operation $\nabla\nabla$ on either separately.

Appendix C

FINITE DIFFERENCES

1. Polynomial representation of a continuous function

The functions occurring in the equations for physics are usually single-valued, finite and continuous at all points in the range considered. However, the experimental data corresponding to these functions are known at only discrete points of the function space. Theory and experiment can be compared at these discrete points only, so that it is frequently convenient to reshape the theoretical expressions into a form suitable for numerical manipulation over discrete intervals of the function space.

The first step is the converse of this process. Suppose a continuous function $F = F_0, F_1, \ldots, F_{k-1}, F_k, F_{k+1}, \ldots, F_n$ at points $R_x = 0, h, \ldots, (k-1)h, kh, (k+1)h, \ldots, nh$ for a single independent variable. It is assumed that the function F can be expressed as a finite power series (or polynomial). Thus,

$$F = \sum_{k=0,1,\ldots,n} C_k R_x{}^k \tag{1.1}$$

The coefficients C_k are adjusted to such values that F assumes the values F_k at points $R_x = kh$, but otherwise the values of F conform with those given by C(1.1). This polynomial is continuous, with continuous derivatives up to the n'th, and so satisfies all the required conditions for the function.

Several techniques have been evolved to find the values of the C_k in terms of the F_k, k, h. Usually factorial expressions are used [93, 94, 77]. Thus, with

$$\phi_k(R_x) = R_x(R_x-h)\ldots[R_x-(k-1)h][R_x-(k+1)h]\ldots(R_x-nh)$$
$$\phi_k(kh) = (-1)^{(n-k)}k!(n-k)!h^n$$

then,

$$F = \sum_{k=0,1,\ldots,n} [\phi_k(R_x)/\phi_k(kh)]F_k \tag{1.2}$$

Thus, when $R_x = kh$ then $F = F_k$, since the coefficient of F_k is unity, while the coefficient of each F_r when $r \neq k$ is zero. The expansion of this expression gives the form C(1.1) with the coefficients C_k in terms of the F_k and h.

2. Differentiation with finite differences

This process is as old as the differential calculus, but, even so, fresh progress has been made recently. W. G. Bickley, in 1941 [94], studied the accuracy of differentiation at the point $R_x = 0$ when various numbers of the values F_k are considered in the process. A few values such as $F_0, F_1, \ldots, F_5$ proved sufficient for differentiation up to the fourth order, for example. The inclusion of F_k's with $k > 5$ leads to elaborate formulæ not justified by the slight increase in accuracy for most cases.

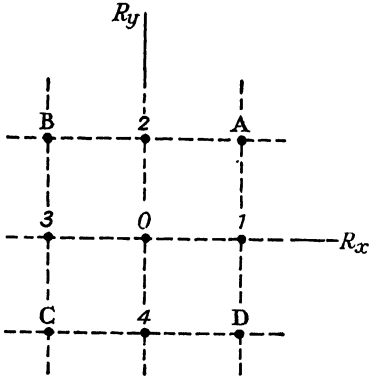

FIG. C,2.1—Two-dimensional relaxation *local* grid. All points are h apart along the grid lines. The eight points around the central point are sufficient to define all the partial-differential coefficients up to the second order.

2.1. **Two-dimensional.** Using a two-dimensional grid for cartesian axes OR_xR_y and notation as in reference [77] gives the discrete points at distance h apart as in Fig. C,2.1. Differentiation of such as C(1.1) gives [94], with the least possible number of F_k's, the partial-differential coefficients at the point *0* as

$$\left.\begin{aligned}(F_{;x})_0 &= (F_1 - F_3)/(2h)\\ (F_{;xx})_0 &= (F_1 + F_3 - 2F_0)/h^2\end{aligned}\right\} \qquad (2.1)$$

$$\left.\begin{aligned}(F_{;y})_0 &= (F_2 - F_4)/(2h)\\ (F_{;yy})_0 &= (F_2 + F_4 - 2F_0)/h^2\end{aligned}\right\} \qquad (2.2)$$

$$(F_{;xy})_0 = (F_A - F_B + F_C - F_D)/(4h^2) \qquad (2.3)$$

2.2 **Three-dimensional.** The forms of the partial-differential coefficients are obvious, but, for brevity, it is convenient to modify

the notation. Thus, modify Fig. C,2.1 to give Fig. C,2.2, which is the plane $R_z = 0$ and is the typical plane of the three for the cartesian, orthogonal axes $OR_1R_2R_3$ or OR_x briefly. Thus, the special sequence $x = 1, 2, 3$, $y = 2, 3, 1$, $z = 3, 1, 2$ has been used as in the principal notation. Now, similar to equations C(2.1) to C(2.3),

$$(F_{;x})_0 = (F_x - F_{-x})/(2h) \tag{2.4}$$

$$\left.\begin{aligned}(F_{;xx})_0 &= (F_x + F_{-x} - 2F_0)/h^2 \\ (F_{;xy})_0 &= (F_{xy} - F_{-xy} + F_{-x-y} - F_{x-y})/(4h^2)\end{aligned}\right\} \tag{2.5}$$

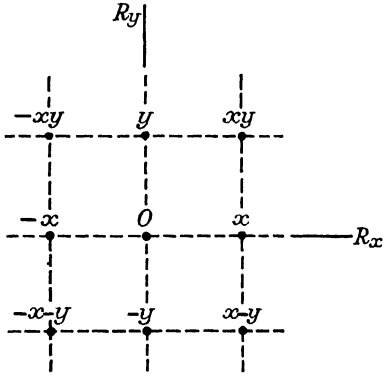

FIG. C,2.2.—Three-dimensional relaxation *local* grid. All points are h apart along the grid lines. This is a typical plane (R_x, R_y) or $R_z = 0$ of the three such planes. The special sequence $x = 1, 2, 3$, $y = 2, 3, 1$, $z = 3, 1, 2$ is used here as elsewhere. The introduction of negative numerals simplifies and abbreviates the three-dimensional formulæ compared with their form if a notation such as that in Fig. C,2.1 is used.

and these apply generally when the appropriate numerals are substituted for x, y. Thus, with $x = 2$, $y = 3$, for example,

$$(F_{;23})_0 = (F_{23} - F_{-23} + F_{-2-3} - F_{2-3})/(4h^2)$$

3. Laplacian operator

This operator occurs frequently in the deformation equations, so that its explicit statement in finite-difference form is convenient.

3.1. **Two-dimensional.** From C(2.1).2 and C(2.2).2

$$(\nabla^2 F)_0 = (F_{;xx})_0 + (F_{;yy})_0 = (F_1 + F_2 + F_3 + F_4 - 4F_0)/h^2 \tag{3.1}$$

This was given by C. Runge, in 1908, and others since[76].

R. V. Southwell [77.3] has generalised this sort of expression to the case where either 3, 4 or 6 points are those adjacent to *0* and are equally spaced around a circle of radius h. The resulting triangular and hexagonal grids for 3 and 6 points on the circle are useful in some problems but usually the square grid, of Fig. C,2.1 for 4 points, is used.

Equation C(3.1) applies to one point and its locality in a continuous field of the function F.

3.2. **Three-dimensional.** The three-dimensional form follows from adding together the three expressions C(2.5).1 to give

$$(\nabla^2 F)_0 = \left(\sum_x F_{;xx}\right)_0 = \left[\sum_x (F_x + F_{-x}) - 6F_0\right]/h^2 \qquad (3.2)$$

where the F_x values are all at distance h from *0*.

4. Solution of simultaneous, linear, algebraic equations

4.1. **Iteration of the wanted functions.** The iterative method of solving simultaneous, linear, algebraic equations began with Gregory's method, given in 1674 [93.1], to extract the square and cube roots of algebraic equations. The solution of the lagrangian frequency equations proved difficult and a matrix iterative method was given by W. J. Duncan & A. R. Collar [98] in 1934. However, this method proved laborious with a large number of independent variables.

4.2. **Escalation.** J. Morris & J. W. Head, in 1942 [99], sought to overcome this difficulty by devising their escalator method, which avoids successive approximation by considering a sub-set of the equations and suitably reducing the number of variables in each. The roots found from these equations are used to find other roots for a larger sub-set and so on until the full number of variables is considered. The escalator method is applied to simultaneous, linear, algebraic equations by J. Morris (1947 [96]).

4.3. **Finite differences.** The solution of the boundary-value problems of theoretical physics for various differential equations was sought by various methods [100],† including finite differences [93.2].

† Other methods include the choice of arbitrary values for the wanted functions satisfying some of the conditions of the problem and then finding the adjustment necessary by *minimising the error*. S. Ödman considered this in detail in 1948 and in a survey in 1953 [101].

The problem is thus reduced to the solution of simultaneous, linear, algebraic equations for which iterative methods are applicable [95].

4.4. **Iteration of errors in the wanted functions.** A fresh approach was initiated by the Hardy Cross method of *moment distribution* given in 1930 [97]. This is a physico-mathematical method to solve for the bending moments in the equilibrium of joints of rigid-jointed frames. A good approximation is found to the moments and then these values are 'fixed' temporarily. Now, one joint is 'released' so that it can rotate to an equilibrium position under the moments in the members radiating from the joint. The previous moment in excess of that for equilibrium has the excess distributed appropriately to the other ends of the members. The joint is again fixed and the distribution of the excess moment performed at another joint. The process is continued until the excess moment at each joint is negligibly small. The process is *iteration of errors* in place of iteration of the wanted quantities in the simultaneous, linear, equilibrium equations.

R. V. Southwell, in 1935 [103], used the iteration of errors to analyse frameworks and named it the *relaxation method.* In 1938 [104], D. G. Christopherson & R. V. Southwell extended the method to two independent variables as in equation C(3.1), for example. An exponent of iterative methods [95] has described the relaxation process as '. . . a sort of brute-force, cut-and-try numerical method of attack' [105]. There may be some justification for this, since elaborate methodological rules of manipulation are not formulated; there are involved only simple arithmetical processes that are within the grasp of the least skilled of computers. This is a powerful argument *for* the method!

4.5. **Spirit of the relaxational approach.** Orthodox mathematics seeks the general solution of a given, governing differential equation: (i) at all points within and on the boundary of the function space, and (ii) the exact values of the wanted function, with (iii) precisely specified values of the wanted function and/or its derivatives at the boundary.

R. V. Southwell [77] observes that for the formulation of a theory in mathematical physics and its subsequent examination '. . . the data must be obtained by physical measurement, *therefore can be neither exact nor complete*' [77.10]. Again, 'From the practical

standpoint a function is *sufficiently* determined when its values are known within tolerable margins of uncertainty and at a number of points which is large enough to define the trend of its values elsewhere' [77.11]. And again he gives '. . . a contention which underlies the whole argument . . . that nothing in our definition of a function requires the mathematical form . . . to be known' [77.10]. On this basis Southwell concludes that in physical problems orthodox differential equations can be replaced by finite-difference forms without appreciable error, since the intervals can be chosen as small as we please [77.9]. Again, it is not necessary to solve the finite-difference equations *exactly*, '. . . *since it is always possible to account for the data within their estimated margins of uncertainty*' [77.9]. This leads to '. . . a systematic sequence of operations, each entailing localised alteration of the wanted function, which steadily reduces the magnitudes of quantities termed "residuals", thereby accounting for the data more and more completely' [77.9]. Therefore, the '. . . task will be ended when all residuals have been brought (sensibly) to zero at internal points' [77.12] and so that '. . . any problem that can be formulated can be solved' [77.13].

The relaxation procedure is described in article C,5.3, where it is noted that there is no mathematical proof of convergence to a unique solution from *any* arbitrary initial values and prescribed boundary conditions. Article C,7.2 shows that convergence does not occur in all cases and article C,7.3 gives examples of pseudo-harmonic functions. The deformation problem in article VII,6 relates the harmonic and pseudo-harmonic functions.

5. Two-dimensional Poisson's equation solved by the iteration of errors

R. V. Southwell [77.4] describes the method by analogy to an initially plane net with transverse forces at the nodes. There appears to be no mathematical proof of convergency of the relaxation process to *unique* values of F. Appeal is made to the fact that the physical net adopts a configuration consistent with minimum strain energy, while the problems considered have physically unique solutions [77.5, 77.6, 77.7]. The following direct arithmetical approach seems shorter than the net analogue.†

† Author, 1945. This is an obvious description but does not seem to be given in the literature.

Poisson's equation, with the right-hand side as a known, continuous function G, is

$$\nabla^2 F = G \tag{5.1}$$

Substituting C(3.1) gives, for point $R_x = 0$,

$$\tfrac{1}{4}(F_1+F_2+F_3+F_4)-F_0-\tfrac{1}{4}h^2G_0 = 0 \tag{5.2}$$

When the values $F_0, \ldots, F_4$ are known exactly, then this equation is satisfied identically.

5.1. **First approximation.** Allocate arbitrary values (usually chosen to suit some intuitive knowledge) F^P, F^Q, ... on the grid,

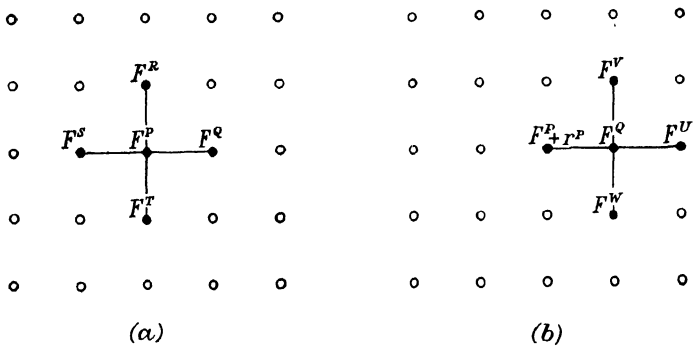

FIG. C,5.1.—Two-dimensional relaxation grid with distance h between the nodes along the grid lines. Five arbitrary, initial values of the wanted function are shown in (*a*) with P as the central point to which the *local* difference equation applies. The residue at P is liquidated and added to the initial value of F as in (*b*). The point Q is now taken as the central point to which the *local* difference equation will apply. The initial residue at P is now seen to influence the value of the residue at Q for this second approximation to the field of values for F.

with nodal points P, Q, ... as in Fig C,5.1(*a*). Apply equation C(5.2), but, since the F^P, ... values are not correct (generally), the right-hand side is not zero but equals the *residue* r_0^P, say. Thus,

$$\tfrac{1}{4}(F_1^Q+F_2^R+F_3^S+F_4^T)-(F_0^P+r_0^P)-\tfrac{1}{4}h^2G_0^P = 0 \tag{5.3}$$

Therefore, if the residue is added to the value F^P, then the five values (F^P+r^P), F^Q, ..., F^T constitute an exact local solution of C(5.2).

5.2. **Second approximation.** Now, regard the set of values of F as those for a fresh beginning. Firstly apply C(5.2) to the

original values before liquidation of the residue at P. Let r_0^Q be this residue to give

$$\tfrac{1}{4}(F_1^U+F_2^V+F_3^P+F_4^W)-(F_0^Q+r_0^Q)-\tfrac{1}{4}h^2G_0^Q=0 \qquad (5.4)$$

Since point P is now point 3 on the local grid, denote the *initial* residue at P by r_3^P and add and subtract $\frac{1}{4}r_3^P$ to C(5.4). This gives

$$\tfrac{1}{4}[F_1^U+F_2^V+(F_3^P+r_3^P)+F_4^W]-(F_0^Q+r_0^Q+\tfrac{1}{4}r_3^P)-\tfrac{1}{4}h^2G_0^Q=0 \quad (5.5)$$

Now apply C(5.2) to the values shown in Fig. C,5.1(b) as those after liquidation of the residue at P. This gives just C(5.5) with the residue $(r_0^Q+\frac{1}{4}r_3^P)$. Therefore, the liquidation of the residue at P *increases* the residue at Q by $\frac{1}{4}r_3^P$.

Similarly, the liquidation of the residue at P effectively increases that at each of the points R, S, T by $\frac{1}{4}r_0^P$ when they are considered in turn.

5.3. **Relaxation procedure.** Fig. C,5.2(a) combines the two Figs. C,5.1(a), (b), while Fig. C,5.2(b) gives numbers as an illustration. The values of F^P, F^Q, ..., F^W have been chosen as 1, 2, ..., 8. The residues are $r^P=2\frac{1}{2}$, $r^Q=3\frac{1}{2}$ on using initial values of F and with G chosen as zero. Each residue has been liquidated at its point and distributed to the adjacent four points. The columns are added on each side of a point to give the modified values of the function and the residue. The liquidation of the residue at each point then gives the new set of values $4\frac{3}{8}$, $6\frac{1}{8}$, ..., $8\frac{7}{8}$ in Fig. C,5.2(c) to be taken as the set for further relaxation by liquidation of the largest residues as and where they occur. Now $r^P=\frac{5}{8}$, $r^Q=\frac{7}{8}$ are smaller than they were, so that temporary local satisfaction of the governing equation is closer.

The description of the process makes it seem complicated, but a trial by the reader will show its simplicity.

5.4. **Boundaries.** The relaxation procedure is continued until the residues are small enough to be considered as negligible within the boundary of the function space.

This leads to the necessity of defining the boundary for finite differences of position. With the grid of discrete points shown in Fig. C,5.3 the 'boundary' points are those nearest to the *actual boundary* (AB) and define the *equivalent boundary* (EB). Boundaries AB and EB are brought closer to coincidence as the grid spacing h is reduced.

The function F and/or its derivatives, as given in article C,2.

must have special values at the boundary. When the derivatives are involved then there must be found a suitable number of values of F outside the boundary as in Fig. C,5.3. We are concerned with all derivatives up to the second order, so that it is necessary to have eight points surrounding each point of EB for

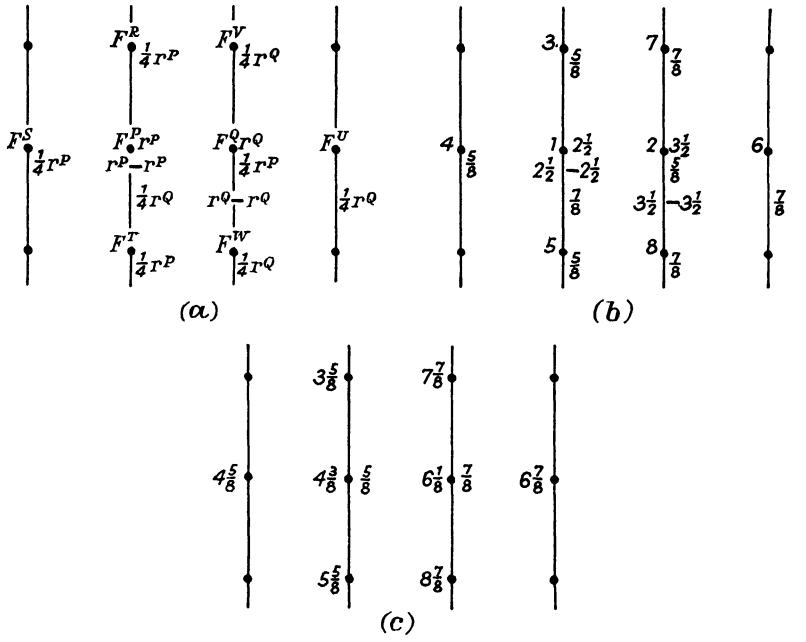

FIG. C,5.2.—Example of a relaxation computation for a laplacian distribution with the algebraic representation in (*a*), the first approximation to the wanted function, the residuals and their distribution in (*b*), the liquidation of all residuals and recalculation of the current residues gives the second approximation to the wanted function in (*c*). Note the rapid reduction in the residues between (*b*) and (*c*) for only one sequence of liquidation for the two points P and Q.

a square mesh. The outer members of these points define the *fictitious boundary* (FB) which tends to coincide with AB as the grid spacing is reduced.

The relaxation procedure † is thus seen to involve the 'dispersal'

† The foregoing description of boundaries differs considerably from that given by R. V. Southwell [77]. Southwell introduces *fictitious nodes* beyond the actual boundary, but these are not considered as joined to form a 'fictitious boundary' as here. The strings of the analogic net are terminated at the actual boundary and this leads to the necessity for the *unequal star*

of the original errors to points beyond the boundary FB. Errors of any magnitude whatever have no effect on the solution of a problem so long as they are not in the function space.

5.5. **Analogues to solve Poisson's equation.** *A net:* The infinitesimal transverse displacement of an initially flat membrane and the distributed normal force causing the displacement are

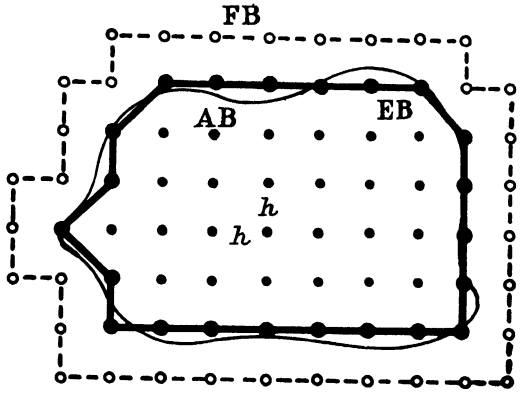

FIG. C,5.3.—Two-dimensional function space relaxation grid with grid length h. The *actual boundary* (AB) is replaced by the *equivalent boundary* (EB) defined by the grid nodal points closest to AB. The points on the *fictitious boundary* (FB) are such that each point on EB is surrounded by eight points: four in the grid lines directions and four in the diagonal directions. These eight points allow the definition of all the arbitrary partial-differential coefficients, up to the second order, of the wanted function at EB. (If it is required to impose arbitrary boundary conditions on the partial-differential coefficients up to the fourth order then the FB must be two lengths h outside EB.) As h becomes smaller, then so AB, EB, FB approach more nearly to coincidence.

related by a Poisson's equation [23.11, 77.8, 106]. R. V. Southwell, in 1938 [77.4], expressed this in finite differences, so that the membrane became a net loaded at its nodal points. Numbering the nodes as in Fig. C,2.1 and viewing, in the direction $-OR_y$, a section of the

grid technique. Further [77.14], '. . . *there is nothing to prohibit multiple values at "fictitious nodes"* . . .'. The present author feels that the complication of manipulation and thought introduced by not considering the fictitious boundary as part of the single-valued function space is unwarranted. Again, it is not clear how to set up the analogic electrical networks of articles C,5.5, C,6.2 if multiple values were allowed at fictitious nodes.

net along axis OR_x gives Fig. C,5.4. Force $\frac{1}{4}h^2G_0$ is applied in direction OR_z to the node at *0*. The small transverse displacements induced are F_0, F_1, F_2, F_3, F_4 considering the four points around *0*. Tensile force L, say, is induced in *each* of the four strings. It is readily shown geometrically that the component in the direction OR_z of the tension in string *01* is $\frac{1}{4}(F_1-F_0)$. All four such forces, when added, give $\frac{1}{4}(F_1+F_2+F_3+F_4)-F_0$ and this balances the applied force $\frac{1}{4}h^2G_0$. Therefore, equation

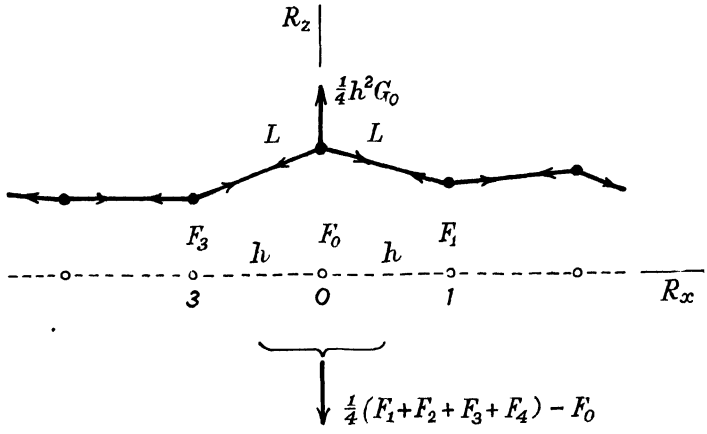

FIG. C,5.4.—The analogic, initially plane net (as in Fig. C,2.1) sectioned along the axis OR_x to show the small transverse deflections due to transverse loading applied to each nodal point. The deflected net is shown as a firm line and the corresponding unloaded net is shown dotted. At the typical node *0* there acts the force shown and this is balanced by the transverse components of the equal tensions L acting in each of the four strings radiating from *0*. The deflections of the central point *0* and the four surrounding points *1, 2, 3, 4* are $F_0, \ldots, F_4$ of the same values as the wanted function at each point.

C(5.2) is satisfied exactly if such a net is constructed, the appropriate forces $\frac{1}{4}h^2G_0$ applied and the transverse displacements measured. Suitable boundary conditions must also be imposed to solve particular problems.

An electrical network: T. K. Hogan, in 1943[107], gave the analogy for an electrical network, as in Fig. C,5.5 with $F_0, \ldots, F_4$, G_0 as potentials and the 'grid length' h is $\sqrt{(r/R)}$ by analogy. The resistance R is large compared with r; that is, 100 to 1000 or more times greater. Equation C(5.2) is satisfied exactly. S. C.

Redshaw, in 1946 [108], extended the analogy, constructed an instrument with a 10 by 10 mesh and performed experiments showing good accuracy.

6. Three-dimensional Poisson's equation solved by the iteration of errors

When the functions F, G are three-dimensional in

$$\nabla^2 F = G \tag{6.1}$$

then the three-dimensional laplacian operator of article C,3.2 gives

$$\tfrac{1}{6}\sum_x (F_x + F_{-x}) - F_0 - \tfrac{1}{6}h^2 G_0 = 0 \tag{6.2}$$

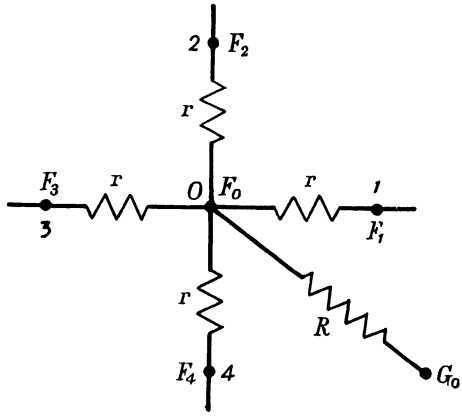

FIG. C,5.5. A typical star of the electrical network analogue to solve the two-dimensional Poisson's equation expressed in finite differences (after T. K. Hogan [107]). Potentials F_0, ..., F_4 correspond to the wanted function when applied potential G_0 is the non-zero right-hand side of Poisson's equation. Potential G_0 must be large when compared with the F's and so resistance R is large when compared with r. The 'grid length' is $\sqrt{(r/R)}$ by analogy.

6.1. **Relaxation procedure.** Similar to the procedure in article C,5 a set of values F_x', say, are guessed for all the nodal points. Then, the right-hand side of C(6.2), instead of being zero, equals the residue r_0', say, to give

$$\tfrac{1}{6}\sum_x (F_x' + F_{-x}') - (F_0' + r_0') - \tfrac{1}{6}h^2 G_0 = 0 \tag{6.3}$$

The liquidated residue r_0' added to F_0' must be distributed equally between the six points x around the current point 0.

That $\frac{1}{6}r_0'$ must be added to the current residues at each of the six points x is clear from the argument similar to that in article C,5.2.

This procedure continues with the greatest (usually) residue liquidated and distributed at each step until the residues become negligibly small within the function space when the boundary conditions are satisfied.

6.2. **Analogues.** The extension from a plane, physical net to a cubical net does not appear to follow simply, but the electrical analogue for three dimensions is simple:

An electrical network: Fig. C,6.1 is an isometric view of the

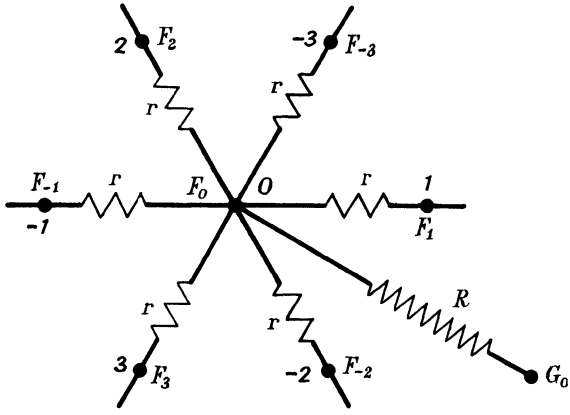

FIG. C,6.1.—An isometric view of the typical, *orthogonal* star of the electrical network for the analogic solution of the three-dimensional Poisson's equation expressed in finite differences with 'grid length' $\sqrt{(r/R)}$. Applied potential G_0 corresponds to the non-zero right-hand side of Poisson's equation and the F's are the potentials of the same values as the wanted function. Potential G_0 must be large compared with the F's, so that the resistance R is also large compared with r.

three-dimensional orthogonal star with six equal resistance arms r which are small compared with the starpoint feeder resistance R. Denote current in the arm x by I_x due to potentials F_0, F_x. Then,

$$F_0 - F_x = rI_x$$

so that, on adding these six terms,

$$6F_0 - \sum_x (F_x + F_{-x}) = r\sum_x (I_x + I_{-x}) \qquad (6.4)$$

But, with current I_0 in the feeder arm, since electricity cannot accumulate at 0, then

$$\sum_x (I_x + I_{-x}) + I_0 = 0 \tag{6.5}$$

while

$$I_0 = (G_0 - F_0)/R \doteq G_0/R \tag{6.6}$$

provided G_0 *is large compared with* F_0. Substituting C(6.6), C(6.5) in C(6.4) and then multiplying by $-\frac{1}{6}$ gives

$$\tfrac{1}{6}\sum_x (F_x + F_{-x}) - F_0 - \tfrac{1}{6}\frac{r}{R}G_0 = 0 \tag{6.7}$$

This is precisely C(6.3) when the grid length $h = \sqrt{(r/R)}$. Therefore, the nodal voltages for a distribution of such stars throughout the function space supply an exact solution of the Poisson equation provided that the appropriate boundary conditions are satisfied.

S. C. Redshaw [108] found experimental difficulty in matching the two-dimensional network resistances r. This difficulty can be avoided by using an electrically resisting continuum (solid or fluid) as the function space. The outer boundary of the continuum needs to be sufficiently far from the region in which the nodal points are to be defined so that the resistance r will be the same between any two points at the same distance apart. That is, the boundary must be at infinity, theoretically, so that it does not influence the resistance r. Now, setting up conducting nodal *points* as in Fig. C,6.1, the resisting continuum acts as r between each pair of points so that Fig. C,6.1 is then the equivalent mesh. The application of potential G_0 through the large resistance R at each nodal point completes the continuum form of the mesh. Much work has been done [51] using a tank of conducting fluid to solve Laplace's equation (i.e. with $G_0 = 0$) but the simple extension of the technique to include Poisson's equation as here appears to have not been done previously.

7. Laplace's equation solved by the iteration of errors

Poisson's two-dimensional equation expressed in finite differences is given in article C,5. When $G = 0$ then Poisson's equation becomes Laplace's equation

$$\nabla^2 F = 0 \tag{7.1}$$

or, for finite differences,

$$F_0 = \tfrac{1}{4}(F_1 + F_2 + F_3 + F_4) \tag{7.2}$$

independent of the grid length h.

7.1. **One-dimensional Laplace's equation.** Suppose F is independent of R_y and then, from Fig. C,2.1, $F_2 = F_0 = F_4$ and then, from C(7.2),

$$F_0 = \tfrac{1}{2}(F_1+F_3) \tag{7.3}$$

consistent with C(2.1).2. Now, the formal Laplace's equation is

$$\nabla^2 F = F_{;xx} = 0 \tag{7.4}$$

Integration gives, with arbitrary constant A, B,

$$F = AR_x+B \tag{7.5}$$

Clearly, the finite-difference equation C(7.3) is satisfied exactly, with zero residues, when the F_k's fall on this linear curve.

7.2. **Pseudo - harmonic functions.** Now, suppose some values F_k' in C(7.3) give

$$\tfrac{1}{2}(F_1'+F_3')-F_0' = r_0' \doteq 0 \tag{7.6}$$

with the residue r_0' as *quasi-zero* in comparison with the 'observed', discrete values of the wanted function F. The values F_k' constitute an harmonic-function solution of the Laplace's equation expressed in finite-difference form in conformity with the spirit of the relaxational approach, as discussed in article C,4.5.

But C(7.6) is satisfied on any continuous curve merely by choosing the F_3', F_0', F_1' sufficiently close together. Notice that the grid length h has disappeared from C(7.3), since the right-hand side of C(7.4) is zero. Thus, any continuous function of R_x constitutes a pseudo-harmonic solution of the finite-difference Laplace's equation.

Any set of discrete values of F (spaced even distances apart) will be 'smoothed' on to a continuous curve which is a pseudo-harmonic solution of C(7.3).† Therefore, the question arises of whether the relaxational technique leads to *convergence* to a unique solution of Laplace's equation for any particular problem.

7.3. **Examples of pseudo - harmonic functions.** For example, with

$$F \doteq \cos R_x \tag{7.7}$$

discrete values of F can be chosen from trigonometric tables to satisfy C(7.3) very closely with r_0' in C(7.6) as small as we wish so that 'practically' it is quasi-zero but is never absolutely zero.

† Author, 1951.

But, formally, C(7.7) in C(7.4) gives

$$-\cos R_x = 0 \tag{7.8}$$

but the left-hand side is *not zero* except at $R_x = \pm\frac{1}{2}\pi$, so that C(7.4) is not satisfied in general although its finite-difference equivalent C(7.3) is quasi-satisfied within 'practical' limits.

More generally,

$$F = \cos nR_x \tag{7.9}$$

is a satisfactory pseudo-harmonic solution of C(7.3) giving the same terminal values of F for suitable, different values of n. Thus, more than one solution of C(7.3) is possible with the same boundary values for F.

7.4. **An artifice to transform Laplace's equation to a Poisson's equation.** Laplace's equation is

$$\nabla^2 F = 0 \tag{7.10}$$

If the operator ∇^2 is two-dimensional, then, with an arbitrary constant G,

$$\nabla^2 \tfrac{1}{4}(\mathbf{R}\cdot\mathbf{R})G = \nabla^2 \tfrac{1}{4}(R_x^2 + R_y^2)G = G \tag{7.11}$$

With function $H(R_x, R_y)$, suppose that

$$H = F + \tfrac{1}{4}G\mathbf{R}\cdot\mathbf{R} \tag{7.12}$$

and then,

$$\nabla^2 H = G \tag{7.13}$$

which is Poisson's equation with the right-hand side constant.† Boundary conditions on F and/or its derivatives are now transformed to conditions on H and $\frac{1}{4}G\mathbf{R}\cdot\mathbf{R}$ as in equation C(7.13).

The net analogue then gives G as a force of the same, but arbitrary, value at each node, while the electrical analogue gives the same-valued potential applied to each of the starpoint arms. Such a physical situation has a unique solution, so that the difficulty about convergence to a unique solution, as presented in articles C,7.2, C,7.3, appears to be avoided. However, the boundary conditions have not been discussed. This is best done by examples, of which one is given in article VII,6.

This artifice overcomes the difficulty that, if C(7.10) is to apply throughout a singly connected plane, for example, then the transverse forces on the net are zero and the analogy does not apply.

† Author, 1951. It is unlikely that such a simple artifice has not been anticipated, but the present author has no other reference to it. The exponents of the relaxation method and analogues do not mention it. (See references [77, 108].)

R. V. Southwell [77] does not discuss the difficulty. Again, when applying the electrical network to Laplace's equation, then S. C. Redshaw [108] introduces a feeder connection into the centre of the field. This is a discontinuity in the laplacian field, so that Poisson's equation must be applied at that point and a 'barrier' boundary used to exclude it from the rest of the field, which then becomes doubly connected and so does not satisfy the requirement of single-connectivity.

If equation C(7.13) is taken as three-dimensional, then,

$$H = F + \tfrac{1}{6} G\mathbf{R}\cdot\mathbf{R} \tag{7.14}$$

with the three-dimensional position vector **R**.

Appendix D

FOURIER SERIES

1. Fourier series

The representation of continuous or *discontinuous* periodic functions by a series of trigonometric terms was given by Fourier in 1811 [110].† Thus, under the conditions prevailing (or which we arrange to prevail), a function $E(\theta)$, say, is *represented* by the Fourier series $F(\theta)$, say, so that

$$E(\theta) = F(\theta) \qquad (-\pi \leqq \theta \leqq \pi) \tag{1.1}$$

with

$$F(\theta) = \tfrac{1}{2}A_0 + \sum_{n=1,\ldots,\infty} (A_n \cos n\theta + B_n \sin n\theta) \tag{1.2}$$

when the constant coefficients, independent of θ, are given by

$$\left.\begin{aligned} A_n &= \frac{1}{\pi}\int_{-\pi}^{\pi} E(\theta)\cos n\theta\, d\theta \qquad (n = 0, 1, \ldots) \\ B_n &= \frac{1}{\pi}\int_{-\pi}^{\pi} E(\theta)\sin n\theta\, d\theta \qquad (n = 1, 2, \ldots) \end{aligned}\right\} \tag{1.3}$$

For the *equality* of E and F it is necessary that $E(\pi) = E(-\pi)$ and that E is continuous in the range [111.1].

1.1. **Discontinuous functions.** If E is discontinuous within or at the end-points of its periodic interval, then, with the sign for 'correspondence',

$$E \sim F \tag{1.4}$$

Let a discontinuity occur at $\theta = \theta_0$ and then at this point [111.1]

$$F_0 = \tfrac{1}{2}[E(\theta_0+0)+E(\theta_0-0)] \tag{1.5}$$

Fig. D,1.1 shows the state diagrammatically.

† This mode of representation proved so unpalatable to Fourier's contemporaries that its publication was delayed some twelve years while the ideas were revised on what constitutes a function. The beginnings of modern analysis resulted.

2. Differentiation and integration of Fourier series

The Fourier series is differentiable term by term when

$$E = F \qquad (-\pi \leqq \theta \leqq \pi) \tag{2.1}$$

and $dE/d\theta$ is also differentiable [111.2]. In the deformation problem these conditions are satisfied (or arranged).

2.1. **Derivatives from the right and the left at a point.** It may happen that the derivative $dE/d\theta$ does not exist at a point

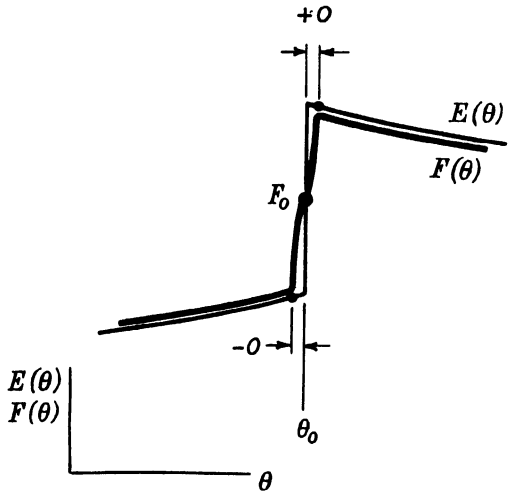

FIG. D,1.1.—The discontinuity in a function E. The Fourier representation F of E converges to F_0, the mean value of E at the discontinuity.

θ_0 where there is a cusp or acute or obtuse 'corner' of the curve $E(\theta)$ vs. θ, for example. However, for the continuous functions we consider there will be a derivative $(dE/d\theta)_{\theta=\theta_0+0}$ to the right of θ_0 and a derivative $(dE/d\theta)_{\theta=\theta_0-0}$ to the left of θ_0. The Fourier series $F(\theta)$ is differentiable termwise at each of these two points and each derivative converges to the appropriate derivative of $E(\theta)$ [111.2]. Thus,

$$\frac{dE}{d\theta} = \frac{dF}{d\theta} \quad \text{when} \begin{Bmatrix} \theta = \theta_0+0 \\ \theta = \theta_0-0 \end{Bmatrix} \tag{2.2}$$

2.2. **Mean derivatives.** The derivative of $F(\theta)$ at any point θ_0 in its periodic interval is always [111.3]

$$\left(\frac{dF}{d\theta}\right)_{\theta=\theta_0} = \tfrac{1}{2}\left[\left(\frac{dE}{d\theta}\right)_{\theta=\theta_0-0} + \left(\frac{dE}{d\theta}\right)_{\theta=\theta_0+0}\right] \tag{2.3}$$

provided that there are right- and left-hand derivatives $d^2E/d\theta^2$ *at* the point. Fig. D,2.1 shows the state diagrammatically. One may think of the 'corner' of F as 'rounded' by not quite fitting the 'corner' in E and with the slope the mean of the two values for E just on each side of the point θ_o.

A similar proof gives the higher-order mean derivative at a point in terms of the right- and left-hand derivatives.

2.3. **Integration.** The conditions imposed on $E(\theta)$ for term-wise integration of $F(\theta)$ are less rigorous than those for differentiation [111.3] but are certainly covered by those already given.

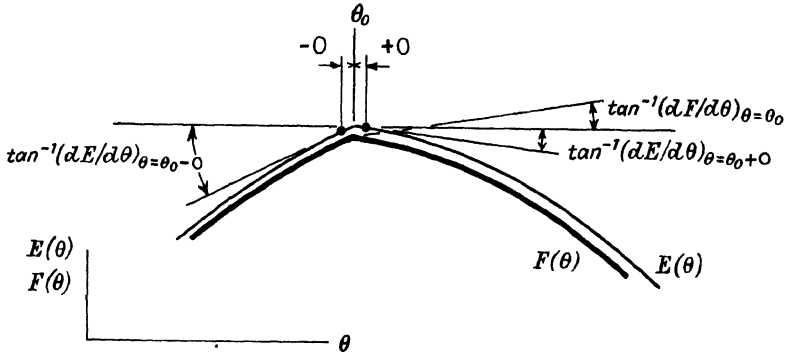

FIG. D,2.1.—A discontinuity of slope in the continuous function E. The slope of the Fourier representation F of E converges to the mean value of the slopes of E at the point.

3. Harmonic analysis

Frequently it is required to express a set of discrete observations $E_k(\theta)$ as lying on a curve $H(\theta)$, say, given by the addition of a *finite* number N of trigonometric terms. Thus, similar to article D,1, there is given the approximate equality,

$$E(\theta) \doteqdot H(\theta) \tag{3.1}$$

with

$$H(\theta) = A_0 + \sum_{n=1,\ldots,N} (A_n \cos n\theta + B_n \sin n\theta) \tag{3.2}$$

The A's and B's are determined, so that the *continuous* function $H(\theta)$ passes through the E_k values. Usually the interval is subdivided into 12 or 24 segments. The method of determining the A's and B's is simple but too lengthy to be given here. A

concise account with methodical tabular working is given by E. T. Whittaker & G. Robinson [93.3], for example.

For a given set of arbitrary observations in the range $a \leqq \theta \leqq b$ there is usually more than one possible choice of interval of periodicity which may be greater than interval (a,b). The choice of interval is frequently governed by the boundary conditions in the physical problem. Whatever choice is made cusps and corners do not occur for $H(\theta)$, so that it is differentiable any number of times, although $E(\theta)$ might appear to have cusps and corners and hence to be undifferentiable at such points. Note carefully that $H \to E$ as closely as we wish by merely subdividing interval (a,b), or sub-intervals in this range, into sufficiently small parts. Thus, from the very nature of the discrete observations in an experiment, they may always be associated with functions that are continuous and differentiable.

REFERENCES

1. SALMON, E. H., *Materials and Structures*, v. I, Longmans, 1931.
   1.1 p. 492
2. UNWIN, W. C., *Testing of Materials of Construction*, Longmans, Green & Co., 1910.
3. SWAINGER, K. H. & TWYMAN, J., *J. Sc. Instr.*, v. 25 (1948), p. 187.
4. ISAAC, P. C. G. & DOBIE, W. B., *Electrical Resistance Strain Gauges*, English Universities Press, Ltd., 1948.
5. SWAINGER, K. H., *Phil. Mag.*, v. 38 (1947), p. 422.
6. PROFESSOR A. C. RUGE, in a private communication of 29th October, 1946, stated that the first modern 'bonded' strain-gauges began to be developed at the California Institute of Technology in 1937, while he, independently, developed a similar device at the Massachusetts Institute of Technology in 1938. See also *The Development of Electrical Strain Gauges*, de Forest, A. V. & Leaderman, H., N.A.C.A. Tech. Note 744.
7. THOMSON, SIR WM. (Lord Kelvin), *Roy. Soc., London, Trans.*, v. 146 (1856), p. 733. (C. A. Coulomb, *Mém. acad. sci., Paris* (1784), anticipates Kelvin to some extent by experiments on the change of electrical resistance of wires under torsion.)
8. SWAINGER, K. H., *Nature*, v. 159 (1947), p. 61.
9. SWAINGER, K. H., *Soc. Exper. Stress Anal., U.S.A., Proc.*, v. 5(2) (1948), p. 1.
10. WEIBULL, W., *Nature*, v. 162 (1948), p. 966.
11. BOAS, W., *Seventh Intern. Congr. Appl. Mech., London, Proc.* (1948), p. 356.
12. KUHN, W., *Kolloidzschr.*, v. 68 (1934), p. 2. (See [13] for further publications up to 1947.)
13. TRELOAR, L. R. G., *Physics of Rubber Elasticity*, Oxford, Clarendon Press, 1949.
    13.1 p. 61 | 13.2 p. 62 | 13.3 p. 236
    13.4 119 |
14. RIVLIN, R. S., *Roy. Soc., London, Phil. Trans.* (*A*), v. 241 (1948), p. 379, and subsequently up to 1951. (See Volume I, reference 24 for a more complete list.) *J. Rational Mech. & Anal.*, v. 2 (1953), p. 53; *Techn. Rpt.* 105 (January 1954) of Brown University, Providence, R.I., U.S.A.

15. REINER, M., *Stand. Inst., Palestine*, 1948.

16. RIVLIN, R. S. & SAUNDERS, D. W., *Roy. Soc., London, Phil. Trans.* (*A*), v. 243 (1951), p. 251.

17. MOONEY, M., *J. Appl. Phys.*, v. 11 (1940), p. 582.

17.1 p. 582 | 17.2 p. 584 | 17.3 p. 585 | 17.4 p. 583

18. HOLT, W. L. & MCPHERSON, A. T., *J. Res. Nat. Bur. Stand.*, v. 17 (1936), p. 657.

19. TODHUNTER, I. & PEARSON, K., *History of the Elasticity and Strength of Materials*, Cambr. Univ. Press, v. I, 1886; v. II, parts 1 and 2, 1893.

19.1	v. I	p. 69	19.2	v. I	p. 869
19.3	II(2)	198	19.4	II(2)	412
19.5	I	361	19.6	I	375
19.7	II(1)	1	19.8	II(1)	166
19.9	II(1)	165	19.10	I	67
19.11	II(1)	167	19.12	II(1)	196
19.13	II(1)	168	19.14	II(1)	169
19.15	I	208	19.16	I	5
19.17	I	6	19.18	I	82
19.19	I	324	19.20	I	865
19.21	II(2)	129			

20. SOKOLNIKOFF, I. S. & E. S., *Higher Mathematics for Engineers and Physicists*, McGraw-Hill, 1939, p. 49, or else a book on Determinants.

21. MILNE-THOMSON, L. M., *Theoretical Hydrodynamics*, Macmillan, 1938.

21.1	p. 176	21.2	p. 143	21.3	p. 144
21.4	145	21.5	149	21.6	268
21.7	158	21.8	156	21.9	248
21.10	249	21.11	120	21.12	122

22. GREENHILL, A. G., *Encycl. Britt.*, 9th ed., v. 12, p. 435.

23. TIMOSHENKO, S., *Theory of Elasticity*, McGraw-Hill, 1934.

23.1	p. 239	23.2	p. 25	23.3	p. 76
23.4	13	23.5	70	23.6	199
23.7	60	23.8	162	23.9	163
23.10	166	23.11	239	23.12	187
23.13	188	23.14	18		

24. NAVIER, C., *Leçons, sur l'application de la mécanique*, Paris, 1864, 3rd ed., edited by Saint-Venant.

25. PRANDTL, L., *Phys. Z.*, v. 4 (1903), p. 758.

26. LARMOUR, J., *Phil. Mag.*, v. 33 (1892), p. 76.

27. URWIN, C. R. & SWAINGER, K. H., *J. Roy. Aero. Soc.*, v. 51 (1947), p. 867.

28. WEATHERBURN, C. E., *Advanced Vector Analysis*, G. Bell & Sons, 1937.

28.1 p. 140

29. SOUTHWELL, R. V., *Theory of Elasticity*, Oxford, 1936.

29.1 p. 384 | 29.2 p. 373 | 29.3 p. 374 | 29.4 p. 137

30. POYNTING, J. H., *Roy. Soc., London, Proc.* (*A*), v. 82 (1909), p. 546; v. 86 (1912), p. 534.

31. TRUESDELL, C., *J. Rational Mech. & Anal.*, v. 1 (1952), pp. 125–300.

32. SAINT-VENANT, B., *Comp. Rend. Acad. Sc., Paris*, v. 70 (1870), p. 473.

33. LÉVY, M., *Comp. Rend. Acad. Sc., Paris*, v. 70 (1870), p. 1323.

34. MISES, R. VON, *Gött. Nachr., math.-phys. Kl.* (1913), p. 582.

35. PRANDTL, L., *First Intern. Congr. Appl. Mech., Delft, Proc.* (1924), p. 43.

36. REUSS, A., *Zeits. ang. Math. Mech.*, v. 10 (1930), p. 266.

37. HILL, R., *Mathematical Theory of Plasticity*, Oxford, Clarendon Press, 1950.

37.1 p. 38 footnote	37.2 p. 15	37.3 p. 33
37.4 34	37.5 40	37.6 116
37.7 303	37.8 22	37.9 307
37.10 129		

38. PRAGER, W. & HODGE, P. G., *Theory of Perfectly Plastic Solids*, John Wiley & Sons, 1951.

39. MURNAGHAN, F. D., *Amer. J. Maths.*, v. 59 (1937), p. 235.

39.1 p. 249

40. MURNAGHAN, F. D., *Finite Deformation of an Elastic Solid*, John Wiley & Sons, 1951.

41. LUDWIK, P., *Elemente der technologischen Mechanic*, Springer, Berlin, 1909.

42. HENCKY, H., *J. Rheol.*, v. 2 (1931), p. 169.

43. ROLLASON, E. C., *Metallurgy for Engineers*, Edward Arnold, 1939.

44. PALM, J., *De Ingenieur*, 1948.

45. OSTWALD, W., *Kolloidzschr.*, v. 40 (1926), p. 58.

46. NADAI, A., *Plasticity*, McGraw-Hill, 1931.
46.1 p. 197 | 46.2 p. 244 | 46.3 p. 183.

47. SWAINGER, K. H., *Phil. Mag.*, v. 36 (1945), p. 443.

48. SWAINGER, K. H., *Eighth Intern. Congr. Appl. Mech., London, Proc.* (1948), p. 49.

49. SOKOLNIKOFF, I. S. & SPECHT, R. D., *Mathematical Theory of Elasticity*, McGraw-Hill, 1946.

50. LOVE, A. E. H., *Mathematical Theory of Elasticity*, Cambr. Univ. Press, 1934.

51. MAXWELL appears to have started the technique; RELF, E. F., *Phil. Mag.*, (series 6) v. 48 (1924), for experimental details in two dimensions; STENSTRÖM, L., 'Three-dimensional Potential Gradient Tank', Saab Aircraft Co., Linköping, Sweden, (1949); elaboration of the technique is given by BOOTHROYD, A. R., CHERRY, E. C. & MAKAR, R., *Inst. Elect. Eng., London, Proc.* (1), v. 96 (1949), p. 163; and CHERRY, E. C., *Symp. on Modern Network Synthesis, Proc.* (1952), Brooklyn Polyt. Inst., U.S.A.

52. REINER, M., *Am. J. Math.*, v. 70 (1948), p. 433; *Hebrew Inst. Techn., Israel, Sc. Publ.*, no. 4 (1950), p. 15; *Bull. Res. C., Israel*, v. 1 (1951), p. 126.

53. SWIFT, H. W., *Engineering*, v. 163 (1947), p. 253.

54. DAVIS, E. A., *J. Appl. Mech.*, v. 10 (1943), p. A-187; v. 12 (1945), p. A-13.

55. NADAI, A., *Inst. Mech. Eng., London, Appl. Mech., Proc.*, v. 157 (1947), p. 121.

56. OSGOOD, W. R., *J. Appl. Mech.*, v. 14 (1947), p. A-147.

57. FRAENKL, S. J., *J. Appl. Mech.*, v. 15 (1948), p. A-453.

58. BRIDGMAN, P. W., *Phil. Mag.*, v. 24 (1912), p. 63.

59. SWAINGER, K. H., *Soc. Exper. Stress Anal., Proc.*, v. 7(1) (1949), p. 117.

60. MORRISON, J. L. M. & SHEPHERD, W. M., *Inst. Mech. Eng., London, Proc.*, v. 163 (1949), p. 1.

61. PETERS, R. W., DOW, N. F. & BATDORF, S. B., *Soc. Exper. Stress Anal., Proc.*, v. 7(2) (1949), p. 127.

62. PRAGER, W., *J. Appl. Mech.*, v. 15; *Am. Soc. Mech. Eng., Trans.*, v. 70 (1948), p. 226.

63. SWAINGER, K. H., discussion in reference [60].

64. SWAINGER, K. H., *Nature*, v. 165 (1950), p. 360.

65. MORRISON, J. L. M. & SHEPHERD, W. M., *Inst. Mech. Eng., London, Proc.*, v. 159 (1948), p. 95.

66. TROUTON, F., *Roy. Soc., London, Proc.* (*A*), v. 77 (1906), p. 326.

67. SWAINGER, K. H., *Nature*, v. 161 (1948), p. 650.

68. SWAINGER, K. H., *Appl. Sc. Res.*, v. A2 (1950), p. 281.

69. GORDON, A. N., *Nature*, v. 166 (1950), p. 657.

70. SWAINGER, K. H., *Nature*, v. 166 (1950), p. 657, reply to polemical letter [69].

71. KIRSCH, G., *V.D.I.*, v. 42 (1898), p. 797.

72. GOLOVIN, H., *Inst. Techn., St. Petersburg, Trans.* (1881).

73. SWAINGER, K. H., *J. Appl. Mech.*, v. 15 (1948), p. A-45.

74. TRELOAR, L. R. G., *Phys. Soc., London, Proc.*, v. 60 (1948), p. 135.

75. SETH, B. R., *Roy. Soc., London, Phil. Trans.* (*A*), v. 234 (1935), p. 231.

76. RUNGE, C., *Z. Math. u. Phys.*, v. 50 (1908), p. 225; LIEBMANN, H., *Sitz. ber. math.-naturw. Abt. bayer. Akad. Wiss. München* (1918), p. 385; THOM, A., *Aero. Res. Comm., Rep. & Mem.* (1928), no. 1194.

77. SOUTHWELL, R. V., *Relaxation Methods in Theoretical Physics*, Oxford, Clarendon Press, 1946.

77.1	p. 19	77.2	p. 20	77.3	p. 23
77.4	40	77.5	45	77.6	46 footnote
77.7	179	77.8	39	77.9	2
77.10	9	77.11	10	77.12	47
77.13	3	77.14	101		

78. MOHR, O., *Ziviling.* (1882), p. 113.

79. COKER, E. G. & FILON, L. N. G., *Photoelasticity*, Cambr. Univ. Press, 1931.

79.1	p. 128	79.2	p. 126

80. FILON, L. N. G., *Roy. Soc., London, Phil. Trans.* (*A*), v. 201 (1903), p. 63.

81. SWAINGER, K. H., Thesis for Ph.D.(Eng.), London (1944).

82. SWAINGER, K. H., *Aero. Res. Comm., Rep. & Mem.* (1945), no. 1999.

83. DRUCKER, D. C., *Stress-strain Relations in the Plastic Range: A Survey of Theory and Experiment*, Brown University, Providence, R.I., U.S.A., 1950.

84. SWAINGER, K. H., *Nature*, v. 158 (1946), p. 165.

85. DRUCKER, D. C. & STOCKTON, F. D., *Instrumentation and Fundamental Experiments in Plasticity*, Brown University, U.S.A., June, 1952.

86. ILYUSHIN, A. A., *Izv. Akad. Nauk S.S.S.R.*, Otd. Tehn. Nauk (1949), p. 1753.

87. KUZNETSOV, V. D., *Physics of Solids*, v. 4, Tomsk Poligraphizdat (1947).

88. RATNER, S. I., *Plasticity and Strength of Metals*, Oborongiz (1949).

89. ILYUSHIN, A. A., *Plasticity*, Gostechizdat (1948).

90. FREUDENTHAL, A. M., *Inelastic Behaviour of Engineering Materials and Structures*, John Wiley & Sons, 1950.

91. KOLSKY, H., *Soc. Glass Techn., Trans.*, v. 36 (1952), p. 56.

92. HERTZ, H., *J. Math. (Crelle's J.)*, v. 92 (1882), p. 156; *Gesammelte Werke*, Leipzig, v. I (1895), p. 155; *Miscellaneous Papers*, Macmillan, 1896.

93. WHITTAKER, E. T. & ROBINSON, G., *Calculus of Observations*, Blackie & Son, 3rd ed., 1940.

93.1 p. 79 | 93.2 p. 363 | 93.3 pp. 260–284

94. BICKLEY, W. G., *Math. Gaz.*, v. 25 (1941), p. 19.

95. SHORTLEY, G., WELLER, R., DARBY, P. & GAMBLE, E. H., *J. Appl. Phys.*, v. 18 (1947), p. 116.

96. MORRIS, J., *The Escalator Method*, Chapman & Hall, 1947; *Phil. Mag.*, v. 36 (1946), p. 106.

97. Cross H., *Am. Soc. Civ. Eng., Proc.*, v. 56 (1930), p. 919.

98. DUNCAN, W. J. & COLLAR, A. R., *Phil. Mag.*, v. 17 (1934), p. 865.

99. MORRIS, J. & HEAD, J. W., *Aircraft Eng.*, v. 14 (1942), p. 313; *Phil. Mag.*, v. 35 (1) (1944), p. 735.

100. LEVY, H. & BAGGOTT, E. A., *Numerical Studies in Differential Equations*, v. I, Watts, 1934.

101. ÖDMAN, S. T. A., Swedish Cement & Concrete Res. Inst., Stockholm, Bull. no. 10 (1948); no. 20 (1953).

102. RAYLEIGH, LORD, *London Math. Soc., Proc.*, v. 17 (1887), p. 4; *Scientific Papers*, v. 2, p. 441.

103. SOUTHWELL, R. V., *Roy. Soc., London, Proc. (A)*, v. 151 (1935), p. 56; v. 153 (1935), p. 41.

104. CHRISTOPHERSON, D. G. & SOUTHWELL, R. V., *Roy. Soc., London, Proc.* (*A*), v. 168 (1938), p. 317.

105. SHORTLEY, G., *Science*, v. 105 (1947), p. 455.

106. SWAINGER, K. H., *Nature*, v. 162 (1948), p. 532.

107. HOGAN, T. K., *J. Inst. Eng., Australia*, v. 15 (1943), p. 89.

108. REDSHAW, S. C., *Inst. Mech. Eng., London, Proc.*, v. 159 (1948), p. 55.

109. FILON, L. N. G., *Roy. Soc., London, Phil. Trans.* (*A*), v. 193 (1899), p. 309.

110. FOURIER, J. B. J., *Théorie de la chaleur*, 1811.

111. CHURCHILL, R. V., *Fourier Series and Boundary Value Problems*, McGraw-Hill, 1941.

111.1 p. 72 | 111.2 p. 78 | 111.3 p. 80

112. KNOPP, K., *Theory and Application of Infinite Series*, Blackie & Son, 1928.

112.1 p. 324

113. GRIFFITH, A. A., *Roy. Soc., London, Phil. Trans.* (*A*), v. 221 (1920), p. 163; *Intern. Congr. Appl. Mech., Delft, Proc.* (1924), p. 55.

114. HOPKINS, W., *Camb. Phil. Soc., Trans.*, v. 8 (1849), p. 456.

115. FROCHT, M. M., *Photoelasticity*, v. I, John Wiley & Sons, 1941.

115.1 p. 13

116. HOUWINK, R., *Elasticity, Plasticity and Structure of Matter*, Cambridge, 1940.

116.1 p. 23 | 116.2 p. 84

117. LÜDERS, W., *Dinglers Polytechn. J.*, v. 155 (1860); *Polytechn. Centralbl.* (1860), cols. 960–4.

118. JOFFÉ, A. F., *Physics of Crystals*, New York, 1928.

119. YAMAGUCHI, K., *Inst. Phys. Chem. Res., Tokyo, Sc. Papers*, v. 8 (1928), p. 289; v. 11 (1929), p. 151 and p. 223.

120. TAYLOR, G. I., *Faraday Soc., Trans.*, v. 24 (1928), p. 121.

121. TAYLOR, G. I., *Roy. Soc., London, Proc.* (*A*), v. 145 (1934), p. 362, p. 388, p. 405; *Fourth Intern. Congr. Appl. Mech., Cambridge, Proc.*, p. 113.

122. POLANYI, M., *Z. Phys.*, v. 89 (1934), p. 660.

123. OROWAN, E., *Z. Phys.*, v. 89 (1934), p. 605, p. 614, p. 634; v. 97 (1935), p. 573; v. 98 (1936), p. 382.

124. GUEST, J. J., *Phil. Mag.*, v. 50 (1900), p. 69.

125. HANCOCK, E. L., *Phil. Mag.*, v. 12 (1906), p. 418; v. 15 (1908), p. 214; v. 16 (1908), p. 720.

126. SCOBLE, W. A., *Phil. Mag.*, v. 12 (1906), p. 533; v. 19 (1910), p. 116, p. 908; *Phys. Soc., Proc.*, v. 20 (1907), p. 374.

127. MASON, W., *Inst. Mech. Eng., London, Proc.*, v. 4 (1909), p. 1205.

128. TURNER, L. B., *Engineering*, v. 87 (1909), p. 169; v. 92 (1911), p. 115.

129. CRAWFORD, W. J., *Roy. Soc., Edinburgh, Proc.*, v. 32 (1911), p. 348.

130. COOK, G. & ROBERTSON, A., *Engineering*, v. 92 (1911), p. 786; *Roy. Soc., London, Proc.* (*A*), v. 88 (1913), p. 462.

131. BECKER, A. J., *Univ. Ill. Eng. Exp. Stn., Bull. no.* 85 (1916), p. 84.

132. SEIGLE, J. & CRETIN, F., *Rev. Mét. Mém.*, v. 22 (1925), p. 374; *Génie Civil* (1925), p. 345.

133. TAYLOR, G. I. & QUINNEY, H., *Roy. Soc., London, Proc.* (*A*), v. 145 (1934), p. 1.

134. MORRISON, J. L. M., *Inst. Mech. Eng., Proc.*, v. 142 (1940), p. 193.

135. GUEST, J. J., *Inst. Auto. Eng., J.*, v. 9 (1940), p. 35.

136. ENNSLIN, M., *Z. Ver. deut. Ing.*, v. 72 (1928), p. 1625.

137. SACHS, G., *Z. Ver. deut. Ing.*, v. 72 (1928), p. 734.

138. COX, H. L. & SOPWITH, D. G., *Phys. Soc., Proc.*, v. 49 (1937), p. 134.

139. DEHLINGER, U., *Z. Metallkunde*, v. 35 (1943), p. 182.

140. SNITKO, N. K., *J. Tech. Phys.*, v. 18 (1948), p. 857.

141. LODE, W., *Z. ang. Math. Mech.*, v. 5 (1925), p. 142; *Z. Phys.*, v. 36 (1926), p. 913; *Forsch. Ver. deut. Ing.*, v. 303 (1928).

142. LESSELLS, J. M. & MACGREGOR, C. W., *J. Franklin Inst.*, v. 230 (1940), p. 163.

143. DAVIS, E. A., *Am. Soc. Mech. Eng., Trans.*, v. 62 (1940), p. 577.

144. LARMOUR, J., *Origin of Clerk Maxwell's Electric Ideas as described in Familiar Letters to William Thomson*, Cambridge, 1937, p. 32.

145. HUBER, M. T., *Czasopismo Technizne*, Lwov (1904).

146. HENCKY, H., *Z. ang. Math. Mech.*, v. 5 (1925), p. 115.

147. WINZER, A. & PRAGER, W., *J. Appl. Mech.*, v. 15 (1948), p. A-187.

148. ILYUSHIN, A. A., *Prikl. Mat. i. Mekh.*, v. 10 (1946), p. 347.

149. TAYLOR, G. I., *Q. J. Mech. Appl. Math.*, v. 1 (1948), p. 103.

150. LAMB, H., *Hydrodynamics*, Cambridge University Press, 6th ed. (1932), reprinted 1953.

151. PRANDTL, L. & TIETJENS, O. G., *Fundamentals of Hydro- and Aeromechanics* and *Applied Hydro- and Aeromechanics*, McGraw-Hill, 1934.

152. YOUNG, T., *A Course of Lectures on Natural Philosophy and the Mechanical Arts*, London, 1807.

153. EULER, L., *Histoirie de l'Académie de Berlin*, 1755.

154. NAVIER, C., *Mém. de l'Acad. des Sciences*, v. 6 (1822), p. 389.

155. CAUCHY, A. L., *Exercices de mathématiques*, v. 2 (1827).

156. GOLDSTEIN, S., as editor of the Fluid Motion Panel of the Aeronautical Research Committee, *Modern Developments in Fluid Dynamics*, vols. I, II, Oxford, Clarendon Press, 1943.

156.1 v. I, p. 55 | 156.2 v. I, p. 60

157. PRANDTL, L., *Essentials of Fluid Dynamics*, Blackie & Son, 1952, p. 107.

GLOSSARY

The primary purpose of this glossary is to collect, for easy reference, the more unfamiliar technical terms introduced by the author to describe the new physico-mathematical ideas of the theory. The commonplace terms of the subject are not given here usually, but are, of course, described in the general text where appropriate.

Stress

Tensile stress is orthogonal to and acting outwards from the surface of an element of volume. This is a positive normal stress.

Compressive stress is orthogonal to and acting inwards to the surface of an element of volume. This is a negative normal stress.

One-stress loading is given to a substance when the stress throughout the body is either simple tensile or simple compressive.

Two-stress loading is given to a substance when the complex stresses at each point of it can be reduced to only two orthogonal normal stresses.

Three-stress loading is the general case. Every complex stress system at a point can be reduced to three mutually orthogonal principal normal stresses (or two, or one, as particular cases).

Stress dyadic with its scalar, principal normal stress components those of the one-stress, two-stress or three-stress loading as appropriate for the point.

Stress invariants are combinations of the scalar stress components of the stress dyadic which retain their arithmetical values for any directions to which the dyadic is referred.

Stress transfer is the rotation of the principal normal stresses at a point relative to the local substance.

Partial-increment stress dyadic is one in which increments of scalar stresses appear but not increments of the unit dyads.

Auxiliary normal stresses at a point are those acting on planes normal to the face diagonals of an elemental cube and, when used appropriately, are 'equivalent' to the complementary shear stresses.

Octahedral stress is a vector stress acting on a plane normal to a stress octahedral direction having equal angles with all three principal normal stress directions defining the *stress-space*.

Octahedral normal stress is the component of the octahedral stress parallel to the stress-space octahedral unit vector. Scalarly, it is $\frac{1}{3}$ the value of the first stress invariant equal to the sum of the normal stresses.

Octahedral shear stress is the component of the octahedral stress normal to the stress-space octahedral unit vector.

Plane stress is plane, two-dimensional two-stress. Thus, it is independent of the coordinate normal to its plane of distribution.

Curvilinear plane stress is two-dimensional two-stress distributed over a curvilinear surface.

Generalised plane stress theory considers stresses and strains averaged over the thickness of a plate. The normal stress on all planes parallel to the stress-free main faces of a plate is hypothesised as identically zero.

Quasi-plane stress theory is similar to the generalised plane stress theory except for fewer arbitrary assumptions. The normal stress on planes parallel to the stress-free main faces of the plate is not hypothesised as zero.

Modified Maxwell stress function is the direct, three-dimensional extension of the Airy two-dimensional stress function. It is given by leaving off the three distinguishing superscripts from the three Maxwell stress functions said to be independent one from another. (Each of the three Maxwell stress functions removes from the stress dyadic the necessary property of invariant transformability and, therefore, they are not acceptable to represent the stress dyadic.)

Strain

Normal strain is suffered by an element when it is initially and currently rectangular. (Generally, the element can be of different curvilinearity in the two states.)

Applied extensile strain usually induces *transverse contractile strain.*

'True' normal strain parallel to the edges of the orthogonal element in one direction is the relative displacement between the ends of these edges per unit length of the currently deformed element.

'Nominal' normal strain is the relative displacement per unit length of the initially undeformed element.

Unit stretch is the relative displacement (absolute-displacement) between the ends of a line element (in general, not in the principal normal strains directions) per unit current length of the line.

Er is coined from 'extension ratio' which is the current length of a line element divided by its initial length.

Ser is coined from 'squared extension ratio' and is $(er)^2$.

Inver is coined from 'inverse extension ratio' and is the initial length of a line element divided by its current length.

Invser is coined from 'inverse squared extension ratio' and is $(inver)^2$.

Strain metric is a scalar relation between the gradients of displacement and the initial and current lengths of any elemental line in the continuous elastic body. Thus, the quadratic strain metric gives the ser when the coordinates are those of the point in the undeformed

elastic body, and the invser when the coordinates refer to the deformed elastic body. The linear strain metric gives the er when the coordinates refer to the undeformed elastic body, and the inver when the coordinates refer to the deformed body.

Strain dyadic has three mutually orthogonal, scalar, principal normal strains of the same values as the unit stretches for the corresponding directions.

Strains for general directions are the coefficients of the strain dyadic when it has been transformed invariantly from its principal directions.

Strain invariants are combinations of scalar strain components and each retains its arithmetical value for any directions to which the strain dyadic is referred.

Strain transfer is the rotation of the principal normal strains directions at a point relative to the deformable substance local to that point.

Partial-strain at a point for a given principal normal strain component is the strain in that direction less the effects of the two transverse partial-strains.

Partial-increment strain dyadic is one having increments of scalar strain but not increments of the unit dyads.

Auxiliary normal strains at a point are those in the directions of the face diagonals of an elemental cube and, when used appropriately, give a measure of the shear strains.

Octahedral strain is best visualised as a vector relative-displacement between the ends of the strain-space octahedral unit vector. (See volume I, article III,10.)

Octahedral normal strain is the component of the octahedral strain parallel to the strain-space octahedral unit vector. Scalarly, it is $\frac{1}{3}$ of the value of the first strain invariant.

Octahedral shear strain is the component of the octahedral strain normal to the stress-space octahedral unit vector.

Reference spaces

Spatially fixed axes are those relative to which the body may move as a whole and obey the Newtonian laws of motion.

Locally convected axes are in the principal normal strains orthogonal directions from a typical point of the deformed body and are also orthogonal in the undeformed body but at some other spatial orientation. If these axes are regarded as imbedded in the local, deformable substance then, generally, they are not orthogonal at any state other than the initially undeformed and currently deformed states.

Deformable reference is a set of orthogonal trajectories given by the aggregate of all the locally convected axes and changing its curvilinearity from the initially undeformed to the currently deformed state but remaining orthogonal at these end states.

Whole-body convected axes are a non-deformable orthogonal set with their origin at an arbitrary point of the body and are tangential to the locally convected axes at that point.

Displacement is the rectilinear vector joining the initial and current positions of a point relative to an arbitrarily chosen reference line, lines or space that can be locally infinitesimal or generally finite.

Spatial-displacement is that relative to the spatially fixed space.

Absolute-displacement is usually given in differential form and is the linewise displacement of one end of an elemental line relative to its other end.

Relative-displacement in differential form is the displacement of one end of an elemental line vector relative to its other end as seen from the locally convected reference space. The three components of the differential relative-displacement relative to the local reference each equals the differential absolute-displacement of the corresponding component of the elemental line vector relative to the locally convected axes. Relative-displacement as an entity is the summation, or integration, of its differentials between the origin of whole-body convected axes and the typical point considered. (Otherwise, it is the line integral of the strain dyadic between the two points.)

Straining-displacement is that relative to the whole-body convected axes.

Spatial convection-displacement is the difference between relative-displacement and spatial-displacement when the origin of the whole-body convected axes does not translate.

Whole-body convection-displacement is the component of spatial convection-displacement given by the difference between straining-displacement and spatial-displacement.

Straining convection-displacement is the component of spatial convection-displacement given by the difference between relative-displacement and straining-displacement. It is due to the distribution of strain at all points of the body other than that typical point on which attention is focussed in the equations.

Deformation-displacement is the elastic-displacement component plus the plastic-displacement component of elasto-plastic straining relative to the whole-body convected axes.

Doublet vector field is one consisting of two added vector fields components of which the solenoidal (rotational) components are equal but of opposite sign. Thus, the doublet is lamellar but each of its components is not lamellar in general. (See article A,32 of volume I.)

Complementary doublet vector fields are equal and all components, whether implicit or explicit, are in one-one correspondence.

Initial positions

Spatially initial position is relative to the spatially fixed axes and is given by current position minus spatial-displacement.

Relatively initial position is relative to the deformable reference and is given by current position minus relative-displacement.

Instantaneously initial position is relative to the whole-body convected axes and is given by the current position minus straining-displacement.

Rotations

Spatial-rotation is that of the locally convected axes relative to the spatially fixed reference.

Straining-rotation is that of the locally convected axes relative to the whole-body convected axes.

Whole-body rotation is that of the whole-body convected axes relative to the spatially fixed reference.

Stress-strain

Stress-strain parameters quadadic has as its scalar coefficients the phenomenological values found to relate the stress and strain partial-increment dyadics. The principal normal strain directions are chosen arbitrarily as those with respect to which the physical parameters are defined. After invariant transformation to general directions the quadadic scalar coefficients include direction cosines for the orientation of the strain dyadic and so are not physical parameters. The quadadic in prefactor double scalar product with the partial-increment stress dyadic gives the partial-increment strain dyadic.

Anisotropic substances are those in which the principal directions of the stress and strain dyadics are not parallel at a typical point.

Isotropic substances are those in which the principal directions of the stress and strain dyadics are parallel at a typical point.

General isotropy is the condition when the stress-strain parameters are not isotropic.

Restricted isotropy is the condition when the stress-strain parameters are isotropic.

Octahedral-parametric surface for a point is that defined by the octahedral shear stress and strain and the isotropic plastic modulus.

Yielding

Equivalent normal stress for yielding hypothetically replaces a complex stress loading. It is only different from octahedral shear stress by a numerical factor.

Stress-tube is the vector sum of the principal normal stresses.

Strain energy

Unit strain energy is the energy of straining per unit current volume. If the unit initial volume is taken then the context distinguishes the two cases.

Zero strain energy function occurs in the straining of incompressible substances. Although of zero magnitude its derivatives with respect to strain are not zero and it is seen to influence the stress-strain relations discussed with respect to strain energy.

AUTHOR INDEX

N.B.—The references given in this index are to the *page numbers* given at the foot of each page, and not to the section headings.

SUBJECT INDEX

N.B.—The references given in this index are to the *page numbers* given at the foot of each page, and not to the section headings.

Indent marks refer to the whole of the previous unindented statement except the page numbers.